UNIVERSITÉ DE TOURS

ÉCOLE DOCTORALE : SSBCV

INSERM UMR1253, iBraiN – Genomics and Pathophysiology of Neurodevelopmental and Motor Disorders

THÈSE présentée par :

Yara ALOJAIMI

soutenue le : **9 décembre 2024**

pour obtenir le grade de : **Docteure de l'université de Tours**

Discipline/ Spécialité : Sciences de la vie et de la santé

Characterization of a therapeutic approach to target TDP-43 in amyotrophic lateral sclerosis using antibody fragments

THÈSE dirigée par :

Mme. BLASCO Hélène	Professeur des Universités, Praticien Hospitalier, Université de Tours

RAPPORTEURS :

M. LEBLANC Pascal	Chargé de Recherche, HDR, Université de Lyon
M. RAOUL Cédric	Directeur de Recherche, Université de Montpellier

---

JURY :

Mme. BLASCO Hélène	Professeur des Universités, Praticien Hospitalier, Université de Tours
M. PRADAT Pierre-François	Praticien Hospitalier, Sorbonne Université
M. LEBLANC Pascal	Chargé de Recherche, HDR, Université de Lyon
M. RAOUL Cédric	Directeur de Recherche, Université de Montpellier
Mme. ALLARD-VANNIER Emilie	Professeur des Universités, Université de Tours

Acknowledgements

I would like to extend my gratitude to the members of my jury for their invaluable time and insightful feedback.

Doctor **Pierre-François Pradat**, Neurologist at the Pitié-Salpêtrière (Paris), Neuroscientist at the Laboratory of Biomedical Imaging (Sorbonne University), and visiting professor at Ulster University (UK). Thank you for agreeing to be the President of the jury of my thesis.

Professor **Pascal Leblanc**, Principal Investigator at NeuroMyoGène Institute (Claude Bernard Lyon 1 University). Thank you for agreeing to be the reviewer of my thesis.

Doctor **Cédric Raoul**, Research Director at the Institute for Neurosciences of Montpellier (University of Montpellier). Thank you for agreeing to be the reviewer of my thesis.

Doctor **Emilie Allard-Vannier**, University Professor at the University of Tours and Researcher in the Laboratory of Galenic Pharmacy (University of Tours). Thank you for agreeing to be the examiner of my thesis.

I would also like to thank the **Région Centre Val de Loire**, **ARSLA**, the **LabEx MAbImprove**, and **Sanofi** for funding this project.

A special thank you as well for the team at Key-Obs (Orléans), Doctor **Jean-Charles Bizot**, Doctor **Fabrice Trovero**, Doctor **Fabienne Masse**, Doctor **Sabrina David**, and Doctor **Norinne Lacerda** for their invaluable help in the management and execution of the preclinical part of the project.

I would also like to thank the team from the metabolomics platform for their assistance. Professor **Patrick Emond**, thank you for your valuable feedback, your ideas and all the discussions we had. **Antoine Lefèvre**, thank you for your patience and your help with the metabolomics part of this project. **Jérémy Monteiro**, we always had very interesting discussions. Thank you for your ideas and for always checking up on how everything is going.

To my dear supervisor, Professor **Hélène Blasco**, I extend to you my deepest and most heartfelt gratitude. Your unwavering support and encouragement throughout this journey have meant more to me than words can express. From the very beginning, your insightful guidance and thoughtful feedback have been essential in helping me navigate the complexities of this big project. Your patience, kindness and dedication to my development as a researcher have inspired me every step of the way. Your constant belief in my abilities gave me the confidence to push forward. Thank you for trusting me throughout these 4 years and including me in many of your projects. For giving me the freedom to explore my capabilities. For teaching me to ask the right questions. For encouraging me to think outside the box. For showing me how to say “I don’t know” and ask for help and advice when needed. For teaching me how to keep trying but also knowing when to stop. I want to also thank you for always being transparent, for offering to help whenever you can, for being understanding and kind, and for always being there whenever I had a problem. I will always be grateful for the major role you’ve played in this journey. Thank you !

Doctor **Débora Lanznaster**, I am lucky to have had you as my co-supervisor at the beginning of my thesis and for the 3 years that followed. Apart from the technical training you gave me,

you taught me how to be patient, to plan ahead, and to stand up for my ideas. You also knew when to slow me down when I was overwhelming myself with too many things at once. You showed me how to maintain a good work-life balance. Your guidance, filled with kindness and understanding, helped me stay focused and motivated, especially during the challenging periods. Your ability to inspire confidence and provide reassurance made this journey much smoother than I imagined. Your constant smile, friendly demeanor, and positivity were always a source of encouragement. Thank you for everything!

Thank you to the Professor **Catherine Belzung**, Director of the INSERM Unit 1253, for welcoming me in your unit, and for your dedication to the PhD students which I had the chance to experience first-hand as a member of the BDE.

Doctor **Frédéric Laumonnier**, team leader of IDeALS. Thank you for welcoming me in your team, for your help in navigating the PhD journey within this lab, for your advice, and for everything you do to maintain and support the cohesiveness of this team (hopefully the Prison Island plan will finally happen!).

A big thank you to Professor **Patrick Vourc'h** for your valuable advice and ideas, your thorough feedback on the project and articles, your availability, and your kindness and encouragement.

Thank you, Professor **Christian Andres**, for the engaging discussions we had, as well as your attention to details, and valuable feedback and insights on various parts of this project.

Doctor **Jean-Michel Escoffre**, thank you for your advice and for always being there to help when needed.

Doctor **Charlotte Veyrat-Durebex**, thank you for your support on this project. Your feedback and suggestions have been a big help.

Doctor **Sylviane Marouillat**, I can't even imagine what the lab would be without you. Thank you for being caring, supportive, kind, and full of positive energy. Thank you so much for always finding time to help and always doing it with a smile. We are very lucky to have someone like you on the team.

Doctor **Rudolf Hergesheimer**, who not only laid the groundwork for this project but also took the time to train and guide me when I first started my thesis. I remember how inspired I felt by the dedication you exhibited for your work. Your willingness to share your knowledge and expertise were instrumental in helping me navigate the complexities of this project. Thank you.

Doctor **Sylvaine Renault**, thank you for your advice, your goodwill and for never hesitating to help whenever you got the chance.

Doctor **Devina Ung**, the famous postdoc of the lab. Thank you for your encouragement and tips whenever things were complicated. And for all the candy bags you kept bringing us!

And speaking of the famous postdocs of the lab, Doctor **Audrey Dangoumeau**. Thank you for your help in this project, your advice, your kindness, and constantly checking up on how everything is going.

Doctor **Thibaut Laboute**, it was great to have someone in the lab working on a topic so closely related to mine. Thank you for all your help and advice, and for patiently answering my countless questions. Keep taking photos of everything — they'll definitely come in handy one day!

Chloé Boisseau, our favorite lab technician. Thank you for all your assistance in the lab and for your help with my project. Your positivity, friendliness, and kindness have brought such great energy to the team. There's never a dull moment when you're around! We can always count on you to keep things lively!

Doctor **Samira Osman**, it's funny how we crossed paths again after all these years. It somehow felt like we were picking up right where we left off (reminiscing about the old times probably helped lol). It really is a small world. You're not just a colleague, you're a friend. Thank you for being caring, for offering your support when needed, and for encouraging me when things were tough. I wish you all the success and happiness in everything you pursue, both personally and professionally!

David Lever, thank you for your reactivity, and for all your help in managing all the administrative and financial side of this thesis from when I first arrived in Tours and throughout the entire time I was here.

To all the PhD students in the lab, both old and new, I wouldn't have wanted to share this experience with anyone else. You were all like a family to me here, and I am grateful for all of you. **Shanez**, thank you for your welcoming spirit and for all the fun moments we had together. I surely do miss having you here and hearing all about your adventures! **Florence**, my four years PhD partner FloFlo. From day one, we went through the ups and downs of this journey together, and I'm so grateful for all the wonderful memories we shared both in and outside the lab. We surely nagged a lot, but we're almost done! Thank you for being there for me, lightning the mood and always having crazy stories to tell! **Sara**, the one who's always losing her things! You're the most spontaneous, always smiling, kind-hearted person I know. I don't know how you managed to do it all, but you did. Never lose that positive energy of yours, it's contagious. **Léa,** my shawarma partner and the person who gets me the most. You never failed to make me smile when things were tough. You never got tired of listening to my stories. I know I can always count on you. Thank you for being the amazing person that you are. And I'll make sure you keep learning Arabic! **Laurine**, papi chinois, the queen of taking great photos! I can't think of many people who are as thoughtful and sincere as you. Your kind gestures never failed to lighten my mood. And thank you for all the French expressions you taught me! **Melissa,** you were only here for a few months, but I am happy I got the chance to meet you and grateful for the time we got to spend together here. Thank you for always being kind and caring. **Perla**, thank you for your kindness, your support and all the desserts we shared while you were here. **Hugo**, I can easily say that I never met anyone who is as timely and organized as you! I'm not sure I'll miss all the trips to Orléans, but I'm really glad for the nice chats and stories we shared on the road. **Yann**, I bet it wasn't always easy being

surrounded by all this feminine energy in the office, good thing you had your earphones! The way you handled this rollercoaster of a PhD was impressive. Thank you for the good times we had, and for always being kind and ready to help.

Marie, you came to the lab as an M2 intern and left as a great friend! I am happy for the time we got to spend together, both in and outside the lab. I hope we get to go on more trips together. For some reason, crazy bike rides and moules frites will now always remind me of you! I wish you all the success in everything you wish to do.

To the most amazing friends in the world, **Nathalie, Rosie, Line**, thank you for always being there for me, whether it was cheering me on during tough times or celebrating the small wins. For believing in me and pushing me forward. Thank you for being just one call away. You all made a world of difference. I love you so much and I can't wait to celebrate with you once this is all over. **Simon**, my number one partner in chocolate overdosing and laughing until we're crying. Being on the other side of the world yourself, you understood things that no one else could. Thank you for always being there and for inspiring me in so many ways!

Nay, not everyone is lucky enough to have a sister-in-law like you. Thank you for being so kind and understanding. You've always been welcoming and a source of comfort and positivity to the point where your place was my go-to whenever I needed a break. Thank you for being there, for encouraging me, for listening, for being part of my family here. I am very grateful for you.

My amazing parents, without whom I wouldn't be here today. **Mom, Pap,** there are no words that can express how thankful I am for the both of you. I cannot thank you enough for the sacrifices you've made to give me the opportunities I have today. Thank you for being there for me no matter what (and for taking super good care of my Masha while I'm gone!). Your belief in me has been a constant source of motivation, reminding me that I'm never alone, no matter how far I am. I know you are proud of me, and I hope to make you even prouder. Bhebkon.

To the bestest, most amazing brother, **Rami**. When people ask me who my role model is, my answer is always you. You've always been my biggest cheerleader. I cannot think of a time where you haven't been there for me, whether it was through your advice (yes, even when you were harsh and annoying) or simply being a shoulder to lean on. Thank you for believing in me even when I doubted myself, and for always knowing how to make me smile. Thank you for being my inspiration to always be the best I can be and to go for what I want and to aim higher. And I can't wait to celebrate all of our successes together. Love you!

My dearest friend, **Marc Msallem**, I wish you were still here to celebrate this with me. I was not prepared to lose you at the beginning of my thesis, but you made sure to give me all the positivity in the world before you left. I miss you always.

And to all the people whose support has meant the world to me. **Samira**, **May, Layal, Joséphine, Melissa, Joelle, Aline, Ahmad, Antonio**, thank you for everything.

Table of Contents

Acknowledgements **4**
List of abbreviations **12**
Résumé **14**
Abstract **17**
List of publications **20**
List of figures **21**
Introduction **22**
I. Amyotrophic Lateral Sclerosis 23
A. Overview of ALS 23
B. Epidemiology 24
C. Aetiology 25
D. Pathophysiology 30
E. ALS in the clinics 50
F. ALS biomarkers 54
II. TDP-43 : a major target in ALS 55
Publication 1: 57
III. Therapeutic development in ALS 77
A. Riluzole 77
B. Edaravone 78
C. Therapies targeting the CNS 79
Publication 2: 83
D. Why are clinical trials failing? 114
Aims and Objectives **117**
Results **119**
I. Effect of pH alterations on TDP-43 in ALS 120
Publication 4: 120
II. Development of scFvs targeting TDP-43 133

Publication 5 133
III. Development of SPION-scFv complexes for guided intracellular delivery of the scFv 180
A. Résumé en Français 180
B. Context 181
C. Materials and methods 182
D. Results 186
E. Discussion 190
IV. Characterization of a transgenic TDP-43 mouse model of ALS 194
Publication 6 194
V. AAV-mediated delivery of the scFvs B1, D7 and 13R4. 241
A. Résumé en Français 241
B. Context 242
C. Materials and methods 242
D. Results 244
E. Discussion 247
General discussion 248
Conclusion and perspectives 262
References 265

List of abbreviations

6*His	6*Histidine tag
ALS	Amyotrophic lateral sclerosis
ALSFRS-R	ALS Functional Rating Scale revised
AMPAR	α-amino-3-hydroxy-5-methyl-4-isoxazolepropionic acid receptor
ARE	Antioxidant responsive element
ASO	Antisense oligonucleotide
BBB	Blood-brain barrier
BMI	Body mass index
C9ORF72	Chromosome 9 open reading frame 72
CNS	Central nervous system
CSF	Cerebrospinal fluid
EAAT2	Excitatory amino acid transporter 2
EMG	Electromyography
ER	Endoplasmic reticulum
Fab	Fragment antigen binding
fALS	Familial ALS
Fc	Fragment crystallizable
FDA	Food and drug administration
FTD	Frontotemporal dementia
FUS	Fused in sarcoma
GluR2	Glutamate receptor subunit 2
GPX4	Glutathione peroxidase 4
HEK293T	Human embryonic kidney 293T cells
HSP	Heat shock protein
iPSC	Induced pluripotent stem cell
Kir4.1	Inwardly rectifying potassium channel 4.1
LMN	Lower motor neuron
MCT1	Monocarboxylate transporter 1

MRI	Magnetic resonance imaging
NCT	Nucleocytoplasmic transport
NfH	Neurofilament heavy
NfL	Neurofilament light
NF-κB	Nuclear factor kappa B
NGF	Nerve growth factor
NMDA	N-methyl-D-aspartate
NMJ	Neuromuscular junction
NRF2	Nuclear factor erythroid 2-related factor 2
PEG	Polyethylene glycol
PET	Positron emission tomography
pNfH	Phosphorylated neurofilament heavy
RBP	RNA binding protein
RNP	Ribonucleoprotein
ROS	Reactive oxygen species
RRM1-2	RNA recognition motifs 1 and 2
sALS	Sporadic ALS
scFv	Single chain variable fragment
SG	Stress granule
SOD1	Superoxide dismutase 1
SPION	Superparamagnetic iron oxide nanoparticle
TDP-43	Transactive response DNA binding protein 43
UMN	Upper motor neuron
UPR	Unfolded protein response
UPS	Ubiquitin proteasome system
VH	Variable heavy
VL	Variable light

Résumé

La Sclérose Latérale Amyotrophique (SLA) est une maladie neurodégénérative progressive affectant les neurones moteurs et conduisant à une paralysie totale. L'un des principaux marqueurs pathologiques de la SLA est l'accumulation anormale de la protéine TDP-43 dans les neurones et les cellules gliales retrouvée dans 97 % des patients SLA. Impliquée dans le métabolisme de l'ARN, cette protéine a un rôle clé dans la physiopathologie de la SLA de par son changement de localisation et son agrégation dans le cytoplasme. Ces modifications contribuent à une perte globale d'homéostasie et donc à une neurodégénérescence. Ces arguments font de cette protéine une cible thérapeutique prometteuse mais contrainte par les limites de l'accessibilité au système nerveux central (Publications 1, 2 et 3).

Dans ce projet, nous avons exploré plusieurs stratégies pour mieux comprendre la SLA en tant que protéinopathie liée à TDP-43 et nous avons développé des thérapies ciblant TDP-43. L'ambition de ce projet de thèse était ainsi de développer des biomédicaments ciblant TDP-43 et de les évaluer *in vitro* afin de comprendre les effets protecteurs potentiels, avant de proposer l'évaluation i*n vivo* des candidats thérapeutiques.

D'abord, nous nous sommes intéressés à la cible et nous avons montré que l'altération du pH intracellulaire augmentent la délocalisation de TDP-43 et son accumulation dans des punctas cytoplasmiques dans un modèle cellulaire de SLA, impactant ainsi le métabolisme (Publication 4). Ensuite, nous avons centré notre attention sur des candidats biomédicaments ciblant TDP-43 qui avaient été développés dans une précédente Thèse du Laboratoire (Hergesheimer, 2021). Nous avons choisi de caractériser deux fragments d'anticorps à chaîne unique (scFv), B1 et D7, qui ciblent TDP-43 humain entier. Le scFv D7, en particulier, réduit les niveaux du fragment pathologique TDP-35 insoluble, et est capable de restaurer certaines altérations métaboliques, notamment lipidiques associées à TDP-43 dans des HEK293T surexprimant TDP-43 (Publication 5).

Les effets protecteurs *in vitro* des candidats intracorps étant convaincants, nous avons débuté le projet d'évaluation préclinique, qui passe dans un premier temps par une meilleure caractérisation du modèle souris TDP-43. Nous avons ainsi étudié le modèle murin Prp-TDP-43^{A315T} afin d'identifier des paramètres phénotypiques, moléculaires et métabolomiques qui sont altérés à différents stades de la maladie et qui nous permettraient de mieux comprendre

l'évolution de ce modèle mais aussi d'identifier des paramètres objectifs et quantifiables de réponse aux candidats thérapeutiques. Ce modèle a reproduit des symptômes moteurs et des agrégats de TDP-43, avec des altérations métabolomiques et lipidomiques détectées dans différents tissus même avant l'apparition des symptômes. Cela fait de ce modèle un outil précieux pour explorer de nouvelles thérapies ciblant la protéinopathie TDP-43 comme les scFv identifiés dans cette étude (Publication 6).

En raison des difficultés à cibler le système nerveux central par les biothérapies, notamment à cause de la barrière hémato-encéphalique, nous avons exploré différentes méthodes pour améliorer l'administration du scFv. Nous avons développé des nanoparticules magnétiques à base d'oxides de fer (SPIONs) PEGylés complexés avec le scFv afin d'améliorer le ciblage du système nerveux central et en particulier le cortex moteur. Nous avons montré que les complexes SPION-scFv n'étaient pas toxiques dans des modèles in vitro et leur utilisation a permis d'améliorer l'internalisation cellulaire du scFv. En parallèle et après différents essais infructueux de voies d'administration de scFv dans des modèles murins précédemment cités nous avons utilisé des vecteurs viraux adéno-associés (AAV), notamment l'AAV.CAP-B10, pour exprimer les scFv dans le système nerveux central des souris. Ces AAV ont permis une bonne expression du scFv dans le cerveau et la moelle épinière, sans affecter les tissus périphériques. Ainsi, ces AAV sont actuellement utilisés pour administrer nos candidats intracorps dans le modèle murin Prp-TDP-43^{A315T} en utilisant les paramètres préalablement identifiés comme marqueurs de suivi.

En résumé, notre travail a exploré divers aspects de la protéinopathie liée à TDP-43 à la fois *in vitro* et *in vivo*. Les scFv identifiés semblent présenter des effets protecteurs in vitro directement contre TDP-43 et indirectement sur les altérations métaboliques induites par TDP-43. Nous avons également examiné différentes méthodes d'administration du scFv dans des modèles murins TDP-43 finement caractérisés et nous avons souligné l'importance de considérer la SLA comme une maladie systémique avec une interaction dynamique entre différents mécanismes physiopathologiques impliquant différents types cellulaires et différents tissus. Ce projet a ouvert des perspectives de développement de nouveaux marqueurs de suivi de thérapeutiques et a également permis de valoriser l'utilisation d'AAV pour administrer des biomédicaments.

Abstract

Amyotrophic Lateral Sclerosis (ALS) is a progressive neurodegenerative disease that affects motor neurons, leading to progressive paralysis. One of the main pathological markers of ALS is the abnormal accumulation of TDP-43 in the neurons and glial cells of 97% of ALS patients, making TDP-43 a promising therapeutic target. This protein, which is normally involved in RNA metabolism, becomes mislocalized and aggregated in the cytoplasm, contributing to a global loss of homeostasis and consequently, neurodegeneration. This makes this protein a major promising therapeutic target in ALS. However, targeting it in comes with some limitations such as the delivery of therapeutics through the blood-brain barrier and into the CNS (Publications 1, 2 and 3)

In this project, we explored several strategies to better understand ALS as a TDP-43 proteinopathy and develop therapies targeting TDP-43. The overall project of this thesis was based on the development of biotherapeutics that target TDP-43 and assess them *in vitro* in order to understand their potential protective effects, before evaluating them in a preclinical model of ALS.

First, we were interested in better understanding TDP-43, and we demonstrated that alterations in intracellular pH increase the mislocalization of TDP-43 and its accumulation in cytoplasmic puncta in a cellular model of ALS, implicating metabolic alterations in the functioning of TDP-43 (Publication 4). Next, we focused on potential biotherapeutics targeting TDP-43 which were identified in a previous thesis project in our laboratory (Hergesheimer, 2021). We decided to characterize two single-chain variable fragments (scFv), B1 and D7, which target full-length human TDP-43. The scFv D7, in particular, reduced levels of the insoluble pathological fragment TDP-35 and restored certain lipid metabolites that were altered in HEK293T cells overexpressing TDP-43, suggesting a protective effect (Publication 5).

Given that the protective effects of the scFv were demonstrated *in* vitro, we decided to start the preclinical evaluation project, which requires first a better characterization of the TDP-43 animal model of ALS. We therefore studied the Prp-TDP-43^{A315T} mouse model to identify phenotypic, molecular, and metabolomic parameters that are altered at different stages of the disease. This will allow us to identify objective and quantifiable parameters that we can use to measure the effects of the scFv. This model reproduced motor symptoms and aggregates of TDP-43, with metabolomic and lipidomic alterations detected in several tissues

even before the onset of symptoms. This makes this model a valuable tool for exploring new therapies targeting TDP-43 proteinopathy, such as the scFvs identified in this study (Publication 6).

Finally, given that targeting the central nervous system is complicated by the presence of the blood-brain barrier, we explored different possible methods to enhance the administration of the scFv to target tissues. We developed PEGylated iron oxide-based magnetic nanoparticles (SPIONs) complexed with the scFv to enhance targeting of the central nervous system, particularly the motor cortex. We showed that the SPION-scFv complexes were non-toxic to cells and improved cellular internalization of the scFv. In parallel, and after several inconclusive tests of different routes of administration of the scFv in the mouse model previously evaluated, we used adeno-associated viral (AAV) vectors, notably AAV.CAP-B10, to express the scFv in the central nervous system of mice. These AAVs allowed for good expression of the scFv in the brain and spinal cord without affecting peripheral tissues and are currently being tested in the Prp-TDP-43^{A315T} mouse model based on the parameters already identified for follow-up.

Overall, our work investigated various aspects of TDP-43 proteinopathy both *in vitro* and *in vivo*. The scFv molecules that were identified seem to exhibit protective effects directly against TDP-43 and indirectly against TDP-43-induced metabolic alterations. Additionally, we explored different methods of scFv administration in a well-characterized TDP-43 mouse model, and highlighted the importance of looking at ALS as a systemic disorder implicating a dynamic interplay between many physiopathological mechanisms in various cell types and tissues. This project has opened up perspectives for the development of new markers to track therapeutic responses, and highlighted the potential of using AAV for the delivery of biologics.

List of publications

- **Publication 1:**

  Al Ojaimi, Y., Dangoumau, A., Alarcan, H., Hergesheimer, R., Vourc'h, P., Corcia, P., ... Lanznaster, D., & Blasco, H. (2022). TAR DNA-binding protein of 43 kDa (TDP-43) and amyotrophic lateral sclerosis (ALS): a promising therapeutic target. *Expert Opinion on Therapeutic Targets*, 1-18.

- **Publication 2:**

  Al Ojaimi, Y., Blin, T., Lamamy, J., Gracia, M., Pitiot, A., Denevault-Sabourin, C., ... & Sécher, T. (2021). Therapeutic antibodies–natural and pathological barriers and strategies to overcome them. *Pharmacology & Therapeutics*, 108022.

- **Publication 3:**

  Alarcan, H., **Al Ojaimi, Y.,** Lanznaster, D., Escoffre, J. M., Corcia, P., Vourc'h, P., ... & Blasco, H. (2022). Taking Advantages of Blood–Brain or Spinal Cord Barrier Alterations or Restoring Them to Optimize Therapy in ALS?. *Journal of Personalized Medicine*, *12*(7), 1071.

- **Publication 4:**

  Al Ojaimi, Y., Slek, C., Osman, S., Alarcan, H., Marouillat, S., Corcia, P., ... & Blasco, H. (2024). The effect of pH alterations on TDP-43 in a cellular model of amyotrophic lateral sclerosis. *Biochemistry and Biophysics Reports*, *38*, 101664.

- **Publication 5:**

  Al Ojaimi, Y., Hergesheimer, R., Chami, A., Augros, J., Alarcan, H., Dangoumau, A., ... Lanznaster, D., & Blasco, H. scFv intrabody targeting wildtype TDP-43 presents protective effects in a cellular model of TDP-43 proteinopathy. (Under review)

- **Publication 6:**

  Al Ojaimi, Y., Osman, S., Alarcan, H., Emond, P., Veyrat-Durebex, C., Lanznaster, D., … Blasco, H. Characterization of functional and biological parameters in a longitudinal study of Prp-TDP-43^{A315T} transgenic mice, a model of amyotrophic lateral sclerosis. (Submitted)

- **Publication 7:**

  Al Ojaimi, Y., Vallet, N., Dangoumau, A., Lanznaster, D., Bruno, C., Lefèvre, A., … & Blasco, H. Metabolomic and proteomic profiling of serum-derived extracellular vesicles from early-stage amyotrophic lateral sclerosis. (Submitted)

List of figures

Figure 1 : Schematic representation of the progression of ALS 24

Figure 2 : Interplay between genetic and environmental factors contirbuting to the development of ALS 26

Figure 3 : Known ALS-causative genes in fALS and sALS 28

Figure 4 : The cumulative discovery of ALS-related genes from 1990 to 2022 29

Figure 5 : Pathophysiological mechanisms involved in ALS 31

Figure 6 : Schematic representation of the main mechanisms contributing to neuronal hyperexcitability and excitotoxicity in ALS 34

Figure 7 : Astrocytic and microglial dysfuntion in ALS 36

Figure 8 : Oligodendrocyte dysfunction in ALS 38

Figure 9 : The interplay between oxidative stress and mitochondrial damage in ALS 42

Figure 10 : Schematic representation of dysfunctional nucleocytoplasmic transport and RNA metabolism in ALS 47

Figure 11 : Schematic representation of the impact of ALS-associated proteins on the proteostatic dysfunction 50

Figure 12 : Neuronal circuits that are involved in ALS 52

Figure 13 : Schematic representation of an immunoglobulin (IgG), and scFv and an intrabody 108

Figure 14 : Representation of SPIONs as theranostic nanoparticles 114

Figure 15 : Purification of the scFv 186

Figure 16 : Characterization of the SPION, scFv, and SPION-scFv complexes 187

Figure 17 : Detection of uncomplexed scFv 188

Figure 18 : Cellular viability of HEK293T cells treated with SPIONs and/or scFv 189

Figure 19 : Internalization of the SPION and the scFv D7 into HEK293T cells following 4 hrs of treatment 190

Figure 20 : Exclusive AAV-mediated expression of the scFv in the CNS at 4 weeks post-administration 245

Figure 21 : Exclusive AAV-mediated expression of the scFv in the CNS at 8 weeks post-administration 246

Figure 22 : RT-qPCR reuslts showing scFv expression exclusively in the CNS at 8 weeks post-AAV administration 246

Introduction

I. Amyotrophic Lateral Sclerosis

A. Overview of ALS

Amyotrophic lateral sclerosis (ALS) is a fatal paralytic neurodegenerative disease that is characterized by the progressive and selective loss of both the upper (located in the motor cortex) and lower (located in the brainstem and spinal cord) motor neurons (Fig.1). It is known as Charcot's disease in French-speaking countries, particularly in Europe, in reference to the physician and neurobiologist Jean-Martin Charcot who was the first to describe the clinico-pathological aspects of the disease in 1869 (Duyckaerts et al., 2021). In the United States, the disease is more commonly known as Lou Gehrig's disease, named after the famous baseball player Lou Gehrig who was diagnosed with ALS in 1939 (Kasarskis & Winslow, 1989). The term amyotrophic lateral sclerosis described by J.M. Charcot refers to the muscle atrophy (amyotrophy) that occurs as a result of the condition and to the hardening or scarring that develops in the lateral columns of the spinal cord (lateral sclerosis) (Rowland, 2001).

Since the initial description of ALS in the 19th century, extensive progress has been made in the understanding of the pathological processes underlying the disease, the uncovering of several genes associated with it, the identification of risk factors, the development of potential therapeutic approaches, and the improvement of patient care.

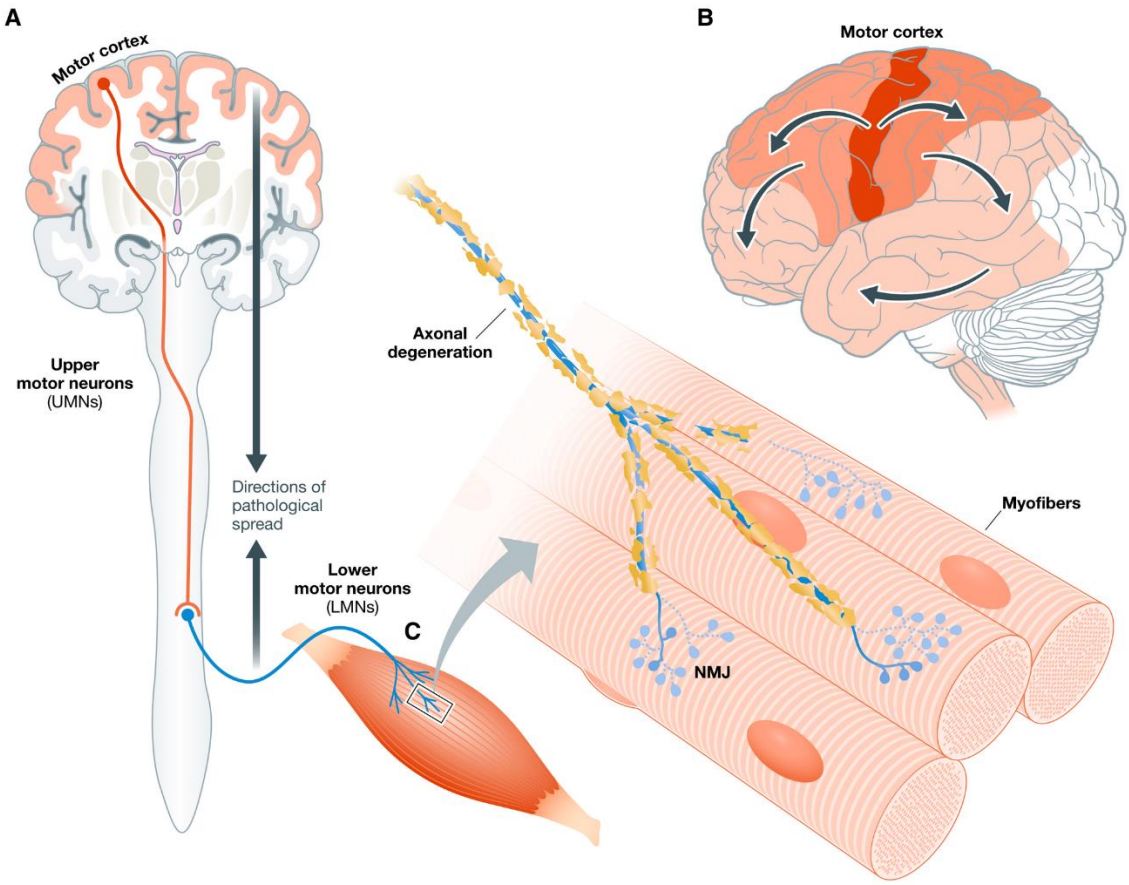

Figure 1: Schematic representation of the progression of ALS. A) Representation of the corticospinal tract comprising the upper motor neurons (UMN) originating in the motor cortex (dark red) and the lower motor neurons (LMN) (in blue) that innervate the skeletal muscle fibres. **B)** Lateral view of the brain showing the spread of ALS pathology starting from the motor cortex to nearby regions. **C)** As the axons of the LMN start to degenerate, the neuromuscular junctions become disrupted, leading to muscle denervation and atrophy. Reproduced from (Cicardi et al., 2021).

B. Epidemiology

ALS is recognized as the most common disease of the motor neuron in adults (Bäumer et al., 2014). It is also the third most common neurodegenerative disease following Alzheimer's disease and Parkinson's disease (Renton et al., 2014). Worldwide, the overall ALS prevalence is 4.42 per 100,000 while its incidence is 1.59 per 100,000 person-years, with values varying between subcontinents (Xu et al., 2020). Like other neurodegenerative diseases, the risk of developing ALS increases in an age-dependent manner up until 70-79 years, after which it decreases (Turner et al., 2012; Xu et al., 2020). Males have been reported to be more susceptible to developing ALS than females, with a lifetime risk of 1.5 per 1000

males compared to 1.2 per 1000 females (Ryan et al., 2019). In addition, the number of ALS cases has been estimated to increase by 69% from 2015 to 2040, primarily due to the ageing of the population (Arthur et al., 2016).

The current understanding of ALS is that it is mainly sporadic in nature, with 90% of cases being apparently sporadic (sALS) and the remaining 10% having a familial history of the disease (fALS) (Talbott et al., 2016). The means age of symptoms onset is estimated at 58-63 years for sALS while that of fALS is at 40-60 years (Logroscino et al., 2010).

C. Aetiology

ALS is a complex disorder with a multifactorial nature. The interplay between environmental risks and genetic backgrounds has been well demonstrated in ALS. This is highlighted by the differences observed in ALS incidence, male/female ratio, age at diagnosis, site of onset, clinical manifestation, and survival time between different geographical areas (Al-Chalabi & Hardiman, 2013; Logroscino et al., 2018; Marin, Boumédiene, et al., 2016; Marin, Logroscino, et al., 2016).

In neurodegenerative diseases like ALS, genetic pleiotropy which is the influence of a single gene on multiple phenotypic traits, is observed by the shared genetic mutations across different neurodegenerative diseases. This is the case for many genes such as *KIF5A* (Nicolas et al., 2018), *VCP* (Abrahao et al., 2016), *TMEM106B* (Nicholson & Rademakers, 2016), *C9ORF72* (Breevoort et al., 2022). These observations suggest that the same genetic alteration can lead to different phenotypic outcomes depending on other factors, such as genetic background and environmental exposures.

In addition to the hypothesis of the gene-environment interactions that is widely described in the field of neurodegeneration (Bogers et al., 2023; Migliore & Coppedè, 2022; Sarkar, 2021), the factor of time and ageing has been recently added to the equation to create the gene-environment-time hypothesis of ALS aetiology (Bradley et al., 2018; Dey et al., 2024) (Fig.2). Age is an important factor to consider in the aetiology of ALS, given that the risk of developing ALS increases progressively with age until 79 (Turner et al., 2012; Xu et al., 2020). Interestingly, motor neurons have been found to be particularly vulnerable to both intrinsic

and extrinsic factors (Ovsepian et al., 2023), which makes them particularly susceptible to environmental insults, genetic alterations (mutational or epigenetic), and the ageing process.

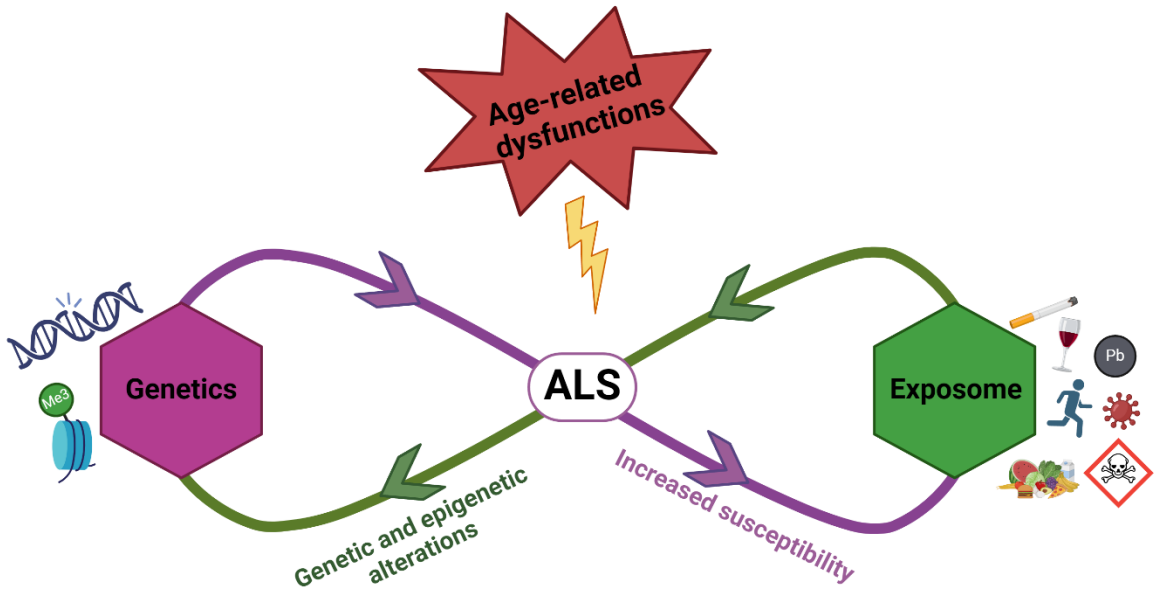

Figure 2: Interplay between genetic and environmental factors contributing to the development of ALS. Genetic background can predispose some individuals to become more susceptible to common environmental risk factors. In turn, environmental factors can influence the expression and modulation of some genes through DNA damage or epigenetic modulation. Over time, the cumulative effects of these environmental influences can interact with genetic predispositions, causing the onset of ALS. Age itself is a critical factor, as the risk of neurodegeneration increases with time due to the gradual wear and tear on neural systems and the dysfunction in several homeostatic mechanisms, alongside the long-term impact of both genetic and environmental factors. Created with BioRender.com.

a. Environmental factors

The exposome is the set of environmental factors to which an individual is exposed (Wild, 2005). Lifestyle factors such as dietary intake (D'Antona et al., 2021), smoking (H. Wang et al., 2011), coffee intake (Beghi et al., 2011), alcohol consumption (X. Yu et al., 2020), and physical activity and athleticism (Julian et al., 2021) can have an effect on the development of ALS. In addition, exposure to some chemical neurotoxic compounds such as lead (Fang et al., 2010), manganese (Roos et al., 2021), pesticides (Andrew et al., 2021), BMAA (Anzilotti et al., 2023; Pablo et al., 2009), as well as some biological exposures like enterovirus (Berger et al., 2000) and herpesvirus infections (Cermelli et al., 2002), seem to play a role in the risk of

developing ALS. The period at which an exposure takes place is also an important factor to consider. In one study for example, metal dysregulation from early childhood was shown to impact the risk of developing ALS later on in life, highlighting the importance of temporal considerations when investigating environmental factors (Figueroa-Romero et al., 2020).

Studies have found some discrepancies related to the contribution of some environmental factors to the risk of developing ALS. For instance, some studies found a positive correlation between physical activity, particularly intense exercise, and the risk of developing ALS (Daneshvar et al., 2021; Gamez & Carmona, 2021; Lehman et al., 2012; Raymond et al., 2021), while other studies failed to make that correlation (Korner et al., 2019; Savica et al., 2012). Also, some environmental factors might not have the same effect on all individuals. For example, the risk to develop ALS seems to be higher among female smokers than male smokers (Weisskopf, 2004). Such inconsistencies can be due to the relatively small number of study participants, but they pinpoint to the fact that different individuals with different genetic backgrounds do not have the same susceptibility to the same environmental factor. Additionally, some environmental exposures not only seem to affect the risk of developing ALS, but also the severity and prognosis of the disease if developed. For instance, lead exposure has been associated with a faster disease progression and shorter survival in ALS patients (T.-W. Wang et al., 2023).

It remains difficult to label an environmental factor as an ALS-causing factor due to the inability to conduct studies with placebo-controlled exposures in humans. In addition, several factors that are not easy to control make it difficult to conclude the role of an environmental factor in ALS. Such factors include the big size of the human exposome, the exact dose an individual is exposed to, the period of life during which the exposure took place, and the combined or synergistic effects of different environmental exposures. But overall, understanding how environmental factors are associated with and influence ALS can help in developing preventive strategies and improving management plans for those affected by the disease.

b. Genetic factors

ALS has a complex genetic landscape with numerous genes implicated in its pathogenesis. The disease can be both monogenic or oligogenic, depending on the case (Van

Blitterswijk et al., 2012; Van Daele et al., 2023). Although only about 10% of ALS cases are familial, with a predominant Mendelian pattern of inheritance, mutations in the same genes are also observed in sALS albeit at lower percentages (Veldink, 2017) (Fig.3). Mutations in four major genes (*C9ORF72*, *SOD1*, *TARDBP*, and *FUS*) have been found to contribute to 47.7% of all fALS cases, and 5.2% of all sALS cases (Zou et al., 2017). Interestingly, a study found that different populations had different frequencies of genetic mutations in both fALS and sALS (Zou et al., 2017). For instance, mutations in the *C9ORF72* gene were the most commonly observed in European populations, while mutations in the *SOD1* gene were the most commonly observed in Asian populations (Zou et al., 2017). This highlights even further the genetic heterogeneity in ALS and the importance of considering ethnic differences in the genetic studies of the disease.

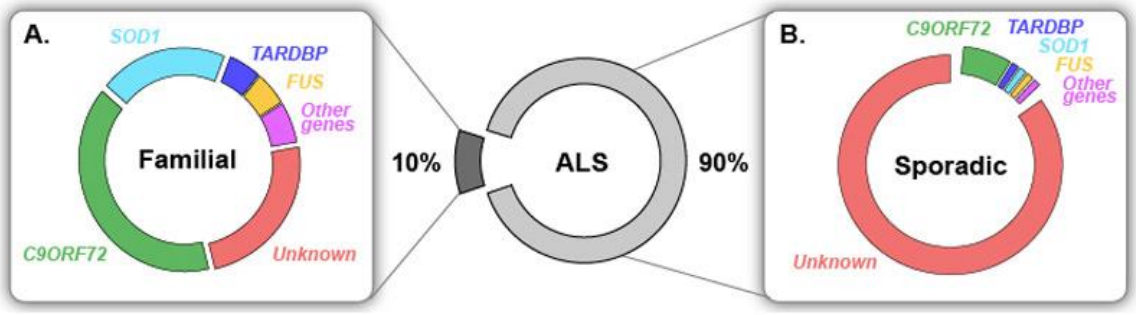

Figure 3: Known ALS-causative genes in fALS and SALS. 90% of ALS cases are sporadic while only 10% are familial. Mutations in the *C9ORF72, SOD1, TARDBP*, and *FUS* genes are the main genetic causes of ALS. However, in most ALS cases, an identified genetic cause is still missing. Reproduced from (Laferriere & Polymenidou, 2015).

The first ALS-causing mutation was identified in the *SOD1* gene in 1993 (Rosen et al., 1993), followed by *TARDBP* in 2008 (Sreedharan et al., 2008). Since then, advancements in genetic and sequencing techniques have largely accelerated the rate of gene discovery, leading to the identification of around 690 genes associated with ALS, and more than 40 causative genes (Gregory et al., 2020; Ilieva et al., 2023; Nicolas et al., 2018; Wood, 2022; S. Zhang et al., 2022) (Fig.4). Nevertheless, there is still an important knowledge gap in the understanding of the contribution of genetic factors in the development of ALS.

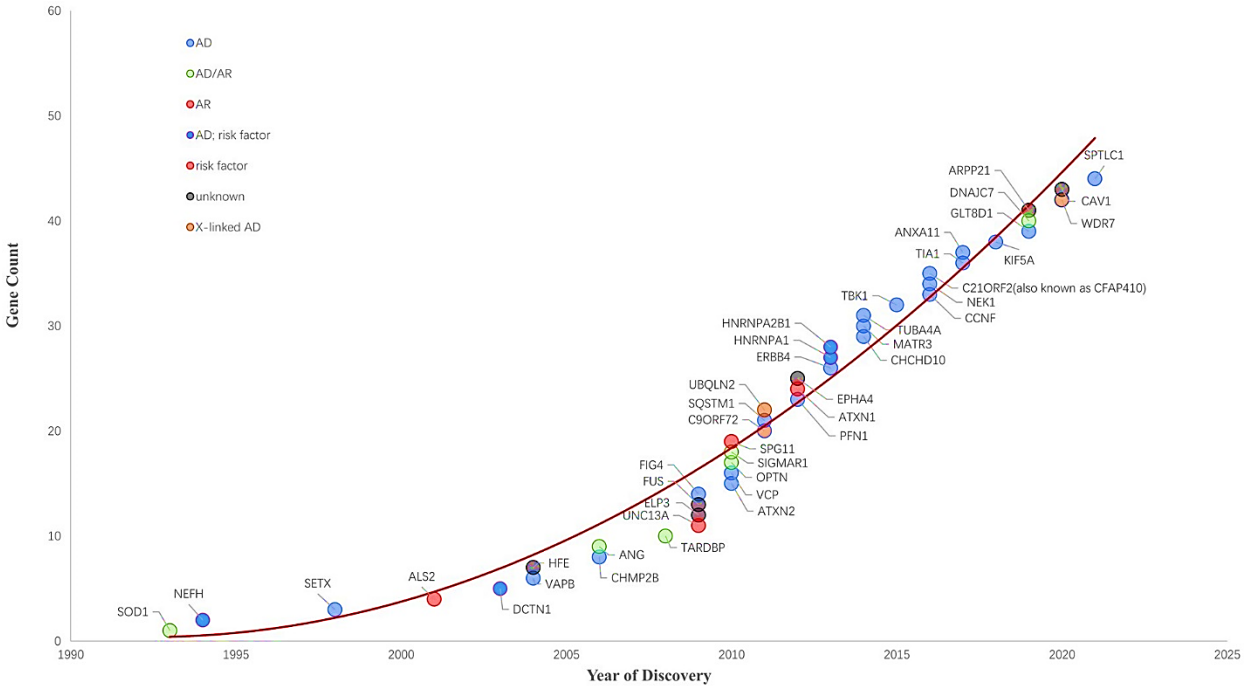

Figure 4: The cumulative discovery of ALS-related genes from 1990 to 2022. Each gene is represented by a circle, with different colors indicating their respective inheritance patterns (AD: autosomal dominant; AR: autosomal recessive; or X-linked). Reproduced from (Wang et al., 2023).

When talking about the contribution of genetics in the development of ALS, one should not only consider genetic mutations, but also epigenetic changes which alter the expression of genes without alterations in the DNA sequence itself. The epigenome can capture the cumulative environmental exposures over a person's lifetime and age-related changes in gene expression, which can provide insights into the contribution of these factors to the development of ALS (Cavalli & Heard, 2019). In addition, the concept of epigenetic inheritance, which is the passing on of epigenetic changes from the parents to the offspring (Lacal & Ventura, 2018), might also play a role in the susceptibility of individuals to certain stressors. Various epigenetic alterations have been detected in ALS such as aberrant DNA methylation (Z. Cai et al., 2022; Hop et al., 2022; Nabais et al., 2020; Ruf et al., 2022), histone modifications (Basavarajappa & Subbanna, 2021; Belzil et al., 2013; Pegoraro et al., 2020; Tibshirani et al., 2015), and alterations in non-coding RNA-associated gene regulation (Nishimoto et al., 2013; Pegoraro et al., 2020; Rajabi et al., 2024; Ruffo et al., 2021). Understanding the epigenome in the context of ALS can help link environmental, genetic, and ageing factors in the development of ALS even in the absence of known mutations.

Another important concept that has been studied is the heritability of ALS. It refers to the proportion of the variation in the risk of developing ALS that can be attributed to genetic differences within a population. This was examined by Al-Chalabi and his colleagues (2010) using monozygotic and dizygotic twins data (Al-Chalabi et al., 2010). They reported that the heritability of sALS was 0.61, meaning that approximately 60% of the risk of developing ALS is attributed to genetic elements, while the remaining 40% was due to distinct environmental factors. In 2014, another study using genome-wide analysis estimated the overall heritability of ALS to be 0.21 (Keller et al., 2014). Similarly, Ryan and her colleagues showed that half of the risk of developing ALS was attributed to genetic elements (Ryan et al., 2019). Overall, all these studies suggest that genetic factors play a significantly larger role in the development of ALS than previously understood, and that inherited and non-inherited factors can contribute almost equally to the development of the disease.

The identification of ALS-causative and -associated genes has improved our understanding of the pathophysiology of the disease by unravelling disease pathways that overlap with those observed in sALS, such as alterations in RNA processing, axonal transport, proteostasis, and the cellular response to stress. It also contributed to the development of cellular and animal models of ALS for investigating these pathways and testing potential therapeutics.

D. Pathophysiology

Extensive research has been conducted to decipher the wide array of cellular and molecular mechanisms that contribute to the development and progression of the disease. Initially, it was thought that ALS was mainly restricted to the motor neuron. Nowadays, our understanding of the pathophysiology of ALS implicates other cell types, including glial cells, immune cells, and myocytes (Fig.5). However, it should be noted that a single pathophysiological mechanism is unable to explain the heterogeneity and nuances observed in ALS. In the last decade, major progress has been made in understanding the key pathogenic pathways implicated in ALS, but the exact causes of ALS are still not well understood. In addition, it is unclear whether some of the implicated pathways are a cause of the disease or a phenomenon secondary to the disease.

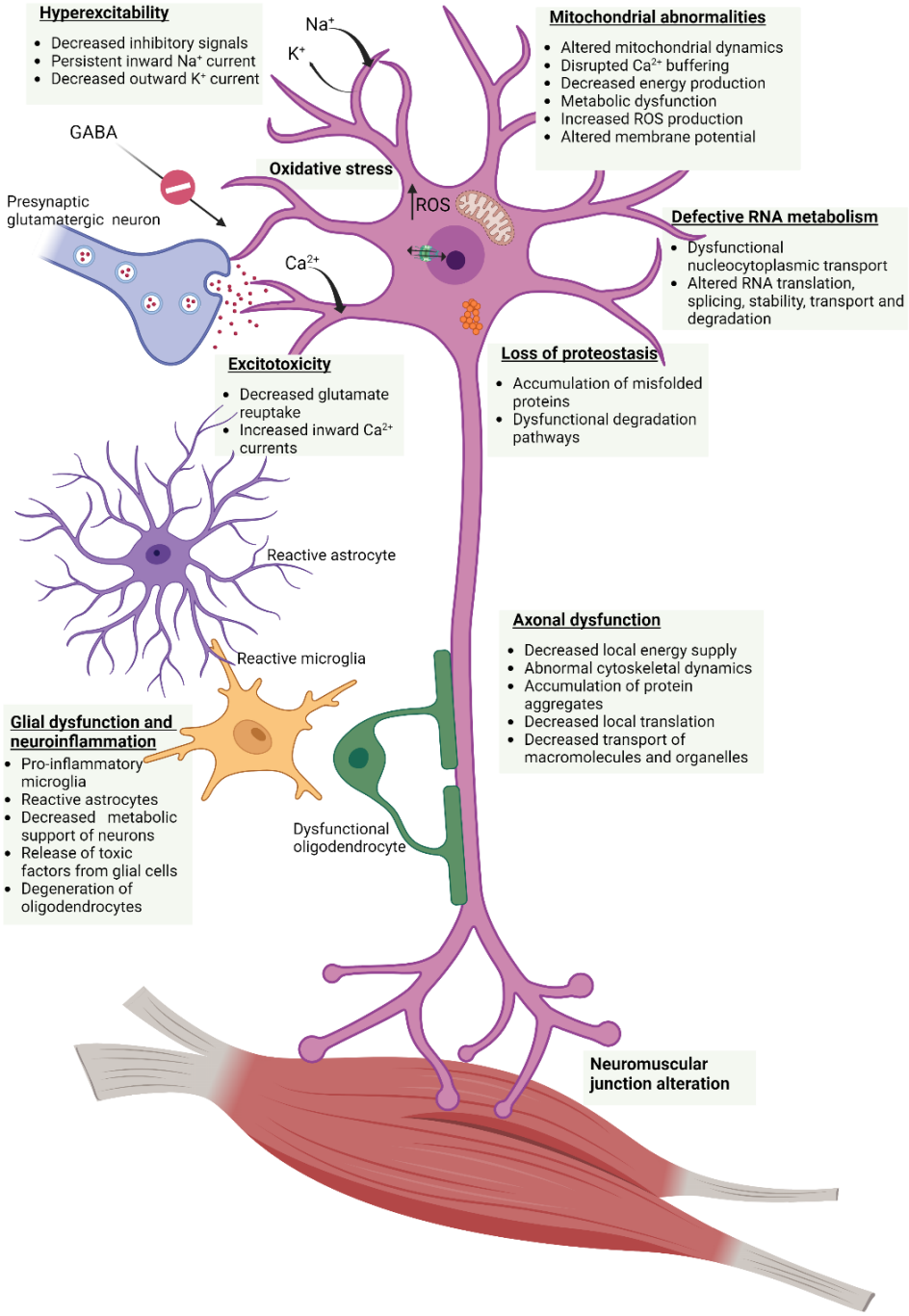

Figure 5: Pathophysiological mechanisms involved in ALS. Key processes include excitotoxicity, neuronal hyperexcitability, mitochondrial dysfunction, oxidative stress, the accumulation of misfolded proteins, impaired RNA metabolism, disrupted axonal transport, neuroinflammation, and NMJ alterations. The interplay between these mechanisms leads to the progressive loss of motor neurons, resulting in the characteristic muscle weakness and paralysis observed in ALS. Created with BioRender.com

a. Excitotoxicity

Two concepts that are key in the pathophysiology of ALS are hyperexcitability and excitotoxicity, and the interplay between the two. Hyperexcitability is the exaggerated responsiveness of neurons to stimuli (Bülow et al., 2022). It is one of the major and earliest phenomena observed both in fALS (Blair et al., 2010; Vucic et al., 2008; Williams et al., 2013) and sALS (Kannan A. Nith, 1998; Menon et al., 2015). The increase in neuronal activity and spontaneous firing is linked to the initial symptoms of fasciculations and muscle stiffness observed in patients (De Carvalho & Swash, 2013).

The exact mechanisms of hyperexcitability are not fully deciphered yet, but it seems to stem from a loss of balance between excitatory and inhibitory circuits (Van Den Bos et al., 2018). For instance, loss of modulatory interneurons, and the resulting dysregulation of inhibitory/excitatory circuits, have been demonstrated in ALS (Allodi et al., 2021; Q. Chang & Martin, 2009; Salamatina et al., 2020). Studies have also demonstrated the impairment of the GABAergic signalling in ALS, leading to decreased inhibitory currents (Khademullah et al., 2020; Lloyd et al., 2000; McGown et al., 2013; Moser et al., 2013; Nieto-Gonzalez et al., 2011; Petri et al., 2003). Moreover, alterations in ion channel currents, such as enhanced persistent Na^+ currents (Kuo et al., 2005; Pieri et al., 2009; Vucic & Kiernan, 2010) and reduced outward K^+ currents (Y. Jiang et al., 2005; Kanai et al., 2006; Shibuya et al., 2011) have been reported to contribute to neuronal hyperexcitability in ALS.

Hyperexcitability usually leads to excessive release of the excitatory neurotransmitter glutamate by the pre-synaptic neurons, which overstimulates post-synaptic neurons leading to excitotoxic damage. Glutamate-induced excitotoxicity is mediated by the increase in intracellular Ca^{2+} and the limited Ca^{2+} buffering capacity of motor neurons, which triggers a cascade of cytotoxic events (Pivovarova & Andrews, 2010). This is the main pathway that is thought to be targeted by Riluzole, the primary treatment option for ALS (Doble, 1996).

Several mechanisms that contribute to excitotoxicity have been described in ALS. Normally, AMPA receptors (AMPAR) are Ca^{2+}-impermeable (Wright & Vissel, 2012). However, researchers have reported an increase in Ca^{2+}-permeable AMPAR, and a subsequent increase in Ca^{2+} influx into neurons (Kawahara et al., 2004; Sommer et al., 1991). This phenomenon was found to induce astrogliosis and the selective death of motor neurons while preserving

the ALS-resistant oculomotor neurons (Hideyama et al., 2010; Naito et al., 2023). Concomitantly, it was found that in ALS patients, neurons with Ca^{2+}-permeable AMPAR were also positive for TDP-43 cytoplasmic inclusions, partly due to the Ca^{2+}-induced activation of proteases like calpain that cleave TDP-43 (Aizawa et al., 2010; Hideyama et al., 2012). Astrocytes are also important players in the excitotoxic injury to neurons given their role in regulating the environment around neurons. Studies in ALS have reported a reduction of astrocytic glutamate clearance and reuptake from synapses (Diaper et al., 2013; Fomin et al., 2018; Lagier-Tourenne et al., 2012; Lin et al., 1998; Pardo et al., 2006; Rothstein et al., 1995; Tollervey et al., 2011), and an abnormal buffering of extracellular K^+ by astrocytes (Bataveljić et al., 2012; Kaiser et al., 2006), which can additionally contribute to glutamate-induced excitotoxicity.

The combination of all these dysfunctions negatively affects motor neurons, particularly at the level of the mitochondria and the endoplasmic reticulum (ER), eventually leading to their excitotoxic death (Pivovarova & Andrews, 2010). A feed-forward cycle can be established, whereby the increase in intracellular calcium causes an increase in the production of reactive oxygen species (ROS), which in turn alters the ability of astrocytes to regulate synaptic glutamate levels, causing increased glutamate-induced activation of neurons and Ca^{2+} influx. Excitotoxicity in ALS, in addition to the early detection of cortical hyperexcitability support the “dying-forward” hypothesis of ALS which suggests that ALS begins at the level of the cortex and progresses outward towards the distal parts of the motor neurons (Eisen, 2021). The main mechanisms involved in neuronal hyperexcitability and excitotoxicity in ALS are represented in Fig.6.

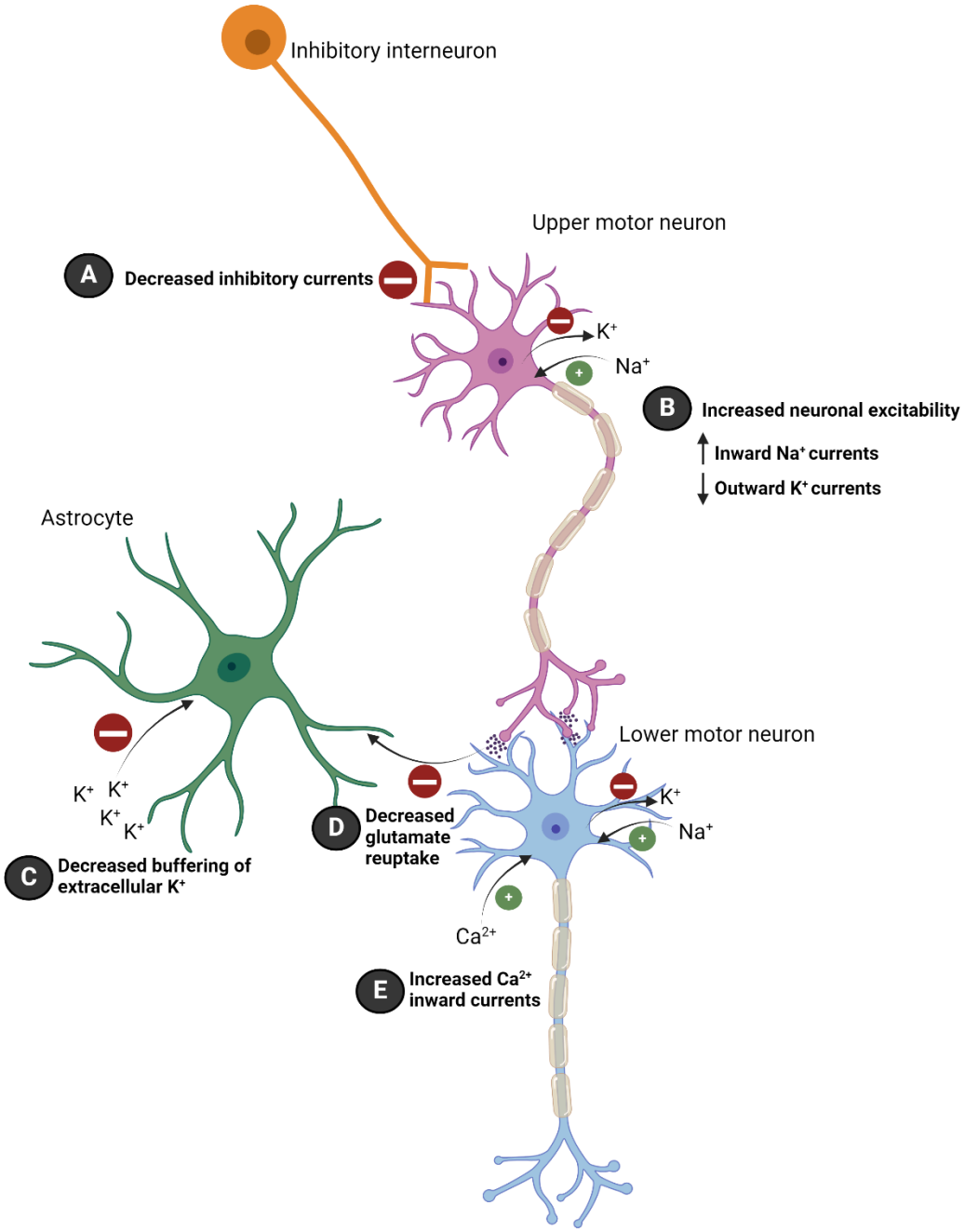

Figure 6: Schematic representation of the main mechanisms contributing to neuronal hyperexcitability and excitotoxicity in ALS. A combination of A) decreased inhibitory currents from interneurons, B) perturbed inward and outward ionic currents, C) decreased astrocytic buffering of extracellular K^+, D) decreased astrocytic reuptake of glutamate, and E) and a glutamate-induced increase in inward Ca^{2+} currents all lead to the hyperexcitability of motor neurons and subsequent excitotoxic damage. Created with BioRender.com.

b. Glial dysfunction and neuroinflammation

- **Microglia and astrocytes:** Several microglial and astrocytic dysfunctions have been observed and are thought to play a major role in the pathology of ALS (Fig.7). Microglia are important in maintaining the homeostasis of the CNS by responding to stressors and modulating the immunological response (Wolf et al., 2017). Astrocytes play a plethora of functions essential for forming the blood-brain barrier (BBB), supporting neurons, regulating synapses and neuronal activity, maintaining the microenvironment of the CNS, and participating in the immune response (Gradisnik & Velnar, 2023). A dysfunction in the crosstalk between neurons and these two types of neuroglia contribute to the pathogenesis of ALS. Astrogliosis and microgliosis are both reported in ALS, with the interplay between the two contributing to the observed neuroinflammatory profile (Calafatti et al., 2023; Guttenplan et al., 2020; Liddelow et al., 2017; Ouali Alami et al., 2018; Zürcher et al., 2015).

As the disease progresses, microglia seem to shift their phenotype from a neuroprotective, anti-inflammatory M2 phenotype to a neurotoxic pro-inflammatory M1 phenotype (Gravel et al., 2016; B. Liao et al., 2012). For instance, mutant TDP-43 or SOD1 caused the activation of microglia into an M1 phenotype (Beers et al., 2006; Boillée et al., 2006; C. Huang et al., 2012; Swarup, Phaneuf, Bareil, et al., 2011; Swarup, Phaneuf, Dupré, et al., 2011). One of the consequences was the activation of the NF-κB signalling pathway in microglia, leading to motor neuron death (Frakes et al., 2014; Swarup, Phaneuf, Dupré, et al., 2011).

Similar findings have been reported in astrocytes which acquire a neurotoxic, pro-inflammatory A1 reactive phenotype in ALS (LaRocca et al., 2019; Ziff et al., 2022). For instance, both the overexpression and loss-of-function of TDP-43 in astrocytes was shown to alter their function from neuroprotective to neurotoxic (S. Lee et al., 2020; Peng et al., 2020). There seems to be a transcriptomic shift in ALS astrocytes where there is an up-regulation of deleterious genes related to inflammation, ER stress, and hypoxia, and a down-regulation of homeostatic genes related to glutamate metabolism and synaptic support (Ziff et al., 2022). For instance, the main glutamate transporter, the excitatory amino acid transporter EAAT2, was reported to be significantly decreased in ALS astrocytes, causing a decrease in glutamate reuptake by these cells (Bruijn et al., 1997; Rothstein et al., 1995). In addition, some factors

released by reactive astrocytes and microglia were shown to be particularly toxic to motor neurons (Nagai et al., 2007; Vahsen et al., 2023).

Astrocytic mitochondrial abnormalities are also observed in ALS (Cassina et al., 2008; Martínez-Palma et al., 2019; Miquel et al., 2012), which might exacerbate oxidative stress and impair energy metabolism. Moreover, a decrease in the astrocytic metabolic support of neurons was also demonstrated in ALS (Z. Chen et al., 2023; Ferraiuolo et al., 2011; Madji Hounoum et al., 2017; Stella et al., 2021). For instance, it is thought that the antioxidant activity of astrocytes is stronger than that of neurons, and that neurons rely mainly on astrocytes in cases of increased oxidative stress (Shih et al., 2003). In this context, enhancing the antioxidant activity of astrocytes could help rescue motor neuron death (Cassina et al., 2008; Pehar et al., 2006).

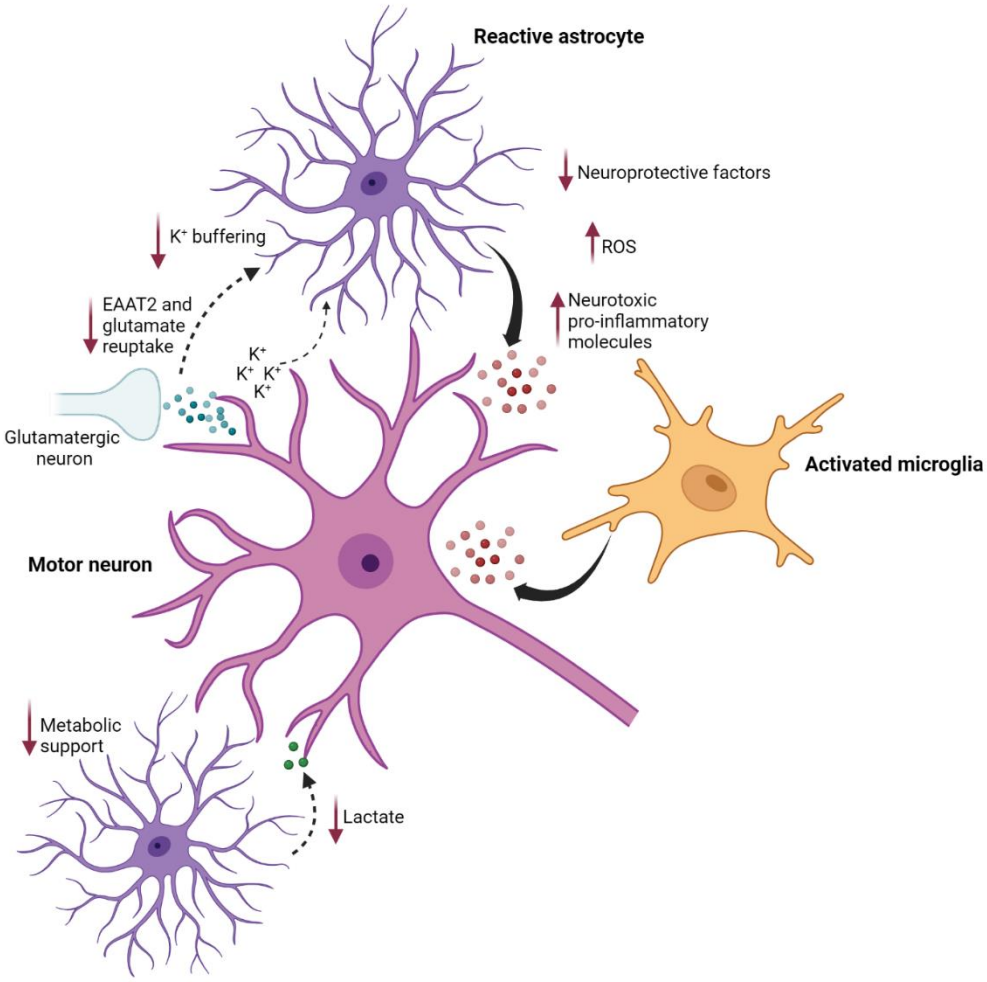

Figure 7: Astrocytic and microglial dysfunction in ALS. Astrocytes exhibit reduced glutamate uptake due to decreased expression of the EAAT2 transporter, leading to excitotoxicity and motor neuron damage. Additionally, astrocytes fail to regulate extracellular K+ and provide inadequate metabolic support to neurons, such as reduced release of lactate. Reactive astrocytes release pro-inflammatory

cytokines, worsening neuroinflammation and oxidative stress. Microglia become chronically activated, transitioning to a pro-inflammatory state that releases neurotoxic factors, exacerbating oxidative damage and further contributing to neuronal injury. Together, these glial dysfunctions create a hostile environment that accelerates motor neuron degeneration in ALS. Created with BioRender.com.

- **Oligodendrocytes**: Oligodendrocytes play a key role in maintaining axonal health. They contribute not only to the myelination of axons, but also to their metabolic support through the buffering of extracellular K^+ concentrations and providing glycolysis products to active neurons (Larson et al., 2018; Looser et al., 2024; Philips & Rothstein, 2017; Saab et al., 2016). The involvement of oligodendrocytes, which are closely associated with the axons of motor neurons, has been widely reported in ALS (Jamet et al., 2024). Aggregation of ALS-linked proteins like TDP-43, FUS and SOD1 have been detected in ALS oligodendrocytes and have been suggested to be able to be transferred to neuronal axons (Brettschneider et al., 2014; Fatima et al., 2015; Ferraiuolo et al., 2016; Ishii et al., 2017; Scekic-Zahirovic et al., 2017). The degeneration of oligodendrocytes was also detected in the motor cortex and spinal cord of ALS patients (S. H. Kang et al., 2013; Philips et al., 2013). In ALS, oligodendrocytes seem to have a high turnover rate, with enhanced proliferation of oligodendrocyte precursor NG2+ cells, and decreased maturation, making them dysfunctional (S. H. Kang et al., 2010, 2013). Furthermore, oligodendrocyte dysfunction results in decreased energy supply to motor neurons through decreased supply of glucose and lactate (Ferraiuolo et al., 2016; Y. Lee et al., 2012; N. Meyer et al., 2018; Saab et al., 2016). For instance, the monocarboxylate transporter MCT1, which is responsible for the release of lactate from oligodendrocytes, has been found to be downregulated in ALS (Y. Lee et al., 2012). In addition, the inward rectifying K^+ channels Kir4.1, which are sensitive to extracellular K^+ concentrations, were also downregulated in oligodendrocytes in the case of ALS, suggesting a decreased buffering of extracellular K^+ and a subsequent decrease in axonal metabolic support (Kelley et al., 2018; Peric et al., 2021). Based on all these observations, oligodendrocytes seem to play a significant role in the pathophysiology of ALS and this requires further exploration (Fig.8).

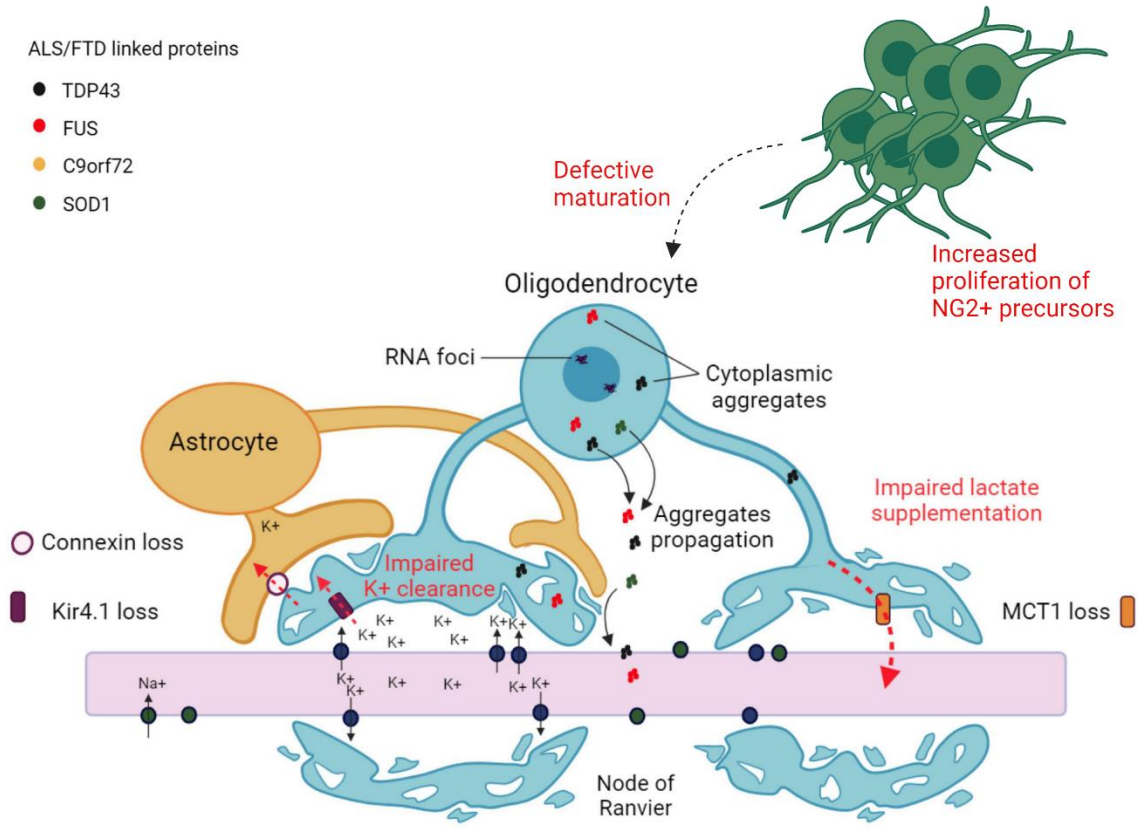

Figure 8: Oligodendrocyte dysfunction in ALS. In ALS, functional interactions between oligodendrocytes and neuronal axons are significantly altered. There is a decrease in the maturation of NG2+ cells into functional oligodendrocytes. Reduced levels of Kir4.1 channels and connexins lead to dysfunctional extracellular K^+ buffering. Lower MCT1 expression leads to inadequate metabolic support of axons by decreasing the release of lactate. Pathological aggregates can also spread from the oligodendrocytes into the axons. Adapted from (Jamet et al., 2024). Edited with BioRender.com.

c. Axonal dysfunction and neuromuscular junction impairment

Dysfunctions at the level of the axon, and more particularly retrograde and anterograde axonal trafficking, have been extensively reported in ALS. Some ALS-associated genes encode proteins that are directly involved in axonal cytoskeletal dynamics like kinesin (KIF5*)* (Baron et al., 2022), neurofilament heavy *(*NfH*)* (Figlewicz et al., 1994), alsin (ALS2) (Y. Yang et al., 2001), a subunit of dynactin (DCTN1) (Borg et al., 2023), α-tubulin (TUB4A) (Ganne et al., 2023), profilin (PFN1) (Schmidt et al., 2021), and peripherin (PRPH) (Corrado et al., 2011), highlighting the role of proper cytoskeletal function in maintaining motor neuron health.

Some studies showed that the axons of motor neurons start to die back before the cell body is lost (Fischer et al., 2004). These findings support the "dying-back" hypothesis of ALS, which suggests that the degeneration of the motor neurons start at the neuromuscular junctions (NMJ) and distal axons and moves upwards towards to cell body (Dadon-Nachum et al., 2011). Abnormalities at the level of NMJ have been described in ALS, sometimes even before the onset of symptoms (Cappello et al., 2012; Clark et al., 2016; Dzieciolowska et al., 2017; Mejia Maza et al., 2021; Pollari et al., 2014; Rocha et al., 2013; So et al., 2018; R. Xia et al., 2012). Interestingly, there seems to be some subtypes of motor neurons that are selectively susceptible to NMJ dysfunctions related to ageing and ALS, with this susceptibility being at least partially linked to ER stress, TDP-43 and the cytoskeleton-regulating protein CRMP-4a (Saxena et al., 2009; Valdez et al., 2012). Additionally, it was shown that some motor neurons try to compensate for the loss of synapses at the NMJ by creating new axonal branches (Martineau et al., 2018; Schaefer et al., 2005).

These findings however cannot exclude the possibility that pathological changes in the soma are occurring before the degeneration of axons, and that they contribute, whether directly or indirectly, to dysfunctions in the distal axon and NMJ. For instance, abnormal splicing activity of TDP-43 contributes to a decrease of stathmin-2, a microtubule regulator needed for the growth and regeneration of axons (Klim et al., 2019; Melamed et al., 2019). Furthermore, the communication between the cell body and the distal axon is indispensable for the good functioning of motor neurons. Disruptions in some major proteins in ALS like TDP-43, SOD1, and C9ORF72 have been found to alter the transport of macromolecules (Briese et al., 2020; L. Fumagalli et al., 2021; Nagano et al., 2020) and organelles (e.g. mitochondria, endosomes) (De Vos et al., 2007; Magrané et al., 2012, 2014; Sleigh et al., 2020). They were also found to negatively affect the local translation and protein synthesis in axons (Altman et al., 2021; Briese et al., 2020; Piol et al., 2023). Additionally, abnormal mitochondrial bioenergetics (discussed below) decreases the amount of energy available for proper axonal function and trafficking (L. Cheng et al., 2023; B. Wang et al., 2021).

d. Mitochondrial dysfunction and oxidative stress

Mitochondria play a major role in maintaining cellular homeostasis through ionic, metabolic, bioenergetic, and redox functions, and are particularly crucial for neuronal health. Several aspects of mitochondrial malfunctioning have been described in ALS, with some

researchers reporting mitochondrial defects as one of the earliest events in ALS (Gautam, Xie, et al., 2019; Günther et al., 2022; Matveeva et al., 2024; T. Singh et al., 2021). Mitochondrial dynamics including increased aggregation and fragmentation, as well as abnormal mitophagy and biogenesis were also reported to be altered in ALS (Gautam, Xie, et al., 2019; W. Liu et al., 2013; Moore & Holzbaur, 2016; W. Song et al., 2013; W. Wang et al., 2013). In one study using induced pluripotent stem cells (iPSC)-derived motor neurons from ALS patients, researchers detected higher levels of ROS, decreased levels of ATP, impaired mitochondrial import, aberrant oxidative phosphorylation and depolarized mitochondrial membrane potentials in ALS patients compared to controls (T. Singh et al., 2021). Studies have also shown that some ALS-associated proteins directly alter mitochondrial functions. For example, mutant SOD1 protein accumulates in the mitochondria and negatively affects the mitochondrial respiratory chain (Higgins et al., 2002; Mattiazzi et al., 2002; Vande Velde et al., 2008; Vijayvergiya et al., 2005). TDP-43 was also shown to interact directly with mitochondrial proteins, accumulate in mitochondria, alter mitophagy, cause defects in mitochondrial morphology, inhibit the activity of complex I, decrease ATP production, increase ROS production, and activate the mitochondrial unfolded protein response (Davis et al., 2018; P. Wang et al., 2019; W. Wang et al., 2016). Additionally, FUS was also found to alter the expression of mitochondrial respiratory chain complexes by sequestering their mRNAs and preventing their translation, as well as inhibiting the activity of the ATP synthase and inducing the unfolded protein response of the mitochondria (Deng et al., 2018; Tsai et al., 2020). Mitochondrial defects, including mitochondrial DNA alterations and a decreased complex IV activity, were also observed in the skeletal muscles of ALS patients (Echaniz-Laguna et al., 2006; Vielhaber, 2000). Similarly, reduced activities of complexes I, II, III, and IV were observed in the spinal cord of ALS patients (Wiedemann et al., 2002).

In addition to the ER, the mitochondria is another organelle that plays a key role in regulating intracellular Ca^{2+} levels (Hirabayashi et al., 2017; Kwon et al., 2016; Marland et al., 2016). When the mitochondrial capacity to buffer Ca^{2+} is compromised, due to high intracellular Ca^{2+} concentration or abnormal mitochondrial functioning, this can lead to mitochondrial Ca^{2+} overload, mitochondrial alterations, ROS production and eventually cell death (Calvo-Rodriguez et al., 2020; Malyala et al., 2019; Pivovarova et al., 2004; Strubbe-Rivera et al., 2021; Tadić et al., 2019). Motor neurons are selectively vulnerable to Ca^{2+}

dysregulations (Lewinski & Keller, 2005). As previously discussed, motor neuron excitation and the glutamate-induced increase in intracellular Ca^{2+} can largely contribute to Ca^{2+} overload in the mitochondria, which eventually leads to excitotoxic cell death. Indeed, impaired Ca^{2+} homeostasis have been repeatedly observed in ALS (Bergmann & Keller, 2004; De Marco et al., 2022; Jaiswal et al., 2009; Nahm et al., 2020; Tradewell et al., 2011; Zhou et al., 2019).

Dysfunctional mitochondria and inflammation are also highly interconnected with oxidative stress in ALS (Rojas et al., 2015). Evidence of oxidative stress and damage have been widely reported in ALS patients (Babu et al., 2008; Blasco, Garcon, et al., 2017; Mitsumoto et al., 2008; Shaw et al., 1995; Shibata et al., 2001; Simpson et al., 2004; Tohgi et al., 1999; Weishaupt et al., 2006). For instance, Edaravone which is approved for the treatment of ALS, exerts its effects mainly by counteracting oxidative stress through scavenging free radicals and activating the nuclear factor erythroid 2-related factor 2 (NRF2) (Z. Liu et al., 2018; Moujalled et al., 2017). The transcription factor NRF2 binds to antioxidant responsive element (ARE) to regulate the expression of specific genes involved in the cellular response to oxidative stress (Zgorzynska et al., 2021). In postmortem tissues from ALS patients, NRF2 expression was found to be decreased in motor neurons in the cortex and spinal cord, suggesting a failure of these cells in responding to oxidative stress (Sarlette et al., 2008). Interestingly, motor neurons have been found to be particularly susceptible to bioenergetic defects and oxidative stress due to their high energy demands, low levels of antioxidant enzymes and reduced glutathione, decreased NRF2 levels, and increased activity of NADPH oxidases (Blasco, Garcon, et al., 2017; Boas et al., 2021; Chi et al., 2007; Kraft et al., 2004; Mimoto et al., 2012; D.-C. Wu et al., 2006). Additionally, NRF2 plays a role in inhibiting cell death and helping cells resist against excitotoxic insults (J.-M. Lee et al., 2003; Niture & Jaiswal, 2012; Shih et al., 2005; Y. Zhao et al., 2021). Decreased NRF2 activity and depletion of the antioxidant enzyme glutathione peroxidase 4 (GPX4) in motor neurons were also found to mediate a form of iron-dependent programmed cell death called ferroptosis (T. Wang et al., 2022; B. Yang et al., 2023). Additionally, aberrant TDP-43 function was found to decrease the translation of the Nrf2 transcripts in the spinal cord of an ALS mouse model (Moujalled et al., 2017).

These findings highlight the interplay between mitochondrial dysfunction, metabolic dysfunction and oxidative stress, which creates a vicious cycle, amplifying neurodegenerative processes and accelerating disease progression (Fig.9).

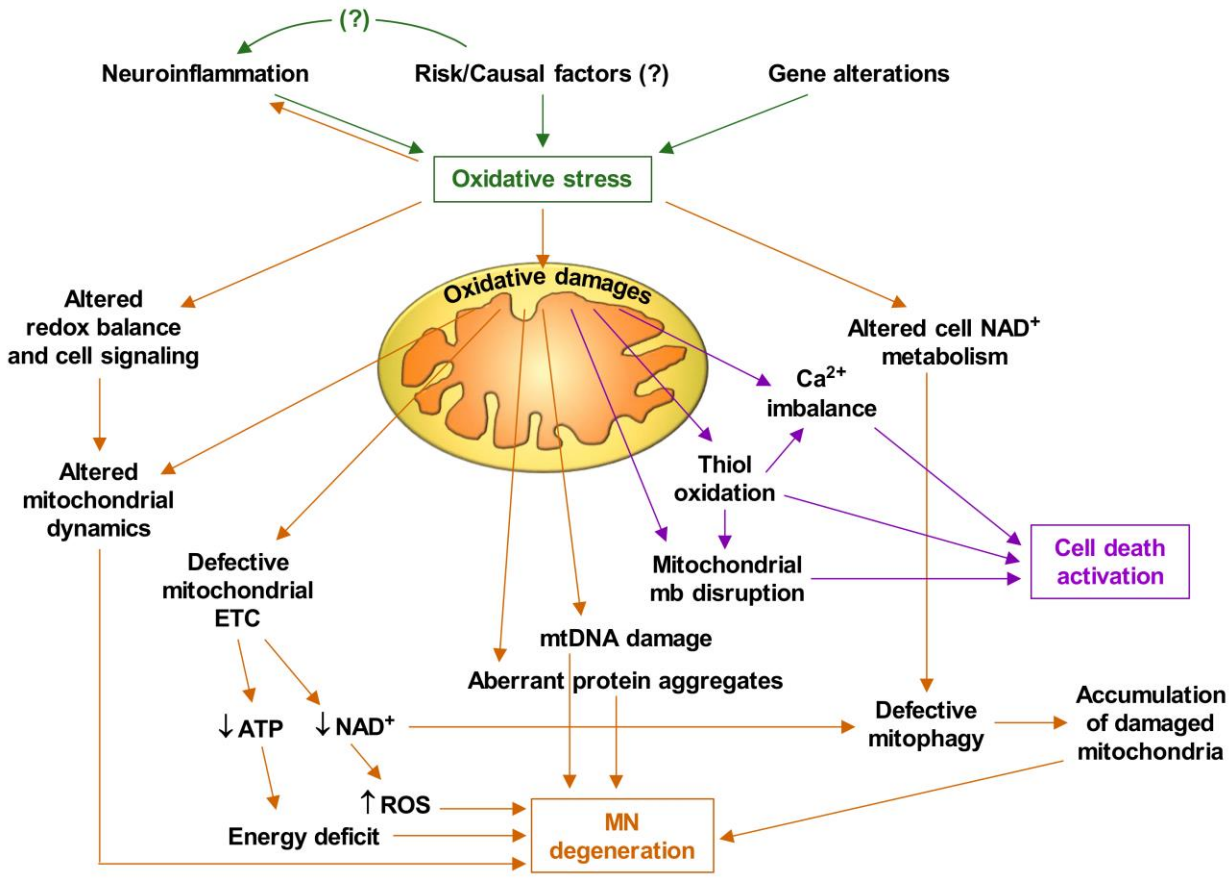

Figure 9: The interplay between oxidative stress and mitochondrial damage in ALS. Factors like neuroinflammation, environmental factors and genetic alterations contribute to oxidative stress, which in turn damages various cellular components, including lipids, proteins, and DNA. Mitochondria are both a major source of ROS and a primary target of oxidative damage. When mitochondria become impaired due to oxidative stress, their ability to produce energy efficiently is compromised, and they generate even more ROS. Defective mitochondria also fail to regulate intracellular Ca^{2+}, contributing to excitotoxic cellular damage. Additionally, they can release pro-apoptotic factors, further promoting neuronal injury and death. This cyclical relationship between oxidative stress and mitochondrial damage is a key factor in the progression of ALS, leading to the degeneration of motor neurons. Reproduced from (Obrador et al., 2021).

e. Metabolic alterations in ALS

The mitochondrial defects described above lead to significant metabolic alterations that have been widely reported in ALS patients (Cistaro et al., 2014; Goutman et al., 2020; Lawton et al., 2014; Steyn et al., 2018). Interestingly, presymptomatic ALS gene carriers had significant metabolic alterations that preceded any changes in the levels of neurofilaments (Dorst et al., 2023). There are still a lot of discrepancies related to metabolic alterations in ALS patients,

which can be due to the heterogeneity of the disease and other confounding factors such as age, gender, drugs, and co-morbidity factors (Godoy-Corchuelo et al., 2022; Jové et al., 2021). One major observation in ALS is the presence of a state of systemic hypermetabolism, an increase in resting energy expenditure, in sALS and fALS patients, which was correlated with a worse disease prognosis (Bouteloup et al., 2009; Desport et al., 2001; Fayemendy et al., 2021; Steyn et al., 2018). The cause of hypermetabolism in ALS is still unknown, especially that patients have a decreased fat-free mass. Different factors might be playing a role including hypothalamic atrophy (Gabery et al., 2021; Gorges et al., 2017), muscle fasciculations and cortical hyperexcitability (Menon et al., 2015; Vázquez-Costa et al., 2018), and mitochondrial dysfunction (Nelson & Trotti, 2022).

Altered lipid profiles have also been reported in ALS patients (i.e. dyslipidemia), including increased levels of serum LDL, cholesterol, and triglycerides compared to controls (Pardo-Moreno et al., 2023). The observed dyslipidemia can be linked to inflammatory processes and oxidative stress (Godoy-Corchuelo et al., 2022; González-Guevara et al., 2020; H. Lee et al., 2021). Various lipidomic changes such as increased levels of cholesterol, phosphatidylcholine, ceramides, and glucoceramides were also observed in the cerebrospinal fluid (CSF) of ALS patients (Abdel-Khalik et al., 2017; Blasco, Veyrat-Durebex, et al., 2017). Some studies have found that TDP-43 played a role in the regulation of cholesterol metabolism in the CNS, providing a potential link between cholesterol dysmetabolism and TDP-43 proteinopathy (Egawa et al., 2022; Ho et al., 2021).

Hypotheses about disturbances in the glucose metabolism have been largely explored as well. Metabolic reprogramming, a switch from glucose to lipid consumption, particularly fatty acid oxidation has been reported in ALS, and is thought to be a compensatory mechanism to abnormal glucose metabolism (Bayer et al., 2017; Fergani et al., 2007; Palamiuc et al., 2015; Pradat et al., 2010; Szelechowski et al., 2018). A decrease in cortical glucose metabolism has been repeatedly described in ALS patients even at the presymptomatic stage (Pagani et al., 2014; Popuri et al., 2021; Van Laere et al., 2014). For instance, Riluzole has been found to enhance the metabolism of glucose in the CNS, possibly contributing to its protective effects (G. M. Chowdhury et al., 2008; Daniel et al., 2013). Insulin resistance and aberrant insulin signalling have also been reported in ALS patients, with some studies showing a link between TDP-43 proteinopathy and these abnormalities (Ahmed et al., 2019; Araki et al., 2019; Pradat

et al., 2010). The overall consequences of metabolic reprogramming and hypermetabolism in ALS can include weight loss, increased muscle wasting, malnutrition, and increased oxidative stress due to the elevated consumption of oxygen, all of which contribute to the worsening of the patient's condition (D'Amico et al., 2021; Ludolph et al., 2023; Obrador et al., 2021). This might explain why a high body mass index (BMI) at diagnosis is associated with a slower progression and an increased survival in ALS patients (W. Cao et al., 2023; J. Chang et al., 2023; Dardiotis et al., 2018).

Metabolic alterations in ALS are multi-faceted and contribute to both disease progression and symptomatology. Overall, mitochondrial dysfunction, hypermetabolism, dyslipidemia, and altered glucose metabolism create a cycle of energy imbalance and oxidative stress, further accelerating motor neuron degeneration.

f. RNA metabolism and nucleocytoplasmic transport dysregulations

RNA metabolism is deeply implicated in the pathogenesis of ALS. Key players in RNA metabolism, such as RNA-binding proteins (RBPs) like TDP-43 and FUS, are commonly mutated in ALS (Da Cruz & Cleveland, 2011). For instance TDP-43 was shown to regulate, both directly and indirectly, more than 6000 coding and non-coding RNA targets (De Conti et al., 2015; Polymenidou et al., 2011; Tollervey et al., 2011). Mutations in the glycine-rich domain of TDP-43, which are the most common mutations in this protein, can affect the binding of TDP-43 to RNA molecules (Ishiguro & Ishihama, 2023). Less frequent mutations in other RBP-encoding genes like *TAF15* (J. Chen et al., 2022), *ATAXN2* (Laffita-Mesa et al., 2013; Salmon et al., 2022), *TIA1* (Mackenzie et al., 2017), *HNRNPA1* (Beijer et al., 2021), *MATR3* (Boehringer et al., 2017), and *EWSR1* (J. Lee et al., 2019) have also been reported in ALS. RBPs are critical for numerous aspects of RNA metabolism, including RNA splicing, transport, localization, stability, translation and assembly into RNA-protein membrane-less organelles, making them a major player in ALS (Kelaini et al., 2021).

For RNA metabolism to function normally, RNA molecules, associated proteins and ribonucleoprotein (RNP) complexes need to move to and from the nucleus through the nuclear pore complex (Sloan et al., 2016). Several studies have reported altered nucleocytoplasmic transport (NCT) in ALS, including aberrant expression, aggregation and/or localization of NCT proteins, abnormal nuclear morphology, and abnormal localization of NCT

cargoes (Aizawa et al., 2019; Chou et al., 2018; Freibaum et al., 2015; Gautam, Jara, et al., 2019; Giampetruzzi et al., 2019; Solomon et al., 2018). All these alterations can have detrimental effects on RNA metabolism (Sloan et al., 2016). For instance, a hallmark of ALS is the loss of RBP from the nucleus and their aggregation in the cytoplasm. In this regard, the most prominent RBP in ALS is TDP-43 which forms cytoplasmic inclusions in 97% of fALS and sALS cases (Neumann et al., 2006; Winton et al., 2008). A dysfunction in either TDP-43 or FUS was found to affect the processing of several long pre-mRNAs and mRNAs encoding proteins that are critical for neuronal health such as EAAT2, neurexin, and various ataxins (Lagier-Tourenne et al., 2012).

Through aberrant loss- and gain-of-function mechanisms, RBPs in neurons can alter various mechanisms including the formation of membrane-less RNA granules, and the transport of RNP complexes along the axon for local translation (Alami et al., 2014; Buchan & Parker, 2009; Imperatore et al., 2020; Ishiguro et al., 2016; Liu-Yesucevitz et al., 2010; Nagano et al., 2020). In fact, RBPs have the capacity to undergo liquid-liquid phase separation, leading to the formation of membrane-less organelles, particularly stress granules (SGs) that transiently sequester certain proteins and RNAs into liquid-like droplets, regulating their usage when the cell experiences stress (Wolozin & Ivanov, 2019). Chronic stress and/or a dysfunction in RBP can therefore affect SG dynamics and enhance the formation of persistent toxic cytoplasmic inclusions that lack the ability to properly control RNA translation (Baron et al., 2013; Chew et al., 2019; Khalfallah et al., 2018; H. J. Kim et al., 2013; Liu-Yesucevitz et al., 2014; Mackenzie et al., 2017; Reineke & Neilson, 2019). In addition to a loss-of-function of the proteins found in cytoplasmic inclusions, there is also a gain-of-function due to the sequestration of essential proteins, RBP, and RNA molecules important for neuronal homeostasis (Liu-Yesucevitz et al., 2010; Verdile et al., 2023). For example, NCT can be impaired by SGs, which sequester factors involved in nuclear import and export (Woerner et al., 2016; K. Zhang et al., 2018). The RBP Ataxin-2, which is implicated in ALS, was also shown to sequester TDP-43 into cytoplasmic condensates, affecting the stability and translation of various mRNA targets important for motor neuron survival (Inagaki et al., 2020; Wijegunawardana et al., 2023).

RNA splicing defects were also observed in ALS following the mislocalization of RBP, NCT defects, and abnormal assembly of the splicing machinery (Luisier et al., 2018; Rossi et al.,

2020; S. Yin et al., 2017). For instance, the loss of FUS from the nucleus and its aggregation in the cytoplasm led to a skipping of neuron-specific exons, a decrease in intron retention, and an increase in cryptic exon splicing (Rezvykh et al., 2023). ALS-associated mutations in the splicing factor HNRNPA1 protein also lead to abnormal splicing of thousands of transcripts involved in neuronal homeostasis (Y. J. Lee & Rio, 2024). Moreover, aberrant TDP-43 function was found to cause the mis-splicing and cryptic exon inclusion in different mRNA like *UNC13A* and *STMN2* that result in a decrease of the normal protein level (Brown et al., 2022; Koike et al., 2023; Krus et al., 2022).

Another aspect of disrupted RNA metabolism in ALS is observed at the level of microRNAs (miRNAs). miRNAs are small non-coding RNA molecules that regulate gene expression at the post-transcriptional level (Cai et al., 2009). Aberrant miRNA expression can lead to the misregulation of key proteins involved in axonal transport, mitochondrial function, and neuromuscular junction integrity (Rinchetti et al., 2018; Si et al., 2018). In recent years, miRNA have been investigated for their potential use as a biomarker in ALS (Banack et al., 2022; Waller et al., 2017).

Overall, disruptions in NCT and RNA metabolism can lead to the mislocalization and aggregation of RBPs, splicing errors, impaired RNA transport, and instability of RNA molecules, which eventually contribute to motor neuron degeneration (Fig.10).

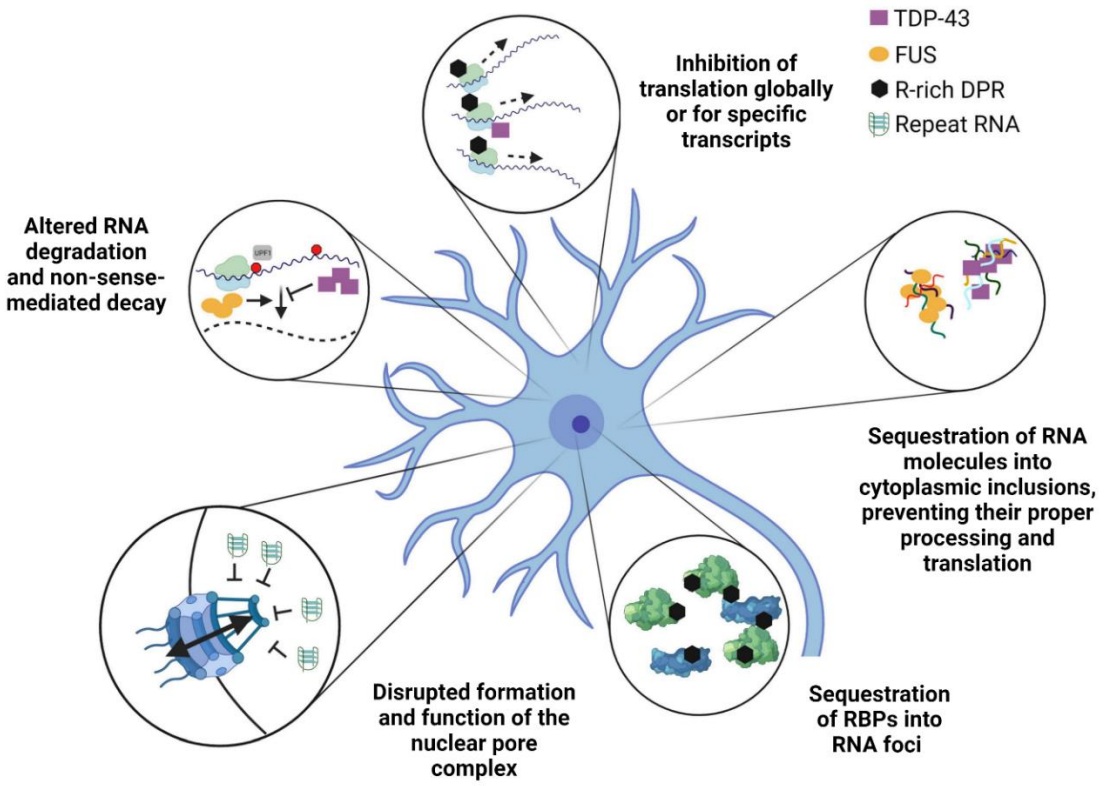

Figure 10: Schematic representation of dysfunctional nucleocytoplasmic transport and RNA metabolism in ALS. Numerous RNA pathways are dysregulated in ALS including RNA splicing, transport, translation and degradation. The exact mechanisms behind these disruptions are not fully understood, but the aberrant function of various ALS-related proteins, with some of them being RBPs like FUS and TDP-43, can negatively affect these processes. In addition, dysfunctional NCT can negatively affect the localization of RNA molecules and RNA-associated proteins, further aggravating the problem. Abbreviations: DPR, dipeptide repeats. Adapted from (Zaepfel & Rothstein, 2021). Edited with BioRender.com

g. Abnormal proteostasis

Proteostasis, or protein homeostasis, involves the coordination of several cellular processes to regulate protein synthesis, folding, degradation, and trafficking. This process is essential for cellular function and survival and is largely impacted in ALS, causing proteotoxicity. ALS is characterized by the accumulation of misfolded proteins and protein aggregates in motor neurons, contributing to their dysfunction and death. Several factors can drive the accumulation of misfolded proteins such as genetic mutations, dysregulated transcription/translation, oxidative stress, protein overexpression, aberrant post-translational modifications, and alterations in the protein quality control system.

When proteins misfold or accumulate within the ER, a condition known as ER stress occurs. To cope with this stress, cells activate a signalling network called the unfolded protein response (UPR) (X. Chen et al., 2023). The UPR aims to restore ER homeostasis but can lead to cell death if the stress is not resolved (X. Chen et al., 2023). In neurodegenerative diseases like ALS, chronic ER stress and a maladaptive UPR contribute to disease pathology. In fact, it was shown that in the motor neurons impacted in ALS, enhanced ER stress coupled with UPR were detected, suggesting an accumulation of misfolded proteins (Dafinca et al., 2021; Farg et al., 2012; Sasaki, 2010; Saxena et al., 2009).

Molecular chaperones and co-chaperones, such as the heat shock proteins (HSP) family, are needed to ensure the proper folding of proteins, prevent aberrant protein-protein interactions, assist in refolding damaged proteins, and drive the degradation of misfolded proteins through the ubiquitin-proteasome system (UPS) or autophagy (Hu et al., 2022). In ALS, numerous reports have described a dysfunction of chaperones and a sequestration of HSPs in cytoplasmic aggregates (Filareti et al., 2017; François-Moutal et al., 2022; F. Liu et al., 2022; Lu et al., 2022). Moreover, the activity and expression of chaperones in the brain have been found to be decreased with ageing (Brehme et al., 2014). Such alterations exacerbate the vulnerability of neurons to stress conditions which can contribute to the increased risk of developing ALS with age. Furthermore, the motor neurons impacted in ALS seem to have a lower tolerance to protein quality control abnormalities. They intrinsically express lower levels of HSPs compared to other cells (Batulan et al., 2003). It was also found that the network of aggregation-prone proteins involved in ALS is in a supersaturated state in the motor neurons of the spinal cord, contrary to the ALS-resistant oculomotor neurons (Ciryam et al., 2015; Yerbury et al., 2019). Supersaturated proteins are proteins that exist in a state where their concentration in the cell is higher than their solubility limit under normal physiological conditions, making them prone to aggregation if not properly managed by cellular mechanisms (Ciryam et al., 2015). These proteins are therefore easily aggregated when the protein quality control system is dysregulated such is the case in ALS.

When chaperones become dysfunctional or overwhelmed, they fail to maintain the proper folding of proteins and direct them to the degradation pathways of the cell (Brehme et al., 2014). However, there seems to be an initial dysfunction of the UPS in ALS followed by a dysfunction in the autophagy system as the disease progresses, contributing to proteostatic

collapse (Tadokoro et al., 2021). Various ALS-related mutations have been detected in genes involved in the degradation pathways such as *UBQLN2, SQSTM1, VCP,* and *OPTN* (Fecto, 2011; Feng et al., 2019; Koppers et al., 2012; J. J. Wu et al., 2020). Moreover, proteins known to be key players in ALS including TDP-43, FUS, SOD1, and C9ORF72 have been shown to interact with the degradation machinery such as the UPS and autophagy system, leading to their dysfunction (Dzik et al., 2024; Farrawell et al., 2020; Riemenschneider et al., 2022; Soo & Atkin, 2015; Yamakawa et al., 2015; P. Yin et al., 2021). Additionally, various stress conditions can lead to a loss of proteostasis. For instance, the formation of SG can be initially protective by isolating misfolded proteins from the rest of the cellular components. However, if not efficiently cleared, due to dysfunctional chaperons for example, these structures can mature into insoluble inclusions and toxic aggregates (Mateju et al., 2017; A. Patel et al., 2015).

Another factor is the aberrant post-translational modifications to aggregation-prone proteins, which can occur following a perturbation of the intracellular environment. For example, oxidative stress can modify proteins like TDP-43 leading to their aggregation and the subsequent collapse of proteostasis (Pirie et al., 2021; Zuo et al., 2021). Similarly, by increasing intracellular Ca^{2+}, glutamate-induced excitotoxicity can cause the activation of enzymes like the protease calpain, which can cleave TDP-43 into pathological aggregation-prone fragments (Yamashita & Kwak, 2014). A dysregulation in intracellular metal ions can also alter proteins like TDP-43 and SOD1 and drive their misfolding and aggregation (Ash et al., 2019; Garnier et al., 2017; Y. Huang et al., 2006; Sheng et al., 2013).

The disruption of the delicate proteostatic balance in ALS leads to a vicious cycle that exacerbates cellular damage. The accumulation of misfolded aggregation-prone proteins overwhelms the cellular machinery responsible for maintaining proteostasis, including molecular chaperones and degradation pathways. As these systems become compromised, their ability to clear misfolded proteins diminishes, resulting in increased aggregation and proteotoxic stress. This stress further impairs cellular functions, including mitochondrial activity, which leads to elevated oxidative stress and additional protein damage. The heightened oxidative stress exacerbates protein misfolding, creating a vicious cycle of proteostatic collapse. As motor neurons are particularly susceptible to this cycle, the

continuous accumulation of damaged proteins and cellular stress ultimately leads to their dysfunction and death, driving the progression of ALS (Fig.11).

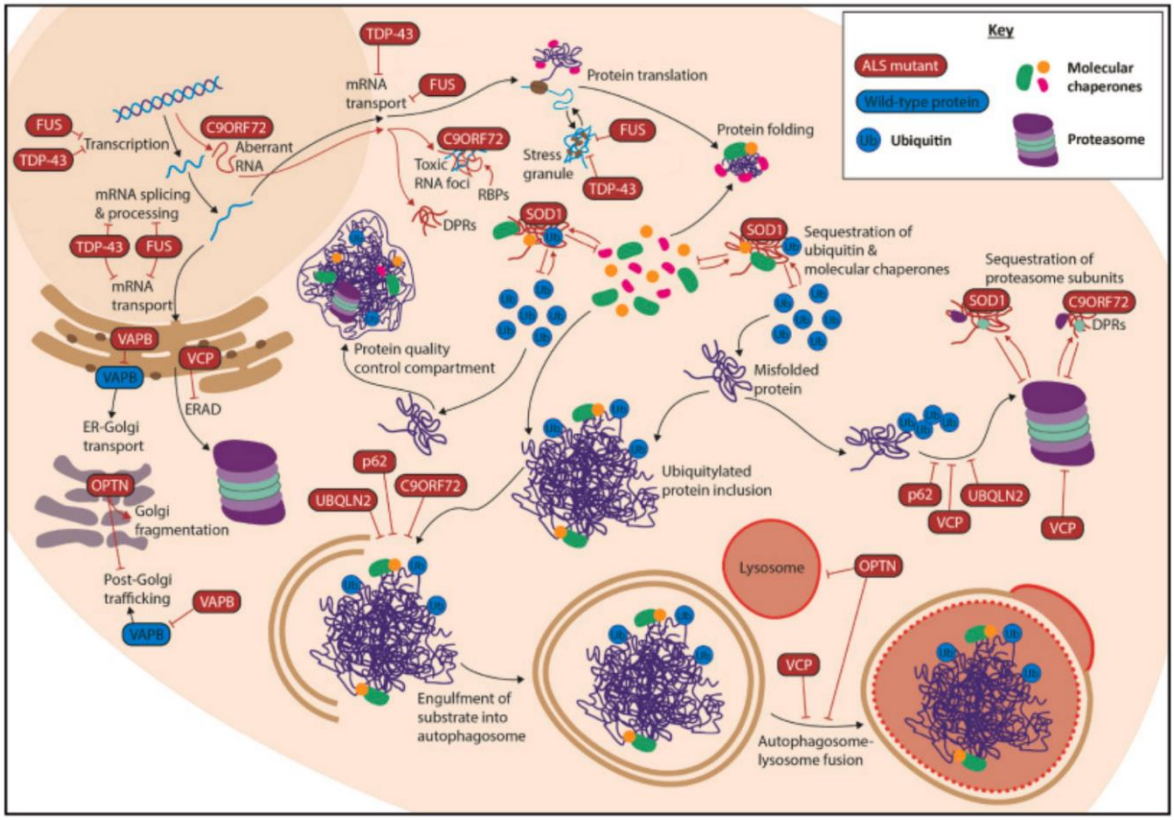

Figure 11: Schematic representation of the impact of ALS-associated proteins on the proteostatic dysfunction. Chaperones play a crucial role in assisting the folding of newly synthesized polypeptides into their proper native structures, preventing the aggregation of misfolded proteins, and guiding irreversibly misfolded proteins toward degradation via the UPS and autophagy pathways. Under pathological and stressful conditions, the accumulation of misfolded proteins can overwhelm the protein quality control systems including chaperones-assisted refolding and degradation pathways. Reproduced from (Lambert-Smith et al., 2022).

E. ALS in the clinics

a. Clinical manifestations of ALS

ALS presents with progressive atrophy of skeletal muscles, and paralysis that eventually leads to the death of the patient from diaphragmatic and respiratory failure, 2 to 5 years following the onset of symptoms (Mehta et al., 2017). Several neuronal circuits can be affected but they primarily involve the corticospinal tract which encompasses both the upper motor

neurons (UMN) in the brain and the lower motor neurons (LMN) in the spinal cord which innervate the skeletal muscles (Lemon, 2008).

ALS is a heterogenous disease that can affect multiple systems and present with symptoms that vary greatly from one patient to another and change as the disease progresses (Grad et al., 2017) (Fig.12). In addition, the rate of progression differs widely among patients (Witzel et al., 2021). The clinical manifestation of ALS varies depending on which neurons are affected first, leading to the recognition of two main clinical phenotype variants: bulbar-onset ALS, and limb-onset ALS (Brooks, 1994). Limb-onset ALS encompasses around two thirds of ALS cases (Logroscino et al., 2010). Patients initially experience nonspecific mild symptoms in the upper or lower limbs such as muscle weakness, cramping, stiffness, and fasciculations, then develop bulbar symptoms as the disease progresses (Gwathmey et al., 2023; Zarei et al., 2015). Patients with bulbar-onset ALS experience spasticity, exaggerated reflexes in the affected muscles, as well as weakness, atrophy, and fasciculations in the muscles of the face, tongue, and throat (Gwathmey et al., 2023). Patients typically present with slurred speech (dysarthria), difficulties in swallowing (dysphagia), hoarseness, excessive saliva flow (sialorrhea), facial weakness, and respiratory issues as the disease progresses (Shellikeri et al., 2017). Patients with bulbar-onset ALS seem to be predominately females and tend to have a poorer prognosis and a shorter survival time (<2 years) compared to limb-onset ALS (Z. He et al., 2022; Turner et al., 2010). A third and rare type of ALS that affects only 3-5% of patients is respiratory-onset ALS, which is associated with difficulty breathing due to the weakening of the respiratory muscles and diaphragm (Gwathmey et al., 2023; Pinto et al., 2023). Surprisingly, the survival time of these patients, who are predominately males, was not found to differ significantly from that of bulbar- or limb-onset ALS patients (Shoesmith et al., 2007).

It was first thought that ALS only affects the motor neurons in the spinal cord and the brain, particularly the pyramidal cortical neurons and the corticospinal tract neurons, while sparing neurons related to oculomotor, sensory, and autonomic functions (Chipika et al., 2022; Štětkářová & Ehler, 2021). However, patients who survive for a long time with the disease start showing alterations in these latter functions as well (Swinnen & Robberecht, 2014). This highlights the extra-motor impairments in ALS and implies that ALS should not be considered solely a motor neuron disease. In addition, up to 50% of ALS patients experience some neuropsychological symptoms and cognitive deficits such as memory impairment,

personality changes, executive dysfunction, behavioural changes, language difficulties, and others (Goldstein & Abrahams, 2013; Phukan et al., 2012). Cognitive dysfunction seems to be more common in patients with bulbar-onset ALS (Shellikeri et al., 2017). The observation in ALS of these symptoms, which are features of a disease known as frontotemporal lobar degeneration (FTD) led to the description of an ALS-FTD disease continuum (Lomen-Hoerth et al., 2002; Strong et al., 2017).

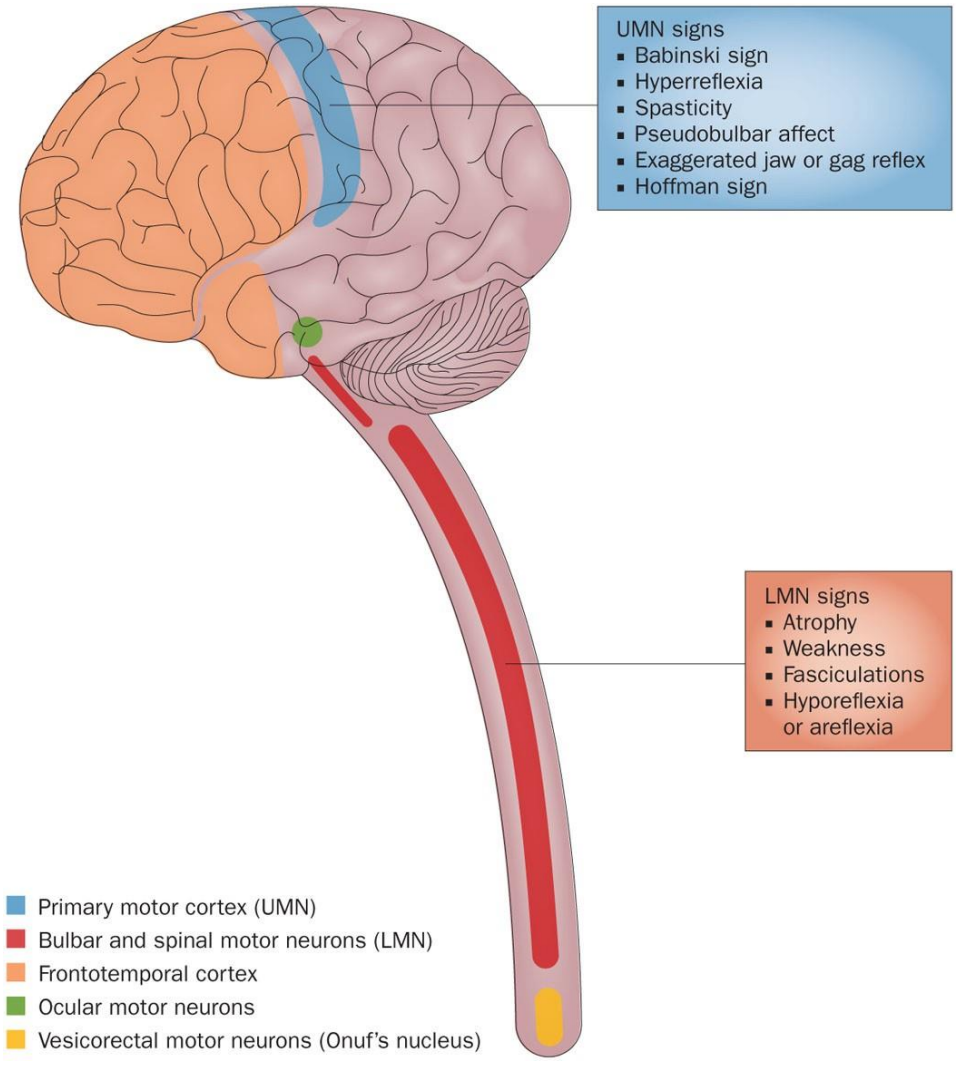

Figure 12: Neuronal circuits that are involved in ALS. The main neuronal populations that are involved in ALS are the UMN (in blue) and the LMN (in red). Involvement of the frontotemporal cortex (in orange) leads to symptoms of the ALS-FTD spectrum. The ocular motor neurons (in green) and the vesicorectal motor neurons (in yellow) are usually not involved except in patients with a prolonged disease. Reproduced from (Swinnen & Robberecht, 2014).

b. Diagnosis and management

The diagnosis of ALS is mainly a clinical one which uses a combination of medical history, physical examination, clinical findings, and various tests to rule out other conditions. Due to the lack of specific ALS biomarkers and the non-specificity of symptoms, there is a diagnostic delay ranging from 10 to 16 months following the onset of symptoms (Richards et al., 2020). A set of criteria has been established to guide physicians in the diagnosis of ALS and its differentiation from ALS mimickers such as primary lateral sclerosis, myasthenia gravis, compressive neuropathies, spinobulbar muscular atrophy, inclusion body myositis, multifocal motor neuropathy, and multiple sclerosis (N. Singh et al., 2018). These criteria have been revised and modified several times following the improvement in the classification of ALS subtypes and the advancement in diagnostic technologies. The most commonly used sets of diagnostic guidelines are the El Escorial criteria (1994) (Brooks, 1994) and their revised version (2000) (Brooks et al., 2000), as well as the Amaji-Shima criteria (2008) (De Carvalho et al., 2008). When an ALS diagnosis is suspected following clinical and neurological examination, electromyography (EMG) can be used to detect motor neuron lesions, particularly at the level of the LMN (Štětkářová & Ehler, 2021). However, these guidelines were mainly intended for therapeutic trials rather than ALS diagnosis, and lacked sensitivity (Rutter-Locher et al., 2016; Traynor et al., 2000; Zoccolella et al., 2006). A few years ago, new guidelines known as the Gold Coast criteria (2020) emerged and addressed some limitations of the original criteria to enhance diagnostic accuracy (Shefner et al., 2020).

The evaluation of the physical status of ALS patients relies on a standardized clinical tool known as the ALS Functional Rating Scale in its revised form (ALSFRS-R) (Cedarbaum et al., 1999). It's a questionnaire comprising 12 questions, each rated from 0 (inability) to 4 (normal function), that assesses the patient's bulbar function, gross and fine motor functions, as well as respiratory function (Cedarbaum et al., 1999). It is considered as a valuable tool to evaluate the severity of the disease, its progression rate, and the effectiveness of potential therapeutic and interventional approaches (Genge et al., 2024; Kollewe et al., 2008).

As for the management of ALS, it is primarily focused on slowing the progression of the disease, managing the symptoms, and improving the quality of life of patients. It therefore requires a comprehensive multidisciplinary approach in order to address the multitude of symptoms and challenges that are faced by them. It therefore requires the collaboration of a

team of healthcare professionals comprising neurologists, respiratory specialists, occupational and speech-language therapists, physical therapists, nutritionists, as well as social workers (Sukockienė et al., 2020).

F. ALS biomarkers

The progressive nature of ALS and the lack of reliable disease biomarkers make it particularly challenging for patients, healthcare givers, and researchers. Recently, neurofilament proteins in the blood and CSF, which are markers of neuronal and axonal damage, have become increasingly investigated as potential biomarkers in ALS. However, these proteins are considered to be non-specific because their levels are increased following neuronal injury regardless of its cause (Dietmann et al., 2023; Fisse et al., 2021; J Lukiw, 2021; Mortensen et al., 2023). Interestingly, a recent study found that CSF and/or blood levels of phosphorylated neurofilament heavy chain (pNfH) and more importantly NfL can be used to distinguish ALS from other ALS mimics, differentiate clinical subtypes of ALS, and estimate prognosis (Behzadi et al., 2021). However although promising, more work is needed to validate the use of neurofilaments in the diagnosis of ALS. Despite the relevance of NfL largely described in the literature, even in presymptomatic patients (Benatar et al., 2018, 2019; Smith et al., 2024), or in clinical trials to monitor drug response (e.g. Tofersen) (T. Meyer et al., 2024; Weishaupt et al., 2024), the use of this biomarker is still not done in routine practice in France.

The invasiveness of exploring biomarkers in the CSF has led researchers to consider peripheral biofluids that are less invasive to collect. They can allow for a longitudinal follow-up and reflect the state of the CNS. In recent years, interest has grown in exploring the potential of exosomes as potential biomarkers in ALS. Exosomes are small extracellular vesicles, typically 30-100 nm in size, that are released by various cell types into the extracellular space and can be found in biofluids (Thakur et al., 2022). They are involved in cell-to-cell communication and carry a variety of molecular cargoes, including proteins, lipids, and nucleic acids (such as mRNA, microRNA, and DNA) (H. Wei et al., 2021). Because of their ability to reflect the physiological state of their cells of origin, exosomes have earned significant interest as potential biomarkers in various neurodegenerative diseases including ALS (Afonso et al., 2023; Gschwendtberger et al., 2023). In fact, brain-derived exosomes have been successfully detected and isolated from the plasma (Picciolini et al., 2018). Studies have reported miRNA differences in serum-derived extracellular vesicles from ALS patients

compared to controls, suggesting an ALS-specific miRNA profile in these vesicles (Y.-F. Cheng et al., 2023; J.-A. Kim et al., 2023). Moreover, ALS-related proteins like TDP-43, phosphorylated TDP-43, FUS, SOD1, as well as neurofilaments and miRNA have been differentially detected in CNS-derived exosomes in ALS compared to controls (Darabi et al., 2024). However, no one molecule was sufficient to be used alone as a biomarker (Darabi et al., 2024). Recently, our group examined exosome-enriched extracellular vesicles derived from patient's serum at an early disease stage through an omics (proteomics and metabolomics) and bioinformatics approach, which was not explored before. In this proof-of-concept study, the aim was to identify potential biomarkers that were differently present in exosomes from patients compared to healthy controls using a small volume of non-invasively collected biological sample (Publication 7).

II. TDP-43 : a major target in ALS

TDP-43 is a critical therapeutic target in ALS due to the central role it plays in the pathogenesis and progression of the disease. In fact, TDP-43 proteinopathy is present in the majority of ALS cases, both sporadic and familial. For this reason, by targeting this protein, therapies could potentially address a common underlying mechanism in a wide range of patients. However, this approach also comes with several challenges and obstacles. These are mainly linked to the complexity of TDP-43 functions and its implication in numerus cellular processes. In fact, therapeutic approaches must ensure target specificity, meaning that they only target pathological TDP-43 without affecting its normal functions. In addition, given the ubiquitous nature of TDP-43, potential toxicity and off-target effects should be carefully considered.

In the following review article (Publication 1), we describe the structure and normal function of TDP-43. We also discuss the consequences of TDP-43 proteinopathy on various cellular pathways, in both neuronal and non-neuronal cells. Finally, we present the strategies that are being developed to target TDP-43 in ALS and the promise they hold in improving the pathophysiological mechanisms of the disease.

Briefly, TDP-43 is a ubiquitous 414 amino acid protein that plays a key role in cellular homeostasis starting from early embryonic development stages. It consists of four domains: two RNA-recognition motifs (RRM1 and RRM2), the N- and the C-terminal domains. TDP-43 is

mainly found in the nucleus where it regulates gene transcription and participates in DNA repair mechanisms. It also plays a pivotal role in the regulation of both coding and non-coding RNA. It participates in the biogenesis of non-coding RNA, as well as the stabilization, trafficking, splicing, and translation of coding RNA transcripts. Neurons seem to have an increased vulnerability to TDP-43 pathology, partly due to their intrinsic low ability to adapt to cellular stress. Several therapeutic strategies have been developed to target, either directly or indirectly, the pathological cellular changes linked to TDP-43 dysfunctions. These include stabilizing the native functional form of TDP-43, decreasing its export from the nucleus, enhancing its nuclear functions particularly pre-mRNA splicing, decreasing the aggregation of TDP-43 by enhancing the activity of molecular chaperones or enhancing the clearance of aggregates, regulating the formation of TDP-43-containing stress granules, and finally modulating the pathological post-translational modifications to TDP-43. This review discusses all these aspects of TDP-43 as a therapeutic target in ALS.

Publication 1:

Al Ojaimi, Y., Dangoumau, A., Alarcan, H., Hergesheimer, R., Vourc'h, P., Corcia, P., ... Lanznaster, D., & Blasco, H. (2022). TAR DNA-binding protein of 43 kDa (TDP-43) and amyotrophic lateral sclerosis (ALS): a promising therapeutic target. ***Expert Opinion on Therapeutic Targets*****, 1-18.**

Taylor & Francis
Taylor & Francis Group

Expert Opinion on Therapeutic Targets

ISSN: (Print) (Online) Journal homepage: https://www.tandfonline.com/loi/iett20

TAR DNA-binding protein of 43 kDa (TDP-43) and amyotrophic lateral sclerosis (ALS): a promising therapeutic target

Yara Al Ojaimi, Audrey Dangoumau, Hugo Alarcan, Rudolf Hergesheimer, Patrick Vourc'h, Philippe Corcia, Débora Lanznaster & Hélène Blasco

To cite this article: Yara Al Ojaimi, Audrey Dangoumau, Hugo Alarcan, Rudolf Hergesheimer, Patrick Vourc'h, Philippe Corcia, Débora Lanznaster & Hélène Blasco (2022) TAR DNA-binding protein of 43 kDa (TDP-43) and amyotrophic lateral sclerosis (ALS): a promising therapeutic target, Expert Opinion on Therapeutic Targets, 26:6, 575-592, DOI: 10.1080/14728222.2022.2083958

To link to this article: https://doi.org/10.1080/14728222.2022.2083958

View supplementary material

Published online: 02 Jun 2022.

Submit your article to this journal

Article views: 237

View related articles

View Crossmark data

Full Terms & Conditions of access and use can be found at
https://www.tandfonline.com/action/journalInformation?journalCode=iett20

EXPERT OPINION ON THERAPEUTIC TARGETS
2022, VOL. 26, NO. 6, 575–592
https://doi.org/10.1080/14728222.2022.2083958

Taylor & Francis
Taylor & Francis Group

REVIEW

Check for updates

TAR DNA-binding protein of 43 kDa (TDP-43) and amyotrophic lateral sclerosis (ALS): a promising therapeutic target

Yara Al Ojaimi[a], Audrey Dangoumau[a], Hugo Alarcan[a,b], Rudolf Hergesheimer[a], Patrick Vourc'h[a,b], Philippe Corcia[b,c], Débora Lanznaster [a] and Hélène Blasco[a,b]

[a]UMR 1253 iBrain, Université de Tours, Tours, France; [b]Laboratoire de biochimie et biologie moléculaire, CHRU Bretonneau, Tours, France; [c]Service de neurologie, CHRU Bretonneau, Tours, France

ABSTRACT

Introduction: Amyotrophic Lateral Sclerosis (ALS) is a fatal neurodegenerative disease that lacks an effective treatment. Aggregates of the TAR DNA-binding protein-43 (TDP-43) are observed in 97% of all ALS cases, thus making this protein a major therapeutic target in ALS.

Areas covered: The authors describe the major cellular functions of TDP-43 and the features and consequences of TDP-43 proteinopathy. Drawing from fundamental and preclinical studies on cellular and animal TDP-43 models of ALS and selected clinical trials, the major pathways that have been targeted for the mitigation of TDP-43 pathology in ALS are discussed. The authors provide insights on the approaches targeting the tendency of TDP-43 for aggregation, defective nucleocytoplasmic transport, dysfunctional proteostasis, abnormal stress granule dynamics, and pathological post-translational modifications of TDP-43.

Expert opinion: The complexity of ALS and TDP-43 proteinopathy generates challenges for the development of novel therapeutic approaches. However, the critical involvement of TDP-43 in the initiation and progression of ALS, makes it a promising therapeutic target. Further research should be centered on the development of precision strategies, consideration of patient subgroups, the prevention of the mislocalization of TDP-43 and restoration of the lost functions of TPD-43.

ARTICLE HISTORY
Received 3 April 2022
Accepted 26 May 2022

KEYWORDS
Aggregation; ALS; mislocalization; neurodegeneration; proteinopathy; TDP-43; therapeutics

1. Introduction

Amyotrophic Lateral Sclerosis (ALS), also known as Lou Gehrig's disease is a fast-progressing paralytic neurodegenerative disease that leads to the irreversible degeneration of the upper and lower motor neurons. It is the most common motor neuron disease. 90% of ALS cases are sporadic (sALS), while only 10% are familial cases (fALS). Various disease-causing mutations have been identified with the most common pathogenic variants occurring in the *C9ORF72, SOD1, TARDBP* and *FUS* genes. The pathogenesis of ALS is complex and still poorly understood. An interplay between genetics and environmental factors is likely to contribute to the disease. Several pathological mechanisms have been identified so far, including glutamate excitotoxicity, oxidative stress, mitochondrial dysfunction, neuroinflammation, alterations of mRNA processing, and the accumulation of protein aggregates such as Transactive response DNA binding Protein (TDP-43). TDP-43 is an evolutionary conserved protein that is involved in transcriptional and post-transcriptional regulation. Under normal physiological conditions, TDP-43 is mainly localized in the nucleus. However, toxic cytoplasmic aggregates of TDP-43 have been found in several neuropathologies, particularly in ALS where 97% of patients displayed such aggregates in neurons and glial cells, making it a hallmark of the disease [1,2].

ALS remains a fatal disease with an average life expectancy of 2 to 5 years following the appearance of symptoms. There is still no effective treatment to reverse or stop the progression of ALS. The only two FDA-approved drugs, Rilutek® (Riluzole) and Radicava® (Edaravone), produce mild effects on slowing down disease progression. One of the major pathological consequences of TDP-43 pathology is the depletion of nuclear TDP-43 and its subsequent effects on alternative splicing and protein expression. Therefore, one of the main aims of targeting TDP-43 proteinopathy is to restore the lost nuclear functions of the protein. For this reason, the development of new therapeutic strategies such as antisense oligonucleotides (ASO) seemed promising, but clinical translation remains challenging [3–5]. Therefore, intense research is still being conducted to find reliable ALS biomarkers and innovative potential treatments targeting the most relevant pathophysiological factors that can alter the course of the disease. In this review, we will discuss the physiological role of TDP-43 and the subsequent effects of TDP-43 proteinopathy. We then present the advances made in the therapeutic strategies targeting TDP-43 pathology in ALS.

2. Structure and function of TDP-43

TDP-43 is encoded by the *TARDBP* gene. It plays an important role in the development and maintenance of the nervous system from early embryonic stages to adulthood.

CONTACT Hélène Blasco helene.blasco@univ-tours.fr UMR 1253 iBrain, Université de Tours, Tours, France.
Supplemental data for this article can be accessed online at https://doi.org/10.1080/14728222.2022.2083958.
© 2022 Informa UK Limited, trading as Taylor & Francis Group

Article highlights

- TDP-43 plays a major role in the initiation and progression of ALS and hence is a promising therapeutic target.
- TDP-43 is crucial for cellular homeostasis, particularly in motoneurons where it plays a key role in the processing of mRNA, the biogenesis of miRNA, mitochondrial function, the cellular response to stress, and axonal transport.
- TDP-43 proteinopathy seems to be mainly mediated by the loss of the protein's normal function and autoregulation, which are due to its nuclear depletion and cytoplasmic aggregation.
- Most therapeutic approaches indirectly target TDP-43 by regulating nucleocytoplasmic transport and nuclear functions of TDP-43, the cellular response to stress, RNA-TDP-43 interactions, the degradation pathways of the cell, and the post-translational modifications of TDP-43.
- TDP-43-specific fragments of antibodies are recently being developed to directly target pathological TDP-43 for degradation.
- It is important to determine which mechanism of TDP-43 pathology (e.g. loss of nuclear function, aggregation, cytoplasmic mislocalization, etc.) should be targeted to obtain the best therapeutic effects with the least potential side effects.

This box summarizes key points contained in the article.

In fact, homozygous knockout of *TARDBP* in embryos is lethal. This ubiquitous protein belongs to the heterogeneous nuclear ribonucleoprotein (hnRNP) family and regulates RNA metabolism including processing, splicing, transport and stability. TDP-43 is involved in the regulation of several thousand transcripts, as well as the autoregulation of its own mRNA [6,7].

TDP-43 consists of 414 amino acids forming four main domains: a N-terminal domain (NTD), two RNA recognition motifs (RRM1 and RRM2), and a C-terminal domain (CTD). The NTD is a well-folded globular domain, important for the homodimerization of the protein. It mediates TDP-43 self-assembly and is crucial for its splicing activity [8]. The RRM1 and 2 of TDP-43 can interact with a large variety of RNA and single-stranded DNA, preferentially through UG and TG repeats, respectively [9]. They might also play an important role in the aggregation of the protein [10]. The CTD is a glycine-rich low complexity domain (LCD) that mediates homo- and heterotypic protein-protein interactions and TDP-43 oligomerization [11]. This domain, particularly its glycine-rich region was recently found to interact directly with G-quadruplex RNA to mediate their long distance transport in neurons [12]. The CTD can be cleaved to generate different fragments of TDP-43 that accumulate in cytoplasmic inclusions [13]. In addition, most ALS-associated mutations have been detected in the CTD [14]. The structure and domains of full-length and 35- and 25-kDa C-terminal fragments (CTF) of TDP-43 are represented in Figure 1.

Under normal physiological conditions, TDP-43 mainly resides in the nucleus with a small fraction constantly shuttling between the nucleus and the cytoplasm. In the nucleus, TDP-43 regulates gene transcription through its association with sites of transcription and its interaction with transcription regulators [15]. TDP-43 also participates in the repair of double-stranded DNA breaks [16]. In addition, it is important for pre-mRNA splicing through the regulation of exon skipping and inclusion, the repression of cryptic exons, and the regulation of its own mRNA [3]. The autoregulation of TDP-43 occurs via the nuclear fraction of the protein which normally promotes the splicing of cryptic introns in the TDP-43 pre-mRNA and subsequent nonsense-mediated mRNA decay (NMD) [7]. TDP-43 was also shown to be involved in the processing of non-coding RNA such as the biogenesis of micro-RNA (miRNA) and the association with long non-coding RNA (lncRNA) [17,18]. In the cytoplasm, TDP-43 controls the stability of the mRNA through its binding to 3' untranslated regions. It is also essential for the regulation of mRNA translation by associating with translation initiation and elongation factors or recruiting translational inhibiting complexes [19]. Moreover, in neurons TDP-43 is involved in mRNA trafficking, particularly in dendrites and axons [20].

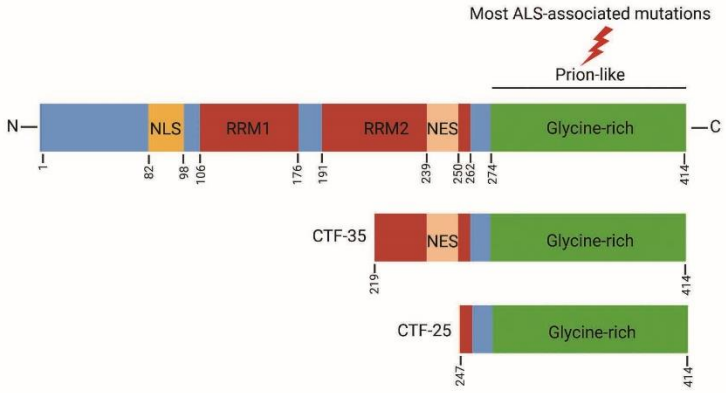

Figure 1. Schematic representation of the structural organization of full-length, 35kDa and 25kDa fragmented TDP-43.
CTF: C-terminal fragment; NES: nuclear export signal; NLS: Nuclear localization signal; RRM: RNA recognition motifs.

3. Features of TDP-43 pathology in ALS

3.1. Mechanisms and consequences of TDP-43 pathology

TDP-43 mutations account for 1.5% of sALS cases and 3% of fALS cases, directly implicating this protein in the pathogenesis of ALS [14]. TDP-43 pathologies are characterized by the abnormal translocation of TDP-43 from the nucleus to the cytoplasm, leading to a nuclear depletion of the protein and a cytoplasmic accumulation of insoluble and modified TDP-43. These aggregates mainly contain abnormally phosphorylated and ubiquitinated TDP-43, in addition to truncated 25 and 35 kDa CTF. These pathological variants of TDP-43, in addition to the mutated forms of the protein, play an important role in disease initiation and progression [14]. In fact, it was recently observed that a more severe TDP-43 proteinopathy, particularly an increased density of phosphorylated TDP-43 (pTDP-43) inclusions in the spinal cord is associated with a faster disease progression in ALS patients [21].

At the protein level, purified full-length and CTF of TDP-43 display an intrinsic tendency to aggregate in solution, and ALS-linked CTD mutations further increase this aggregation [22]. Several mechanisms exist in cells in order to monitor the levels of TDP-43. For example, in stressed HEK293T cells, a redistribution of TDP-43 from the nucleus to the cytoplasm causes a decrease in the levels of miRNAs, particularly those that suppress the expression of TDP-43, leading to increased TDP-43 levels and an exacerbation of TDP-43 pathology [23]. In addition, the loss of nuclear TDP-43 affects the ability of the protein to control the splicing of its own pre-mRNA and regulate its expression [7]. The levels of TDP-43 need to be tightly regulated and in ALS, TDP-43 loses the ability to autoregulate leading to its accumulation and subsequent aggregation. Since TDP-43 is known to extensively regulate various cellular processes, a dysregulation of TDP-43 is expected to have deleterious effects on various pathways.

For instance, TDP-43 plays an important role in the nucleus through the regulation of transcription and the response to DNA damage, which are dysregulated in ALS [16]. The mislocalization of TDP-43 into the cytoplasm was associated with abnormal shuttling between the nucleus and the cytoplasm. In fact, abnormal nucleocytoplasmic transport has been reported in several age-related neurodegenerative diseases including ALS with TDP-43 pathology [24]. Fibroblasts, iPSC-derived neurons and brain tissues from ALS patients with TDP-43 pathology showed morphologically defective nuclear membranes and nuclear pore complexes [25]. It is still not well understood if TDP-43 aggregates lead to nucleocytoplasmic transport defects or vice versa. On one hand, cytoplasmic TDP-43 aggregates were shown to sequester specific nucleoporins and transport factors, thus altering the normal nuclear import of proteins and export of RNA, exacerbating the depletion of TDP-43 from the nucleus and causing cell death [25]. On the other hand, defective nucleocytoplasmic transport was found to trigger TDP-43 proteinopathy and cytoplasmic aggregation [26]. Exclusion of TDP-43 from the nucleus will have global effects on mRNA alternative splicing, including transcripts that are crucial for the survival of neurons.

Another mechanism for the accumulation of misfolded and aggregated TDP-43 is the altered function of cellular proteostasis mechanisms in ALS. The presence of polyubiquitinated TDP-43-containing cytoplasmic inclusions in ALS means that these proteins have been marked for degradation but that the cell was unable to degrade them. For example, some TDP-43 mutants exhibit increased stability and longer half-lives, and were correlated to earlier disease onset in patients [27]. In addition, the aggregation and loss of nuclear function of TDP-43 impairs the functions of the ubiquitin-proteasome system (UPS) and autophagy-lysosome pathway (ALP), particularly in motoneurons [28], further exacerbating the problem.

TDP-43 pathology also affects other critical biochemical pathways in the cell. For example, 80% of mitochondria displayed abnormal morphology and structure in the brains of TDP-43-pathology patients which was also confirmed in animal and cellular models of ALS [29]. TDP-43 was found to abnormally localize to the mitochondria in cellular and animal models of ALS as well as in ALS patients, impairing the expression of complex I of the electron transport chain and the production of ATP, as well as increasing oxidative and nitrosative stress [30,31]. Moreover, metabolic alterations have been reported in animal and cellular models of ALS, as well as patients exhibiting TDP-43 proteinopathy [32,33].

3.2. Prion-like behavior of TDP-43

The CTD of TDP-43 contains an amino acid sequence that is similar to that of prion proteins [6]. Researchers have investigated the prion-like propagation of TDP-43, including the seeding of TDP-43 aggregates and cell-to-cell spreading [14,31,34]. The intercellular spreading of pathogenic TDP-43 is thought to occur through two main mechanisms: the neuronal connectome and synapses [35], and/or exosomes [36]. Interestingly, postmortem studies revealed that pTDP-43 seems to spread in a sequential pattern along axonal pathways, enabling the identification of four neuropathological stages of ALS [37].

Contrary to the prion-like spreading of the insoluble oligomeric form of TDP-43, Braak and his colleagues suggested that soluble TDP-43 might be able to spread through synaptic connections from one neuron to the next, primarily originating in cortical Betz cells and progressing into α-motoneurons [38]. TDP-43 does not seem to form cytoplasmic aggregates in Betz cells, leading to the assumption that soluble cytoplasmic TDP-43 is able to spread via trans-synaptic transmission from Betz cells to subcortical neurons where it becomes toxic [38].

3.3. Selective neuronal vulnerability to TDP-43 pathology

The toxicity of TDP-43 in neurons is proportional to the levels of TDP-43, with higher protein levels correlating with a more severe neurodegeneration [39]. In comparison to other cells, neurons seem to be particularly vulnerable to TDP-43 pathology, which might be due to some intrinsic properties of neurons, as well as neuron-specific TPD-43 functions. For instance, TDP-43 displays a longer half-life in neurons

(18 hours) compared to other cell types such as fibroblasts (4–11 hours) [39], which might explain the selective vulnerability of motoneurons in ALS. In addition, neurons have a decreased capacity to respond to stress and degrade misfolded proteins, partially due to their high threshold for stress before triggering a response [40]. Moreover, in neurons, the translation and trafficking of RNA are linked to the transport of specific RNA sequences along dendrites and axons, including the neuromuscular junction, for local translation. Studies also showed that TDP-43 is involved in the transport of some mRNAs along neurites and axons where they are locally translated in response to a stimulus or injury, a function that is impaired in TDP-43 proteinopathies [20]. In fact, cortical and motoneurons with impaired TPD-43 function display abnormal cytoskeletal integrity, shorter axons, and smaller growth cone size [41]. A decreased function of TDP-43 was shown to reduce the expression of genes involved in synaptic activity [42]. Moreover, neurons have high energy demands and therefore strongly depend on proper mitochondrial function, making them especially vulnerable to TDP-43-induced mitochondrial and energetical deficiencies [29].

3.4. TDP-43 pathology in non-neuronal cells

Several studies pointed toward the effects of TDP-43 pathologies in cells other than neurons. For instance, ALS has been described as a neurovascular disease given the abnormalities observed at the level of blood vessels in the brain and spinal cord [43]. TDP-43 has been associated with some of these changes [44], and TDP-43 deposits were observed in the blood vessels of the spinal cord and motor cortex [45]. In a recent study, TDP-43 overexpression in a non-transgenic mouse using intracranial injection of AAV-serotype 9 (AAV9) as delivery agents led to impaired motor learning, reduced number of neurons in the frontal cortex, increased astrocyte activation, microgliosis, enhanced BBB permeability, and inflammation [44]. These findings support the implication of TDP-43 proteinopathy in the loss of BBB integrity and central nervous system (CNS) homeostasis. In addition, pTDP-43 aggregates were recently observed in Schwann cells in ALS patients, even prior to histopathological changes and axonal degeneration [46].

TDP-43 proteinopathy was also detected in the periphery. For instance, aggregates of pTDP-43 have been detected in the axial skeletal muscles of sALS and fALS patients [47]. Mitochondrial dysfunction and inflammation in muscle cells were also found to be mediated by such TDP-43 alterations [48]. Moreover, abnormal TDP-43 accumulation was observed in the myenteric plexus of TDP-43 transgenic mice, and was correlated with lethal intestinal malfunctioning [49].

The exact mechanisms through which TDP-43 lead to neuronal degeneration are still unclear (Figure 2). The relocalization of TDP-43 to the cytoplasm suggests the driver of TDP-43 pathology to either be a toxic gain of function, a loss of normal function, or a combination of both. Indeed, studies on transgenic mice have shown that the overexpression of wildtype or mutated TDP-43 [14] as well as the targeted depletion of TDP-43 [50] both lead to ALS-like phenotypes. For this reason, targeting TDP-43 and its pathological variants is a promising strategy for the treatment of ALS.

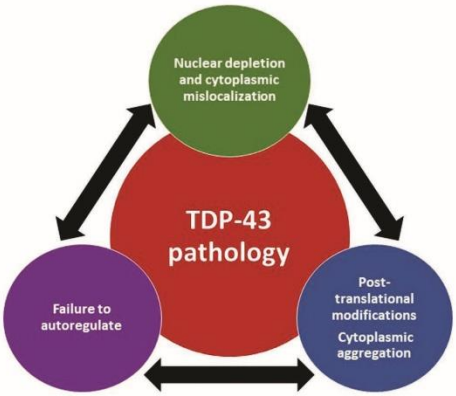

Figure 2. Schematic representation of the main pathways involved in the pathology of TDP-43. The nuclear depletion and cytoplasmic translocation of TPD-43 enhance the formation of cytoplasmic aggregates of the protein. Insoluble cytoplasmic TDP-43 loses the ability to autoregulate, leading to a vicious cycle of nuclear depletion and loss of normal function.

4. Therapeutic approaches to target TDP-43 in ALS

Given how TDP-43 is implicated in several homeostatic pathways in the cell (Figure 3), an impairment of the normal function and metabolism of TDP-43 is expected to have deleterious effects on cells, particularly neurons. Therefore, several approaches have been developed to target TDP-43 proteinopathy, such as the stabilization of the soluble form of TDP-43, the enhancement of the nuclear localization and function of the protein, the removal of TDP-43 cytoplasmic aggregates, the regulation of stress granule formation, and the mitigation of pathological post-translation modifications of TDP-43 (Figure 4). A list of therapeutic approaches targeting TDP-43 in the context of ALS is provided in Table 1.

4.1. Stabilizing the functional form of TDP-43

TDP-43 self-associates and normally functions as a dimer [8]. One approach to target TDP-43 proteinopathy would be to stabilize the correctly folded TDP-43 dimers, thus preventing the misfolding and aggregation of the protein. Researchers have therefore tried to identify and isolate molecules that are capable of interacting with TDP-43 and stabilizing its native functional form.

It was recently shown that specific RNA binding to TDP-43 can enhance the liquid properties of TDP-43-containing granules and prevent them from being converted into solid-like complexes [51]. Other studies also confirmed that the binding of TDP-43 to its target RNA sequences, including its own RNA, is able to increase its solubility [52,53]. Several mechanisms have been proposed to explain these observations including the role of nucleic acids as molecular chaperones, the allosteric prevention of interaction between aggregation-prone domains, and

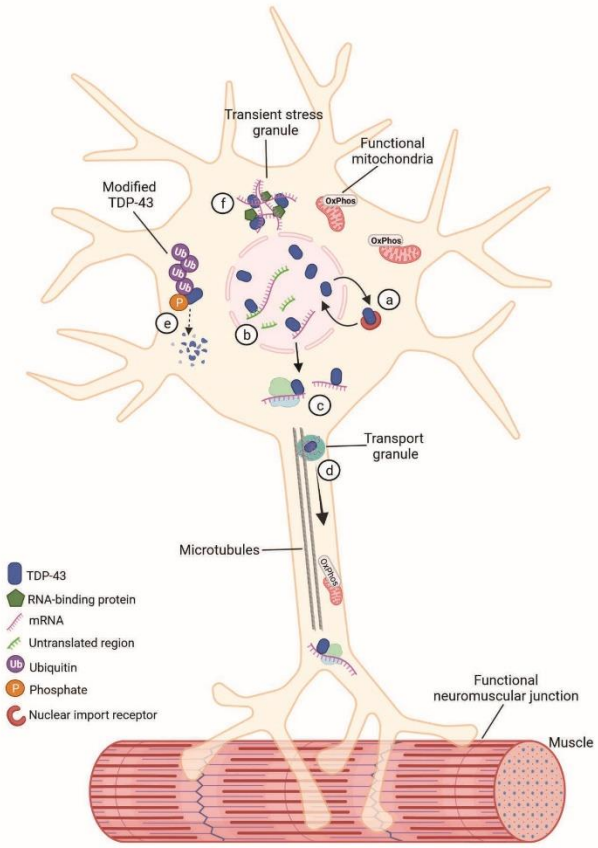

Figure 3. Main physiological pathways implicating TDP-43 in neurons: TDP-43 mainly localizes in the nucleus and constantly shuttles between the nucleus and cytoplasm (a). In the nucleus, TDP-43 controls the processing and splicing of the pre-mRNA (b) and in the cytoplasm, it is involved in the association of the mRNA with the translation machinery (c). TDP-43 plays an important role in the local translation in neurons by associating with mRNA in transport granules that move mRNA along neuronal axons (d). When TDP-43 undergoes abnormal post-translational modifications, it is targeted for degradation by the ALS and UPS (e). Under stressful conditions, TDP-43 undergoes liquid-liquid phase separation and associates with transient SGs containing mRNA and other RNA-binding proteins (f). OxPhos: Oxidative phosphorylation. Created with BioRender.com.

competitive inhibition of TDP-43 homo-oligomerization. Accordingly, ALS-linked mutations that decrease the binding capacity of TDP-43 to RNA or single-stranded (ss)DNA targets seem to enhance the oligomerization and aggregation of TDP-43 [54]. In fact, it was suggested that the self-oligomerization of TDP-43 through its free RRM domains is an initial step that seeds subsequent aggregation of the protein through its NTD or CTD [55]. These findings also explain why TDP-43 remains soluble in the nucleus where the RNA/protein ratio is high but starts to aggregate in the cytoplasm where the RNA/protein ratio is much lower.

Conversely, various studies suggested that the binding of TDP-43 to RNA can decrease TDP-43 turnover, enhance stress granule (SG) formation and aggravate TDP-43-induced toxicity [56], especially in the presence of excess nonspecific RNA lacking long UG repeats [53]. Some small molecules that disrupt RNA-TDP-43 interactions seem to mitigate TDP-43-induced cytotoxicity [57,58]. Therefore, it seems like the effect that RNA binding to TDP-43 has on the cell is influenced by several confounding factors, including the specific types of RNA, their length, their binding affinity to TDP-43, their relative abundance, and the context of TDP-43 proteinopathy (e.g. overexpression, hyperphosphorylation, mutated protein, etc.).

Given the role that the RRM domains play in the dimerization of TDP-43, altering their normal interaction with RNA should consider the effect that such alterations can have on the self-assembly and normal functioning of TDP-43. Specific aptamers or 'bait oligonucleotides' can be used to mimic the binding of TDP-43 to its endogenous RNA targets, making them a potential therapeutic strategy to counteract TDP-43 aggregation, particularly in the context of TDP-43 overexpression. This approach should also investigate the potential off-target effects on the other RNA-binding proteins that are normally found in the cell.

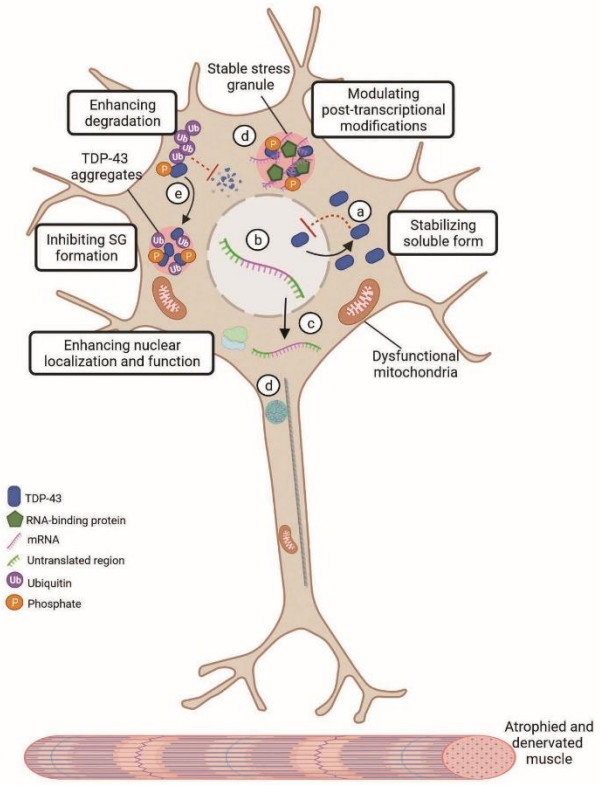

Figure 4. Main pathological pathways impacted by TDP-43 proteinopathy in neurons and potential therapeutic approaches: Abnormal nucleocytoplasmic shuttling of TDP-43 leads to its mislocalization from the nucleus to the cytoplasm (a). Nuclear depletion of TDP-43 leads to dysfunctional pre-mRNA processing and splicing (b) as well as abnormal mRNA translation (c). Pathological TDP-43 leads to impaired axonal transport and subsequent impairment of the local translation of mRNA in neurons (d). Modifications of TDP-43 and dysfunctional protein degradation pathways mediate the accumulation of insoluble TDP-43 inclusions in the cytoplasm (e). Under stressful conditions, SGs can recruit TDP-43 and seed its aggregation in the cytoplasm (f). Created with BioRender.com.

4.2. Enhancing the nuclear localization and function of TDP-43

The mislocalization of TDP-43 can be due to a deficient nuclear import of cytoplasmic TDP-43, an enhanced export of nuclear TDP-43, or a combination of both. Some studies suggest that TDP-43 proteinopathy is due to a loss of nuclear TDP-43 rather than an accumulation of toxic cytoplasmic TDP-43 inclusions [59].

4.2.1. Restoring the nuclear function of TDP-43

TDP-43 plays a major in the nucleus, mainly through the control of gene expression via the regulation of pre-mRNA splicing and processing. Therefore, in addition to decreasing the accumulation of toxic aggregates of TDP-43 in the cytosol, restoring the nuclear localization of the protein is crucial to restore its normal functions in the nucleus. For example, defective TDP-43-mediated cryptic exon splicing was detected in the brain of ALS patients [60]. Based on this observation, Ling and his colleagues attempted to replace the depleted TDP-43 from the nucleus by creating a chimeric TDP-43 protein fused with the splicing repressor domain of the ribonucleoprotein Raver 1. The chimera was found to localize to the nucleus and retain the normal splicing function of TDP-43, thus compensating for the loss of native TDP-43 from the nucleus and rescuing TDP-43-deficient mouse embryonic stem cells, highlighting the indispensable role of TDP-43 in the nucleus [60]. Another approach that has recently gained increased interest is the use of ASO to restore the normal expression of proteins involved in ALS. This technique has already shown promising results when targeting other ALS-causing proteins such as superoxide dismutase 1 (*SOD1*) [3], *C9orf72* [5] and the hnRNP fused in sarcoma (*FUS*) [4]. However, silencing of TDP-43 would have detrimental effects on cells so scientists are trying to target proteins downstream of TDP-43, through the compensation of the lost normal RNA splicing. For instance, stathmin-2 is a crucial protein involved in axonal regeneration and neurite outgrowth that was found to be decreased in TDP-43-mediated neurodegeneration

Table 1. Recent therapeutic approaches targeting TDP-43 pathology in ALS.

Therapeutic approach	Molecule	Disease model/Trial phase	Observed effects	Reference
Stabilizing the functional form of TDP-43	TDP-43-target RNA sequences	In vitro HEK293T cells overexpressing TDP-43	Increased liquid-like properties of TDP-43	[51]
	GU-rich RNA repeats	In vitro HeLa cells expressing wildtype or mutated TDP-43	Increased solubility of TDP-43	[52]
Enhancing the nuclear function of TDP-43	Chimeric TDP-RAVER1 (splicing repressor domain)	Mouse TDP-43-deficient embryonic stem cells	Recovered repression of cryptic exon Increased cell viability	[60]
	Lentivirus carrying stathmin-2-encoding gene	iPSC-derived motor neurons with reduced TDP-43 and stathmin-2 expression	Restoration of normal axonal regeneration	[61]
Decreasing TDP-43 nuclear export	SINEs: KPT-276 and KPT-335	Mouse primary cortical neurons expressing TDP-43^{Q331K} or TDP-CTF Transgenic TDP-43 ^{WT} TDP-43^{G298S} Drosophila larvae	Restoration of normal nuclear morphology Increased cellular viability Improved locomotor activity	[25]
	SINEs: KPT-335 and KPT-350	Rat primary cortical neurons overexpressing TDP-43 ^{WT} or TDP-43^{A315T}	Moderate improval of neuronal survival of TDP-43 ^{WT} but not TDP-43^{A315T}-expressing rats	[64]
Enhancing TDP-43 nuclear import	Increased cytosolic calcium	Drosophila overexpressing arginine-rich dipeptide repeat proteins (C9orf72 ALS model)	Restoration of nuclear TDP-43 localization Rescued larval locomotion	[66]
Preventing the accumulation of TDP-43 aggregates using heat shock proteins	Potentiated Hsp104 variants with disaggregase activity	Transformed yeast cells overexpressing TDP-43	Decreased TDP-43 aggregation and mislocalization	[69]
	Overexpression of the Hsp40 Sis-1	Transformed yeast cells overexpressing TDP-43	Reduced TDP-43-induced oxidative stress	[70]
	Upregulation of HSPB8	NSC-34 cells overexpressing TDP-43	Decreased accumulation and mislocalization of TDP-43 fragments	[71]
		Drosophila overexpressing full length or fragmented TDP-43	Decreased toxicity and accumulation of cytoplasmic TDP-43	
	Increased HSF1 expression and/or activity	Cultured tibialis anterior muscle cells, NSC-34, or QBI-293 cells overexpressing TDP-43	Reduced TDP-43 aggregation	[48]
	Increased HSF1 expression	HEK293T and SH-SY5Y cells overexpressing TDP-43	Increased solubility of TDP-43 Decreased levels of hyperphosphorylated TDP-43 Increased cell viability	[74]
	17-AAG (activator of HSF1)	Drosophila expressing human TDP-43 or truncated TDP-25	Decreased aggregation of TDP-43. Depletion of TDP-25 fragments. Increased cell viability	[77]
	Upregulation of HSPB8	NSC-34 cells overexpressing TDP-43	Decreased accumulation and mislocalization of TDP-43 fragments	[71]
		Drosophila overexpressing full length or fragmented TDP-43	Decreased toxicity and accumulation of cytoplasmic TDP-43	
	Increased HSF1 expression and/or activity	Cultured tibialis anterior muscle cells, NSC-34, or QBI-293 cells overexpressing TDP-43	Reduced TDP-43 aggregation	[48]
	Increased HSF1 expression	HEK293T and SH-SY5Y cells overexpressing TDP-43	Increased solubility of TDP-43 Decreased levels of hyperphosphorylated TDP-43 Increased cell viability	[74]
	17-AAG (activator of HSF1)	Drosophila expressing human TDP-43 or truncated TDP-25	Decreased aggregation of TDP-43. Depletion of TDP-25 fragments. Increased cell viability	[77]

(*Continued*)

Table 1. (Continued).

Therapeutic approach	Molecule	Disease model/Trial phase	Observed effects	Reference
Decreasing TDP-43 aggregates by activating the ALP	BIX02189 (downregulator of MEK5)	Neuro-2A cells overexpressing TDP- 43 ^{WT} or TDP-43^{Q331K} or TDP-43^{M337V}	Decreased cytoplasmic accumulation of TDP-43 Decreased neuronal toxicity	[79]
	Trehalose	SH-SY5Y cells overexpressing TDP-43 ^{WT} or TDP-43^{Q331K}	Reduced TDP-43 aggregation	[80]
	Berberine	Neuro-2A cells overexpressing TDP-25	Reduced TDP-43 aggregation	[81]
	Diallyl trisulfdide	NSC-34 cells overexpressing TDP-43 ^{WT} or TDP-43^{Q331K} or TDP-43^{M337V} or TDP-25	Decreased levels of TDP-43 or TDP-25 Reduced oxidative stress	[82]
	Methotrimeprazine (MTM) or Fluphenazine (FPZ)	Primary rat cortical neurons overexpressing TDP-43 ^{WT} or TDP-43^{A315T}	Reduced TDP-43 ^{WT} and TDP-43^{A315T} levels, and cytoplasmic mislocalization and aggregation Increased cell viability	[39]
		iPSC-derived motoneurons and astrocytes from patients carrying TDP-43^{M337V}	Increased cell viability	
	Rapamycin, spermidine, carbamazepin, or tamoxifen	TDP-43 transgenic mice	Decreased cytosolic full-length and fragmented TDP-43 inclusions Increased neuron survival Slowing down of motor function loss	[83]
	Ibudilast	NSC-34 cells HEK293T overexpressing TDP-43 or TDP-25	Reduced TDP-43 aggregation Decreased neuronal toxicity	[84]
	Withaferin-A	Transgenic TDP-43^{G348C} mouse model	Decreased cytoplasmic accumulation of TDP-43 in the brain Decreased neuroinflammation Improved cognitive functions	[85]
	Overexpression of SQSTM1	Mice injected with AAV-TARDBP-25^{M337V} into the cortex Monkeys injected with AAV-TARDBP-25^{M337V} into the substantia nigra and motor cortex	Decreased aggregation of TDP-25 Decreased damage in the substantia nigra and motor cortex Decreased accumulation of TDP-25	[86]
	Colchicine or Doxorubicin	SH-SY5Y cells overexpressing TDP-43 or TDP-25	Decreased aggregation of TDP-43 or TDP-25	[87]
	Colchicine	Phase II clinical trial	NA	NCT03693781
Decreasing TDP-43 aggregates by activating the UPS	Overexpression of PABPN1	Yeast overexpressing TDP-43	Increased cell viability	[93]
		Neuro-2A overexpressing TDP-CTF, TDP-43 ^{WT}, or TDP-43^{Q331K} or TDP-43^{M337V}	Decreased cytoplasmic aggregation and mislocalization of TDP-43	
		Primary cortical neurons overexpressing TDP-43 ^{WT}, TDP-43^{Q331K}, TDP-43^{M337V} or TDP-43^{A382T} or fragmented TDP-CTF	Decreased of pre-formed TDP-43 aggregates Increased cell viability	
	Thioridazine	HEK293T and SH-SY5Y cells expressing TDP-43 with 12Q/N repeats	Reduced TDP-43 aggregation Recovered TDP-43 splicing function	[94]
		Drosophila expressing TDP-43 with 12Q/N repeats	Rescued locomotive function	
Decreasing TDP-43 aggregates with scFv	3B12A scFv	HEK293A cells overexpressing TDP-43^{mNLS}, TDP-43$^{C173S/C175S}$	Reduced mutant TDP-43 cytoplasmic aggregation Increased cell viability	[95]
		Murine embryonic cerebral cortex in utero	Reduced mutant TDP-43 cytoplasmic aggregation	
	VH7VK9 scFv	TDP-43^{A315T} transgenic mice	Decreased cytoplasmic aggregation and mislocalization of TDP-43 Restoration of TDP-43 splicing activity Ameliorated cognitive impairment and motor defects Decreased neuroinflammation	[96]

(*Continued*)

Table 1. (Continued).

Therapeutic approach	Molecule	Disease model/Trial phase	Observed effects	Reference
Regulating stress granule formation	XAV-939, G007-LK or IWR1-endo (Tankyrase inhibitors)	Cos-7 cells and primary rat cortical neurons subjected to sodium arsenite-induced oxidative stress	Reduced TDP-43 cytoplasmic aggregation	[103]
	Inhibition of CDK2 phosphorylation by Olomoucin, aminopurvalanol A, CDK2 Inhibitor I, or roscovitine	SH-SY5Y cells subjected to paraquat-induced stress	Inhibition of TDP-43 accumulation into SGs	[104]
	Inhibition of eIF2α phosphorylation by GSK2606414	Primary rat cortical neurons overexpressing TDP-43	Increased cell viability	[105]
		Drosophila expressing ataxin-2 with expanded poly-Q repeat	Improved locomotor function	
	Compounds with planar moieties (e.g. Mitoxantone)	H4 neuroglioma and HEK293xT cells expressing TDP-43 lacking the NLS	Decreased localization of TDP-43 to stress granules	[106]
		iPSC-derived motor neurons from ALS patients	Decreased cytoplasmic accumulation of TDP-43aggregates	
		Mouse primary neurons expressing TDP-43^{M337V}	Increased cell viability	
	Knockdown of ataxin-2 using ASO or siRNA	U2OS cells subjected to sodium arsenite-induced stress	Inhibition of TDP-43 accumulation into SGs	[107]
			Reduced TDP-43 cytoplasmic aggregation	
		TDP-43 transgenic mice	Improved motor function	
			Prolonged survival	

(*Continued*)

Table 1. (Continued).

Therapeutic approach	Molecule	Disease model/Trial phase	Observed effects	Reference
Targeting TDP-43 post-translational modifications	Tideglusib (inhibitor of GSK-3β)	SH-SY5Y subjected to ethacrynic acid-induced stress	Decreased amount of phosphorylate TDP-43 and TDP-35 Increased cell viability	[110]
		Lymphoblasts from ALS patients	Decreased amount of pTDP-43 Decreased cytoplasmic mislocalization of TDP-43	
		TDP-43^{A315T} transgenic mice	Decreased amount of pTDP-43	
	Mercaptopurine-based inhibitors of CDC7	SH-SY5Y subjected to ethacrynic acid-induced stress	Increased cell viability Decreased amount of phosphorylated TDP-43 Decreased cytoplasmic mislocalization of TDP-43	[111]
		C. *elegans* expressing TDP-43	Decreased amount of phosphorylated TDP-43	
		TDP-43^{A315T} transgenic mice	Improved motor function Decreased amount of phosphorylated TDP-43 in the spinal cord	
	ERP1.14a and ERP1.28a (inhibitors of CDC7)	Immortalized lymphocytes from ALS patients	Decreased amount of pTDP-43 Decreased cytoplasmic accumulation of TDP-43 Recovered nuclear function of TDP-43	[112]
	IGS-2.7 (Inhibitor of CK-1δ)	TDP-43^{A315T} transgenic mice	Delayed weight loss Decreased amount of phosphorylated TDP-43 in the spinal cord Decreased microgliosis and astrogliosis Increased motoneuron viability in the spinal cord	[113]
		Immortalized lymphocytes from ALS patients	Decreased cytoplasmic accumulation of TDP-43 Decreased amount of phosphorylated TDP-43	
	Pyrrolopyrimidine derivatives (inhibitors of TTBK1)	SH-SY5Y subjected to ethacrynic acid-induced stress	Decreased amount of phosphorylated TDP-43 Decreased cytoplasmic accumulation of TDP-43 Increased cell viability	[114]
		TDP-43^{A315T} transgenic mice	Increased motoneuron viability in the spinal cord Decreased amount of phosphorylated TDP-43 Decreased microgliosis and astrogliosis	
		Immortalized lymphocytes from ALS patients	Decreased amount of phosphorylated TDP-43 Recovery of nuclear TDP-43	
	Inhibition of caspase-4 by LEVD-fmk or siRNA	SH-SY5Y cells subjected to tunicamycin-induced stress	Decreased cytoplasmic accumulation of TDP-43 Decreased levels of TPD-35 and TPD-25	[115]
		Lysates of TDP-43 ^{M337V}-injected monkey brains	Increased cell viability Decreased levels of TPD-35 and TPD-25	

AAV, Adeno-associated virus; ASO, Antisense oligonucleotide; CTF, C-terminal fragment; iPSC, Induced pluripotent stem cells; NLS, Nuclear localization signal; scFv, Single chain variable fragment; WT, wildtype.

following abnormal splicing of its pre-mRNA [61]. Based on this observation, several ongoing projects are currently trying to use ASO to restore the normal levels of stathmin-2. In addition, nuclear depletion of TDP-43 was directly associated with a decreased expression of UNC13A, an essential pre-synaptic protein associated with ALS. This decrease was found to affect disease progression and was mediated by cryptic exon inclusion following mis-splicing of *UNC13A* in the absence of TDP-43 both in cultured neurons and in the spinal cords and brains of ALS patients [62]. These findings make *UNC13A* a promising target for ASO directed at restoring its normal expression in TDP-43 pathologies.

4.2.2. Decreasing TDP-43 export

One therapeutic strategy would be to inhibit TDP-43 export from the nucleus. Orally administered reversible inhibitors of Exportin 1 were able to enhance the nuclear retention of neuroprotective transcription factors while decreasing the nuclear export of molecules associated with neuronal damage in murine models of axonopathies [63]. Using this approach to target TPD-43 proteinopathies might be interesting in the context of ALS. In fact, selective inhibitors of nuclear export (SINE) that target Exportin-1, such as KPT-276 and KPT-335, were able to attenuate TDP-43-induced cellular toxicity in Drosophila and mice primary cortical neurons [25]. Another study showed that other SINEs were also able to provide modest neuroprotection in primary neurons and rats overexpressing TDP-43, albeit without significantly affecting TDP-43 localization [64].

Contrary to these studies, it was shown that the nuclear egress of TDP-43 is size-dependent and happens through passive diffusion rather than active transport [65]. The nuclear export signal (NES) of TDP-43 was found to not be accessible to export receptors and is therefore considered nonfunctional [65]. Complementary to these findings, Archbold et al suggested that overlapping pathways regulate the nuclear export of TDP-43 and therefore preventing the accumulation of cytoplasmic TDP-43 would require targeting several of these mechanisms at the same time [64]. Studies that linked the decreased cellular toxicity of TDP-43 to a mutated NES or to inhibited export receptors did not consider the indirect effects of such changes on mechanisms such as TDP-43 solubility, RNA processing, SG formation, or the export of other nuclear proteins. Consequently, enhancing the nuclear retention of TDP-43 seems to be a more reliable strategy to reduce TDP-43 mislocalization than inhibiting the nuclear export of TDP-43.

4.2.3. Enhancing TDP-43 import

Another therapeutic strategy to reduce the cytoplasmic localization of TDP-43 would be the enhancement of TDP-43 nuclear import. The calcium-Calpain A-Imp α3 was identified as a potential pathway that affects TDP-43 localization and likely precedes the sequestration of nucleocytoplasmic receptors into TDP-43 aggregates, making it a potential target for the early prevention of TDP-43 cytoplasmic mislocalization [66]. The upregulation of this pathway through increased cytosolic calcium was able to restore the nuclear localization of TDP-43 and mitigate the locomotor defects in an ALS fly model [66]. Interestingly, in addition to their role in nucleocytoplasmic transport, nuclear import receptors are thought to act as chaperones that disaggregate cytoplasmic proteins bearing a nuclear localization sequence (NLS) [67,68]. Increasing the level of the nuclear import receptors Karyopherin-β1 and Importin-α was able to prevent and even reverse the fibrillization of TDP-43. This effect was abolished by TDP-43 fragments lacking the NLS [67]. Although promising, this observation implies that such an approach might have limited effects in cases where TDP-43 is extensively fragmented into insoluble CTFs that lack the NLS.

4.3. Preventing the accumulation of TDP-43 aggregates

Preventing the accumulation of misfolded proteins relies on an interplay between different proteostatic pathways, particularly molecular chaperones and degradation pathways such as the UPS and ALP.

4.3.1. Molecular chaperones: heat shock proteins

One way to decrease the aggregation of TDP-43 is to direct molecular chaperones such as heat shock proteins (Hsp) against the misfolded protein. Some studies suggest that when Hsp's fail to properly refold a protein, they recruit co-chaperones that mark these proteins for degradation by the UPS or ALP. Hsp104, a yeast chaperone with a disaggregase activity, was successfully modified to efficiently remove TDP-43 aggregates and restore the nuclear localization of the protein in a yeast model of TDP-43 proteinopathy [69]. The Hsp104 chaperone has no homologue in humans and therefore, strategies aiming at modifying existing human heat shock proteins that have a disaggregase activity such as Hsp70, Hsp110, and Hsp40 can render them more potent in specifically removing TDP-43 aggregates. Several studies have focused on increasing the activity of Hsp's, to induce the degradation of pathological TDP-43 in cellular or animal models of TDP-43 proteinopathy and reduce TDP-43-mediated toxicity and oxidative stress [70,71]. An interesting study recently described the essential role of Hsp70 in the assembly of aggregation-prone TDP-43 into anisosomes which are spherical droplets with liquid properties [72]. Anisosomes are formed from a self-interacting RNA-unbound TDP-43 shell surrounding an Hsp70 core that maintains the liquidity of these droplets. A drop in cellular ATP levels decreases the activity of Hsp70 chaperones and leads to the conversion of anisosomes into protein aggregates, similar to those observed in ALS [72]. Therefore, maintaining the normal function of Hsp70 chaperones can be used as an early therapeutic intervention that inhibits the progression of TDP-43 droplets into aggregates.

The ability to increase the activity of Hsp's in neurons is limited given the high threshold of stress-induced Hsp response activation in motoneurons and their subsequent resistance to Hsp activators [40]. In addition, given the complexity of the Hsp networks and the interaction of chaperones with several other co-chaperones implies that approaches targeting the expression and/or activity of one Hsp might

not be able to effectively target misfolded TDP-43 [73]. Therefore, pharmacological targeting of an upstream transcription factor that regulates several chaperones, such as heat shock factor 1 (HSF1) which is reduced in the neurons of ALS patients [74], might prove to be more successful.

Arimoclomol, a hydroxylamine derivative that can cross the BBB and specifically stabilize HSF1 in stressed cells, was first found to delay the progression of ALS [75] possibly through a mechanism that can decrease TDP-43 aggregates [48]. However, a phase III clinical trial for Arimoclomol failed to show significant efficacy in ALS patients (NCT00706147). Recently, it was shown that combining Arimoclomol with a histone deacetylase inhibitor could enhance and prolong the efficacy of the treatment in ALS models, which can be attributed to overcoming the resistance of neurons to activating the Hsp stress response [76]. Another study demonstrated that the overexpression of HSF1 enhances the survival of cellular models overexpressing TDP-43 by dramatically decreasing the levels of hyperphosphorylated and aggregated TDP-43 [74]. 17-AAG, another activator of HSF1, also successfully decreased the aggregation and toxicity of TDP-43 in the motoneurons of a Drosophila model of TDP-43 pathology [77].

4.3.2. The autophagy-lysosome pathway

Evidence points toward a bidirectional interplay between the normal function of TDP-43 and the normal function of the ALP [78]. Several studies successfully used autophagy activators to target TDP-43 proteinopathy. For example, downregulation of the mitogen-activated kinase 5 (MEK5) by BIX02189 activated the ALP and decreased the cytoplasmic accumulation of overexpressed wildtype or mutated TDP-43 and their subsequent toxicity in neuronal cells [79]. Similar results were obtained upon treatment of cellular and animal ALS models with autophagy inducers such as trehalose [80], berberine [81], diallyl trisulfide [82], methotrimeprazine (MTM), fluphenazine (FPZ), and 10-(4′-(N-diethylamino)butyl)-2-chlorophenoxazine (NCP) [39]. In addition, rapamycin was able to decrease the mislocalization and aggregation of TDP-43 and its cleavage products in neuronal cell lines overexpressing TDP-43, as well as mitigate motoneuron death and motor dysfunction in mice with TDP-43 proteinopathy [83]. Other autophagy activators such as spermidine, carbamazepine, tamoxifen, ibudilast, and withaferin-A showed similar effects [83–85]. Another recent study revealed that pathological TDP-43 selectively decreases the levels of the autophagy receptor protein, sequestosome-1 (SQSTM1), in the non-human primate brain, and that overexpression of this protein is capable of decreasing the cytosolic accumulation of TDP-43 [86]. Interestingly, two FDA-approved drugs, colchicine and doxorubicin, were found to counteract the accumulation of misfolded TDP-43 in a neuronal model of TDP-43 pathology by strongly upregulating HspB8 and other pro-autophagy proteins and activating the ALP [87]. Currently, a phase II clinical trial is being conducted to assess the efficacy of orally administered colchicine in ALS patients and the first results are expected at the end of 2022 (NCT03693781) [88].

Contrary to the previous findings, the activation of the ALP was also linked to an exacerbation of neuronal degeneration in some ALS models and TDP-43 proteinopathies [89], implying that case-by-case studies are needed, and specific isoforms need to be considered. The key is providing a good balance between the stimulation of autophagy and its potential negative effects, as well as maintaining a proper equilibrium between the formation and clearance of autophagic vacuoles. Moreover, enhancing the degradation of TDP-43 by the ALP should also take into consideration the endocytic pathway. A decreased endocytic activity was found to impair the removal of pathological TDP-43 in ALS [90]. In fact, endocytosis and autophagy are interconnected and share a common endpoint at the lysosome. Accordingly, one study found that enhancing endocytosis was more effective than the enhancement of autophagy in mitigating TDP-43 toxicity [91].

4.3.3. The ubiquitin-proteasome system

Targeting TDP-43 for UPS degradation is also an important mechanism for proper turnover of TDP-43. The presence of robust ubiquitinated inclusions of TDP-43 suggests a strong dysfunction of the UPS. Tashiro and his colleagues reported that the degeneration of motoneurons and ALS-like symptoms in mice was primarily due to the impairment of the proteasome rather than autophagy functions [92]. Cleaved TDP-43 products were shown to be mainly degraded by the UPS, and their accumulation disrupts the normal function of this system [27]. Overexpression of poly(A)-binding protein nuclear 1 (PABPN1), a novel interaction partner of TDP-43, was found to increase the turnover of TDP-43 through the UPS, restoring the solubility and nuclear localization of TDP-43 [93]. Another study found that Thioridazine, which was previously used as an antipsychotic drug, was able to induce a proteasome-dependent clearance of TDP-43 aggregates in a cellular model of TDP-43 proteinopathy as well as reverse locomotor defects in a Drosophila model of ALS [94].

4.3.4. Fragments of antibodies

Single-chain variable fragments of antibodies (scFv) have been developed to target the clearance of TDP-43. The 3B12A scFv which recognizes a region in the NES of TDP-43, was able to reduce TDP-43 aggregates in HEK293T cells and embryonic mouse brains in utero. This effect was found to be mediated by the activation of the UPS and chaperone-mediated autophagy [95]. Similarly, the VH7VK9 scFv recognizing the RRM1 of TDP-43 was able to decrease the mislocalization of TDP-43 as well as decrease microglial activation and improve the motor and cognitive functions of a mouse model of TDP-43 proteinopathy [96]. Other scFv constructs with a lysosomal targeting signal and that specifically recognize mislocalized TDP-43 were found to mediate the clearance of TDP-43 aggregates in cells, but were unable to enhance cellular viability [97]. Recently, a single-domain intrabody directed toward intracellular TDP-43 was also generated in an attempt to target TDP-43 pathology [98]. Recently, Cryo-electron microscopic advances have characterized the atomic structure of TDP-43 fibrils, which can contribute to the rational development of intrabodies targeting specific pathogenic fibrillar forms of TDP-43 [99].

The therapeutic effects of removing insoluble TDP-43 aggregates are debatable given that the aggregation of TDP-

43 is not mandatory for TDP-43-induced cellular toxicity [59]. One way through which aggregates might contribute to TDP-43 proteinopathy is through the sequestration of soluble TDP-43, thus limiting the available amount of functional TPD-43 required for cellular homeostasis [94]. In addition, the relative contribution of the ALP and UPS dysfunction in ALS is still unclear. For example, one study found that the degradation of soluble TDP-43 is mainly mediated by the UPS while insoluble aggregates are degraded primarily by ALP [100]. These findings highlight the importance of timely targeting both systems in order to efficiently clear excessive and insoluble TDP-43 while restoring the normal function of the protein.

4.4. Regulating stress granule formation

The presence of an LCD domain in TDP-43 makes it prone to multivalent interactions and aggregation under stressful conditions, leading to the formation of membraneless, cytoplasmic RNP assemblies known as SGs. SGs are thought to have a cytoprotective role in response to environmental stressors. In fact, evidence seems to point to the dysregulation of SG formation and degradation as a pathological mechanism in ALS, rather than the mere formation of SG [101]. TDP-43-containing SGs were detected in the cytoplasm of stressed cultured cells as well as in the brain and spinal cord samples from ALS patients [102]. In order to decrease the formation of TDP-43 aggregates, researchers have tried to inhibit the formation of SGs and their subsequent maturation into insoluble aggregates. Inhibition by small molecules of Tankyrase, which is needed for the assembly of SGs, antagonizes TDP-43 cytoplasmic aggregation and association to SGs [103]. In addition to its role in promoting UPS-mediated turnover of TDP-43. overexpression of PABPN1 also attenuates TDP-43 proteinopathy by regulating the nuclear localization of the protein and interrupting the cycle of TDP-43-induced dysregulation of SG formation [93]. In addition, various protein kinases are known to control the assembly of proteins, including TDP-43, into SGs. Researchers successfully mitigated TDP-43-mediated toxicity by inhibiting these kinases [104,105]. Small molecules that prevent RNA-dependent recruitment of TDP-43 into SGs were also able to decrease the cytoplasmic accumulation of TDP-43 in in vitro experiments [106]. Another interesting study showed that using ASO to reduce the levels of ataxin-2, a protein involved in regulating SG dynamics, and TDP-43 recruitment into SGs, was able to mitigate TDP-43 pathology and extend the lifespan of TDP-43 ALS mouse models [107]. The ASO targeting ataxin-2 (BIIB105) is currently being tested in a phase I clinical trial on ALS patients that should be completed by the end of 2024 (NCT04494256).

However, several researchers have shown that mature TDP-43 aggregates are distinct from SGs. TDP-43 aggregates can form in a SG-independent manner but SGs can in fact act as short-lived intermediates that seed and facilitate the aggregation of TDP-43 [108]. For instance, SGs might indirectly trigger TDP-43 proteinopathy by sequestering other factors involved in proteostasis. Therefore, the efficacy of targeting SGs to reduce TDP-43 pathology in ALS might be decreased at more advanced stages of the disease where TDP-43 aggregates become mature.

4.5. TDP-43 post-translational modifications

TDP-43 undergoes several post-translational modifications such as phosphorylation, ubiquitination, acetylation, and SUMOylation, that affect its structure, function, cellular localization and solubility [14]. Phosphorylation of TDP-43 is one of the most documented modifications which increases the propensity of the protein for aggregation and C-terminal fragmentation [14,109]. Therefore, targeting putative or validated TDP-43 kinases has become a very promising area of research in ALS therapy. GSK-3β is a kinase that was found to be upregulated in ALS patients and was correlated with increased TDP-43 phosphorylation and cytoplasmic mislocalization. Inhibition of GSK-3β by Tideglusib decreased the amount of pTDP-43 and recovered its normal nuclear localization cellular and animal models of TDP-43 pathology [110]. In fact, a phase II clinical trial of Tideglusib in ALS patients is currently underway (NCT05105958). BBB-permeable inhibitors of the cell division cycle kinase 7 (CDC7), a TDP-43 kinase, were also found to mitigate pathological phosphorylation and loss of nuclear function of TDP-43 in cellular models of ALS [111,112]. The inhibition of another kinase, the protein casein kinase-1δ (CK-1δ), by a benzothiazole-based compound (IGS-2.7) was shown to preserve motoneurons, decrease astrogliosis and microgliosis, and reduce TDP-43 phosphorylation and mislocalization in a TDP-43 cellular and animal model of ALS [113]. Tau-tubulin kinase (TTBK1) also plays a major role in the phosphorylation of TDP-43 at disease-relevant sites. Inhibition of this kinase by pyrrolopyrimidine derivatives decreased TDP-43 phosphorylation and enhanced the preservation of motoneurons in the spinal cord of TPD-43 transgenic mice [114].

Another major post-translational modification of TDP-43 is the fragmentation of the protein into 35- and 25- kDa CTF. Recently, LEVD-fmk, an inhibitor of caspase 4, successfully and specifically blocked the cleavage of TDP-43 in lysates of TDP-43-injected monkey brains [115]. Although fragmented TDP-43 largely mediate the toxic mislocalization and aggregation of the protein, not many studies have focused on targeting this aspect of TDP-43 pathology.

5. Conclusion

The interest in TDP-43 as a major therapeutic target in ALS has been growing exponentially. However, the translation of preclinical findings to human trials is still a major problem. Despite the increase in our understanding of TDP-43 proteinopathy and the role it plays in ALS, there are still several challenges to overcome, including the form and location of TDP-43 that should be targeted, the availability of a model representative of the patients' phenotypes, and the identification of specific parameters reflective of therapeutic effectiveness. Successful reversal and/or mitigation of TDP-43 pathology might be achieved by the removal of the already-present TDP-43 aggregates, the inhibition of further aggregation, and/or the restoration of the lost functions of TDP-43. Restoring the homeostatic cellular environment by mitigating TDP-43-mediated dysfunctions hold the potential to halt the progression of the disease, improve some of its symptoms and prolong the survival of ALS patients.

6. Expert opinion

All the findings described in this paper highlight the pivotal role of TDP-43 in the initiation and progression of ALS. Considering the crucial role of TDP-43 in maintaining cellular homeostasis, silencing TDP-43 through ASO for example, would not be an appropriate approach against TDP-43 proteinopathy. For this reason, several strategies are being developed for the treatment of ALS by targeting TDP-43-induced pathological changes, such as mitochondrial dysfunction, oxidative stress, and metabolic dysfunction. However, given the pleiotropic pathways that are regulated by this protein, targeting only one of them will unlikely have significant therapeutic effects. Therefore, focusing on targeting the source – the mislocalization and aggregation of TDP-43 – might prove to be more efficient in regulating the cellular impairments downstream of TDP-43. With the lack of conclusive studies on the relative contribution of these pathways in relation to the tissue affected and the disease stage, it could be interesting to test combinations of molecules to simultaneously target several TDP-43-induced pathological mechanisms in different cell types. In addition, TDP-43 proteinopathy does not always depend on the cytoplasmic aggregation of the protein [59], meaning that therapies should not only focus on removing or preventing the formation of TDP-43 aggregates but also on restoring the normal function of the protein that is lost in ALS. One potential way to achieve this is through the development of ASO that can restore the lost function of TDP-43 in regulating RNA splicing.

In order to successfully develop a therapeutic strategy against TDP-43 pathology, researchers need to overcome several important problems.

One major issue is the failure of animal models to replicate the phenotypes observed in ALS patients. This accounts for the success of many approaches in preclinical studies and their subsequent failure in clinical trials. ALS phenotypes including disease onset, severity, evolution of symptoms, and survival vary greatly among patients, implying the need for several models that can reproduce these different disease subtypes and allow for the development of phenotype-specific therapies. For instance, one of the most widely used ALS animal models is the transgenic mutant SOD1 model. However, it fails to recapitulate the TDP-43 aggregation observed in the majority of ALS patients, making its use in developing ALS therapies debatable [116]. In addition, TDP-43 animal models, which rely on mainly on the overexpression of wildtype or mutated TDP-43, fail to recapitulate all the aspects of the disease observed in ALS patients, which can add several limitations to the development of therapeutic approaches [117]. Another example highlighting the limitation of animal models is the differences in protein sequences among species. For instance, the cryptic poly-adenylation site in intron 1 of stathmin-2 is absent in mice, leading to a failure to reproduce the mis-splicing of this protein observed in TDP-43 pathology [61]. In complex diseases like ALS, a one-size-fits-all treatment approach cannot be applied. Therefore, different strata of patients need to be considered. For example, differentiating patients with a known ALS-causing mutation might allow for an earlier, even pre-symptomatic treatment administration. When the identification of patients in the pre-symptomatic stage cannot be achieved, treatment should begin as early as possible following diagnosis. In a mouse model of TDP-43 proteinopathy, removal of pathological TDP-43 was found to be beneficial even at later stages of the disease through a mechanism that involves the reinnervation of muscle fibers by motoneurons that are intrinsically resistant to TDP-43 pathology [118]. These findings are promising because they suggest the possibility of reversing, at least partially, muscle denervation and ALS symptoms. Moreover, bench-to-bedside translation is complicated in the absence of well-established quantifiable disease-reflective parameters that can be used to assess the effectiveness of therapies targeting TDP-43 pathology. Although multidisciplinary approaches such as imaging and biochemical analyses have been used to establish some correlations between changes in measurable parameters (e.g. cerebrospinal fluid and blood biomarkers, tissue pTDP-43, cortical atrophy, etc.) and the progression of TDP-43 proteinopathy, these approaches still require a lot of improvements and further characterization [119].

Another important consideration is establishing the best location to target TDP-43. This should take into consideration the site of ALS onset and how the disease progresses. Some researchers support the dying-back hypothesis stating that the disease starts at the level of lower motor neurons and neuromuscular junctions and then progresses in a retrograde direction toward the cortex [120]. Other researchers believe that ALS starts by an increased cortical excitability that leads to the degeneration of lower motor neurons suggesting a dying-forward pattern [120]. In both cases, the involvement of TDP-43 in the initiation and progression of the disease has been documented by several groups, even if more evidence seems to be pointing toward a dying-forward hypothesis concomitant with the spreading of TDP-43 [121]. Answering this question will determine if peripheral or central TDP-43 should be targeted, which will therefore depend on the disease stage.

Targeting TDP-43 in the CNS is limited by the presence of the BBB. Therefore, the access of therapies into target cells in the CNS need to consider the local permeability of the BBB and the diffusion capacity of molecules across the CNS. Several strategies have been developed to overcome the BBB and specific BBB alterations in ALS should be considered [43].

TDP-43 proteinopathy is also detected in the periphery and seems to differently affect several systems. Some treatments that successfully prevented the death of motoneurons were not successful in maintaining proper muscle innervation or extending survival [122], implying that motoneurons are mainly involved in the initial stages of the disease, while other cell types such as microglia, astrocytes and oligodendrocytes could drive the progression of the disease at later stages. Such findings emphasize the need of therapies targeting TDP-43 to consider the stage of the disease and not be

limited to exclusively targeting motoneurons. Therefore, different approaches should be considered to target TDP-43 in nonneuronal cells compared to neurons.

As mentioned at the beginning, TPD-43 aggregates are a hallmark of ALS and have been observed in 97% of ALS cases. Strikingly, aggregation of TDP-43 has also been detected in other neurodegenerative diseases including 45% of frontotemporal dementia (FTD) cases, up to 57% of Alzheimer's disease patients, as well as Huntington's and Parkinson's disease patients [123]. This means that in addition to being a major therapeutic target in ALS, treating TDP-43 proteinopathy might prove to be important in other currently incurable neurodegenerative diseases.

Acknowledgments

LabEx MAbImprove, ARD CVL biopharmaceuticals, Région Centre Val de Loire.

Disclosure statement

The authors have no relevant affiliations or financial involvement with any organization or entity with a financial interest in or financial conflict with the subject matter or materials discussed in the manuscript. This includes employment, consultancies, honoraria, stock ownership or options, expert testimony, grants or patents received or pending, or royalties.

Reviewer disclosures

Peer reviewers on this manuscript have no relevant financial or other relationships to disclose.

Funding

This paper was not funded.

ORCID

Débora Lanznaster http://orcid.org/0000-0001-5911-3120

References

Papers of special note have been highlighted as either of interest (•) or of considerable interest (••) to readers.

1. Neumann M, Sampathu DM, Kwong LK, et al. Ubiquitinated TDP-43 in frontotemporal lobar degeneration and amyotrophic lateral sclerosis. Science. 2006;314:130–133.
2. Arai T, Hasegawa M, Akiyama H, et al. TDP-43 is a component of ubiquitin-positive tau-negative inclusions in frontotemporal lobar degeneration and amyotrophic lateral sclerosis. Biochem Biophys Res Commun. 2006;351:602–611.
3. Miller T, Cudkowicz M, Shaw PJ, et al. Phase 1–2 trial of antisense oligonucleotide tofersen for *SOD1* ALS. N Engl J Med. 2020;383:109–119.
4. Korobeynikov VA, Lyashchenko AK, Blanco-Redondo B, et al. Antisense oligonucleotide silencing of FUS expression as a therapeutic approach in amyotrophic lateral sclerosis. Nat Med. 2022;28:104–116.
5. Liu Y, Andreucci A, Iwamoto N, et al. Preclinical evaluation of WVE-004, an investigational stereopure oligonucleotide for the treatment of C9orf72-associated ALS or FTD. Mol Ther. 2022;28:558–570.
6. Narayanan RK, Mangelsdorf M, Panwar A, et al. Identification of RNA bound to the TDP-43 ribonucleoprotein complex in the adult mouse brain. Amyotrophic Lateral Sclerosis Frontotemp Degener. 2013;14:252–260.
7. Sugai A, Kato T, Koyama A, et al. Non-genetically modified models exhibit TARDBP mRNA increase due to perturbed TDP-43 autoregulation. Neurobiol Dis. 2019;130:104534.
8. Wang A, Conicella AE, Schmidt HB, et al. A single N-terminal phosphomimic disrupts TDP-43 polymerization, phase separation, and RNA splicing. EMBO J. 2018;37:e97452.
9. Furukawa Y, Suzuki Y, Fukuoka M, et al. A molecular mechanism realizing sequence-specific recognition of nucleic acids by TDP-43. Sci Rep. 2016;6:20576.
10. Zacco E, Martin SR, Thorogate R, et al. The RNA-recognition motifs of TAR DNA-binding protein 43 may play a role in the aberrant self-assembly of the protein. Front Mol Neurosci. 2018;11:372.
11. Dhakal S, Wyant CE, George HE, et al. Prion-like C-terminal domain of TDP-43 and α-synuclein interact synergistically to generate neurotoxic hybrid fibrils. J Mol Biol. 2021;433:166953.
12. Ishiguro A, Kimura N, Noma T, et al. Molecular dissection of ALS-linked TDP-43 – involvement of the Gly-rich domain in interaction with G-quadruplex mRNA. FEBS Lett. 2020;594:2254–2265.
13. Zhang Y-J, Xu Y-F, Cook C, et al. Aberrant cleavage of TDP-43 enhances aggregation and cellular toxicity. Proc Natl Acad Sci. 2009;106:7607–7612.
14. Hergesheimer RC, Chami AA, de Assis DR, et al. The debated toxic role of aggregated TDP-43 in amyotrophic lateral sclerosis: a resolution in sight? Brain. 2019;142:1176–1194.
15. Morera AA, Ahmed NS, Schwartz JC. TDP-43 regulates transcription at protein-coding genes and Alu retrotransposons. Biochim Biophys Acta. 2019;1862:194434.
16. Mitra J, Guerrero EN, Hegde PM, et al. Motor neuron disease-associated loss of nuclear TDP-43 is linked to DNA double-strand break repair defects. Proc Natl Acad Sci USA. 2019;116:4696–4705.
17. Keihani S, Kluever V, Mandad S, et al. The long noncoding RNA *neuroLNC* regulates presynaptic activity by interacting with the neurodegeneration-associated protein TDP-43. Sci Adv. 2019;5:eaay2670.
18. Kawahara Y, Mieda-Sato A. TDP-43 promotes microRNA biogenesis as a component of the Drosha and Dicer complexes. Proc Natl Acad Sci. 2012;109:3347–3352.
19. Gao J, Wang L, Ren X, et al. Translational regulation in the brain by TDP-43 phase separation. J Cell Biol. 2021;220:e202101019.
20. Ling S-C. Synaptic paths to neurodegeneration: the emerging role of TDP-43 and FUS in synaptic functions. Neural Plast. 2018;2018:1–13.
21. Cathcart SJ, Appel SH, Peterson LE, et al. Fast progression in amyotrophic lateral sclerosis is associated with greater TDP-43 burden in spinal cord. J Neuropathol Exp Neurol. 2021;80:754–763.
22. Johnson BS, Snead D, Lee JJ, et al. TDP-43 is intrinsically aggregation-prone, and amyotrophic lateral sclerosis-linked mutations accelerate aggregation and increase toxicity. J Biol Chem. 2009;284:20329–20339.
23. Hawley ZCE, Campos-Melo D, Strong MJ. Evidence of A negative feedback network between TDP-43 and miRNAs dependent on TDP-43 nuclear localization. J Mol Biol. 2020;432:166695.
24. Kim HJ, Taylor JP. Lost in transportation: nucleocytoplasmic transport defects in ALS and other neurodegenerative diseases. Neuron. 2017;96:285–297.
25. Chou -C-C, Zhang Y, Umoh ME, et al. TDP-43 pathology disrupts nuclear pore complexes and nucleocytoplasmic transport in ALS/FTD. Nat Neurosci. 2018;21:228–239.
26. Anderson EN, Morera AA, Kour S, et al. Traumatic injury compromises nucleocytoplasmic transport and leads to TDP-43 pathology. eLife. 2021;10:e67587.
27. Watanabe S, Kaneko K, Yamanaka K. Accelerated disease onset with stabilized familial amyotrophic lateral sclerosis (ALS)-linked mutant TDP-43 proteins. J Biol Chem. 2013;288:3641–3654.
28. Watanabe Y, Taguchi K, Tanaka M. Ubiquitin, autophagy neurodegener dis. Cells. 2020;9:2022.
29. Wang P, Deng J, Dong J, et al. TDP-43 induces mitochondrial damage and activates the mitochondrial unfolded protein response. PLoS Genet. 2019;15:e1007947.

30. Dafinca R, Barbagallo P, Talbot K. The role of mitochondrial dysfunction and ER stress in TDP-43 and C9ORF72 ALS. Front Cell Neurosci. 2021;15:653688.
31. Pirie E, Oh C, Zhang X, et al. S-nitrosylated TDP-43 triggers aggregation, cell-to-cell spread, and neurotoxicity in hiPSCs and in vivo models of ALS/FTD. Proc Natl Acad Sci USA. 2021;118:e2021368118.
32. Floare M-L, Allen SP. Why TDP-43? Why not? Mechanisms of metabolic dysfunction in amyotrophic lateral sclerosis. J Exp Neurosci. 2020;15:263310552095730.
33. Gautam M, Gunay A, Chandel NS, et al. Mitochondrial dysregulation occurs early in ALS motor cortex with TDP-43 pathology and suggests maintaining NAD+ balance as a therapeutic strategy. Sci Rep. 2022;12:4287.
34. Smethurst P, Newcombe J, Troakes C, et al. In vitro prion-like behaviour of TDP-43 in ALS. Neurobiol Dis. 2016;96:236–247.
35. Ding X, Xiang Z, Qin C, et al. Spreading of TDP-43 pathology via pyramidal tract induces ALS-like phenotypes in TDP-43 transgenic mice. Acta Neuropathol Commun. 2021;9:15.
36. Chen P-C, Wu D, Hu C-J, et al. Exosomal TAR DNA-binding protein-43 and neurofilaments in plasma of amyotrophic lateral sclerosis patients: a longitudinal follow-up study. J Neurol Sci. 2020;418:117070.
37. Schulthess I, Gorges M, Müller H-P, et al. Functional connectivity changes resemble patterns of pTDP-43 pathology in amyotrophic lateral sclerosis. Sci Rep. 2016;6:38391.
38. Braak H, Ludolph AC, Neumann M, et al. Pathological TDP-43 changes in Betz cells differ from those in bulbar and spinal α-motoneurons in sporadic amyotrophic lateral sclerosis. Acta Neuropathol. 2017;133:79–90.
39. Barmada SJ, Serio A, Arjun A, et al. Autophagy induction enhances TDP43 turnover and survival in neuronal ALS models. Nat Chem Biol. 2014;10:677–685.
40. Zhao T, Hong Y, Yin P, et al. Differential HspBP1 expression accounts for the greater vulnerability of neurons than astrocytes to misfolded proteins. Proc Natl Acad Sci USA. 2017;114:E7803–E7811.
41. Asakawa K, Handa H, Kawakami K. Optogenetic modulation of TDP-43 oligomerization accelerates ALS-related pathologies in the spinal motor neurons. Nat Commun. 2020;11:1004.
42. Polymenidou M, Lagier-Tourenne C, Hutt KR, et al. Long pre-mRNA depletion and RNA missplicing contribute to neuronal vulnerability from loss of TDP-43. Nat Neurosci. 2011;14:459–468.
43. Pan Y, Nicolazzo JA. Altered blood–brain barrier and blood–spinal cord barrier dynamics in amyotrophic lateral sclerosis: impact on medication efficacy and safety. Br J Pharmacol. 2022;2022:15802.
44. Zamudio F, Loon AR, Smeltzer S, et al. TDP-43 mediated blood-brain barrier permeability and leukocyte infiltration promote neurodegeneration in a low-grade systemic inflammation mouse model. J Neuroinflammation. 2020;17:283.
45. Ferrer I, Andrés-Benito P, Carmona M, et al. TDP-43 vasculopathy in the spinal cord in sporadic Amyotrophic Lateral Sclerosis (sALS) and frontal cortex in sALS/FTLD-TDP. J Neuropathol Exp Neurol. 2021;80:229–239.
46. Riva N, Gentile F, Cerri F, et al. Phosphorylated TDP-43 aggregates in peripheral motor nerves of patients with amyotrophic lateral sclerosis. Brain. 2022;2022:awab285.
47. Cykowski MD, Powell SZ, Appel JW, et al. Phosphorylated TDP-43 (pTDP-43) aggregates in the axial skeletal muscle of patients with sporadic and familial amyotrophic lateral sclerosis. Acta Neuropathol Commun. 2018;6:28.
48. Wang P, Wander CM, Yuan C-X, et al. Acetylation-induced TDP-43 pathology is suppressed by an HSF1-dependent chaperone program. Nat Commun. 2017;8:82.
49. Guo Y, Wang Q, Zhang K, et al. HO-1 induction in motor cortex and intestinal dysfunction in TDP-43 A315T transgenic mice. Brain Res. 2012;1460:88–95.
50. Iguchi Y, Katsuno M, Niwa J, et al. Loss of TDP-43 causes age-dependent progressive motor neuron degeneration. Brain. 2013;136:1371–1382.
51. Grese ZR, Bastos AC, Mamede LD, et al. Specific RNA interactions promote TDP-43 multivalent phase separation and maintain liquid properties. EMBO Rep. 2021;22:e53632.
52. Rengifo-Gonzalez JC, El Hage K, Clément M-J, et al. The cooperative binding of TDP-43 to GU-rich RNA repeats antagonizes TDP-43 aggregation. eLife. 2021;10:e67605.
53. Zacco E, Graña-Montes R, Martin SR, et al. RNA as a key factor in driving or preventing self-assembly of the TAR DNA-binding protein 43. J Mol Biol. 2019;431:1671–1688.
54. Chen H-J, Topp SD, Hui HS, et al. RRM adjacent TARDBP mutations disrupt RNA binding and enhance TDP-43 proteinopathy. Brain. 2019;142:3753–3770.
55. French RL, Grese ZR, Aligireddy H, et al. Detection of TAR DNA-binding protein 43 (TDP-43) oligomers as initial intermediate species during aggregate formation. J Biol Chem. 2019;294:6696–6709.
56. Flores BN, Li X, Malik AM, et al. An intramolecular salt bridge linking TDP43 RNA binding, protein stability, and TDP43-dependent neurodegeneration. Cell Rep. 2019;27:1133–1150.e8.
57. François-Moutal L, Felemban R, Scott DD, et al. Small molecule targeting TDP-43's RNA recognition motifs reduces locomotor defects in a *drosophila* model of Amyotrophic Lateral Sclerosis (ALS). ACS Chem Biol. 2019;14:2006–2013.
58. Mollasalehi N, Francois-Moutal L, Scott DD, et al. An allosteric modulator of RNA binding targeting the N-terminal domain of TDP-43 yields neuroprotective properties. ACS Chem Biol. 2020;15:2854–2859.
59. Nana AL, Sidhu M, Gaus SE, et al. Neurons selectively targeted in frontotemporal dementia reveal early stage TDP-43 pathobiology. Acta Neuropathol. 2019;137:27–46.
60. Ling JP, Pletnikova O, Troncoso JC, et al. TDP-43 repression of nonconserved cryptic exons is compromised in ALS-FTD. Science. 2015;349:650–655.
61. Melamed Z, López-Erauskin J, Baughn MW, et al. Premature polyadenylation-mediated loss of stathmin-2 is a hallmark of TDP-43-dependent neurodegeneration. Nat Neurosci. 2019;22:180–190.
•• **This article highlights the importance of TDP-43 splicing function in the nucleus, particularly for proteins involved in neuronal homeostasis, in addition to the promising potential of using ASO to correct such dysfunction.**
62. Brown A-L, Wilkins OG, Keuss MJ, et al. TDP-43 loss and ALS-risk SNPs drive mis-splicing and depletion of UNC13A. Nature. 2022;603:131–137.
•• **This article that was recently published in Nature also highlights the role of TDP-43 in mRNA splicing (UNC13A) and subsequent effect on synaptic function.**
63. Haines JD, Herbin O, de la Hera B, et al. Nuclear export inhibitors avert progression in preclinical models of inflammatory demyelination. Nat Neurosci. 2015;18:511–520.
64. Archbold HC, Jackson KL, Arora A, et al. TDP43 nuclear export and neurodegeneration in models of amyotrophic lateral sclerosis and frontotemporal dementia. Sci Rep. 2018;8:4606.
65. Pinarbasi ES, Cağatay T, Fung HYJ, et al. Active nuclear import and passive nuclear export are the primary determinants of TDP-43 localization. Sci Rep. 2018;8:7083.
66. Park JH, Chung CG, Park SS, et al. Cytosolic calcium regulates cytoplasmic accumulation of TDP-43 through Calpain-A and Importin α3. eLife. 2020;9:e60132.
67. Guo L, Kim HJ, Wang H, et al. Nuclear-import receptors reverse aberrant phase transitions of RNA-binding proteins with prion-like domains. Cell. 2018;173:677–692.e20.
68. Odeh HM, Fare CM, Shorter J. Nuclear-import receptors counter deleterious phase transitions in neurodegenerative disease. J Mol Biol. 2022;434:167220.

69. Jackrel ME, DeSantis ME, Martinez BA, et al. Potentiated Hsp104 variants antagonize diverse proteotoxic misfolding events. Cell. 2014;156:170–182.
70. Bharathi V, Bajpai A, Parappuram IT, et al. Elevated constitutive expression of Hsp40 chaperone Sis1 reduces TDP-43 aggregation-induced oxidative stress in Ire1 pathway dependent-manner in yeast TDP-43 proteinopathy model of amyotrophic lateral sclerosis. Biochem Biophys Res Commun. 2022;595:28–34.
71. Crippa V, Cicardi ME, Ramesh N, et al. The chaperone HSPB8 reduces the accumulation of truncated TDP-43 species in cells and protects against TDP-43-mediated toxicity. Hum Mol Genet. 2016;25:3908–3924.
72. Yu H, Lu S, Gasior K, et al. HSP70 chaperones RNA-free TDP-43 into anisotropic intranuclear liquid spherical shells. Science. 2021;371: eabb4309.
73. Lin LT, Razzaq A, Di Gregorio SE, et al. Hsp90 and its co-chaperone Sti1 control TDP-43 misfolding and toxicity. FASEB J. 2021;35: e21594.
74. Chen H-J, Mitchell JC, Novoselov S, et al. The heat shock response plays an important role in TDP-43 clearance: evidence for dysfunction in amyotrophic lateral sclerosis. Brain. 2016;139:1417–1432.
75. Benatar M, Wuu J, Andersen PM, et al. Randomized, double-blind, placebo-controlled trial of arimoclomol in rapidly progressive *SOD1* ALS. Neurology. 2018;90:e565–e574.
76. Kuta R, Larochelle N, Fernandez M, et al. Depending on the stress, histone deacetylase inhibitors act as heat shock protein co-inducers in motor neurons and potentiate arimoclomol, exerting neuroprotection through multiple mechanisms in ALS models. Cell Stress Chaperones. 2020;25:173–191.
77. Gregory JM, Barros TP, Meehan S, et al. The aggregation and neurotoxicity of TDP-43 and its ALS-associated 25 kDa fragment are differentially affected by molecular chaperones in drosophila. PLoS One. 2012;7:e31899.
78. Ormeño F, Hormazabal J, Moreno J, et al. Chaperone mediated autophagy degrades TDP-43 protein and is affected by TDP-43 aggregation. Front Mol Neurosci. 2020;13:19.
79. Jo M, Lee S, Kim K, et al. Inhibition of MEK5 suppresses TDP-43 toxicity via the mTOR-independent activation of the autophagy-lysosome pathway. Biochem Biophys Res Commun. 2019;513:925–932.
80. Wang Y, Liu F-T, Wang Y-X, et al. Autophagic modulation by trehalose reduces accumulation of TDP-43 in a cell model of amyotrophic lateral sclerosis via TFEB activation. Neurotox Res. 2018;34:109–120.
81. Chang C-F, Lee Y-C, Lee K-H, et al. Therapeutic effect of berberine on TDP-43-related pathogenesis in FTLD and ALS. J Biomed Sci. 2016;23:72.
82. Liu C, Leng B, Li Y, et al. Diallyl trisulfide protects motor neurons from the neurotoxic protein TDP-43 via activating lysosomal degradation and the antioxidant response. Neurochem Res. 2018;43:2304–2312.
83. Wang I-F, Guo B-S, Liu Y-C, et al. Autophagy activators rescue and alleviate pathogenesis of a mouse model with proteinopathies of the TAR DNA-binding protein 43. Proc Natl Acad Sci. 2012;109:15024–15029.
84. Chen Y, Wang H, Ying Z, et al. Ibudilast enhances the clearance of SOD1 and TDP-43 aggregates through TFEB-mediated autophagy and lysosomal biogenesis: the new molecular mechanism of ibudilast and its implication for neuroprotective therapy. Biochem Biophys Res Commun. 2020;526:231–238.
85. Kumar S, Phaneuf D, Julien J-P. Withaferin-A treatment alleviates TAR DNA-binding protein-43 pathology and improves cognitive function in a mouse model of FTLD. Neurotherapeutics. 2021;18:286–296.
86. Yin P, Bai D, Deng F, et al. SQSTM1-mediated clearance of cytoplasmic mutant TARDBP/TDP-43 in the monkey brain. Autophagy. 2021;1–14.
87. Crippa V, D'Agostino VG, Cristofani R, et al. Transcriptional induction of the heat shock protein B8 mediates the clearance of misfolded proteins responsible for motor neuron diseases. Sci Rep. 2016;6:22827.
•• **This study sheds light on the FDA-approved drug colchicine that was found to target TDP-43 proteinopathy and is now being tested in a phase II clinical trial in ALS patients.**
88. Mandrioli J, Crippa V, Cereda C, et al. Proteostasis and ALS: protocol for a phase II, randomised, double-blind, placebo-controlled, multicentre clinical trial for colchicine in ALS (Co-ALS). BMJ Open. 2019;9:e028486.
89. Perera ND, Tomas D, Wanniarachchillage N, et al. Stimulation of mTOR-independent autophagy and mitophagy by rilmenidine exacerbates the phenotype of transgenic TDP-43 mice. Neurobiol Dis. 2021;154:105359.
90. Liu G, Byrd A, Warner AN, et al. Cdc48/VCP and endocytosis regulate TDP-43 and FUS toxicity and turnover. Mol Cell Biol. 2020;40:e00256–19.
91. Liu G, Coyne AN, Pei F, et al. Endocytosis regulates TDP-43 toxicity and turnover. Nat Commun. 2017;8:2092.
92. Tashiro Y, Urushitani M, Inoue H, et al. Motor neuron-specific disruption of proteasomes, but not autophagy, replicates amyotrophic lateral sclerosis. J Biol Chem. 2012;287:42984–42994.
93. Chou -C-C, Alexeeva OM, Yamada S, et al. PABPN1 suppresses TDP-43 toxicity in ALS disease models. Hum Mol Genet. 2015;24:5154–5173.
94. Cragnaz L, Spinelli G, De Conti L, et al. Thioridazine reverts the phenotype in cellular and Drosophila models of amyotrophic lateral sclerosis by enhancing TDP-43 aggregate clearance. Neurobiol Dis. 2021;160:105515.
95. Tamaki Y, Shodai A, Morimura T, et al. Elimination of TDP-43 inclusions linked to amyotrophic lateral sclerosis by a misfolding-specific intrabody with dual proteolytic signals. Sci Rep. 2018;8:6030.
96. Pozzi S, Thammisetty SS, Codron P, et al. Virus-mediated delivery of antibody targeting TAR DNA-binding protein-43 mitigates associated neuropathology. J Clin Investig. 2019;129:1581–1595.
• **This study uses RRM1-specific antibody fragments (scFv) to target TDP-43 proteinopathy and improve motor and cognitive functions in mice. scFv's for neurodegenerative diseases are an innovative and promising therapeutic area.**
97. Zhao B, Louadi S, Dijkstra AA, et al. Selective targeting of intracellular, misfolded, pathogenic TDP-43 with rationally designed intrabodies. Alzheimers Dement. 2021;17:e045221.
98. Gilodi M, Lisi S, Dudás F, et al. Selection and modelling of a new single-domain intrabody against TDP-43. Front Mol Biosci. 2022;8:773234.
99. Li Q, Babinchak WM, Surewicz WK. Cryo-EM structure of amyloid fibrils formed by the entire low complexity domain of TDP-43. Nat Commun. 2021;12:1620.
100. Scotter EL, Vance C, Nishimura AL, et al. Differential roles of the ubiquitin proteasome system (UPS) and autophagy in the clearance of soluble and aggregated TDP-43 species. J Cell Sci. 2014;127:1263–1278.
101. Zhang Y, Gu J, Sun Q. Aberrant stress granule dynamics and aggrephagy in ALS pathogenesis. Cells. 2021;10:2247.
102. Ratti A, Gumina V, Lenzi P, et al. Chronic stress induces formation of stress granules and pathological TDP-43 aggregates in human ALS fibroblasts and iPSC-motoneurons. Neurobiol Dis. 2020;145:105051.
103. McGurk L, Gomes E, Guo L, et al. Poly(ADP-Ribose) prevents pathological phase separation of TDP-43 by promoting liquid demixing and stress granule localization. Mol Cell. 2018;71:703–717.e9.
104. Moujalled D, James JL, Yang S, et al. Phosphorylation of hnRNP K by cyclin-dependent kinase 2 controls cytosolic accumulation of TDP-43. Human Mol Genet. 2015;24:1655–1669.
105. Kim H-J, Raphael AR, LaDow ES, et al. Therapeutic modulation of eIF2α phosphorylation rescues TDP-43 toxicity in amyotrophic lateral sclerosis disease models. Nat Genet. 2014;46:152–160.
106. Fang MY, Markmiller S, Vu AQ, et al. Small-molecule modulation of TDP-43 recruitment to stress granules prevents persistent TDP-43 accumulation in ALS/FTD. Neuron. 2019;103:802–819.e11.
107. Becker LA, Huang B, Bieri G, et al. Therapeutic reduction of ataxin-2 extends lifespan and reduces pathology in TDP-43 mice. Nature. 2017;544:367–371.

•• **This study describes the successful targeting of ALS-associated ataxin-2 using ASO, which is now being tested in a phase I clinical trial.**

108. Fernandes N, Nero L, Lyons S, et al. Stress granule assembly can facilitate but is not required for TDP-43 cytoplasmic aggregation. Biomolecules. 2020;10:1367.
109. Zhang Y-J, Gendron TF, Xu Y-F, et al. Phosphorylation regulates proteasomal-mediated degradation and solubility of TAR DNA binding protein-43 C-terminal fragments. Mol Neurodegeneration. 2010;5:33.
110. Martínez-González L, Gonzalo-Consuegra C, Gómez-Almería M, et al. Tideglusib, a non-ATP competitive inhibitor of GSK-3β as a drug candidate for the treatment of amyotrophic lateral sclerosis. IJMS. 2021;22:8975.

•• **This study paved the way for the current phase II clinical trial of Tideglusib in ALS patients which was found to mitigate TDP-43 pathology in animal models.**

111. Rojas-Prats E, Martinez-Gonzalez L, Gonzalo-Consuegra C, et al. Targeting nuclear protein TDP-43 by cell division cycle kinase 7 inhibitors: a new therapeutic approach for amyotrophic lateral sclerosis. Eur J Med Chem. 2021;210:112968.
112. Vaca G, Martinez-Gonzalez L, Fernandez A, et al. Therapeutic potential of novel Cell Division Cycle Kinase 7 inhibitors on TDP-43-related pathogenesis such as Frontotemporal Lobar Degeneration (FTLD) and amyotrophic lateral sclerosis (ALS). J Neurochem. 2021;156:379–390.
113. Martínez-González L, Rodríguez-Cueto C, Cabezudo D, et al. Motor neuron preservation and decrease of in vivo TDP-43 phosphorylation by protein CK-1δ kinase inhibitor treatment. Sci Rep. 2020;10:4449.
114. Nozal V, Martínez-González L, Gomez-Almeria M, et al. TDP-43 modulation by Tau-Tubulin kinase 1 inhibitors: a new avenue for future amyotrophic lateral sclerosis therapy. J Med Chem. 2022;65:1585–1607.
115. Yin P, Guo X, Yang W, et al. Caspase-4 mediates cytoplasmic accumulation of TDP-43 in the primate brains. Acta Neuropathol. 2019;137:919–937.
116. Farrawell NE, Lambert-Smith IA, Warraich ST, et al. Distinct partitioning of ALS associated TDP-43, FUS and SOD1 mutants into cellular inclusions. Sci Rep. 2015;5:13416.
117. Bonifacino T, Zerbo RA, Balbi M, et al. Nearly 30 years of animal models to study amyotrophic lateral sclerosis: a historical overview and future perspectives. IJMS. 2021;22:12236.
118. Spiller KJ, Cheung CJ, Restrepo CR, et al. Selective motor neuron resistance and recovery in a new inducible mouse model of TDP-43 proteinopathy. J Neurosci. 2016;36:7707–7717.
119. Steinacker P, Barschke P, Otto M. Biomarkers for diseases with TDP-43 pathology. Mol Cell Neurosci. 2019;97:43–59.
120. Baker MR. ALS—dying forward, backward or outward? Nat Rev Neurol. 2014;10:660.
121. Eisen A, Braak H, Del Tredici K, et al. Cortical influences drive amyotrophic lateral sclerosis. J Neurol Neurosurg Psychiatry. 2017;88:917–924.
122. Scaricamazza S, Salvatori I, Ferri A, et al. Skeletal muscle in ALS: an unappreciated therapeutic opportunity? Cells. 2021;10:525.
123. de Boer EMJ, Orie VK, Williams T, et al. TDP-43 proteinopathies: a new wave of neurodegenerative diseases. J Neurol Neurosurg Psychiatry. 2021;92:86–95.

Given the interplay between the different TDP-43-related cellular and molecular mechanisms mentioned above, targeting one or more of them can be important to restore the homeostatic balance of the cell. The involvement of TDP-43 in numerous cellular pathways complicates the targeting of this protein but offers the potential to restore the normal function of these pathways if TDP-43 dysfunction is corrected. In addition, since TDP-43 proteinopathy is not only observed in ALS but also in other neurodegenerative diseases like FTD and Alzheimer's disease, targeting TDP-43 can be an interesting therapeutic approach in these diseases as well.

III. Therapeutic development in ALS

Therapeutic development in ALS has made significant strides over the past few decades, driven by an enhanced understanding of the disease's complex pathology and advancements in medical technology. Therapeutic strategies are multifaceted, targeting different aspects of the disease. Initially, treatment options were limited to managing symptoms and improving the quality of life. However, recent years have seen the emergence of more targeted and disease-modifying approaches such as antisense oligonucleotides (ASO). To date, only few treatments have received approval for ALS treatment, reflecting the challenges in developing effective therapies for this complex disease. While the treatments discussed below offer some benefits, the overall impact on the disease course remains limited, highlighting the need for continued research and development of new therapeutic approaches.

A. Riluzole

Riluzole, a lipophilic benzothiazole derivative initially used as an anticonvulsant, is the first drug to be approved in 1995 by the Food and Drug Administration (FDA) for the treatment of ALS (Lacomblez et al., 1996; Saitoh & Takahashi, 2020). Up to date, it remains the gold standard, first-line therapeutic intervention in ALS. Although the exact mechanism of action of this drug is still not fully understood, it seems to exert neuroprotective effects on motor neurons by counteracting glutamate-induced excitotoxicity through several possible mechanisms including blocking Na^+ channels (Lamanauskas & Nistri, 2008; Urbani & Belluzzi, 2000; Y.-J. Wang et al., 2008), decreasing Ca^{2+} currents (Lamanauskas & Nistri, 2008), activating Ca^{2+}-activated K^+ channels (Dimitriadi et al., 2013) , increasing the uptake of glutamate (Azbill et al., 2000; E. Fumagalli et al., 2008), and decreasing glutamate release

(Lamanauskas & Nistri, 2008). The drug apparently exerts protective effects at the level of both the central and peripheral nervous systems, decreasing cortical hyperexcitability and reducing abnormal axonal excitability (Vucic et al., 2013).

Riluzole seems to exhibit a beneficial impact in both bulbar- and limb-onset ALS, without an improvement in muscle strength (Hinchcliffe & Smith, 2017). It had no significant effect on the levels of serum NfL, which suggests that the beneficial effect of Riluzole might not be due a halting of neurodegeneration (Esselin et al., 2022). In one study, it was also shown to decrease the extent of weight loss in ALS patients, which might have a positive impact on their survival (Thakor et al., 2021). In addition, Riluzole is thought to have a protective effect against some aspects of TDP-43 proteinopathy. One study reported the inhibitory effects of Riluzole on protein kinase CK1δ, which is a key enzyme involved in the phosphorylation and mislocalization of TDP-43 (Nonaka et al., 2016), providing a new possible mechanism by which Riluzole can reduce TDP-43 hyperphosphorylation (Bissaro & Moro, 2019). Another study demonstrated that Riluzole inhibited the self-interaction of TDP-43, which could help in decreasing the aggregation of the protein (Oberstadt et al., 2018).

Riluzole is administered at an oral dose of 50 mg, twice daily (Lacomblez et al., 1996), with a bioavailability of 60%, and relatively minor side effects (Liboux et al., 1997; Wymer et al., 2023). After 18 months of treatment, Riluzole improved survival by 2 to 3 months and decreased the risk of tracheostomy by 21% (Bensimon et al., 1994; Lacomblez et al., 1996). However, real-world evidence seems to point towards a much greater improvement of patient survival, from 6 to 19 months (Hinchcliffe & Smith, 2017). Recently, a new formulation of riluzole as an oral film preparation (Exservan™), mainly intended for patients with dysphagia, was approved by the FDA (Wymer et al., 2023). Moreover, attempts are being made to enhance the therapeutic potential of Riluzole by decreasing its side effects and increasing its concentration at the level of the spinal cord using continuous intrathecal infusion (Keifer et al., 2023).

B. Edaravone

Edaravone was first approved by the FDA for intravenous treatment of ALS in 2017 and as an oral treatment in 2022 (The Food and Drug Administration, 2017, 2022). The neuroprotective effects of Edaravone are mainly through its antioxidant activity. It's a potent

free radical-scavenger (K. Watanabe et al., 2018), and an inducer of the antioxidant defence mechanisms of the cell (Jami et al., 2015; Z. Liu et al., 2018; Pan et al., 2019). The antioxidant activity of Edaravone can indirectly preserve the integrity of the components of the BBB (B. J. Lee et al., 2010; J. Liu et al., 2019; Miyamoto et al., 2013; T. Watanabe et al., 1988), decrease the activation of microglia and astrocytes (G.-H. Wang et al., 2011), and preserve mitochondrial function (L. Liu et al., 2015; Takayasu et al., 2007; H.-M. Wang et al., 2017; Yamamura et al., 2013; X. Zhao et al., 2020). One study also reported a decrease in the aggregation of SOD1 in the spinal cord of transgenic mice following Edaravone treatment (Ito et al., 2008).

The effect of Edaravone is considered to be very moderate, with a slight improvement of 33% in the ALSFRS-R score (Abe et al., 2017; M. Gao et al., 2023), an increased median survival of 6 months, and a decreased risk of death of 27% (Brooks, Berry, et al., 2022). Studies have provided some conflicting results concerning the efficacy of Edaravone in patients at different disease stages, with some results suggesting that Edaravone needs to be started early in the disease to be effective and others showing protective effects even at more advanced stages (Abe et al., 2017; Brooks, Heiman-Patterson, et al., 2022; J.-M. Park et al., 2020; The Writing Group on Behalf of the Edaravone (MCI-186) ALS 18 Study Group, 2017). Interestingly, the combined therapy of Edaravone and Riluzole did not show any significant additional clinical benefit for patients (Samadhiya et al., 2022; Witzel et al., 2022).

C. Therapies targeting the CNS

ALS primarily affects motor neurons in the CNS, making it essential to develop therapeutic approaches that can target the brain and spinal cord. However, several barriers complicate CNS-targeted therapies, primarily the BBB which restricts the entry of many traditional drugs. Recently, therapies targeting the CNS in ALS became at the forefront of modern treatment strategies, with a focus on both biotherapeutics and advanced delivery techniques.

Biotherapeutics, such as ASOs or antibodies, have been investigated to target specific ALS-linked abnormalities in the CNS. To overcome the problem of the BBB, various delivery techniques are being developed, including direct administration into the CNS, the use of

nanoparticle-based delivery systems, or AAV vectors capable of crossing the BBB. We discuss below some of these strategies.

a. Tofersen

This is an example of a drug that is administered directly into the CNS through the intrathecal route. Tofersen is an investigational 20-base ASO therapy developed for the treatment of ALS patients carrying a *SOD1* mutation. Mutations in the *SOD1* gene account for 1-2% of sALS cases and 13-20% of fALS (Berdyński et al., 2022), with more than 230 mutations identified to date (De La Cruz et al., 2024). An ASO is a synthetic, short strand of 15-25 nucleotides that hybridizes with the complementary mRNA fragment, forming an RNA-DNA hybrid that activates the degradation of the target mRNA through RNase H (Saini & Chawla, 2024). Given that mutations in the *SOD1* gene confers a toxic gain of function to the protein, the aim of designing anti-*SOD1* ASO was to reduce the burden of the SOD1 protein by decreasing its production (McCampbell et al., 2018).

In a phase 3 clinical trial, intrathecally administered Tofersen was found to decrease the concentrations of the SOD1 protein in the CSF and decrease the levels of NfL in the plasma (Miller et al., 2022). These findings reflected the protective effect of the drug in ALS patients and pushed for its accelerated approval by the FDA in 2023 (The Food and Drug Administration, 2023) (Mullard, 2023). Currently, another phase 3 clinical trial is underway to test if Tofersen, administered in the presymptomatic stage, can delay the onset of symptoms in carriers of a confirmed *SOD1* mutation (ATLAS study; NCT04856982) (Benatar et al., 2022).

b. Antibodies and the blood-brain barrier

Antibodies, which can be targeted against specific proteins or their pathological forms, have gained extensive interest in therapeutic developments. The specificity of the antibodies is pivotal in decreasing the potential off-target effects of drugs. However, delivering therapeutic antibodies involves overcoming several biological barriers to ensure that the antibodies reach their target site in an effective concentration. The following review (Publication 2), published in collaboration with the LabEx MAbImprove, describes primary biological barriers and their impact on the delivery of antibodies to tissues, and discusses techniques to either take advantage of these barriers or circumvent them in both health and disease. In section 3.3. “Endothelial barrier and systemic delivery of antibody”, we address the

main barrier to the CNS – the BBB – and describe strategies that can help antibodies cross the BBB for delivery into the CNS. Although this review mainly focuses on full-length immunoglobulins, many of the approaches that are discussed can also be applied to antibody fragments such as single chain variable fragments (scFvs).

Briefly, the BBB is a highly selective barrier that separates the circulating blood from the brain's extracellular fluid, maintaining the brain's homeostasis and shielding it from potentially harmful substances. Composed of tightly joined endothelial cells, astrocytic end-feet, and a basement membrane, the BBB restricts the passage of most large molecules, including therapeutic antibodies, making it a significant obstacle for treating neurological conditions. In fact, only 0.1% of systematically administered antibodies are able to cross the BBB and an even less amount is able to reach the cortex. Moreover, in various health conditions and diseases, the integrity and function of the BBB can be compromised. This can result in an increase in its permeability, which might allow for an enhanced passage of molecules that cannot cross the BBB under normal conditions.

Various strategies have been employed to enhance the delivery of antibodies to the CNS, including the direct but invasive administration of therapeutics into the CNS, engineering antibodies to bind to receptors that mediate transcytosis across the BBB, temporarily increasing the permeability of the BBB to allow the passage of larger molecules, and bypassing the BBB by using intranasal administration.

Overall, overcoming the BBB is essential for unlocking the full therapeutic potential of antibodies and antibody fragments in treating CNS disorders, addressing unmet medical needs, and improving patient outcomes in a range of debilitating neurological diseases including neurodegenerative diseases like ALS.

In another review published by our group and titled “Taking advantage of blood-brain or -spinal cord barrier alterations or restoring them to optimize therapy in ALS?” (Publication 3) (Alarcan et al., 2022), we tackled the specific alterations of the BBB in the case of ALS and how they can affect therapeutics strategies. Several studies have shown that the BBB becomes dysfunctional in ALS, leading to a compromised barrier. Such alterations include degeneration of endothelial cells, thickening of the basement membrane, formation of extracellular oedema, infiltration of blood circulating cells, astrocytic endfeet degeneration, decreased

tight junctions, and others (Alarcan et al., 2022). These changes have even been observed at the presymptomatic stage, prior to neuromuscular dysfunction and motor neuron loss in animal models of ALS (Yoshikawa et al., 2022; Zhong et al., 2008). In some ALS patients, increased leakage into the CNS of molecules and cells coming from the blood circulation have been described, suggesting an increased permeability of the BBB (Donnenfeld et al., 1984; Engelhardt et al., 1993; J.-Y. Li et al., 2022). It should be noted that alterations in the BBB do not seem to be uniform across all regions of the BBB and are not reported in all ALS patients (Waters et al., 2021). Additionally, an increase in the permeability of the BBB does not directly translate into an increased delivery of potential therapeutic agents into their intended target regions in the CNS. This can be due to an increase in efflux transporters or a decreased diffusion capacity of the drug across the CNS interstitial fluid (Alarcan et al., 2022). Moreover, all these changes in the BBB can affect the pharmacokinetic parameters of drugs intended for the CNS and need to be taken into consideration during drug development. Therefore, two therapeutic approaches can be envisaged: 1) restoring barrier integrity to protect neurons by stabilizing or repairing the BBB, potentially slowing disease progression, and 2) exploiting barrier disruption for enhanced drug delivery, using the increased permeability to facilitate the entry of therapeutic agents that normally wouldn't cross these barriers. The balance between these strategies is crucial, as restoring the barrier might protect against further damage, while taking advantage of its permeability could improve treatment efficacy.

Publication 2:

Al Ojaimi, Y., Blin, T., Lamamy, J., Gracia, M., Pitiot, A., Denevault-Sabourin, C., ... & Sécher, T. (2021). Therapeutic antibodies–natural and pathological barriers and strategies to overcome them. *Pharmacology & Therapeutics*, 108022.

Pharmacology & Therapeutics 233 (2022) 108022

Contents lists available at ScienceDirect

Pharmacology & Therapeutics

journal homepage: www.elsevier.com/locate/pharmthera

Invited Article

Therapeutic antibodies – natural and pathological barriers and strategies to overcome them

Yara Al Ojaimi [a,b,1], Timothée Blin [b,c,1], Juliette Lamamy [b,d,1], Matthieu Gracia [e,1], Aubin Pitiot [b,c], Caroline Denevault-Sabourin [b,d], Nicolas Joubert [b,d], Jean-Pierre Pouget [e], Valérie Gouilleux-Gruart [b,d], Nathalie Heuzé-Vourc'h [b,c,*], Débora Lanznaster [a,b,2], Sophie Poty [e,2], Thomas Sécher [b,c,2]

[a] UMR 1253, iBrain, Inserm, 37000 Tours, France
[b] University of Tours, 37000 Tours, France
[c] UMR 1100, CEPR, Inserm, 37000 Tours, France
[d] GICC, EA7501, 37000 Tours, France
[e] Institut de Recherche en Cancérologie de Montpellier (IRCM), Inserm U1194, Université de Montpellier, Institut Régional du Cancer de Montpellier (ICM), Montpellier F-34298, France

ARTICLE INFO

Available online 20 October 2021

Keywords:
Antibodies
Biological barriers
Pathological barriers
Therapeutic strategies

ABSTRACT

Antibody-based therapeutics have become a major class of therapeutics with over 120 recombinant antibodies approved or under review in the EU or US. This therapeutic class has experienced a remarkable expansion with an expected acceleration in 2021–2022 due to the extraordinary global response to SARS-CoV2 pandemic and the public disclosure of over a hundred anti-SARS-CoV2 antibodies. Mainly delivered intravenously, alternative delivery routes have emerged to improve antibody therapeutic index and patient comfort. A major hurdle for antibody delivery and efficacy as well as the development of alternative administration routes, is to understand the different natural and pathological barriers that antibodies face as soon as they enter the body up to the moment they bind to their target antigen. In this review, we discuss the well-known and more under-investigated extracellular and cellular barriers faced by antibodies. We also discuss some of the strategies developed in the recent years to overcome these barriers and increase antibody delivery to its site of action. A better understanding of the biological barriers that antibodies have to face will allow the optimization of antibody delivery near its target. This opens the way to the development of improved therapy with less systemic side effects and increased patients' adherence to the treatment.

© 2021 Elsevier Inc. All rights reserved.

Contents

1. Introduction . . . 2
2. Extracellular barriers . . . 2
3. FcRn and cellular barriers . . . 9
4. Immune barrier and antibody clearance . . . 14
5. Conclusion . . . 15
Declaration of Competing Interest . . . 16
Acknowledgements . . . 16
References . . . 16

Abbreviations: Aβ, amyloid-β; AD, Alzheimer's disease; ADC, antibody-drug conjugate; BBB, blood-brain barrier; CNS, central nervous system; ECM, extracellular matrix; EU, European union; Fab, fragment antigen-binding; Fc, fragment crystallizable; FcRn, neonatal Fc receptor; FDA, Food and Drug Administration; GI, gastrointestinal; HER2, human epidermal growth factor receptor 2; IA, intra-articular; IdeS, bacteria secreted proteases; IFP, interstitial fluid pressure; IgG, immunoglobulin G; IVIg, intravenous immunoglobulin; mAb, monoclonal antibody; MMP, matrix metalloproteinase; PD, pharmacodynamics; pI, isoelectric point; PK, pharmacokinetic; scFv, single-chain variable fragment; TNF, tumour necrosis factor; VEGF, vascular endothelial growth factor; US, United States.

* Corresponding author.
E-mail address: nathalie.vourch@med.univ-tours.fr (N. Heuzé-Vourc'h).

[1] equally contributed to manuscript writing.
[2] equally contributed to manuscript conception, writing and reviewing.

https://doi.org/10.1016/j.pharmthera.2021.108022
0163-7258/© 2021 Elsevier Inc. All rights reserved.

1. Introduction

Today, recombinant antibodies represent an important therapeutic class in the armamentarium of clinicians, with some products standing as first-line standard of care. Recombinant antibodies exist in diverse forms, whether they are monoclonal or multivalent, full-length IgG or Ab fragments, first-in-class molecule or biosimilar, naked or conjugated to cytotoxic agents (antibody drug conjugate; ADC) (Elshiaty, Schindler, & Christopoulos, 2021). In fact, there are more than 120 molecules approved or in review in the EU and US, most of them being full-length unconjugated mAb from the IgG1, IgG2 and IgG4 subclasses (Vukovic, van Elsas, Verbeek, & Zaiss, 2021). Since 2014, six to twelve new recombinant antibodies are granted first approval (in either the US or EU) each year (https://www.antibodysociety.org/resources/approved-antibodies/). Recombinant antibodies constitute a thriving focus of research in oncology and non-cancer diseases (autoimmune, infectious diseases, ophthalmic, dermatologic, respiratory disorders), as they have already proven their efficiency in a variety of diseases, ranging from small patient populations with orphan diseases to hundreds of thousands of patients. The success of recombinant antibodies relies on: (i) a unique and complex pharmacokinetic profile, with full-length IgG exhibiting long half-lives, (ii) a multifaceted pharmacodynamics (PD) with multiple modes of action, and (iii) a good safety profile, generally well tolerated and with a low risk of unexpected side effects in humans. These qualities often provide a first-to-market advantage, as antibodies can move rapidly from proof-of-concept studies towards commercialization.

The therapeutic response to antibodies relies on their interdependent PK and PD, with PK influencing the magnitude and duration of antibody PD, and PK being influenced by the biology of the target antigen, a concept known as target-mediated drug disposition. PK is characterized by antibody absorption, distribution, metabolism and elimination (Kamath, 2016). Antibody absorption depends mainly on the route of administration. While intravenous injection remains the most commonly used administration route for Ab, there has been an increasing trend towards the development of alternative delivery modalities to treat patients with chronic diseases. This should enable self-administration or caregiver-supported dosing at home in order to reduce hospital/clinical cost while improving patients' quality of life and treatment (Sanchez-Felix, Burke, Chen, Patterson, & Mittal, 2020). It should also improve antibody therapeutic index when the intravenous injection is not adapted to achieve high Ab concentration at the site of action and/or results in undesirable on-target/off-tissue side effects. Since 2009, the subcutaneous route has shown a marked interest. With a third antibody approved in the US, this route is the predominant alternative delivery route, and commonly used to treat immunological chronic diseases, such as asthma, rheumatoid arthritis and psoriasis (Matucci, Vultaggio, & Danesi, 2018). Other administration routes of marketed Ab include intravitreal for anti-vascular endothelial growth factor (VEGF) in ophthalmic disorders, inhalation, oral and intra-articular delivery which constitute a growing focus of research for local-acting antibodies, with several molecules being evaluated in clinical trials (inhalation: NCT04631705, NCT01818024; oral: NCT01205087, NCT01459419; intra-articular: NCT00819572, NCT04731675, NCT04814368). The distribution and subsequent binding of the Ab to its target antigen depends on its partitioning properties in the different body compartments, and are directly impacted by the antibody format, the expression/concentration of the target antigen, the route of administration and biological barriers associated to the physio-pathological conditions. Metabolism of intravenous IgG mainly occurs in the vascular endothelium, following saturation of the FcRn receptor, which is known to rescue IgG Ab from intracellular catabolism. Once in the tissue, antibodies catabolism may take place after interaction with the target antigen (target-mediated drug disposition) or by non-specific mechanisms (Glassman, Abuqayyas, & Balthasar, 2015).

Here, we comprehensively review the different biological barriers that recombinant antibodies must overcome to access their target antigen, associated either to physiological or pathological conditions and encountered depending on the route of administration. Understanding the influence of these biological barriers on the kinetics and partitioning of antibody distribution is necessary for accurate predictions of antibody PK and ultimately therapeutic response. In addition, we describe strategies recently developed to overcome these barriers and improve the efficacy of antibody-based therapeutics.

2. Extracellular barriers

2.1. Extracellular matrix

2.1.1. Structure and functions of the extracellular matrix

In normal and malignant tissues, the extracellular matrix (ECM) is defined as a non-cellular component that provides biochemical and structural support for its cellular constituents (Walker, Mojares, & Del Rio Hernandez, 2018) (Fig. 1). Two main ECM structures can be found: (i) the basement membrane, a very compact ECM found in both epithelial and endothelial tissues (Kruegel & Miosge, 2010); and (ii) the interstitial matrix, a looser matrix found below the basement membrane as well as between connective tissues. Structurally, the ECM core components are collagens, fibronectins, laminins, proteoglycans, hyaluronan, and other (glyco)proteins such as matricellular proteins (Theocharis, Manou, & Karamanos, 2019). Collagens are the most abundant structural proteins of the ECM and are produced by fibroblasts, endothelial and epithelial cells. They are found mainly in the ECM of connective tissues, providing tensile strength. Collagens have been shown to be involved in cell adhesion and migration. Fibronectins are located within the basement membrane and arranged into a mesh of fibrils similar to collagens. They are linked to cell surface receptors (integrins) and play a key role in cell adhesion, embryonic development and wound healing processes. Laminins are important components of the basement membrane that create a network with collagens by bridging molecules such as perlecan. They interact with epithelial cells via surface cell receptors such as integrins or cell surface proteoglycans. Laminins are involved in cell adhesion and play a pivotal role in cell differentiation and migration. Proteoglycans are core proteins onto which a few to hundreds of glycosaminoglycans (e.g., hyaluronan, heparan sulphate) side chains are linked. They are scattered among collagen fibrils. Proteoglycans sequester water within tissues, conferring to them hydration functions. Glycosaminoglycans also bind many growth factors, sequestering them in the ECM. Matricellular proteins are non-structural proteins that encompass thrombospondins, tenascins, fibulins, osteonectin, osteopontin, or periostin. Secreted in the ECM, they can interact with matrix proteins, growth factors and several cell surface receptors. They play a major role in cell-matrix communication. These components are organised in a structural meshwork that interacts with host cells through surface receptors including integrins, discoidin domain receptors, cell surface proteoglycans, or hyaluronic acid receptors such as CD44. The ECM does not only supply cells with a physical structure, but also provides chemical and mechanical signals known to regulate migration, proliferation, survival, as well as differentiation to maintain homeostasis (Koohestani et al., 2013; Pickering, 2001; Quaranta, 2000). The ECM is a highly dynamic structure that goes through continuous remodelling under normal (e.g., wound healing) or pathological conditions. ECM originates from a broad range of cells, but fibroblasts are the major source of ECM during remodelling (Bonnans, Chou, & Werb, 2014). Notably, ECM remodelling occurs after matrix degradation and is critical for the regulation of ECM abundance, composition, structure, as well as the release of biologically active molecules such as growth factors. Matrix-degrading enzymes include matrix metalloproteinases (MMPs), adamalysins (e.g., a-disintegrin and metalloproteinases, ADAMs; and ADAMs with thrombospondin motifs, ADAMTS), meprins, plasminogen activators, and extracellular proteases such as serine proteases, cathepsins and

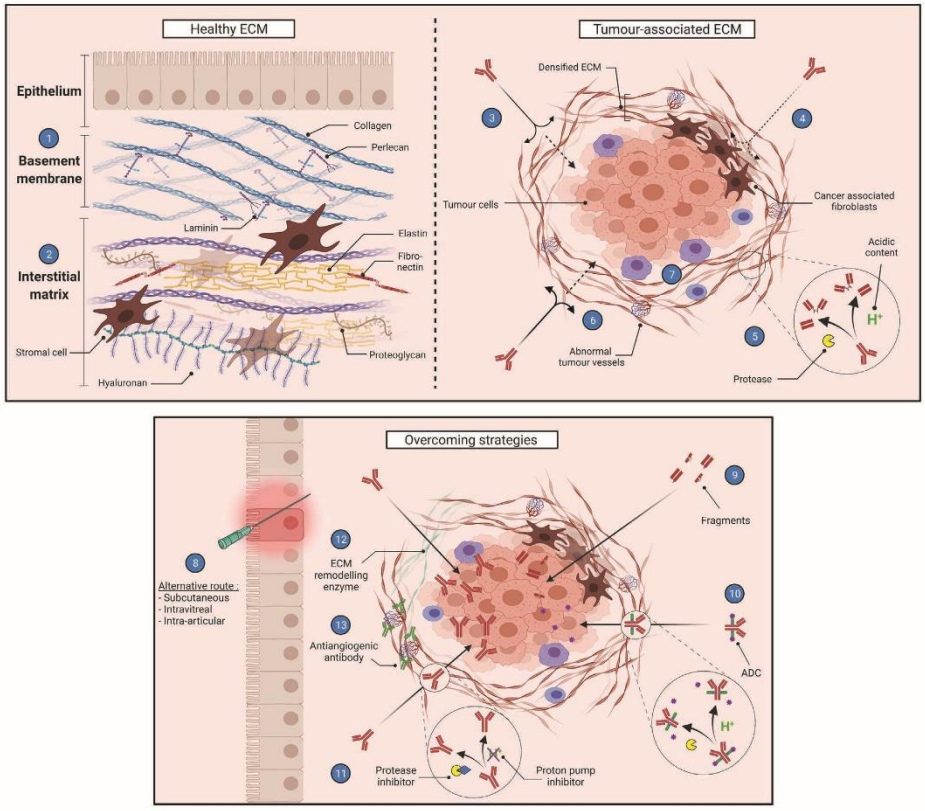

Fig. 1. Schematic representation of the extracellular matrix in healthy condition and in the tumour microenvironment as a barrier to antibodies.
A healthy ECM (left panel), located under the epithelium, consists in two distinct structures. The basement membrane (1) is composed of a very compact network of collagen fibrils and laminins that can self-associate to form a secondary network; perlecan further bridge these networks. The interstitial matrix is a looser matrix mainly composed of collagen fibrils assembled through the participation of fibronectin. Other components, including elastin, proteoglycans, and hyaluronan, contribute to the ECM organisation. Stromal cells present in the interstitial matrix interact with ECM components and growth factors. In cancers (right panel), tumour cells and cancer-associated fibroblast secrete a plethora of ECM proteins (such as collagens, fibronectin, elastin, or laminins), proteoglycans, cytokines, and growth factors. This ECM differs significantly in conformation and composition from that of normal tissues. The excessive accumulation of dense and rigid ECM results in the encapsulation of tumour cell clusters, acting as a physical barrier for antibody diffusion (3) (4). The acidic microenvironment associated with increased concentration of proteases within the ECM (5) represents a biochemical barrier degrading antibodies and reducing ADC efficacy. The increase interstitial pressure contributes to repelling antibodies (6). Finally, ECM-mediated hypoxia and low immune cell infiltrate (7) reduces antibody effectiveness and especially immunotherapy treatments. Strategies to overcome the ECM barrier (lower panel) and increase antibodies distribution and diffusion in the vicinity of the mAb target have been developed. Alternative administration routes have been considered (e.g. subcutaneous, intravitreal, or intra-articular) (8). Antibody fragments exhibit higher diffusion rate through the stroma as compared to full length antibodies (9). ADCs have been specifically designed to manipulate ECM acidic pH and high protease concentration for the efficient release of their payload (10). Combination of mAb with pH pump inhibitors or proteases inhibitors can also be considered to lower ECM-associated biochemical barrier (11). ECM remodelling strategies have been evaluated to increase antibodies diffusion and therapeutic efficacy (12). Finally, antiangiogenic mAbs can be used to restore interstitial fluid pressure and normalize anarchic blood vessels growth in order to enhance antibody delivery (13).

granzymes (Bonnans et al., 2014) (see Section 2.2). Non-proteolytic enzymes involved in ECM remodelling include hyaluronidases and heparanase (Bonnans et al., 2014). It is noteworthy that aberrant ECM remodelling is at the origin of various pathologies. For example, abnormally high ECM breakdown is observed in cardiomyopathy or osteoarthritis (Maldonado & Nam, 2013; Silva, Pereira, Fonseca, Pinto-do, & Nascimento, 2020). On the contrary, excessive ECM production and deposition without balanced degradation can lead to fibrosis in the context of chronic or severe tissue injuries (Herrera, Henke, & Bitterman, 2018). Finally, tumorigenesis is highly associated with alteration of ECM structure, composition, and remodelling.

2.1.2. The ECM as a barrier for antibody delivery and therapeutic efficacy in the context of cancer

In cancers, the ECM differs significantly from that of normal tissues as well as between molecular tumours subtypes (Fig. 1). Many solid tumours demonstrate high expression of ECM proteins such as collagens, fibronectin, elastin or laminins. Moreover, a hyaluronic acid-rich ECM characterizes few cancer types, such as pancreatic ductal adenocarcinoma (Hessmann et al., 2020). The ECM is a major component of the tumour microenvironment, accounting for up to 60% of the tumour mass. Tumour cells are themselves the source of ECM, and to an even greater extend cancer-associated fibroblasts. This desmoplastic reaction is

linked to poor patient prognosis and described as a major driver of cancer therapy resistance.

The excessive accumulation of dense and rigid ECM results in the encapsulation of tumour cell clusters, acting as a physical barrier for the diffusion of therapeutic agents. The role of ECM composition and organization on IgG penetration was assessed *in vivo* in xenograft tumour models (Netti, Berk, Swartz, Grodzinsky, & Jain, 2000). Netti et al. also showed that resistance to IgG penetration is related to tumour rigidity and collagen organization. An inverse correlation between sulphated glycosaminoglycans and IgG penetration was later reported (Davies Cde, Berk, Pluen, & Jain, 2002). 3D *in vitro* co-culture cancer models were recently developed to assess IgG distribution within the ECM (Estrada et al., 2016; Rebelo et al., 2018) and a computational (*in silico*) model was calibrated based on these data (Cartaxo et al., 2020). Such models offer a valuable and modular tool to study the influence of different components of the ECM on antibody transport without the need for *in vivo* models. The ECM barrier impairs the diffusion of oxygen, leading to highly hypoxic regions in the tumour mass. Histological analysis of tumour samples from patients highlighted that hypoxia results in increased collagen deposition and fibrosis in hypoxic regions (Shekhar, Pauley, & Heppner, 2003). The low microvessel density observed in tumours with high ECM deposition further aggravates hypoxia (Edgar, Underwood, Guilkey, Hoying, & Weiss, 2014). This hypoxia factor was used for the activation of prodrugs (Zhou et al., 2019) and the cleavage of ADC linkers (Staudacher & Brown, 2017), but can also confer resistance to ADCs. This was recently showed for trastuzumab-emtansine (T-DM1) in HER2+ breast cancer cells. Indeed, Chandran et al. demonstrated that trastuzumab internalization was reduced in hypoxic conditions due to a redistribution of phosphorylated caveolin-1 from vesicular membrane raft to the plasma membrane (Indira Chandran et al., 2020). Hypoxia is also linked to radiotherapy resistance through different mechanisms such as reduced production of oxygen radical species, reduced fixation of oxygen on DNA radical preventing its repair, or production of hypoxia-inducible factor (HIF-1) that will increase the production of antioxidant and thus buffer radiation-induced reactive oxygen species (Pouget, Georgakilas, & Ravanat, 2018; Pouget, Lozza, Deshayes, Boudousq, & Navarro-Teulon, 2015). Therefore, combating tumour hypoxia is considered as an approach to improve radioimmunotherapy effect (Boreel, Span, Heskamp, Adema, & Bussink, 2021).

Cancer immunotherapy using inhibitory Ab against the cytotoxic T-lymphocyte-associated protein 4 (CTLA4), and the programmed cell death ligand and protein 1 (PD-L1/PD-1) attracted a lot of attention due to the outstanding therapeutic response observed in patients with melanoma or non-small cell lung cancer. However, most cancers remain refractory to this approach. A major limitation of immunotherapy approaches is the need to get both drug and T cells through the ECM to reach tumour cells in order to be effective. Immune cells attracted by tumour-induced cytokine gradient are redirected when confronted with the rigid ECM that surrounds tumour cells clusters. Upon contact with the rigid ECM, lymphocytes will migrate along the fields of elevated rigidity (haptotaxis) (Hallmann et al., 2015). Salmon et al. demonstrated that in human lung tumour samples, the distribution of T cells is dictated by the aligned collagen fibres surrounding tumour islets (Salmon et al., 2012). Therefore, the reduced diffusion of antibody and immune cells throughout the ECM highly contributes to the low response of ECM-rich tumours to immunotherapy treatment.

2.1.2.1. Delivery through cancer ECM: overcoming strategies. Tumour ECM ostensibly contributes to transport resistance, and diffusion coefficient correlates inversely to the molecular hydrodynamic radius of any therapeutics (Xenaki, Oliveira, & van Bergen En Henegouwen, 2017; Yokota, Milenic, Whitlow, & Schlom, 1992). Diffusivity assays with dextrans of molecular weights ranging from 4 to 70 kDa showed a decrease of diffusion throughout the ECM for molecules with high molecular weight (Galgoczy et al., 2014). One could extrapolate this conclusion and hypothesise that antibody fragments should better diffuse in the ECM as compared to full-length IgG, however, there is a current lack of comparative studies to prove this hypothesis. Remodelling the extracellular matrix appears also as an evident strategy to improve the therapeutic efficacy of full-length antibody, ADC or radio-immunoconjugates. Eikenes et al. showed that collagenase treatment in a human osteosarcoma xenograft model resulted in a 2-fold increase in tumour uptake and improved distribution of a specific mAb (Eikenes, Bruland, Brekken, & Davies Cde, 2004). Depletion of hyaluronic acid using a pegylated recombinant human PH20 (PEGPH20) resulted in an increase in natural killer cell access to high-hyaluronic tumour cells, and enhanced antibody-dependent cellular cytotoxicity (ADCC) effect of both trastuzumab and cetuximab *in vitro* (Singha et al., 2015). This approach was translated *in vivo* and resulted in the further inhibition of tumour growth in tumour-bearing mice upon combined treatment of trastuzumab, PEGPH20 and natural killer cells when compared to control groups. Depletion of hyaluronic acid was further assessed for the unmasking of the HER2. Trastuzumab-resistant JIMT1 breast cancer cells were treated with hyaluronidase and 4-methylumbelliferone Degradation of hyaluronan and inhibition of its synthesis were achieved by treating trastuzumab-resistant JIMT1 breast cancer cells with hyaluronidase and 4-methylumbelliferone to degrade hyaluronan and inhibit its synthesis. This combined treatment resulted in the increased uptake of a radiolabelled trastuzumab conjugate ([^{89}Zr]Zr-trastuzumab) and the enhanced efficacy of trastuzumab in JIMT1 xenografts (Pereira et al., 2020).

Numerous ECM targets have been evaluated for the development of therapeutic antibodies, and especially ADCs, with the aim of overcoming ECM pitfalls by exploiting its specific features for the efficient release of the payload. Matsumura and his team described an innovative ADC that targets specifically cancer-associated fibrin using a chimeric mAb (Matsumura, 2012; Yasunaga, Manabe, & Matsumura, 2011; Yasunaga, Manabe, Tarin, & Matsumura, 2011). This chimeric ADC, targeting ECM fibrin, comprised the conjugation of the active metabolite of irinotecan (SN-38) through an acid-labile linker (ester), sensitive to the acidic tumoral microenvironment. This results in a potent antitumor activity by damaging both cancer cells and tumour vasculature (M. Yasunaga, Manabe, & Matsumura, 2011). In a comparable approach, the same group designed a similar ADC targeting collagen IV in the ECM (Yasunaga, Manabe, & Matsumura, 2013). Non-structural ECM proteins, such as Tenascin-C or fibronectin, overexpressed in various human cancers (e.g., epidermoid carcinoma, glioblastoma, non-small cell lung cancer, head and neck cancers and triple negative breast cancers), were further investigated for ADC development. A site-specific ADC was produced from a mAb targeting a splice form of tenascin C, conjugated with monomethyl auristatin E (MMAE) through a protease-sensitive linker. This linker is cleaved by proteases such as cathepsin B, which activity is increased in the tumour microenvironment. Furthermore, the acidic tumour microenvironment may facilitate the extracellular activation of these hydrolytic enzymes. Complete tumour regression was observed in 3 out of 5 mice after 4 administrations of the ADC (7 mg/kg every 3 days) in A431 human epidermoid carcinoma xenografted-BALB/c nude mice (Dal Corso, Cazzamalli, Gebleux, Mattarella, & Neri, 2017). A smaller ADC based on a small immune protein, consisting of a scFv fragment fused to the human IgE εCH4 domain, was developed to target the alternatively spliced Extra Domain A (EDA) of fibronectin (Casi & Neri, 2012, 2015; Gebleux, Wulhfard, Casi, & Neri, 2015; Perrino et al., 2014). This small immune protein was conjugated to two emtansine (DM1) molecules that can be cleaved by the high level of extracellular glutathione in the tumour microenvironment. The resulting ADC led to total remission of tumour mass in 4 out of 5 mice (5 injections at 5 mg/kg), whereas no effect was observed with the control IgG drug conjugate. In the context of refractory and ECM-rich cancers, these studies highlight that the ECM diffusion barrier can be overcomed by targeting ECM non-internalising targets and taking advantage of ECM extracellular stimuli for a sustained ADC payload

release (Joubert, Beck, Dumontet, & Denevault-Sabourin, 2020; Joubert, Denevault-Sabourin, Bryden, & Viaud-Massuard, 2017).

2.1.3. ECM and administration of antibody through the skin

The skin is composed of an outer avascular layer – the epidermis – a core connective tissue layer – the dermis – and finally a subcutaneous layer – the hypodermis (Arda, Goksugur, & Tuzun, 2014). Antibodies exhibit low skin permeability when applied topically (Bruno, Miller, & Lim, 2013). It may be explained by the hydrophobic nature of the keratin, contrasting with the hydrophilic and polar features of antibodies, limiting their diffusivity through the skin. In addition, antibodies exhibit low cellular and transcellular diffusion capabilities. Thus, high doses of antibody may be required by the trans-appendageal route to achieve local therapeutic response. Additional hurdle comprises the nature of products for topical delivery – gel or cream are often intended for topical skin application –, which will require complex formulation engineering to maintain antibodies stability (Stevens & Cowin, 2017). Overall, antibody treatment of lesions with intact skin epithelium remains challenging. New technologies investigate cell-penetrating peptides, physical penetration enhancer or injection with microneedles to help antibody cross the skin barrier (Francis & Thomas, 2017; Gautam et al., 2016; Geh et al., 2019; Lee, Park, & Kim, 2018; Oberli, Schoellhammer, Langer, & Blankschtein, 2014), but none of them already achieved clinical success.

Subcutaneous injection of antibody is particularly attractive, as it has been shown to be safe and valuable for both patients and healthcare workers (Sanchez-Felix et al., 2020). Currently, at least one-third of FDA-approved recombinant antibodies are administered by subcutaneous injection and therefore face this barrier for Ab distribution and efficacy (Viola et al., 2018). The subcutaneous injection of antibodies is predominantly used in immunology for the treatment of chronic diseases such as rheumatoid arthritis or plaque psoriasis, targeting interleukins and their receptors, thus the subcutaneous route is mostly intended for antibody with a systemic action (Sanchez-Felix et al., 2020). When considering a subcutaneous administration, the formulated drug is delivered into the hypodermis interstitial space. The hypodermis is composed of adipose tissue, unevenly distributed blood and lymph vessels, fibroblasts, macrophages and an ECM network rich in collagen, elastin and glycosaminoglycans (Arda et al., 2014). In this context, the ECM constitutes the first physical barrier for subcutaneous delivery, as Ab must pass the ECM to reach the vascular compartment (Viola et al., 2018). Collagen fibrils are positively charged at physiological pH while hyaluronic acid and chondroitin sulfate, two major glycosaminoglycans of the hypodermis ECM, are negatively charged. Despite collagen and glycosaminoglycans having opposite charges, the hypodermis interstitial space is negatively charged due to the presence of negatively charged proteoglycans, rendering the transport of negatively charged drug more rapid thanks to electrostatic repulsion (Viola et al., 2018). One should note that most mAb have an isoelectric point (pI) between 7 and 9, meaning that mAbs are generally positively charged at physiological pH. Bumbaca Yadav et al. evaluated the impact of the variable region charge ($+3/+5$ versus -4) on mAb subcutaneous bioavailability in Cynomolgus monkeys. They reported that positively charged mAb present a reduced subcutaneous bioavailability by 31%, while their negatively charged counterpart demonstrates enhanced subcutaneous bioavailability up to 70% (Bumbaca Yadav et al., 2015). Furthermore, positively charged mAb ($pI = 7.3$; 9.1) showed electrostatic interaction with negatively charged ECM components in another study, leading to 50–60% unrecoverable/tissue bound mAb. Co-injection with hyaluronic acid resulted in the recovery of 70% of soluble Ab, highlighting that hyaluronic acid does compete with mAb binding sites and that such formulation strategy enhances the subcutaneous bioavailability of positively charged mAb (Mach et al., 2011). The ECM negative charges are also responsible for interaction with water molecules and consequently impacts the ECM hydraulic conductivity and interstitial fluid. Because of the latter, subcutaneous injection volume is limited to 2 mL in humans.

2.1.3.1. Subcutaneous delivery: overcoming strategies. To facilitate subcutaneous bulk fluid flow and increase the dispersion and absorption of drugs, a recombinant human hyaluronidase PH20 (rHuPH20) was used to locally and transiently degrade hyaluronan (Locke, Maneval, & LaBarre, 2019). Clinical studies confirmed the potential of this approach to improve the pharmacokinetic profiles of co-administered mAb (e.g. rituximab, trastuzumab, cetuximab) compared to subcutaneous injection without rHuPH20 (Printz et al., 2020; Shpilberg & Jackisch, 2013; Styles et al., 2019). Another study achieved a comparable body exposure to trastuzumab after subcutaneous injection at 8 mg/kg as compared to intravenous injection at 6 mg/kg (Wynne et al., 2013). These studies led to the FDA approvals of rHuPH20 in combination with rituximab in 2017, trastuzumab in 2019 (Locke et al., 2019), and trastuzumab plus pertuzumab in 2021 (Tan et al., 2021). The hypodermis interstitial fluid is mostly composed of plasma water with only about 50% of its protein content. Among these proteins, proteases play a major role in antibody catabolism and therefore reduces antibody subcutaneous bioavailability (see Section 2.2). Once in the hypodermis interstitial space, antibody will be absorbed by convection into lymphatic vessels as their large size prevents them from diffusing directly into the bloodstream. Such knowledge further underlines the relevance of subcutaneous injection for antibody targeting the lymphatic system like interferons or interleukins.

2.1.4. ECM and retinal/eyes delivery of antibody

The prevalence of age-related posterior eye diseases, which most frequent example being age-related macular degeneration, will reach several hundred billion in the next decades (Wong et al., 2014). The delivery of drugs to targets in the retina is challenging and various routes of administration have been considered and investigated to circumvent the complexity of ocular anatomy and physiology.

The anterior part of the eye comprises the cornea, conjunctiva, anterior chamber, ciliary body, aqueous humour, lens and the lachrymal system, which forms a static and dynamic barrier to efficiently prevent foreign particles getting access into the eyes. As a result, non-invasive topical application, mainly through eye drops, leads to a low bioavailability with less than 3% of topically administered drug reaching the vitreous humour and even less in the posterior part of the eye (Boddu, Gupta, & Patel, 2014; Hughes, Olejnik, Chang-Lin, & Wilson, 2005). Several mAbs have been considered for local ocular application (Hu & Koevary, 2016; Ottiger, Thiel, Feige, Lichtlen, & Urech, 2009), with a clinical translation to humans that remains elusive and may require the use of penetration enhancers (see Section 3.2.1) (Thareja, Hughes, Alvarez-Lorenzo, Hakkarainen, & Ahmed, 2021). The posterior part is composed of the vitreous humour, retina, sclera and choroid. The cornea is the transparent front part of the eye, continuous with the sclera, which is composed of five layers comprising epithelium, stroma and endothelium. Since the cornea is negatively charged, it represents a primary barrier to topical administration using eye drops, especially for negatively charged drugs (Kim, Chiang, Wu, & Prausnitz, 2014). The other external parts of the eye, including conjunctival epithelium, sclera and choriocapillaries, represent absorption barriers for macromolecules coming from the systemic circulation with permeability dropping significantly for high-molecular weight drugs. In addition, the intra-ocular environment is protected from the outside by the blood-aqueous barrier and blood-retinal barrier. The blood-aqueous barrier is composed of the iris epithelium, iridial capillaries, ciliary muscle capillaries, and non-pigmented ciliary epithelium while the blood-retinal barrier located in the posterior part of the eye consists of retinal pigment epithelium and the endothelium of the retinal vessels. The two barriers comprise inter-cellular tight junctions restricting drug transfer between the eye and blood circulation (see Section 3.3) (Del Amo et al., 2017;

Thrimawithana, Young, Bunt, Green, & Alany, 2011), especially of proteins and other large molecules.

2.1.4.1. Delivery to the eyes: overcoming strategies. A major step forward in the treatment of retinal diseases was local delivery of antibodies, mainly targeting VEGF, in the internal parts of the eye, by intravitreal injection. It provides a high amount of antibody in the retina and vitreous compartments, while partly protecting the eyes and the rest of the body from antibody exposure. However, the volume of such injection should not exceed 0.1 or 0.2 mL in the anterior chamber or vitreal body, respectively, necessitating specific antibody formulation. Once injected, antibody diffusion is conditioned by the intrinsic characteristics of the vitreous humour, which is mainly composed by a hydrophilic matrix made of water, collagen and hyaluronic acid. The latter being negatively charged, it will restrict the diffusion of positively charged molecules (Q. Xu et al., 2013) (see Section 2.1.1). Bevacizumab (full-length IgG1) and ranibizumab (Fab fragment), two approved therapeutic mAb against age-related macular degeneration are both negatively charged under physiological conditions and will diffuse slowly through the vitreous cavity because of their molecular weight (Crowell et al., 2019). On the contrary, aflibercept (a fusion protein) which has a mild positive charge, will exhibit altered pharmacokinetic properties (Holash et al., 2002). The rheological properties of the vitreous humour are not homogeneous. Changes in the composition occur according to the position in the orbital cavity; the posterior part of the vitreous humour in contact with the retina has more collagen and hyaluronic acid that makes it less fluid-like. Age-related liquefaction of vitreous humour will also affect drug diffusion, especially for those of high molecular weight (Laude et al., 2010). Elimination of drugs after intravitreal injection might occur either by metabolism or by excretion through the systemic circulation. Anti-VEGF mAbs appear preserved from metabolism or degradation in the orbital cavity (Del Amo et al., 2017), but will be eliminated through diffusion to the aqueous chamber (Gal-Or et al., 2016) or the retinal pigment epithelium (Del Amo et al., 2017). Blood-ocular barrier does not allow permeation of antibodies from the systemic circulation, making the intravitreal injection a standard treatment achieving therapeutic drug levels in the retina. However, this invasive route of administration is associated with specific challenges including the crucial necessity to guarantee the absence of ocular toxicity. This requires the development of specific formulations (Elsaid, Jackson, Elsaid, Alqathama, & Somavarapu, 2016), which will allow prolonged action, eventually reducing injection regimen and improving tolerability.

2.1.5. ECM and intra-articular (IA) delivery of antibody

Joint inflammation is one of the leading causes for progressive motor disability. Osteoarthritis and rheumatoid arthritis are the most common forms of joint degeneration with high incidence requiring long-term therapeutic care (Lawrence et al., 1998). The main symptoms of these diseases are joint inflammation, pain and cartilage destruction. Standard care includes systemic administration of analgesic and anti-inflammatory agents, including anti-TNFα antibody (infliximab, etanercept, adalimumab) and anti-IL1β mAb (canakinumab). However, their chronic systemic administration regimen is frequently associated with substantial side effects (Tarner & Muller-Ladner, 2008). Synovial joints, most often affected by osteoarthritis and rheumatoid arthritis, are delimitated by a fibrous capsule and ligaments. They comprised bone endings covered by hyaline cartilage. The cartilage is an avascular tissue, composed of chondrocytes embedded in a highly anionic ECM, which is impermeable to molecules with a molecular weight >50 kDa, depending upon their charge and conformation (Foy & Blake, 2001). Because cartilage is avascular, it is inefficiently targeted by drugs administered systemically that must first reach the synovial fluid and then diffuse through the cartilaginous ECM. The synovial fluid mediates the supply of nutrients to the cartilage. Synovial fluid is mainly composed of hyaluronic acid and lubricin providing lubricating and frictionless mobility of the joint. To enter the joint from the systemic vasculature, a drug must pass through the capillary endothelium of the synovium, the ECM of the synovial intima and the macrophage-like synoviocytes composing the synovial membrane. Both cellular layers are highly fenestrated facilitating the directed exit of drug from the capillaries and the entry into the synovial fluid cavity. The consequence of this small diffusion barrier is a high synovial diffusion of molecules with a molecular weight <10 kDa. For larger molecules, fenestration will dictate a size-dependent restriction on the rate of passage that is 10 times less for IgG as compared to the one of albumin (Kushner & Somerville, 1971). During inflammation, capillary and synovial membrane permeabilities will increase, enhancing the entry of macromolecules in the synovial joint. This is exemplified by the increase in protein content in the synovial fluid from rheumatoid arthritis patients (Furst et al., 1999). The duration of residency in the joint of a therapeutic agent is dictated by the equilibrium between the rate at which the drug reaches and is cleared from the synovial fluid. On the contrary, the removal of macromolecules from joints, mainly driven by lymphatic drainage, is independent of size. Several studies tried to evaluate half-lives of various macromolecules including antibodies within the joints. Values reported ranged from 1–13 h for albumin, more than 25h for hyaluronic acid, 72h for gamma-globulin and 8–12 h for unspecified IgG (Scully et al., 2009). Joint inflammation will accelerate synovial clearance rate (Weinberger & Simkin, 1989). Indeed, for anti-inflammatory antibody, clinical PK data revealed half-lives of approximately 2–4 h (Evans, Kraus, & Setton, 2014).

2.1.5.1. Delivery to the joints: overcoming strategies. The IA administration is attracting as point-of-care therapy from both economics and patient's perspectives. It will achieve high drug concentration in the diseased area while limiting systemic exposure. Eventually, this will lead to a dose reduction and therefore minimization of costs and side effects. Despite these promising features, IA delivery for recombinant antibodies is rare; specific inhibition of the pro-inflammatory cytokines IL-1β and TNFα using anakinra, canakinumab or infliximab (both full-length and scFv fragment) delivered by IA have been clinically tested without conclusive results – which can be explained by the specific prevailing physiologic and anatomic conditions of the joint. The rapid clearance of antibody from the inflamed joint is a major limitation for therapeutics, requiring frequent injections that may be associated with unwanted side effects, patient discomfort and even morbidity. Specific formulations enabling controlled release over time are under consideration for injectable antibody in the joint. These include mainly natural polymers/lipids formulated as hydrogels as described for the anti-TNFα infliximab (Chen et al., 2020) and micro/nano particles (Eswaramoorthy et al., 2012) or *in situ* implants (Lambert & Peck, 1995), which have been used for other therapeutic proteins. However, such strategies do not come without disadvantage; indeed, controlled release formulations are associated with loss of bioactivity mainly due to stability issues (Koerselman et al., 2020). Finally, depending on their size, nanospheres might induce inflammatory reaction that may ultimately accelerate cartilage injury and even induce fibrotic processes (Kang & Im, 2014).

2.2. Proteases

Proteases are catalytic enzymes promoting peptide cleavage of proteins necessary for protein maturation, catabolism and the generation of amino acids. Their molecular pattern encompasses small enzymes (20–30 kDa) to sophisticated protein complexes, like proteasomes (0.7–6 MDa) (Lopez-Otin & Bond, 2008). Proteases are distributed in all living organisms including plants, animals and microorganisms such as bacteria and viruses. In humans, they constitute one of the largest families of enzymes with 2% of the genome encoding proteases. Proteases are classified into six different groups based on the specificity of their active site: aspartate-, cysteine-, glutamate-, metallo-, serine- and threonine-proteases. They can be found in all tissues with both

intra- and extra-cellular site of action. At physiological state, these enzymes are critically involved in the control of multiple biological processes including digestion, cellular communication and proliferation, haemostasis, immunity, wound healing and apoptosis. According to the irrevocability of their mode of action and the pleiotropic functions in which they are involved, proteases need to be tightly regulated. Several mechanisms control their production and secretion, including regulation of biosynthesis, activation of inactive precursors known as proenzymes or zymogens, and the binding of endogenous inhibitors and cofactors (Vasiljeva, Menendez, Nguyen, Craik, & Michael Kavanaugh, 2020). This allows the protease/anti-protease balance to be neutral, except in the gastro-intestinal tract where proteases participate to nutrients digestion, requiring sustained activation. The activation of resident immune cells and the recruitment of leukocytes generate tissue damage and extracellular matrix destruction resulting in a dysregulation of protease homeostasis. Imbalance in the regulation of proteases/proteases inhibitors plays a major role in the development of pathological conditions such as cancer, inflammatory, cardiovascular, neurodegenerative, bacterial, viral and parasitic diseases (Lopez-Otin & Bond, 2008). For example, in inflammatory bowel diseases, inflammation characterized in particular by a neutrophilic and macrophages infiltrate, leads to a highly proteolytic mucosal microenvironment. Neutrophil proteases (elastase and cathepsin G) and metalloproteinases (MMP3, MMP12, and MMP9) are highly up regulated in the inflamed gut (Baugh et al., 1999). In acute respiratory distress syndrome, significant elastase levels have been reported (Hashimoto et al., 2008). In chronic obstructive pulmonary disease (Pandey, De, & Mishra, 2017; Thulborn et al., 2019) and cystic fibrosis (Oriano et al., 2019; Witko-Sarsat et al., 1999), an increase in neutrophil-related proteases activity is observed and more particularly during infectious exacerbations contributing to the decline of respiratory function (Chalmers et al., 2017). In cancer, protracted activation of extracellular proteases, with MMPs representing the most prominent family associated with tumorigenesis, provides additional survival advantages to cancer cells (Kessenbrock, Plaks, & Werb, 2010). Proteases promote angiogenesis, impair anticancer lymphocytes functions and facilitate metastasis through tissue remodelling.

Proteases may be considered as a biological barrier complicating the administration of therapeutic proteins especially in disease conditions. Extracellular proteases such as neutrophil proteases, MMPs or bacteria secreted proteases (Dunnhaupt, Kammona, Waldner, Kiparissides, & Bernkop-Schnurch) have the ability to cleave endogenous immunoglobulins (Brezski & Jordan, 2010; von Pawel-Rammingen, Johansson, & Bjorck, 2002). Several studies have demonstrated such proteolysis both *in vitro* and *in vivo*, hypothesizing that bacterial-secreted or tumour-associated proteases may act as virulence factors to escape the immune response (Plaut, Wistar Jr., & Capra, 1974; Ryan et al., 2008; Senior & Woof, 2005). The proteolytic inactivation of therapeutic antibodies is under-appreciated as a contributor to therapeutic response evasion, but several studies highlighted the critical role of proteases on mAb PD. Proteases (MMP-3, MMP-12 and HNE) affect the integrity of anti-TNFα mAb and compromise their therapeutic capacities in comparison with intact mAb (Biancheri et al., 2015; Curciarello et al., 2020). Proteolysis of mAbs (IgG1 and 4) by MMPs (MMP-12) and IdeS has been shown to be dependent on the incubation time (Deveuve, Lajoie, Barrault, & Thibault, 2020), with long time exposition to proteases being responsible for a decreased efficacy of the anti-HER2 antibody pertuzumab (Hsiao, Fan, Jordan, Zhang, & An, 2018; Kinder et al., 2013). A single proteolytic cleavage in the lower hinge of a humanized IgG1, trastuzumab, or pertuzumab, by MMP-12 also led to a loss of one of the Fc fractions, reducing its effector activity via the immune system and therefore its anti-tumour efficacy *in vivo* (Fan et al., 2012; Hsiao et al., 2018; Zhang et al., 2015).

2.2.1. Proteases: overcoming strategies

The identification of proteolytic cleavage sites could allow the development of mutant antibodies protected against proteases. Indeed, the fact that IgG2 are resistant to MMPs contrary to IgG1 has been associated with differences in amino-acid sequence of the lower hinge region. Specific mutations in the CH2 domain result in resistance to MMPs with restored *in vitro* complement-dependent cytotoxicity and antibody-dependent cellular phagocytosis activities. Thus, engineered antibodies that are resistant to hinge proteolysis hold promise to maintain potent effector functions (Kinder et al., 2013). Another strategy would rely on the use of rescuing antibodies, which bind to hinge neo-epitope generated after proteolytic cleavage and restore the effector functions of the protease-sensitive antibody. This was elegantly demonstrated by Fan et al. with an antibody targeting the hinge neo-epitope of trastuzumab generated by MMP or IdeS proteolysis. Fan et al. demonstrated both *in vitro* and *in vivo* that the rescuing antibody restored antibody-dependent cellular cytotoxicity function of trastuzumab as well as the recruitment of immune effector cells into the tumour microenvironment (Fan et al., 2015). *In vitro*, co-incubation with specific protease inhibitors inhibits antibody proteolysis (Curciarello et al., 2020). *Ex vivo*, TNFα-neutralizing function was restored after incubation of anti-TNFα mAb (infliximab and adalimumab) with MMP inhibitors in the sera from patients with inflammatory bowel disease (Biancheri et al., 2015). These co-treatment strategies with protease inhibitors may represent an interesting way to maintain the antibody functionality in inflammatory contexts. However, numerous proteases coexist in tumour/inflammatory/infected microenvironments complicating the choice of inhibitors as well as their optimal concentration that would need to be defined and adjusted to each pathological context.

2.3. Other extracellular barriers

2.3.1. Mucus and oral or airway administration of antibody

Mucus is a viscoelastic hydrogel located in the airways, the eyes, the gastrointestinal, urogenital and reproductive tracts, and the peritoneal surface of intra-abdominal organs. Continuously produced and secreted by mucous cells, it coats the luminal surface of these different compartments acting as a lubricant and maintains a hydrated layer above the epithelial cells (Leal, Smyth, & Ghosh, 2017). On exposed surfaces, mucus also provides a barrier to pathogens and foreign substances including environmental particles (Lai, Wang, Wirtz, & Hanes, 2009). Mucus is mainly composed of water (>95%), mucins, proteins, DNA, cells and cellular debris (Leal et al., 2017). Mucins are the primary non-aqueous component of mucus. They give to the mucus its three-dimensional mesh network structure mainly stabilized by covalent and noncovalent interactions, including hydrophobic, electrostatic, hydrogen bonds, or other specific binding interactions (Creeth, 1978; Lieleg & Ribbeck, 2011). The homeostasis of its components is highly interdependent and govern mucus main physicochemical properties, as pore size, viscoelasticity, pH, ionic strength and charge (Leal et al., 2017). For example, viscosity may be modified by the hydration, pH level and salt, proteins and ionic concentration (Frohlich & Roblegg, 2014).

It is obvious to imagine mucus acting as a barrier to the transport of drugs and therapeutic molecules administered through oral or inhaled route (Bansil & Turner, 2006; Leal et al., 2017). However, several studies described endogenous immunoglobulins behaviour in respiratory, GI and cervico-vaginal homeostatic mucus suggesting that their diffusion was barely altered in mucus (Olmsted et al., 2001). Intriguingly, the mucus-antibody interplay at mucosal surfaces also acts as a new defence mechanism of antibody during infections. Indeed, pathogen-coated antibodies form weak and transient Fc-mucins bonds – via sugars– and trap pathogens, thereby preventing pathogens to infect epithelial cells and facilitating their physical elimination through mucociliary clearance (Schaefer & Lai, 2021; Wang et al., 2017; Yang et al., 2018). The “muco-trapping function” of antibodies-coated to pathogens has been nicely exemplified with virus-like particles (VLP) of influenza-binding IgG, and the anti-Ebola antibody cocktail ZMapp bound to Ebola VLP in fresh airway mucus from healthy adult. Overall,

"muco-trapping" function of antibody appears as a universal effector function for IgG in major mucus and apply to other immunoglobulin subclasses and extracellular matrix. However, muco-trapping property of antibody implies on a subtle balance partly depending on the rapid IgG diffusion within mucus and binding to pathogen. To date, the capacity of antibody Fc-mucin to crosslink and immobilize pathogen has never been studied in pathological conditions, when mucus is altered. Indeed, in broncho-obstructive diseases such as cystic fibrosis and chronic obstructive pulmonary disease, overproduction of mucus is associated with dehydration and a shrinkage of pore size (Duncan et al., 2016). In cancers, mucins overproduction and heterogeneity has been associated to tumour progression (Hukill & Vidone, 1965). This resulted in modifications of architectural structure and viscoelasticity of the mucus present in the cancer microenvironment and has been described in the context of colonic and gastric adenocarcinoma (Hollingsworth & Swanson, 2004). Inflammatory disorders such as inflammatory bowel disease may also impact mucus architecture secondary to a modification of mucins' glycosylation changing viscoelastic properties, resistance to bacterial degradation, and adhesion (Corfield, Carroll, Myerscough, & Probert, 2001). In summary, mucus structure is often abnormal in various pathological conditions and may impair antibody diffusivity, as previously described for other therapeutics (Braeckmans, Peeters, Sanders, De Smedt, & Demeester, 2003; Ensign et al., 2012; Maisel et al., 2016).

2.3.1.1. Mucus: overcoming strategies. The development of antibodies able to diffuse through the mucus requires an exhaustive knowledge of its structure and its physicochemical properties both in physiological and pathological contexts. Depending on the location of the antibody target, it may be necessary to explore the impact of formulations or co-administrated treatments to improve their deposition and define their efficacy after administration in the nasal, lung and oral mucosa. When the target is located into the mucus or in the organ lumen, formulations conferring mucoadhesive properties on the treatment and prolonging its local stability may be preferred. For example, encapsulation with polymeric non-charged and lipophilic nanoparticles optimizes mucoadhesion, cellular uptake, immune system interactions and cell targeting (Ensign, Cone, & Hanes, 2012). Conversely, when the target is located under the layer of mucus, strategies improving mucosal permeability of drugs must be favoured. These strategies may include the use of mucolytic treatments such as recombinant human deoxyribonuclease (rhDNase) (Macierzanka et al., 2014; Sanders et al., 2000) or N-Acetyl cysteine (Suk et al., 2011; Vukosavljevic et al., 2017) as co-treatments. Nanoparticle-based systems may also be of particular interest allowing protection of drug from degradation mechanisms and the control of surface properties to avoid adhesion or steric hindrance (Dunnhaupt, Kammona, Waldner, Kiparissides, & Bernkop-Schnurch, 2015; Ensign, Cone, & Hanes, 2012; Lai, Wang, & Hanes, 2009). Poly(lactic-co-glycolic acid) PLGA or poly(ethylene glycol) PEGylation have shown their effectiveness to enhance mucus transport of drugs in gastric, intestinal, vaginal, cervicovaginal, respiratory animal mucus and in CF sputum (Suk et al., 2009; Tang et al., 2009; Wang et al., 2008; Yu et al., 2012). Chitosan, a cationic polymer, is also used for oral and nasal drug applications in particular to improve the administration of nasal vaccines (Csaba, Garcia-Fuentes, & Alonso, 2009). Presently, we do not know if it would be relevant to investigate such strategies, since the impact of the pathological context on antibody diffusivity and muco-trapping function of mAb in the mucus remains unknown.

2.3.2. pH and oral administration of antibody

The gastrointestinal tract is essential in digestion and absorption of nutrients while, as other mucosae, it must defend the host against exogenous materials and microorganisms. Consequently, it harbours several non-cellular barriers, which renders oral administration of antibody challenging. After oral administration, drugs are conducted from the mouth to stomach, small intestine and finally conveyed to the colon and expelled into faeces. Each gastrointestinal segments exhibit specific environmental conditions, which may alter antibody efficacy. In the stomach, antibody is subjected to degradation by pepsin, which is activated by the acidic pH (pH=2). The acidic pH will also promote irreversible changes in protein conformation (Lopez et al., 2019). In the small intestine, antibody will be exposed to proteases activated by pH ranging between 6.0–7.3 like trypsin, chymotrypsin, carboxypeptidase, and elastase (see Section 2.2).

2.3.2.1. Oral delivery: overcoming strategies. Therapeutic proteins and peptides are poorly resistant to the acidic and proteolytic content of the stomach, thus protection strategies have been envisioned to overcome these barriers and include enteric coating (Crowe et al., 2019) and encapsulation in nanoparticles (Tashima, 2021). Interestingly, formulations based on coated mini capsules were engineered for the local treatment of inflammatory bowel disease with anti-TNFα antibody and led to high intestinal and colon concentrations with limited systemic exposure (Crowe et al., 2019). Thus, mini capsules may have a huge potential to improve the management of inflammatory bowel disease, which currently require chronic parenteral administration associated with deleterious systemic side effects. Omeprazole, a well-known proton pump inhibitor neutralizing stomach acidity, has been proposed in combination with anti-CD3 mAb foralumab and muromomab, in the treatment of type 2 diabetes and ulcerative colitis, respectively (Boden et al., 2019). Larger studies are required to confirm the benefits of the combination.

2.3.3. Biofilm and anti-infectious antibody

A key virulence factor associated with the development of chronic infections is the ability of pathogens to build organized cells communities (Costerton et al., 2003; Hoiby, Ciofu, & Bjarnsholt, 2010). Biofilms are three-dimensional structured communities of pathogens encased in a self-produced extracellular matrix (Neu et al., 2010), which can adhere on both inert and biotic surfaces (Bowen, 2016; Veerachamy, Yarlagadda, Manivasagam, & Yarlagadda, 2014). Biofilms are mainly composed of an extracellular polymeric substance (del Aguila, Longstreth Jr., McGuire, Koepsell, & van Belle, 2003) including exopolysaccharide (Ciornei et al., 2010), extracellular proteins (Fong, Karplus, Schoolnik, & Yildiz, 2006; Tielker et al., 2005) and extracellular DNA (eDNA) (Montanaro et al., 2011). The importance of the structural biofilm complexity as pathological obstacle to antimicrobial therapeutics is now widely recognized. This recalcitrance is a direct consequence of the physical and biological properties of biofilm. Exopolysaccharides represent 90% of biofilm's biomass, which composition is continuously evolving and differs depending on the bacteria species, and form a diffusion-limiting barrier impairing the penetrance of therapeutics and binding to their respective targets. Thanks to an electrostatically charged net, biofilm is also able to either repulse or trap antimicrobial peptides and proteins (Anaya-Lopez, Lopez-Meza, & Ochoa-Zarzosa, 2013) contributing to its antimicrobial resilience (Koo, Allan, Howlin, Stoodley, & Hall-Stoodley, 2017). Furthermore, a large array of molecules released near the biofilm enable chemical inactivation or degradation of anti-microbial agents (Hall & Mah, 2017; Lewenza, 2013; Stewart & Franklin, 2008). Biofilm also reduces the efficiency of the immune response, especially phagocytosis mediated by macrophages or neutrophils. Target-mediated recognition of microbial molecular pattern by Ig activates phagocytes, which have been recruited to the site of infection, in a phenomenon referred as opsonophagocytosis. However, the steric hindrance induced by exopolysaccharide limits the engulfment of pathogens by phagocytes, thus impeding microbial clearance (Campoccia, Mirzaei, Montanaro, & Arciola, 2019). Therefore, bacteria embedded in biofilm are protected against endogenous antibody-mediated opsonophagocytosis. Finally, in addition to its role as a barrier for penetration, reduced efficacy of antimicrobial treatment against biofilm is also due to the status of cells present inside the biofilm: a large proportion is in a status of reduced metabolism (Wood,

Knabel, & Kwan, 2013) whereas most anti-microbial agents target active cellular processes, including cell wall formation, virulence factors expression, translation or transcription (Mah & O'Toole, 2001). Altogether, these processes, associated with an important heterogeneity of phenotype and genotype of cells embedded in biofilms (Becker, Hufnagle, Peters, & Herrmann, 2001; Besharova, Suchanek, Hartmann, Drescher, & Sourjik, 2016; Cho & Caparon, 2005; Stewart & Franklin, 2008), promote the development of resilient pathogenic populations (Crabbe, Jensen, Bjarnsholt, & Coenye, 2019). Up to now, no demonstration has been provided on the impact of biofilm on antibody ability to reach their pathogenic target. It would be important to take into account the biofilm barrier in the development of anti-infectious antibody.

2.3.4. Tumour blood flow and interstitial pressure

Role of branching and expansion of blood vessels in tumour growth do not need to be proved any longer. However, rapid growth of tumour cells is often unsynchronised from effective vasculature growth, which results in non-vascularised tumour areas (Durand & Aquino-Parsons, 2001). This lack of tumour blood flow near new tumour areas can hinder drug delivery and in particular therapeutic antibodies as the majority of immunotherapies are administered systemically. Thurber and Weissleder in 2011 (Thurber & Weissleder, 2011) have shown that antibody uptake depends on both tumour vasculature and blood flow using sub-saturating antibody concentrations, and on the number of receptors using saturating antibody concentrations. Decrease in vessel diameters, as branching progresses, induces a decrease of blood pressure and blood flow. Moreover, unorganised vessel structure in the tumour microenvironment is associated with blood flow resistance due to vessels tortuosity (irregular network structure), loose of fluidity for red blood cell (hypoxia, acidosis) and retrograde or intermittent blood flow due to anarchic vessel growth. Drug transport by the systemic route is, as a result, considerably impeded (Jain, 1988). A normalization of the blood flow velocity may help to recover a "normal" diffusion. Gao and his team (Gao et al., 2020) have shown that an increase of blood flow velocity enhanced pressure gradient between vessels and interstitial tissue, thereby promoting diffusion of nanoparticles from the blood to the interstitial domain. On the opposite, interstitial fluid pressure in tumour microenvironment is higher than in normal tissue (Gao et al., 2020; Wu et al., 2014). Indeed, an easy transfer of macromolecules from the blood to the interstitial space due to fewer tight junctions and lack of pericyte coverage lead to high pressure (Kerbel, 2006). In addition, a lack of lymphatic function in tumour system reduces the expulsion of fluid and result in high pressure (Padera et al., 2002). In addition to the defective blood and lymph vessels, the increased contractility of cancer-associated fibroblasts and a dense ECM compartment both contribute to the increase and persistence of high interstitial fluid pressure in tumours (Eikenes, Tari, Tufto, Bruland, & de Lange Davies, 2005; Heldin, Rubin, Pietras, & Ostman, 2004). In the context of pancreatic adenocarcinoma, high hyaluronic acid content in the microenvironment has been correlated to increased water molecules retention in the stroma and increased interstitial fluid pressure (Jacobetz et al., 2013). Interstitial fluid pressure further inhibits the transport of drugs from the blood vessels (Ferretti, Allegrini, Becquet, & McSheehy, 2009). Heine et al. (2012) reported a heterogeneous distribution of an anti-EpCAM MOC31 mAb in subcutaneous xenografts with only few regions in the vicinity of perfused blood vessels positive for the mAb. The reduced penetration was correlated to the observation of immature blood vessels together with sparsely existing lymph vessels and an elevated interstitial fluid pressure (three time higher as compared to normal tissue).

2.3.4.1. Blood flow and interstitial pressure: overcoming strategies. Strategies to lower tumour interstitial fluid pressure and regulate blood flow should be considered in order to improve antibody distribution and therapeutic effectiveness. Actually, antiangiogenic mAbs (anti-VEGF or anti-VEGFR2) were used to restore interstitial fluid pressure and normalize anarchic blood vessels growth in order to enhanced small-drug penetration in tumour (Jain, Tong, & Munn, 2007; Tong et al., 2004). The relevance of this strategy in the improvement of anti-cancerous mAb remains to be clinically evaluated.

3. FcRn and cellular barriers

3.1. The role of FcRn

Recombinant antibodies need to cross different cellular barriers to reach the organs in which their target is expressed. All these barriers have in common the expression of the neonatal Fc receptor (FcRn) described by Brambell in 1964 (Brambell, Hemmings, & Morris, 1964) and known since then as a major player in IgG half-life and biodistribution. By analogy to IgG, mAb (and Fc-conjugated protein) PK/PD is also submitted to FcRn control. FcRn is composed of a heavy chain in non-covalent association with β2-microglobulin. The heavy chain is made up of 3 extracellular domains (α1, α 2 and α 3), a transmembrane domain and an intracellular tail. FcRn is an intracellular receptor (over 90%) expressed in the cellular early endosomes (Antohe, Radulescu, Gafencu, Ghetie, & Simionescu, 2001; Ober, Martinez, Vaccaro, Zhou, & Ward, 2004). It is transiently expressed on the cell surface during endosome fusion to the membrane. Indeed, only about 4% of the FcRn pool is expressed at the surface with 2% FcRn non-internalisable by cells (D'Hooghe, Chalmers, Heywood, & Whitley, 2017). FcRn allows the recycling of its two ligands, IgG and albumin, in order to prolong their half-life in blood and tissues. Following their entry into the cell by pinocytosis, monomeric IgG (comprising mAb) and albumin bind to FcRn in a pH-dependent manner, at acidic pH (6.0–6.5) in early endosomes. This pH-dependent binding is mediated by the interaction of the FcRn with residues located in the CH2–CH3 hinge region of the IgG (Kim et al., 1999; Oganesyan et al., 2014; Raghavan, Bonagura, Morrison, & Bjorkman, 1995). IgG are then released at neutral pH into the circulation (Ober et al., 2004). This phenomenon confers protection of IgG from lysosomal degradation and prolongs their half-life (Ko, Jo, & Jung, 2021). The same mechanism is also involved in FcRn-dependent IgG transcytosis in polarized cells or across various tissues (Antohe et al., 2001; Dickinson et al., 1999; Kim et al., 1999).

Interestingly, polymorphism of the FcRn gene may influence the PK/PD of IgG, including therapeutic mAb. FcRn polymorphism, consisting in variable number of tandem repeats (VNTR, five different alleles VNTR1–VNTR5) within the *FCGRT* promoter, influences the quantity of FcRn transcripts (Sachs et al., 2006). Indeed, VNTR3/3 homozygous individuals express more FcRn transcript than VNTR2/3 heterozygous individuals. Finally, VNTR3/3 polymorphism leads to better management of IgG in monocytes due to an increase binding of IgG (Sachs et al., 2006). In this context, Passot et al. showed that VNTR polymorphism was associated with variations in cetuximab PK parameters. Indeed, VNTR3 homozygote patients (high level of FcRn transcripts) had a lower cetuximab distribution clearance than VNTR2/VNTR3 (low level of FcRn transcript) and VNTR3/VNTR4 patients (Passot et al., 2013). VNTR in FcRn promoter also influences the PK of intravenous Ig (IVIg) in patients with Guillain-Barré Syndrome (GBS) or IVIg efficiency in Common-Variable-Immunodeficiency (CVID) patients (Fokkink et al., 2016; Gouilleux-Gruart, et al., 2013).

FcRn is a receptor found in a large variety of epithelial cell types such as hepatocytes, enterocytes, thyrocytes and podocytes. FcRn is also expressed in endothelial and hematopoietic cells (Akilesh, Christianson, Roopenian, & Shaw, 2007; Borvak et al., 1998; Haymann et al., 2000; Israel et al., 1997; Latvala, Jacobsen, Otteneder, Herrmann, & Kronenberg, 2017; Montoyo et al., 2009). This wide cellular expression leads to its ubiquitous presence in organs all over the body, consistent with the functions attributed to FcRn regarding therapeutic antibodies and with its role in overcoming cellular barriers. Its function in each specific tissue will be discussed in the sessions below.

3.2. Epithelial barrier and mucosal delivery of antibody

Non-invasive routes have been investigated for therapeutic antibodies using delivery through mucosa including nasal (Rohrer, Lupo, & Bernkop-Schnurch, 2018), lung (Respaud, Vecellio, Diot, & Heuze-Vourc'h, 2015), buccal (Montenegro-Nicolini & Morales, 2017) and oral mucosa (Vllasaliu, Thanou, Stolnik, & Fowler, 2018) for either topic or systemic-acting drugs. Mucosal surfaces represent an extensive area that face the external environment, require the establishment of anatomic and physiologic barriers, and prevent pathogens and macromolecules from reaching the internal surfaces of the body.

The epithelium represents a barrier for both locally and systemically acting antibody, depending on the antigen target location and route of administration (Ferrati, Wu, Kanapuram, & Smyth, 2018; Homayun, Lin, & Choi, 2019). Mucosal epithelium, which is almost a non-keratinized epithelium (except in specific areas of the oral cavity), is a critical barrier that provides protection for pathogens entering the body. The regulation and exchange of molecules between the environment and the underlying tissues by epithelium is exemplified by nutrient absorption in the gastro-intestinal tract (Turner, 2009) and gas exchange in the airways (Hellings & Steelant, 2020). Directional transport across the epithelium is provided by cellular polarity featuring apical and basolateral domains that are asymmetrical in structure and functions (Farquhar & Palade, 1963). From the apical to basolateral side, the apical junctional complex is composed of tight junctions, adherent junctions, gap junctions and desmosomes (Fig. 2). It is the main regulator of molecular transport across the epithelium. Indeed, epithelium tight junctions dictate the characteristics of paracellular permeability that accepts, with high capacity, molecules with molecular mass <600 Da and size in the range of 8–9 Å in diameter (Watson, Rowland, & Warhurst, 2001). During transient alterations of the epithelium, a leak pathway has also been characterized, allowing less restrictive, low capacity and size-independent transportation (Buschmann et al., 2013; Turner, 2009). Due to their large molecular size and high polarity, paracellular transportation of full-length (Guilleminault et al., 2014) and fragments antibodies (Patil et al., 2018) is estimated low or negligible. Besides paracellular transportation, transcellular transport of larger molecules can occur at the mucosal surface. Macromolecules localised in the lumen can access the lamina propria by specialised cells including microfold cells (in the gastrointestinal tract) and dendritic cells (Kimura, 2018) or by unspecific endocytosis through epithelial cells. Endocytosis may result in partial or total degradation of proteins in acidic and lysosomal compartments (Heyman, Ducroc, Desjeux, & Morgat, 1982). Transcellular transport of antibody (with an Fc domain) mainly occurs through receptor-mediated mechanisms involving FcRn (see section 3.1). In lung mucosa, FcRn is expressed in bronchial and alveolar epithelial cells (Akilesh et al., 2007; Latvala et al., 2017; Sakagami et al., 2006; Spiekermann et al., 2002) where it maintains homeostatic IgG levels (Vogelzang et al., 2016) and allows IgG transcytosis across the mucosal surface (Spiekermann et al., 2002). For inhaled antibodies, FcRn contributes to mAb biodistribution via recycling and transcytosis in the airways (Guilleminault et al., 2014). FcRn is also expressed in human nasal epithelium (Campanari, Bourefis, & Kabashi, 2019) and may mediate transcytosis of mAb across this tissue after nasal administration (Bequignon et al., 2019).

3.2.1. Epithelial barrier: overcoming strategies

According to the target localisation, several strategies have been designed to interface with mucosal surfaces in an attempt to improve or reduce penetration of antibody through the epithelial barrier. Structural simplification of antibody architecture has proven to improve *in vivo* delivery after inhalation. Indeed, anti-IL-13, anti-TNFR1 or anti-RSV F protein antibody fragments display improved tissue penetration and biodistribution after inhalation (Bertok et al., 2012; Detalle et al., 2016; Hacha et al., 2012). Several studies describe the use of delivery carrier systems to overcome the epithelial barrier for proteinaceous drugs. This includes permeation enhancers that will temporarily weaken tight junctions enhancing paracellular permeability (Maher, Mrsny, & Brayden, 2016). They have been successfully used for insulin, liposomes and nanoparticles, but only one study reported a positive impact on IgG delivery. The concomitant intranasal administration of (^{125}I) I-IgG and MMP-9 significantly improved the uptake of antibody into the brain as compared to unformulated antibody (Kumar et al., 2018). However, permeability enhancers should be used with caution as mucosal irritation and toxicity has been reported (Maher et al., 2016; Marttin et al., 1997). Another method consists in improving transcellular transport using cell-penetrating peptides: short-length (5–30 amino-acids) peptides, rich in positive charges and containing hydrophobic tryptophan residues may help translocation across epithelium. This technology has been successfully used mainly for nanotechnologies (Jin et al., 2012; Porsio, Craparo, Mauro, Giammona, & Cavallaro, 2018) and is currently under investigation for antibody delivery across the mucosal epithelium (Zhang et al., 2018; Zhao, Brown, Kohler, & Muller, 2003). When aiming luminal target, prolonging antibody retention may be of particular interest. Conjugation of polyethylene glycol (PEG) chains to antibody will increase the molecular weight lowering transcytosis to the systemic circulation (Patil et al., 2018) by inhibiting its binding to FcRn, as demonstrated for the certolizumab pegol (Mariette et al., 2018). In addition, it will enhance stability and mucoadhesion, while avoiding the uptake by phagocytes (see Section 2.3.1.1) improving antibody PK profile (Koussoroplis et al., 2014). When considering the mucosal route of administration to deliver a drug acting at the systemic level, it would be beneficial to use the FcRn-mediated transcytosis. Indeed Fc-conjugated drugs, like Epo-, IFNb- of FSH-Fc have shown both improved transepithelial transport or half-life in the airways and in the plasma (Rath et al., 2015). However, it is noteworthy that antibody epithelium-to-endothelium diffusion after inhalation delivery is slow, indicating that other parameters may contribute to airway-blood passage (Guilleminault et al., 2014; Respaud et al., 2016).

3.3. Endothelial barrier and systemic delivery of antibody

The endothelium is a cell monolayer lining blood vessel walls that not only controls the vascular tone, haemostasis and angiogenesis but also cell behaviour, innate immunity, cell-cell interactions, and cell metabolism in the vessel wall (Xu et al., 2021). Vascular endothelium cells act like a gatekeeper controlling the flow of molecules and fluid into and out of a tissue. In this section, we will discuss how vascular endothelium and more specifically the blood-brain barrier (BBB) limit antibody delivery.

3.3.1. Structure of blood vessels

The structure of blood vessels is commonly described with three tunicae characterised by morphological differences: intima, media and adventitia (from the most internal to the most external tunic). Microvasculature, the main place for exchanges, is composed by intima tunica with endothelial cells for the most important part and pericytes localized at the outside with basal membrane. The growth of this network is dependent of angiogenesis phenomenon, which allows neo-vessels growth from pre-existing structures (one of the ways used by tumour cells to increase neo-vessels proliferation) (Raza, Franklin, & Dudek, 2010; Tennant & McGeachie, 1990). Blood vessels are essential to protect tissues from molecules present in the bloodstream circulation. Nevertheless, a non-negligible proportion of drugs must diffuse through the micro-vessel wall to reach their targets. Drug diffusion depends both on micro-vessel structure and on drug diffusion abilities. Due to their features (hydrophilicity and large size), antibodies are restricted in their ability to pass through endothelial vessel cells. Studies in mice have shown that FcRn is expressed in the endothelium of small arterioles and capillaries, but not in larger vessels like central vein and portal vasculature (Borvak et al., 1998). FcRn is expressed on the walls of endothelial cell endocytosis vesicles (pinocytosis) in the human vascular

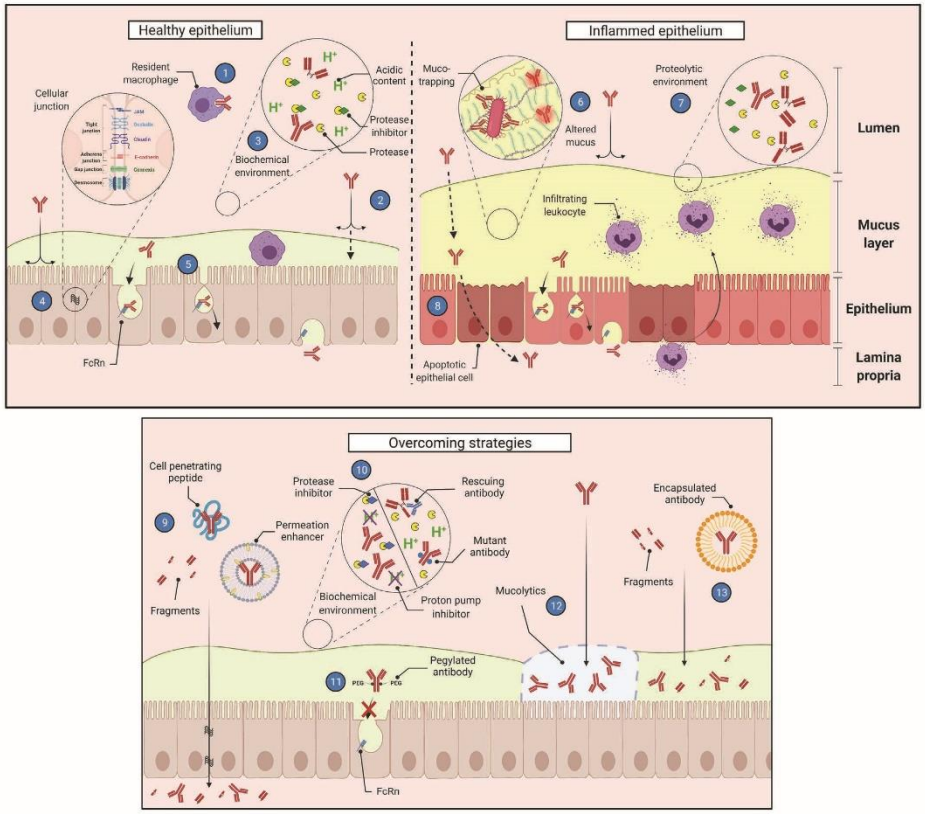

Fig. 2. Schematic representation of epithelial barriers to antibodies in healthy and disease conditions.
At steady state (left panel), mAbs present in the lumen may encounter biological barriers at the mucosal surface limiting their bioavailability. Resident macrophages (1) patrolling the mucosa could phagocytose mAbs leading to their degradation or denaturation. The mucus (2) covering the epithelium can partly repel Abs. In homeostatic conditions, balance between proteases and anti-proteases is neutral (3), except in the gastro-intestinal tract where the acidic pH will activate specific proteases and alter mAb conformation. Once the epithelium is reached, tight junctions between epithelial cells (4) prevent paracellular transport of mAb. mAbs can cross the epithelial surface by transcytosis, mainly through their binding with FcRn (5) resulting in improvement or decrease in the mAb bioavailability depending on the location of its target. In inflammatory conditions (right panel), mucus structure and composition are altered (6) with thicker layer and tighter pores decreasing the diffusion of mAbs. The activation of resident immune cells and the recruitment of leukocytes generate a dysregulation of proteases / protease-inhibitors balance (7) leading to a proteolytic environment favoring mAb proteolysis. Local inflammation leads to cellular damage and epithelial apoptosis promoting para- and trans-cellular leakage of mAbs (8). Several strategies have been investigated trying to solve mucosal barrier problems. In order to circumvent epithelium impermeability, cell-penetrating or permeation enhancer strategies have been considered as well as reducing mAb size, using small fragments, in order to improve mAb trans-epithelial passage (9). The use of protease inhibitors, proton-pump inhibitors or rescuing mAb may protect from degradation and denaturation (10). When considering local target, mAb-pegylation will lower transcytosis and increase mAb retention within mucosa (11). In order to improve mAb diffusion through the mucus, the addition of mucolytics (12), the encapsulation of mAb in nanovectors or the use of small fragments have been investigated (13).

endothelium (Paintaud, 2009). After membrane invagination, mAb bind this specific receptor. FcRn expression in blood vessels leads to sustainable IgG serum half-life by recycling them to the blood, including mAb (Pyzik et al., 2019). For tumour vasculature, there is a paradoxical situation. On the one hand, the inflamed environment combined with the rapid tumour vasculature growth induce an increase in the number and size of gaps, a decrease in the quality of basal membrane and a reduced number of pericytes that facilitates diffusion through intima tunica of tumour microenvironment capillaries (Azzi & Gavard, 2014; Ribatti et al., 2005). On the other hand, tumour vasculature tortuosity and unorganised microcirculation structure decreases diffusion capacity by flow resistance mechanism. In fact, even if the vascular density is high in tumour microenvironment, thanks to hypersecretion of growth factor (VEGF for example), the unstructured network could be an important obstacle for drugs delivery (Dewhirst & Secomb, 2017), as illustrated in Section 2.c.iv for antibodies.

3.3.2. The blood-brain barrier (BBB): the wall between the blood and the central nervous system (CNS)

The CNS is protected by three main barriers that separate it from the rest of the body: the BBB, the blood-cerebrospinal fluid barrier, and the arachnoid barrier. The BBB is found at the interface between the cerebral systemic circulation and the brain (Wolburg, Noell, Mack, Wolburg-Buchholz, & Fallier-Becker, 2009; Zlokovic, 2008). Given the high sensitivity of neurons to changes in their microenvironment and the low regenerative capacity of the nervous system, a disruption of the BBB can have detrimental effects on the CNS. The BBB strictly modulates the passage of molecules into and from the brain parenchyma.

This barrier is mainly made up of specialised endothelial cells characterised by the lack of fenestrae, reduced pinocytosis and transcytosis, the expression of specific metabolising enzymes, and the presence of energy-dependent efflux transporters, such as the FcRn, ATP-binding cassette transporters and low-density lipoprotein receptor-related protein 1 (LRP1) (Deane et al., 2004; Higgins, 2001; Salameh & Banks, 2014). Therefore, these cells demonstrate a high transendothelial electrical resistance, coupled with low paracellular and transcellular permeability (Maherally et al., 2018). This electrical resistance is largely due to the presence of continuous junctional complexes, and particularly tight junctions between endothelial cells (Bazzoni & Dejana, 2004). Tight junctions enhance the selective transport of molecules across the BBB through two main mechanisms: (i) conferring endothelial cells their polarity by separating their apical and basolateral surfaces, each of which has a different expression of transporters, and (ii) restricting paracellular transport pathways and forcing molecules to move transcellularly through specific transporters (Tsukita, Furuse, & Itoh, 2001). The BBB endothelial cells are surrounded by pericytes and perivascular astrocytic end-feet. Pericytes share the basal lamina of endothelial cells and act like vascular smooth muscle cells to regulate blood flow through BBB capillaries (Jespersen & Ostergaard, 2012). They also release signalling molecules that modulate tight junctions' density and astrocytic end-feet polarisation (Armulik et al., 2010) (Fig. 3). The basal lamina is in turn composed of a mixture of laminin, fibronectin, type IV collagen, and heparin sulphate, which further regulate the permeability of the BBB (see Section 2.1.1) (Milner et al., 2008). The BBB is not static and is finely modulated in both healthy and disease conditions. Its permeability is influenced by several cell types including endothelial cells, pericytes, astrocytes, microglia, and neurons, which morphologically and molecularly interact together to form the functional neurovascular unit (Luissint, Artus, Glacial, Ganeshamoorthy, & Couraud, 2012).

It is estimated that less than 0.1% of systematically administered antibody enter the CNS through nonspecific pathways (Atwal et al., 2011; Poduslo, Curran, & Berg, 1994). An even lower amount of 0.009% of the injected dose reaches the cortex (St-Amour et al., 2013). This may be partly attributable to the presence of FcRn (Cooper et al., 2013). In the BBB, FcRn is expressed in microvascular endothelium and in choroid plexus epithelium that constitute the BBB (Schlachetzki, Zhu, & Pardridge, 2002), but not in neurons, astrocytes, or microglia (Akilesh

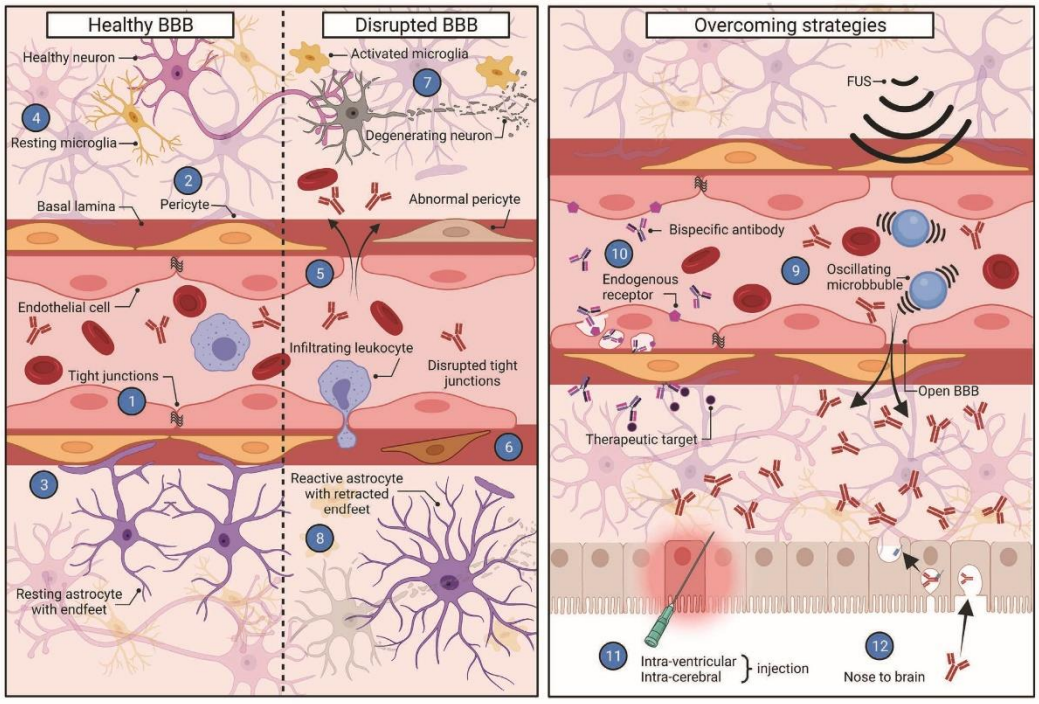

Fig. 3. Schematic representation of the blood-brain barrier (BBB) to antibodies in healthy and disease conditions, and the strategies developed to overcome this barrier.
A healthy BBB (left panel) is composed of endothelial cells that are tightly sealed by tight junctions (1) and prevent paracellular transport, hindering antibodies from reaching the CNS. Pericytes (2), which share the basal lamina with endothelial cells, help maintain the BBB and regulate blood flow through the capillaries. Astrocytes interact with BECs through their end-feet (3) and contribute to the maintenance of the BBB integrity. Resting microglia (4) are motile and highly ramified surveillant cells that are constantly scanning the brain environment to maintain its homeostasis. In pathological conditions (middle panel), the BBB becomes hyper-permeable to blood-born cells and molecules, including antibodies. Tight junctions between endothelial cells are disrupted (5), leading to a loss of endothelial cell polarity and uncontrolled paracellular transport. Pericytes are lost and detach from endothelial cells (6). Activated microglia (7) and reactive astrocytes (8) undergo molecular and morphological changes and adopt a pro-inflammatory phenotype. Studies suggest that BBB permeability increases with age, therefore increasing the passage of antibodies from the periphery to the CNS. Strategies to overcome the BBB (right panel) and increase antibodies distribution into the CNS were developed, including brain-focused ultrasound (FUS) combined with administration of microbubbles that open reversibly the BBB (9); bispecific antibodies (10) that target endogenous receptors expressed in the BBB and facilitate transcytosis; invasive, direct injection to the brain (11) via intra-cerebroventricular or intra-cerebral administrations; and nose-to-brain delivery (12), where antibodies are delivered to the nose and cross the olfactory epithelium, reaching the brain.

et al., 2007; Stamou, Grodzki, van Oostrum, Wollscheid, & Lein, 2018). FcRn in the brain is involved in reverse transcytosis of IgG across the BBB by a rapid efflux of IgG secreted in the brain to blood direction (Cooper et al., 2013; Schlachetzki et al., 2002). However, despite numerous studies in brain endothelial cells, the role of FcRn in IgG recycling and transcytosis from blood to brain has not yet been clearly demonstrated (Abuqayyas & Balthasar, 2013; Chen et al., 2014; Deane et al., 2005; Yip et al., 2014). For example, it was reported that systemically injected Ab in FcRn knockout mice presented similar plasma to brain ratio compared to wild-type mice (Garg & Balthasar, 2009). More recently, a study performed in brain endothelial-like cells derived from human induced pluripotent stem cells showed that transcytosis occurs independently of FcRn, as IgGs lacking human FcRn recognition presented the same permeability as a full-length control IgG (Ruano-Salguero & Lee, 2020). Even if several studies demonstrated that FcRn rapidly promotes efflux of therapeutic antibody and hamper their therapeutic potential, studies performed in Alzheimer's disease models suggest that FcRn can actually improve the therapeutic effect of antibodies targeting amyloid-β (Aβ) plaques by promoting the efflux of anti-Aβ antibody/Aβ immune complexes (Deane et al., 2005; Deane, Bell, Sagare, & Zlokovic, 2009). Intriguingly, studies performed in a transgenic AD mouse model suggested that FcRn expression decreases with age (Deane et al., 2005). The putative occurrence of such decrease in the human ageing brain suggests two scenarios: (i) Ab administered at the periphery would present a lower efflux ratio than described so far; or (ii) Ab/antigen complexes would be trapped in the CNS thus preventing any therapeutic effect induced by immunotherapy.

Disruptions in the BBB have been reported in several pathological conditions (Zlokovic, 2008), involving several cellular and molecular actors, like proteases (Yang & Rosenberg, 2011), ultimately resulting in the increased permeability of the BBB (Fig. 3), associated to the disruption of tight junctions (Gaillard, de Boer, & Breimer, 2003) and changes in pericytes (Bohannon et al., 2020). Studies also reported an age-associated increase in the BBB permeability, which implies a potential age- and disease-induced increase in the antibody uptake (Bell et al., 2010; Erickson & Banks, 2019; Popescu et al., 2009). Among the consequences of increased BBB permeability is the leakage of serum proteins including antibodies (Gray & Woulfe, 2015; Nelson, Sweeney, Sagare, & Zlokovic, 2016; Wenting et al., 2020; Zamudio et al., 2020) and the infiltration of peripheral cells such as T cells, macrophages, neutrophils, and red blood cells (Blair et al., 2015; Zamudio et al., 2020). These changes lead to the activation of microglia and astrocytes, and an inflammatory cascade exacerbating the condition and leading to a vicious cycle whereby the BBB disruption causes an inflammatory response, which in turn disrupts the integrity of the BBB (Chan-Ling et al., 2007; Oksanen et al., 2019; Tuppo & Arias, 2005). Studies on neurodegenerative diseases reported an enhanced uptake of drugs that usually are unable to cross the BBB (Kortekaas et al., 2005). For example, trastuzumab uptake increased by 18-fold in metastatic brain lesions once the tumour size was superior to 0.5 mm (Dijkers et al., 2010), which is enough to cause a disruption of the BBB (Ni, Chen, & Lu, 2018). Other antibodies have also been successfully delivered to ischemic brain regions following a stroke-induced BBB opening and showed significant therapeutic and prognostic results (Irving et al., 2005; Macrez et al., 2011; Rust et al., 2019). However, alterations in the BBB permeability in CNS disorders do not always favour an increased permeability for peripheral antibodies (Bien-Ly et al., 2015; Wahl et al., 2020).

Despite promising results in experimental models of CNS diseases, where peripherally administered antibodies were able to reduce symptoms (Atwal et al., 2011; Bard et al., 2000; Buttini et al., 2005; Masliah et al., 2011), there seems to be many difficulties to translate them in humans. Several clinical trials involving anti-Aβ mAbs were terminated after interim analysis indicating that systemically administered mAbs were unlikely to meet they primary endpoint (Blennow et al., 2012; Doody, et al., 2014; Ostrowitzki et al., 2017; Rinne et al., 2010; Salloway et al., 2021). One of the reasons why these mAbs failed in clinical trials is the need to administer large mAb doses to achieve a therapeutic effect in the CNS, which increases the risk of side effects. Recently, Aducanumab became the first anti-Aβ mAb to be approved by the FDA for the management of Alzheimer's disease. However, the effectiveness of this intravenously administered mAb is still controversial and its approval debatable due to its considerable side effects and unproven therapeutic potential (Mullard, 2021).

3.3.2.1. Blood-brain barrier: overcoming strategies. Since peripherally administrated mAbs that target the CNS have been facing lack of success, several strategies have been evaluated to overcome the BBB and are reviewed below.

Direct delivery into the CNS: Direct antibody delivery into the brain and therapeutic effects were successfully achieved after intracerebroventricular injection (Cheng et al., 2017; Du et al., 2020; Gros-Louis, Soucy, Lariviere, & Julien, 2010; Klyubin et al., 2005; Qiang et al., 2018; Thakker et al., 2009; Yadav et al., 2017), intracerebral injection (Brendza et al., 2005; Grossi et al., 2003; Lombardo et al., 2003; Wilcock et al., 2003) and convection-enhanced delivery (Nwagwu, Immidisetti, Bukanowska, Vogelbaum, & Carbonell, 2020; Shoji et al., 2016; Souweidane et al., 2018). Although potentially effective, such neurosurgical methods are technically challenging, highly invasive, and raise serious safety concerns (Cohen-Pfeffer et al., 2017; Pardridge, 2007). In addition, such techniques show limited diffusion and distribution capacities of the antibody in the brain parenchyma (Nagaraja et al., 2005; Salvatore et al., 2006; Yan et al., 1994).

Antibody engineering: In an attempt to increase the uptake of peripherally injected antibody by the CNS, bispecific antibodies have been developed. As their name imply, they are capable of simultaneously recognizing two different epitopes or antigens. To improve BBB crossing, one antibody-binding site would recognise an endogenous BBB receptor and therefore acting as a Trojan horse, while the other site would recognise a therapeutic target inside the CNS. The ideal target receptor for this receptor-mediated transcytosis across the BBB needs to be highly and specifically expressed on brain endothelial cells (Choudhari et al., 2021; Pardridge, 2017). Several receptors for receptor-mediated transcytosis across the BBB have been considered so far as antigen for bispecific antibodies, such as the insulin receptor, LRP1 and LRP2 CD98hc (Zuchero et al., 2016), but the transferrin receptor remains the most widely targeted delivery system (Tashima, 2020) with promising results in Alzheimer's disease models (Yu et al., 2014).

Artificial ways to reversibly increase the permeability of BBB: Other techniques can be used in combination to intravenously administered antibodies with the aim to reversibly increase BBB permeability. Recently, Lesniak and co-workers reported a high brain uptake of bevacizumab following intra-arterial administration and mannitol-induced BBB opening (Lesniak et al., 2019). This old technique is resurfacing for the delivery of antibody to the brain and is currently being tested in three clinical trials (NCT02861898, NCT02800486, NCT01269853).

A new technique, which uses brain-focused ultrasound (FUS) (Costa, Joaquim, Forlenza, Talib, & Gattaz, 2019) to sonicate systematically administered microbubbles, can reversibly and locally disrupt tight junctions (Shang, Wang, Liu, Zhang, & Xue, 2011; Sheikov, McDannold, Sharma, & Hynynen, 2008) and increase active transcytosis in the BBB (Sheikov et al., 2006), allowing antibody transport from the blood to specific brain regions. This method was found to be safe in non-human primates (McDannold, Arvanitis, Vykhodtseva, & Livingstone, 2012; Nwagwu et al., 2020), and recently in humans (Abrahao et al., 2019; Carpentier et al., 2016). In addition, brain-focused ultrasound was found to downregulate the efflux transporter, P-glycoprotein, in the targeted brain regions (Cho et al., 2016). Since 2004, when Sheikov and his colleagues demonstrated for the first time that brain-focused ultrasound allowed BBB permeabilization to molecules as large as IgG (Sheikov, McDannold, Vykhodtseva, Jolesz, & Hynynen, 2004), there has been several studies demonstrating the relevance of brain-focused ultrasound to improve the delivery of systematically administered

antibody into specific brain areas, particularly in tumours and Alzheimer's disease (Dubey et al., 2020; Janowicz, Leinenga, Gotz, & Nisbet, 2019; Jordao et al., 2010; Kinoshita, McDannold, Jolesz, & Hynynen, 2006; Kobus, Zervantonakis, Zhang, & McDannold, 2016; Leinenga, Bodea, Koh, Nisbet, & Gotz, 2020; Liu et al., 2016; Park, Zhang, Vykhodtseva, & McDannold, 2012; Raymond et al., 2008; Sheybani et al., 2021). Overall, brain-focused ultrasound seems to be a promising technique to deliver antibody to targeted areas in the CNS, but the secondary effects of this technique on the brain still need to be further assessed (Todd et al., 2020).

Bypassing the BBB: Finally, intracerebral drug delivery through the nasal interface ("Nose-to-brain") is a way to bypass the BBB. Drugs are deposited in the olfactory region of the nares where, after crossing the olfactory epithelium, they travel to the brain via mechanisms that still need to be fully determined. Disorders that may benefit from this novel route of administration include neurodegenerative diseases, post-traumatic stress disorder, pain and glioblastoma. In an *ex vivo* porcine model, endogenous Ig as well as various mAb were shown to diffuse through the nasal mucosa in an FcRn-dependent mechanism (see Section 3.1) (Ladel et al., 2018). In a murine model, administration of anti-Aβ3 mAb by intranasal route allowed a better intracerebral bioavailability than the intraperitoneal route (Chauhan & Chauhan, 2015), while maintaining its therapeutic properties (Cattepoel, Hanenberg, Kulic, & Nitsch, 2011). This has motivated the EU to launch the N2B-patch program in 2017 aiming at developing a mAb for the treatment of multiple sclerosis through the nose-to-brain route (https://cordis.europa.eu/project/id/721098). In 2021, another program, Bio2Brain, was also launched by the EU to enhance the bioavailability of mAb targeting the CNS (https://cordis.europa.eu/project/id/956977). Even if promising, this groundwork on nose-to-brain delivery still exposes mAb to the cellular and extracellular barriers of the nasal mucosa (see Section 2). Lately, a combination of brain-focused ultrasound and intranasal drug administration was found to enhance the delivery of antibodies to gliomas in mice (Ye, Yuan, Yue, Rubin, & Chen, 2021). Ferreira and her colleagues also showed that nanoparticles coated with a mAb targeting EGFR were successfully delivered to glioblastoma following intranasal administration (Ferreira et al., 2021). Further optimisation is needed to increase the retention time at the nasal surface and to enhance the penetration of the nasal epithelium.

4. Immune barrier and antibody clearance

Among the different types of cells engaged in the immune responses, macrophages are at the crossroad between innate and adaptive immunity. Tissue-resident macrophages are found in various tissues through the body, like Kupffer cells in the liver, microglia in the brain, osteoclasts in bones, or alveolar macrophages in the lungs. Some tissue-resident macrophages are known to have a major role in IgG transport, biodistribution or metabolism and may be considered as an immune barrier against recombinant antibodies.

Only antibody fragments (Waldmann, Strober, & Mogielnicki, 1972), which have low-molecular weight as compared to full-length IgG/mAb above the glomerular cut-off threshold can be filtered by the kidneys. Consequently, antibody clearance occurs mainly through intracellular catabolism, which includes upstream engulfment of antibody through non-specific pinocytosis, target-mediated or FcγR-mediated endocytosis (W. Wang, Wang, & Balthasar, 2008). This latter process is mediated through binding of IgG Fc region or immune-complexes to FcγR-expressing cells such as phagocytes from mononuclear phagocytic system, including notably Kupffer cells, Langherans cells in the skin and alveolar macrophages. This binding will result in antibody lysosomal proteolysis. Kupffer cells represent the largest population of tissue macrophages (Nguyen-Lefebvre & Horuzsko, 2015). They are mainly found in the lumen of hepatic sinusoids and exhibit endocytic activity against blood material entering the liver (Naito, Hasegawa, Ebe, & Yamamoto, 2004) including immune-complexes via FcγR-dependent uptake (Johansson et al., 2002). Similarly, there is evidence indicating that alveolar macrophages are involved in IgG catabolism. Indeed, Lombry et al. showed that clodronate-treated mice where alveolar macrophages were depleted, exhibited several-fold enhancement in systemic absorption of intratracheally-administered IgG (Lombry, Edwards, Preat, & Vanbever, 2004). Antibodies are supposed to cross slowly the epithelial-capillary barrier and consequently can remain within parenchyma for prolonged period as compared to small molecules, giving more time to resident phagocytes to engulf them. FcγR binding alone is not expected to have a major impact on IgG PK. Indeed, studies with FcγR-/- mice showed that FcγR-mediated clearance played only a minor role (Abuqayyas & Balthasar, 2012). However, in some circumstances antibody binding to FcγR may limit its bioavailability, for example: (i) when phagocyte infiltration is increased due to inflammatory or infectious triggers, (ii) when considering larger antibody structure, like ADC that tend to have a better binding to FcγR (Lux, Yu, Scanlan, & Nimmerjahn, 2013), and (iii) when considering engineered antibody with improved affinity to FcγR. Preclinical studies reported a contribution of Fc–FcγR interactions between ADCs and tumour-associated macrophages, suggesting that they can contribute to ADC processing through FcγR interaction and may induce off target cytotoxicity (Li et al., 2017). It has been showed that trastuzumab emtansine exhibited faster clearance in mice and humans compared to native antibody; this was suggested to be attributable to a better recognition and internalisation of antibody by FcγR-expressing phagocytes from the mononuclear phagocytic system (Burris 3rd et al., 2011; Leyland-Jones et al., 2003). Other factors like larger patient body mass or tumour burden, associated with increased mononuclear phagocytic system function, may accelerate antibody clearance (Bruno et al., 2005; Quartino et al., 2016). This should be put into perspective with the fact that for complex antibody-like structures like bispecific antibodies, rapid clearance was not attributable to target binding nor involved mononuclear phagocytic system but to binding with liver sinusoidal endothelial cells (Datta-Mannan et al., 2016). Overall, the exact contribution of FcγR-expressing phagocytes to antibody elimination remains not fully understood.

In addition, many immune cells express FcRn: myeloid lineage such as dendritic cells, monocytes/macrophages and neutrophils (Akilesh et al., 2007; Zhu et al., 2001) mainly express FcRn while it is detected at a lower level in lymphoid cells (T and B lymphocytes) (van Bilsen et al., 2010). In bone marrow chimera experiments using FcRn wild-type and knockout mice, Akilesh et al. showed that FcRn expression in bone marrow-derived cells plays a significant role in regulating IgG serum half-life and homeostasis (Akilesh et al., 2007). Nevertheless, the loss of FcRn expression in B cells and dendritic cells had no significant effect on IgG homeostasis, in mice. The role of macrophages in the recycling and homeostasis of IgG (Challa et al., 2019) may be more prominent as they express FcγR and the highest level of FcRn. Additional factors including antibody glycosylation, aggregation, and sensitivity to proteolysis, (Jiang et al., 2011) may be involved in phagocyte-mediated clearance and further studies are warranted to better understand and delineate the contribution of immune cells in antibody homeostasis.

4.1. Immune barrier: overcoming strategies

The dual role of FcR in IgG catabolism and PK/PD makes any modifications of IgG affinity to FcγR or FcRn susceptible to ultimately alter mAb efficacy. Thus, protein engineering in the Fc domain of IgG must be considered with caution, depending on the target localization and pathological context, which will profoundly affect the nature and the magnitude of the immune cell populations encountered by mAb. Interestingly, a recent study took the advantage of the phagocytic pathways to achieve therapeutic efficacy. Kasturirangan et al. showed that a bispecific/biparatopic antibody construct generated with two antibodies targeting different epitopes of IL-6 was much rapidly internalised and degraded by Kupffer cells as compared to parental antibodies. This

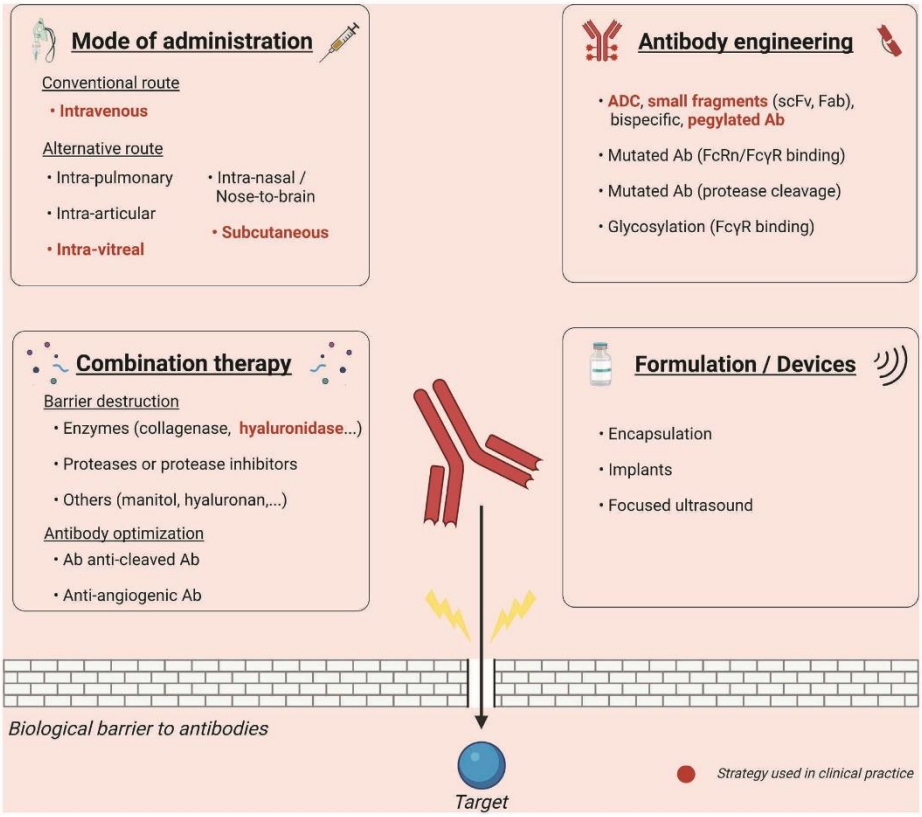

Fig. 4. Therapeutic strategies to overcome barriers to antibodies.
Depending on its location, different therapeutic strategies have been developed or are under consideration to help mAb reaching their target through the modulation of biological barriers. The choice of the mode of administration or specific tools and devices may allow a direct access to the target location. mAb engineering and/or formulation will help lowering the detrimental impact of barrier components. Finally, the administration of mAb in combination with a co-treatment will either destroy the barrier or improve mAb stability, favouring its access to its target.

describing novel approach will both promote neutralisation but also clearance of soluble targets (Kasturirangan et al., 2017).

5. Conclusion

In most cases, antibodies have to face several cellular and non-cellular barriers after entering the human body to reach their target antigens. The barriers that antibody may encounter depends on:

i) the delivery route. Although, the intravenous route may not be optimal to efficiently deliver antibody to specific organ or tissues, like the brain, lungs, gastro-intestinal tract, eye or the joints, exposing antibody to low-permeable barriers, antibody delivered by alternative routes are also confronted with cellular and non-cellular barriers, which should be considered during antibody-drug development.
ii) the antibody format/structure, which confers different partitioning properties in the different body compartment parts. Although IgG may benefit from FcRn uptake for transcytosis, their high molecular weight may be detrimental for diffusion across non-cellular barriers as compared to antibody fragments. More comparative studies addressing the impact of antibody format/structure on barrier crossing would be valuable but difficult to implement since the format/structure is also modifying antibody half-life.
iii) the pathological conditions and inter-individual variability response to disease. As oncology is a major medical application field for recombinant antibody, the impact of tumour stroma on antibody diffusion has constituted a thriving focus of research. In contrast other barriers, which can be altered in non-cancerous pathological conditions, such as proteases, mucus, biofilm have driven lower attention so far and should be taken into consideration to avoid antibody clinical failure.
iv) aging, which is certainly an under-appreciated parameter in antibody response. The present review briefly mentioned the impact of aging on the decreased function of organs, like the brain, as well as the significant decline in the efficacy of the immune system that may ultimately leads to age-associated diseases (Erdo, Denes, & de Lange, 2017; Owyong et al., 2018). The influence of ageing on the nature and magnitude of the biological barriers and response to antibodies has been poorly characterized so far and may certainly require more attention especially

Table 1
Approved strategies to overcome biologicals barriers for therapeutic antibodies

Indication	Generic name (trade name)	Sponsoring company	Antibody target	Antibody format	Combined molecule	Date of approval	Route of administration
HER2+ metastatic breast cancer	Herceptin	Roche	HER2	Full-length		2013	
Primary immunodeficiency	HYQVIA	Shire Pharmaceuticals	IgG replacement	Full-length		2013	
HER2+ early/metastatic breast cancer	Phesgo	Roche	HER2	Full-length	rHuPH20	2021	Subcutaneous
Non-Hodgkin lymphoma	Rituxan Hycela / Rituxan SC / MabThera SC	Roche	CD20	Full-length		2014	
Age-related macular degeneration	Avastin	Genentech	VEGF	Full-length	–	Off-label use	Intravitreal
	Eylea	Regeneron pharmaceuticals	VEGF/PlGF	Full-length		2011	
Rhumatoid arthritis / Crohn disease / Psiorasis	Lucentis	Genentech	VEGF	Fab		2006	
	Cimzia	UCB Pharma	TNF	Fab	PEG	2008	
Hodgkin lymphoma	Adcetris	Seagen (Seattle Genetics)	CD30	ADC, protease sensitive linker	MMAE	2011	
HER2+ metastatic breast cancer	Enhertu	Daiichi Sankyo	HER2	ADC, protease sensitive linker	DXd	2019	
Urotelial cancer	Padcev	Astellas	Nectin-4	ADC, protease sensitive linker	MMAE	2019	
Diffuse large B-cell lymphoma	Polivy	Roche	CD79b	ADC, protease sensitive linker	MMAE	2019	
Cervical cancer	Tivdak	Genmab	Tissue factor	ADC, protease sensitive linker	MMAE	2021	
Diffuse large B-cell lymphoma	Zynlonta	ADC therapeutics	CD19	ADC, protease sensitive linker	PBD	2021	
Acute lymphoblastic leukemia	Besponsa	Pfizer	CD22	ADC, pH-sensitive linker	Calicheamicin	2017	
Triple-negative breast cancer	Trodelvy	Immunomedics	TROP-2	ADC, pH-sensitive linker	SN38	2020	
Acute myeloid leukemia	Mylotarg	Pfizer	CD33	ADC, pH-sensitive linker	Calicheamicin	2017	Intraveinous

ADC, antibody-drug conjugate; DXd, topoisomerase I inhibitor; in.v, intravitreal; i.v, intravenous; MMAE, Monomethyl auristatin E; MMAF, Monomethyl auristatin F; PBD, pyrrolobenzodiazepine; PEG, polyethylene glycol; rHUPH20, hyaluronidase; SN38, irinotecan.

with the increased ageing of populations and the relevance of antibodies in the treatment of age-associated diseases.

As illustrated (Fig. 4), many strategies have been or can be investigated to overcome both natural and pathological barriers to improve antibody distribution and ultimately their therapeutic response. However, few of them have been materialised in the clinic successfully (Table 1). A better understanding of the consequences of each barrier/barrier component on antibody partitioning will be required to help develop antibodies with novel clinical applications or delivery routes.

Declaration of Competing Interest

YA, TB, JL, MG, AP, CDS, NJ, JPP, VGG, DL, SP, TS, have nothing to declare. NHV is co-founder and scientific expert for Cynbiose Respiratory. In the past two years, she received consultancy fees from Eli Lilly, Argenx, Novartis.

Acknowledgements

This work was supported by the French National Research Agency as part of the "Investissements d'Avenir" program (LabEx MAbImprove, ANR-10-LABX-53-01). Figures were created in BioRender.com.

References

Abrahao, A., Meng, Y., Llinas, M., Huang, Y., Hamani, C., Mainprize, T., ... Zinman, L. (2019). First-in-human trial of blood-brain barrier opening in amyotrophic lateral sclerosis using MR-guided focused ultrasound. *Nature Communications 10*, 4373.

Abuqayyas, L., & Balthasar, J. P. (2012). Application of knockout mouse models to investigate the influence of FcgammaR on the tissue distribution and elimination of 8C2, a murine IgG1 monoclonal antibody. *International Journal of Pharmaceutics 439*, 8–16.

Abuqayyas, L., & Balthasar, J. P. (2013). Investigation of the role of FcgammaR and FcRn in mAb distribution to the brain. *Molecular Pharmaceutics 10*, 1505–1513.

del Aguila, M. A., Longstreth, W. T., Jr., McGuire, V., Koepsell, T. D., & van Belle, G. (2003). Prognosis in amyotrophic lateral sclerosis: A population-based study. *Neurology 60*, 813–819.

Akilesh, S., Christianson, G. J., Roopenian, D. C., & Shaw, A. S. (2007). Neonatal FcR expression in bone marrow-derived cells functions to protect serum IgG from catabolism. *Journal of Immunology 179*, 4580–4588.

Anaya-Lopez, J. L., Lopez-Meza, J. E., & Ochoa-Zarzosa, A. (2013). Bacterial resistance to cationic antimicrobial peptides. *Critical Reviews in Microbiology 39*, 180–195.

Antohe, F., Radulescu, L., Gafencu, A., Ghetie, V., & Simionescu, M. (2001). Expression of functionally active FcRn and the differentiated bidirectional transport of IgG in human placental endothelial cells. *Human Immunology 62*, 93–105.

Arda, O., Goksugur, N., & Tuzun, Y. (2014). Basic histological structure and functions of facial skin. *Clinics in Dermatology 32*, 3–13.

Armulik, A., Genove, G., Mae, M., Nisancioglu, M. H., Wallgard, E., Niaudet, C., ... Betsholtz, C. (2010). Pericytes regulate the blood-brain barrier. *Nature 468*, 557–561.

Atwal, J. K., Chen, Y., Chiu, C., Mortensen, D. L., Meilandt, W. J., Liu, Y., ... Watts, R. J. (2011). A therapeutic antibody targeting BACE1 inhibits amyloid-beta production in vivo. *Science Translational Medicine 3* 84ra43.

Azzi, S., & Gavard, J. (2014). Blood vessels in cancer: Can't stop whispering. *Medical Science (Paris) 30*, 408–414.

Bansil, R., & Turner, B. (2006). Mucin structure, aggregation, physiological functions and biomedical applications. *Current Opinion in Colloid & Interface Science 11*, 164–170.

Bard, F., Cannon, C., Barbour, R., Burke, R. L., Games, D., Grajeda, H., ... Yednock, T. (2000). Peripherally administered antibodies against amyloid beta-peptide enter the central nervous system and reduce pathology in a mouse model of Alzheimer disease. *Nature Medicine 6*, 916–919.

Baugh, M. D., Perry, M. J., Hollander, A. P., Davies, D. R., Cross, S. S., Lobo, A. J., ... Evans, G. S. (1999). Matrix metalloproteinase levels are elevated in inflammatory bowel disease. *Gastroenterology 117*, 814–822.

Bazzoni, G., & Dejana, E. (2004). Endothelial cell-to-cell junctions: Molecular organization and role in vascular homeostasis. *Physiological Reviews 84*, 869–901.

Becker, P., Hufnagle, W., Peters, G., & Herrmann, M. (2001). Detection of differential gene expression in biofilm-forming versus planktonic populations of Staphylococcus aureus using micro-representational-difference analysis. *Applied and Environmental Microbiology 67*, 2958–2965.

Bell, R. D., Winkler, E. A., Sagare, A. P., Singh, I., LaRue, B., Deane, R., & Zlokovic, B. V. (2010). Pericytes control key neurovascular functions and neuronal phenotype in the adult brain and during brain aging. *Neuron 68*, 409–427.

Bequignon, E., Dhommee, C., Angely, C., Thomas, L., Bottier, M., Escudier, E., ... Gouilleux-Gruart, V. (2019). FcRn-dependent transcytosis of monoclonal antibody in human nasal epithelial cells in vitro: A prerequisite for a new delivery route for therapy? *International Journal of Molecular Sciences 20*.

Bertok, S., Wilson, M. R., Morley, P. J., de Wildt, R., Bayliffe, A., & Takata, M. (2012). Selective inhibition of intra-alveolar p55 TNF receptor attenuates ventilator-induced lung injury. *Thorax 67*, 244–251.

Besharova, O., Suchanek, V. M., Hartmann, R., Drescher, K., & Sourjik, V. (2016). Diversification of gene expression during formation of static submerged biofilms by Escherichia coli. *Frontiers in Microbiology 7*, 1568.

Biancheri, P., Brezski, R. J., Di Sabatino, A., Greenplate, A. R., Soring, K. L., Corazza, G. R., ... MacDonald, T. T. (2015). Proteolytic cleavage and loss of function of biologic agents that neutralize tumor necrosis factor in the mucosa of patients with inflammatory bowel disease. *Gastroenterology 149*(1564–1574) e1563.

Bien-Ly, N., Boswell, C. A., Jeet, S., Beach, T. G., Hoyte, K., Luk, W., ... Watts, R. J. (2015). Lack of widespread BBB disruption in Alzheimer's disease models: Focus on therapeutic antibodies. *Neuron 88*, 289–297.

van Bilsen, K., Bastiaans, J., Dik, W. A., De Haas, E. F., Baarsma, S. G., Kuipers, R. W., & van Hagen, P. M. (2010). The neonatal Fc receptor is expressed by human lymphocytes. *Journal of Translational Medicine 8*, P1.

Blair, L. J., Frauen, H. D., Zhang, B., Nordhues, B. A., Bijan, S., Lin, Y. C., ... Dickey, C. A. (2015). Tau depletion prevents progressive blood-brain barrier damage in a mouse model of tauopathy. *Acta Neuropathologica Communications 3*, 8.

Blennow, K., Zetterberg, H., Rinne, J. O., Salloway, S., Wei, J., Black, R., ... Investigators, A. A. B. (2012). Effect of immunotherapy with bapineuzumab on cerebrospinal fluid biomarker levels in patients with mild to moderate Alzheimer disease. *Archives of Neurology 69*, 1002–1010.

Boddu, S. H., Gupta, H., & Patel, S. (2014). Drug delivery to the back of the eye following topical administration: An update on research and patenting activity. *Recent Patents on Drug Delivery & Formulation 8*, 27–36.

Boden, E. K., Canavan, J. B., Moran, C. J., McCann, K., Dunn, W. A., Farraye, F. A., ... Snapper, S. B. (2019). Immunologic alterations associated with oral delivery of anti-cd3 (okt3) monoclonal antibodies in patients with moderate-to-severe ulcerative colitis. *Crohn's & Colitis 360*(1) otz009.

Bohannon, D. G., Okhravi, H. R., Kim, J., Kuroda, M. J., Didier, E. S., & Kim, W. K. (2020). A subtype of cerebrovascular pericytes is associated with blood-brain barrier disruption that develops during normal aging and simian immunodeficiency virus infection. *Neurobiology of Aging 96*, 128–136.

Bonnans, C., Chou, J., & Werb, Z. (2014). Remodelling the extracellular matrix in development and disease. *Nature Reviews Molecular Cell Biology 15*, 786–801.

Boreel, D. F., Span, P. N., Heskamp, S., Adema, G. J., & Bussink, J. (2021). Targeting oxidative phosphorylation to increase the efficacy of radio- and immune-combination therapy. *Clinical Cancer Research 27*, 2970–2978.

Borvak, J., Richardson, J., Medesan, C., Antohe, F., Radu, C., Simionescu, M., ... Ward, E. S. (1998). Functional expression of the MHC class I-related receptor, FcRn, in endothelial cells of mice. *International Immunology 10*, 1289–1298.

Bowen, W. H. (2016). Dental caries - not just holes in teeth! A perspective. *Molecular Oral Microbiology 31*, 228–233.

Braeckmans, K., Peeters, L., Sanders, N. N., De Smedt, S. C., & Demeester, J. (2003). Three-dimensional fluorescence recovery after photobleaching with the confocal scanning laser microscope. *Biophysical Journal 85*, 2240–2252.

Brambell, F. W., Hemmings, W. A., & Morris, I. G. (1964). A theoretical model of gamma-globulin catabolism. *Nature 203*, 1352–1354.

Brendza, R. P., Bacskai, B. J., Cirrito, J. R., Simmons, K. A., Skoch, J. M., Klunk, W. E., ... Holtzman, D. M. (2005). Anti-Abeta antibody treatment promotes the rapid recovery of amyloid-associated neuritic dystrophy in PDAPP transgenic mice. *The Journal of Clinical Investigation 115*, 428–433.

Brezski, R. J., & Jordan, R. E. (2010). Cleavage of IgGs by proteases associated with invasive diseases: An evasion tactic against host immunity? *MAbs 2*, 212–220.

Bruno, B. J., Miller, G. D., & Lim, C. S. (2013). Basics and recent advances in peptide and protein drug delivery. *Therapeutic Delivery 4*, 1443–1467.

Bruno, R., Washington, C. B., Lu, J. F., Lieberman, G., Banken, L., & Klein, P. (2005). Population pharmacokinetics of trastuzumab in patients with HER2+ metastatic breast cancer. *Cancer Chemotherapy and Pharmacology 56*, 361–369.

Bumbaca Yadav, D., Sharma, V. K., Boswell, C. A., Hotzel, I., Tesar, D., Shang, Y., ... Kelley, R. F. (2015). Evaluating the use of antibody variable region (Fv) charge as a risk assessment tool for predicting typical cynomolgus monkey pharmacokinetics. *The Journal of Biological Chemistry 290*, 29732–29741.

Burris, H. A., 3rd, Rugo, H. S., Vukelja, S. J., Vogel, C. L., Borson, R. A., Limentani, S., ... O'Shaughnessy, J. A. (2011). Phase II study of the antibody drug conjugate trastuzumab-DM1 for the treatment of human epidermal growth factor receptor 2 (HER2)-positive breast cancer after prior HER2-directed therapy. *Journal of Clinical Oncology 29*, 398–405.

Buschmann, M. M., Shen, L., Rajapakse, H., Raleigh, D. R., Wang, Y., Wang, Y., ... Weber, C. R. (2013). Occludin OCEL-domain interactions are required for maintenance and regulation of the tight junction barrier to macromolecular flux. *Molecular Biology of the Cell 24*, 3056–3068.

Buttini, M., Masliah, E., Barbour, R., Grajeda, H., Motter, R., Johnson-Wood, K., Khan, K., Seubert, P., Freedman, S., Schenk, D., & Games, D. (2005). Beta-amyloid immunotherapy prevents synaptic degeneration in a mouse model of Alzheimer's disease. *The Journal of Neuroscience 25*, 9096–9101.

Campanari, M. L., Bourefis, A. R., & Kabashi, E. (2019). Diagnostic challenge and neuromuscular junction contribution to ALS pathogenesis. *Frontiers in Neurology 10*, 68.

Campoccia, D., Mirzaei, R., Montanaro, L., & Arciola, C. R. (2019). Hijacking of immune defences by biofilms: A multifront strategy. *Biofouling 35*, 1055–1074.

Carpentier, A., Canney, M., Vignot, A., Reina, V., Beccaria, K., Horodyckid, C., ... Idbaih, A. (2016). Clinical trial of blood-brain barrier disruption by pulsed ultrasound. *Science Translational Medicine 8* 343re342.

Cartaxo, A. L., Almeida, J., Gualda, E. J., Marsal, M., Loza-Alvarez, P., Brito, C., & Isidro, I. A. (2020). A computational diffusion model to study antibody transport within reconstructed tumor microenvironments. *BMC Bioinformatics 21*, 529.

Casi, G., & Neri, D. (2012). Antibody-drug conjugates: Basic concepts, examples and future perspectives. *Journal of Controlled Release 161*, 422–428.

Casi, G., & Neri, D. (2015). Noninternalizing targeted cytotoxics for cancer therapy. *Molecular Pharmaceutics 12*, 1880–1884.

Cattepoel, S., Hanenberg, M., Kulic, L., & Nitsch, R. M. (2011). Chronic intranasal treatment with an anti-Abeta(30-42) scFv antibody ameliorates amyloid pathology in a transgenic mouse model of Alzheimer's disease. *PLoS One 6* e18296.

Challa, D. K., Wang, X., Montoyo, H. P., Velmurugan, R., Ober, R. J., & Ward, E. S. (2019). Neonatal Fc receptor expression in macrophages is indispensable for IgG homeostasis. *MAbs 11*, 848–860.

Chalmers, J. D., Moffitt, K. L., Suarez-Cuartin, G., Sibila, O., Finch, S., Furrie, E., ... Fardon, T. C. (2017). Neutrophil elastase activity is associated with exacerbations and lung function decline in bronchiectasis. *American Journal of Respiratory and Critical Care Medicine 195*, 1384–1393.

Chan-Ling, T., Hughes, S., Baxter, L., Rosinova, E., McGregor, I., Morcos, Y., van Nieuwenhuyzen, P., & Hu, P. (2007). Inflammation and breakdown of the blood-retinal barrier during "physiological aging" in the rat retina: A model for CNS aging. *Microcirculation 14*, 63–76.

Chauhan, M. B., & Chauhan, N. B. (2015). Brain uptake of neurotherapeutics after intranasal versus intraperitoneal delivery in mice. *Journal of Neurology and Neurosurgery 2*.

Chen, W., Li, Z., Wang, Z., Gao, H., Ding, J., & He, Z. (2020). Intraarticular injection of infliximab-loaded thermosensitive hydrogel alleviates pain and protects cartilage in Rheumatoid arthritis. *Journal of Pain Research 13*, 3315–3329.

Chen, X., Guo, X., Huang, R., Zheng, Z., Chen, Y., & Shang, H. F. (2014). An exploratory study of serum creatinine levels in patients with amyotrophic lateral sclerosis. *Neurological Sciences 35*, 1591–1597.

Cheng, L., Zhang, J., Li, X. Y., Yuan, L., Pan, Y. F., Chen, X. R., ... Qi, J. S. (2017). A novel antibody targeting sequence 31-35 in amyloid beta protein attenuates Alzheimer's disease-related neuronal damage. *Hippocampus 27*, 122–133.

Cho, H., Lee, H. Y., Han, M., Choi, J. R., Ahn, S., Lee, T., ... Park, J. (2016). Localized down-regulation of P-glycoprotein by focused ultrasound and microbubbles induced blood-brain barrier disruption in rat brain. *Scientific Reports 6*, 31201.

Cho, K. H., & Caparon, M. G. (2005). Patterns of virulence gene expression differ between biofilm and tissue communities of Streptococcus pyogenes. *Molecular Microbiology 57*, 1545–1556.

Choudhari, M., Hejmady, S., Narayan Saha, R., Damle, S., Singhvi, G., Alexander, A., Kesharwani, P., & Kumar Dubey, S. (2021). Evolving new-age strategies to transport therapeutics across the blood-brain-barrier. *International Journal of Pharmaceutics 599*, 120351.

Ciornei, C. D., Novikov, A., Beloin, C., Fitting, C., Caroff, M., Ghigo, J. M., ... Adib-Conquy, M. (2010). Biofilm-forming Pseudomonas aeruginosa bacteria undergo lipopolysaccharide structural modifications and induce enhanced inflammatory cytokine response in human monocytes. *Innate Immunity 16*, 288–301.

Cohen-Pfeffer, J. L., Gururangan, S., Lester, T., Lim, D. A., Shaywitz, A. J., Westphal, M., & Slavc, I. (2017). Intracerebroventricular delivery as a safe, long-term route of drug administration. *Pediatric Neurology 67*, 23–35.

Cooper, P. R., Ciambrone, G. J., Kliwinski, C. M., Maze, E., Johnson, L., Li, Q., ... Hornby, P. J. (2013). Efflux of monoclonal antibodies from rat brain by neonatal Fc receptor, FcRn. *Brain Research 1534*, 13–21.

Corfield, A. P., Carroll, D., Myerscough, N., & Probert, C. S. (2001). Mucins in the gastrointestinal tract in health and disease. *Frontiers in Bioscience 6*, D1321–D1357.

Costa, A. C., Joaquim, H. P. G., Forlenza, O., Talib, L. L., & Gattaz, W. F. (2019). Plasma lipids metabolism in mild cognitive impairment and Alzheimer's disease. *The World Journal of Biological Psychiatry 20*, 190–196.

Costerton, W., Veeh, R., Shirtliff, M., Pasmore, M., Post, C., & Ehrlich, G. (2003). The application of biofilm science to the study and control of chronic bacterial infections. *The Journal of Clinical Investigation 112*, 1466–1477.

Crabbe, A., Jensen, P. O., Bjarnsholt, T., & Coenye, T. (2019). Antimicrobial tolerance and metabolic adaptations in microbial biofilms. *Trends in Microbiology 27*, 850–863.

Creeth, J. M. (1978). Constituents of mucus and their separation. *British Medical Bulletin 34*, 17–24.

Crowe, J. S., Roberts, K. J., Carlton, T. M., Maggiore, L., Cubitt, M. F., Ray, K. P., ... West, M. R. (2019). Oral delivery of the anti-tumor necrosis factor alpha domain antibody, V565, results in high intestinal and fecal concentrations with minimal systemic exposure in cynomolgus monkeys. *Drug Development and Industrial Pharmacy 45*, 387–394.

Crowell, S. R., Wang, K., Famili, A., Shatz, W., Loyet, K. M., Chang, V., ... Kelley, R. F. (2019). Influence of charge, hydrophobicity, and size on vitreous pharmacokinetics of large molecules. *Translational Vision Science & Technology 8*, 1.

Csaba, N., Garcia-Fuentes, M., & Alonso, M. J. (2009). Nanoparticles for nasal vaccination. *Advanced Drug Delivery Reviews 61*, 140–157.

Curciarello, R., Sobande, T., Jones, S., Giuffrida, P., Di Sabatino, A., Docena, G. H., ... Kok, K. (2020). Human neutrophil elastase proteolytic activity in ulcerative colitis favors the loss of function of therapeutic monoclonal antibodies. *Journal of Inflammation Research 13*, 233–243.

Dal Corso, A., Cazzamalli, S., Gebleux, R., Mattarella, M., & Neri, D. (2017). Protease-cleavable linkers modulate the anticancer activity of noninternalizing antibody-drug conjugates. *Bioconjugate Chemistry 28*, 1826–1833.

Datta-Mannan, A., Croy, J. E., Schirtzinger, L., Torgerson, S., Breyer, M., & Wroblewski, V. J. (2016). Aberrant bispecific antibody pharmacokinetics linked to liver sinusoidal endothelium clearance mechanism in cynomolgus monkeys. *MAbs 8*, 969–982.

Davies Cde, L., Berk, D. A., Pluen, A., & Jain, R. K. (2002). Comparison of IgG diffusion and extracellular matrix composition in rhabdomyosarcomas grown in mice versus

in vitro as spheroids reveals the role of host stromal cells. *British Journal of Cancer 86*, 1639–1644.
Deane, R., Bell, R. D., Sagare, A., & Zlokovic, B. V. (2009). Clearance of amyloid-beta peptide across the blood-brain barrier: Implication for therapies in Alzheimer's disease. *CNS & Neurological Disorders Drug Targets 8*, 16–30.
Deane, R., Sagare, A., Hamm, K., Parisi, M., LaRue, B., Guo, H., ... Zlokovic, B. V. (2005). IgG-assisted age-dependent clearance of Alzheimer's amyloid beta peptide by the blood-brain barrier neonatal Fc receptor. *The Journal of Neuroscience 25*, 11495–11503.
Deane, R., Wu, Z., Sagare, A., Davis, J., Du Yan, S., Hamm, K., ... Zlokovic, B. V. (2004). LRP/amyloid beta-peptide interaction mediates differential brain efflux of Abeta isoforms. *Neuron 43*, 333–344.
Del Amo, E. M., Rimpela, A. K., Heikkinen, E., Kari, O. K., Ramsay, E., Lajunen, T., ... Urtti, A. (2017). Pharmacokinetic aspects of retinal drug delivery. *Progress in Retinal and Eye Research 57*, 134–185.
Detalle, L., Stohr, T., Palomo, C., Piedra, P. A., Gilbert, B. E., Mas, V., ... Depla, E. (2016). Generation and characterization of ALX-0171, a potent novel therapeutic nanobody for the treatment of respiratory syncytial virus infection. *Antimicrobial Agents and Chemotherapy 60*, 6–13.
Deveuve, Q., Lajoie, L., Barrault, B., & Thibault, G. (2020). The proteolytic cleavage of therapeutic monoclonal antibody hinge region: More than a matter of subclass. *Frontiers in Immunology 11*, 168.
Dewhirst, M. W., & Secomb, T. W. (2017). Transport of drugs from blood vessels to tumour tissue. *Nature Reviews Cancer 17*, 738–750.
D'Hooghe, L., Chalmers, A. D., Heywood, S., & Whitley, P. (2017). Cell surface dynamics and cellular distribution of endogenous FcRn. *PLoS One 12* e0182695.
Dickinson, B. L., Badizadegan, K., Wu, Z., Ahouse, J. C., Zhu, X., Simister, N. E., ... Lencer, W. I. (1999). Bidirectional FcRn-dependent IgG transport in a polarized human intestinal epithelial cell line. *The Journal of Clinical Investigation 104*, 903–911.
Dijkers, E. C., Oude Munnink, T. H., Kosterink, J. G., Brouwers, A. H., Jager, P. L., de Jong, J. R., ... de Vries, E. G. (2010). Biodistribution of 89Zr-trastuzumab and PET imaging of HER2-positive lesions in patients with metastatic breast cancer. *Clinical Pharmacology and Therapeutics 87*, 586–592.
Doody, R. S., Thomas, R. G., Farlow, M., Iwatsubo, T., Vellas, B., Joffe, S., ... Alzheimer's Disease Cooperative Study Steering, C., & Solanezumab Study, G (2014). Phase 3 trials of solanezumab for mild-to-moderate Alzheimer's disease. *The New England Journal of Medicine 370*, 311–321.
Du, B., Liang, M., Zheng, H., Fan, C., Zhang, H., Lu, X., Du, Z., Lian, Y., Zhang, Y., & Bi, X. (2020). Anti-mouse CX3CR1 antibody alleviates cognitive impairment, neuronal loss and myelin deficits in an animal model of brain ischemia. *Neuroscience 438*, 169–181.
Dubey, S., Heinen, S., Krantic, S., McLaurin, J., Branch, D. R., Hynynen, K., & Aubert, I. (2020). Clinically approved IVIg delivered to the hippocampus with focused ultrasound promotes neurogenesis in a model of Alzheimer's disease. *Proceedings of the National Academy of Sciences of the United States of America 117*, 32691–32700.
Duncan, G. A., Jung, J., Joseph, A., Thaxton, A. L., West, N. E., Boyle, M. P., ... Suk, J. S. (2016). Microstructural alterations of sputum in cystic fibrosis lung disease. *JCI Insight 1* e88198.
Dunnhaupt, S., Kammona, O., Waldner, C., Kiparissides, C., & Bernkop-Schnurch, A. (2015). Nano-carrier systems: Strategies to overcome the mucus gel barrier. *European Journal of Pharmaceutics and Biopharmaceutics 96*, 447–453.
Durand, R. E., & Aquino-Parsons, C. (2001). Clinical relevance of intermittent tumour blood flow. *Acta Oncologica 40*, 929–936.
Edgar, L. T., Underwood, C. J., Guilkey, J. E., Hoying, J. B., & Weiss, J. A. (2014). Extracellular matrix density regulates the rate of neovessel growth and branching in sprouting angiogenesis. *PLoS One 9* e85178.
Eikenes, L., Bruland, O. S., Brekken, C., & Davies Cde, L. (2004). Collagenase increases the transcapillary pressure gradient and improves the uptake and distribution of monoclonal antibodies in human osteosarcoma xenografts. *Cancer Research 64*, 4768–4773.
Eikenes, L., Tari, M., Tufto, I., Bruland, O. S., & de Lange Davies, C. (2005). Hyaluronidase induces a transcapillary pressure gradient and improves the distribution and uptake of liposomal doxorubicin (Caelyx) in human osteosarcoma xenografts. *British Journal of Cancer 93*, 81–88.
Elsaid, N., Jackson, T. L., Elsaid, Z., Alqathama, A., & Somavarapu, S. (2016). PLGA microparticles entrapping chitosan-based nanoparticles for the ocular delivery of ranibizumab. *Molecular Pharmaceutics 13*, 2923–2940.
Elshiaty, M., Schindler, H., & Christopoulos, P. (2021). Principles and current clinical landscape of multispecific antibodies against cancer. *International Journal of Molecular Sciences 22*.
Ensign, L. M., Cone, R., & Hanes, J. (2012). Oral drug delivery with polymeric nanoparticles: The gastrointestinal mucus barriers. *Advanced Drug Delivery Reviews 64*, 557–570.
Ensign, L. M., Tang, B. C., Wang, Y. Y., Tse, T. A., Hoen, T., Cone, R., & Hanes, J. (2012). Mucus-penetrating nanoparticles for vaginal drug delivery protect against herpes simplex virus. *Science Translational Medicine 4* 138ra179.
Erdo, F., Denes, L., & de Lange, E. (2017). Age-associated physiological and pathological changes at the blood-brain barrier: A review. *Journal of Cerebral Blood Flow and Metabolism 37*, 4–24.
Erickson, M. A., & Banks, W. A. (2019). Age-associated changes in the immune system and blood(-)brain barrier functions. *International Journal of Molecular Sciences 20*.
Estrada, M. F., Rebelo, S. P., Davies, E. J., Pinto, M. T., Pereira, H., Santo, V. E., ... Brito, C. (2016). Modelling the tumour microenvironment in long-term microencapsulated 3D co-cultures recapitulates phenotypic features of disease progression. *Biomaterials 78*, 50–61.
Eswaramoorthy, R., Chang, C. C., Wu, S. C., Wang, G. J., Chang, J. K., & Ho, M. L. (2012). Sustained release of PTH(1-34) from PLGA microspheres suppresses osteoarthritis progression in rats. *Acta Biomaterialia 8*, 2254–2262.
Evans, C. H., Kraus, V. B., & Setton, L. A. (2014). Progress in intra-articular therapy. *Nature Reviews Rheumatology 10*, 11–22.
Fan, X., Brezski, R. J., Deng, H., Dhupkar, P. M., Shi, Y., Gonzalez, A., ... An, Z. (2015). A novel therapeutic strategy to rescue the immune effector function of proteolytically inactivated cancer therapeutic antibodies. *Molecular Cancer Therapeutics 14*, 681–691.
Fan, X., Brezski, R. J., Fa, M., Deng, H., Oberholtzer, A., Gonzalez, A., ... An, Z. (2012). A single proteolytic cleavage within the lower hinge of trastuzumab reduces immune effector function and in vivo efficacy. *Breast Cancer Research 14*, R116.
Farquhar, M. G., & Palade, G. E. (1963). Junctional complexes in various epithelia. *The Journal of Cell Biology 17*, 375–412.
Ferrati, S., Wu, T., Kanapuram, S. R., & Smyth, H. D. C. (2018). Dosing considerations for inhaled biologics. *International Journal of Pharmaceutics 549*, 58–66.
Ferreira, N. N., de Oliveira Junior, E., Granja, S., Boni, F. I., Ferreira, L. M. B., Cury, B. S. F., ... Gremiao, M. P. D. (2021). Nose-to-brain co-delivery of drugs for glioblastoma treatment using nanostructured system. *International Journal of Pharmaceutics 603*, 120714.
Ferretti, S., Allegrini, P. R., Becquet, M. M., & McSheehy, P. M. (2009). Tumor interstitial fluid pressure as an early-response marker for anticancer therapeutics. *Neoplasia 11*, 874–881.
Fokkink, W. J., Haarman, A. E., Tio-Gillen, A. P., van Rijs, W., Huizinga, R., van Doorn, P. A., & Jacobs, B. C. (2016). Neonatal Fc receptor promoter gene polymorphism does not predict pharmacokinetics of IVIg or the clinical course of GBS. *Annals of Clinical Translational Neurology 3*, 547–551.
Fong, J. C., Karplus, K., Schoolnik, G. K., & Yildiz, F. H. (2006). Identification and characterization of RbmA, a novel protein required for the development of rugose colony morphology and biofilm structure in Vibrio cholerae. *Journal of Bacteriology 188*, 1049–1059.
Foy, B. D., & Blake, J. (2001). Diffusion of paramagnetically labeled proteins in cartilage: Enhancement of the 1-D NMR imaging technique. *Journal of Magnetic Resonance 148*, 126–134.
Francis, D. M., & Thomas, S. N. (2017). Progress and opportunities for enhancing the delivery and efficacy of checkpoint inhibitors for cancer immunotherapy. *Advanced Drug Delivery Reviews 114*, 33–42.
Frohlich, E., & Roblegg, E. (2014). Mucus as barrier for drug delivery by nanoparticles. *Journal of Nanoscience and Nanotechnology 14*, 126–136.
Furst, D. E., Lindsley, H., Baethge, B., Botstein, G. R., Caldwell, J., Dietz, F., ... Yocum, D. (1999). Dose-loading with hydroxychloroquine improves the rate of response in early, active rheumatoid arthritis: A randomized, double-blind six-week trial with eighteen-week extension. *Arthritis and Rheumatism 42*, 357–365.
Gaillard, P. J., de Boer, A. B., & Breimer, D. D. (2003). Pharmacological investigations on lipopolysaccharide-induced permeability changes in the blood-brain barrier in vitro. *Microvascular Research 65*, 24–31.
Galgoczy, R., Pastor, I., Colom, A., Gimenez, A., Mas, F., & Alcaraz, J. (2014). A spectrophotometer-based diffusivity assay reveals that diffusion hindrance of small molecules in extracellular matrix gels used in 3D cultures is dominated by viscous effects. *Colloids and Surfaces. B, Biointerfaces 120*, 200–207.
Gal-Or, O., Dotan, A., Dachbash, M., Tal, K., Nisgav, Y., Weinberger, D., Ehrlich, R., & Livnat, T. (2016). Bevacizumab clearance through the iridocorneal angle following intravitreal injection in a rat model. *Experimental Eye Research 145*, 412–416.
Gao, Y., Shi, Y., Fu, M., Feng, Y., Lin, G., Kong, D., & Jiang, B. (2020). Simulation study of the effects of interstitial fluid pressure and blood flow velocity on transvascular transport of nanoparticles in tumor microenvironment. *Computer Methods and Programs in Biomedicine 193*, 105493.
Garg, A., & Balthasar, J. P. (2009). Investigation of the influence of FcRn on the distribution of IgG to the brain. *The AAPS Journal 11*, 553–557.
Gautam, A., Nanda, J. S., Samuel, J. S., Kumari, M., Priyanka, P., Bedi, G., ... Raghava, G. P. (2016). Topical delivery of protein and peptide using novel cell penetrating peptide IMT-P8. *Scientific Reports 6*, 26278.
Gebleux, R., Wulhfard, S., Casi, G., & Neri, D. (2015). Antibody format and drug release rate determine the therapeutic activity of noninternalizing antibody-drug conjugates. *Molecular Cancer Therapeutics 14*, 2606–2612.
Geh, K. J., Stelzl, A., Grone, A., Wagner, L., Forster, B., & Winter, G. (2019). Development of a sprayable hydrogel formulation for the skin application of therapeutic antibodies. *European Journal of Pharmaceutics and Biopharmaceutics 142*, 123–132.
Glassman, P. M., Abuqayyas, L., & Balthasar, J. P. (2015). Assessments of antibody biodistribution. *Journal of Clinical Pharmacology 55*(Suppl. 3), S29–S38.
Gouilleux-Gruart, V., Chapel, H., Chevret, S., Lucas, M., Malphettes, M., Fieschi, C., ... group, D. s (2013). Efficiency of immunoglobulin G replacement therapy in common variable immunodeficiency: Correlations with clinical phenotype and polymorphism of the neonatal Fc receptor. *Clinical and Experimental Immunology 171*, 186–194.
Gray, M. T., & Woulfe, J. M. (2015). Striatal blood-brain barrier permeability in Parkinson's disease. *Journal of Cerebral Blood Flow and Metabolism 35*, 747–750.
Gros-Louis, F., Soucy, G., Lariviere, R., & Julien, J. P. (2010). Intracerebroventricular infusion of monoclonal antibody or its derived Fab fragment against misfolded forms of SOD1 mutant delays mortality in a mouse model of ALS. *Journal of Neurochemistry 113*, 1188–1199.
Grossi, P. M., Ochiai, H., Archer, G. E., McLendon, R. E., Zalutsky, M. R., Friedman, A. H., ... Sampson, J. H. (2003). Efficacy of intracerebral microinfusion of trastuzumab in an athymic rat model of intracerebral metastatic breast cancer. *Clinical Cancer Research 9*, 5514–5520.
Guilleminault, L., Azzopardi, N., Arnoult, C., Sobilo, J., Herve, V., Montharu, J., Guillon, A., Andres, C., Herault, O., Le Pape, A., Diot, P., Lemarie, E., Paintaud, G., Gouilleux-Gruart, V., & Heuze-Vourc'h, N. (2014). Fate of inhaled monoclonal antibodies after the deposition of aerosolized particles in the respiratory system. *Journal of Controlled Release 196*, 344–354.

Hacha, J., Tomlinson, K., Maertens, L., Paulissen, G., Rocks, N., Foidart, J. M., ... Cataldo, D. D. (2012). Nebulized anti-IL-13 monoclonal antibody Fab' fragment reduces allergen-induced asthma. *American Journal of Respiratory Cell and Molecular Biology 47*, 709–717.

Hall, C. W., & Mah, T. F. (2017). Molecular mechanisms of biofilm-based antibiotic resistance and tolerance in pathogenic bacteria. *FEMS Microbiology Reviews 41*, 276–301.

Hallmann, R., Zhang, X., Di Russo, J., Li, L., Song, J., Hannocks, M. J., & Sorokin, L. (2015). The regulation of immune cell trafficking by the extracellular matrix. *Current Opinion in Cell Biology 36*, 54–61.

Hashimoto, S., Okayama, Y., Shime, N., Kimura, A., Funakoshi, Y., Kawabata, K., Ishizaka, A., & Amaya, F. (2008). Neutrophil elastase activity in acute lung injury and respiratory distress syndrome. *Respirology 13*, 581–584.

Haymann, J. P., Levraud, J. P., Bouet, S., Kappes, V., Hagege, J., Nguyen, G., ... Sraer, J. D. (2000). Characterization and localization of the neonatal Fc receptor in adult human kidney. *Journal of the American Society of Nephrology 11*, 632–639.

Heine, M., Freund, B., Nielsen, P., Jung, C., Reimer, R., Hohenberg, H., ... Schumacher, U. (2012). High interstitial fluid pressure is associated with low tumour penetration of diagnostic monoclonal antibodies applied for molecular imaging purposes. *PLoS One 7* e36258.

Heldin, C. H., Rubin, K., Pietras, K., & Ostman, A. (2004). High interstitial fluid pressure - an obstacle in cancer therapy. *Nature Reviews Cancer 4*, 806–813.

Hellings, P. W., & Steelant, B. (2020). Epithelial barriers in allergy and asthma. *The Journal of Allergy and Clinical Immunology 145*, 1499–1509.

Herrera, J., Henke, C. A., & Bitterman, P. B. (2018). Extracellular matrix as a driver of progressive fibrosis. *The Journal of Clinical Investigation 128*, 45–53.

Hessmann, E., Buchholz, S. M., Demir, I. E., Singh, S. K., Gress, T. M., Ellenrieder, V., & Neesse, A. (2020). Microenvironmental determinants of pancreatic cancer. *Physiological Reviews 100*, 1707–1751.

Heyman, M., Ducroc, R., Desjeux, J. F., & Morgat, J. L. (1982). Horseradish peroxidase transport across adult rabbit jejunum in vitro. *The American Journal of Physiology 242*, G558–G564.

Higgins, C. F. (2001). ABC transporters: Physiology, structure and mechanism–an overview. *Research in Microbiology 152*, 205–210.

Hoiby, N., Ciofu, O., & Bjarnsholt, T. (2010). Pseudomonas aeruginosa biofilms in cystic fibrosis. *Future Microbiology 5*, 1663–1674.

Holash, J., Davis, S., Papadopoulos, N., Croll, S. D., Ho, L., Russell, M., ... Rudge, J. S. (2002). VEGF-Trap: A VEGF blocker with potent antitumor effects. *Proceedings of the National Academy of Sciences of the United States of America 99*, 11393–11398.

Hollingsworth, M. A., & Swanson, B. J. (2004). Mucins in cancer: Protection and control of the cell surface. *Nature Reviews Cancer 4*, 45–60.

Homayun, B., Lin, X., & Choi, H. J. (2019). Challenges and recent progress in oral drug delivery systems for biopharmaceuticals. *Pharmaceutics 11*.

Hsiao, H. C., Fan, X., Jordan, R. E., Zhang, N., & An, Z. (2018). Proteolytic single hinge cleavage of pertuzumab impairs its Fc effector function and antitumor activity in vitro and in vivo. *Breast Cancer Research 20*, 43.

Hu, S., & Koevary, S. (2016). Efficacy of antibody delivery to the retina and optic nerve by topical administration. *Journal of Ocular Pharmacology and Therapeutics 32*, 203–210.

Hughes, P. M., Olejnik, O., Chang-Lin, J. E., & Wilson, C. G. (2005). Topical and systemic drug delivery to the posterior segments. *Advanced Drug Delivery Reviews 57*, 2010–2032.

Hukill, P. B., & Vidone, R. A. (1965). Histochemistry of mucus and other polysaccharides in tumors. I. Carcinoma of the bladder. *Laboratory Investigation 14*, 1624–1635.

Indira Chandran, V., Mansson, A. S., Barbachowska, M., Cerezo-Magana, M., Nodin, B., Joshi, B., ... Belting, M. (2020). Hypoxia attenuates trastuzumab uptake and trastuzumab-emtansine (T-DM1) cytotoxicity through redistribution of phosphorylated caveolin-1. *Molecular Cancer Research 18*, 644–656.

Irving, E. A., Vinson, M., Rosin, C., Roberts, J. C., Chapman, D. M., Facci, L., ... Parsons, A. A. (2005). Identification of neuroprotective properties of anti-MAG antibody: A novel approach for the treatment of stroke? *Journal of Cerebral Blood Flow and Metabolism 25*, 98–107.

Israel, E. J., Taylor, S., Wu, Z., Mizoguchi, E., Blumberg, R. S., Bhan, A., & Simister, N. E. (1997). Expression of the neonatal Fc receptor, FcRn, on human intestinal epithelial cells. *Immunology 92*, 69–74.

Jacobetz, M. A., Chan, D. S., Neesse, A., Bapiro, T. E., Cook, N., Frese, K. K., ... Tuveson, D. A. (2013). Hyaluronan impairs vascular function and drug delivery in a mouse model of pancreatic cancer. *Gut 62*, 112–120.

Jain, R. K. (1988). Determinants of tumor blood flow: A review. *Cancer Research 48*, 2641–2658.

Jain, R. K., Tong, R. T., & Munn, L. L. (2007). Effect of vascular normalization by antiangiogenic therapy on interstitial hypertension, peritumor edema, and lymphatic metastasis: Insights from a mathematical model. *Cancer Research 67*, 2729–2735.

Janowicz, P. W., Leinenga, G., Gotz, J., & Nisbet, R. M. (2019). Ultrasound-mediated blood-brain barrier opening enhances delivery of therapeutically relevant formats of a tau-specific antibody. *Scientific Reports 9*, 9255.

Jespersen, S. N., & Ostergaard, L. (2012). The roles of cerebral blood flow, capillary transit time heterogeneity, and oxygen tension in brain oxygenation and metabolism. *Journal of Cerebral Blood Flow and Metabolism 32*, 264–277.

Jiang, X. R., Song, A., Bergelson, S., Arroll, T., Parekh, B., May, K., ... Schenerman, M. (2011). Advances in the assessment and control of the effector functions of therapeutic antibodies. *Nature Reviews Drug Discovery 10*, 101–111.

Jin, Y., Song, Y., Zhu, X., Zhou, D., Chen, C., Zhang, Z., & Huang, Y. (2012). Goblet cell-targeting nanoparticles for oral insulin delivery and the influence of mucus on insulin transport. *Biomaterials 33*, 1573–1582.

Johansson, A., Erlandsson, A., Eriksson, D., Ullen, A., Holm, P., Sundstrom, B. E., ... Stigbrand, T. (2002). Idiotypic-anti-idiotypic complexes and their in vivo metabolism. *Cancer 94*, 1306–1313.

Jordao, J. F., Ayala-Grosso, C. A., Markham, K., Huang, Y., Chopra, R., McLaurin, J., ... Aubert, I. (2010). Antibodies targeted to the brain with image-guided focused ultrasound reduces amyloid-beta plaque load in the TgCRND8 mouse model of Alzheimer's disease. *PLoS One 5* e10549.

Joubert, N., Beck, A., Dumontet, C., & Denevault-Sabourin, C. (2020). Antibody-drug conjugates: The last decade. *Pharmaceuticals (Basel) 13*.

Joubert, N., Denevault-Sabourin, C., Bryden, F., & Viaud-Massuard, M. C. (2017). Towards antibody-drug conjugates and prodrug strategies with extracellular stimuli-responsive drug delivery in the tumor microenvironment for cancer therapy. *European Journal of Medicinal Chemistry 142*, 393–415.

Kamath, A. V. (2016). Translational pharmacokinetics and pharmacodynamics of monoclonal antibodies. *Drug Discovery Today: Technologies 21–22*, 75–83.

Kang, M. I., & Im, G. I. (2014). Drug delivery systems for intra-articular treatment of osteoarthritis. *Expert Opinion on Drug Delivery 11*, 269–282.

Kasturirangan, S., Rainey, G. J., Xu, L., Wang, X., Portnoff, A., Chen, T., ... Gao, C. (2017). Targeted Fcgamma receptor (FcgammaR)-mediated clearance by a biparatopic bispecific antibody. *The Journal of Biological Chemistry 292*, 4361–4370.

Kerbel, R. S. (2006). Antiangiogenic therapy: A universal chemosensitization strategy for cancer? *Science 312*, 1171–1175.

Kessenbrock, K., Plaks, V., & Werb, Z. (2010). Matrix metalloproteinases: Regulators of the tumor microenvironment. *Cell 141*, 52–67.

Kim, J. K., Firan, M., Radu, C. G., Kim, C. H., Ghetie, V., & Ward, E. S. (1999). Mapping the site on human IgG for binding of the MHC class I-related receptor, FcRn. *European Journal of Immunology 29*, 2819–2825.

Kim, Y. C., Chiang, B., Wu, X., & Prausnitz, M. R. (2014). Ocular delivery of macromolecules. *Journal of Controlled Release 190*, 172–181.

Kimura, S. (2018). Molecular insights into the mechanisms of M-cell differentiation and transcytosis in the mucosa-associated lymphoid tissues. *Anatomical Science International 93*, 23–34.

Kinder, M., Greenplate, A. R., Grugan, K. D., Soring, K. L., Heeringa, K. A., McCarthy, S. G., ... Brezski, R. J. (2013). Engineered protease-resistant antibodies with selectable cell-killing functions. *The Journal of Biological Chemistry 288*, 30843–30854.

Kinoshita, M., McDannold, N., Jolesz, F. A., & Hynynen, K. (2006). Noninvasive localized delivery of Herceptin to the mouse brain by MRI-guided focused ultrasound-induced blood-brain barrier disruption. *Proceedings of the National Academy of Sciences of the United States of America 103*, 11719–11723.

Klyubin, I., Walsh, D. M., Lemere, C. A., Cullen, W. K., Shankar, G. M., Betts, V., ... Rowan, M. J. (2005). Amyloid beta protein immunotherapy neutralizes Abeta oligomers that disrupt synaptic plasticity in vivo. *Nature Medicine 11*, 556–561.

Ko, S., Jo, M., & Jung, S. T. (2021). Recent achievements and challenges in prolonging the serum half-lives of therapeutic IgG antibodies through Fc engineering. *BioDrugs 35*, 147–157.

Kobus, T., Zervantonakis, I. K., Zhang, Y., & McDannold, N. J. (2016). Growth inhibition in a brain metastasis model by antibody delivery using focused ultrasound-mediated blood-brain barrier disruption. *Journal of Controlled Release 238*, 281–288.

Koerselman, M., Warmink, K., Korthagen, N. M., van Midwoud, P., Verrips, T., Weinans, H. H., & Karperien, M. (2020). Intra-articular drug depots for controlled release of heavy chain only antibodies blocking joint inflammation. *2020 OARSI world congress on osteoarthritis. 28.*. Messe Wien Exhibition & Congress Center, Vienna, Austria: Elsevier S37.

Koo, H., Allan, R. N., Howlin, R. P., Stoodley, P., & Hall-Stoodley, L. (2017). Targeting microbial biofilms: Current and prospective therapeutic strategies. *Nature Reviews Microbiology 15*, 740–755.

Koohestani, F., Braundmeier, A. G., Mahdian, A., Seo, J., Bi, J., & Nowak, R. A. (2013). Extracellular matrix collagen alters cell proliferation and cell cycle progression of human uterine leiomyoma smooth muscle cells. *PLoS One 8* e75844.

Kortekaas, R., Leenders, K. L., van Oostrom, J. C., Vaalburg, W., Bart, J., Willemsen, A. T., & Hendrikse, N. H. (2005). Blood-brain barrier dysfunction in parkinsonian midbrain in vivo. *Annals of Neurology 57*, 176–179.

Koussoroplis, S. J., Paulissen, G., Tyteca, D., Goldansaz, H., Todoroff, J., Barilly, C., ... Vanbever, R. (2014). PEGylation of antibody fragments greatly increases their local residence time following delivery to the respiratory tract. *Journal of Controlled Release 187*, 91–100.

Kruegel, J., & Miosge, N. (2010). Basement membrane components are key players in specialized extracellular matrices. *Cellular and Molecular Life Sciences 67*, 2879–2895.

Kumar, N. N., Lochhead, J. J., Pizzo, M. E., Nehra, G., Boroumand, S., Greene, G., & Thorne, R. G. (2018). Delivery of immunoglobulin G antibodies to the rat nervous system following intranasal administration: Distribution, dose-response, and mechanisms of delivery. *Journal of Controlled Release 286*, 467–484.

Kushner, I., & Somerville, J. A. (1971). Permeability of human synovial membrane to plasma proteins. Relationship to molecular size and inflammation. *Arthritis and Rheumatism 14*, 560–570.

Ladel, S., Flamm, J., Zadeh, A. S., Filzwieser, D., Walter, J. C., Schlossbauer, P., ... Schindowski, K. (2018). Allogenic Fc domain-facilitated uptake of IgG in nasal lamina propria: Friend or foe for intranasal CNS delivery? *Pharmaceutics 10*.

Lai, S. K., Wang, Y. Y., & Hanes, J. (2009). Mucus-penetrating nanoparticles for drug and gene delivery to mucosal tissues. *Advanced Drug Delivery Reviews 61*, 158–171.

Lai, S. K., Wang, Y. Y., Wirtz, D., & Hanes, J. (2009). Micro- and macrorheology of mucus. *Advanced Drug Delivery Reviews 61*, 86–100.

Lambert, W. J., & Peck, K. D. (1995). Development of an in situ forming biodegradable poly-lactide-coglycolide system for the controlled release of proteins. *Journal of Controlled Release 33*, 189–195.

Latvala, S., Jacobsen, B., Otteneder, M. B., Herrmann, A., & Kronenberg, S. (2017). Distribution of FcRn across species and tissues. *The Journal of Histochemistry and Cytochemistry 65*, 321–333.

Laude, A., Tan, L. E., Wilson, C. G., Lascaratos, G., Elashry, M., Aslam, T., ... Dhillon, B. (2010). Intravitreal therapy for neovascular age-related macular degeneration and inter-individual variations in vitreous pharmacokinetics. *Progress in Retinal and Eye Research 29*, 466–475.
Lawrence, R. C., Helmick, C. G., Arnett, F. C., Deyo, R. A., Felson, D. T., Giannini, E. H., ... Wolfe, F. (1998). Estimates of the prevalence of arthritis and selected musculoskeletal disorders in the United States. *Arthritis and Rheumatism 41*, 778–799.
Leal, J., Smyth, H. D. C., & Ghosh, D. (2017). Physicochemical properties of mucus and their impact on transmucosal drug delivery. *International Journal of Pharmaceutics 532*, 555–572.
Lee, H., Park, J., & Kim, Y. C. (2018). Enhanced transdermal delivery with less irritation by magainin pore-forming peptide with a N-lauroylsarcosine and sorbitan monolaurate mixture. *Drug Delivery and Translational Research 8*, 54–63.
Leinenga, G., Bodea, L. G., Koh, W. K., Nisbet, R. M., & Gotz, J. (2020). Delivery of antibodies into the brain using focused scanning ultrasound. *The Journal of Visualized Experiments 18*(161). https://doi.org/10.3791/61372.
Lesniak, W. G., Chu, C., Jablonska, A., Du, Y., Pomper, M. G., Walczak, P., & Janowski, M. (2019). A distinct advantage to intraarterial delivery of (89)Zr-bevacizumab in PET imaging of mice with and without osmotic opening of the blood-brain barrier. *Journal of Nuclear Medicine 60*, 617–622.
Lewenza, S. (2013). Extracellular DNA-induced antimicrobial peptide resistance mechanisms in Pseudomonas aeruginosa. *Frontiers in Microbiology 4*, 21.
Leyland-Jones, B., Gelmon, K., Ayoub, J. P., Arnold, A., Verma, S., Dias, R., & Ghahramani, P. (2003). Pharmacokinetics, safety, and efficacy of trastuzumab administered every three weeks in combination with paclitaxel. *Journal of Clinical Oncology 21*, 3965–3971.
Li, F., Ulrich, M., Jonas, M., Stone, I. J., Linares, G., Zhang, X., ... Law, C. L. (2017). Tumor-associated macrophages can contribute to antitumor activity through FcgammaR-mediated processing of antibody-drug conjugates. *Molecular Cancer Therapeutics 16*, 1347–1354.
Lieleg, O., & Ribbeck, K. (2011). Biological hydrogels as selective diffusion barriers. *Trends in Cell Biology 21*, 543–551.
Liu, H. L., Hsu, P. H., Lin, C. Y., Huang, C. W., Chai, W. Y., Chu, P. C., ... Wei, K. C. (2016). Focused ultrasound enhances central nervous system delivery of bevacizumab for malignant glioma treatment. *Radiology 281*, 99–108.
Locke, K. W., Maneval, D. C., & LaBarre, M. J. (2019). ENHANZE((R)) drug delivery technology: A novel approach to subcutaneous administration using recombinant human hyaluronidase PH20. *Drug Delivery 26*, 98–106.
Lombardo, J. A., Stern, E. A., McLellan, M. E., Kajdasz, S. T., Hickey, G. A., Bacskai, B. J., & Hyman, B. T. (2003). Amyloid-beta antibody treatment leads to rapid normalization of plaque-induced neuritic alterations. *The Journal of Neuroscience 23*, 10879–10883.
Lombry, C., Edwards, D. A., Preat, V., & Vanbever, R. (2004). Alveolar macrophages are a primary barrier to pulmonary absorption of macromolecules. *American Journal of Physiology. Lung Cellular and Molecular Physiology 286*, L1002–L1008.
Lopez, E., Scott, N. E., Wines, B. D., Hogarth, P. M., Wheatley, A. K., Kent, S. J., & Chung, A. W. (2019). Low pH exposure during immunoglobulin G purification methods results in aggregates that avidly bind fcgamma receptors: Implications for measuring Fc dependent antibody functions. *Frontiers in Immunology 10*, 2415.
Lopez-Otin, C., & Bond, J. S. (2008). Proteases: Multifunctional enzymes in life and disease. *The Journal of Biological Chemistry 283*, 30433–30437.
Luissint, A. C., Artus, C., Glacial, F., Ganeshamoorthy, K., & Couraud, P. O. (2012). Tight junctions at the blood brain barrier: Physiological architecture and disease-associated dysregulation. *Fluids and Barriers of the CNS 9*, 23.
Lux, A., Yu, X., Scanlan, C. N., & Nimmerjahn, F. (2013). Impact of immune complex size and glycosylation on IgG binding to human FcgammaRs. *Journal of Immunology 190*, 4315–4323.
Mach, H., Gregory, S. M., Mackiewicz, A., Mittal, S., Lalloo, A., Kirchmeier, M., & Shameem, M. (2011). Electrostatic interactions of monoclonal antibodies with subcutaneous tissue. *Therapeutic Delivery 2*, 727–736.
Macierzanka, A., Mackie, A. R., Bajka, B. H., Rigby, N. M., Nau, F., & Dupont, D. (2014). Transport of particles in intestinal mucus under simulated infant and adult physiological conditions: Impact of mucus structure and extracellular DNA. *PLoS One 9* e95274.
Macrez, R., Obiang, P., Gauberti, M., Roussel, B., Baron, A., Parcq, J., ... Ali, C. (2011). Antibodies preventing the interaction of tissue-type plasminogen activator with N-methyl-D-aspartate receptors reduce stroke damages and extend the therapeutic window of thrombolysis. *Stroke 42*, 2315–2322.
Mah, T. F., & O'Toole, G. A. (2001). Mechanisms of biofilm resistance to antimicrobial agents. *Trends in Microbiology 9*, 34–39.
Maher, S., Mrsny, R. J., & Brayden, D. J. (2016). Intestinal permeation enhancers for oral peptide delivery. *Advanced Drug Delivery Reviews 106*, 277–319.
Maherally, Z., Fillmore, H. L., Tan, S. L., Tan, S. F., Jassam, S. A., Quack, F. I., ... Pilkington, G. J. (2018). Real-time acquisition of transendothelial electrical resistance in an all-human, in vitro, 3-dimensional, blood-brain barrier model exemplifies tight-junction integrity. *The FASEB Journal 32*, 168–182.
Maisel, K., Reddy, M., Xu, Q., Chattopadhyay, S., Cone, R., Ensign, L. M., & Hanes, J. (2016). Nanoparticles coated with high molecular weight PEG penetrate mucus and provide uniform vaginal and colorectal distribution in vivo. *Nanomedicine (London, England) 11*, 1337–1343.
Maldonado, M., & Nam, J. (2013). The role of changes in extracellular matrix of cartilage in the presence of inflammation on the pathology of osteoarthritis. *BioMed Research International 2013*, 284873.
Mariette, X., Forger, F., Abraham, B., Flynn, A. D., Molto, A., Flipo, R. M., ... Chakravarty, E. F. (2018). Lack of placental transfer of certolizumab pegol during pregnancy: Results from CRIB, a prospective, postmarketing, pharmacokinetic study. *Annals of the Rheumatic Diseases 77*, 228–233.
Marttin, E., Verhoef, J. C., Cullander, C., Romeijn, S. G., Nagelkerke, J. F., & Merkus, F. W. (1997). Confocal laser scanning microscopic visualization of the transport of dextrans after nasal administration to rats: Effects of absorption enhancers. *Pharmaceutical Research 14*, 631–637.
Masliah, E., Rockenstein, E., Mante, M., Crews, L., Spencer, B., Adame, A., ... Schenk, D. (2011). Passive immunization reduces behavioral and neuropathological deficits in an alpha-synuclein transgenic model of Lewy body disease. *PLoS One 6* e19338.
Matsumura, Y. (2012). Cancer stromal targeting (CAST) therapy. *Advanced Drug Delivery Reviews 64*, 710–719.
Matucci, A., Vultaggio, A., & Danesi, R. (2018). The use of intravenous versus subcutaneous monoclonal antibodies in the treatment of severe asthma: A review. *Respiratory Research 19*, 154.
McDannold, N., Arvanitis, C. D., Vykhodtseva, N., & Livingstone, M. S. (2012). Temporary disruption of the blood-brain barrier by use of ultrasound and microbubbles: Safety and efficacy evaluation in rhesus macaques. *Cancer Research 72*, 3652–3663.
Milner, R., Hung, S., Wang, X., Berg, G. I., Spatz, M., & del Zoppo, G. J. (2008). Responses of endothelial cell and astrocyte matrix-integrin receptors to ischemia mimic those observed in the neurovascular unit. *Stroke 39*, 191–197.
Montanaro, L., Poggi, A., Visai, L., Ravaioli, S., Campoccia, D., Speziale, P., & Arciola, C. R. (2011). Extracellular DNA in biofilms. *The International Journal of Artificial Organs 34*, 824–831.
Montenegro-Nicolini, M., & Morales, J. O. (2017). Overview and future potential of buccal mucoadhesive films as drug delivery systems for biologics. *AAPS PharmSciTech 18*, 3–14.
Montoyo, H. P., Vaccaro, C., Hafner, M., Ober, R. J., Mueller, W., & Ward, E. S. (2009). Conditional deletion of the MHC class I-related receptor FcRn reveals the sites of IgG homeostasis in mice. *Proceedings of the National Academy of Sciences of the United States of America 106*, 2788–2793.
Mullard, A. (2021). Landmark Alzheimer's drug approval confounds research community. *Nature 594*, 309–310.
Nagaraja, T. N., Patel, P., Gorski, M., Gorevic, P. D., Patlak, C. S., & Fenstermacher, J. D. (2005). In normal rat, intraventricularly administered insulin-like growth factor-1 is rapidly cleared from CSF with limited distribution into brain. *Cerebrospinal Fluid Research 2*, 5.
Naito, M., Hasegawa, G., Ebe, Y., & Yamamoto, T. (2004). Differentiation and function of Kupffer cells. *Medical Electron Microscopy 37*, 16–28.
Nelson, A. R., Sweeney, M. D., Sagare, A. P., & Zlokovic, B. V. (2016). Neurovascular dysfunction and neurodegeneration in dementia and Alzheimer's disease. *Biochimica et Biophysica Acta 1862*, 887–900.
Netti, P. A., Berk, D. A., Swartz, M. A., Grodzinsky, A. J., & Jain, R. K. (2000). Role of extracellular matrix assembly in interstitial transport in solid tumors. *Cancer Research 60*, 2497–2503.
Neu, T. R., Manz, B., Volke, F., Dynes, J. J., Hitchcock, A. P., & Lawrence, J. R. (2010). Advanced imaging techniques for assessment of structure, composition and function in biofilm systems. *FEMS Microbiology Ecology 72*, 1–21.
Nguyen-Lefebvre, A. T., & Horuzsko, A. (2015). Kupffer cell metabolism and function. *Journal of Enzymology and Metabolism 1*.
Ni, W., Chen, W., & Lu, Y. (2018). Emerging findings into molecular mechanism of brain metastasis. *Cancer Medicine 7*, 3820–3833.
Nwagwu, C. D., Immidisetti, A. V., Bukanowska, G., Vogelbaum, M. A., & Carbonell, A. M. (2020). Convection-enhanced delivery of a first-in-class anti-beta1 integrin antibody for the treatment of high-grade glioma utilizing real-time imaging. *Pharmaceutics 13*.
Ober, R. J., Martinez, C., Vaccaro, C., Zhou, J., & Ward, E. S. (2004). Visualizing the site and dynamics of IgG salvage by the MHC class I-related receptor, FcRn. *Journal of Immunology 172*, 2021–2029.
Oberli, M. A., Schoellhammer, C. M., Langer, R., & Blankschtein, D. (2014). Ultrasound-enhanced transdermal delivery: Recent advances and future challenges. *Therapeutic Delivery 5*, 843–857.
Oganesyan, V., Damschroder, M. M., Cook, K. E., Li, Q., Gao, C., Wu, H., & Dall'Acqua, W. F. (2014). Structural insights into neonatal Fc receptor-based recycling mechanisms. *The Journal of Biological Chemistry 289*, 7812–7824.
Oksanen, M., Lehtonen, S., Jaronen, M., Goldsteins, G., Hamalainen, R. H., & Koistinaho, J. (2019). Astrocyte alterations in neurodegenerative pathologies and their modeling in human induced pluripotent stem cell platforms. *Cellular and Molecular Life Sciences 76*, 2739–2760.
Olmsted, S. S., Padgett, J. L., Yudin, A. I., Whaley, K. J., Moench, T. R., & Cone, R. A. (2001). Diffusion of macromolecules and virus-like particles in human cervical mucus. *Biophysical Journal 81*, 1930–1937.
Oriano, M., Terranova, L., Sotgiu, G., Saderi, L., Bellofiore, A., Retucci, M., ... Blasi, F. (2019). Evaluation of active neutrophil elastase in sputum of bronchiectasis and cystic fibrosis patients: A comparison among different techniques. *Pulmonary Pharmacology & Therapeutics 59*, 101856.
Ostrowitzki, S., Lasser, R. A., Dorflinger, E., Scheltens, P., Barkhof, F., Nikolcheva, T., ... Investigators, S. C. R. (2017). A phase III randomized trial of gantenerumab in prodromal Alzheimer's disease. *Alzheimer's Research & Therapy 9*, 95.
Ottiger, M., Thiel, M. A., Feige, U., Lichtlen, P., & Urech, D. M. (2009). Efficient intraocular penetration of topical anti-TNF-alpha single-chain antibody (ESBA105) to anterior and posterior segment without penetration enhancer. *Investigative Ophthalmology & Visual Science 50*, 779–786.
Owyong, M., Efe, G., Owyong, M., Abbasi, A. J., Sitarama, V., & Plaks, V. (2018). Overcoming barriers of age to enhance efficacy of cancer immunotherapy: The clout of the extracellular matrix. *Frontiers in Cell and Development Biology 6*, 19.
Padera, T. P., Kadambi, A., di Tomaso, E., Carreira, C. M., Brown, E. B., Boucher, Y., ... Jain, R. K. (2002). Lymphatic metastasis in the absence of functional intratumor lymphatics. *Science 296*, 1883–1886.

Paintaud, G. (2009). Pharmacokinetics (PK) of mAbs. *Medical Science (Paris) 25*, 1057–1062.
Pandey, K. C., De, S., & Mishra, P. K. (2017). Role of proteases in chronic obstructive pulmonary disease. *Frontiers in Pharmacology 8*, 512.
Pardridge, W. M. (2007). Blood-brain barrier delivery. *Drug Discovery Today 12*, 54–61.
Pardridge, W. M. (2017). Delivery of biologics across the blood-brain barrier with molecular Trojan horse technology. *BioDrugs 31*, 503–519.
Park, E. J., Zhang, Y. Z., Vykhodtseva, N., & McDannold, N. (2012). Ultrasound-mediated blood-brain/blood-tumor barrier disruption improves outcomes with trastuzumab in a breast cancer brain metastasis model. *Journal of Controlled Release 163*, 277–284.
Passot, C., Azzopardi, N., Renault, S., Baroukh, N., Arnoult, C., Ohresser, M., Boisdron-Celle, M., Gamelin, E., Watier, H., Paintaud, G., & Gouilleux-Gruart, V. (2013). Influence of FCGRT gene polymorphisms on pharmacokinetics of therapeutic antibodies. *MAbs 5*, 614–619.
Patil, H. P., Freches, D., Karmani, L., Duncan, G. A., Ucakar, B., Suk, J. S., ... Vanbever, R. (2018). Fate of PEGylated antibody fragments following delivery to the lungs: Influence of delivery site, PEG size and lung inflammation. *Journal of Controlled Release 272*, 62–71.
von Pawel-Rammingen, U., Johansson, B. P., & Bjorck, L. (2002). IdeS, a novel streptococcal cysteine proteinase with unique specificity for immunoglobulin G. *The EMBO Journal 21*, 1607–1615.
Pereira, P. M. R., Ragupathi, A., Shmuel, S., Mandleywala, K., Viola, N. T., & Lewis, J. S. (2020). HER2-targeted PET imaging and therapy of hyaluronan-masked HER2-overexpressing breast cancer. *Molecular Pharmaceutics 17*, 327–337.
Perrino, E., Steiner, M., Krall, N., Bernardes, G. J., Pretto, F., Casi, G., & Neri, D. (2014). Curative properties of noninternalizing antibody-drug conjugates based on maytansinoids. *Cancer Research 74*, 2569–2578.
Pickering, J. G. (2001). Regulation of vascular cell behavior by collagen : Form is function. *Circulation Research 88*, 458–459.
Plaut, A. G., Wistar, R., Jr., & Capra, J. D. (1974). Differential susceptibility of human IgA immunoglobulins to streptococcal IgA protease. *The Journal of Clinical Investigation 54*, 1295–1300.
Poduslo, J. F., Curran, G. L., & Berg, C. T. (1994). Macromolecular permeability across the blood-nerve and blood-brain barriers. *Proceedings of the National Academy of Sciences of the United States of America 91*, 5705–5709.
Popescu, B. O., Toescu, E. C., Popescu, L. M., Bajenaru, O., Muresanu, D. F., Schultzberg, M., & Bogdanovic, N. (2009). Blood-brain barrier alterations in ageing and dementia. *Journal of the Neurological Sciences 283*, 99–106.
Porsio, B., Craparo, E. F., Mauro, N., Giammona, G., & Cavallaro, G. (2018). Mucus and cell-penetrating nanoparticles embedded in nano-into-micro formulations for pulmonary delivery of ivacaftor in patients with cystic fibrosis. *ACS Applied Materials & Interfaces 10*, 165–181.
Pouget, J. P., Georgakilas, A. G., & Ravanat, J. L. (2018). Targeted and off-target (bystander and abscopal) effects of radiation therapy: Redox mechanisms and risk/benefit analysis. *Antioxidants & Redox Signaling 29*, 1447–1487.
Pouget, J. P., Lozza, C., Deshayes, E., Boudousq, V., & Navarro-Teulon, I. (2015). Introduction to radiobiology of targeted radionuclide therapy. *Frontiers of Medicine (Lausanne) 2*, 12.
Printz, M. A., Dychter, S. S., DeNoia, E. P., Harrigan, R., Sugarman, B. J., Zepeda, M., ... Maneval, D. C. (2020). A phase I study to evaluate the safety, tolerability, pharmacokinetics, and pharmacodynamics of recombinant human hyaluronidase PH20 administered intravenously in healthy volunteers. *Current Therapeutic Research, Clinical and Experimental 93*, 100604.
Pyzik, M., Sand, K. M. K., Hubbard, J. J., Andersen, J. T., Sandlie, I., & Blumberg, R. S. (2019). The neonatal Fc receptor (FcRn): A misnomer? *Frontiers in Immunology 10*, 1540.
Qiang, M., Dong, X., Zha, Z., Zuo, X. K., Song, X. L., Zhao, L., ... Lerner, R. A. (2018). Selection of an ASIC1a-blocking combinatorial antibody that protects cells from ischemic death. *Proceedings of the National Academy of Sciences of the United States of America 115*, E7469–E7477.
Quaranta, V. (2000). Cell migration through extracellular matrix: Membrane-type metalloproteinases make the way. *The Journal of Cell Biology 149*, 1167–1170.
Quartino, A. L., Hillenbach, C., Li, J., Li, H., Wada, R. D., Visich, J., ... Lum, B. L. (2016). Population pharmacokinetic and exposure-response analysis for trastuzumab administered using a subcutaneous "manual syringe" injection or intravenously in women with HER2-positive early breast cancer. *Cancer Chemotherapy and Pharmacology 77*, 77–88.
Raghavan, M., Bonagura, V. R., Morrison, S. L., & Bjorkman, P. J. (1995). Analysis of the pH dependence of the neonatal Fc receptor/immunoglobulin G interaction using antibody and receptor variants. *Biochemistry 34*, 14649–14657.
Rath, T., Baker, K., Dumont, J. A., Peters, R. T., Jiang, H., Qiao, S. W., ... Blumberg, R. S. (2015). Fc-fusion proteins and FcRn: Structural insights for longer-lasting and more effective therapeutics. *Critical Reviews in Biotechnology 35*, 235–254.
Raymond, S. B., Treat, L. H., Dewey, J. D., McDannold, N. J., Hynynen, K., & Bacskai, B. J. (2008). Ultrasound enhanced delivery of molecular imaging and therapeutic agents in Alzheimer's disease mouse models. *PLoS One 3* e2175.
Raza, A., Franklin, M. J., & Dudek, A. Z. (2010). Pericytes and vessel maturation during tumor angiogenesis and metastasis. *American Journal of Hematology 85*, 593–598.
Rebelo, S. P., Pinto, C., Martins, T. R., Harrer, N., Estrada, M. F., Loza-Alvarez, P., ... Brito, C. (2018). 3D-3-culture: A tool to unveil macrophage plasticity in the tumour microenvironment. *Biomaterials 163*, 185–197.
Respaud, R., Marchand, D., Pelat, T., Tchou-Wong, K. M., Roy, C. J., Parent, C., ... Heuze-Vourc'h, N. (2016). Development of a drug delivery system for efficient alveolar delivery of a neutralizing monoclonal antibody to treat pulmonary intoxication to ricin. *Journal of Controlled Release 234*, 21–32.
Respaud, R., Vecellio, L., Diot, P., & Heuze-Vourc'h, N. (2015). Nebulization as a delivery method for mAbs in respiratory diseases. *Expert Opinion on Drug Delivery 12*, 1027–1039.
Ribatti, D., Nico, B., Floris, C., Mangieri, D., Piras, F., Ennas, M. G., ... Sirigu, P. (2005). Microvascular density, vascular endothelial growth factor immunoreactivity in tumor cells, vessel diameter and intussusceptive microvascular growth in primary melanoma. *Oncology Reports 14*, 81–84.
Rinne, J. O., Brooks, D. J., Rossor, M. N., Fox, N. C., Bullock, R., Klunk, W. E., ... Grundman, M. (2010). 11C-PiB PET assessment of change in fibrillar amyloid-beta load in patients with Alzheimer's disease treated with bapineuzumab: A phase 2, double-blind, placebo-controlled, ascending-dose study. *Lancet Neurology 9*, 363–372.
Rohrer, J., Lupo, N., & Bernkop-Schnurch, A. (2018). Advanced formulations for intranasal delivery of biologics. *International Journal of Pharmaceutics 553*, 8–20.
Ruano-Salguero, J. S., & Lee, K. H. (2020). Antibody transcytosis across brain endothelial-like cells occurs nonspecifically and independent of FcRn. *Scientific Reports 10*, 3685.
Rust, R., Gronnert, L., Gantner, C., Enzler, A., Mulders, G., Weber, R. Z., ... Schwab, M. E. (2019). Nogo-A targeted therapy promotes vascular repair and functional recovery following stroke. *Proceedings of the National Academy of Sciences of the United States of America 116*, 14270–14279.
Ryan, M. H., Petrone, D., Nemeth, J. F., Barnathan, E., Bjorck, L., & Jordan, R. E. (2008). Proteolysis of purified IgGs by human and bacterial enzymes in vitro and the detection of specific proteolytic fragments of endogenous IgG in rheumatoid synovial fluid. *Molecular Immunology 45*, 1837–1846.
Sachs, U. J., Socher, I., Braeunlich, C. G., Kroll, H., Bein, G., & Santoso, S. (2006). A variable number of tandem repeats polymorphism influences the transcriptional activity of the neonatal Fc receptor alpha-chain promoter. *Immunology 119*, 83–89.
Sakagami, M., Omidi, Y., Campbell, L., Kandalaft, L. E., Morris, C. J., Barar, J., & Gumbleton, M. (2006). Expression and transport functionality of FcRn within rat alveolar epithelium: A study in primary cell culture and in the isolated perfused lung. *Pharmaceutical Research 23*, 270–279.
Salameh, T. S., & Banks, W. A. (2014). Delivery of therapeutic peptides and proteins to the CNS. *Advances in Pharmacology 71*, 277–299.
Salloway, S., Farlow, M., McDade, E., Clifford, D. B., Wang, G., Llibre-Guerra, J. J., ... Dominantly Inherited Alzheimer Network-Trials, U. (2021). A trial of gantenerumab or solanezumab in dominantly inherited Alzheimer's disease. *Nature Medicine 27*, 1187–1196.
Salmon, H., Franciszkiewicz, K., Damotte, D., Dieu-Nosjean, M. C., Validire, P., Trautmann, A., ... Donnadieu, E. (2012). Matrix architecture defines the preferential localization and migration of T cells into the stroma of human lung tumors. *The Journal of Clinical Investigation 122*, 899–910.
Salvatore, M. F., Ai, Y., Fischer, B., Zhang, A. M., Grondin, R. C., Zhang, Z., ... Gash, D. M. (2006). Point source concentration of GDNF may explain failure of phase II clinical trial. *Experimental Neurology 202*, 497–505.
Sanchez-Felix, M., Burke, M., Chen, H. H., Patterson, C., & Mittal, S. (2020). Predicting bioavailability of monoclonal antibodies after subcutaneous administration: Open innovation challenge. *Advanced Drug Delivery Reviews 167*, 66–77.
Sanders, N. N., De Smedt, S. C., Van Rompaey, E., Simoens, P., De Baets, F., & Demeester, J. (2000). Cystic fibrosis sputum: A barrier to the transport of nanospheres. *American Journal of Respiratory and Critical Care Medicine 162*, 1905–1911.
Schaefer, A., & Lai, S. K. (2021). The biophysical principles underpinning muco-trapping functions of antibodies. *Human Vaccines & Immunotherapeutics*, 1–10.
Schlachetzki, F., Zhu, C., & Pardridge, W. M. (2002). Expression of the neonatal Fc receptor (FcRn) at the blood-brain barrier. *Journal of Neurochemistry 81*, 203–206.
Scully, M., Soderman, A., Schneider, M., Makropoulos, D., Blake, S., Picha, K., & Ort, T. (2009). Pharmacokinetics of an antibody following intra-articular and systemic delivery in rodents. *Osteoarthritis and cartilage. 17*. (pp. S61–S62). Elsevier.
Senior, B. W., & Woof, J. M. (2005). Effect of mutations in the human immunoglobulin A1 (IgA1) hinge on its susceptibility to cleavage by diverse bacterial IgA1 proteases. *Infection and Immunity 73*, 1515–1522.
Shang, X., Wang, P., Liu, Y., Zhang, Z., & Xue, Y. (2011). Mechanism of low-frequency ultrasound in opening blood-tumor barrier by tight junction. *Journal of Molecular Neuroscience 43*, 364–369.
Sheikov, N., McDannold, N., Jolesz, F., Zhang, Y. Z., Tam, K., & Hynynen, K. (2006). Brain arterioles show more active vesicular transport of blood-borne tracer molecules than capillaries and venules after focused ultrasound-evoked opening of the blood-brain barrier. *Ultrasound in Medicine & Biology 32*, 1399–1409.
Sheikov, N., McDannold, N., Sharma, S., & Hynynen, K. (2008). Effect of focused ultrasound applied with an ultrasound contrast agent on the tight junctional integrity of the brain microvascular endothelium. *Ultrasound in Medicine & Biology 34*, 1093–1104.
Sheikov, N., McDannold, N., Vykhodtseva, N., Jolesz, F., & Hynynen, K. (2004). Cellular mechanisms of the blood-brain barrier opening induced by ultrasound in presence of microbubbles. *Ultrasound in Medicine & Biology 30*, 979–989.
Shekhar, M. P., Pauley, R., & Heppner, G. (2003). Host microenvironment in breast cancer development: Extracellular matrix-stromal cell contribution to neoplastic phenotype of epithelial cells in the breast. *Breast Cancer Research 5*, 130–135.
Sheybani, N. D., Breza, V. R., Paul, S., McCauley, K. S., Berr, S. S., Miller, G. W., ... Price, R. J. (2021). ImmunoPET-informed sequence for focused ultrasound-targeted mCD47 blockade controls glioma. *Journal of Controlled Release 331*, 19–29.
Shoji, T., Saito, R., Chonan, M., Shibahara, I., Sato, A., Kanamori, M., Sonoda, Y., Kondo, T., Ishii, N., & Tominaga, T. (2016). Local convection-enhanced delivery of an anti-CD40 agonistic monoclonal antibody induces antitumor effects in mouse glioma models. *Neuro-Oncology 18*, 1120–1128.
Shpilberg, O., & Jackisch, C. (2013). Subcutaneous administration of rituximab (MabThera) and trastuzumab (Herceptin) using hyaluronidase. *British Journal of Cancer 109*, 1556–1561.

Silva, A. C., Pereira, C., Fonseca, A., Pinto-do, O. P., & Nascimento, D. S. (2020). Bearing my heart: The role of extracellular matrix on cardiac development, homeostasis, and injury response. *Frontiers in Cell and Development Biology 8*, 621644.

Singha, N. C., Nekoroski, T., Zhao, C., Symons, R., Jiang, P., Frost, G. I., ... Shepard, H. M. (2015). Tumor-associated hyaluronan limits efficacy of monoclonal antibody therapy. *Molecular Cancer Therapeutics 14*, 523–532.

Souweidane, M. M., Kramer, K., Pandit-Taskar, N., Zhou, Z., Haque, S., Zanzonico, P., ... Dunkel, I. J. (2018). Convection-enhanced delivery for diffuse intrinsic pontine glioma: A single-centre, dose-escalation, phase 1 trial. *The Lancet Oncology 19*, 1040–1050.

Spiekermann, G. M., Finn, P. W., Ward, E. S., Dumont, J., Dickinson, B. L., Blumberg, R. S., & Lencer, W. I. (2002). Receptor-mediated immunoglobulin G transport across mucosal barriers in adult life: Functional expression of FcRn in the mammalian lung. *The Journal of Experimental Medicine 196*, 303–310.

Stamou, M., Grodzki, A. C., van Oostrum, M., Wollscheid, B., & Lein, P. J. (2018). Fc gamma receptors are expressed in the developing rat brain and activate downstream signaling molecules upon cross-linking with immune complex. *Journal of Neuroinflammation 15*, 7.

St-Amour, I., Pare, I., Alata, W., Coulombe, K., Ringuette-Goulet, C., Drouin-Ouellet, J., Vandal, M., Soulet, D., Bazin, R., & Calon, F. (2013). Brain bioavailability of human intravenous immunoglobulin and its transport through the murine blood-brain barrier. *Journal of Cerebral Blood Flow and Metabolism 33*, 1983–1992.

Staudacher, A. H., & Brown, M. P. (2017). Antibody drug conjugates and bystander killing: Is antigen-dependent internalisation required? *British Journal of Cancer 117*, 1736–1742.

Stevens, N. E., & Cowin, A. J. (2017). Overcoming the challenges of topical antibody administration for improving healing outcomes: A review of recent laboratory and clinical approaches. *Wounds Practice and Research 25*.

Stewart, P. S., & Franklin, M. J. (2008). Physiological heterogeneity in biofilms. *Nature Reviews Microbiology 6*, 199–210.

Styles, I. K., Feeney, O. M., Nguyen, T. H., Brundel, D. H. S., Kang, D. W., Clift, R., ... Porter, C. J. H. (2019). Removal of interstitial hyaluronan with recombinant human hyaluronidase improves the systemic and lymphatic uptake of cetuximab in rats. *Journal of Controlled Release 315*, 85–96.

Suk, J. S., Lai, S. K., Boylan, N. J., Dawson, M. R., Boyle, M. P., & Hanes, J. (2011). Rapid transport of muco-inert nanoparticles in cystic fibrosis sputum treated with N-acetyl cysteine. *Nanomedicine (London, England) 6*, 365–375.

Suk, J. S., Lai, S. K., Wang, Y. Y., Ensign, L. M., Zeitlin, P. L., Boyle, M. P., & Hanes, J. (2009). The penetration of fresh undiluted sputum expectorated by cystic fibrosis patients by non-adhesive polymer nanoparticles. *Biomaterials 30*, 2591–2597.

Tan, A. R., Im, S. A., Mattar, A., Colomer, R., Stroyakovskii, D., Nowecki, Z., ... FeDeriCa study, g. (2021). Fixed-dose combination of pertuzumab and trastuzumab for subcutaneous injection plus chemotherapy in HER2-positive early breast cancer (FeDeriCa): A randomised, open-label, multicentre, non-inferiority, phase 3 study. *The Lancet Oncology 22*, 85–97.

Tang, B. C., Dawson, M., Lai, S. K., Wang, Y. Y., Suk, J. S., Yang, M., ... Hanes, J. (2009). Biodegradable polymer nanoparticles that rapidly penetrate the human mucus barrier. *Proceedings of the National Academy of Sciences of the United States of America 106*, 19268–19273.

Tarner, I. H., & Muller-Ladner, U. (2008). Drug delivery systems for the treatment of rheumatoid arthritis. *Expert Opinion on Drug Delivery 5*, 1027–1037.

Tashima, T. (2020). Smart strategies for therapeutic agent delivery into brain across the blood-brain barrier using receptor-mediated transcytosis. *Chemical & Pharmaceutical Bulletin (Tokyo) 68*, 316–325.

Tashima, T. (2021). Delivery of orally administered digestible antibodies using nanoparticles. *International Journal of Molecular Sciences 22*.

Tennant, M., & McGeachie, J. K. (1990). Blood vessel structure and function: A brief update on recent advances. *The Australian and New Zealand Journal of Surgery 60*, 747–753.

Thakker, D. R., Weatherspoon, M. R., Harrison, J., Keene, T. E., Lane, D. S., Kaemmerer, W. F., ... Shafer, L. L. (2009). Intracerebroventricular amyloid-beta antibodies reduce cerebral amyloid angiopathy and associated micro-hemorrhages in aged Tg2576 mice. *Proceedings of the National Academy of Sciences of the United States of America 106*, 4501–4506.

Thareja, A., Hughes, H., Alvarez-Lorenzo, C., Hakkarainen, J. J., & Ahmed, Z. (2021). Penetration enhancers for topical drug delivery to the ocular posterior segment-a systematic review. *Pharmaceutics 13*.

Theocharis, A. D., Manou, D., & Karamanos, N. K. (2019). The extracellular matrix as a multitasking player in disease. *The FEBS Journal 286*, 2830–2869.

Thrimawithana, T. R., Young, S., Bunt, C. R., Green, C., & Alany, R. G. (2011). Drug delivery to the posterior segment of the eye. *Drug Discovery Today 16*, 270–277.

Thulborn, S. J., Mistry, V., Brightling, C. E., Moffitt, K. L., Ribeiro, D., & Bafadhel, M. (2019). Neutrophil elastase as a biomarker for bacterial infection in COPD. *Respiratory Research 20*, 170.

Thurber, G. M., & Weissleder, R. (2011). Quantitating antibody uptake in vivo: Conditional dependence on antigen expression levels. *Molecular Imaging and Biology 13*, 623–632.

Tielker, D., Hacker, S., Loris, R., Strathmann, M., Wingender, J., Wilhelm, S., ... Jaeger, K. E. (2005). Pseudomonas aeruginosa lectin LecB is located in the outer membrane and is involved in biofilm formation. *Microbiology (Reading) 151*, 1313–1323.

Todd, N., Angolano, C., Ferran, C., Devor, A., Borsook, D., & McDannold, N. (2020). Secondary effects on brain physiology caused by focused ultrasound-mediated disruption of the blood-brain barrier. *Journal of Controlled Release 324*, 450–459.

Tong, R. T., Boucher, Y., Kozin, S. V., Winkler, F., Hicklin, D. J., & Jain, R. K. (2004). Vascular normalization by vascular endothelial growth factor receptor 2 blockade induces a pressure gradient across the vasculature and improves drug penetration in tumors. *Cancer Research 64*, 3731–3736.

Tsukita, S., Furuse, M., & Itoh, M. (2001). Multifunctional strands in tight junctions. *Nature Reviews Molecular Cell Biology 2*, 285–293.

Tuppo, E. E., & Arias, H. R. (2005). The role of inflammation in Alzheimer's disease. *The International Journal of Biochemistry & Cell Biology 37*, 289–305.

Turner, J. R. (2009). Intestinal mucosal barrier function in health and disease. *Nature Reviews Immunology 9*, 799–809.

Vasiljeva, O., Menendez, E., Nguyen, M., Craik, C. S., & Michael Kavanaugh, W. (2020). Monitoring protease activity in biological tissues using antibody prodrugs as sensing probes. *Scientific Reports 10*, 5894.

Veerachamy, S., Yarlagadda, T., Manivasagam, G., & Yarlagadda, P. K. (2014). Bacterial adherence and biofilm formation on medical implants: A review. *Proceedings of the Institution of Mechanical Engineers. Part H 228*, 1083–1099.

Viola, M., Sequeira, J., Seica, R., Veiga, F., Serra, J., Santos, A. C., & Ribeiro, A. J. (2018). Subcutaneous delivery of monoclonal antibodies: How do we get there? *Journal of Controlled Release 286*, 301–314.

Vllasaliu, D., Thanou, M., Stolnik, S., & Fowler, R. (2018). Recent advances in oral delivery of biologics: Nanomedicine and physical modes of delivery. *Expert Opinion on Drug Delivery 15*, 759–770.

Vogelzang, A., Lozza, L., Reece, S. T., Perdomo, C., Zedler, U., Hahnke, K., ... Kaufmann, S. H. (2016). Neonatal Fc receptor regulation of lung immunoglobulin and CD103+ dendritic cells confers transient susceptibility to tuberculosis. *Infection and Immunity 84*, 2914–2921.

Vukosavljevic, B., Murgia, X., Schwarzkopf, K., Schaefer, U. F., Lehr, C. M., & Windbergs, M. (2017). Tracing molecular and structural changes upon mucolysis with N-acetyl cysteine in human airway mucus. *International Journal of Pharmaceutics 533*, 373–376.

Vukovic, N., van Elsas, A., Verbeek, J. S., & Zaiss, D. M. W. (2021). Isotype selection for antibody-based cancer therapy. *Clinical and Experimental Immunology 203*, 351–365.

Wahl, A. S., Correa, D., Imobersteg, S., Maurer, M. A., Kaiser, J., Augath, M. A., & Schwab, M. E. (2020). Targeting therapeutic antibodies to the CNS: A comparative study of intrathecal, intravenous, and subcutaneous anti-Nogo A antibody treatment after stroke in rats. *Neurotherapeutics 17*, 1153–1159.

Waldmann, T. A., Strober, W., & Mogielnicki, R. P. (1972). The renal handling of low molecular weight proteins. II. Disorders of serum protein catabolism in patients with tubular proteinuria, the nephrotic syndrome, or uremia. *The Journal of Clinical Investigation 51*, 2162–2174.

Walker, C., Mojares, E., & Del Rio Hernandez, A. (2018). Role of extracellular matrix in development and cancer progression. *International Journal of Molecular Sciences 19*.

Wang, W., Wang, E. Q., & Balthasar, J. P. (2008). Monoclonal antibody pharmacokinetics and pharmacodynamics. *Clinical Pharmacology and Therapeutics 84*, 548–558.

Wang, Y. Y., Harit, D., Subramani, D. B., Arora, H., Kumar, P. A., & Lai, S. K. (2017). Influenza-binding antibodies immobilise influenza viruses in fresh human airway mucus. *The European Respiratory Journal 49*.

Wang, W., Wang, E. Q., & Balthasar, J. P. (2008). *Clin. Pharmacol. Ther. 84*(5), 548–558. https://doi.org/10.1038/clpt.2008.170.

Watson, C. J., Rowland, M., & Warhurst, G. (2001). Functional modeling of tight junctions in intestinal cell monolayers using polyethylene glycol oligomers. *American Journal of Physiology: Cell Physiology 281*, C388–C397.

Weinberger, A., & Simkin, P. A. (1989). Plasma proteins in synovial fluids of normal human joints. *Seminars in Arthritis and Rheumatism 19*, 66–76.

Wenting, Z., Ling, Z., Chengrui, A., Rongrong, W., Liqun, Y., Weifeng, Y., Peiying, L., & Yanqin, G. (2020). The blood brain barrier in cerebral ischemic injury – disruption and repair. *Brain Hemorrhages 1*, 34–53.

Wilcock, D. M., DiCarlo, G., Henderson, D., Jackson, J., Clarke, K., Ugen, K. E., ... Morgan, D. (2003). Intracranially administered anti-Abeta antibodies reduce beta-amyloid deposition by mechanisms both independent of and associated with microglial activation. *The Journal of Neuroscience 23*, 3745–3751.

Witko-Sarsat, V., Halbwachs-Mecarelli, L., Schuster, A., Nusbaum, P., Ueki, I., Canteloup, S., ... Nadel, J. A. (1999). Proteinase 3, a potent secretagogue in airways, is present in cystic fibrosis sputum. *American Journal of Respiratory Cell and Molecular Biology 20*, 729–736.

Wolburg, H., Noell, S., Mack, A., Wolburg-Buchholz, K., & Fallier-Becker, P. (2009). Brain endothelial cells and the glio-vascular complex. *Cell and Tissue Research 335*, 75–96.

Wong, W. L., Su, X., Li, X., Cheung, C. M., Klein, R., Cheng, C. Y., & Wong, T. Y. (2014). Global prevalence of age-related macular degeneration and disease burden projection for 2020 and 2040: A systematic review and meta-analysis. *The Lancet Global Health 2*, e106–e116.

Wood, T. K., Knabel, S. J., & Kwan, B. W. (2013). Bacterial persister cell formation and dormancy. *Applied and Environmental Microbiology 79*, 7116–7121.

Wu, M., Frieboes, H. B., Chaplain, M. A., McDougall, S. R., Cristini, V., & Lowengrub, J. S. (2014). The effect of interstitial pressure on therapeutic agent transport: Coupling with the tumor blood and lymphatic vascular systems. *Journal of Theoretical Biology 355*, 194–207.

Wynne, C., Harvey, V., Schwabe, C., Waaka, D., McIntyre, C., & Bittner, B. (2013). Comparison of subcutaneous and intravenous administration of trastuzumab: A phase I/II trial in healthy male volunteers and patients with HER2-positive breast cancer. *Journal of Clinical Pharmacology 53*, 192–201.

Xenaki, K. T., Oliveira, S., & van Bergen En Henegouwen, P. M. P. (2017). Antibody or antibody fragments: Implications for molecular imaging and targeted therapy of solid tumors. *Frontiers in Immunology 8*, 1287.

Xu, Q., Boylan, N. J., Suk, J. S., Wang, Y. Y., Nance, E. A., Yang, J. C., ... Hanes, J. (2013). Nanoparticle diffusion in, and microrheology of, the bovine vitreous ex vivo. *Journal of Controlled Release 167*, 76–84.

Xu, S., Ilyas, I., Little, P. J., Li, H., Kamato, D., Zheng, X., ... Weng, J. (2021). Endothelial dysfunction in atherosclerotic cardiovascular diseases and beyond: From mechanism to pharmacotherapies. *Pharmacological Reviews 73*, 924–967.

Yadav, D. B., Maloney, J. A., Wildsmith, K. R., Fuji, R. N., Meilandt, W. J., Solanoy, H., ... Atwal, J. K. (2017). Widespread brain distribution and activity following i.c.v. infusion of anti-beta-secretase (BACE1) in nonhuman primates. *The British Journal of Pharmacology 174*, 4173–4185.

Yan, Q., Matheson, C., Sun, J., Radeke, M. J., Feinstein, S. C., & Miller, J. A. (1994). Distribution of intracerebral ventricularly administered neurotrophins in rat brain and its correlation with trk receptor expression. *Experimental Neurology 127*, 23–36.

Yang, B., Schaefer, A., Wang, Y. Y., McCallen, J., Lee, P., Newby, J. M., ... Lai, S. K. (2018). ZMapp reinforces the airway mucosal barrier against Ebola virus. *The Journal of Infectious Diseases 218*, 901–910.

Yang, Y., & Rosenberg, G. A. (2011). Blood-brain barrier breakdown in acute and chronic cerebrovascular disease. *Stroke 42*, 3323–3328.

Yasunaga, M., Manabe, S., & Matsumura, Y. (2011). New concept of cytotoxic immunoconjugate therapy targeting cancer-induced fibrin clots. *Cancer Science 102*, 1396–1402.

Yasunaga, M., Manabe, S., & Matsumura, Y. (2013). Tumor stromal barrier and cancer stromal targeting therapy. *Microvascular Reviews and Communications 6*, 2–8.

Yasunaga, M., Manabe, S., Tarin, D., & Matsumura, Y. (2011). Cancer-stroma targeting therapy by cytotoxic immunoconjugate bound to the collagen 4 network in the tumor tissue. *Bioconjugate Chemistry 22*, 1776–1783.

Ye, D., Yuan, J., Yue, Y., Rubin, J. B., & Chen, H. (2021). Focused ultrasound-enhanced delivery of intranasally administered anti-programmed cell death-ligand 1 antibody to an intracranial murine glioma model. *Pharmaceutics 13*.

Yip, V., Palma, E., Tesar, D. B., Mundo, E. E., Bumbaca, D., Torres, E. K., ... Boswell, C. A. (2014). Quantitative cumulative biodistribution of antibodies in mice: Effect of modulating binding affinity to the neonatal Fc receptor. *MAbs 6*, 689–696.

Yokota, T., Milenic, D. E., Whitlow, M., & Schlom, J. (1992). Rapid tumor penetration of a single-chain Fv and comparison with other immunoglobulin forms. *Cancer Research 52*, 3402–3408.

Yu, T., Wang, Y. Y., Yang, M., Schneider, C., Zhong, W., Pulicare, S., ... Hanes, J. (2012). Biodegradable mucus-penetrating nanoparticles composed of diblock copolymers of polyethylene glycol and poly(lactic-co-glycolic acid). *Drug Delivery and Translational Research 2*.

Yu, Y. J., Atwal, J. K., Zhang, Y., Tong, R. K., Wildsmith, K. R., Tan, C., ... Watts, R. J. (2014). Therapeutic bispecific antibodies cross the blood-brain barrier in nonhuman primates. *Science Translational Medicine 6* 261ra154.

Zamudio, F., Loon, A. R., Smeltzer, S., Benyamine, K., Navalpur Shanmugam, N. K., Stewart, N. J. F., ... Selenica, M. B. (2020). TDP-43 mediated blood-brain barrier permeability and leukocyte infiltration promote neurodegeneration in a low-grade systemic inflammation mouse model. *Journal of Neuroinflammation 17*, 283.

Zhang, J. F., Xiong, H. L., Cao, J. L., Wang, S. J., Guo, X. R., Lin, B. Y., ... Xia, N. S. (2018). A cell-penetrating whole molecule antibody targeting intracellular HBx suppresses hepatitis B virus via TRIM21-dependent pathway. *Theranostics 8*, 549–562.

Zhang, N., Deng, H., Fan, X., Gonzalez, A., Zhang, S., Brezski, R. J., ... An, Z. (2015). Dysfunctional antibodies in the tumor microenvironment associate with impaired anticancer immunity. *Clinical Cancer Research 21*, 5380–5390.

Zhao, Y., Brown, T. L., Kohler, H., & Muller, S. (2003). MTS-conjugated-antiactive caspase 3 antibodies inhibit actinomycin D-induced apoptosis. *Apoptosis 8*, 631–637.

Zhou, F., Fu, T., Huang, Q., Kuai, H., Mo, L., Liu, H., Wang, Q., Peng, Y., Han, D., Zhao, Z., Fang, X., & Tan, W. (2019). Hypoxia-activated PEGylated conditional aptamer/antibody for cancer imaging with improved specificity. *Journal of the American Chemical Society 141*, 18421–18427.

Zhu, X., Meng, G., Dickinson, B. L., Li, X., Mizoguchi, E., Miao, L., ... Blumberg, R. S. (2001). MHC class I-related neonatal Fc receptor for IgG is functionally expressed in monocytes, intestinal macrophages, and dendritic cells. *Journal of Immunology 166*, 3266–3276.

Zlokovic, B. V. (2008). The blood-brain barrier in health and chronic neurodegenerative disorders. *Neuron 57*, 178–201.

Zuchero, Y. J., Chen, X., Bien-Ly, N., Bumbaca, D., Tong, R. K., Gao, X., ... Watts, R. J. (2016). Discovery of novel blood-brain barrier targets to enhance brain uptake of therapeutic antibodies. *Neuron 89*, 70–82.

Several strategies are being explored to overcome the BBB for effective delivery of antibodies to the CNS. Direct delivery methods such intracerebroventricular and intracerebral injections show promise but invasive and have limited distribution capacity. Antibody engineering has led to the development of bispecific antibodies that can use receptor-mediated transcytosis to cross the BBB. Reversible BBB permeability enhancement techniques such as mannitol-induced opening and brain-focused ultrasound allow better antibody transport to the brain. Intranasal delivery also offers a non-invasive route od bypassing the BBB, although it can face challenges like the nasal mucosal barrier. Other methods such as the use nanoparticles also show promise for antibody delivery.

The potential that the use of antibodies has for the specific targeting of pathologically relevant proteins and the availability of methods allowing them to cross the BBB led us to consider this a similar approach to target TDP-43. However, TDP-43 is mainly an intracellular protein, which poses a problem for the use of full-length antibodies that are generally designed to function in the extracellular space or the bloodstream. For this reason, using antibody fragments such as scFvs seems to be more suitable for intracellular delivery because their smaller size allows them to be internalized more readily by cells.

c. scFv intrabodies

An immunoglobulin is a Y-shaped protein consisting of two identical heavy chains, and two identical light chains, held together by disulfide bonds. Each antibody has two Fragment antigen-binding (Fab) domains, which include the variable regions of the heavy (VH) and light (VL) chains, and a Fragment crystallizable (Fc) domain which is composed of the constant regions of the heavy chains (Schroeder & Cavacini, 2010) (Fig.13). The Fab is responsible for the recognition and binding of the antibody to its specific antigen, while the Fc is responsible for effector functions by interacting with cell surface receptors and proteins of the complement system (Chiu et al., 2019).

Through recombinant protein engineering, researchers have been able to modify immunoglobulins and create smaller antibody formats such as scFvs. An scFv molecule is an engineered antibody fragment composed of the variable regions of the VH and VL of immunoglobulins. Instead of being connected by a disulfide bond, the VH and VL are connected together by a short flexible linker peptide of 10-25 amino acids (Glockshuber et al.,

1990). These fragments retain the antigen-binding specificity of the full antibody (Sheets et al., 1998). When used as intrabodies, scFvs are expressed within the cells to target and bind specific intracellular proteins (Fig.13). They can modify protein functions, prevent harmful protein-protein interactions, or direct the degradation of target proteins (Lo et al., 2008). This approach is particularly useful in research and therapeutic settings for studying and potentially treating diseases caused by abnormal intracellular protein activities.

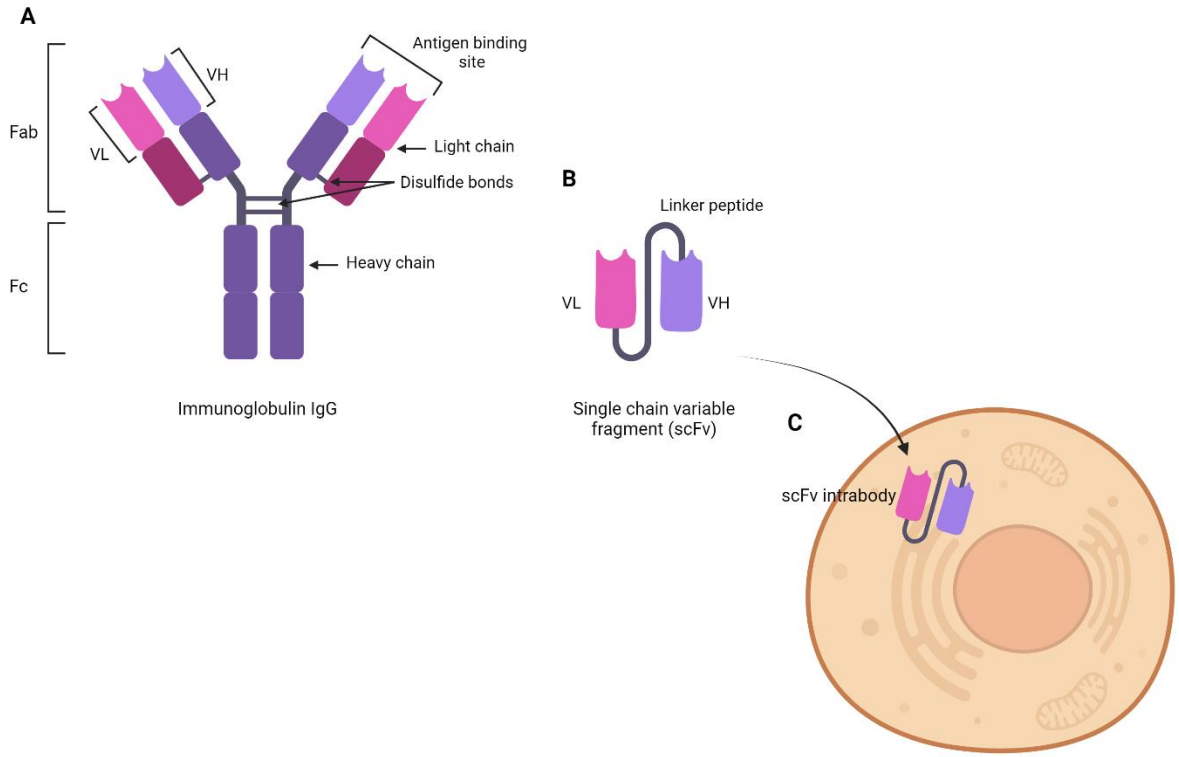

Figure 13: Schematic representation of an immunoglobulin (IgG), an scFv, and an intrabody. A) The IgG is made up of a heavy chain (purple) and a light chain (pink) that are linked together by disulfide bonds. Each of these chains contains a variable region (VH and VL) that allows for the formation of the antigen binding site. **B)** The scFv is made up the VH and VL regions, connected together by a linker peptide chain. **C)** Once the scFv is expressed inside cells, it becomes known as an intrabody. Created with BioRender.com.

Both scFvs and full immunoglobulins present with advantages and disadvantages that make them suitable for different purposes. The scFv is almost 6 times smaller than a full antibody, with a size of 25 kDa for the scFv compared to 150 kDa for a full antibody. The reduced size of the scFv allows for better tissue penetration and rapid blood clearance, making

them useful for diagnostic imaging, therapeutic targeting, and research applications (M. Bordeau & P. Balthasar, 2021; Thurber et al., 2007). In addition, due to their recombinant nature, scFvs can be easily modified genetically to enhance their stability, binding affinity, and/or specificity (Pirkalkhoran et al., 2023). They are also easy to produce in prokaryotic systems (Gupta & Shukla, 2017). Because scFvs are smaller and more versatile than immunoglobulins, they can be engineered to penetrate cellular compartments, like the cytoplasm or nucleus, that traditional antibodies cannot easily reach (Pirkalkhoran et al., 2023). scFvs also tend to be less immunogenic than full-length antibodies, mainly due to their lack of the constant Fc region that interacts with immune cells and complement proteins, potentially triggering an immune response (Bates & Power, 2019). Moreover, when scFvs are used as intrabodies, they are less likely to be exposed to the immune system. Compared to full antibodies, scFvs are also less complex and have fewer potential glycosylation sites, reducing potential immunogenic epitopes (Ghaderi et al., 2023).

In the context of neurodegenerative diseases, scFvs hold significant therapeutic potential. They can be engineered to target and neutralize pathological proteins such as tau or amyloid-beta in Alzheimer's disease (S. Li et al., 2021; Qian et al., 2023; Rodrigues Martins et al., 2023; Selles et al., 2023; C. Song et al., 2023), or α-synuclein in Parkinson's disease (Fassler et al., 2022; Schlichtmann et al., 2023). Some scFv molecules have also been developed in the context of ALS. For example, scFvs targeting misfolded SOD1 in the CNS, mainly as intrabodies, were able to improve some disease outcomes by decreasing gliosis, rescuing motor neurons, delaying the onset of the disease and/or prolonging survival (Bakavayev et al., 2023; Dong et al., 2018; Ghadge et al., 2019; P. Patel et al., 2014). As for TDP-43, an scFv targeting the RRM2 domain of TDP-43 was developed, which enhanced the clearance of TDP-43 aggregates in an embryonic TDP-43 mouse model (Tamaki et al., 2018). Another group developed an scFv targeting the RRM1 domain of TDP-43 which was able to decrease TDP-43 aggregation, neuroinflammation, NMJ denervation and symptom severity in a mouse model of ALS (Pozzi et al., 2019). Recently, an scFv clone directed against an epitope specific to mislocalized and aggregated TDP-43 mediated the clearance of TDP-43 aggregates in a cellular HEK293T model of ALS (B. Zhao et al., 2021).

By binding to misfolded proteins, scFvs can prevent their aggregation, promote their clearance, and mitigate the associated neurotoxicity. Moreover, their small size can allow for

better penetration of the BBB, enhancing their efficacy in targeting brain tissues (Güell-Bosch et al., 2020; Roda et al., 2020; Spencer et al., 2018). Recent advances in gene therapy and delivery methods, such as the use of viral vectors (Goodwin et al., 2021; Qian et al., 2023; Selles et al., 2023; Y. Zhang et al., 2022) or bispecific antibodies (Faresjö et al., 2021; Gustavsson et al., 2023; Rofo et al., 2022), have further expanded the potential of scFvs, offering new avenues for the treatment of neurodegenerative disorders that currently lack effective therapeutic options.

In addition to their use as therapeutic agents, the characteristics of scFvs make them also useful for imaging purposes. They can be conjugated with various imaging agents such as fluorescent dyes (Tateo et al., 2023; Tsirkas et al., 2022; Velappan et al., 2021; Yun et al., 2024), radionuclides (Bozorgchami et al., 2024; Joukar et al., 2022; D. Li et al., 2024) as well as nanoparticles (Bonnet et al., 2021; Sun et al., 2021), to enable their detection by different imaging modalities including fluorescent imaging, positron emission tomography (PET), and magnetic resonance imaging (MRI). They can therefore be used in research settings to study the distribution and progression of neurodegenerative markers in animal models. In clinical settings, they have the potential to be developed into diagnostic imaging tools for early detection and monitoring of neurodegenerative diseases. For instance, a group of researchers successfully developed labelled scFv molecules that allow the specific detection of amyloid beta and tau in the brain of Alzheimer's disease mice (Banka et al., 2023), while another group was able to visualize extracellular deposits of α-synuclein in the brain of Parkinson's disease mice (Roshanbin et al., 2022).

Overall, while full-length antibodies remain valuable in many applications due to their high affinity and long half-life, scFvs offer unique advantages that make them preferable in situations requiring smaller, more versatile, and less immunogenic molecules.

d. Techniques to enhance scFv delivery to the CNS

As previously discussed, the targeting of intracellular proteins in the CNS is complicated by the presence of the BBB and the need to get the biotherapeutic internalized into target cells. Researchers have developed several techniques to enhance these two processes, including guided nanoparticle delivery systems, and adeno-associated viral vectors for direct biotherapeutic delivery into specific cells. These two techniques were tested in our study.

- **Superparamagnetic iron oxide nanoparticles (SPIONs):** They are a type of nanomaterial with unique magnetic properties, making them useful in various biomedical applications. These nanoparticles, typically composed of magnetite (Fe_3O_4) and/or maghemite (γ-Fe_2O_3), and range in size from 10 to 100 nm in diameter (Wahajuddin & Arora, 2012). They exhibit superparamagnetism, a size-dependent characteristic making them magnetized only in the presence of an external magnetic field and rapidly lose their magnetism once the field is removed. This property makes SPIONs particularly advantageous for use in medical and biological fields (Surpi et al., 2023) (Fig.14).

  The superparamagnetism of SPIONs means that they do not have residual magnetism without an external magnetic field, reducing the risk of aggregation in biological environments (Wahajuddin & Arora, 2012). The strong magnetisation they exhibit in the presence of an external magnetic field allows for their targeted manipulation and control (Cristofolini et al., 2020; M. Wu et al., 2015). SPIONs can be coated with biocompatible materials like dextran, polyethylene glycol (PEG), or silica to enhance their stability, reduce their toxicity and facilitate their functionalization with targeting ligands, drugs, or imaging agents (Boyer et al., 2010). In medical applications, SPIONs serve as MRI contrast agents, enhancing image contrast and enabling targeted imaging for detecting tumors and inflammation (Nosrati et al., 2021; Oberdick et al., 2023; L. Xia et al., 2022). They also facilitate targeted drug delivery, directing therapeutic agents to specific sites using an external magnetic field, and are used in hyperthermia treatments for cancer by generating localized heat to kill cancer cells (Luque-Michel et al., 2021; Nieciecka et al., 2021; Nosrati et

al., 2021; Reyes-Ortega et al., 2021). Because they can be used for both diagnostic and therapeutic purposes, SPIONs are said to have theranostic properties.

The effect of SPIONs is largely dependent on their physiochemical properties (composition, surface charge, size, shape), dose, and coating (Friedrich et al., 2023; Vangijzegem et al., 2023). An increasing number of studies have been developing SPIONs for use in neurodegenerative diseases. SPIONs alone, mainly when having a negative surface charge, have been reported to reduce the formation of amyloid fibrils in solution (Mahmoudi et al., 2013; Naik et al., 2015). Low doses of PEGylated SPIONs were also shown to mitigate the fibrillation of amyloid-β, decrease ROS production, and improve memory impairment in an animal model of Alzheimer's disease (Sanati et al., 2021). To enhance their properties and tailor them for specific applications, SPIONs can be functionalized by attaching on their surface various molecules like polymers (e.g. PEG, dextran, chitosan), biomolecules (e.g. antibodies, antibody fragments, peptides), ligands, and fluorescent dyes (Chaparro et al., 2023). For example, several groups developed functionalized SPIONs that can cross the BBB and detect amyloidogenic species in the brain by MRI to diagnose Alzheimer's disease, Parkinson's disease and Huntington's disease (K. K. Cheng et al., 2015; X. Liu et al., 2019; X.-G. Liu et al., 2020; Sillerud et al., 2013), while others used functionalized SPIONs to enhance the clearance of amyloidogenic oligomers or deliver therapeutic molecules (Amanzadeh Jajin et al., 2021; Y. Li et al., 2018; X.-G. Liu et al., 2020; Ruan et al., 2022).

SPION nanoparticles hold significant promise in various biomedical fields due to their unique magnetic properties and versatility. However, challenges such as toxicity, long-term safety, regulatory approval, and efficient targeting need to be addressed. Ongoing research and development continue to advance SPION-based technologies, paving the way for innovative diagnostic and therapeutic applications.

- **Adeno-associated viral vectors (AAV):** AAVs are a type of viral vector derived from the adeno-associated virus, which is a small, non-enveloped virus belonging to the Parvoviridae family. AAV vectors are widely used in gene therapy and biomedical research for delivering genetic material into cells (E. A. Chowdhury et al., 2021). These vectors are particularly valued for their ability to achieve long-term gene expression,

as they can deliver genetic material into target cells. AAVs generally do not integrate into the host genome. Instead, the genetic material delivered by AAV vectors typically remains as episomal DNA, which means it exists as a separate, non-integrated DNA structure within the nucleus, making it a safer option compared to other types of virus vectors like retroviruses (Anson, 2004). AAV vectors exhibit broad tissue tropism, meaning different serotypes can infect a wide range of cell types and tissues, such as the liver, muscle, retina, and central nervous system (Castle et al., 2016). This versatility makes them effective for targeting specific tissues in gene therapy. Additionally, AAV vectors can be designed to typically provoke a low immune response, reducing the risk of adverse reactions and enabling the possibility of repeated administration (Hamilton & Wright, 2021).

AAV vectors have emerged as a highly promising platform for delivering therapeutic molecules into the CNS. They are particularly well suited for this purpose due to their ability to transduce different cells, including neurons, with long lasting expression of therapeutic genes. A key advantage of AAV is their capacity to cross the BBB and efficiently target specific regions of the CNS (Bunuales et al., 2024; W. Chen et al., 2021; D. Liu et al., 2021) which is a critical challenge in the development of treatments for diseases like ALS. By encoding therapeutic proteins such antibodies or antibody fragments (e.g. scFv), AAVs offer a means to deliver treatments directly into the brain and the spinal cord, areas that are central to ALS pathology. Several studies have used AAV-encoded scFvs to target proteins in the CNS such as amyloid-β oligomers (Selles et al., 2023), tau (Goodwin et al., 2021; Ising et al., 2017), SOD1 (Bakavayev et al., 2023; Ghadge et al., 2019; P. Patel et al., 2014), and TDP-43 (Pozzi et al., 2019; Tamaki et al., 2018). Therefore, by using AAV vector for the delivery of biotherapeutics, researchers address one of the main hurdles in ALS treatment, which is crossing the BBB and ensuring that therapeutic molecules reach the critical regions of the CNS in an efficient and sustained manner.

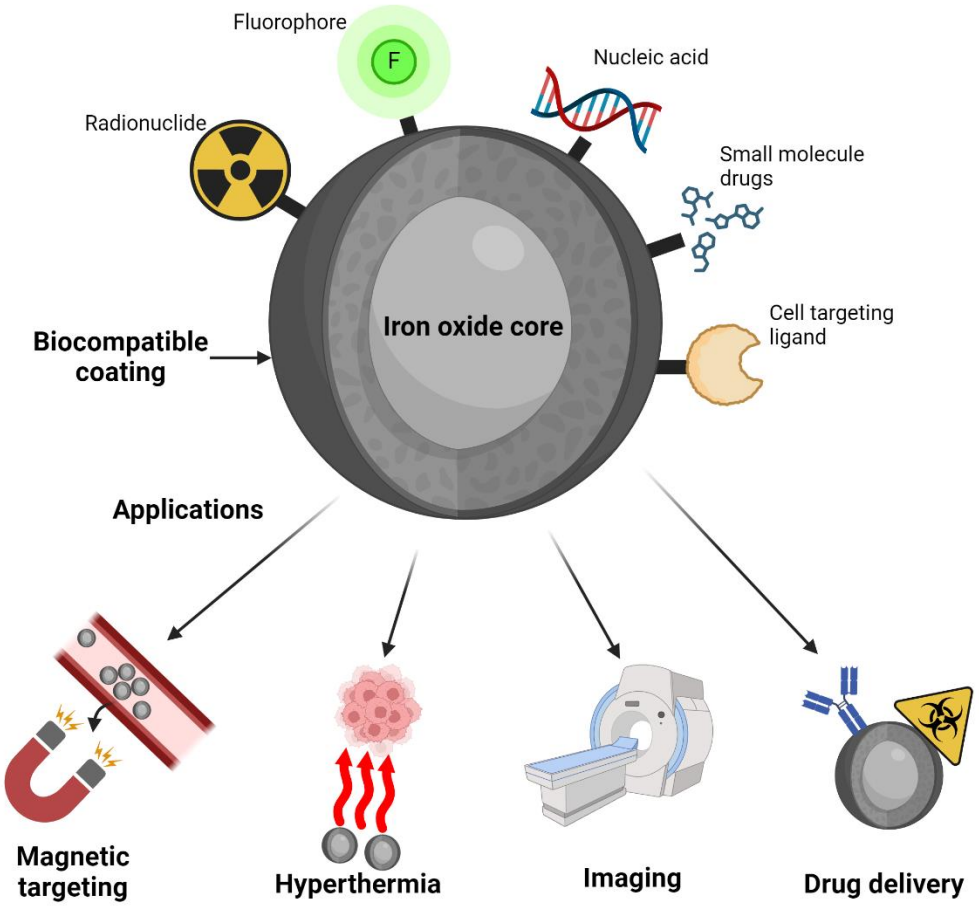

Figure 14: Representation of SPIONs as theranostic nanoparticles. SPIONs can be coated with several materials to enhance their stability and biocompatibility. They can also be functionalized to allow for their use in specific diagnostic and therapeutic applications such as magnetic targeting, hyperthermia cancer therapy, MRI or PET imaging, and targeted drug delivery. Created with BioRender.com.

D. Why are clinical trials failing?

Despite over 150 years since Charcot's initial description of ALS, there is still no treatment that can effectively slow down the disease or reverse its course. The significant challenges and the high failure rate observed in ALS clinical trials can be traced back to several factors:

- **Late diagnosis and neurodegenerative nature:** the diagnosis of ALS is mainly a diagnosis of exclusion, which is complicated by the non-specificity of symptoms and the lack of specific early ALS biomarkers. It relies on evaluating clinical symptoms, which only become apparent following the death of a significant number of motor

neurons, limiting the window for effective intervention. Motor neurons are challenging to regenerate or repair once damaged. Therefore, for a drug to be effective, it needs to be administered very early in the disease or at the pre-symptomatic stage, in order to prevent the degeneration of motor neurons and maintain the proper function of the remaining motor neurons. Researchers are trying to identify several parameters that can help them detect the disease in its pre-symptomatic stage. For example, some studies have shown that NfL levels increased prior to phenoconversion in carriers of ALS-causing mutations, and that they can be used to predict the timing of phenoconversion (Benatar et al., 2018, 2019). Imaging abnormalities like atrophy and decreased white matter integrity was also detected in some pre-symptomatic patients (Gorges et al., 2017; Le Blanc et al., 2020; S. E. Lee et al., 2017; Ng et al., 2008). Electrophysiological studies also revealed some abnormalities such as cortical hyperexcitability in the pre-symptomatic stage (Geevasinga et al., 2015; Vucic et al., 2008). Such information can help patients access some experimental treatments while in the pre-symptomatic phase, increasing the likelihood of a more positive outcome. However, more studies are still required because most of those parameters are non-specific and do not allow for a definitive diagnosis.

- **Lack of reliable biomarkers**: a reliable and specific biomarker for ALS progression and treatment response is lacking. In addition to delaying diagnosis and reducing the opportunity for early therapeutic intervention, the lack of a reliable biomarker also makes it difficult to monitor the effects of an intervention accurately, complicating the design and interpretation of clinical trials. As discussed earlier, NfL levels, which correlate with the extent of neuronal damage, are emerging as an important objective measurement to evaluate treatments effects (Benatar et al., 2023). Although this marker is not specific enough for diagnostic purposes, it can be a valuable tool to assess the outcome of clinical trials (Verde et al., 2021).
- **Multifactorial and complex disease mechanisms:** the identification of more than 600 genes that are associated with ALS, and the implication of environmental and possibly infectious factors suggest that ALS is a disease spectrum rather than a single disease. Several pathological cellular mechanisms seem to converge into a common cellular phenotype leading to motor neuron dysfunction and cell death. As a result, the

inability to determine the exact contribution of each mechanism in individual patients means that a one-size-fits-all approach with a single drug is ineffective. This highlights the need for treatments to focus on addressing the underlying molecular alterations and the predominant dysfunctional pathway in each patient, rather than just targeting the final cellular manifestations and clinical symptoms.

- **Disease heterogeneity:** Genetic and exposome variability among patients makes it difficult to find a one-size-fits-all treatment for ALS. In addition, ALS progression varies widely among patients, complicating the assessment of treatment efficacy. It is crucial to develop precise methods for patient subtyping, through the identification of specific genetic or biomarker profiles, in order to address the heterogeneity of the disease. For instance, baseline NfL levels could be used as part of the inclusion criteria or as a method to stratify patients enrolled in clinical trials. This could achieve more homogenous patient populations, potentially reducing variability and increasing the power to detect treatment effects.
- **Limitations of preclinical models**: animal models of ALS do not fully recapitulate the disease in humans, leading to discrepancies between preclinical and clinical trials outcomes. In fact, animal models of ALS, which often involve genetic manipulation to replicate human ALS mutations, can be considered as target models rather than disease models because they do not replicate the complexity of human ALS.

Understanding and addressing these challenges is crucial for the development of effective ALS therapies. As advances in understanding the genetic basis of ALS are gradually unfolding, this enables more targeted approaches in developing treatments, recruiting participants for clinical trials, and managing the disease effectively.

Aims and Objectives

The overall aim of this thesis project is to develop a deeper understanding of ALS pathophysiology, with a specific focus on TDP-43 proteinopathy, and to explore potential therapeutic strategies targeting TDP-43. The project's objectives are broad and multifaceted, involving both fundamental research on the behavior of TDP-43 in disease models, and the development and preclinical testing of novel therapeutic approaches. The key aims and objectives can be outlined as follows:

1. To understand TDP-43 dynamics under pathological conditions: since metabolic alterations are widely reported in ALS, and since intracellular pH is closely linked to cellular metabolism, our first objective was to evaluate the effect of intracellular pH alterations on the localization and aggregation of TDP-43 in a cellular model of ALS.
2. To characterize novel biotherapeutics targeting TDP-43: building on previous work from the laboratory, the project evaluates two scFv molecules (B1 and D7) that specifically target human wildtype TDP-43. Our second objective was to assess the therapeutic potential of these scFvs both directly on TDP-43 and indirectly on pathways downstream of TDP-43 in a cellular model of TDP-43 proteinopathy.
3. To develop a nanoparticle-based delivery system for scFv: the administration of the scFvs to target cells can be complicated by their limited crossing of the BBB and internalization into cells. Our third objective was to develop SPION-based nanoparticles that can be complexed with the scFvs for an enhanced delivery into the target cells.
4. To undertake a detailed evaluation of a preclinical mouse model of ALS: before testing the scFvs *in vivo*, we wanted to establish and characterize an animal model that accurately mimics ALS pathology, particularly in respect to TDP-43 proteinopathy. Therefore, our fourth objective was to evaluate key phenotypic, molecular, and metabolomic changes occurring at different stages of ALS progression in order to identify quantifiable biomarkers that can be used to assess the efficacy of potential therapeutics.
5. To test the scFv *in vivo*: given the difficulty of delivering drugs into the CNS, our final objective was to test AAV-mediated delivery systems, particularly the CNS-specific AAV-CAP.B10 variant, in order to deliver the scFv specifically to the CNS prior to the start of the preclinical trial in the previously characterized mouse model.

Results

Metabolic alterations are widely described in ALS and can lead to various alterations in the intracellular environment, including pH changes. These changes can have significant effects on macromolecules inside the cell, especially proteins like TDP-43. Therefore, the first step of this project was to study the effect of changes in intracellular pH on the localization and solubility of TDP-43 in the context of ALS.

IV. Effect of pH alterations on TDP-43 in ALS

Publication 4:

The effect of pH alterations on TDP-43 in a cellular model of amyotrophic lateral sclerosis (2024), *Biochemistry and Biophysics Reports.*

a. Resumé en Français

TDP-43 joue un rôle clé dans la réponse cellulaire à divers stress, y compris les stress métaboliques, bioénergétiques et oxydatifs. En plus, ces stress peuvent altérer la fonction de TDP-43 si la cellule ne parvient pas à rétablir l'homéostasie. Des altérations métaboliques, incluant des changements dans le métabolisme du pyruvate, NAD^+, glutathione, carnitines tyrosine, sérine, et le cycle de Krebs ont été observées dans le cortex moteur de modèles murins TDP-43 de SLA (Gautam et al., 2022). Une activation de la voie AMPK a aussi été détectée, favorisant la délocalisation de TDP-43 (Lim et al., 2012; Liu et al., 2015).

Dans la SLA, ces différents mécanismes pathologiques peuvent potentiellement affecter le pH intracellulaire, entraînant d'autres perturbations de l'homéostasie. Une augmentation des niveaux de l'anhydrase carbonique I, une enzyme importante pour la régulation du pH, ont été observés dans les motoneurones de la moelle épinière chez les patients atteints de SLA, suggérant des altérations du pH cellulaire (Liu et al., 2016). Chez les souris SOD1, un état d'acidose progressive a été détecté dans le système nerveux central (SNC), particulièrement marqué au niveau de la moelle épinière, et associé à diverses altérations métaboliques (Dodge et al., 2013). Les variations de pH peuvent perturber la structure et la fonction des protéines, compromettant ainsi les processus métaboliques et entraînant potentiellement la mort cellulaire. Étant donné l'interaction entre TDP-43 et le métabolisme d'une part, et entre le

métabolisme et le pH d'autre part, nous nous sommes intéressés à évaluer l'effet des altérations de pH sur TDP-43 dans le contexte de la SLA.

Des HEK293T, utilisées comme modèle cellulaire, ont été transfectées avec un plasmide exprimant TDP-43 fusionné à la GFP. Après une incubation d'une heure dans des solutions de pH 6.4, 7.2, et 8, la viabilité cellulaire a été testée par un essai MTT, montrant aucune modification significative (Fig.1). La localisation de TDP-43 a révélé une délocalisation cytoplasmique accrue dans les conditions de pH 6.4 et 8 (Fig.2 A, B). Le nombre de cellules avec des inclusions cytoplasmiques de TDP-43 a également augmenté sous ces conditions (Fig.2 A, C). L'analyse par western blot n'a montré aucune différence significative dans les niveaux de TDP-43 total, de ses fragments C-terminaux ou de sa forme phosphorylée que ça soit dans la fraction protéique insoluble (Fig. 3, 4) ou soluble (Fig.5).

Plusieurs études antérieures ont évalué l'impact du pH sur la structure et le repliement de TDP-43, mais la plupart de ces études ont été menées sur des domaines recombinants et purifiés de la protéine, plutôt que sur sa forme complète (Babinchak et al., 2019; Carter et al., 2021; Conicella et al., 2016; Mompeán et al., 2016; Patni & Jha, 2023). Cependant, des travaux récents ont montré que le comportement de la protéine TDP-43 entière diffère de celui de ses domaines isolés, suggérant que les études sur des domaines recombinants ne reflètent pas fidèlement le comportement de TDP-43 (Staderini et al., 2022, 2024). De plus, ces recherches sont souvent menées en solution, en dehors du contexte cellulaire, et ne tiennent pas compte des interactions moléculaires ni des modifications post-traductionnelles (fragmentations, phosphorylation, ubiquitination, etc…) observées dans les cellules (Ciazynska, 2023; Y. Wei et al., 2016). En plus, dans un contexte pathologique comme la SLA, TDP-43, lorsqu'elle est surexprimée et délocalisée dans le cytoplasme, pourrait ne pas réagir de la même manière aux changements de pH que la protéine en condition normale. Notre étude a montré pour la première fois qu'un changement de pH extracellulaire, se traduisant par un changement plus faible de pH intracellulaire (Bouyer et al., 2004; Buckler et al., 1991; Putnam, 2001), peut entraîner une augmentation de la délocalisation de TDP-43 et de son inclusion dans des punctas cytoplasmiques. L'augmentation des punctas positives pour TDP-43 suite à des fluctuations de pH pourrait indiquer un rôle de TDP-43 dans la réponse des cellules aux variations de pH, ou bien une altération structurelle induite par le pH, entraînant la séparation

de phase liquide-liquide de TDP-43. Cependant, une limitation de notre étude est la durée limitée d'exposition des cellules à ces conditions de pH modifié (1 heure), car des traitements plus longs ont causé une mortalité cellulaire trop importante. Un autre point à améliorer serait l'impact possible des tags GFP et 6*His sur le comportement de TDP-43 surexprimé. Une prochaine étape intéressante serait d'étudier l'effet des altérations prolongées du pH intracellulaire sur la protéinopathie de TDP-43 et d'analyser l'impact de TDP-43 sur le pH intracellulaire. Cela pourrait offrir de nouvelles pistes pour le développement d'interventions thérapeutiques.

b. Context

An interplay exists between TDP-43 and cellular metabolism. TDP-43 is known to play a key role in the cellular response to different types of stressors including metabolic, bioenergetic, and oxidative stress. In turn, these stressors can have a detrimental effect on the function of TDP-43 when the cell fails to restore homeostasis. For example, loss of function of TDP-43 was found to cause bioenergetic failure and a reprogramming of the lipid metabolism in human iPSC-derived neurons (Ceron-Codorniu et al., 2024). Although few studies on TDP-43 mouse models of ALS are focused on metabolism, changes in the metabolism of pyruvate, NAD^+, glycine, tyrosine, serine, glutathione, carnitines, and the citric acid cycle were reported in the motor cortex of a TDP-43 mouse model of ALS (Gautam et al., 2022). Metabolic dysfunctions were also shown to contribute to aberrant energy signalling in ALS, leading to the activation of the AMPK signalling pathway, which can contribute to the mislocalization of TDP-43 (Lim et al., 2012; Liu et al., 2015).

In ALS, these different pathological mechanisms can potentially impact intracellular pH, leading to further homeostatic disturbances. Intracellular pH is a critical aspect of cellular homeostasis, and it is found to be altered in different pathological conditions. Increased levels of the carbonic anhydrase I enzyme, which is important in pH regulation, have been observed in the spinal cord motor neurons of ALS patients, suggesting cellular pH alterations (X. Liu et al., 2016). In SOD1 mice, a state of progressive acidosis was detected in the CNS, most prominently at the level of the spinal cord, and was linked to various metabolic alterations (Dodge et al., 2013). Deviations from physiological pH can lead to alterations in protein structure and function, disrupting metabolic processes and potentially leading to cell damage

or death. Given the interplay between TDP-43 and the metabolism on one hand, and between the metabolism and pH on the other hand, we were interested in evaluating the effect of pH fluctuations on the behaviour, localization and aggregation of TDP-43 in the context of ALS.

c. Summary of materials and methods

We used HEK293T cells as a cellular model of ALS because it's a human cell line with a very good transfection efficiency, allowing to study the effects of the overexpression of TDP-43 in cells. Before transfection, 300,000 cells were plated in six-well plates. Once they reached 60-70% confluency, they were transfected for 48 hours with 3 µg of plasmid expressing GFP-TDP-43-6*His (GTH). Before the assays, cells were incubated for one hour with different solutions at pH 6.4, 7.2, and 8. Cell viability was evaluated using an MTT reduction assay. The localization of TDP-43 and its inclusion into TDP-43-positive puncta were assessed using fluorescence microscopy. The solubility and aggregation of TDP-43 was examined via western blotting by using the soluble and insoluble protein fractions of treated cells. For the western blots, three different plasmids were used as controls. An empty pcDNA6.2 plasmid was used to control for the transfection, while plasmid expressing TDP-43-6*His and GFP were used to control for the effect of the 6*His tag and GFP tag, respectively.

d. Summary of results

The MTT assay revealed that cells overexpressing GTH and treated for 1 hour with the different pH solutions had no significant change in viability (Fig.1). Concerning the localization of TDP-43, we found that the overexpressed protein was mislocalized into the cytoplasm in some cells. Following the incubation of cells with solutions of pH 6.4 or 8, we observed an increase in the percentage of cells with mislocalized TDP-43 compared to the control pH of 7.2 (Fig.2 A,B), in addition to an increase in the number of cells with cytoplasmic TDP-43-positive puncta (Fig.2 A,C). Western blot analysis showed no change in the levels of full-length TDP-43, its C-terminal fragment, or phosphorylated TDP-43 in either the insoluble (Fig.3, 4) or soluble (Fig.5) protein fractions.

Biochemistry and Biophysics Reports 38 (2024) 101664

Contents lists available at ScienceDirect

Biochemistry and Biophysics Reports

journal homepage: www.elsevier.com/locate/bbrep

The effect of pH alterations on TDP-43 in a cellular model of amyotrophic lateral sclerosis

Yara Al Ojaimi [a,*], Charlotte Slek [a], Samira Osman [a], Hugo Alarcan [a,b], Sylviane Marouillat [a], Philippe Corcia [b], Patrick Vourc'h [a,b], Débora Lanznaster [a], Hélène Blasco [a,b]

[a] UMR 1253, iBrain, Université de Tours, INSERM, Tours, France
[b] Service de Biochimie et Biologie Moléculaire, CHRU de Tours, France

ARTICLE INFO

Keywords:
Amyotrophic lateral sclerosis
TDP-43
Aggregates
Mislocalization
pH

ABSTRACT

Amyotrophic Lateral Sclerosis (ALS) is the most common neurodegenerative disease affecting motor neurons. The pathophysiology of ALS is not well understood but TDP-43 proteinopathy (aggregation and mislocalization) is one of the major phenomena described. Several factors can influence TDP-43 behavior such as mild pH alterations that can induce conformational changes in recombinant TDP-43, increasing its propensity to aggregate. However to our knowledge, no studies have been conducted yet in a cellular setting, in the context of ALS. We therefore tested the effect of cellular pH alterations on the localization, aggregation, and phosphorylation of TDP-43. HEK293T cells overexpressing wildtype TDP-43 were incubated for 1 h with solutions of different pH (6.4, 7.2, and 8). Incubation of cells for 1 h in solutions of pH 6.4 and 8 led to an increase in TDP-43-positive puncta. This was accompanied by the mislocalization of TDP-43 from the nucleus to the cytoplasm. Our results suggest that small alterations in cellular pH affect TDP-43 and increase its mislocalization into cytoplasmic TDP-43-positive puncta, which might suggest a role of TDP-43 in the response of cells to pH alterations.

1. Introduction

Amyotrophic lateral sclerosis (ALS) is a neurodegenerative disease characterized by the progressive death of motor neurons. This disease leads to the paralysis of skeletal muscles and ultimately respiratory muscles, resulting in the death of patients within 3–5 years following the onset of symptoms [1]. Abnormal aggregation of various proteins, particularly the TAR DNA binding protein 43 (TDP-43) has been reported in motor neurons and glial cells of ALS patients.

TDP-43 is a heterogenous nuclear ribonucleoprotein (hnRNP) that plays an essential role in transcriptional and post-translational regulation [2]. Physiological TDP-43 primarily acts as a nuclear protein, that shuttles between the nucleus and the cytoplasm. However, in pathological conditions, TDP-43 mislocalizes to the cytoplasm where it undergoes post-translational modifications and aggregation. These modifications have been associated with toxic loss and gain of function of this protein, leading to homeostatic imbalances.

pH changes have been described to have significant implications on the pathophysiology of neurodegenerative disorders [3]. Pathological mechanisms observed in ALS, such as ischemia, mitochondrial alterations, glutamate-mediated excitotoxicity and oxidative stress, all of which can affect intracellular pH, have been associated with the cytoplasmic mislocalization and aggregation of TDP-43 [4–6]. Concomitantly, several studies have shown that alterations in the pH can affect the structure of purified recombinant TDP-43 [7,8]. However, no studies have assessed the effect of such pH alterations on cellular TDP-43 in the context of ALS. The goal of our study was to assess the impact of pH alterations on the localization and solubility of cellular TDP-43, which emphasizes the importance of pH control when considering therapeutic strategies.

2. Materials and methods

2.1. Cells and transfection

HEK293T cells (ATCC, USA) were cultured in Dulbecco's modified

Abbreviations: ALS, Amyotrophic lateral sclerosis; BCECF, 2′-7′-bis(carboxyethyl)-5(6)-carboxyfluorescein; CTD, C-terminal domain; HEK293T, Human embryonic kidney cells 293T; hnRNP, Heterogenous nuclear ribonucleoprotein; LLPS, Liquid-liquid phase separation; TDP-43, TAR DNA binding protein 43.

* Corresponding author.
E-mail address: yara.alojaimi@univ-tours.fr (Y. Al Ojaimi).

https://doi.org/10.1016/j.bbrep.2024.101664
Received 11 December 2023; Received in revised form 5 February 2024; Accepted 11 February 2024
2405-5808/© 2024 The Authors. Published by Elsevier B.V. This is an open access article under the CC BY-NC-ND license (http://creativecommons.org/licenses/by-nc-nd/4.0/).

Eagle's medium (DMEM) supplemented with 10% (*v/v*) fetal bovine serum and 1% non-essential amino acids at 37 °C and 5% CO_2 and plated in six-well plates at a concentration of 0.3 × 10^6 cells/well the day before transfection.

Cells were transfected at 60–70% confluency using the JetPEI transfection reagent (Polyplus transfection) following the manufacturer's protocol. Briefly, a volume of JetPEI equivalent to twice the amount (μg) of the plasmid was used. The plasmid and JetPEI were prepared in sterile 150 mM NaCl. Following gentle mixing and an incubation for 15 min at RT, the mix was added drop by drop to the cells. All transfections used 3 μg of plasmids unless otherwise mentioned, and lasted 48 h.

2.2. pH solutions

pH solutions were prepared to induce changes in intracellular pH, as previously described [9]. The stock solution was prepared with 125 mM NaCl, 4.5 mM KCl, 20 mM Hepes, 20 mM MES, 1 mM $CaCl_2$ and 1 mM $MgCl_2$. Once this solution was obtained, the pH was adjusted with NaOH or HCl in order to obtain two different solutions of pH 6.4, 7.2, and 8. Cells were incubated with these solutions for 1 h before different assays were performed to determine the effect of pH changes on cell viability and TDP-43 localization and aggregation.

2.3. Cell viability

Cell viability was examined using the MTT reduction assay. 48 h after transfection, and following incubation with the different pH solutions, the cell medium was removed, and cells were incubated with 0.5 mg/mL MTT for 30 min at 37 °C. The MTT solution was then removed and DMSO was added to the cells. The plate was wrapped in foil and put on an orbital shaker for 10 min. Absorbance was then measured at 570 nm using a microplate reader (Biorad).

2.4. Assessment of TDP-43 localization and aggregation

To study the effect of intracellular acidification on the localization of TDP-43, HEK293T cells were plated on coverslips pre-treated with poly-D-lysine (10 μg/mL) and transfected with the plasmid expressing GFP-wtTDP-43-6*His (3 μg, GTH). 48 h post-transfection, cells were incubated for 1 h with the different pH solutions (6.4, 7.2 and 8) as previously described. Cells were then incubated with 1 μL of Hoechst 33342 (1:1000) for 10 min before reading the fluorescence. Afterwards, cells were fixed for 20 min with 4% paraformaldehyde solution (diluted in PBS). Images were obtained by confocal microscopy (Leica SP8) where 100 cells per condition were analysed for TDP-43 localization (nuclear, cytoplasmic, or both) and aggregation.

Western blot was used to assess the solubility of TDP-43. HEK293T cells were transiently transfected with 3 μg of plasmids coding for TDP-43-6*His (TH), or 3 μg of plasmids coding for GFP-TDP-43-6*His (GTH). The empty pcDNA6.2 plasmid and a GFP-coding plasmid were used as control (3 μg). 48 h after transfection, cells were treated for 1 h with the different pH solutions before protein extraction.

The medium of HEK293T cells was removed and the cells were scraped off in ice-cold PBS and centrifuged at 900×*g* for 5 min at 4 °C. Cells were then resuspended in 100 μL of cold lysis buffer (PBS pH = 8.0, 1% Triton-X 100, 10 mM $MgCl_2$, 1 mM DTT) supplemented with 1X Halt Protease and Phosphatase Inhibitor Cocktails (*Thermo Fisher Scientific*) and Pierce Universal Nuclease (*Thermo Fisher Scientific*). After 30 min, 50 μL of lysate was centrifuged at 13,000×*g* for 5 min. The pellet, which makes up the insoluble protein fraction, was resuspended in RIPA supplemented with 6 M urea. 10 μg of proteins were migrated by SDS-PAGE, transferred onto a 0.2 μm PVDF membrane, and blocked with 5% fat-free milk in TBS-Tween (0.1%) for 1 h at room temperature. Membranes were then probed overnight at 4 °C with a primary antibody diluted in the blocking solution at 1:5000 targeting either the C-terminus of TDP-43 (Rabbit, 12892-1-AP, *Proteintech*) or phosphorylated TDP-43 (Rabbit, 22309-1-AP, *Proteintech)*. The following day, membranes were incubated for 1 h at room temperature with a complementary HRP-conjugated secondary antibody diluted at 1:10000 in the blocking solution. Detection of proteins was achieved following 5 min incubation with Enhanced Chemiluminescence (ECL) reagent and exposed using a ChemiDoc imaging system (BioRad). Loading control was performed by normalizing the target protein to the stain-free images of total protein. All bands were quantified using the BioRad Image Lab software version 6.1.0.

2.5. Statistical analysis

All statistical analyses were carried out using the GraphPad Prism 8 software. Data is reported as mean ± Standard Error of the Mean (SEM) for 3–5 independent experiments. The localization of the TDP-43 protein was analysed using a two-way ANOVA test. The influence of pH on TDP-43 puncta were analysed using the Kruskal-Wallis test. Analysis of the western blot results was done using the Wilcoxon test. Results were considered to be statistically significant at $*p$ values < 0.05.

3. Results

3.1. pH-dependent cell viability

We first assessed the effect of extracellular pH changes on the viability of cells in order to determine the right incubation time. The incubation of HEK293T cells with different pH conditions for 1 h does not decrease the viability of cells (Fig. 1A). On the other hand, 4 h and 24 h incubation reduces the viability of the cells by more than 50% (results not shown). Therefore, the timepoint used in this study was limited to 1 h of incubation. The viability of HEK293T cells transfected with 3 μg of plasmid expressing either GFP, TDP-43-6*His (TH), or GFP-TDP-43-6*His (GTH) and incubated with the different pH solutions for 1 h was also assessed. No change in cellular viability was observed under these different conditions (Fig. 1B–D).

3.2. pH-dependent TDP-43 localization

We then examined the effect of pH alterations on the localization of overexpressed TDP-43. At pH 7.2, most cells had TDP-43 mainly localized in the nucleus, with a small percentage of cells showing both nuclear and cytoplasmic TDP-43. Following a 1 h incubation with solutions at pH 6.4 or pH 8, we detected an increase of around 6% in cells showing TDP-43 mislocalized to the cytoplasm compared to the control condition at pH 7.2 (Fig. 2 A,B). We also observed an increase in the % of cells showing TDP-43-positive puncta at pH 6.4 (15.3 ± 1.8 %) and pH 8 (13.8 ± 0.9 %) compared to pH 7.2 (Fig. 2 A,C).

3.3. pH-dependent TDP-43 aggregation and phosphorylation

We assessed by western blot the amounts of total and phosphorylated TDP-43 in the soluble and insoluble protein fractions. There was no change in the solubility of GFP under different pH conditions, indicating that the GFP tag has no effect on the solubility of TDP-43 under these conditions. Concomitantly, there was no difference in the solubility of TDP-43 when cells were overexpressing GTH compared to TH, confirming the lack of effect of GFP on TDP-43 solubility. We detected no change in either TDP-43 (Fig. 3 A,B) nor its 35-kDa C-terminal fragment (Fig. 3 A,C) at pH 6.4 or pH 8 compared to pH 7.2. Similar results were observed for the insoluble 70-kDa GTH (Fig. 3A,D).

As for the insoluble phosphorylated TDP-43, we detected two main bands on the blots, with one being at 45-kDa and the other at 50 kDa (Fig. 4A). No change in these TDP-43 species, nor the insoluble 70 kDa phosphorylated GTH were detected when cells were incubated with different pH conditions (Fig. 4B-D).

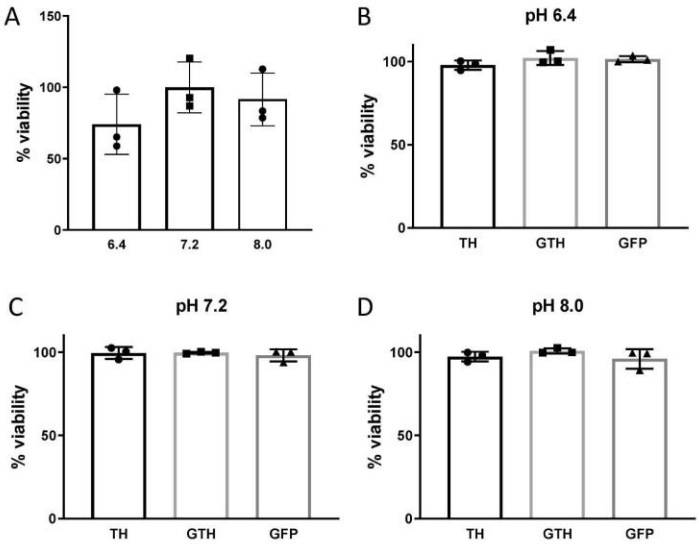

Fig. 1. The viability of HEK293T cells is not decreased under different pH conditions
A) MTT reduction assay of untransfected HEK293T cells incubated for 1 h with different pH conditions. Values are expressed as percentage viability compared to pH 7.2 condition. Kruskall-Wallis test (N = 3). **B-D)** MTT reduction assay of HEK293T cells transfected with 3 μg of plasmid expressing TDP-43-6*His (TH), GFP-TDP-43-6*His (GTH) or GFP and incubated for 1 h at pH 6.4, 7.2 or 8. Values are expressed as percentage of viability compared to control (empty vector). Kruskal-Wallis test (N = 3).

The amount of soluble total and phosphorylated TDP-43 was also assessed. We observed no change in the levels of soluble full-length TDP-43 (Fig. 5A,B) nor its 35-kDa fragment which was only detected in the TH condition (Fig. 5A,C). Interestingly, we detected a different band pattern for phosphorylated TDP-43 in the soluble fraction compared to the insoluble fraction (Fig. 5D). We only observed a band at 45-kDa. The bands corresponding to the 50-kDa phosphorylated TDP-43 and the 70-kDa phosphorylated GTH were not detected. However, there was no effect of pH changes on the amount of soluble phosphorylated TDP-43 (Fig. 5E).

4. Discussion

Extracellular pH alterations have been shown to induce parallel but less pronounced changes in the intracellular pH [10–13]. The change in intracellular pH was verified in our cells using the pH-sensitive BCECF (data not shown). How intracellular pH induces TDP-43 mislocalization and aggregation has not been well investigated. Since TDP-43 is known for its ability to spontaneously aggregate, particularly through its intrinsically disordered C-terminal domain (CTD) [14,15], it is complicated to assess the effect of microenvironmental alterations on the full-length protein. Therefore, most studies that investigated the effect of pH on TDP-43 folding have used isolated protein domains rather than the full-length protein [15–17]. In addition, the results obtained seem to vary according to the recombinant TDP-43 forms used and the protocols applied (i.e. protein concentration, temperature, buffer pH, salt concentration). Although several studies show that TDP-43 domains can be structurally altered upon pH changes [18–21], the impact observed on separate protein domains might not be reproducible in the full-length protein given the presence of complex intra- and inter-molecular interactions [22,23]. In addition, all these studies were performed on recombinant purified proteins, and not in cellular models of TDP-43 proteinopathy. Given the extensive post-translational modifications that TDP-43 can undergo inside cells [23], such studies do not take into consideration these modifications that can highly affect the structure and solubility of proteins.

Here we showed, for the first time, that pH alterations in the cellular environment can affect the cytoplasmic mislocalization of TDP-43. In cells overexpressing TDP-43, we observed a decrease in the nuclear localization of TDP-43 and an increase in the number of cells with TDP-43-positive puncta at pH 6.4 and 8 compared to the physiological pH. Western blot analysis revealed no significant change in the amount of TDP-43 or its phosphorylated forms in the soluble or insoluble fractions following pH alterations in HEK293T cells overexpressing TDP-43. This discrepancy in the results observed through western blot and those observed through fluorescence microscopy can be explained by the differing accuracy of these two methods in detecting real insoluble aggregates. In fact, Barmada and his colleagues demonstrated that the TDP-43-positive puncta observed by immunofluorescence can sometimes be removed by detergent treatment, indicating that they can't always be considered as insoluble TDP-43 aggregates [24]. These results suggest that studying TDP-43 aggregation by immunofluorescence can lead to its overestimation and that western blot analysis might be a more accurate method.

TDP-43 is particularly sensitive to changes in its environment which can shift the equilibrium towards favouring the formation of oligomeric forms [7]. Under stressful cellular conditions, TDP-43 undergoes liquid-liquid phase separation (LLPS) and is recruited to stress granules [23,24]. For instance, stress granules can be formed in the context of metabolic dysfunction caused by starvation, hypoxia, or mitochondrial abnormalities [25–29], which can enhance TDP-43 LLPS and subsequent aggregation. For instance, a recent study has shown that the regulation of the oxidative status of TDP-43 particularly at the level of the CTD, which is largely affected by the metabolic status of the cell, affects the conformation of TDP-43 and its self-assembly [30]. Metabolic stressors are partly linked to intracellular pH changes and can affect the protonation state of charged amino acid residues and therefore alter the structure and conformation of proteins [31,30]. Such modifications

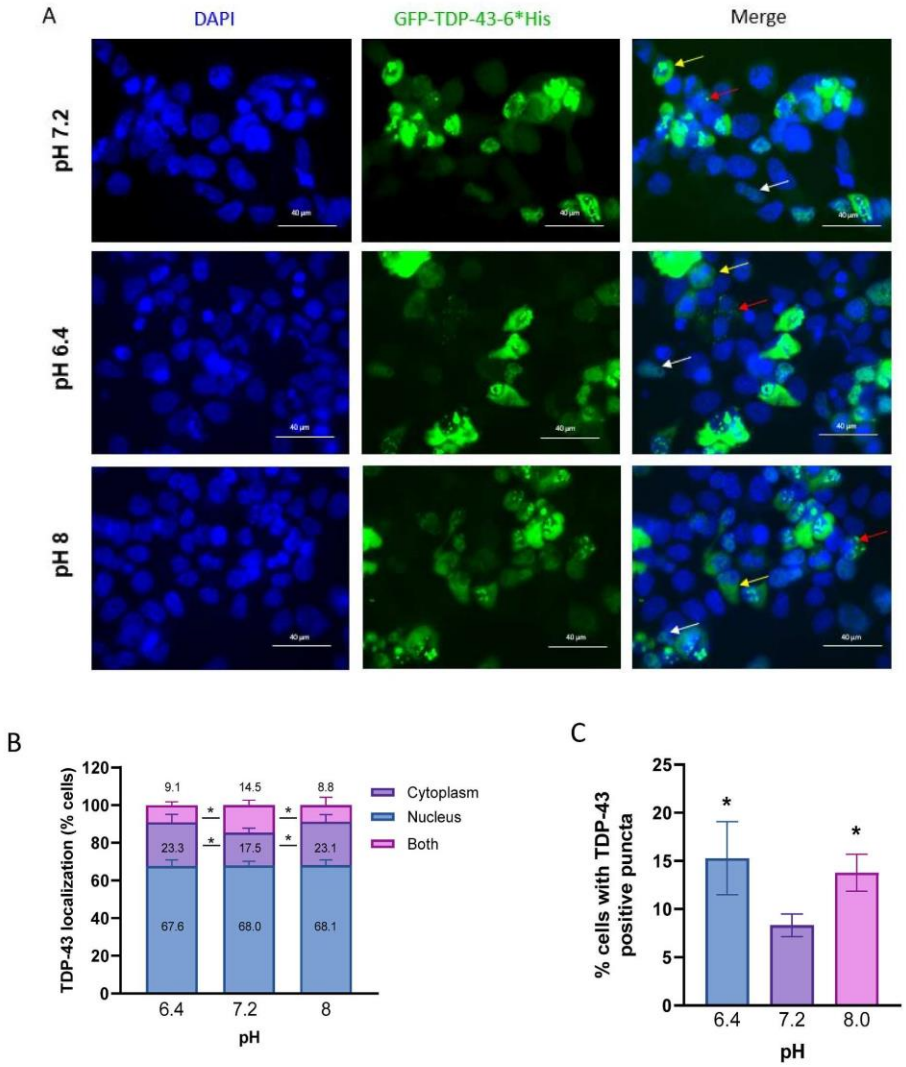

Fig. 2. Changes in intracellular pH affect the localization of TDP-43
A) Immunofluorescence of HEK293T cells overexpressing GFP-wtTDP-43-6*His, following a 1 h incubation at pH 7.2 or pH 6.4. White arrow: nuclear TDP-43; Yellow arrow: cytoplasmic TDP-43. Red arrow: TDP-43-positive puncta. Scale bar = 40 μm. **B)** Percentage of cells with TDP-43-positive puncta. *p = 0.04, Kruskal-Wallis test, N = 4. **C)** Localization of TDP-43 under different pH conditions. *p = 0.04, two-way ANOVA, N = 4. (For interpretation of the references to colour in this figure legend, the reader is referred to the Web version of this article.)

might allow proteins like TDP-43 to act as biosensors of alterations in the intracellular environment [32]. Our results therefore suggest that an acute change in intracellular pH is associated with increased mis-localization of TDP-43 and its assembly into cytoplasmic puncta, possibly as part of the cellular response to the pH stress. This highlights the importance of controlling for cellular pH when assessing potential therapeutic approaches in ALS. In addition, different cell types react differently to metabolic alterations and pH changes, with more or less efficient buffering mechanisms. Therapeutic approaches should therefore be designed accordingly and consider restoring cellular homeostasis in a cell-specific way. Future studies should give more focus to the effect of pH alterations on TDP-43 in neurons, which are particularly sensitive to changes in their environment, and assess the effect of regulating cellular pH on the proteinopathy associated with TDP-43.

Data availability

Data generated in this study is available upon reasonable request to

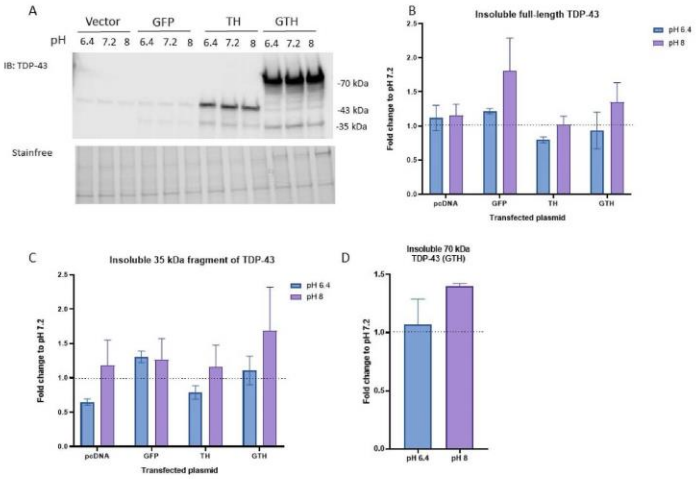

Fig. 3. No change in the insolubility of TDP-43 following a 1 h incubation with different pH conditions. Immunoblot (A) and quantification of insoluble full-length TDP-43 (B), 35 kDa fragment of TDP-43 (C), and the 70 kDa GTH (D) in HEK293T cells transfected with 3 μg of empty vector or plasmid expressing GFP, TDP-43-6*His (TH), GFP-TDP-43-6*His (GTH) and incubated for 1 h with different pH conditions. Values were normalized to the corresponding pH 7.2 condition. Wilcoxon test, N = 3.

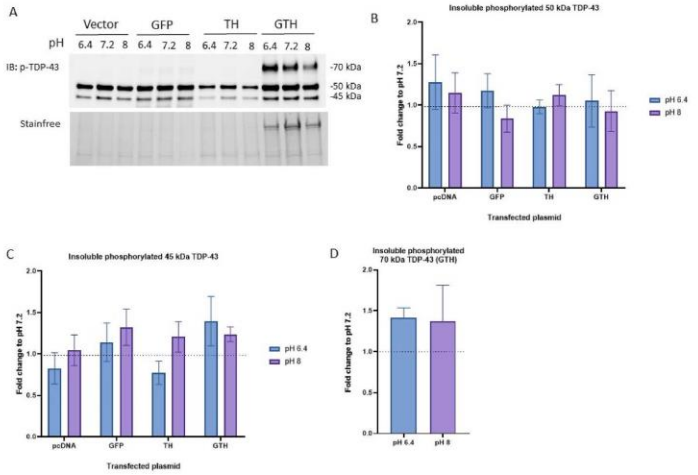

Fig. 4. No change in the amount of insoluble phosphorylated TDP-43 (p-TDP-43) following a 1 h incubation with different pH **conditions.** Insoluble phosphorylated full-length TDP-43 was detected at 45- and 50 kDa. Immunoblot (A) and quantification of insoluble phosphorylated 50 kDa TDP-43 (B), phosphorylated 45 kDa TDP-43 (C), and the phosphorylated 70 kDa GTH (D) in HEK293T cells transfected with 3 μg of empty vector or plasmid expressing GFP, TDP-43-6*His (TH), GFP-TDP-43-6*His (GTH) and incubated for 1 h with different pH conditions. Values were normalized to the corresponding pH 7.2 condition. Wilcoxon test, N = 3.

the corresponding author.

CRediT authorship contribution statement

Yara Al Ojaimi: Writing – original draft, Formal analysis, Data curation. **Charlotte Slek:** Writing – original draft, Formal analysis, Data curation. **Samira Osman:** Writing – review & editing. **Hugo Alarcan:** Data curation, Conceptualization. **Sylviane Marouillat:** Data curation. **Philippe Corcia:** Conceptualization. **Patrick Vourc'h:** Writing – review & editing. **Débora Lanznaster:** Formal analysis, Data curation. **Hélène Blasco:** Writing – original draft, Supervision, Conceptualization.

Declaration of competing interest

The authors declare that they have no known competing financial interests or personal relationships that could have appeared to influence

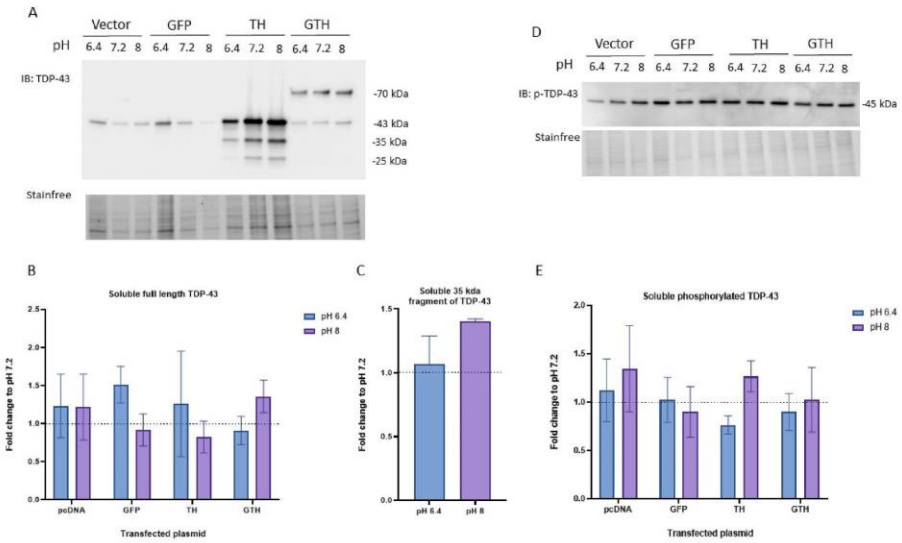

Fig. 5. No change in the amount of soluble TDP-43 following a 1 h incubation with different pH conditions. Immunoblot (A) and quantification of soluble full-length TDP-43 (B), and 35-kDa fragment of TDP-43 (observed only in the TH condition) (C); and immunoblot (D) and quantification (E) of soluble phosphorylated TDP-43 (p-TDP-43) in HEK293T cells transfected with 3 μg of empty vector or plasmid expressing GFP, TDP-43-6*His (TH), GFP-TDP-43-6*His (GTH) and incubated for 1 h with different pH conditions. Values were normalized to the corresponding pH 7.2 condition. Wilcoxon test, N = 3.

the work reported in this paper.

Acknowledgements

The authors would like to thank LabEx MAbImprove (ANR-10-LABX-53-01) and the Région Centre Val de Loire for their financial support.

References

[1] O. Hardiman, et al., Correction: amyotrophic lateral sclerosis, Nat. Rev. Dis. Prim. 3 (1) (Oct. 2017) 17085, https://doi.org/10.1038/nrdp.2017.85.
[2] R.C. Hergesheimer, et al., The debated toxic role of aggregated TDP-43 in amyotrophic lateral sclerosis: a resolution in sight? Brain 142 (5) (May 2019) 1176–1194, https://doi.org/10.1093/brain/awz078.
[3] A. Majdi, J. Mahmoudi, S. Sadigh-Eteghad, S.E.J. Golzari, B. Sabermarouf, S. Reyhani-Rad, Permissive role of cytosolic pH acidification in neurodegeneration: a closer look at its causes and consequences, J. Neurosci. Res. 94 (10) (Oct. 2016) 879–887, https://doi.org/10.1002/jnr.23757.
[4] P. Wang, et al., TDP-43 induces mitochondrial damage and activates the mitochondrial unfolded protein response, PLoS Genet. 15 (5) (May 2019) e1007947, https://doi.org/10.1371/journal.pgen.1007947.
[5] W. Wang, et al., The ALS disease-associated mutant TDP-43 impairs mitochondrial dynamics and function in motor neurons, Hum. Mol. Genet. 22 (23) (Dec. 2013) 4706–4719, https://doi.org/10.1093/hmg/ddt319.
[6] J. Gao, L. Wang, T. Yan, G. Perry, X. Wang, TDP-43 proteinopathy and mitochondrial abnormalities in neurodegeneration, Mol. Cell. Neurosci. 100 (Oct. 2019) 103396, https://doi.org/10.1016/j.mcn.2019.103396.
[7] A.A. Doke, S.K. Jha, Effect of *in vitro* solvation conditions on inter- and intramolecular assembly of full-length TDP-43, J. Phys. Chem. B 126 (26) (Jul. 2022) 4799–4813, https://doi.org/10.1021/acs.jpcb.2c02203.
[8] M. Mompeán, A. Chakrabartty, E. Buratti, D.V. Laurents, Electrostatic repulsion governs TDP-43 C-terminal domain aggregation, PLoS Biol. 14 (4) (Apr. 2016) e1002447, https://doi.org/10.1371/journal.pbio.1002447.
[9] P. Swietach, A. Hulikova, S. Patiar, R.D. Vaughan-Jones, A.L. Harris, Importance of intracellular pH in determining the uptake and efficacy of the weakly basic chemotherapeutic drug, doxorubicin, PLoS One 7 (4) (Apr. 2012) e35949, https://doi.org/10.1371/journal.pone.0035949.
[10] P. Bouyer, S.R. Bradley, J. Zhao, W. Wang, G.B. Richerson, W.F. Boron, Effect of extracellular acid-base disturbances on the intracellular pH of neurones cultured from rat medullary raphe or hippocampus: effect of acid-base disturbances on neurones, J. Physiol. 559 (1) (Aug. 2004) 85–101, https://doi.org/10.1113/jphysiol.2004.067793.
[11] K. Glunde, H. Dussmann, H.-P. Juretschke, D. Leibfritz, Na+/H+ exchange subtype 1 inhibition during extracellular acidification and hypoxia in glioma cells, J. Neurochem. 80 (1) (Jan. 2002) 36–44, https://doi.org/10.1046/j.0022-3042.2001.00661.x.
[12] K.J. Buckler, R.D. Vaughan-Jones, C. Peers, D. Lagadic-Gossmann, P.C. Nye, Effects of extracellular pH, PCO2 and HCO3- on intracellular pH in isolated type-I cells of the neonatal rat carotid body, J. Physiol. 444 (1) (Dec. 1991) 703–721, https://doi.org/10.1113/jphysiol.1991.sp018902.
[13] R.W. Putnam, Intracellular pH regulation of neurons in chemosensitive and nonchemosensitive areas of brain slices, Respir. Physiol. 129 (1–2) (Dec. 2001) 37–56, https://doi.org/10.1016/S0034-5687(01)00281-X.
[14] B.S. Johnson, D. Snead, J.J. Lee, J.M. McCaffery, J. Shorter, A.D. Gitler, TDP-43 is intrinsically aggregation-prone, and amyotrophic lateral sclerosis-linked mutations accelerate aggregation and increase toxicity, J. Biol. Chem. 284 (30) (Jul. 2009) 20329–20339, https://doi.org/10.1074/jbc.M109.010264.
[15] H.I. Ingólfsson, et al., Multiscale simulations reveal TDP-43 molecular level interactions driving condensation, Biophys. J. (Oct. 2023) S0006349523006525, https://doi.org/10.1016/j.bpj.2023.10.016.
[16] M. Pillai, S.K. Jha, Early metastable assembly during the stress-induced formation of worm-like amyloid fibrils of nucleic acid binding domains of TDP-43, Biochemistry 59 (3) (Jan. 2020) 315–328, https://doi.org/10.1021/acs.biochem.9b00780.
[17] D. Patni, S.K. Jha, Protonation–deprotonation switch controls the amyloid-like misfolding of nucleic-acid-binding domains of TDP-43, J. Phys. Chem. B 125 (30) (Aug. 2021) 8383–8394, https://doi.org/10.1021/acs.jpcb.1c03262.
[18] M. Pillai, S.K. Jha, The folding and aggregation energy landscapes of tethered RRM domains of human TDP-43 are coupled via a metastable molten globule-like oligomer, Biochemistry 58 (6) (Feb. 2019) 608–620, https://doi.org/10.1021/acs.biochem.8b01013.
[19] M. Mompeán, et al., The TDP-43 N-terminal domain structure at high resolution, FEBS J. 283 (7) (Apr. 2016) 1242–1260, https://doi.org/10.1111/febs.13651.
[20] P.S. Tsoi, et al., The N-terminal domain of ALS-linked TDP-43 assembles without misfolding, Angew. Chem. Int. Ed. 56 (41) (Oct. 2017) 12590–12593, https://doi.org/10.1002/anie.201706769.
[21] H.-R. Li, T.-C. Chen, C.-L. Hsiao, L. Shi, C.-Y. Chou, J. Huang, The physical forces mediating self-association and phase-separation in the C-terminal domain of TDP-43, Biochim. Biophys. Acta Protein Proteonomics 1866 (2) (Feb. 2018) 214–223, https://doi.org/10.1016/j.bbapap.2017.10.001.
[22] Y. Wei, L. Lim, L. Wang, J. Song, Inter-domain interactions of TDP-43 as decoded by NMR, Biochem. Biophys. Res. Commun. 473 (2) (Apr. 2016) 614–619, https://doi.org/10.1016/j.bbrc.2016.03.158.
[23] K. Ciazynska, TDP-43 folds shape disease, Nat. Struct. Mol. Biol. 30 (10) (Oct. 2023), https://doi.org/10.1038/s41594-023-01135-z, 1406–1406.
[24] S.J. Barmada, G. Skibinski, E. Korb, E.J. Rao, J.Y. Wu, S. Finkbeiner, Cytoplasmic mislocalization of TDP-43 is toxic to neurons and enhanced by a mutation

associated with familial amyotrophic lateral sclerosis, J. Neurosci. 30 (2) (Jan. 2010) 639–649, https://doi.org/10.1523/JNEUROSCI.4988-09.2010.
[25] C. Colombrita, et al., TDP-43 is recruited to stress granules in conditions of oxidative insult, J. Neurochem. 111 (4) (Nov. 2009) 1051–1061, https://doi.org/10.1111/j.1471-4159.2009.06383.x.
[26] Y. Khalfallah, R. Kuta, C. Grasmuck, A. Prat, H.D. Durham, C. Vande Velde, TDP-43 regulation of stress granule dynamics in neurodegenerative disease-relevant cell types, Sci. Rep. 8 (1) (May 2018) 7551, https://doi.org/10.1038/s41598-018-25767-0.
[27] J.A. Riback, et al., Stress-triggered phase separation is an adaptive, evolutionarily tuned response, Cell 168 (6) (Mar. 2017) 1028–1040, https://doi.org/10.1016/j.cell.2017.02.027, e19.
[28] N.G. Farny, N.L. Kedersha, P.A. Silver, Metazoan stress granule assembly is mediated by P-eIF2α-dependent and -independent mechanisms, RNA 15 (10) (Oct. 2009) 1814–1821, https://doi.org/10.1261/rna.1684009.
[29] S. Jain, J.R. Wheeler, R.W. Walters, A. Agrawal, A. Barsic, R. Parker, ATPase-modulated stress granules contain a diverse proteome and substructure, Cell 164 (3) (Jan. 2016) 487–498, https://doi.org/10.1016/j.cell.2015.12.038.
[30] J. Gu, et al., Oxidative regulation of TDP-43 self-association by a β-to-α conformational switch, Proc. Natl. Acad. Sci. U.S.A. 120 (41) (Oct. 2023) e2311416120, https://doi.org/10.1073/pnas.2311416120.
[31] A.M.A. van der Laan, et al., mRNA cycles through hypoxia-induced stress granules in live Drosophila embryonic muscles, Int. J. Dev. Biol. 56 (9) (2012) 701–709, https://doi.org/10.1387/ijdb.103172al.
[32] C. Rabouille, S. Alberti, Cell adaptation upon stress: the emerging role of membrane-less compartments, Curr. Opin. Cell Biol. 47 (Aug. 2017) 34–42, https://doi.org/10.1016/j.ceb.2017.02.006.

e. Discussion

We investigated whether changes in intracellular pH can impact TDP-43. Previous studies that evaluated the effect of pH on TDP-43 were mainly done on recombinant, purified domains of TDP-43 rather than the full-length protein (Babinchak et al., 2019; Carter et al., 2021; Conicella et al., 2016; Mompeán et al., 2016; Patni & Jha, 2023). Recently, Staderini and his colleagues investigated the assembly of purified full-length TDP-43 in solution, and showed that the behaviour of the full-length protein is different from that of its CTD, suggesting that studies conducted on recombinant TDP-43 domains do not represent the behaviour of full-length TDP-43 (Staderini et al., 2022, 2024). Another downside of the studies performed on purified domains is that they are not performed in cells (Ingólfsson et al., 2023; Patni & Jha, 2021; Pillai & Jha, 2020). Therefore, they do not take into consideration the inter- and intra-molecular interactions that occur in the full-length protein, nor the post-translational modifications and cellular adaptations that take place inside cells in response to a stress condition (Ciazynska, 2023; Y. Wei et al., 2016). In addition, TDP-43 in a pathological context (e.g. overexpressed and cytoplasmically mislocalized) would probably not respond to pH changes in a similar way as non-pathological TDP-43 which is in its native functional form. Our study showed for the first time that a change in extracellular pH, which translates into a smaller change in intracellular pH (Bouyer et al., 2004; Buckler et al., 1991; Putnam, 2001), can increase the mislocalization of TDP-43 and its inclusion in cytoplasmic puncta. This observation suggests 1) a role of TDP-43 in the response of cells to intracellular pH fluctuations, and/or 2) a pH-induced alteration in the structure or function of TDP-43 leading to its sequestration into intracellular inclusions. One limitation of this study is that cells were submitted to altered pH conditions for only 1 hour. Treatments of 4 and 24 hours led to significant cell death, causing us to exclude these conditions. Another limitation is that overexpressed TDP-43 contained two tags which might impact the behaviour of the protein even though we tried to control for these factors. An interesting next step would be to understand how prolonged intracellular pH alterations affect TDP-43 proteinopathy and to assess the effect of TDP-43 proteinopathy on intracellular pH. Answering these questions can provide a new avenue for therapeutic interventions. Moreover, they highlight the importance of considering intracellular pH when developing biotherapeutics, because it can affect the stability, affinity, and effect of the different molecules on their target. By understanding how

these factors might be altered in the context of TDP-43 proteinopathy, one might also reconsider some disease models to make them more suitable and representative of the disease.

Building on the work that was previously done in the laboratory and that identified by phage display scFv clones specific for TDP-43 (thesis of Rudolf Hergesheimer, 2021), this second part of the project focused on evaluating the possible therapeutic effects of two scFvs (B1 and D7) in a cellular model of ALS.

V. Development of scFvs targeting TDP-43

Publication 5

scFv intrabody targeting wildtype TDP-43 presents protective effects in a cellular model of TDP-43 proteinopathy (Submitted, under review).

a. Résumé en français

La dysfonction et l'agrégation de TDP-43 sont étroitement liées à la dégénérescence des motoneurones et cette agrégation de TDP-43, présente dans toutes les formes de SLA, joue un rôle central dans la maladie. Ainsi, TDP-43 représente une cible thérapeutique prometteuse. Cependant, cibler TDP-43 se heurtent à des limites, notamment l'accès au compartiment intracellulaire de la protéine et la nécessité d'une action spécifique sur TDP-43. Notre objectif était d'identifier des fragments variables à chaîne unique (scFv) capables de se lier à la TDP-43 sauvage qui est la forme la plus souvent retrouvée dysfonctionnelle dans les patients atteints de SLA, et d'évaluer leurs effets.

Contrairement aux études antérieures utilisant des scFv pour cibler les domaines spécifiques RRM1 et RRM2 de TDP-43 (Pozzi et al., 2019; Tamaki et al., 2018), nous avons utilisé une approche non ciblée pour identifier des scFv capables de se lier à d'autres régions 3D de TDP-43 qui sont potentiellement pertinents à la SLA. Un criblage par phage display a permis de tester 10^{12} clones de scFv pour leur liaison à TDP-43 sous sa forme entière. Parmi ces clones, quatre scFv (B1, A2, B6, et D7) ont été identifiés, et les clones B1 et D7 ont été retenus pour des expériences ultérieures. L'analyse *in silico* a révélé que B1 pouvait se lier à une région comprenant le domaine RRM1 et la région riche en glycine de TDP-43, tandis que D7 ciblait une région comprenant le domaine N-terminal et les domaines RRM1 et RRM2 (Fig.1). Les tests ELISA ont confirmé que ces scFv interagissaient physiquement avec TDP-43

(Fig.2). Pour déterminer les épitopes exacts, de futures études devront utiliser des versions de TDP-43 mutées dans les sites de liaison prédits. Dans les cellules, les scFv étaient principalement localisés dans le cytoplasme, sans cytotoxicité détectée (Fig.3). Lorsqu'ils étaient co-exprimés avec TDP-43, ils se colocalisaient avec la TDP-43 qui était délocalisée dans le cytoplasme et agrégée (Fig.4). Les scFv B1 et D7 n'avaient aucun effet sur TDP-43 total et soluble (Fig.5). Cela, en plus de la localisation principalement cytoplasmique des scFv, suggèrent qu'ils n'altèrent pas la protéine fonctionnelle non pathologique. Le scFv D7 était associé à une diminution du fragment C-terminal de 35-kDa de TDP-43 (TDP-35 CTF) dans la fraction insoluble, sans effet similaire pour B1 ou le scFv contrôle. Cet effet étant aboli par l'inhibition du protéasome mais pas par l'inhibition de l'autophagie (Fig.6) indique que D7 favorise la dégradation protéasomale de TDP-35 CTF. Le scFv B1 n'a pas eu d'effet direct sur TDP-43 et a été exclus de l'étude pour l'instant. Il est encore à éclaircir pourquoi D7, qui se lie à TDP-43 entier recombinant semble n'affecter que TDP-35 CTF à l'intérieur des cellules. Cette différence pourrait être liée à des conformations ou stabilités différentes de TDP-43 entier et TDP-35 CTF dans les cellules, entraînant des affinités de liaison variables de D7. Étant donné que TDP-35 est un fragment cytoplasmique, connu pour former des agrégats qui séquestrent TDP-43 entier et des ARN (M. Che et al., 2011a; M.-X. Che et al., 2015; Nishimoto et al., 2010), il représente une cible thérapeutique importante tout en épargnant la TDP-43 fonctionnelle.

Les altérations métaboliques, notamment celles liées au métabolisme lipidique, sont largement rapportées dans la SLA (Goutman et al., 2022; Lanznaster et al., 2019, 2020) et ont été liées à la protéinopathie de TDP-43 (Andrés-Benito et al., 2021; Ceron-Codorniu et al., 2024; Floare & Allen, 2020; Lanznaster et al., 2019). Nous avons donc étudié l'impact de D7 sur les altérations métabolipidomiques induites par TDP-43, et avons détecté des changements dans le métabolisme des lipides, en particulier les glycérophospholipides et les carnitines. Trois métabolites altérés par la surexpression de TDP-43 sont revenus à des niveaux normaux lorsque D7 a été co-exprimé, suggérant un effet protecteur en aval de TDP-43.

Notre étude propose une nouvelle molécule scFv qui peut cibler divers aspects de la protéinopathie TDP-43, notamment les agrégats cytoplasmiques et les altérations métaboliques. Elle souligne également l'importance d'identifier de nouveaux paramètres, au-

delà de la simple agrégation de TDP-43 ou de la mort cellulaire, pour évaluer l'effet des médicaments ciblant TDP-43, notamment aux premiers stades de la maladie.

b. Context

The dysfunction and aggregation of TDP-43 is closely linked to the degeneration of motor neurons and is a key feature of ALS. Because TDP-43 proteinopathy is present in both sporadic and familial ALS, it serves as a common factor in the disease, making it a particularly promising target for therapeutic intervention. However, targeting TDP-43 presents several challenges. Some of these challenges are the intracellular localization of TDP-43 and the specificity required to target the pathological forms of the protein without affecting its normal functions. For this reason, we aimed to identify scFv clones and use them as intrabodies that can bind to wildtype TDP-43, which is the form most commonly found dysfunctional in ALS, and alter some of its pathological behaviors. Unlike previous studies that have used a targeted approach to develop intrabodies specifically against the RRM1 or RRM2 domains of TDP-43 (Pozzi et al., 2019; Tamaki et al., 2018), we used a non-targeted approach to screen for scFv clones that can potentially bind to new pathologically relevant domains on the full-length human wildtype TDP-43. The effect of the identified clones on TDP-43 proteinopathy was assessed in a HEK293T cellular model of ALS overexpressing TDP-43.

c. Summary of materials and methods

By means of a high throughput phage display screening, a library of 10^{12} scFv clones were screened for their binding to full length human wildtype TDP-43. Following the generation of a 3D model of full-length TDP-43, *in silico* binding site prediction allowed us to identify the potential binding sites of the scFv on TDP-43. ELISA was then used to confirm the binding of the purified selected scFvs to recombinant TDP-43. The scFv 13R4, which binds to β-galactosidase, was used as a control scFv. The identified scFvs were cloned into plasmid vectors to allow for their expression as intrabodies in human cells. HEK293T cells overexpressing wildtype human TDP-43 were used as a cellular model of ALS. Overexpression of plasmids were maintained for 48 hours. The effect of the intrabodies on total, soluble and insoluble TDP-43, as well as its C-terminal fragments was tested using western blot. The metabolipidomic profile of HEK293T cells overexpressing TDP-43 alone, the scFv alone, or co-

overexpressing TDP-43 with the scFv was examined in order to identify potential metabolipidomic markers that were modified when TDP-43 and/or the scFv were overexpressed.

d. Summary of results

The phage display screening identified four distinct scFv clones (called B1, A2, B6 and D7). Following their successful expression in HEK293T cells, two (B1 and D7) out of the four clones were retained. *In silico* binding site prediction revealed the potential binding sites of B1 and D7 to TDP-43 (Fig.1). By ELISA, we confirmed the physical interaction of the scFvs with TDP-43 (Fig.2). When expressed in cells, the scFvs were mainly localized in the cytoplasm and the MTT reduction assay revealed that they were not toxic to cells (Fig.3). Upon their co-expression in cells that also overexpressed TDP-43, the intrabodies colocalized particularly with mislocalized and aggregated cytoplasmic TDP-43 (Fig.4). When assessing the effect of the intrabodies on TDP-43, we first verified that the levels of total and soluble TDP-43 were not altered by any scFv (Fig.5). As for the insoluble protein fraction, the scFv D7 was found to cause a decrease in the insoluble 35-kDa C-terminal fragment of TDP-43 (TDP-35 CTF) that seemed to be mediated by the proteasome (Fig.6). The scFv B1 had no effect on the levels of TDP-43 and was therefore eliminated at this stage of the study and the metabolipidomic analysis was performed for D7 only. A total of 220 metabolites were detected in HEK293T cells. The 10% that were most upregulated and downregulated for each condition were identified. Of the metabolites that were altered by the overexpression of TDP-43 and the scFv, we identified three (L-palmitoylcarnitine, PC[36:4], 4-hydroxy-phenylglycine) that returned to basal levels when D7 but not the control was present (Fig. 7).

scFv intrabody targeting wildtype TDP-43 presents protective effects in a cellular model of TDP-43 proteinopathy

Yara Al Ojaimi[1,*], Rudolf Hergesheimer[1,*], Anna A. Chami[1], Hugo Alarcan[1], Johanna Augros[1], Audrey Dangoumau[1], Shanez Haouari[1], Jérôme Bourgeais[2], Antoine Lefevre[1], Samira Osman[1], Patrick Emond[1,3], Patrick Vourc'h[1,4], Christian R. Andres[1,4], Philippe Corcia[1,5], Olivier Herault[2], Pierre Martineau[6], Débora Lanznaster[1#], Hélène Blasco[1,3#]

*, # These authors contributed equally to this work.

[1] Université de Tours, INSERM, Imaging Brain & Neuropsychiatry iBraiN U1253, 37032, Tours, France.

[2] Université de Tours, NRS ERL7001, EA 7501 GICC, Tours, France.

[3] CHU de Tours, Service de Médecine Nucléaire In Vitro, Tours, France.

[4] CHU de Tours, Service de Biochimie et Biologie Moléculaire, Tours, France.

[5] CHU de Tours, Service de Neurologie, Tours, France.

[6] IRCM, Univ Montpellier, Inserm, ICM, Montpellier, France.

Corresponding author: Yara Al Ojaimi
INSERM iBrain UMR1253/University of Tours
10 Boulevard Tonnellé, 37000 - Tours, France
Tel: (33) 07 58 57 10 95
E-mail: yara.alojaimi@univ-tours.fr

Short title: Phage-display-derived intrabody targeting TDP-43 proteinopathy.

Conflict of interest statement: The authors declare no conflict of interest.

Abstract

TDP-43 proteinopathies are a set of neurological disorders characterized by the abnormal accumulation and mislocalization of TDP-43 in the cytoplasm, leading to the disruption of the normal function of the protein. In most of the cases, it is the wildtype (wt) form of the protein that is involved. An untargeted high-throughput screen of a single-chain variable fragment (scFv) library was performed using phage display against human full-length wt TDP-43. Two scFvs (B1 and D7) were retained following cellular expression (then termed intrabodies) and colocalization with cytoplasmic TDP-43 *in vitro.* We generated a 3D structure of full length wt TDP-43 *in silico*, and used it for epitope mapping. In a cellular model of TDP-43 proteinopathy, D7 enhanced the proteasomal degradation of the insoluble 35-kDa C-terminal fragment TDP-43 and reversed some TDP-43-induced metabolomic alterations, particularly relating to the lipid metabolism. Our findings offer a new scFv intrabody that bind to human wtTDP-43 and modify cellular pathways associated with TDP-43 proteinopathies.

1. Introduction

TDP-43 is a DNA/RNA-binding protein encoded by the TARDBP gene, and is essential for cell homeostasis (Hergesheimer et al., 2019; Polymenidou et al., 2011). Under physiological conditions, TDP-43 is mostly localized in the nucleus and shuttles between the nucleus and cytoplasm. TDP-43 was mainly linked to amyotrophic lateral sclerosis (ALS), where 97% of patients present with cytoplasmic aggregates of the protein, regardless of their mutational status (Hergesheimer et al., 2019). However, the protein was later found to be dysregulated in several other neurodegenerative diseases like frontotemporal dementia (FTD) (Neumann et al., 2006), Alzheimer's (Arai et al., 2009), Parkinson's (Chanson et al., 2010), and Huntington's disease (Schwab et al., 2008), and limbic-predominant age-related TDP-43 encephalopathy (LATE) (Besser et al., 2020). These diseases became therefore collectively known as TDP-43 proteinopathies. In these diseases, it is TDP-43 in its wild-type (wt) form that is found mislocalized and aggregated in the cytoplasm.

TDP-43 aggregates mainly include full-length and 35-kDa and 25-kDa C-terminal fragments (CTF) of TDP-43 (Arai et al., 2006; Neumann et al., 2006). The C-terminal fragments are a result of proteolytic cleavage or alternative splicing and have been widely implicated in toxic gain- or loss-of function mechanisms (Chhangani et al., 2021). Dysregulation of TDP-43 was found to induce metabolic alterations, particularly in pathways involving energy metabolism, lipids, and neurotransmission (Floare & Allen, 2020; Loganathan et al., 2022). Moreover, there seems to be a bidirectional interplay between the function of the degradation pathways of the cell, particularly the ubiquitin-proteasome system and TDP-43 proteinopathy, suggesting a key role of these pathways in TDP-43 dysfunction (Ormeño et al., 2020; Tashiro et al., 2012). However, targeting TDP-43 pathology is complicated by the plethora of cellular pathways affected by the protein and its role in maintaining cellular homeostasis (Ojaimi et al., 2022). For instance, knockdown of TDP-43 by siRNA was found to be associated with impaired axonal transcriptome (Briese et al., 2020), increased inflammation (Dunker et al., 2021; LaRocca et al., 2019) , and dysregulation of the expression of important proteins implicated in cell homeostasiss (Fiesel et al., 2010; Prpar Mihevc et al., 2016). Similarly, antisense oligonucleotides (ASO) that downregulate TDP-43 in mice resulted in synaptic dysfunction and increased neuronal vulnerability (Polymenidou et al., 2011).

Researchers are therefore trying to develop new strategies such as single-chain variable fragments (scFvs) to better regulate this protein is TDP-43 proteinopathies.

scFvs are generated by fusing the variable V_H and V_L regions of an IgG antibody with a linker peptide, resulting in an antibody fragment of 25-35 kDa that lacks the constant regions of the 150-kDa IgG yet still retains antigen-binding specificity. Due to their small size, scFvs haven been used as intracellular antibodies, called intrabodies. In recent years, important developments have been made in the use of scFvs for passive immunization targeting proteinopathies in many neurodegenerative diseases (Chen et al., 2021; Esquerda-Canals et al., 2019; Goodwin et al., 2021; Güell-Bosch et al., 2020; S. Li et al., 2021; Zha et al., 2016).

Our aim for this project was to apply an innovative, untargeted high-throughput strategy based on a scFv screening method to target full length wtTDP-43, and to evaluate diverse cellular variables to elucidate their effects. We used phage display to screen an scFv library against recombinant human full-length wt TDP-43. Since no 3D structure of full length TDP-43 was available, one was generated *in silico* externally, which we used to identify pathologically relevant epitopes. The retained scFv was investigated for its cellular localization, its impact on cell viability and the expression and solubility of TDP-43, as well as its effect on other subtle cellular alterations that might occur earlier in TDP-43 proteinopathies, such as metabolic alterations.

2. Materials and Methods

2.1 Plasmids and cloning

We had previously cloned a full-length human wtTDP-43 cDNA(Lanznaster et al., 2019) into the pcDNA3.3-TOPO TA vector (Invitrogen). Starting from this clone, we added a 6xHis tag to the 3' end by performing PCR on the plasmid using the following primers (Eurogentec): forward (5'-TCTGAATATATTCGGGTAACCGAAG-3') and reverse (5'-CTAGTGATGGTGATGGTGATGAGAACCCCCCATTCCCCAGCCAGAAGACTTAG–3'). The resulting amplicon was then integrated into the Vivid Colors pcDNA 6.2/C-EmGFP-GW/TOPO Mammalian Expression Vector (Invitrogen), which added GFP to the 5' end and yielded GFP-wtTDP-43-6xHis to permit mammalian cell expression and downstream purification for phage display. To clone the sequence for the control antigen for phage display, GFP-6xHis, a similar

approach was taken by first performing PCR on the plasmid containing GFP-wtTDP-43-6xHis using the following primers (Eurogentec): forward (5'–GCCACCATGGTGAGCAAGGGCGAGGA–3') and reverse (5'–CTAGTGGTGATGGTGATGATGAGAACCCCCCTTGTACAGCTCGTCCATGCC–3'). Then, the GFP-6xHis sequence was integrated into an empty pcDNA3.3-TOPO plasmid.

As for scFv cloning, using the NcoI and NotI restriction sites surrounding the 5' and 3' ends of the scFv cDNA sequence, respectively, the pHEN-HuscI plasmid was digested to completion. The liberated scFv sequence was then integrated into previously digested empty pET-23NN vector using T4 DNA Ligase (Thermo Fisher Scientific). This vector added a c-myc and 6xHis tag at the 3' end of the clone, which permitted expression and purification from BL21(DE3)pLysS bacteria (New England BioLabs). From the integrated pET-23NN vector, we cloned the scFv sequence with the 3' tags into pcDNA3.3-TOPO plasmid to permit mammalian cell expression according to the manufacturer's instructions (Thermo Fisher Scientific). For the PCR step, the following primers were used (Eurogentec): forward (5'–GCCACCATGGCCGAGGTGCAGCTG–3') and reverse (5'-CTAATGGTGATGATGGTGATGTGCGG–3').

2.2 Mammalian Cell Culture

HEK-293T human cells (ATCC) were the main cell line of choice due to their high transfection efficiency and common application in studies on TDP-43 proteinopathy. The cells were maintained in Dulbecco's Modified Eagle's Medium (DMEM) supplemented with 5% (*v/v*) fetal bovine serum (FBS) at 37 °C and 5% CO_2. Cells were split once they reached 90% confluency.

2.3 Purification of antigens from HEK-293T cells

The recombinant proteins GFP-6xHis and GFP-wtTDP-43-6xHis were overexpressed for 48h in HEK293T cells plated at a density of 0.44×10^6 cells/T-150 flask. At 70% confluency, the cells were transfected with 60 µg of expression plasmid mixed with Lipofectamine-2000 in a ratio of 1:2 (Invitrogen), following the manufacturer's protocol. The cells were harvested and centrifuged at 500 × g for 10 min at 4° C then resuspended in cold denaturing lysis buffer (500 mM NaCl, PBS pH 8.0, 10% glycerol, 0.1% Brij-35, 6 M urea, 1 mM DTT) supplemented with 1X Halt Protease Inhibitor Cocktail (Thermo Fisher Scientific). Four freeze-thaw cycles using liquid

nitrogen and a 37° C water bath were applied to the cells, then Pierce Universal Nuclease (250 U/µL, Invitrogen) and 10 mM $MgCl_2$ were added to the lysate. After 15 min of agitation at 4° C, the lysate was centrifuged at 15,000 × g for 20 min at 4° C. The supernatant was passed through an equilibrated Ni-NTA resin column (Thermo Fisher Scientific). The column was then washed with cold lysis buffer supplemented with 25 mM imidazole. Finally, the recombinant protein was eluted by the addition of cold lysis buffer supplemented with 250 mM imidazole. The fractions containing recombinant protein were identified by SDS-PAGE and pooled.

The pooled eluate was transferred to dialysis tubing (CelluSepH1, Membrane Filtration Products) with a molecular-weight cutoff (MWCO) of 15 kDa and incubated in 500 mL of dialysis buffer (50 mM Tris-HCl pH 7.4, 10% glycerol, 150 mM NaCl, 0.1 mM EDTA, 2 mM β-mercaptoethanol) at 4° C for 16 h to permit the refolding of the purified protein. The buffer was then replaced with 500 mL of fresh buffer for another incubation for 2 h at 4° C. The dialyzed solution containing refolded protein was concentrated using an Amicon Ultra tube (Merck Millipore) with a MWCO of 10 kDa at 4° C. The concentration of the purified refolded protein was determined by Bradford assay (Thermo Fisher Scientific) following the manufacturer's protocol.

To characterize the size of the purified recombinant proteins, a sample of 100 µL was injected into an FPLC AKTA Purifier10 (GE Healthcare) with a 25-mL Superdex 200 Increase 10/300 GL column (GE Healthcare) equilibrated in dialysis buffer at 4° C; 500-µL fractions were collected at a flow rate of 0.5 mL/min. The identity of the purified recombinant protein was confirmed by western blot using a 6xHis tag antibody (HRP-66005, Proteintech).

2.4 HuscI phage library and control scFv

The HuscI (Human scFv Intrabody Library) library provided by Dr. Pierre Martineau from the Montpellier Cancer Research Institute(Martineau et al., 1998; Robin et al., 2014; Robin & Martineau, 2012) is a human synthetic library with a diversity of 3×10^9 functional clones. The library is cloned in vector pHEN1 (pHEN-HuscI), resulting in M13 phage clones expressing single-chain variable fragments (scFvs) at the N-terminal extremity of pIII protein. Each scFv consists of a variable heavy (VH) and light (VL) chain connected by a linker sequence (GGGGSGGGGSGGGGS). The molecular weight of the scFvs ranges from 25 to 30 kDa. The scFv

employed as the control in this work is the anti-β-galactosidase scFv, termed 13R4, described by Martineau and his colleagues(Martineau et al., 1998).

2.5 Phage display and polyclonal selection

Before panning on GFP-wtTDP-43-6xHis (GTH), the HuscI scFv library was depleted on anti-GFP and GFP-His protein. Three wells of a Nunc Maxisorp 96-well plate (Thermo Fisher Scientific) were coated with 10 µg/mL of anti-GFP antibody (Roche, 11814460001) diluted in PBS, for 24 h at 4 °C. After 5 washes in PBS-Tween 0.1% (PBST) and one wash in PBS, the wells were saturated in 4% powdered milk in PBS (MPBS) for 2 h at RT. After washing, the first well was incubated with 50 µL of MPBS and 50 µL of the HuscI phage library. In parallel, the second well was incubated with 10 µg/mL of purified GFP-6xHis diluted in 100 µL of PBST. After 2 h, the supernatant from the first well was transferred to the second well for another 2-h incubation. During this time, the third well was incubated with 5 µg/mL of purified GFP-wtTDP-43-6xHis diluted in 100 µL of PBST. After 2 h, the supernatant from the second well was transferred to the third well to begin the first round of selection.

Following 2 h of incubation in the third well at RT, the supernatant was discarded and the well was washed 20 times with PBST and 3 times with PBS. Next, 100 µL of elution buffer (50 mM Tris pH = 8.0, 1 mM $CaCl_2$) containing 125 µg/mL of trypsin (TPCK-treated, Sigma-Aldrich) was added to the well for 15 min at RT. The supernatant was transferred to 200 µL of 2xYT medium (Sigma-Aldrich) containing TG1 *E. Coli* at an optical density (OD) of 0.5. After 1 h at 37 °C with shaking, the bacteria were centrifuged at 3000 × g for 10 min at RT and resuspended in 500 µL of 2xYT/2% glucose/100 µg mL^{-1} ampicillin. The bacteria were allowed to grow at 30 °C with shaking for 16 h, then 20 µL of the culture were added to 1 mL of fresh 2xYT/2% glucose/100 µg mL^{-1} ampicillin and shaken at 37 °C. After reaching an OD of 0.5, the culture was infected with 20 µL of KM13 helper phage(Kristensen & Winter, 1998) comprising approximately 10^{11} TU/mL. Following shaking at 37 °C for 1 h, the bacteria were centrifuged at 3000 × g for 10 min at RT and resuspended in 1 mL of 2xYT with 100 µg/mL ampicillin and 25 µg/mL kanamycin. The culture was shaken at 30 °C for 16 h, then 500 µL of this culture was centrifuged at 10,000 × g for 10 min at 4 °C. Next, 400 µL of the supernatant containing new phage was added to 100 µL of 20% polyethylene glycol-8000 (PEG) and sterile 2.5 M NaCl at 4°C to precipitate the phage. After 15 min on ice, the solution was centrifuged at 13,000 rpm

for 20 min at 4 °C. The pellet was resuspended in 200 µL of 15% sterile glycerol diluted in PBS. The phage titer was calculated using the following formula:

number of virions/mL = $(A_{269} – A_{320}) \times 10^{13}$

Next, 50 µL of the new phage stock containing approximately 10^{11} to 10^{12} phage was added to 50 µL of MPBS in a new well coated with 5 µg/mL of GFP-wtTDP-43-6xHis to undergo the second round of selection. In total, 4 rounds of selection were performed.

2.6 Phage display: monoclonal selection

A flowchart of the phage display strategy for identifying the hits against wtTDP-43 is represented in **Fig.S1**. HB2151 cells (a strain allowing the expression of soluble unfused scFv, provided by Dr. Pierre Martineau's group) at an optical density of 0.5 were infected with 10^6 phage from polyclonal selection round 4. After 30 min at 37 °C without shaking, infected bacteria were plated on LB/agar with 1% glucose and 100 µg/mL ampicillin and incubated at 37 °C for 16 h. Ninety-six isolated HB2151 colonies were transferred to wells of a 96-well deep-well plate (Thermo Fisher Scientific) containing 300 µL of 2xYT, 100 µg/mL ampicillin, and 1% glucose. The plate was incubated at 37 °C with agitation for 16 h, then 2–5 µL of culture from each well was transferred to a new flat-bottom plate (Thermo Fisher Scientific) containing 200 µL of 2xYT, 100 µg/mL ampicillin, and 0.1% glucose in each well. At an optical density of 0.6, 25 µL of fresh medium supplemented with 9 mM IPTG (Sigma-Aldrich) was added to each well for induction. Induction lasted 24 h at 30 °C with shaking.

The plate was centrifuged at 1800 × g for 10 min. The supernatant contained soluble scFv with a C-terminal myc tag; 50 µL of each supernatant were added to 50 µL of 4% MPBS in each well of a 96-well plate pre-coated with 1.0 µg/mL of GTH and GH antigen (2 plates total). After a 1-h incubation at RT, the wells were washed 3 times in PBS, and 100 µL of anti-c-Myc antibody (9E10, Thermo Fisher Scientific) diluted 2000-fold in saturation solution was added to each well and incubated for 1 h at RT. The wells were washed 3 times with PBST and 1 time with PBS, and 100 µL of TMB-ELISA Substrate Solution (Thermo Fisher Scientific) was then added for an incubation of 5–15 min at RT in the dark. The reaction was halted with 50 µL of 1 M H_2SO_4. Absorbance was measured at 450 nm using an iMark Microplate Absorbance Reader (Bio-Rad).

For the alternative monoclonal selection, the glycerol stock of TG1 infected with phage from round 4 of selection was incubated in 2xYT/2% glucose/100 µg/mL ampicillin for overnight shaking at 37 °C. A small volume of the culture was then plated on LB agar with 100 µg/mL ampicillin. After 16 h at 37 °C, 95 colonies were transferred to each well of a deep-well 96-well plate containing 300 µL of 2xYT/1% glucose/100 µg mL^{-1} ampicillin. Following 16 h of shaking at 37 °C, 5 µL of culture from each well was transferred to another flat-bottom 96-well plate with 200 µL of 2xYT/2% glucose/100 µg mL^{-1} ampicillin. At an OD of 0.5, the cultures were infected with KM13 helper phage, as described previously.

The cultures were then centrifuged at 3000 × g for 10 min and resuspended in fresh medium supplemented with 25 µg/mL kanamycin. After 16 h at 30 °C with shaking, the cultures were centrifuged again, and 50 µL of supernatant was added to 50 µL of MPBS and incubated in a 96-well plate pre-coated with 1.0 µg/mL GFP-6xHis and another plate pre-coated with 1.0 µg/mL GFP-wtTDP-43-6xHis. Following 1 h at RT, the wells were washed 3 times with PBST and 1 time with PBS, and 100 µL of 4% MPBS containing HRP-conjugated anti-M13 bacteriophage antibody (Sino Biological) at 1/2000 dilution was added to each well for an incubation at RT for 1 h. The same washing procedure was applied before adding 100 µL of TMB-ELISA Substrate Solution (Thermo Fisher Scientific) for an incubation of 5–15 min at RT in the dark. The reaction was halted with 50 µL of 1 M H_2SO_4. Absorbance was measured at 450 nm.

2.7 In silico epitope mapping

The potential binding sites of the scFv of interest were predicted *in silico* for wtTDP-43 by MAbSilico (Nouzilly, France). Given that no 3D structure of full-length TDP-43 was found, it was generated by combining the resolved structures of the separate domains of TDP-43 and homologous proteins available on the RCSB PDB Protein Data Bank. Residues 1–88 were modeled by region 1–102 of TDP-43 (PDB file 5MRG)(Mompeán et al., 2017). Residues 89–102 were modeled by the structure of nuclear ribonucleoprotein L (PDB file 2MQN)(Blatter et al., 2015). Residues 103–177 and 191–258 were modeled by both RRM domains of TDP-43 (PDB file 4BS2)(Lukavsky et al., 2013). Residues 259–306 were modeled by U1 small nuclear ribonucleoprotein 70 (PDB file 5UZ5)(X. Li et al., 2017). Residues 307–346 were modeled by the hydrophobic helix, prion-like domain of TDP-43 (PDB file 2N2C). Finally, residues 347–413 were modeled by human splicing factor (PDB file 4WIJ)(Lee et al., 2015).

Briefly, epitope mapping was based on a docking method(Bourquard et al., 2018). The probability of an interaction for each residue involved in the top 30 conformations of the scFv-TDP-43 complex was also evaluated.

2.8 Overexpression of recombinant proteins in mammalian cells

Six-well plates (CytoOne) were each seeded with 0.3 × 10^6 cells in DMEM/5% FBS/pyruvate/1% non-essential amino acids. When the cells reached 60% confluency, they were transfected for 48h (Polyplus transfection) using jetPEI transfection reagent (Polyplus transfection) following the manufacturer's protocol. Regarding transfections, a total of 4.5 µg of plasmids were always used. For the TDP-43 condition, 3.0 µg of wt-TDP-43-expressing plasmid with 1.5 µg of empty plasmid was used. For the intrabodies alone condition, 1.5 µg of scFv-expressing plasmids and 3 µg of empty plasmid were used. With respect to TDP-43/scFv co-transfections, 3.0 µg of wtTDP-43 was mixed with 1.5 µg of scFv-expressing plasmid. Unless noted otherwise, all TDP-43 transfections included the untagged, full-length, wild-type form.

2.9 Immunofluorescence

For immunofluorescence experiments, an 8-well Nunc Lab-Tek II plate (No. 1.5 borosilicate glass, Thermo Fisher Scientific) that was pre-coated with 50 µg/mL of poly-D-lysine (Sigma-Aldrich) was seeded with 0.02 × 10^6 HEK293T cells. After 24 h, transfection was performed as described previously with 0.2 µg of TDP-43 plasmid or empty plasmid and 0.1 µg of scFv plasmid. Following 48 h of overexpression, the cells were fixed in 4% paraformaldehyde and 2% sucrose for 20 min at RT. The cells were washed 3 times in PBS. The fixed cells were permeabilized using 0.2% Triton-X 100 diluted in PBS for 15 min at RT. Then they were saturated in permeabilization buffer supplemented with 10% donkey serum (ab7475, Abcam) for 1 h at RT. Next, 1000-fold diluted rabbit anti-TDP-43 primary antibody (12892-1-AP, Proteintech), and 1000-fold diluted mouse anti-6xHis primary antibody (66005-1-Ig, Proteintech) were added to the cells for an incubation of 2 h at RT. Cells were washed 5 times the incubated wtih 500-fold diluted goat anti-rabbit Alexa Fluor 488 (A-11034, Thermo Fisher Scientific) and 500-fold diluted donkey anti-mouse Alexa Fluor 594 (A-11005, Thermo Fisher Scientific) for 1 h at RT away from light. Following 4 washes, the slides were mounted using Vectashield Antifade Mounting Medium with DAPI (H-1200-10, Vector Laboratories).

then visualized with a SP8 confocal microscope (Leica Microsystems) using a magnification of 60X. A table of all the antibodies used in this study is presented in **Table S1**.

2.10 Cell viability

Following 48 h of overexpression, the culture medium was withdrawn and replaced with 0.5 mg/mL MTT (3-(4,5-dimethylthiazol-2-yl)-2,5-diphenyltetrazolium bromide, Sigma-Aldrich) diluted in HBSS (Gibco). After 30 min of incubation at 37 °C with 5% CO_2, the medium was discarded and replaced with 500 µL of DMSO (Sigma-Aldrich), in which the formazan crystals were dissolved. The absorbance was recorded at 570 nm.

2.11 Purification of scFv from BL21(DE3)pLysS

A culture for a given clone was started in LB containing 1% glucose and 100 µg/mL ampicillin and incubated for 16 h at 37 °C with shaking. At an OD of 0.6, 12 mL of culture was added to an auto-inducible medium consisting of fresh LB containing 100 µg/mL ampicillin, 2 mM $MgSO_4$, 20mM 50x5052 (2.7 M glycerol, 0.14 M glucose, 0.28 M α-lactose monohydrate), and 20mM of solution 50xM (1.3 M Na_2HPO_4, 1.3 M KH_2PO_4, 2.5 M NH_4Cl, 0.25 M Na_2SO_4). The culture was incubated at 37 °C with shaking for 3 h, then moved to 22 °C for 16 h. The bacteria were pelleted by centrifugation at 5000 × g for 10 min at 4 °C and resuspended in lysis buffer (PBS pH 8.0, 1% Brij-35, 1.0 mM EDTA, 10 mM $MgCl_2$, 1.0 mM DTT). To this solution were added 1% Halt Protease Inhibitor Cocktail (Thermo Fisher Scientific), Pierce Universal Nuclease (Thermo Fisher Scientific), and 0.1 M of lysozyme. After 15 min of agitation at 4 °C, the bacteria were lysed by sonication. The lysate was centrifuged at 15,000 × g for 20 min at 4 °C. The supernatant was passed through a of Ni-NTA resin column (Thermo Fisher Scientific) equilibrated in lysis buffer with 10 mM imidazole. The column was then washed with cold lysis buffer supplemented with 25 mM imidazole. The scFv was eluted using cold lysis buffer supplemented with 250 mM imidazole. Fractions containing the scFv were identified by SDS-PAGE and pooled, then dialyzed in MilliQ water. The dialyzed product was quantified by Bradford assay and concentrated to 0.5–1.0 mg/mL if necessary. The final product was stored at 4 °C. The identity of the scFv was confirmed by western blot.

2.12 Enzyme-linked immunosorbent assay (ELISA) on purified scFv

Wells of a Nunc MaxiSorp 96-well plate (Thermo Fisher Scientific) were coated overnight at 4 °C with commercial human wtTDP-43 (Abcam, ab224788) diluted to 1 µg/mL in

PBS. Wells were washed 3 times in 0.2% PBST, and blocked using PBS Tween-20(0.02%) and 5% fat-free milk for 2 h at RT. The wells were washed 3 times then incubated with purified scFv diluted to 1, 5, or 10 µg/mL for 1 h at RT. Following 3 washes, HRP-conjugated mouse anti-6xHis antibody (66005, Proteintech) diluted 10,000-fold in PBS-T(0.02%) was then added to the wells and incubated for 1 h at RT, after which the wells were washed 5 times. Next, TMB-ELISA Substrate Solution (Thermo Fisher Scientific) was added for an incubation of 10–15 min at RT in the dark. The reaction was halted with 2 M H_2SO_4. Absorbance was measured at 450 nm using an iMark Microplate Absorbance Reader (Bio-Rad).

2.13 TDP-43 solubility

Following 48 h of overexpression in HEK293T, the cells were lysed using ice cold lysis buffer (PBS pH 8.0, 1% Triton-X 100, 10 mM $MgCl_2$, 1 mM DTT) supplemented with 1X Halt Protease Inhibitor Cocktail (Thermo Fisher Scientific) and Pierce Universal Nuclease (Thermo Fisher Scientific). After a 30 min incubation at 4 °C, the lysates were centrifuged at 13,000 × g for 20 min at 4 °C. The supernatant (soluble fraction) was transferred to a new tube, while the pellet (insoluble fraction) was resuspended in the same volume as the supernatant of ice cold lysis buffer supplemented with 6 M urea. The protein concentrations of the crude extracts of the lysates were measured by the detergent-compatible Pierce 660nm Protein Assay reagent (Thermo Fisher Scientific). For western blot analysis, 10 µg of crude extract along with equivalent volumes of the insoluble fractions, were run on an SDS-PAGE gel, transferred to a PVDF membrane, and blocked in TBS-Tween20 (0.1%). TDP-43 was stained overnight at 4 °C by a rabbit primary antibody targeted against the C-terminus (12892-1-AP, Proteintech) diluted 5000-fold. Then, a 1-h incubation at RT was performed with HRP-conjugated goat anti-rabbit secondary antibody (W401B, Promega) diluted 10,000-fold. The 6xHis tag of the scFv was stained for 1 h at RT with the HRP-conjugated mouse anti-6xHis antibody (66005-1-Ig, Proteintech) diluted 100,000-fold.

2.14 TDP-43 degradation

Following wtTDP-43 and/or scFv overexpression in HEK293T cells, the medium was replaced with OptiMEM (Gibco, Thermo Fisher Scientific) and the cells were treated for 6 hours with 10 µg/mL cycloheximide (Sigma-Aldrich) with either 300 nM bafilomycin A1

(Merck, Sigma-Aldrich) or 0.5 µM MG-132 (Sigma-Aldrich). Protein extraction and western blots were performed as described previously.

2.15 Metabolomics analysis

After 48 h of overexpression in HEK293T, the cells were harvested and washed twice in ice-cold PBS. The dry cell pellet was frozen at −80 °C until the day of analysis. Cells were thawn on ice and resuspended in 150 µL of MeOH:H_2O (1:1) followed by centrifugation for 5 min at 4 °C. Liquid chromatography in tandem with high-performance mass spectrometry (LC-HPMS) was performed as previously described by our group (Diémé et al., 2017; Lanznaster et al., 2019).

2.16 Data analyses

Unless otherwise stated, results are shown as mean ± standard deviation (SD). When relevant, a Mann–Whitney non-parametric t-test or an ANOVA test was applied using Prism v.7.0 (GraphPad Software, San Diego, CA, USA). The results were considered significant when $p < 0.05$.

For metabolomics analysis, each overexpression condition was normalized to the empty vector condition and the mean of the normalization ratios was calculated. We selected the 10% of the metabolites that increased the most and the 10% of the metabolites that decreased the most. A Venn diagram allowed us to identify the common and specific metabolites impacted by the scFv in comparison with those in naïve cells. We also normalized within each series to the “TDP-43 condition” and conducted the same process to observe the metabolites impacted by the scFv on TDP-43 overexpression. Moreover, we built the Venn diagrams between the increased and the decreased metabolites on scFv-TDP-43 versus scFv-empty vector. Finally, among the metabolites impacted by TDP-43 overexpression alone, we selected the ones also impacted by the scFv.

3. Results.

3.1 Identification of four anti–TDP-43 clones

The purification of recombinant GFP-TDP43-6xHis antigen for phage display yielded highly pure monomer **(Fig.S2)**. Following four rounds of bio-panning, we observed the highest enrichment of bound phage at round 4 (**Fig.S3.A**). Therefore, round 4 phage were selected for the monoclonal screen phase. ELISA of 96 retained phage from round 4 revealed 9 clones showing strong positive signals for TDP-43 and not for the control GFP-6xHis antigen, suggesting specific binding to TDP-43. Fifty four clones displayed positive signals for GFP, and 33 clones showing no signal (**Fig.S3.B,C**). Sanger sequencing of the V_H and V_L domains from the 9 phages revealed 4 distinct scFv clones, which we named B1, A2, B6, and D7.

3.2 Generation of a 3D model of TDP-43 and prediction of scFv binding sites

Given that no 3D structure of the full-length TDP-43 protein was found, a homology model was built using 6 different structures **(Fig. 1A)**. Difficulties were encountered with the relative orientations of the different domains **(Fig. 1B)**. The relative orientation of the N-terminal and RRM1 domains and structure of the hinge 1 region were taken from the resolved structure of hnRNP L (PDB ID: 2MQN), which consists of two RRM domains, the first having homologies with the N-terminal domain of TDP-43. The relative orientation of the RRM2 and prion-like domains and the structure of the hinge 2 region were taken from *S. cerevisiae* U1 snRNP (PDB ID: 5UZ5), which consists of one RRM domain, a hinge, a prion-like domain, and a C-terminal helix. The C-terminal helix was modeled from human splicing factor (PDB ID: 4WIJ), which consists of one RRM domain, a hinge, a prion-like domain, and a C-terminal helix. Since the homologies in these regions were stronger with 5UZ5, it was used to model their orientations. However, the C-terminal helix of 4WIJ is much longer and was therefore used to model the part of this helix that is absent from 5UZ5.

The *in silico* binding site prediction required the 3D modeling of the scFv using templates for the V_H and V_L domains, with the orientation between the V_H and V_L domains being based on the V_H template orientation (data not shown). We then generated 30 ranked predicted conformations for the complex formed by the scFv with TDP-43 **(Fig.1C)**. From the top 30 ranked docking models, the residues of TDP-43 were scored for their probability of belonging to the epitope, and the residues of the scFv were scored for their probability of belonging to the paratope (data not shown). The scFv B1 could target a site containing the RRM1 domain and the prion-like domain **(Fig. 1D, blue line)**. As for the scFv D7, it was found

to potentially bind a site consisting of the N-terminal domain, as well as the RRM1 and the RRM2 domains **(Fig. 1D, violet line)**.

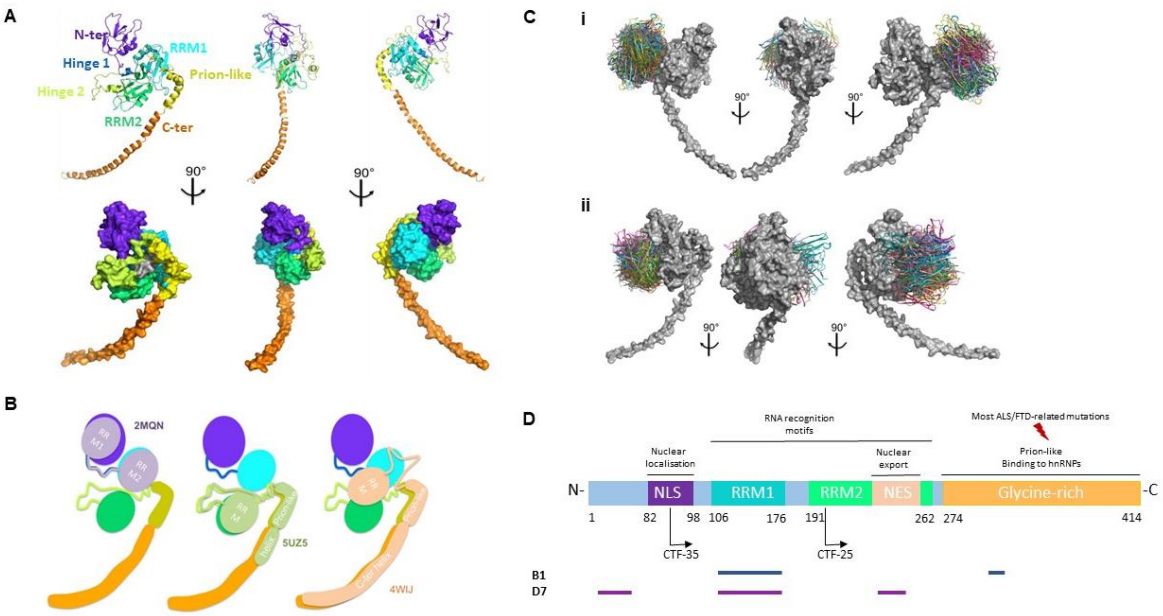

Figure 1: TDP-43 modeling and *in silico* epitope mapping. A) 3D model of full-length TDP-43. B) Templates used for modeling the relative orientations of the different domains of TDP-43. C) . View of the top 30 ranked predicted conformations for the complex between B1 and TDP-43 (i), and D7 and TDP-43 (ii). TDP-43 is shown in grey and the scFv in colors. D) *In silico* prediction of the interacting regions of TDP-43 with the scFvs B1 and D7.

3.3 scFvs B1 and D7 bound wtTDP-43.

To verify whether the scFvs B1 and D7 interact with human wtTDP-43, we conducted an indirect ELISA on recombinant human full-length wtTDP-43 using purified B1, D7, and the control scFv, 13R4. The control wells containing increasing amounts of 13R4 showed no significant binding to TDP-43. However relative to the equivalent quantity of the control scFv, the wells incubated with increasing amounts of B1 and D7 exhibited a significant dose-dependent increase in absorbance **(Fig.2)**. Upon incubation with 5 µg/mL of B1 and D7, the signals increased 5-fold and 2-fold, respectively (B1, $p = 0.004$; D7, $p = 0.03$). Upon incubation with 10 µg/mL of B1 and D7, the signals increased 3-fold and 2-fold, respectively (B1, $p = 0.004$; D7, $p = 0.005$). In addition, surface plasmon resonance confirmed the binding of B1 and D7 to

TDP-43, with a KD value in the 10^{-8} M range (data not shown). These results confirm that B1 and D7 physically interact with human wtTDP-43.

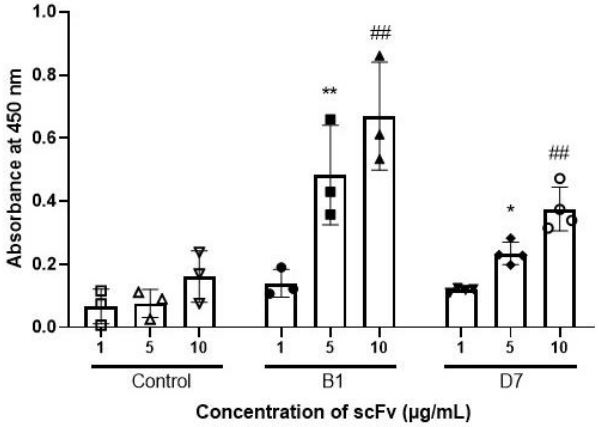

Figure 2: ELISA of purified scFv reveal the binding of B1 and D7 to recombinant wtTDP-43. Wells of 96-well plate coated with wtTDP-43 diluted to 1 µg/mL were incubated with the control scFv, B1, or D7 at increasing concentrations of 1 µg/mL, 5 µg/mL, and 10 µg/mL (x-axis). The control scFv did not show signs of binding to TDP-43 at any concentration, while B1 and D7 showed binding via increasing absorbances. Mann Whitney test: ** p=0.004 or * p=0.03 versus 5 µg of control scFv; ## p<0.005 versus 10 µg of control scFv. N=6-7.

In cells not overexpressing TDP-43 and in which TDP-43 was mainly nuclear, the intrabodies seemed to be localized in the nucleus and the cytoplasm (**Fig.3A**). However, when TDP-43 was overexpressed and subsequently mislocalized to the cytoplasm (**Fig.4 A,B**), the localization of the intrabodies became mainly cytoplasmic, and colocalized with aggregated TDP-43 (**Fig3A**) MTT reduction assays revealed that the intrabodies had no significant toxicity on HEK293T cells **(Fig.3B)**. Similarly, the overexpression of TDP-43 with or without the selected intrabodies did not have an effect on cellular viability (**Fig.4C**). Interestingly, it was also noted that the turnover of the intrabodies of interest, but not the control, was much higher in the presence of pathological, overexpressed TDP-43 compared to control conditions **(Fig.S4)**.

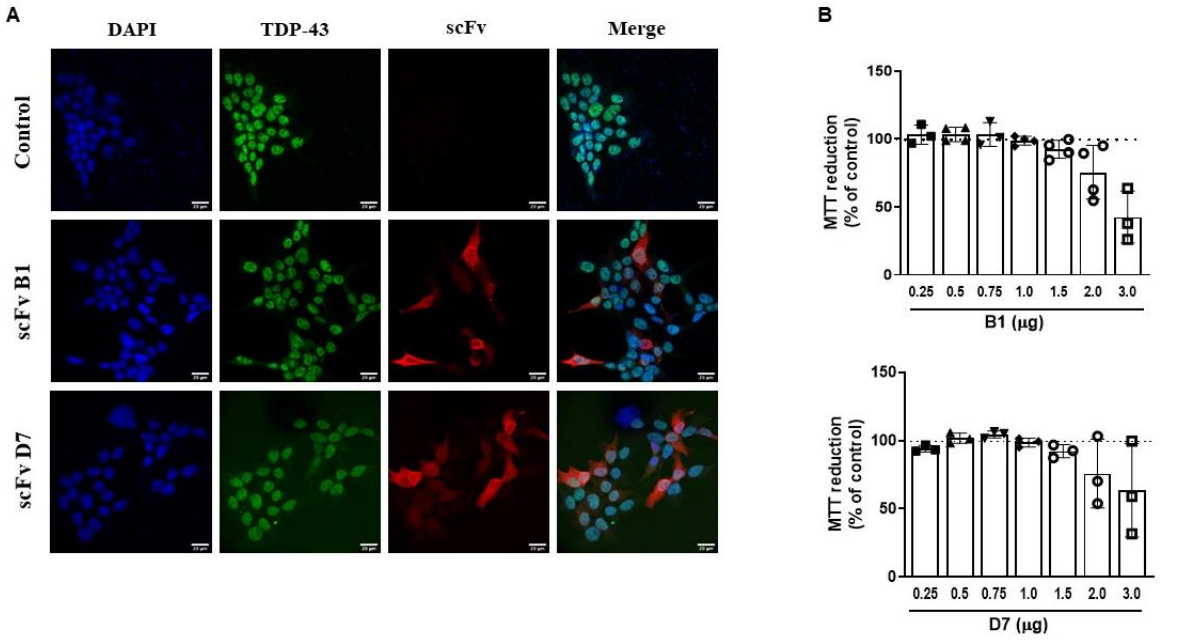

Figure 3: Expression and lack of cellular toxicity of the intrabodies. A) Immunofluorescence of HEK293T cells expressing the intrabodies. Scale bar = 20 µm (N=3). B) MTT reduction assay reveals the absence of toxicity of the intrabodies in HEK293T cells. Control: non-transfected cells. Quantity of scFv reflects the amount of plasmid transfected. One-way ANOVA, $p<0.05$, (N=3).

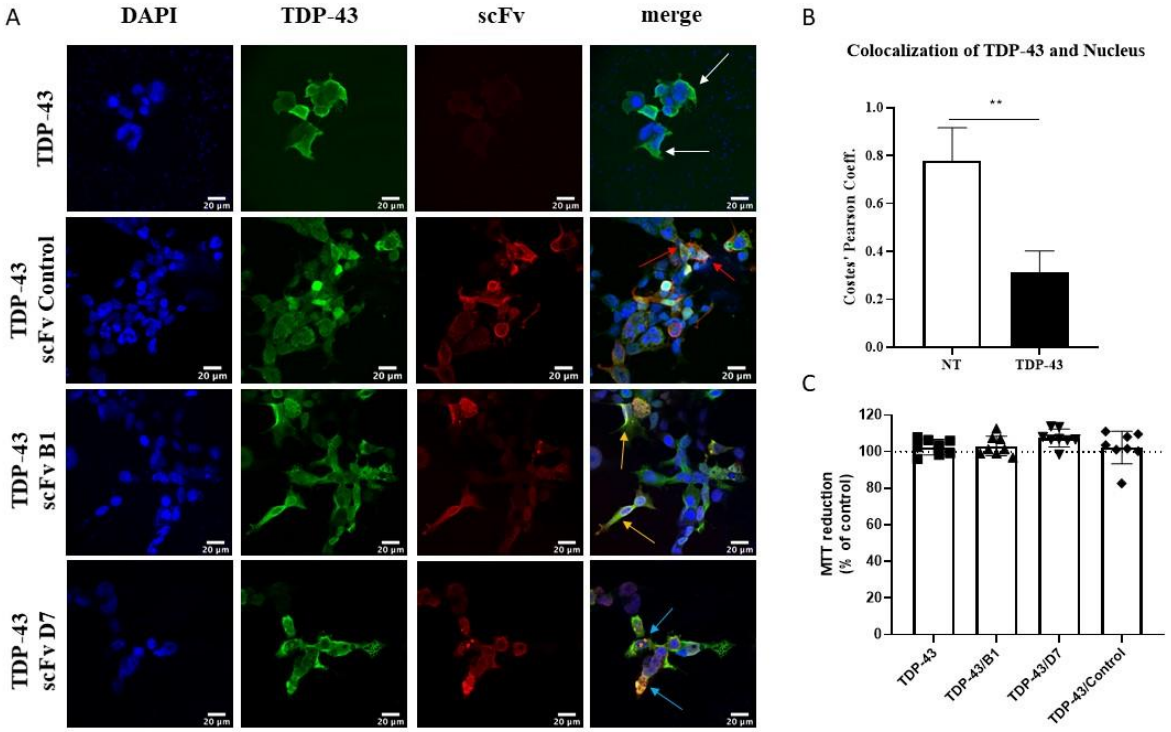

Figure 4: Intrabodies colocalize with mislocalized TDP-43 in the cytoplasm. A) Immunofluorescence of HEK293T cells co-transfected with TDP-43 (3 µg) and scFv (1.5 µg). White arrows: accumulation of TDP-43 in the cytoplasm. Red arrows: colocalization of control scFv with TDP-43. Orange arrows:

colocalization of scFv B1 with TDP-43. Blue arrows: colocalization of scFv D7 with TDP-43. Scale bar = 20 µm (N=3). B) Colocalization of TDP-43 with the nucleus. Mann-Whitney test, **p=0.0016 (N=6). C) MTT reduction assay on HEK293T cells co-transfected with TDP-43 and scFv. Control = cells transfected with empty vector. Quantity of scFv reflects the amount of plasmid transfected. One-way ANOVA, p>0.5 (N=8).

3.4 D7 decreased the amount of the insoluble 35-kDa fragment.

We quantified by Western blot the amount of full-length TDP-43 (TDP-43), the 35-kDa C-terminal fragment (TDP-35 CTF), and the 25-kDa C-terminal fragment (TDP-25 CTF) in the total lysate, soluble and insoluble fractions of HEK293T lysates. Upon transfection of cells with the plasmid overexpressing TDP-43, we observed a clear increase in the amounts of TDP-43 and TDP-35 CTF, as well as the appearance of TDP-25 CTF compared to the control (empty vector). The co-overexpression of the scFv D7 had no effect on the amount of either full-length TDP-43 nor its C-terminal fragments in the total or soluble protein fractions compared **(Fig.5)**. The intrabody B1 had no significant effect on the amount or solubility of TDP-43.

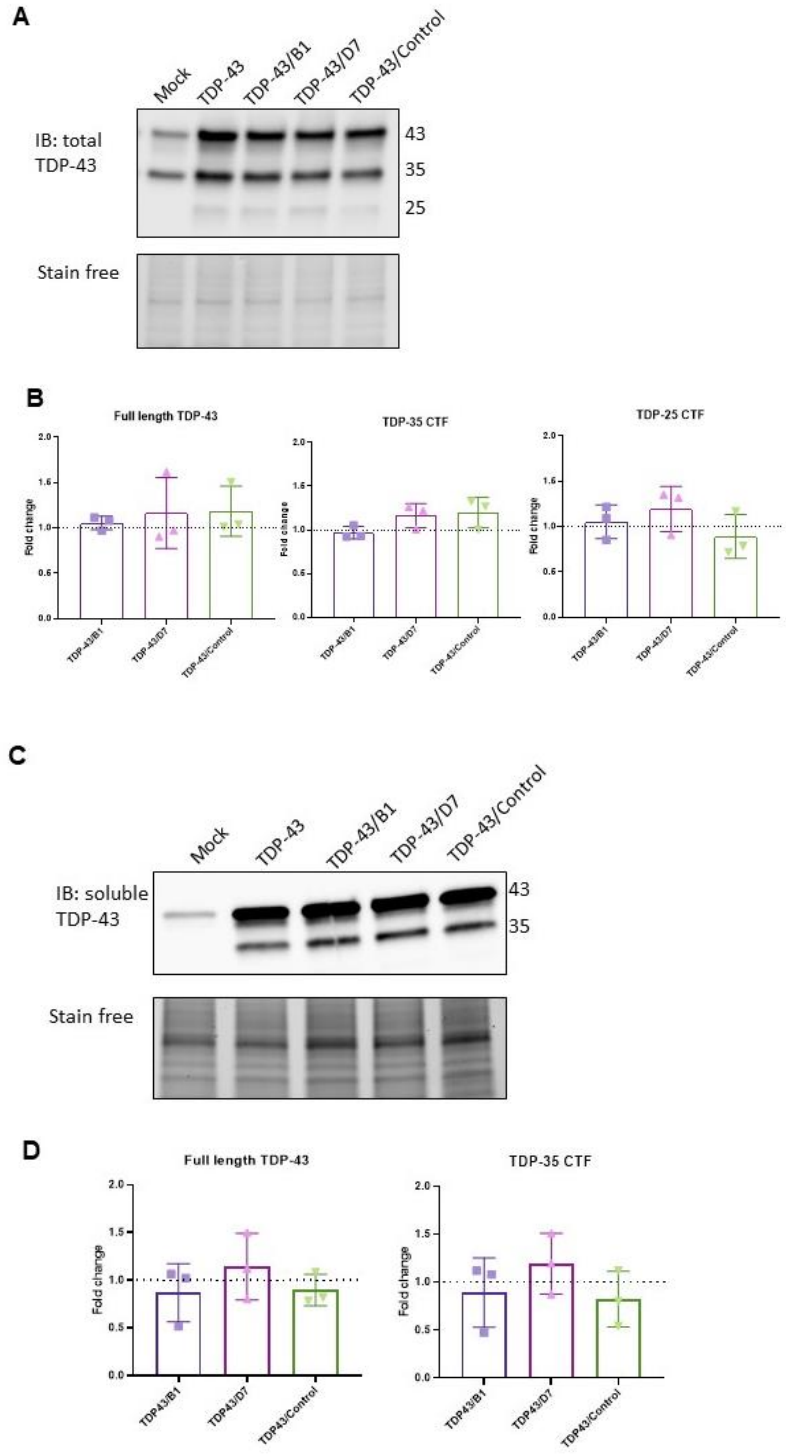

Figure 5: B1 and D7 have no significant effect on total and soluble TDP-43 or its CTFs. Immunoblots of TDP-43 in the total (A) and soluble (C) protein lysates of HEK293T cells. Quantification of TDP-43 forms in the total (B) and soluble (D) lysates normalized to the TDP-43 condition (dotted line). Mock: empty vector. TDP-43 condition: cells transfected with TDP-43-expressing plasmid and empty vector. TDP-43/B1, TDP-43/D7 and TDP-43/control: TDP-43-expressing plasmid and intrabody-expressing plasmid. Mann-Whitney test, p>0.5, (N=3).

In the insoluble protein fraction of HEK293T cells overexpressing TDP-43, we observed TDP-43 and TDP-35 CTF but not TDP-25 CTF **(Fig.6)**. The quantity of insoluble TDP-43 did not change upon overexpression of D7 (not shown), but the amount of insoluble TDP-35 CTF was significantly decreased (**Fig.6A,B**, $p = 0.02$). Interestingly, this effect of D7 was abolished when the cells were also treated with the proteasome inhibitor MG-132 (**Fig.6C,D**; $p = 0.02$). This effect was not observed with the autophagy inhibitor Bafilomycin A1 ($p = 0.1$). Concomitantly, when TDP-43 was overexpressed, the insoluble fraction of full-length TDP-43 and of TDP-35 CTF seemed to be mainly degraded by the proteasome, as evident by their significant increase when proteasomal degradation but not autophagy was inhibited (**Fig.6E,F**; $p = 0.0286$).

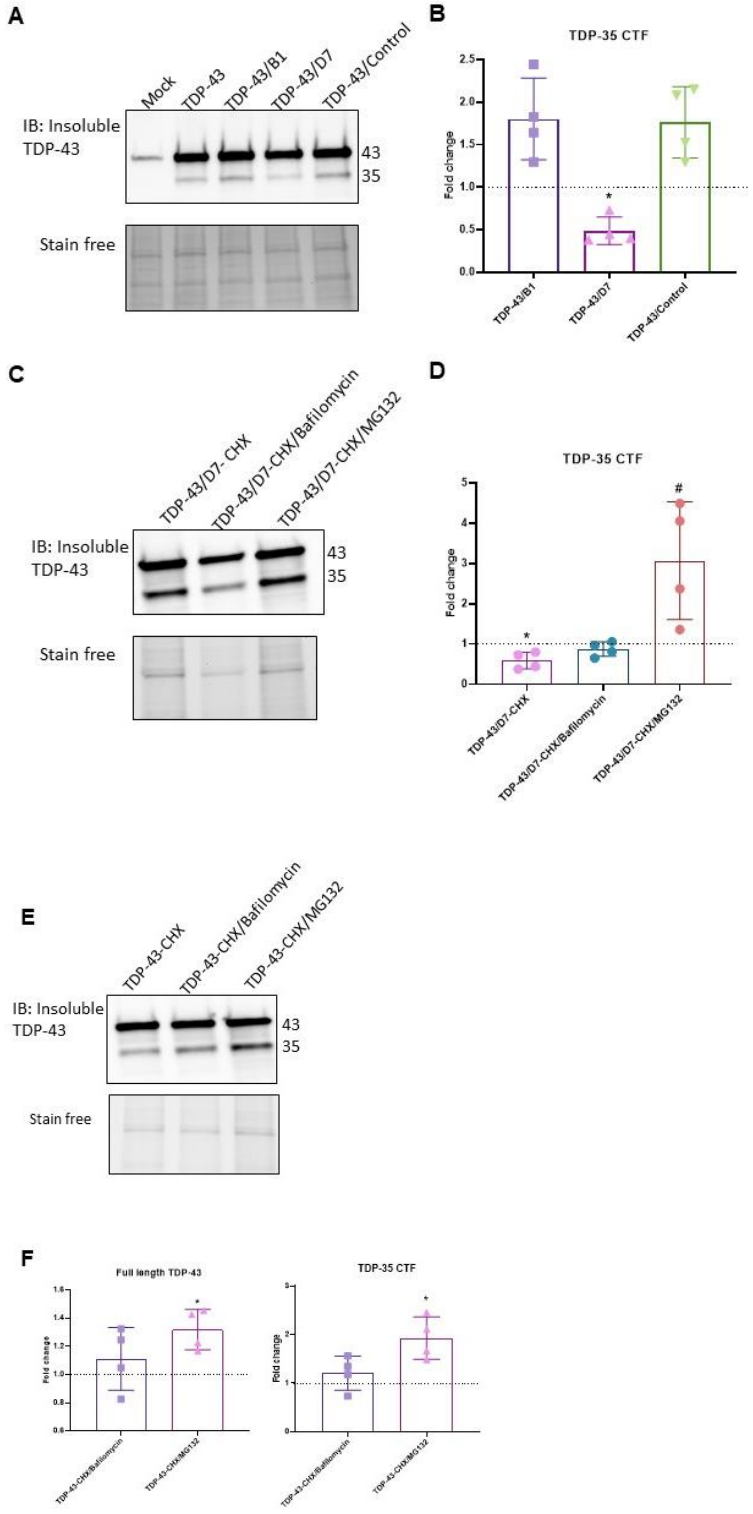

Figure 6: scFv D7 mediates the proteasomal degradation of the insoluble TDP-35 CTF. Immunoblots of TDP-43 in the insoluble protein fraction of HEK293T cells overexpressing TDP-43 and the intrabody in the absence (A) and presence (C) of autophagy and proteasome inhibitors. Quantification of the insoluble TDP-35 CTF normalized to the TDP43 condition (dotted line) in the absence (B) and presence (D) of autophagy and proteasome inhibitors. CHX: cycloheximide (10 µg/mL), Bafilomycin A1 (300 nM), MG-132 (0.5 µM). *p=0.0286 vs TDP43; #p=0.0286 vs TDP43/D7; Mann-Whitney test (N=4). E)

Immunoblot of TDP-43 in the insoluble protein fraction of HEK293T cells overexpressing TDP-43 and treated with autophagy or proteasome inhibitors. F) Quantification of insoluble TDP-43 forms normalized to the vehicle condition (dotted line). *p=0.0286, Mann-Whitney test (N=4).

3.5 The metabolomic profile of cells was affected by TDP-43 and scFv expression.

We analyzed the metabolomic profiles of HEK293T transfected either with TDP-43 plasmid alone or co-transfected with TDP-43 plasmid and each intrabody plasmid (D7, control 13R4) to evaluate (1) the metabolic effect of scFv administration, (2) metabolic modification associated with TDP-43 overexpression, and (3) correction of TDP-43–linked metabolic changes by D7. We identified a total of 220 metabolites in HEK293T cells. Lists of the 10% of metabolites that were the most upregulated and downregulated are presented in **Tables S2 and S3**, respectively. Compared with cells transfected with the empty vector, the majority of the metabolites impacted seem to be common to the two intrabodies **(Fig. 7A)**. They represent the global effect of the overexpression of an scFv on naïve cells, with only a few metabolites specific to D7. The same was observed when comparing the conditions of TDP-43 overexpression and TDP-43/scFv co-transfection, with a majority of metabolites being common to the two intrabodies **(Fig.7B)**. The metabolic effects of D7 also seemed to vary depending on whether TDP-43 was overexpressed or not **(Fig.7C)**, suggesting different effects when TDP-43 is pathological. We were able to identify three metabolites (L-palmitoylcarnitine, PC[36:4], 4-hydroxy-phenylglycine) that were altered when TDP-43 was overexpressed and that returned to baseline levels (empty vector condition) when the scFv D7 was co-expressed **(Fig.7D)**.

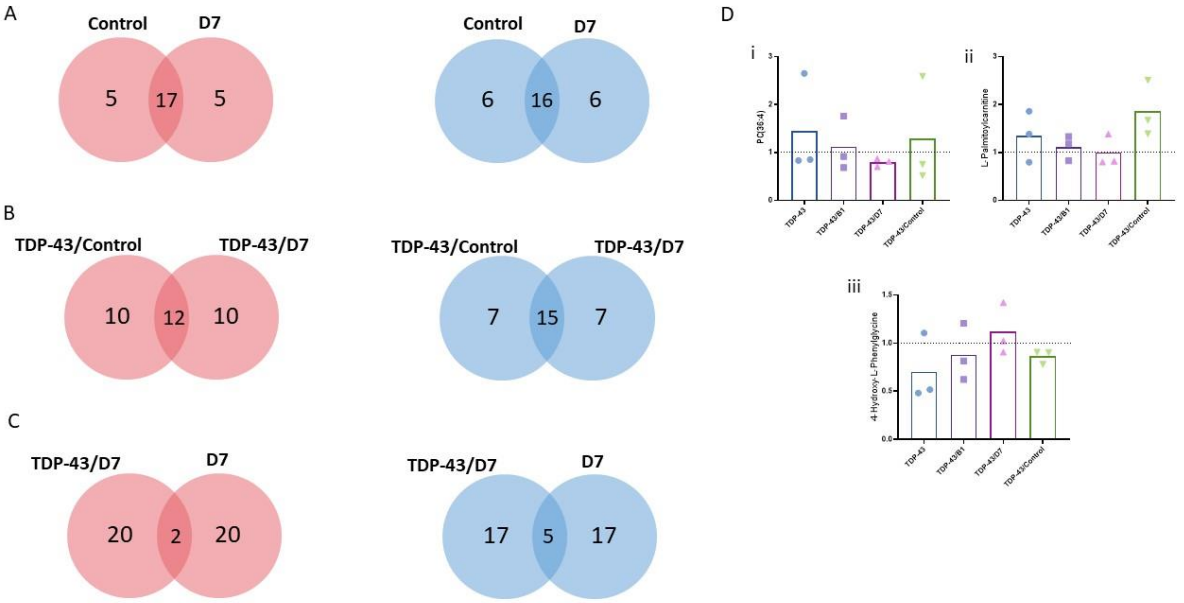

Figure 7: Metabolomic profiles of HEK293T cells. Venn diagram representing the number of specific and common metabolites that increased (red) or decreased (blue) within each condition upon A) overexpression of the scFv (values normalized to the mock condition), (B) overexpression of TDP-43 and the scFv together (values normalized to the TDP-43 condition), C) transfection with the scFv with or without TDP-43 overexpression (values normalized to the TDP-43 condition). D) Quantification of some of the metabolites of interest. i) PC(36:4), ii) L-palmitoylcarnitine, iii) 4-hydroxy-L-Phenylglycine. Values were normalized to the vehicle condition (dotted line).

4. Discussion.

TDP-43 plays a crucial role in maintaining cellular homeostasis by regulating gene expression, RNA processing, and RNA stability (Hergesheimer et al., 2019). In disease states, the protein is found mislocalized to the cytoplasm where it undergoes fragmentation and post-translational modifications and aggregates. Targeting TDP-43 proteinopathy has been the focus of many research groups given the important role that this protein plays in many neurodegenerative diseases (Francois-Moutal et al., 2021; Ojaimi et al., 2022).

scFv intrabodies can offer a highly specific approach to directly target intracellular antigens and have gained growing interest as a therapeutic approach for neurodegenerative diseases (Messer & Butler, 2020). Two previous studies have selected scFvs for their specific binding to the RRM1 and RRM2 domains of TDP-43(Pozzi et al., 2019; Tamaki et al., 2018). Similarly, another team used *in silico* predictions to design nanobodies that intracellularly target the RRM domains of TDP-43(Gilodi et al., 2022). In 2020, a study used phage display to select diagnostic scFv clones that can recognize TDP-43 variants found in FTD (Venkataraman et al., 2020). These studies highlight how targeting TDP-43 can pave the way for developing broad-spectrum therapies that might be effective across various conditions, but can also help in the diagnosis of TDP-43 proteinopathies.

We decided to follow an untargeted high-throughput screening approach using a synthetic scFv phage display library. This technique allows the screening of big libraries that are not biased towards a specific antigen, in order to identify scFvs against different potential sites on TDP-43. In addition, we based our screening on wtTDP-43, which is the form most commonly implicated in TDP-43 proteinopathies (Hergesheimer et al., 2019). We were able to identify four different TDP-43-specific scFv clones, two of which (B1 and D7) were retained for subsequent experiments. By not engineering the scFvs against a specific domain of TDP-43,

we were able to generate two clones that targets different sites of TDP-43 spanning various 3D folded domains.

After verifying that the scFvs D7 and B1 specifically bind to wtTDP-43, we expressed them intracellularly as intrabodies in a HEK293T cell model of TDP-43 proteinopathy. A main challenge of scFvs targeting TDP-43 is ensuring that they do not target functional nuclear TDP-43. In our case, the intrabodies were found to be mainly cytoplasmic in the presence of mislocalized TDP-43. The intrabodies B1 and D7 also colocalized with aggregated TDP-43, which was not the case for the control intrabody. We also detected no effect of our intrabodies on soluble TDP-43 by western blot.

Given that overexpressing TDP-43 for 48 h in HEK293T cells did not lead to significant cell death compared to the control, we could not use cellular viability as a main criterion to assess the effect of the intrabodies on TDP-43-induced cellular toxicity. We confirmed however that our intrabodies did not negatively affect the viability of cells that were already under TDP-43-induced stress. Given the progressive and complex nature of ALS, and the interplay between several malfunctioning mechanisms, it would be interesting to assess more subtle cellular and metabolic changes to evaluate the effectiveness of some TDP-43-targeting approaches. In our case where TDP-43 and the intrabodies are co-overexpressed at the same time and only for 48 h, we can assume that the effect of the scFv occurs on pathological changes that appear at the earliest stages of the disease.

TDP-43 aggregation was represented by the amount of protein recovered in the detergent-insoluble fraction of cell lysates. One study has previously demonstrated that visible TDP-43 inclusions under confocal microscopy were not necessarily insoluble (Barmada et al., 2010); based on this data we used western blot analyses to quantify TDP-43 insolubility. Overexpression of TDP-43 led to the fragmentation of the protein, with the appearance of TDP-35 and TDP-25 CTF. Interestingly, the overexpression of the intrabody D7 led to a decrease in the amount of insoluble TDP-35 CTF in HEK293T cells while the total amount of TDP-43 remained unchanged. The intrabody B1 did not have any effect on the amount or insolubility of TDP-43. The effect of D7 on the insoluble TDP-35 CTF level was reversed upon inhibition of the proteasome, but not upon inhibition of autophagy. This is in line with our observation that upon overexpression of TDP-43 alone, the detergent-insoluble fraction of TDP-43 and TDP-35 CTF was mainly degraded by the proteasome. Together, these results

suggest that D7 enhances the proteasomal degradation of the detergent-insoluble TDP-35 CTF while sparing functional TDP-43. It remains unclear to us why D7 targeted TDP-35 CTF instead of TDP-43, but we speculate that it might be due to different conformations of TDP-43 and TDP-35 inside cells making the epitopes on TDP-35 more accessible to D7. For conditions like TDP-43 proteinopathy, promoting the degradation of toxic aggregation-prone proteins can alleviate cellular stress.

CTFs of TDP-43 have been found to be associated with several neurological disorders such ALS (Neumann et al., 2006), FTD (Igaz et al., 2008), Alzheimer's disease, corticobasal degeneration (Riku et al., 2022), Pick's disease (Rohn & Kokoulina, 2009), Parkinson's disease (Kokoulina & Rohn, 2010), and traumatic brain injury(Wang et al., 2015). TDP-35 CTF is a product of the proteolytic cleavage of TDP-43 at the level of its N-terminus (Chhangani et al., 2021; Kametani et al., 2016). Given that TDP-35 CTF includes the RNA-binding domains of TDP-43, particularly the RRM1 domain, this fragment retains its ability to associate strongly with different RNA species (Kuo et al., 2014). TDP-35 lacks the nuclear localization signal of TDP-43, and predominately localize in the cytoplasm and form stress granules or aggregates that negatively affect RNA processing (Nishimoto et al., 2010). One study showed that TDP-35 CTF can redirect TDP-43 from its normal nuclear location to cytoplasmic aggregates, and that this process depends crucially on RNA binding (M. Che et al., 2011; M.-X. Che et al., 2015). In addition, TDP-35 was found to be even more aggregation-prone than TDP-43 or TDP-25, and to seed to aggregation of TDP-43(M. Che et al., 2011). All these studies highlight the importance of targeting TDP-35 CTF as a strategy to counteract or halt the progression of TDP-43 proteinopathy.

The dysfunction of TDP-43 in neurodegenerative diseases is known to cause significant cellular alterations including disturbances in the metabolipidomics profile (Andrés-Benito et al., 2021; Floare & Allen, 2020; Gautam et al., 2022). D7 exhibited the ability to restore the levels of different metabolites altered by TDP-43 overexpression. In HEK293T cells, L-palmitoylcarnitine and glycerophospholipid PC(36:4) were decreased and restored back to basal levels by D7. Interestingly, our group previously reported perturbations in the levels of numerous carnitines and glycerophospholipids in HEK293T cells overexpressing TDP-43 (Lanznaster et al., 2019). L-palmitoylcarnitine is a 23-carbon acylcarnitine that is increased is ALS (Goutman et al., 2022; Manzo et al., 2018), suggesting an impaired beta-oxidation.

Phosphatidylcholine PC(36:4) was also one of the main molecules that increased in ALS patients compared to controls, and was found to correlate with disease progression (Blasco et al., 2017; Sol et al., 2021). D7 also seemed to increase back to normal the level of 4-hydroxy-phenylglycine, a known inhibitor of carnitine palmitoyltransferase-1 (CPT1) (Yano et al., 2010). Various studies have pinpointed alterations in CPT1 in TDP-43 proteinopathies (Manzo et al., 2018; Torres et al., 2022). For instance, downregulation of CPT1 was found to alleviate pathological alterations and symptoms in a mouse model of ALS (Trabjerg et al., 2021). Metabolomic analysis seems to point towards a clear involvement of lipid metabolism in TDP-43 proteinopathy which was targeted by D7.

5. Conclusions.

Using phage-display, we identified two main scFv clones that can bind to human wtTDP-43. Of the identified scFvs, intrabody D7 was able to reduce the toxic burden of TDP-43 in cells, particularly by decreasing the levels of insoluble TDP-35 CTF, and alleviate some metabolic alterations linked to TDP-43 proteinopathy. This can serve as tool to help decipher the role of TDP-35 CTF in health and disease and the importance of targeting cellular alterations linked to TDP-43 proteinopathy such as metabolomic changes.

Acknowledgements: The authors would like to thank Professor Giles Lalmanach for helpful discussions about the ELISA test; Dr Eric Reiter and Dr Anne Poupon for the MAbSilico analyses; and Professor Hervé Watier and all the LabEx network for their support. This publication has been funded with support from Région Centre Val de Loire and the French National Research Agency under the program “Investissements d’avenir” Grant Agreement LabEx MAbImprove: ANR-10-LABX-53. We would like to thank the ARSLA for financial support. Funding sources had no participation in study design; in the collection, analysis, and interpretation of data; in the writing of the report; and in the decision to submit the article for publication.

Author Contributions. Y.A.O., R.H.: Conceptualization, data curation, formal analysis, investigation, methodology, visualization, writing (original draft); **H.A.**: formal analysis, methodology, visualization, writing (original draft). **A.C, J.A., A.D., S.H., J.B. and A.L**.: investigation; **A.D., S.O., P.E., P.V., C.R.A., P.C. and O.H.**: writing (review & editing); **P.M.**: Supervision, resources, writing (review & editing); **D.L.**: conceptualization**,** methodology, investigation, validation, supervision, writing (review & editing); **H.B.**: supervision, project administration, funding acquisition, writing (review & editing). All authors read and approved the final manuscript.

References

Andrés-Benito, P., Gelpi, E., Jové, M., Mota-Martorell, N., Obis, È., Portero-Otin, M., Povedano, M., Pujol, A., Pamplona, R., & Ferrer, I. (2021). Lipid alterations in human frontal cortex in ALS-FTLD-TDP43 proteinopathy spectrum are partly related to peroxisome impairment. *Neuropathology and Applied Neurobiology*, *47*(4), 544–563. https://doi.org/10.1111/nan.12681

Arai, T., Hasegawa, M., Akiyama, H., Ikeda, K., Nonaka, T., Mori, H., Mann, D., Tsuchiya, K., Yoshida, M., Hashizume, Y., & Oda, T. (2006). TDP-43 is a component of ubiquitin-positive tau-negative inclusions in frontotemporal lobar degeneration and amyotrophic lateral sclerosis. *Biochemical and Biophysical Research Communications*, *351*(3), 602–611. https://doi.org/10.1016/j.bbrc.2006.10.093

Arai, T., Mackenzie, I. R. A., Hasegawa, M., Nonoka, T., Niizato, K., Tsuchiya, K., Iritani, S., Onaya, M., & Akiyama, H. (2009). Phosphorylated TDP-43 in Alzheimer's disease and dementia with Lewy bodies. *Acta Neuropathologica*, *117*(2), 125–136. https://doi.org/10.1007/s00401-008-0480-1

Barmada, S. J., Skibinski, G., Korb, E., Rao, E. J., Wu, J. Y., & Finkbeiner, S. (2010). Cytoplasmic Mislocalization of TDP-43 Is Toxic to Neurons and Enhanced by a Mutation Associated with Familial Amyotrophic Lateral Sclerosis. *Journal of Neuroscience*, *30*(2), 639–649. https://doi.org/10.1523/JNEUROSCI.4988-09.2010

Besser, L. M., Teylan, M. A., & Nelson, P. T. (2020). Limbic Predominant Age-Related TDP-43 Encephalopathy (LATE): Clinical and Neuropathological Associations. *Journal of Neuropathology & Experimental Neurology*, *79*(3), 305–313. https://doi.org/10.1093/jnen/nlz126

Blasco, H., Veyrat-Durebex, C., Bocca, C., Patin, F., Vourc'h, P., Kouassi Nzoughet, J., Lenaers, G., Andres, C. R., Simard, G., Corcia, P., & Reynier, P. (2017). Lipidomics Reveals Cerebrospinal-Fluid Signatures of ALS. *Scientific Reports*, *7*(1), 17652. https://doi.org/10.1038/s41598-017-17389-9

Blatter, M., Dunin-Horkawicz, S., Grishina, I., Maris, C., Thore, S., Maier, T., Bindereif, A., Bujnicki, J. M., & Allain, F. H.-T. (2015). The Signature of the Five-Stranded vRRM Fold Defined by Functional, Structural and Computational Analysis of the hnRNP L Protein. *Journal of Molecular Biology*, *427*(19), 3001–3022. https://doi.org/10.1016/j.jmb.2015.05.020

Bourquard, T., Musnier, A., Puard, V., Tahir, S., Ayoub, M. A., Jullian, Y., Boulo, T., Gallay, N., Watier, H., Bruneau, G., Reiter, E., Crépieux, P., & Poupon, A. (2018). MAbTope: A Method for Improved Epitope Mapping. *The Journal of Immunology*, *201*(10), 3096–3105. https://doi.org/10.4049/jimmunol.1701722

Briese, M., Saal-Bauernschubert, L., Lüningschrör, P., Moradi, M., Dombert, B., Surrey, V., Appenzeller, S., Deng, C., Jablonka, S., & Sendtner, M. (2020). Loss of Tdp-43 disrupts the axonal transcriptome of motoneurons accompanied by impaired axonal translation and mitochondria function. *Acta Neuropathologica Communications*, *8*(1), 116. https://doi.org/10.1186/s40478-020-00987-6

Chanson, J.-B., Echaniz-Laguna, A., Vogel, T., Mohr, M., Benoilid, A., Kaltenbach, G., & Kiesmann, M. (2010). TDP43-Positive Intraneuronal Inclusions in a Patient with Motor Neuron Disease and Parkinson's Disease. *Neurodegenerative Diseases*, *7*(4), 260–264. https://doi.org/10.1159/000273591

Che, M., Jiang, Y., Xie, Y., Jiang, L., & Hu, H. (2011). Aggregation of the 35-kDa fragment of TDP-43 causes formation of cytoplasmic inclusions and alteration of RNA processing. *The FASEB Journal*, *25*(7), 2344–2353. https://doi.org/10.1096/fj.10-174482

Che, M.-X., Jiang, L.-L., Li, H.-Y., Jiang, Y.-J., & Hu, H.-Y. (2015). TDP-35 sequesters TDP-43 into cytoplasmic inclusions through binding with RNA. *FEBS Letters*, *589*(15), 1920–1928. https://doi.org/10.1016/j.febslet.2015.06.009

Chen, Y.-H., Wu, K.-J., Hsieh, W., Harvey, B. K., Hoffer, B. J., Wang, Y., & Yu, S.-J. (2021). Administration of AAV-Alpha Synuclein NAC Antibody Improves Locomotor Behavior in Rats Overexpressing Alpha Synuclein. *Genes*, *12*(6), 948. https://doi.org/10.3390/genes12060948

Chhangani, D., Martín-Peña, A., & Rincon-Limas, D. E. (2021). Molecular, functional, and pathological aspects of TDP-43 fragmentation. *iScience*, *24*(5), 102459. https://doi.org/10.1016/j.isci.2021.102459

Diémé, B., Lefèvre, A., Nadal-Desbarats, L., Galineau, L., Madji Hounoum, B., Montigny, F., Blasco, H., Andres, C. R., Emond, P., & Mavel, S. (2017). Workflow methodology for rat brain metabolome exploration using NMR, LC–MS and GC–MS analytical platforms. *Journal of Pharmaceutical and Biomedical Analysis*, *142*, 270–278. https://doi.org/10.1016/j.jpba.2017.03.068

Dunker, W., Ye, X., Zhao, Y., Liu, L., Richardson, A., & Karijolich, J. (2021). TDP-43 prevents endogenous RNAs from triggering a lethal RIG-I-dependent interferon response. *Cell Reports*, *35*(2), 108976. https://doi.org/10.1016/j.celrep.2021.108976

Esquerda-Canals, G., Roda, A. R., Martí-Clúa, J., Montoliu-Gaya, L., Rivera-Hernández, G., & Villegas, S. (2019). Treatment with scFv-h3D6 Prevented Neuronal Loss and Improved Spatial Memory in Young 3xTg-AD Mice by Reducing the Intracellular Amyloid-β Burden. *Journal of Alzheimer's Disease*, *70*(4), 1069–1091. https://doi.org/10.3233/JAD-190484

Fiesel, F. C., Voigt, A., Weber, S. S., Van Den Haute, C., Waldenmaier, A., Görner, K., Walter, M., Anderson, M. L., Kern, J. V., Rasse, T. M., Schmidt, T., Springer, W., Kirchner, R., Bonin, M., Neumann, M., Baekelandt, V., Alunni-Fabbroni, M., Schulz, J. B., & Kahle, P. J. (2010). Knockdown of transactive response DNA-binding protein (TDP-43) downregulates histone deacetylase 6. *The EMBO Journal*, *29*(1), 209–221. https://doi.org/10.1038/emboj.2009.324

Floare, M.-L., & Allen, S. P. (2020). Why TDP-43? Why Not? Mechanisms of Metabolic Dysfunction in Amyotrophic Lateral Sclerosis. *Neuroscience Insights*, *15*, 263310552095730. https://doi.org/10.1177/2633105520957302

Francois-Moutal, L., Scott, D. D., & Khanna, M. (2021). Direct targeting of TDP-43, from small molecules to biologics: The therapeutic landscape. *RSC Chemical Biology*, *2*(4), 1158–1166. https://doi.org/10.1039/D1CB00110H

Gautam, M., Gunay, A., Chandel, N. S., & Ozdinler, P. H. (2022). Mitochondrial dysregulation occurs early in ALS motor cortex with TDP-43 pathology and suggests maintaining NAD+ balance as a therapeutic strategy. *Scientific Reports*, *12*(1), 4287. https://doi.org/10.1038/s41598-022-08068-5

Gilodi, M., Lisi, S., F. Dudás, E., Fantini, M., Puglisi, R., Louka, A., Marcatili, P., Cattaneo, A., & Pastore, A. (2022). Selection and Modelling of a New Single-Domain Intrabody Against TDP-43. *Frontiers in Molecular Biosciences*, *8*, 773234. https://doi.org/10.3389/fmolb.2021.773234

Goodwin, M. S., Sinyavskaya, O., Burg, F., O'Neal, V., Ceballos-Diaz, C., Cruz, P. E., Lewis, J., Giasson, B. I., Davies, P., Golde, T. E., & Levites, Y. (2021). Anti-tau scFvs Targeted to the Cytoplasm or Secretory Pathway Variably Modify Pathology and Neurodegenerative Phenotypes. *Molecular Therapy*, *29*(2), 859–872. https://doi.org/10.1016/j.ymthe.2020.10.007

Goutman, S. A., Guo, K., Savelieff, M. G., Patterson, A., Sakowski, S. A., Habra, H., Karnovsky, A., Hur, J., & Feldman, E. L. (2022). Metabolomics identifies shared lipid pathways in independent amyotrophic lateral sclerosis cohorts. *Brain*, *145*(12), 4425–4439. https://doi.org/10.1093/brain/awac025

Güell-Bosch, J., Lope-Piedrafita, S., Esquerda-Canals, G., Montoliu-Gaya, L., & Villegas, S. (2020). Progression of Alzheimer's disease and effect of scFv-h3D6 immunotherapy in the 3xTg-AD mouse model: *An in vivo longitudinal study using Magnetic Resonance Imaging and Spectroscopy*. *NMR in Biomedicine*, *33*(5), e4263. https://doi.org/10.1002/nbm.4263

Hergesheimer, R. C., Chami, A. A., de Assis, D. R., Vourc'h, P., Andres, C. R., Corcia, P., Lanznaster, D., & Blasco, H. (2019). The debated toxic role of aggregated TDP-43 in amyotrophic lateral sclerosis: A resolution in sight? *Brain*, *142*(5), 1176–1194. https://doi.org/10.1093/brain/awz078

Igaz, L. M., Kwong, L. K., Xu, Y., Truax, A. C., Uryu, K., Neumann, M., Clark, C. M., Elman, L. B., Miller, B. L., Grossman, M., McCluskey, L. F., Trojanowski, J. Q., & Lee, V. M.-Y. (2008). Enrichment of C-Terminal Fragments in TAR DNA-Binding Protein-43 Cytoplasmic Inclusions in Brain but not in Spinal Cord of Frontotemporal Lobar Degeneration and Amyotrophic Lateral Sclerosis. *The American Journal of Pathology*, *173*(1), 182–194. https://doi.org/10.2353/ajpath.2008.080003

Kametani, F., Obi, T., Shishido, T., Akatsu, H., Murayama, S., Saito, Y., Yoshida, M., & Hasegawa, M. (2016). Mass spectrometric analysis of accumulated TDP-43 in amyotrophic lateral sclerosis brains. *Scientific Reports*, *6*(1), 23281. https://doi.org/10.1038/srep23281

Kokoulina, P., & Rohn, T. T. (2010). Caspase-cleaved transactivation response DNA-binding protein 43 in Parkinson's disease and dementia with Lewy bodies. *Neuro-Degenerative Diseases*, *7*(4), 243–250. https://doi.org/10.1159/000287952

Kristensen, P., & Winter, G. (1998). Proteolytic selection for protein folding using filamentous bacteriophages. *Folding and Design*, *3*(5), 321–328. https://doi.org/10.1016/S1359-0278(98)00044-3

Kuo, P.-H., Chiang, C.-H., Wang, Y.-T., Doudeva, L. G., & Yuan, H. S. (2014). The crystal structure of TDP-43 RRM1-DNA complex reveals the specific recognition for UG- and TG-rich nucleic acids. *Nucleic Acids Research*, *42*(7), 4712–4722. https://doi.org/10.1093/nar/gkt1407

Lanznaster, D., Bourgeais, J., Bruno, C., Hergesheimer, R. C., Thepault, R.-A., Vourc'h, P., Corcia, P., Andres, C. R., Herault, O., & Blasco, H. (2019). TDP-43-Mediated Toxicity in HEK293T Cells: A Fast and Reproducible Protocol To Be Employed in the Search of New Therapeutic Options against Amyotrophic Lateral Sclerosis. *Cells*, *9*(1), 68. https://doi.org/10.3390/cells9010068

LaRocca, T. J., Mariani, A., Watkins, L. R., & Link, C. D. (2019). TDP-43 knockdown causes innate immune activation via protein kinase R in astrocytes. *Neurobiology of Disease*, *132*, 104514. https://doi.org/10.1016/j.nbd.2019.104514

Lee, M., Sadowska, A., Bekere, I., Ho, D., Gully, B. S., Lu, Y., Iyer, K. S., Trewhella, J., Fox, A. H., & Bond, C. S. (2015). The structure of human SFPQ reveals a coiled-coil mediated polymer essential for functional aggregation in gene regulation. *Nucleic Acids Research*, *43*(7), 3826–3840. https://doi.org/10.1093/nar/gkv156

Li, S., Yi, Y., Cui, K., Zhang, Y., Chen, Y., Han, D., Sun, L., Zhang, X., Chen, F., Zhang, Y., & Yang, Y. (2021). A Single-Chain Variable Fragment Antibody Inhibits Aggregation of Phosphorylated Tau and Ameliorates Tau Toxicity in vitro and in vivo. *Journal of Alzheimer's Disease*, *79*(4), 1613–1629. https://doi.org/10.3233/JAD-191266

Li, X., Liu, S., Jiang, J., Zhang, L., Espinosa, S., Hill, R. C., Hansen, K. C., Zhou, Z. H., & Zhao, R. (2017). CryoEM structure of Saccharomyces cerevisiae U1 snRNP offers insight into alternative splicing. *Nature Communications*, *8*(1), 1035. https://doi.org/10.1038/s41467-017-01241-9

Loganathan, S., Wilson, B. A., Carey, S. B., Manzo, E., Joardar, A., Ugur, B., & Zarnescu, D. C. (2022). TDP-43 Proteinopathy Causes Broad Metabolic Alterations including TCA Cycle Intermediates and Dopamine Levels in Drosophila Models of ALS. *Metabolites*, *12*(2), 101. https://doi.org/10.3390/metabo12020101

Lukavsky, P. J., Daujotyte, D., Tollervey, J. R., Ule, J., Stuani, C., Buratti, E., Baralle, F. E., Damberger, F. F., & Allain, F. H.-T. (2013). Molecular basis of UG-rich RNA recognition by the human splicing factor TDP-43. *Nature Structural & Molecular Biology*, *20*(12), 1443–1449. https://doi.org/10.1038/nsmb.2698

Manzo, E., O'Conner, A. G., Barrows, J. M., Shreiner, D. D., Birchak, G. J., & Zarnescu, D. C. (2018). Medium-Chain Fatty Acids, Beta-Hydroxybutyric Acid and Genetic Modulation of the Carnitine Shuttle Are Protective in a Drosophila Model of ALS Based on TDP-43. *Frontiers in Molecular Neuroscience*, *11*, 182. https://doi.org/10.3389/fnmol.2018.00182

Martineau, P., Jones, P., & Winter, G. (1998). Expression of an antibody fragment at high levels in the bacterial cytoplasm. *Journal of Molecular Biology*, *280*(1), 117–127. https://doi.org/10.1006/jmbi.1998.1840

Messer, A., & Butler, D. C. (2020). Optimizing intracellular antibodies (intrabodies/nanobodies) to treat neurodegenerative disorders. *Neurobiology of Disease*, *134*, 104619. https://doi.org/10.1016/j.nbd.2019.104619

Mompeán, M., Romano, V., Pantoja-Uceda, D., Stuani, C., Baralle, F. E., Buratti, E., & Laurents, D. V. (2017). Point mutations in the N-terminal domain of transactive response DNA-binding protein 43 kDa (TDP-43) compromise its stability, dimerization, and functions. *Journal of Biological Chemistry*, *292*(28), 11992–12006. https://doi.org/10.1074/jbc.M117.775965

Neumann, M., Sampathu, D. M., Kwong, L. K., Truax, A. C., Micsenyi, M. C., Chou, T. T., Bruce, J., Schuck, T., Grossman, M., Clark, C. M., McCluskey, L. F., Miller, B. L., Masliah, E., Mackenzie, I. R., Feldman, H., Feiden, W., Kretzschmar, H. A., Trojanowski, J. Q., & Lee, V. M.-Y. (2006). Ubiquitinated TDP-43 in Frontotemporal Lobar Degeneration and Amyotrophic Lateral Sclerosis. *Science*, *314*(5796), 130–133. https://doi.org/10.1126/science.1134108

Nishimoto, Y., Ito, D., Yagi, T., Nihei, Y., Tsunoda, Y., & Suzuki, N. (2010). Characterization of Alternative Isoforms and Inclusion Body of the TAR DNA-binding Protein-43. *Journal of Biological Chemistry*, *285*(1), 608–619. https://doi.org/10.1074/jbc.M109.022012

Ojaimi, Y. A., Dangoumau, A., Alarcan, H., Hergesheimer, R., Vourc'h, P., Corcia, P., Lanznaster, D., & Blasco, H. (2022). TAR DNA-binding protein of 43 kDa (TDP-43) and amyotrophic lateral sclerosis (ALS): A promising therapeutic target. *Expert Opinion on Therapeutic Targets*, *26*(6), 575–592. https://doi.org/10.1080/14728222.2022.2083958

Ormeño, F., Hormazabal, J., Moreno, J., Riquelme, F., Rios, J., Criollo, A., Albornoz, A., Alfaro, I. E., & Budini, M. (2020). Chaperone Mediated Autophagy Degrades TDP-43 Protein and Is Affected by TDP-43 Aggregation. *Frontiers in Molecular Neuroscience*, *13*, 19. https://doi.org/10.3389/fnmol.2020.00019

Polymenidou, M., Lagier-Tourenne, C., Hutt, K. R., Huelga, S. C., Moran, J., Liang, T. Y., Ling, S.-C., Sun, E., Wancewicz, E., Mazur, C., Kordasiewicz, H., Sedaghat, Y., Donohue, J. P., Shiue, L., Bennett, C. F., Yeo, G. W., & Cleveland, D. W. (2011). Long pre-mRNA depletion and RNA missplicing contribute to neuronal

vulnerability from loss of TDP-43. *Nature Neuroscience*, *14*(4), 459–468. https://doi.org/10.1038/nn.2779

Pozzi, S., Thammisetty, S. S., Codron, P., Rahimian, R., Plourde, K. V., Soucy, G., Bareil, C., Phaneuf, D., Kriz, J., Gravel, C., & Julien, J.-P. (2019). Virus-mediated delivery of antibody targeting TAR DNA-binding protein-43 mitigates associated neuropathology. *Journal of Clinical Investigation*, *129*(4), 1581–1595. https://doi.org/10.1172/JCI123931

Prpar Mihevc, S., Baralle, M., Buratti, E., & Rogelj, B. (2016). TDP-43 aggregation mirrors TDP-43 knockdown, affecting the expression levels of a common set of proteins. *Scientific Reports*, *6*(1), 33996. https://doi.org/10.1038/srep33996

Riku, Y., Iwasaki, Y., Ishigaki, S., Akagi, A., Hasegawa, M., Nishioka, K., Li, Y., Riku, M., Ikeuchi, T., Fujioka, Y., Miyahara, H., Sone, J., Hattori, N., Yoshida, M., Katsuno, M., & Sobue, G. (2022). Motor neuron TDP-43 proteinopathy in progressive supranuclear palsy and corticobasal degeneration. *Brain*, *145*(8), 2769–2784. https://doi.org/10.1093/brain/awac091

Robin, G., & Martineau, P. (2012). Synthetic Customized scFv Libraries. In P. Chames (Ed.), *Antibody Engineering* (Vol. 907, pp. 109–122). Humana Press. https://doi.org/10.1007/978-1-61779-974-7_6

Robin, G., Sato, Y., Desplancq, D., Rochel, N., Weiss, E., & Martineau, P. (2014). Restricted Diversity of Antigen Binding Residues of Antibodies Revealed by Computational Alanine Scanning of 227 Antibody–Antigen Complexes. *Journal of Molecular Biology*, *426*(22), 3729–3743. https://doi.org/10.1016/j.jmb.2014.08.013

Rohn, T. T., & Kokoulina, P. (2009). Caspase-cleaved TAR DNA-binding protein-43 in Pick's disease. *International Journal of Physiology, Pathophysiology and Pharmacology*, *1*(1), 25–32.

Schwab, C., Arai, T., Hasegawa, M., Yu, S., & McGeer, P. L. (2008). Colocalization of Transactivation-Responsive DNA-Binding Protein 43 and Huntingtin in Inclusions of Huntington Disease. *Journal of Neuropathology & Experimental Neurology*, *67*(12), 1159–1165. https://doi.org/10.1097/NEN.0b013e31818e8951

Sol, J., Jové, M., Povedano, M., Sproviero, W., Domínguez, R., Piñol-Ripoll, G., Romero-Guevara, R., Hye, A., Al-Chalabi, A., Torres, P., Andres-Benito, P., Area-Gómez, E., Pamplona, R., Ferrer, I., Ayala, V., & Portero-Otín, M. (2021). Lipidomic traits of plasma and cerebrospinal fluid in amyotrophic lateral sclerosis correlate with disease progression. *Brain Communications*, *3*(3), fcab143. https://doi.org/10.1093/braincomms/fcab143

Tamaki, Y., Shodai, A., Morimura, T., Hikiami, R., Minamiyama, S., Ayaki, T., Tooyama, I., Furukawa, Y., Takahashi, R., & Urushitani, M. (2018). Elimination of TDP-43 inclusions linked to amyotrophic lateral sclerosis by a misfolding-specific intrabody with dual proteolytic signals. *Scientific Reports*, *8*(1), 6030. https://doi.org/10.1038/s41598-018-24463-3

Tashiro, Y., Urushitani, M., Inoue, H., Koike, M., Uchiyama, Y., Komatsu, M., Tanaka, K., Yamazaki, M., Abe, M., Misawa, H., Sakimura, K., Ito, H., & Takahashi, R. (2012). Motor Neuron-specific Disruption of Proteasomes, but Not Autophagy, Replicates Amyotrophic Lateral Sclerosis. *Journal of Biological Chemistry*, *287*(51), 42984–42994. https://doi.org/10.1074/jbc.M112.417600

Torres, P., Pamplona, R., & Portero-Otin, M. (2022). Cell senescence, loss of splicing, and lipid metabolism in TDP-43-related neurodegenerative processes. *Neural Regeneration Research*, *0*(0), 0. https://doi.org/10.4103/1673-5374.363832

Trabjerg, M. S., Andersen, D. C., Huntjens, P., Oklinski, K. E., Bolther, L., Hald, J. L., Baisgaard, A. E., Mørk, K., Warming, N., Kullab, U. B., Kroese, L. J., Pritchard, C. E. J., Huijbers, I. J., & Nieland, J. D. V. (2021). Downregulating carnitine palmitoyl transferase 1 affects disease progression in the SOD1 G93A mouse model of ALS. *Communications Biology*, *4*(1), 509. https://doi.org/10.1038/s42003-021-02034-z

Venkataraman, L., He, P., Khan, G., Harris, B. T., & Sierks, M. R. (2020). Isolation and characterization of antibody fragments selective for human FTD brain derived TDP-43 variants. *BMC Neuroscience*, *21*(1), 36. https://doi.org/10.1186/s12868-020-00586-0

Wang, H.-K., Lee, Y.-C., Huang, C.-Y., Liliang, P.-C., Lu, K., Chen, H.-J., Li, Y.-C., & Tsai, K.-J. (2015). Traumatic brain injury causes frontotemporal dementia and TDP-43 proteolysis. *Neuroscience*, *300*, 94–103. https://doi.org/10.1016/j.neuroscience.2015.05.013

Yano, H., Oyanagi, E., Kato, Y., Samejima, Y., Sasaki, J., & Utsumi, K. (2010). L-Carnitine is essential to β-oxidation of quarried fatty acid from mitochondrial membrane by PLA2. *Molecular and Cellular Biochemistry*, *342*(1–2), 95–100. https://doi.org/10.1007/s11010-010-0472-z

Zha, J., Liu, X., Zhu, J., Liu, S., Lu, S., Xu, P., Yu, X., & Liu, R. (2016). A scFv antibody targeting common oligomeric epitope has potential for treating several amyloidoses. *Scientific Reports*, *6*(1), 36631. https://doi.org/10.1038/srep36631

Supplementary figures

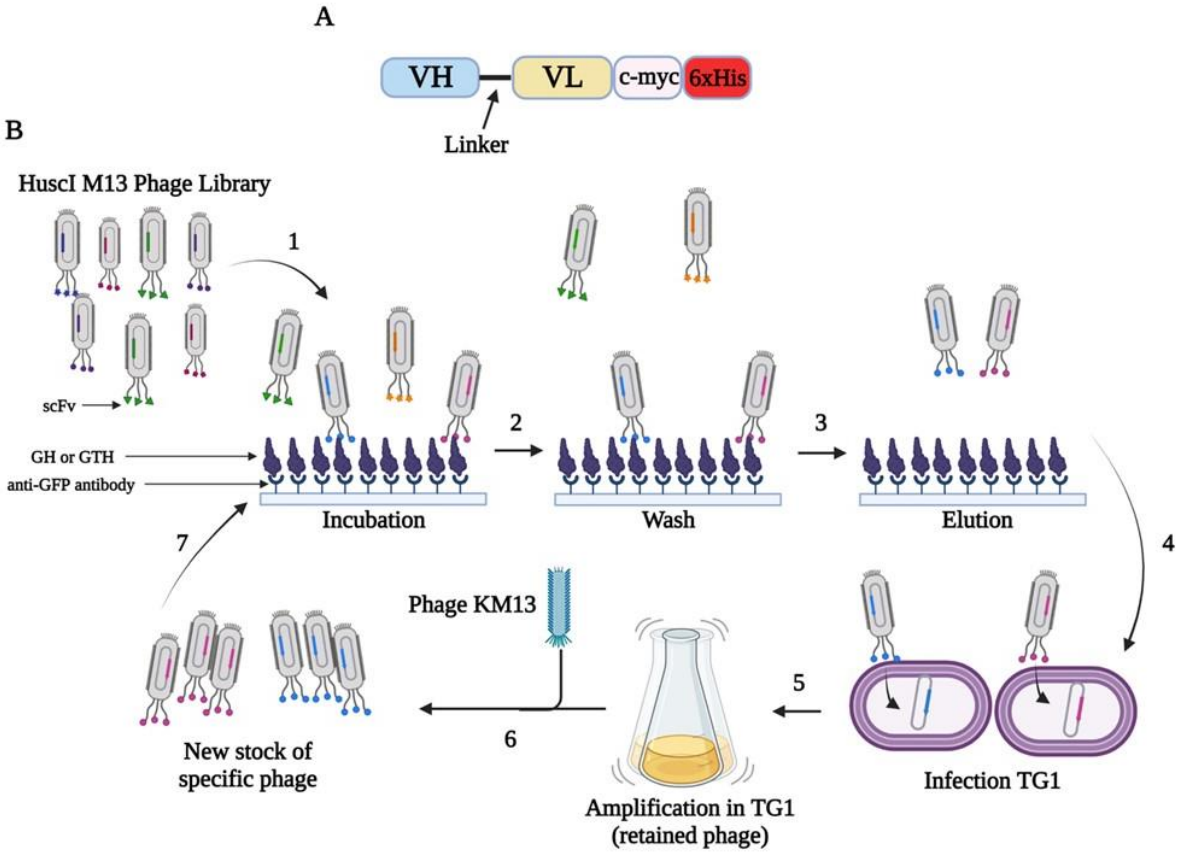

Figure S1: Flow chart illustrating the phage display screening strategy of scFv molecules. A) General structure of scFv protein. Once expressed as protein isolated from phage, it contains C-terminal c-myc and 6xHis tags. B) The HuscI library contained M13 phage that expressed copies of one scFv at their tail. The library that was depleted against anti-GFP antibody and against GFP-6xHis (GH) was incubated with GFP-wtTDP-43-6xHis (GTH) immobilized on anti-GFP antibody (1). After washing (2), the adhered phage were eluted by trypsin (3) and induced to infect TG1 (4). Following amplification of infected TG1 (5), new phage particles were produced (6) containing amplified specific phage. These phage were re-incubated with GTH (7). The cycle was repeated a total of 5 times. Figure made with Biorender.com.

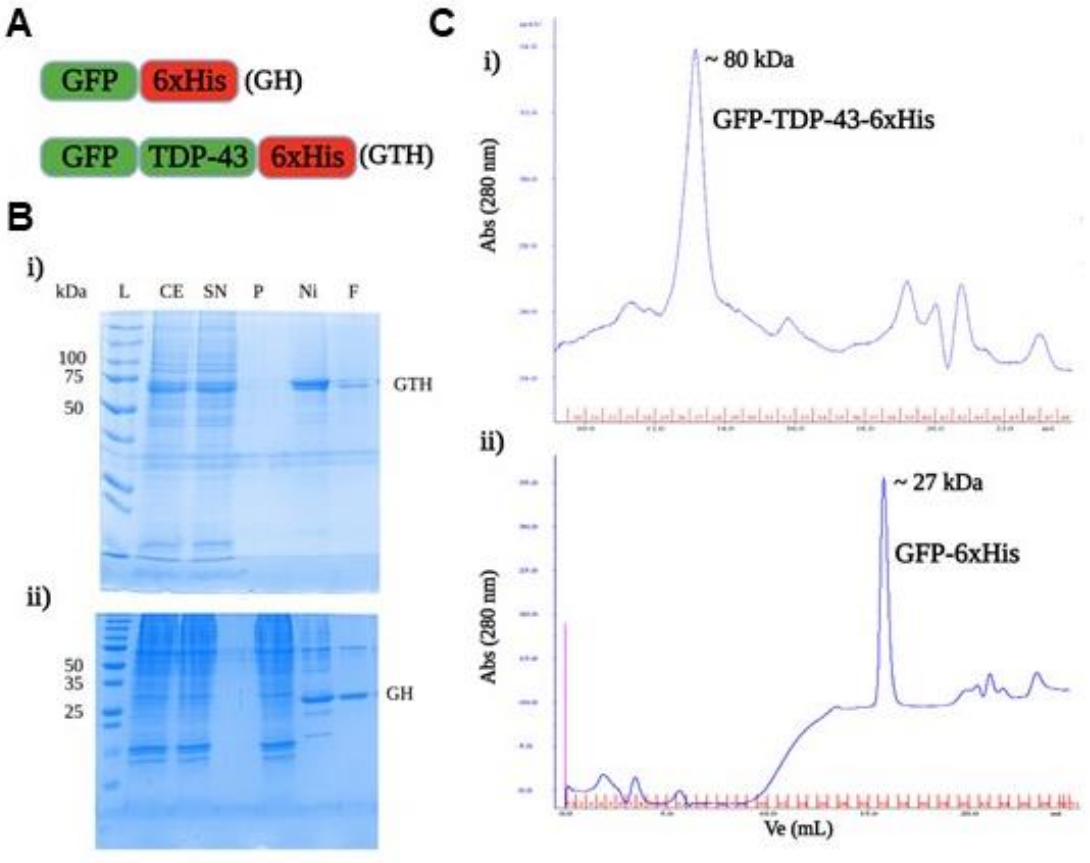

Figure S2: Purification of recombinant antigens for phage display. A) Structures of the recombinant proteins GFP-6xHis (GH) and GFP-TDP-43-6xHis (GTH) of 28 kDa and 75 kDa, respectively. B) SDS-PAGE gel stained by Coomassie reagent representing the purification of i) GTH and ii) GH. L: ladder; CE: crude extract of lysate. SN: supernatant of lysate. P: pellet of lysate. Ni: pooled eluted protein from affinity chromatography. F: final product following dialysis. C) Gel filtration profile of dialyzed i) GTH and ii) GH. The chromatogram reflects highly pure monomers of each protein. Ve: elution volume.

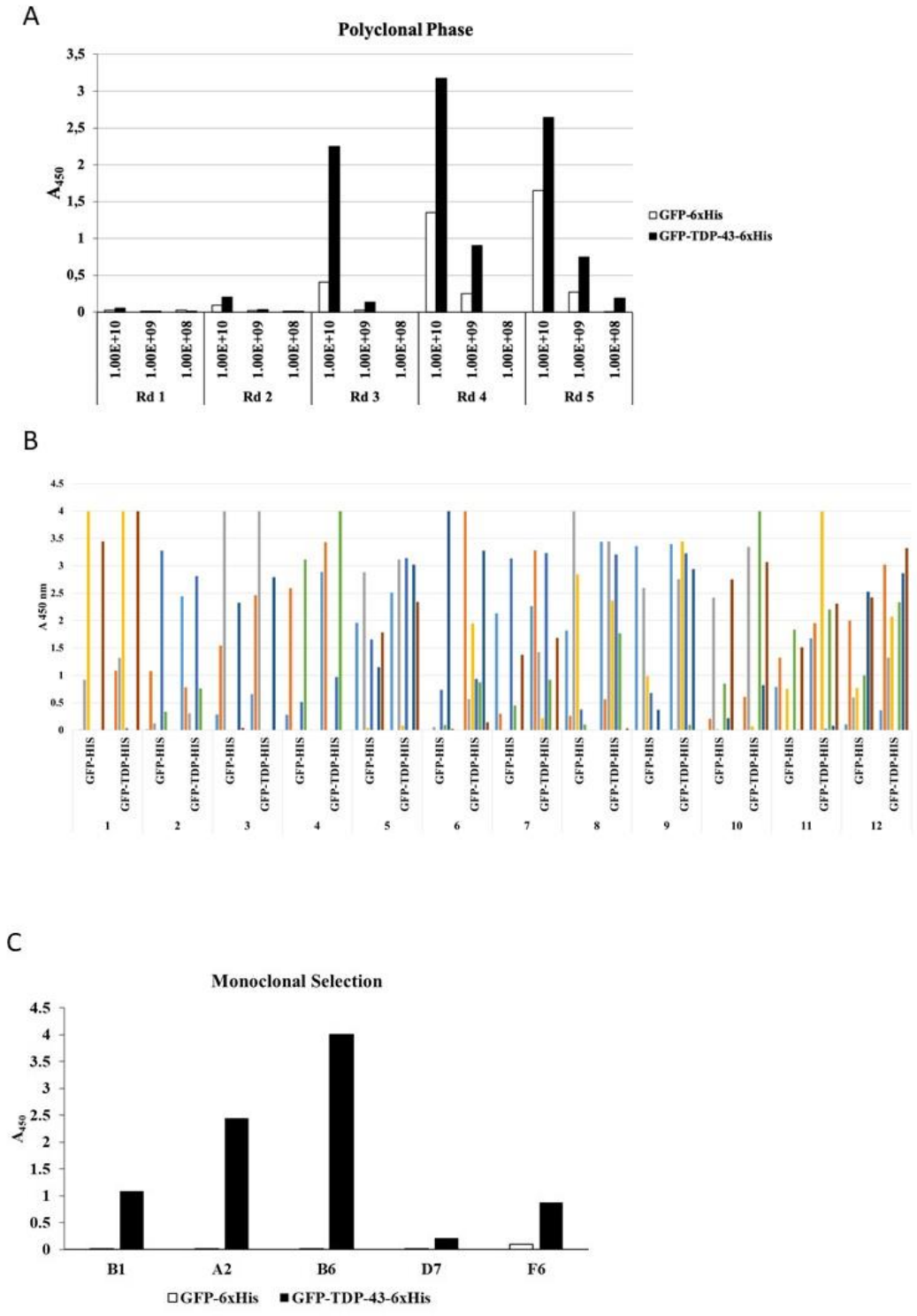

Figure S3: A) Amplification of polyclonal phage against GTH. Each round of eluted phage was tested by ELISA on wells coated with GH and GTH antigen. The x-axis represents the 3 dilutions in phage/mL used on coated wells. The white bar represents the absorbance at 450 nm for GH incubation, while the black bar represents the absorbance for GTH incubation. Round 4 appears to contain the most phage with affinity for GTH. B) Monoclonal screen of selected phage from round 4 for binding to GH and GTH. C)

Identification of monoclonal anti-TDP-43 scFv-phage display from TG1. Phage with distinct scFv sequences from wells B1, A2, B6, and D7 were identified as anti-TDP-43 because no absorbance was detected with GH. Phage from well F6 is represented as an example of non-specific binding because absorbance was also detected when incubated with the GH control.

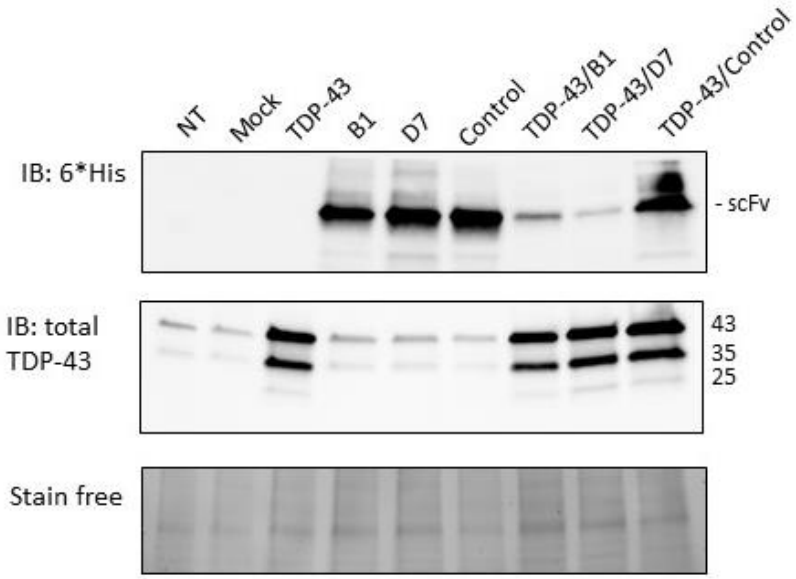

Figure S4: Overexpression of 6*His scFv and TDP-43 in HEK293T cells. Immunoblots showing the expression of the intrabody when expressed alone and when co-overexpressed with TDP-43. NT: non-transfected. Mock: cells transfected with the empty vector. TDP-43: cells transfected with TDP-43-expressing plasmid and empty vector. B1, D7, control: cells transfected with intrabody-expressing plasmid and empty vector. TDP-43/B1, TDP-43/D7 and TDP-43/control: cells transfected with TDP-43-expressing plasmid and intrabody-expressing plasmid.

Supplementary tables

Table S1: List of antibodies used in this study

Name of the antibody	Manufacturer (catalog #)	Species raised in	Dilution
HRP-conjugated anti-6*His	Proteintech (HRP-66005)	Mouse monoclonal	1:100 000 (WB) 1:10 000 (ELISA)
Anti-6*His	Proteintech (HRP-66005-1-Ig)	Mouse monoclonal	1:1000 (IF)
Anti-c-Myc	Thermo Fisher Scientific (13-2500)	Mouse monoclonal	1:2000 (ELISA)
HRP-conjugated M13 bacteriophage	Sino Biological (11973-MM05T-H)	Mouse monoclonal	1:2000 (ELISA)
Anti-TDP-43 (C-terminal)	Proteintech (12892-1-AP)	Rabbit polyclonal	1 :1000 (IF) 1 :5000 (WB)
Anti-NFκB Antibody, p65 subunit	Sigma Aldrich (MAB3026)	Mouse monoclonal	1:1000 (WB)
Alexa Fluor™ 488-conjugated anti-rabbit	Thermo Fisher Scientific (A-11034)		1 :500 (IF)
Alexa Fluor™ 594-conjugated anti-mouse	Thermo Fisher Scientific (A-11005)		1:500 (IF)
HRP-conjugated anti-rabbit	Promega (W401B)		1:10 000 (WB)
HRP-conjugated anti-mouse	Promega (W402B)		1:10 000 (WB)

Table S2: List of most upregulated metabolites within each condition in HEK293T cells

TDP-43 vs Empty	13R4 vs Empty	D7 vs Empty	TDP-43/13R4 vs TDP-43	TDP-43/D7 vs TDP-43
Creatine phosphate	Deoxyadenosine monophosphate	Deoxyadenosine monophosphate	Cysteic acid	Cysteic acid
Citicoline	Inosine	7-dehydrocholesterol	Ornithine	Diethanolamine
PC(36:4)	N-alpha-acetyl-lysine	L-oleoyl-rac-glycerol	Urocanic acid	Glucose-1-phosphate
L-glutamine	C14-carnitine	Inosine	L-histidinol	L-histidinol
Glycerophosphocholine	Galactitol	LysoPE(20:4)	C14-carnitine	Urocanic acid
L-palmitoylcarnitine	L-histidinol	Galactitol	Homogentisate	Trigonelline
Cortisone	Elaidic acid	Ornithine	3-methylglutaric acid	PC(35:4)
C14-carnitine	7-dehydrocholesterol	LysoPE(18:0)	Diethanolamine	Spermidine
Aminoadipic acid	L-oleoyl-rac-glycerol	Elaidic acid	Spermidine	Methyl jasmonate
Sarcosine	LysoPE(20:4)	Thymidine	PC(36:5)	4-hydroxy-L-phenylglycine
7-dehydrocholesterol	Thymidine	SM(32:2)	L-serine	N-acetylmannosamine
Urocanic acid	Pterin	LysoPE(16:0)	Succinic acid	3-methylglutaric acid
Creatinine	Ornithine	N-acetylneuraminate	PC(35:4)	Spermine
L-proline	N-acetylneuraminate	PE(16:0/18:2)	Spermine	D-galactosamine
Taurine	4-hydroxy-L-phenylglycine	N-acetyl-L-methionine	Glucose-1-phosphate	LysoPC(20:4)
LysoPE(20:4)	PC(36:4)	PC(36:4)	Glyceraldehyde-3-phosphate diethyl acetal	Tyramine
C18-carnitine	SM(32:2)	Pterin	PC(37:4)	PC(37:5)
Oxoglutaric acid	LysoPE(18:0)	PAF-C16	Methyl jasmonate	10-hydroxy capric acid
L-aspartic acid	Glucose-1-phosphate	PC(40:9)	L-palmitoyl-carnitine	Omega-hydroxydodecanoic acid

N-aceyl-L-phenylalanine	LysoPC(14:0)	N-alpha-acetyl-lysine	C18-carnitine	Sorbate
Inosine	Xanthine	LysoPC(16:0)	Trigonelline	All-trans-retinoic acid
Alpha-glucose	N-acetyl-L-methionine	4-hydroxy-L-phenylglycine	LysoPC(20:4)	LysoPE(20:4)

Table S3: List of most downregulated metabolites within each condition in HEK293T cells

TDP-43 vs Empty	**13R4 vs Empty**	**D7 vs Empty**	**TDP-43/13R4 vs TDP-43**	**TDP-43/D7 vs TDP-43**
Glucose-1-phosphate	Aminoadipic acid	Phosphorylcholine	Inosine-5'monophosphate	Inosine
Spermidine	Uridine-5'-diphosphoglucose	Citicoline	7-dehydroxycholesterol	Inosine-5'monophosphate
Deoxyadenosine monophosphate	Citicoline	Aminoadipic acid	PE(22:6/18:1)	PE(16:0/22:6)
Trigonelline	Spermidine	Uridine-5'-diphosphoglucose	Inosine	PC(40:9)
Spermine	Creatine phosphate	Spermidine	Cytidine	Uracil
4-hydroxy-L-phenylglycine	Phosphorylcholine	Creatine phosphate	Fumarate	Cytidine
PC(40:8)	L-glutamine	L-glutamine	Lactate	Pyridoxal-5'-phosphate
Sphinganine	Glutathione	Oxoglutaric acid	Glutathione	Uridine
Uridine-5'-monophosphate	O-succinyl-L-homoserine	Trigonelline	Pyridoxal-5'-phosphate	Lactate
Nicotinic acid	Propionylcarnitine	Creatinine	Uracil	PC(36:4)
Methyl jasmonate	S-adenosylmethionine	Propionylcarnitine	Malate	L-acetylcarnitine
Ornithine	L-acetylcarnitine	L-acetylcarnitine	PC(40:9)	7-dehydroxycholesterol
PC(37:4)	Creatinine	PC(o-20:4/2:0)	Uridine	PC(31:0)
PC(40:1)	Thiamine	SM(38:1)	Glucosamine-6-phosphate	Citicoline

Glyceraldehyde-3-phosphate diethyl acetal	Oxoglutaric acid	PC(o-20:6/2:0)	L-proline	L-palmitoylcarnitine
SM(38:2)	3-dehydroxycarnitine	Succinic acid	L-arabitol	Fumarate
Riboflavin	Allantoin	Butyrylcarnitine	L-acetylcarnitine	Hypoxanthine
PC(39:4)	Glutamate	3-dehydroxycarnitine	PE(16:0/22:6)	Glycerophosphocholine
L-serine	L-aspartic acid	Glutathione	N-acetyl-L-glutamic acid	Uridine-5'-diphosphoglucose
PC(38:8)	PC(35:4)	Sarcosine	Glycerophosphocholine	N-acetyl-L-methionine
All-trans-retinoic acid	Creatine	PC(35:4)	Uridine-5'-diphosphoglucose	Succinic acid
Elaidic acid	Sarcosine	Thiamine	L-methionine	Glutathione

e. Discussion

The targeting of TDP-43 using antibodies and antibody fragments has gained extensive interest in the last years. Several monoclonal antibodies targeting the C-terminal domain of TDP-43 have been developed, and were able to increase the uptake of TDP-43 by microglia as well as decrease the spread of TDP-43 pathology in mice (Afroz et al., 2023; Audrain et al., 2023; Chevalier et al., 2024). In another study, active immunization of an ALS mouse model against the C-terminal peptide of TDP-43 was able to decrease NfL levels and slightly improve the neuroinflammatory profile of mice (Riemenschneider et al., 2023). Monoclonal antibodies mainly function in the extracellular space and exert their effect on released TDP-43. Therefore, such approach leverages the prion-like behaviour of TDP-43 (Nonaka & Hasegawa, 2020) aiming to neutralize or prevent its harmful effects. Another approach would be to target intracellular TDP-43, which requires molecules smaller than full-length immunoglobulins to be internalized by cells. For this reason, researchers started designing anti-TDP-43 antibody fragments. scFv molecules specifically targeting the RRM1 and RRM2 domains of TDP-43 have been developed and were found to decrease TDP-43 aggregation and improve disease states in mice (Pozzi et al., 2019; Tamaki et al., 2018). Monoclonal antibody-derived scFvs targeting an epitope on the N-terminal domain that becomes exposed in cytoplasmically aggregated TDP-43 were also designed and were able to decrease TDP-43 aggregates (B. Zhao et al., 2021). In 2022, Gilodi and her colleagues used *in* silico prediction models to design and optimize a single domain intrabody against TDP-43 (Gilodi et al., 2022). An interesting feature of antibody fragments is that their small size allows them to target epitopes on TDP-43 that cannot be accessed by larger immunoglobulins. All these studies highlight the therapeutic potential of targeting TDP-43 using different antibody formats in ALS.

We were interested in developing scFv molecules that can target wildtype human TDP-43, which is the form most commonly found to be implicated in ALS, both in familial and sporadic forms. We followed a different approach using a non-targeted high throughput phage display screening against the full-length wildtype human TDP-43, in an attempt to identify new clones that can potentially target novel sites on TDP-43. Indeed, *in silico* predictions revealed new 3D target regions spanning various domains. Future studies will use

TDP-43 with mutations in the predicted binding sites to accurately identify the epitopes and their potential contribution to the function of TDP-43.

When studying the effect of the scFvs *in vitro*, it was not clear to us why D7 was able to bind to recombinant full-length TDP-43 outside cells but its effect inside cells was limited to the TDP-35 CTF. We believe that it might be due to different conformations and/or stability of full-length TDP-43 and TDP-35 CTF inside cells and subsequently, different binding affinities and/or sites of D7 to these proteins. The therapeutic potential of targeting TDP-35 is interesting given the detrimental effects of TDP-35 on the cell. It's a fragment that mainly localizes in the cytosol because it lacks the nuclear localization signal, and forms cytoplasmic aggregates that can sequester full-length TDP-43 and various RNA molecules (M. Che et al., 2011a; M.-X. Che et al., 2015; Nishimoto et al., 2010). All these observations make TDP-35 CTF a valid and important therapeutic target that can spare functional, full-length, and nuclear TDP-43.

In addition to the direct effect of the scFv on TDP-43, we investigated its effect on the metabolomic profile of cells. In fact, TDP-43 proteinopathy has been linked to various metabolic alterations (Andrés-Benito et al., 2021; Ceron-Codorniu et al., 2024; Floare & Allen, 2020; Lanznaster et al., 2019). We mainly detected changes related to the metabolism of lipids, particularly glycerophospholipids and carnitines. Three of the detected metabolites that were altered following TDP-43 overexpression returned to normal levels when the scFv was co-overexpressed with TDP-43, suggesting protective effects downstream of TDP-43. Despite the limited data that can be collected from cells in culture, these results reinforce the potential of using metabolomics to monitor the effect of targeting TDP-43 proteinopathy in early drug development.

Overall, our study offers a new scFv molecule that can target different aspects of TDP-43 proteinopathy including cytoplasmic aggregation and metabolomic changes. They also highlight the importance of identifying new parameters other than TDP-43 mislocalization/aggregation or cell death to study the effect of drugs on TDP-43, especially at earlier stages of the disease.

Following the identification of protective effects for the scFv *in vitro*, the next question was enhancing the delivery of the scFv into cells. Therefore, the third part of the project focused on increasing the internalization of the scFv into cultured cells using biocompatible nanoparticles called SPIONs which could be used in subsequent steps to allow the targeted delivery of the scFv into specific regions of the CNS *in vivo*.

VI. Development of SPION-scFv complexes for guided intracellular delivery of the scFv

A. Résumé en Français

Les scFv ont une petite taille (25-30 kDa), ce qui permet leur livraison intracellulaire, mais ils ne sont pas facilement internalisés par les cellules, ce qui complique leur utilisation pour cibler des protéines intracellulaires (E. G. Kim et al., 2020; J. Li et al., 2024). De plus, la courte demi-vie des scFv (Hutt et al., 2012; Z. Li & Shah, 2019) présente un obstacle à leur livraison aux tissus cibles et nécessite l'administration de grandes quantités, augmentant ainsi le risque d'effets secondaires. La barrière hémato-encéphalique (BHE) pose aussi un obstacle majeur, avec moins de 0,1% des anticorps administrés par voie périphérique pouvant la traverser. Pour résoudre ces problèmes et améliorer la stabilité des scFv, des complexes PEGylés SPION-scFv ont été développés dans cette partie du projet. Les SPIONs (nanoparticules magnétiques à base d'oxide de fer) peuvent être internalisés par les cellules et dirigés vers une région spécifique du corps via un champ magnétique (Balk et al., 2021; Gu et al., 2011; Gusliakova et al., 2024; Prijic et al., 2010). Des études précédentes ont fonctionnalisé de manière covalente des SPIONs avec des scFv pour cibler des récepteurs spécifiques de la surface des cellules (Hervé-Aubert et al., 2018; X. Liu et al., 2019; Nguyen et al., 2020). Cependant, l'utilisation des SPIONs pour délivrer des scFv thérapeutiques vers des cibles intracellulaires n'a pas encore été explorée.

Le scFv D7 a été purifié à partir de cellules E. coli (BL21(DE3)pLysS). Les SPIONs PEGylés ont été synthétisés et fonctionnalisés avec des fluorophores et des molécules de PEG par l'équipe Nanomédicaments et Nanosondes de l'université de Tours (Alric et al., 2016; Hervé et al., 2008; Nguyen et al., 2020). Nous avons évalué le diamètre hydrodynamique, le potentiel zeta et la capacité à retenir le scFv de différentes formulations ayant des rapports de masse

(MR = m_{Fe}/m_{scFv}) différents allant de 20 à 100. Les paramètres des formulations de MR50 et MR73.5 étaient les mieux adaptés à une bonne internalisation cellulaire potentielle, nous poussant à utiliser ces deux formulations dans les expériences qui suivent. La complexation du scFv avec les SPIONs a réduit la taille des scFv (qui sont facilement agrégés en solution) tout en diminuant leur charge négative. L'analyse de décomplexation par héparine a confirmé une bonne complexation entre les SPIONs et le scFv D7, se basant sur des forces électrostatiques faibles, avec libération du scFv en présence de l'héparine qui est négativement chargée. Les complexes SPION-scFv, avec un diamètre hydrodynamique inférieur à 100 nm et une charge de surface neutre, ont montré une bonne rétention du scFv à 37°C, mais des études supplémentaires sont nécessaires pour tester leur stabilité en présence de sérum.

Les tests de cytotoxicité sur des HEK293T ont montré qu'après 4 heures de traitement, les complexes SPION-scFv ne sont pas toxiques pour les cellules. Toutefois, une réduction de 50% de la viabilité cellulaire a été observée après 24 heures à des concentrations élevées de SPION-scFv, mais pas de SPION ou de D7 seuls. Cela peut être due à un stress cellulaire plus élevé lié à leur combinaison. Lors d'un test préliminaire, nous avons observé l'internalisation des SPIONs et des scFv dans des cellules HEK293T, avec une meilleure efficacité pour le MR73.5 comparé au MR50. Les SPIONs ont aussi augmenté l'internalisation des scFv, même sans utilisation de champ magnétique ou fonctionnalisation avec un ligand spécifique (Luo et al., 2018; Tan et al., 2023; X. Xiao et al., 2020). Ces résultats devront être validés, et des études futures devront examiner la localisation intracellulaire des SPION-scFv et leur impact sur la protéinopathie liée à TDP-43.

B. Context

The small size of scFvs allows for their intracellular delivery to target cytoplasmic proteins. However, these scFvs are not readily internalized by cells, therefore complicating their use to target proteins like TDP-43. In addition, the short half-life of scFvs (Hutt et al., 2012; Z. Li & Shah, 2019) complicates their delivery to target tissues and necessitates the administration of large amounts, thus increasing the risk of off-target side effects. To overcome these obstacles, we decided to develop PEGylated SPION-scFv complexes. The

potential of SPIONs lies in their ability to be internalized by cells, and to be directed towards a specific region in the body using a localized magnetic field (Balk et al., 2021; Gu et al., 2011; Gusliakova et al., 2024; Prijic et al., 2010). Previous studies have covalently functionalized SPIONs to scFv molecules that target specific cell receptors, allowing for these SPIONs to be internalized by specific cell types (Hervé-Aubert et al., 2018; X. Liu et al., 2019; Nguyen et al., 2020). However, the use of SPIONs to deliver scFv molecules to intracellular targets has not been explored yet.

C. Materials and methods

a. Purification of the scFv from BL21(DE3)pLysS E.coli

The purification of the scFv D7 from BL21(DE3)pLysS cells was performed as previously described in [Publication 5]. Briefly, a starter culture of BL21(DE3) pLysS E.coli transformed with the D7-coding plasmid in sterile LB broth containing 1% glucose and 100 µg/mL ampicillin was incubated in a shaker at 37°C. When the OD at 600 nm reached a value of 0.4-0.6, the starter culture was transferred to 500 mL of fresh sterile LB broth supplemented with autoinducing medium, 2 mM $MgCl_2$ and 100 µg/mL ampicillin. The culture was incubated at 37°C for 3 hours then at 22°C overnight. The pelleted bacteria were resuspended in lysis buffer and incubated on a shaker for 15 minutes at 4°C, then sonicated on ice. The lysate was centrifuged at 15,000 x g for 20 minutes at 4°C and the supernatant was collected. 1 mL of equilibrated Ni-NTA resin was mixed gently with the supernatant for 1 hour at 4°C. The lysate/Ni-NTA resin mixture was loaded into a column washed with ice cold lysis buffer supplemented with 25 mM imidazole. The scFv was then eluted using cold lysis buffer supplemented with 250 mM imidazole. Following analysis by SDS-PAGE for the presence of the scFv, the selected fractions were pooled and dialyzed against distilled water overnight at 4°C. The dialyzed product was concentrated to 0.5 mg/mL and stored at 4°C for up to 3 weeks.

b. PEGylated SPION synthesis and nanocomplex formulation

PEGylated SPIONs were provided to us by the team “Nanomédicaments et Nanosondes” of the Faculty of Pharmacy of the University of Tours. The synthesis of the nanoparticles was performed according to a previously published protocol (Alric et al., 2016; Hervé et al., 2008).

Briefly, SPIONs were synthesized following the Massart protocol (Massart, 1981), then silanized by bonding the hydroxyl group on the surface of SPIONs to aminated trialkoxysilane. The silanized SPIONs were successively functionalized with fluorescent dye (sulfocyanine-5 NHS) and PEG molecules (methoxypoly(ethylene glycol) 5000 propionic acid N-succinimidyl ester, CH3O-PEG-NHS) in DMSO for 24 hours. The suspension of fluorescent PEGylated nanoparticles was dialyzed against water for 48h at 4°C, with a change in the acceptor volume of water every 1 hour (Nguyen et al., 2020). After dialysis, the aqueous suspension of nanoparticles was reconcentrated by Vivaspin (cut-off 30kDa) and the total iron concentration was determined by atomic absorption spectrophotometry. The hydrodynamic diameter and the polydispersity index of suspension were determined using a Nanosizer apparatus (Zetasizer, Malvern Instrument).

The complexation was performed on ice in MilliQ water containing 0.1% Tween (v/v). The formulation was prepared by adding the solution containing the scFv to an equal volume of the solution containing the SPIONs in order to obtain the desired mass ratio (m_{Fe}/m_{scFv}) and a final scFv concentration of 20 µg/mL.

c. Hydrodynamic diameter and zeta potential analyses

The hydrodynamic diameter (D_H) and the zeta potential were measured using a Nanosizer apparatus (Zetasizer®, Malvern Instrument, UK). To fix the ionic strength, the SPION-scFv formulations were diluted at 1:25 (v/v) in 0.01 M $NaNO_3$. All the measurements were performed at 25°C in triplicates. Results are presented as mean ± SD.

d. Complexation analysis

To verify the complexation of the scFv to the SPIONs in formulations with different MR values, we resolved the equivalent of 200 ng of D7 using 4-20% precast stain-free gels (Biorad). The proteins were then transferred to a 0.2 µm PVDF membrane. After blocking with 5% non-fat dry milk dissolved in TBS-T (0.1%, Tween 20) for 1 hour at room temperature, the blot was incubated with primary anti-6*His antibody coupled to horseradish peroxidase (1:10,000 ; HRP-66005; Proteintech) for 1 hour at room temperature to detect the free, uncomplexed scFv. Visualization of the protein bands was achieved using the Clarity Max™ Western ECL Blotting (Bio-Rad) on a ChemiDoc™ Touch Imaging System (Bio-Rad).

e. Heparin decomplexation assay

To release the scFv from the SPION and verify their integrity after formulation, heparin was added to each formulation, at a final concentration of 3 mg/mL or 5 mg/mL, at a temperature of either 4°C or 37°C. The equivalent of 200 ng of scFv was deposited on a gel, and Western blot was performed as previously described.

f. Cell culture

HEK293T cells (ATCC® CRL-3216™) were maintained at 37°C and 5% CO2 in DMEM (Gibco) supplemented with 5% FBS. The cells were harvested using Trypsin and passaged once they reached a confluency of 90%.

g. Cell treatment

For subsequent experiments, once cells reached 60% confluency, they were treated with the equivalent of 160 ng/cm^2 or 320 ng/cm^2 of scFv either complexed to SPIONs at MR values of 50 and 73.5, or complexed to the commercial cationic polymer PULSin (Polyplus Transfection®). For the SPION-scFv treatment, the solution was added directly to the culture medium (DMEM, 5% FBS) and left for 4 or 24 hours. The PULSin-scFv treatment was done according to the manufacturer's protocol. Briefly, the treated cells were left in a reduced serum medium Opti-MEM (Gibco) for 4 hours. The cells were then either used for subsequent experiments (t=4 hrs) or incubated back in DMEM supplemented with 5% FBS for an additional 20 hrs (t=24 hrs).

h. Cytotoxicity assay

Cell viability was assessed using the MTT reduction assay. HEK293T cells were seeded at a density of 15,000 cells/well in a 96-well plate. Cells were treated with scFv complexed to either SPION or PULSin according to the protocol described in section 2b. Cell treatments with equivalent concentration of SPIONs alone were also performed. Cells treated with the vehicle solution were used as a negative control while cells treated with 10 mM H_2O_2 were used as a positive control. The medium was then removed, and the cells were incubated for 30 minutes

at 37°C with 5% CO2 with 100 µL of 0.5 mg/mL MTT (Sigma-Aldrich®) dissolved in DMEM/5% FBS. The MTT was removed and 100 µL of DMSO was added to each well. The plate was agitated in the dark until the solutions became homogeneous, and the absorbance was measured at 570 nm. Duplicate measurements of 6 independent experiments were performed. Results are presented as mean ± SD.

i. Internalization assay

HEK293T cells were seeded in a 12-well plate. When they reached 60% confluency, they were treated for 4 hours with the equivalent of 160 ng/cm^2 of scFv complexed to SPIONs at MR values of either 50 or 73.5. The internalization of the SPION into cells was assessed via flow cytometry by detecting the fluorescent signal of the sulfocyanine-5. Briefly, cells were harvested and counted using trypan blue in a cell counting chamber slide (Invitrogen, Carlsbad, CA). The cells were then washed twice by centrifuging them at 110 rpm for 5 min and resuspending them in PBS. A total of 300,000 cells were then used for flow cytometry analysis. We were unable to specifically detect the scFv using flow cytometry. For this reason, the remaining cells were lysed in ice-cold RIPA supplemented with 1X Halt Protease Inhibitor Cocktail (Thermo Fisher Scientific), and an SDS-PAGE using an antibody anti-6*His tag was performed to detect the internalization of the scFv. Protein concentrations were measured using Pierce® 660nm Protein Assay reagent (Thermo Fisher Scientific). A total of 40 µg of proteins was migrated by SDS-PAGE then transferred to a 0.2 µm nitrocellulose membrane. The membranes were blocked for 2 hours using TBS-Tween20 (0.1%) containing 5% non-at dry milk and incubated at 4°C overnight with an HRP-conjugated mouse anti-6xHis antibody (66005-1-Ig, Proteintech®) diluted 100,000-fold. Visualization of bands was realized with Clarity MaxTM Western ECL Blotting (Bio-Rad) on a ChemiDocTM Touch Imaging System (Bio-Rad).

j. Statistical analysis

GraphPad Prism 8 was used for statistical analyses. Values were expressed as mean ± standard deviation (SD). For cytotoxicity assays, Kruskal-Wallis was used to compare treatment groups to the non-treated group at the same time point. Values were considered to be statistically significant when p-value < 0.05.

D. Results

a. Size and zeta potential analyses

The purification of the scFv D7 yielded a protein at approximately 28 kDa (Fig.15). In an aqueous solution containing Tween-20 at 0.1% (v/v), the D_H of the SPION alone and the scFv alone were 47.5 ± 2.4 nm and 306.7 ± 54.6 nm, respectively. The addition of SPIONs to the scFv solution yielded much smaller complex sizes ranging from 69.4 ± 0.6 to 125.2 ± 0.9 nm. Moreover, the complexation of the scFv to the SPION led to a decrease in the negative surface charge of the molecule, going from -11 ± 1.2 mV to relatively neutral values.

SPION-scFv complexes with MR values of 50 and 73.5 had the lowest polydispersity index (PdI) of 0.2 ± 0.0005 and 0.26 ± 0.02, respectively. They also had the smallest D_H, with values of 69.4 ± 0.6 nm for MR 50 and 74.4 ± 1.6 nm for MR 73.5, making them more suitable for biological assays (Fig.16). For these reasons, the experiments that followed were focused on these two MR values.

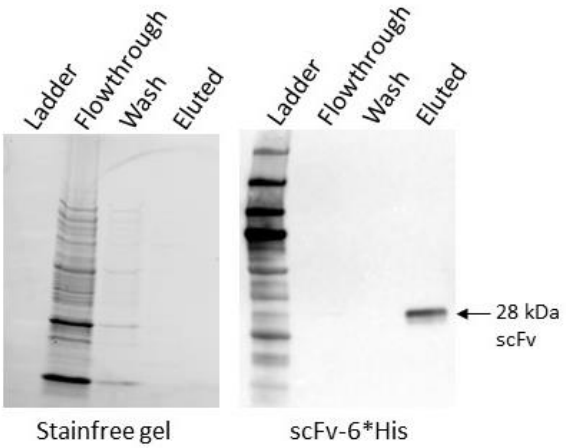

Figure 15: Purification of the scFv. Stainfree and immunoblot of the 6*His-tagged scFv D7 showing the purification process of the scFv. A single 28 kDa fragment was detected in the eluted fraction.

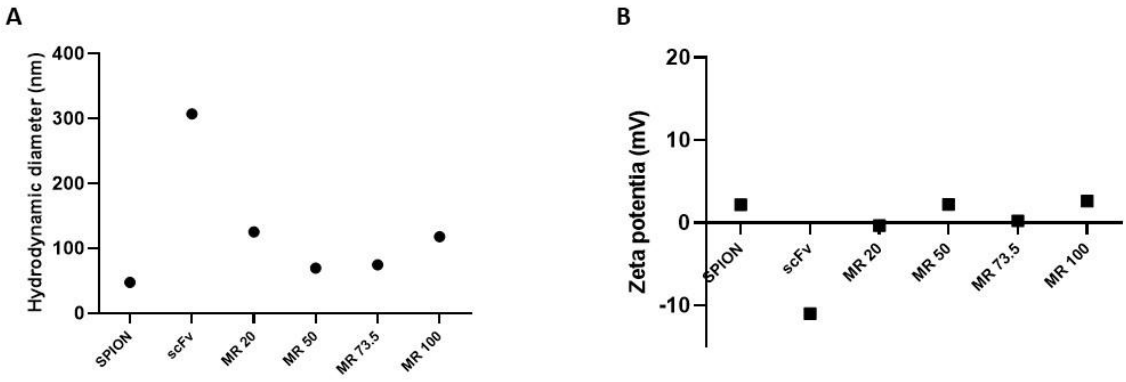

C

Formulation	Hydrodynamic Diameter (nm)	Polydispersity Index (PdI)	Zeta Potential (mV)
SPION	47.5 ± 2.4	0.5 ± 0.06	2.2 ± 0.1
scFv	306.7 ± 54.6	0.6 ± 0.08	-11 ± 1.2
SPION-scFv (MR 20)	125.2 ± 0.9	0.5 ± 0.02	0.3 ± 0.2
SPION-scFv (MR 50)	69.4 ± 0.6	0.2 ± 0.0005	2.2 ± 0.06
SPION-scFv (MR 73.5)	74.4 ± 1.6	0.26 ± 0.02	0.2 ± 0.1
SPION-scFv (MR 100)	117.9 ± 4.5	0.41 ± 0.06	2.62 ± 0.3

Figure 16: Characteristics of the SPION, scFv, and SPION-scFv complexes. **A)** Hydrodynamic diameter (nm) and **B)** zeta potential (mV) of the SPION alone, the scFv alone, and the SPION-scFv complexes at MR20, MR50, MR73.5, and MR100. **C)** Hydrodynamic diameter, polydispersity index (PdI), and zeta potential (mV) values of the different formulations tested.

b. SPION-scFv complexation and heparin decomplexation assay

To study the retention of D7 in the SPION-scFv complexes, we performed an SDS-PAGE. Free scFv is able to migrate in the gel while complexed scFv remains blocked in the loading wells. In order to release the scFv from SPIONs, a heparin decomplexation assay was performed. As evident in Fig. 17, the migration of the scFv was significantly reduced in the absence of heparin at MR50 and MR73.5, indicating a good complexation of the scFv to SPIONs, both at 4°C and 37°C. Upon the addition of heparin at either concentration of temperature, D7 were released from the complexes and were able to migrate in the gel.

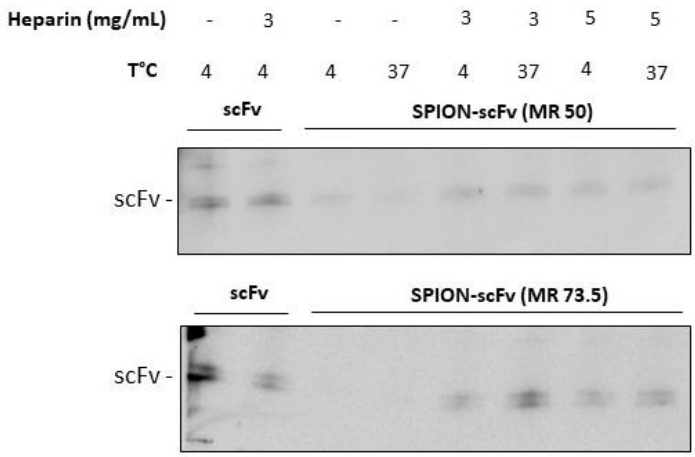

Figure 17: **Detection of free scFv**. Immunoblot to detect the free scFv D7 in SPION-scFv complexes at MR50 and MR73.5, in the presence (3 or 5 mg/mL) and absence (-) of heparin at 4°C or 37°C.

c. Cytotoxicity of the scFv and SPION-scFv complexes

We first ensured that the scFv itself is not toxic to cells following its internalization using commercial PULSin. It should be noted that the PULSin-scFv treatment needs to be done in serum-reduced media like Opti-MEM according to the manufacturer's protocol. Therefore, the cells could only be exposed to the PULSin-scFv for 4 hours, after which the culture medium needed to be changed back to fresh DMEM/5%FBS. We noted no cytotoxicity of D7 on these cells following treatment with 160 ng/cm^2 and 320 ng/cm^2 (Fig.18). We then assessed the toxicity of those same scFv concentrations following treatment with the SPION-scFv complexes having MR values of 50 and 73.5 for 4 and 24 hours. In this case, given that the SPION-scFv complexes could be added directly to DMEM supplemented with FBS, no culture medium change was done. Following 4 hours of treatment, no toxicity of the SPION-scFv was detected for concentrations equivalent to 160 ng/cm^2 and 320 ng/cm^2 of scFv and MR values of 50 and 73.5. However, following 24 hours the viability of the cells was decreased by half when they were treated with 320 ng/cm2 of D7 at either MR 50 (*p=0.03) or MR 73.5 (**p=0.009). This toxicity was not observed for 160 ng/cm2 of scFv for those same MR values (Fig.18). We also assessed the toxicity of SPIONs alone in amounts equivalent to those used in our formulations, which revealed no toxicity in the absence of the scFv at higher concentrations after 24 hours of treatment (data not shown).

Given the absence of cytotoxicity for all treatments of 4 hours, we decided to use this timepoint for subsequent experiments.

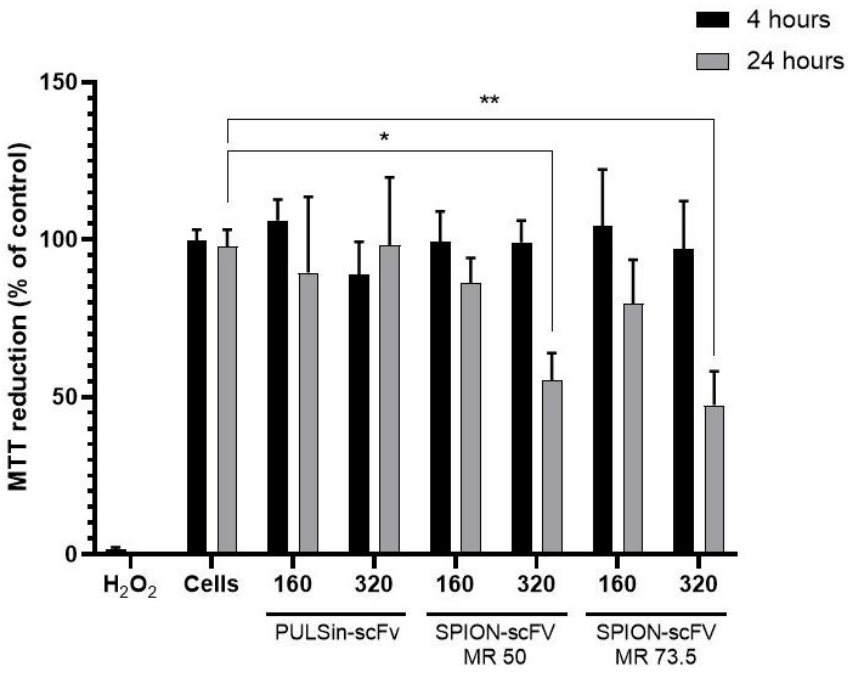

Figure 18: Cellular viability of HEK293T cells treated with SPIONs and/or scFv for 4 or 24 hrs with different formulations (MR50 and MR73.5) and concentrations (160ng/cm^2 and 320 ng/cm^2) of SPION-scFv complexes. Untreated cells were used as negative control. Cells treated with 10 mM H_2O_2 were used as positive control. Cells treated with PULSin-scFv were used to control for the scFv toxicity.

d. Internalization of the SPION-scFv complexes

When HEK293T cells were incubated with SPION-scFv complexes at MR50 and 73.5, a shift to the right in the sulfocyanine-5 signal detected by flow cytometry was observed, indicating that the SPION was internalized into the cells. A slightly bigger shift was observed for cells treated with complexes at MR 73.5, indicating a higher internalization of the SPIONs with this condition (Fig.19.A). We tried to detect the scFv inside cells using flow cytometry and a fluorophore-conjugated antibody targeting the 6*His tag. However, the signal was unspecific, leading us to consider another method to detect the scFv in cells. Western blot analysis also detected the presence of the 6*His-tagged D7 inside the same treated cells, indicating a parallel internalization of the scFv into these cells (Fig.19.B).

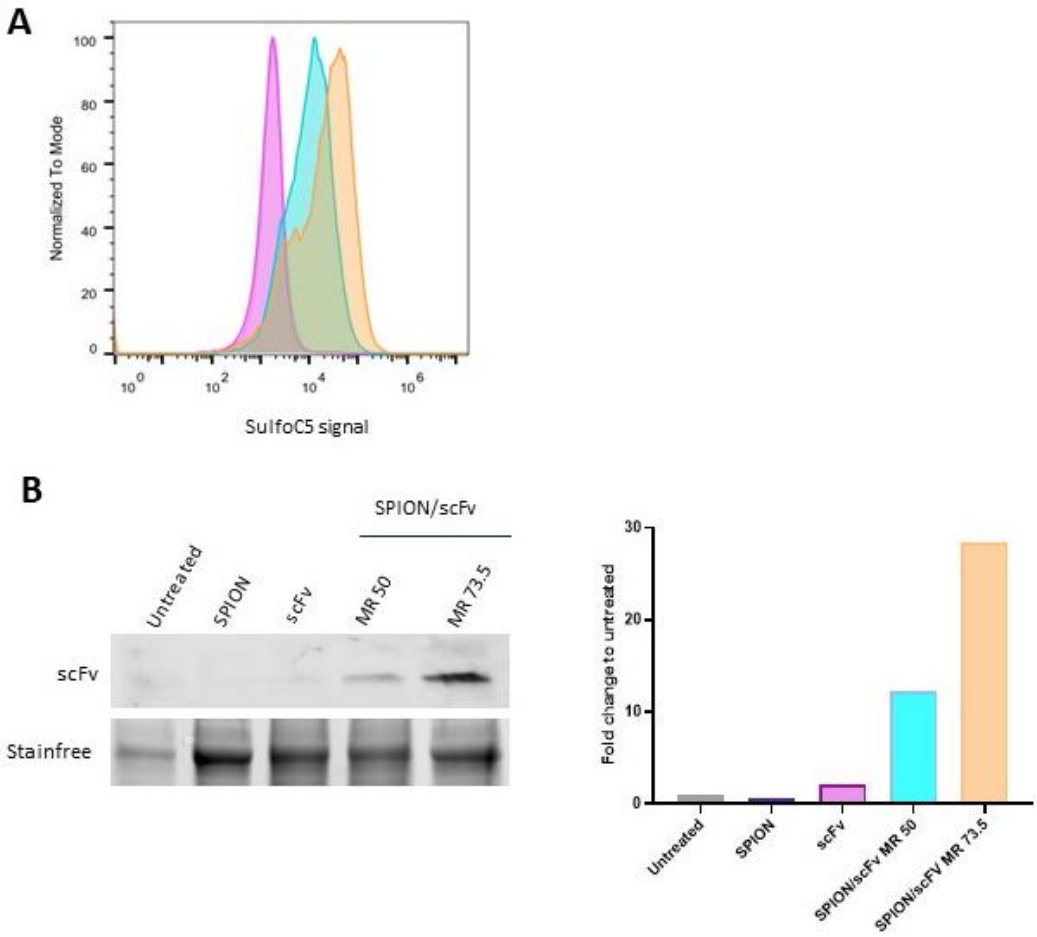

Figure 19: Internalization of the SPION and the scFv D7 into HEK293T cells following 4 hours of treatment. **A)** Flow cytometry analysis of the sulfocyanine-5 fluorescence in treated HEK293T cells. **B)** Immunoblot and quantification of the 6*His-tagged scFv in treated HEK293T cells. Fold change was calculated following normalization of each condition to the corresponding stainfree lane, then comparing it to the untreated condition. Grey: untreated cells; pink: cells treated with PULSin-delivered scFv; Blue: Cells treated with 160ng/cm2 of SPION-scFv at MR50; Orange: Cells treated with 160ng/cm2 of SPION-scFv at MR73.5. N=1.

E. Discussion

While using scFvs to target intracellular proteins like TDP-43 seems like a promising strategy due to their good affinity and small size, delivering the scFv into the target cells is more complicated, especially when targeting the CNS. The half-life of scFvs *in vivo* is generally short, typically ranging from few minutes to few hours. This is mainly due to their small size (about 25-30 kDa) which leads to rapid renal clearance and reduced serum stability compared to full-length antibodies (Go et al., 2024; Kontermann, 2009; Schneider et al., 2016). In

addition, scFvs are not easily internalized into cells, especially when they do not target surface receptors (E. G. Kim et al., 2020; J. Li et al., 2024; Neve et al., 2001). Moreover, delivering biotherapeutics to the CNS has always been a major challenge due to the fact that less than 0.1% of peripherally administered antibodies can cross the BBB, necessitating large amounts to be administered, and increasing the risk of potential side effects (P. Zhao et al., 2022). For all these reasons, we decided to use PEGylated SPIONs in order to enhance the use of the scFv for TDP-43 targeting in the CNS. The PEG coating of the nanoparticles increases their biocompatibility and size, making them more soluble and less toxic, increasing their circulation half-life by decreasing their rapid clearance by the kidneys, and decreasing their take up by phagocytic cells (L. Xia et al., 2022). We selected SPION-scFv complexes with a hydrodynamic diameter smaller than 100 nm and a relatively neutral surface charge, to increase their chances of being taken up by cells. These nanocomplexes at MR50 and MR73.5 had a good scFv retention capacity at 37°C but further experiments still need to assess the stability of such complexation in solutions with different concentrations of serum. The fact that the scFv was released from the nanocomplexes upon the addition of heparin, a competitive negatively charged glycosaminoglycan, indicates that the scFv is associated with SPIONs mainly through electrostatic interactions, and that the stability of the nanocomplexes can be compromised by negatively charged molecules (Egberink et al., 2023). The MTT reduction assays that were performed indicated a certain degree of toxicity when treating cells with higher concentrations of SPION-scFv complexes, whether at MR50 or MR73.5. The fact that such toxicity was not observed for cells treated with the equivalent amount of scFv or SPIONs indicate that the combination of both was probably too stressful for cells, overwhelming them and leading to their cytotoxic death. In a preliminary assay, we were able to detect the internalization of both the SPION and the scFv into HEK293T cells. The detection of the scFv was done by western blot because it was not successful by flow cytometry, probably due to the lack of specificity in flow cytometry of the different anti-6*His antibodies that we tested. An interesting finding was that the SPIONs increased significantly the internalization of the scFv even without the application a guiding magnetic field or the functionalization of the SPION to a cell surface receptor ligand (Luo et al., 2018; Tan et al., 2023; X. Xiao et al., 2020). These results will need to be validated. Future studies will also need to assess the internalization of the SPION-scFv into cells, examine their intracellular localization, and evaluate their effect on TDP-43 proteinopathy in a HEK293T cell model.

The targeting of extracellular proteins using SPIONs covalently conjugated to scFvs has been previously tested in some neurodegenerative diseases. For example, SPIONs conjugated to anti-amyloid β precursor protein have shown great diagnostic and therapeutic potentials in Alzheimer's disease mouse models, by both detecting and promoting the clearance of amyloid β plaques (X.-G. Liu et al., 2020, 2020). However, to our knowledge, the reversible complexation of the scFv to SPIONs has not been tested. The non-covalent physical adsorption of the scFv to SPIONs relies on weak interactions such as electrostatic attractions, and presents with several advantages and disadvantages (Di Nardo et al., 2019; J. H. Lee et al., 2023). The technique is relatively simple and does not require extensive chemical modifications (Owen et al., 2013; J. Park et al., 2020). This preserves the native structure and functional properties of the scFv. In addition, the interaction is reversible, which is beneficial for certain applications where temporary complexation is desired. In our case, the goal is to maintain the complexation until the SPION-scFv complex reaches the target cells, where it can dissociate upon internalization and contact with the intracellular environment (e.g. cytoplasm or lysozomes). Future steps in our study will need to assess the intracellular localization of the SPION and scFv and optimize their intracellular behavior. For instance, to ensure that the scFv is liberated in the cytoplasm, cationic polymers like chitosan or poly-arginine can be added to the formulation to allow for a better complexation of anionic molecules like our scFv, thus enhancing the stability of the SPION-scFv complex (Ben Djemaa et al., 2018; Bruniaux et al., 2017; Plianwong et al., 2013). In addition, these polymers can enhance the delivery of therapeutic molecules to the cytoplasm and allow for the endosomal escape of the nanocomplex through their proton sponge effect (Bruniaux et al., 2017; Wojnilowicz et al., 2019). Briefly, following the uptake of nanocomplexes via endocytosis, they become trapped in endosomes which the cell attempts to acidify by pumping in protons (Shirsat et al., 2024). Cationic polymers buffer these protons, causing more protons, chloride ions and water to enter the endosome. This leads to increased osmotic pressure and swelling, ultimately causing the endosomal membrane to rupture and release the nanoparticles into the cytoplasm, therefore preventing their degradation in lysosomes (Shirsat et al., 2024).

The administration of the scFv via SPIONs might present with some complications. Since non-covalent physisorption between the scFv and SPION is based on weak interactions, it has some disadvantages such decreased stability and increased sensitivity to environmental

changes like pH, ionic strength, and complex biological environments (Di Nardo et al., 2019). In addition, it is harder to control, resulting in possible reproducibility issues (Oliveira et al., 2019). Moreover, despite the fact that PEG is generally safe for coating nanoparticles, some studies have detected anti-PEG antibodies following repeated administration of PEG-coated nanoparticles, resulting in accelerated blood clearance (W.-A. Chen et al., 2023; Ju et al., 2022; H. Wang, Wang, et al., 2023). For all these reasons, the PEGylated SPION-scFv nanocomplexes might be better suited for MRI-based diagnostic or follow-up purposes, such as detecting TDP-43 aggregates, where sustained high tissue concentrations and frequent administrations are not needed. Otherwise, we can envision covalently conjugating the scFv to the SPIONs to test their behaviour in targeting cytoplasmic TDP-43.

The demonstrated protective effects of the scFv in a cellular model of ALS led us to take this project into the next step, which is the preclinical assessment of the scFv. However, in order to assess the effect of the scFv on the full spectrum of ALS pathology, we needed a detailed characterization of a TDP-43 mouse model at different disease timepoints in order to identify quantifiable parameters that are associated with ALS progression and that can be used to evaluate the effect of the scFv. For this reason, the fourth objective of our project focused on undertaking a detailed evaluation of the Prp-TDP-43^{A315T} ALS mouse model using phenotypic, molecular and omics approaches.

VII. Characterization of a transgenic TDP-43 mouse model of ALS

Publication 6

Characterization of functional and biological parameters in a longitudinal study of TDP-43^{A315T} transgenic mice, a preclinical model of amyotrophic lateral sclerosis (Submitted, under review).

a. Résumé en Français

Le développement de modèles animaux de la SLA a été crucial pour comprendre la physiopathologie de la maladie et explorer des stratégies thérapeutiques. Les modèles les plus utilisés sont les souris transgéniques exprimant des formes mutées du gène humain SOD1. Cependant, ces modèles ne répliquent pas une caractéristique clé de la majorité des cas de SLA : la protéinopathie liée à TDP-43. Les modèles murins de TDP-43 de la SLA surexpriment généralement la forme sauvage ou mutée de TDP-43, provoquant des phénotypes similaires à la SLA. Cette étude se concentre sur le modèle Prp-TDP-43^{A315T}, qui surexprime la TDP-43^{A315T} mutée dans le système nerveux sous le contrôle du promoteur de la protéine prion. L'objectif était de fournir une analyse phénotypique et moléculaire détaillée de ce modèle pour mieux comprendre les conséquences de la protéinopathie TDP-43 et identifier de nouveaux marqueurs thérapeutiques potentiels.

Deux cohortes de souris femelles transgéniques (Tg) et sauvages (WT) ont été utilisées. La première (cohorte 1) a été suivie de 50 à 400 jours, avec trois points d'évaluation principaux: avant l'apparition des symptômes (T0), au début des symptômes (T1), et au stade

terminal de la maladie (T2). Des analyses phénotypiques telles que le poids corporel, la force de préhension, la position de la queue et l'altération de la démarche ont été effectuées sur cette cohorte. Une IRM a été également réalisée pour détecter des changements structurels dans la moelle épinière, et des analyses métabolomiques et lipidomiques ont été menées sur du sérum et du sang sur buvard. La deuxième cohorte (cohorte 2) a été utilisée pour une caractérisation moléculaire approfondie à l'apparition des symptômes (T1'). Pour cette cohorte, une analyse par western blot de différentes protéines a été effectuée sur les fractions protéiques totale et insoluble du cerveau et de la moelle épinière. Le sérum, le cerveau, le foie, et le muscle gastrocnémien ont été collectés pour des analyses métabolipidomiques.

Les souris Tg ont commencé à présenter des symptômes à T1 vers 150 jours, avec une diminution significative du poids corporel, de la force de préhension, et une altération de la démarche et de la position de la queue (Fig.1). Aucune modification structurelle de la moelle épinière n'a été détectée par IRM, bien que la TDP-43 insoluble ait augmenté dès le stade pré-symptomatique (T0) (Fig.2). Cela peut suggérer que la protéinopathie TDP-43 peut survenir sans changements structurels détectables dans cet organe. L'analyse métabolomique a révélé des profils distincts entre les souris WT et Tg à chaque temps étudié. Plus de 20 métabolites ont été significativement modifiés chez les souris Tg en phase présymptomatique (T0) dans le sérum (Fig.3). Des altérations de la PC(33_1) ont été détectées à T2 dans les échantillons de sang sur buvard (Fig.3). Dans la cohorte 2 qui a été évaluée à T1', une augmentation de TDP-43 totale et insoluble et de ses fragments C-terminaux a été observée dans le cerveau et la moelle épinière à T1' (Fig.4, 6). De même, une augmentation de TDP-43 phosphorylée a été détectée (Fig.5, 7). L'augmentation de TDP-43 totale et insoluble dans le cerveau et la moelle épinière reflète une protéinopathie généralisée. Cependant, des différences dans les bandes observées des fragments C-terminaux et de TDP-43 phosphorylée entre le cerveau et la moelle épinière indiquent des mécanismes distincts de régulation de TDP-43 dans ces tissus (Berning & Walker, 2019). Dans le cerveau, les niveaux de GFAP et de NRF2 ont augmenté (Fig.8), reflétant une astrogliose et une réponse au stress oxydatif (Habas et al., 2013), tandis que le rapport pAMPK/AMPK a diminué (Fig.8), suggérant une réponse inadéquate au stress énergétique (Barnaba et al., 2023; Muraleedharan & Dasgupta, 2022; J.-M. Park et al., 2023). Aucun changement similaire n'a été observé dans la moelle épinière. L'analyse métabolomique de la cohorte 2 a révélé des altérations dans le sérum, le cerveau et le muscle

des souris Tg par rapport aux WT à T1'. Des niveaux différents de D-glucose, taurine et D-xylose ont été détectés dans le cerveau (Fig.9), et des modifications importantes de lipides, comme les diacylglycérols, phosphatidylcholines et triglycérides, ont été observées dans le muscle (Fig.10). Ces résultats montrent une altération du métabolisme lipidique, associée à la fonction cytosquelettique, à l'inflammation, au développement neuronal et à l'apoptose.

Le modèle Prp-TDP-43^{A315T} que nous avons étudié reproduit plusieurs aspects clés de la protéinopathie TDP-43 dans la SLA, notamment l'agrégation de la TDP-43 et des changements métabolomiques et lipidomiques. De plus, notre utilisation de souris femelles permet une durée d'analyse plus longue et offre des informations complémentaires par rapport aux autres études réalisées souvent sur des mâles. Les souris Tg ont montré un dysfonctionnement moteur et un état hypermétabolique, similaire à ce qui est observé chez les patients atteints de SLA (Fayemendy et al., 2021; J. He et al., 2022). Tous ces résultats suggèrent que ce modèle est un outil important pour mieux comprendre la SLA et faciliter le développement de thérapies, car il reproduit d'importants changements phénotypiques, moléculaires, métabolomiques et lipidomiques associés à la maladie.

b. Context

The development of animal models of ALS has been crucial for understanding the pathophysiology of the disease and exploring potential therapeutic strategies. The most widely used models are transgenic mice that express mutated forms of the human SOD1 gene. These models closely mimic the clinical and pathological features of ALS, including motor neuron degeneration, muscle atrophy and progressive paralysis. However, they do not necessarily replicate a key feature of the majority of ALS cases, which is TDP-43 proteinopathy. TDP-43 mouse models of ALS typically overexpress the wildtype or the mutant form of TDP-43, either ubiquitously or in specific neuronal populations, causing ALS-like phenotypes. In this study, we focused on the Prp-TDP-43^{A315T} mouse model which overexpresses the mutated human TDP-43^{A315T} in the nervous system under the control of the prion promoter. The aim of this study was to provide a detailed phenotypic and molecular analysis of this model in order to better understanding the consequences of TDP-43 proteinopathy and possibly identify new markers for therapeutic developments.

c. Summary of materials and methods

Two cohorts of female Prp-TDP-43^{A315T} transgenic (Tg) and C57BL/6J wildtype (WT) mice were used. The first one (cohort 1) was monitored for disease progression from 50 to 400 days, at three main timepoints: before the onset of symptoms (T0), at the onset of symptoms (T1), and at the end-stage disease (T2). For this cohort, we performed weekly phenotypic characterization such as the measurement of body weight, and the recording of grip strength, tail position, and the degree of gait impairment. MRI was also performed at these same timepoints to detect any potential structural changes at the level of the spinal cord. We also collected serum at T0 and dry blood spots at T1 and T2 for metabolomic and lipidomic analyses. The second cohort (cohort 2) was used to undertake a deeper characterization of these mice at the molecular level upon the onset of symptoms at T1 (called T1'). For these mice, the brain and the spinal cord were collected for western blot analysis of TDP-43 and phosphorylated TDP-43 in the total and insoluble protein fractions, as well as other ALS-related proteins (NRF2, AMPK, pAMPK, GFAP, LC3). Additionally, the serum, brain, liver, and gastrocnemius samples were collected for metabolomic and lipidomic analyses.

d. Summary of results

The Tg mice of cohort 1 started developing symptoms at T1 around 150 days of age where they began showing a significant decrease in body weight, associated with a reduced grip strength, a lowered tail position, and an increase in gait impairment (Fig.1). Diffusion MRI data did not detect any significant changes at the level of the spinal cord of these mice at any timepoint (Fig.2). However, an increase in insoluble TDP-43 was detected in the spinal cord from the pre-symptomatic stage (T0) (Fig.2). The multivariate analysis of the serum and dry blood spots revealed two clearly distinct metabolomic profiles for the WT and Tg mice at all timepoints. Furthermore, univariate analysis revealed more than 20 metabolites that were significantly altered in the serum of Tg mice compared to the WT at T0 (Fig.3). We also detected PC(33_1) to be significantly different at T2 in dry blood sports form Tg mice compared to the WT (Fig.3).

For cohort 2 which was studied upon the onset of symptoms at T1', we observed a significant increase in total and insoluble TDP-43 and its C-terminal fragments in the brain and

spinal cord (Fig.4,6). A similar increase was observed for phosphorylated TDP-43 (Fig.5, 7). Different band patterns for TDP-43 were detected in the spinal cord compared to the brain. In the brain, there was an increase in GFAP and NRF2, and a decrease in the ratio of pAMPK/AMPK (Fig.8). No similar changes were observed in the spinal cord. Multivariate analysis of metabolites from the serum, brain, liver and gastrocnemius revealed an obvious separation of metabolomic profiles between Tg and WT mice at T1'. No discriminating metabolites were detected for the muscle or the liver. However, different levels of D-glucose, taurine and D-xylose were observed in the brain following univariate analysis (Fig.9). As for lipidomic analysis, a significant change in many lipids belonging to various lipid subsets such as diacyglycerols, phosphatidylcholine, phosphatidylethanolamine, fatty acyls, and triglycerides was detected in the muscle at T1'.

Characterization of functional and biological parameters in a longitudinal study of Prp-TDP-43^{A315T} transgenic mice, a model of amyotrophic lateral sclerosis.

Yara Al Ojaimi *[1], Samira Osman *[1], Hugo Alarcan [1,2], Patrick Emond [1,3], Charlotte Veyrat-Durebex [1,2], Debora Lanznaster [1], Antoine Lefèvre [1], Gabrielle Chicheri [1], Sandra Meme [4], Rudy Clemencon [4], Laurent Galineau [1], Philippe Corcia [1,5], Christian Andres [1,2], Patrick Vourc'h [1,2], Fabienne Masse [6], Fabrice Trovero [#6], Hélène Blasco [#1,2]

Affiliations

[1] Université de Tours, INSERM, Imaging Brain & Neuropsychiatry iBraiN U1253, Tours, France.

[2] CHU de Tours, Service de Biochimie et Biologie Moléculaire, Tours, France

[3] CHU de Tours, Service de Médecine Nucléaire In Vitro, Tours, France.

[4]CBM, Orléans

[5]CHU de Tours, Service de Neurologie, Tours, France.

[6] Key-Obs, Orléans, France

* [#] These authors contributed equally to this work

Corresponding author: Yara Al Ojaimi

E-mail: yara.alojaimi@univ-tours.fr

Present address: Université de Tours, INSERM, Imaging Brain & Neuropsychiatry iBraiN U1253, Tours, France.

Abstract

Introduction: One of the major hallmarks of ALS is the presence of cytoplasmic aggregates of the TAR DNA-binding protein 43 (TDP-43) in patients. The successive failures of clinical trials suggest a reconsideration of standard parameters to evaluate drug responses in animal models. Thus, our aim was to investigate phenotypic, molecular, and biochemical characteristics of a mouse model hemizygous for the Prp-TDP-43^{A315T} transgene.

Methodology: Prp-TDP-43^{A315T} transgenic and C57BL/6J wildtype mice were monitored from 50 to 400 days postnatal. One cohort of mice was used to monitor disease evolution, phenotypic parameters and MRI activity across three timepoints: before symptom onset, symptom onset, and end-stage disease. The second cohort was used to validate findings from cohort 1 during the established symptomatic period of the disease. At symptomatic stages, tissue samples were collected for Omics analyses, and to examine ALS-related markers.

Results: Following symptom development (T1), we observed that Tg mice from cohort 1 showed reduced body weight, decreased grip strength and tail position, as well as an increased gait impairment. Changes in brain and spinal cord of (p)TDP-43, NRF2, GFAP, and pAMPK were found in brain samples of Tg mice in cohort 2 at T1'. Metabolomic analysis highlighted shifts in specific metabolites in the brain of Tg mice. Lipidomic analysis revealed changes in Tg mice across subsets of lipid classes in the muscle.

Conclusion: The Prp-TDP-43^{A315T} mouse model recapitulates features described in other models with endogenous TDP-43 genetic variants, supporting the physiological relevance of these findings.

Keywords: Amyotrophic lateral sclerosis, TDP-43, mouse model, characterization

Introduction:

Amyotrophic lateral sclerosis (ALS) is a multifactorial fatal neurodegenerative disease characterized by the progressive degeneration of both upper and lower motor neurons, ultimately leading to the complete loss of voluntary movement and control. Patients inflicted with this disease lose the ability to move, speak, eat and breathe. ALS is mostly considered a sporadic disease, with only 5 - 10% of cases demonstrating patterns of inheritance (Shepheard et al., 2021). The incidence of ALS ranges from 2 - 3 cases per 100,000 individuals in Europe (Hardiman et al., 2017). Additionally, mostly due to the absence of current therapies, the life expectancy of patients diagnosed with ALS is a meagre 2 - 5 years following onset of symptoms (Shepheard et al., 2021), making crucial the deeper understanding of this disease and development of targeted therapies. To this end, murine models have played a key role in furthering our knowledge in the pathophysiology of ALS and have served as important platforms for the testing of potential therapeutic interventions.

One of the major pathological proteins leading to aggregates and motor neuron inclusions in ALS is the TAR DNA-binding protein 43 (TDP-43). Observed cytoplasmic aggregation of this protein has been considered as the hallmark feature of 97% of ALS patients(Mackenzie et al., 2007; Neumann et al., 2006). This discovery has marked a major event in ALS research, and as a result, has led to the generation of approximately 20 mouse models associated with this gene(Lutz, 2018). Thus, the precise phenotypic characterization of behavioral and molecular aspects of animal models with pathogenic variants in the TAR DNA-binding protein gene (*TARDBP)* gene encoding TDP-43 could increase their preclinical relevance in research and drug discovery related to ALS. In fact, in complex diseases like ALS, going beyond the standard parameters used to assess disease progression is important in order to gain a better understanding of the effect of therapeutic interventions on the various pathways directly or indirectly implicated in the disease.

Among the different TDP43 transgenic mice used in ALS studies, we focused our attention on the Prp-TDP-43^{A315T} model. The mouse prion protein (mPrp) promoter/enhancer region has been used to modelize inherited forms of neurodegenerative diseases, accomplished by driving the overexpression of transgenes in the nervous system(Wegorzewska & Baloh, 2011). In this study, we aimed to investigate the phenotypic,

molecular and biochemical characteristics of a mouse model hemizygous for the Prp-TDP-43^{A315T} transgene based on omics strategies and targeted approaches. This model overexpresses a mutant human TDP-43 cDNA harboring an N-terminal Flag tag and an A315T amino acid substitution that is associated with familial ALS. Our objectives were to provide quantitative readouts of disease progression, to determine changes in protein markers in organs/tissue affected by ALS and to determine differences in the metabolic evolution induced by the overexpression of TDP-43. These findings merit attention as they may bring new insights in two aspects: 1) in the better understanding of TDP-43 pathologies, and 2) in the assisted identification of new markers for innovative therapeutics targets.

Methods

Mice

Two cohorts of mice were used for this characterization study. The first cohort (cohort 1) included: adult, female Prp-TDP-43^{A315T} (Jax #010700) Tg mice (n=27), and adult, female C57BL/6J WT mice (n=27)(Hatzipetros et al., 2014; Wegorzewska et al., 2009). These mice were monitored for disease evolution across three different timepoints: before symptom onset (T0), symptom onset (T1), and end-stage symptom development (T2). The second cohort (cohort 2) included: adult, female Prp-TDP-43^{A315T} Tg mice (n=11), and adult, female C57BL/6J WT mice (n=10). This cohort was used to validate specific findings from cohort 1 during the established symptomatic period of the disease (T1).

Mice were housed in groups of 3-5 per cage under a 12-h light/dark cycle, with ad libitum access to food and water. Both groups of mice were maintained on DietGel(R) Boost (ClearH2O) to prevent intestinal occlusion, as described previously(Herdewyn et al., 2014). All animal experiments followed current European Union regulations (Directive 2010/63/EU), as recommended by the regional ethics committee for animal experimentation (CEEA APAFIS#31121-2021042115179336 v3).

The genetic background of Tg and WT mice used in this study was confirmed using the KAPA HotStart® (Roche) genotyping kit, according to the manufacturer's instructions. A schematic representation of the experimental protocol is shown in Diagram 1.

Diagram 1: Schematic representation of the experimental protocol used in this study.

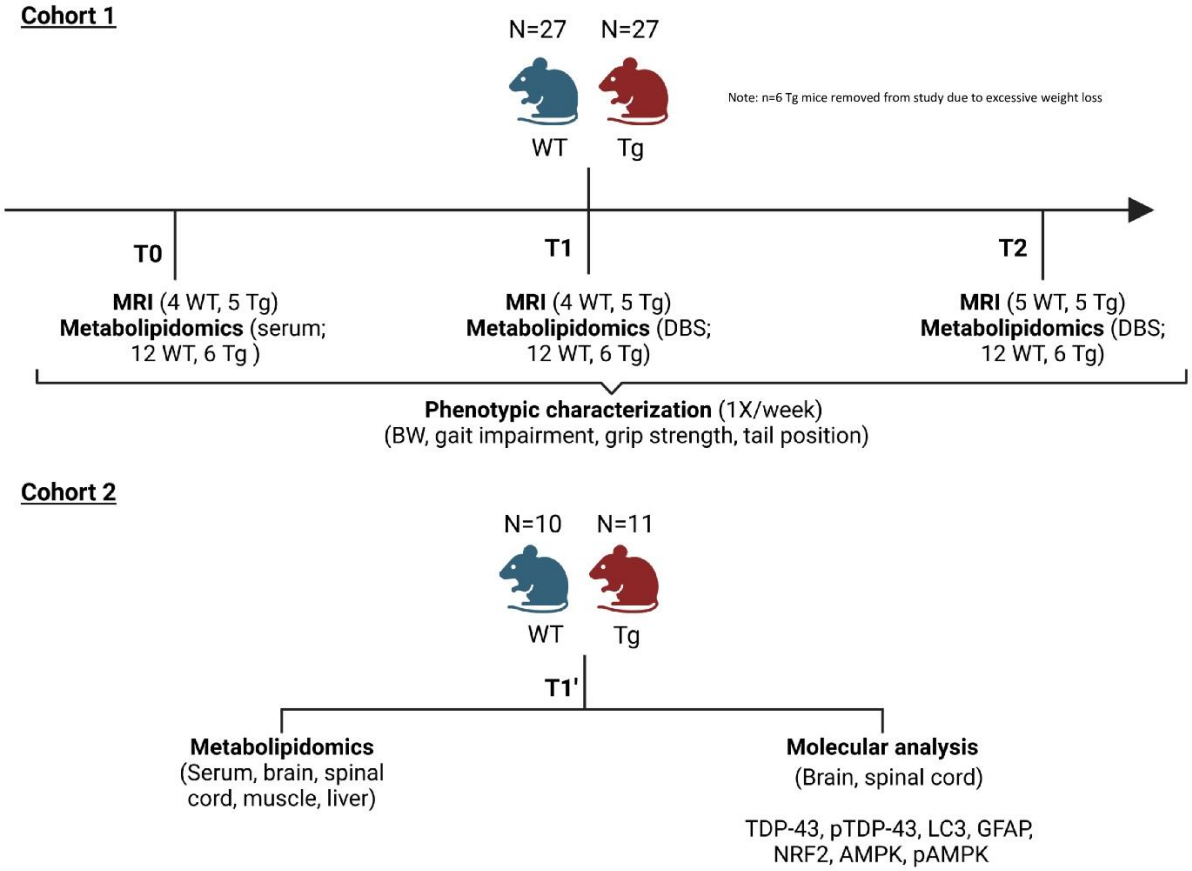

Diagram 1: Schematic representation of the experimental protocol used in this study.

Behavioral phenotypic characterization

Behavioral phenotypic characterization of Tg and WT mice was performed weekly. We analysed changes in body weight, grip strength, gait impairment, and tail position as previously described(Gautam et al., 2019; Hatzipetros et al., 2014; Yu et al., 2020). Tg mice were monitored until the end of disease evolution (i.e: end stages of life), characterized by a weight loss of more than 20% and/or motionless animal with piloerection and eyes closed and/or the moment at which mice could no longer move sideways within a 30 second timeframe. At this point, mice were euthanized by cervical dislocation.

Sample collections

For cohort 1: blood samples were initially collected from the submandibular vein at T0. However, upon disease progression (during the T1 and T2 stages) we switched blood sample collection from submandibular vein to dried blood spots (DBS) from the tail vein (two drops per mouse), as this was considered to be less invasive for mice developing symptoms.

Unfortunately, of the n=12 Tg mice reserved for Omic studies, n=6 Tg mice were required to be euthanized at the beginning of the study due to excessive weight loss following blood collection from the submandibular vein at T0. These mice were removed from the study, thus, all data (excluding MRI data) portrayed for cohort 1 only included n=6 Tg mice. Three groups of mice from cohort 1 were used for terminal MRI and associated western blot analyses of the spinal cord at T0 (WT n=4, Tg n=5), T1 (WT n=4, Tg n=5), and T2 (WT n=5, Tg n=5).

For cohort 2: brain, spinal cord, liver, and muscle tissues were collected at T1 for western blot and omics analyses. This was done following isoflurane anaesthesia and cardiac perfusion using 1x phosphate buffered saline (PBS). As these mice were being sacrificed, blood was collected for later omics analyses.

All samples were stored on dry ice, then moved to a -80ºC freezer.

Magnetic Resonance Imaging (MRI)

Diffusion MRI uses contrast that can identify structural changes in the spinal cord in neurodegenerative diseases, including ALS. Axial images of the spinal cords of WT and Tg mice were obtained for diffusion-weighted imaging at T0, T1 and T2. One WT mouse at T0 and one at T1 were excluded from the study due to stereotypies, leaving 4 WT mice for T0 and T1. MRI acquisition was performed on a 9.4T horizontal ultra-shielded superconducting magnet dedicated to small-animal imaging (94/20 USR Bruker Biospec, Wissembourg, France) and equipped with a 950 mT/m gradient set. A birdcage coil (35 mm inner diameter) was used for both proton transmission and reception. Mice were anesthetized during the MRI experiment with 1.5% isoflurane and a mixture of O2/air (1:1) at an output of 0.5 L/min. Respiration was monitored during the entire experiment, and body temperature was maintained at 37˚C using a warm-water circulation system.

A spin echo diffusion-weighted sequence was applied to the mice using the following parameters: TE/TR = 27/1500ms, flip angle = 90˚, FOV size = 2.5 × 2.5 cm, matrix size = 128 × 128, b values = 8, 200 and 400 s/mm2 in x, y and z directions. Diffusion (D) coefficients Dx, Dy and Dz in x, y and z direction, respectively, were calculated with Bruker Paravision 5.1 software. They correspond to the slope of the decreasing line after the representation of ln(S/S0) = f(b), where S0 corresponds to the grey levels mean of the spinal cord region of interest ROI without diffusion and S the grey levels mean of the spinal cord ROI with diffusion.

Protein extraction

Tissues were homogenized using ceramic beads-filled precellys tubes in an appropriate volume of ice-cold Cell Disruption Buffer (PARIS kit, Invitrogen™) supplemented with 1X Halt Protease and Phosphatase Inhibitor Cocktail (Thermo Fisher Scientific™) and Pierce Universal Nuclease (Thermo Fisher Scientific™). Crude homogenates were left on ice for 15 minutes then centrifuged at 900 x g for 5 minutes at 4ºC to remove cellular debris. Half the supernatant was then centrifuged at 13,000 x g for 5 minutes to separate the detergent-soluble and -insoluble fractions. The pellet, which corresponds to the detergent-insoluble fraction was then resuspended in RIPA with 6M urea. Protein quantification was performed using the Pierce™ 660 nm Protein Assay Reagent (Thermo Fisher Scientific).

Western Blot

20 µg of proteins were resolved using 4-20% precast stain-free gels (Biorad) under reducing conditions and transferred to either a 0.2 µm PVDF or nitrocellulose membrane (depending on the antibody of interest). Membranes were incubated in a 5% solution of non-fat dry milk dissolved in TBS-T (0.1% Tween 20, 100 mM Tris pH 7.5; 150 nM NaCl) for 1 hr at room temperature. Membranes were then incubated overnight in the primary antibody of interest at 4°C. The following day, blots were washed in TBS-T for 15 min and incubated with the complementary secondary antibody for 1 hr at room temperature. After a final 15 min wash in TBS-T, blots were developed for 5 min with enhanced chemiluminescence (Biorad) and exposed using a ChemiDoc imaging system (BioRad). All blots were quantified using the BioRad Image Lab software version 6.1.0. The list of antibodies and dilutions used can be found in Table 1.

Metabo-lipidomic analyses

Metabolite extraction and acquisition

The methodology used for this study was based on that proposed by our group for sample preparation, data preprocessing and processing (Martias et al., 2021). Two modes of acquisition were used: C18 and hydrophilic interaction liquid chromatography (HILIC).

For C18 acquisition, metabolites were extracted from blood serum using 400µL of methanol (MeOH) added to 25µL of serum. After 5 sec of vortex, and centrifugation (3000 rpm, 30 min), the supernatant was collected (350µL) and transferred into the 96 wells plate. Evaporation (40°C, 30 min, N2) was performed and acetonitrile/distilled water (ACN/dH2O) (2:8, 100µL was added). A part of the sample (10µL) was used to constitute the pool for quality control, then 5µL of sample was injected for C18+ mode and for C18- mode. For HILIC acquisition, 75µL of ACN was added to 25µL of serum. After 5 sec of vortex, and centrifugation (3000 rpm, 30 min), the supernatant was collected (75µL) and transferred into a vial. A part of the sample (10µL) was used to constitute the pool for quality control (QC), then 5µL of sample was injected for HILIC mode + acquisition.

For dried blood spot (DBS): two 3mm punches were extracted with 200µL of ACN/MeOH/dH_2O (4:4:2), then the sample was vortexed during 1 min. After 1 hr planar agitation at high speed, the sample was centrifuged (10,000 x g for 5 min/4°C). Later, 150µL of supernatant were aliquoted and dried under vacuum (SpeedVac) for 2 hr/40°C. The dried extract was dissolved in 75µL of solvent (C18 +/- = 100µL ACN/dH2O (2:8); HILIC + = 100µL ACN/dH2O (2:8)). Samples were then vortexed for 1 min and left on planar agitation for 20 min at high speed. 10µL of each sample were injected into the mass spectrometer.

Tissue samples were lyophilized for 48hrs. After which dry weight of the samples was measured, and 1000µL of MeOH/dH2O (5:5) was added. The samples were vortexed for 5 sec, shaken up (30 min/4°C) and centrifuged (15000 g, 15 min/4°C). Later, 900 µL of supernatant was collected and transferred into 2 tubes depending on the acquisition used. For the C18 mode: evaporation of 450µL of the sample previously prepared (speed vac 4 hrs/40°C), then 100µL ACN/dH2O (2:8) was added. Samples were centrifuged (15000 g, 10 min/4°C), and then 80µL was transferred into a 96-well plate. Collection of 5µL was done for the QC pool and sample injection of 5µL was done for C18+ and C18- modes. For HILIC: evaporation of 450µL of the sample previously prepared (SpeedVac 4hrs/40°C), then addition of 100µL ACN/dH2O (2:8), samples were transferred into amber vials. Collection of 5µL was also done for the QC pool and sample injection of 5µL was done for the HILIC + mode.

Mass spectrometry

Mass spectrometry analysis was based on an UPLC Ultimate WPS-3000 system (Dionex, Germany) coupled to a Q-Exactive mass spectrometer (Thermo Fisher Scientific, Bremen,

Germany). Positive (ESI+) and negative (ESI−) electrospray ionization modes were used for this analysis. Liquid chromatography used 2 different columns: a Phenomenex Kinetex 1.7 µm XB – C18 column (150 mm x 2.10 mm) maintained at 55°C and HILIC column (150 mm x 2.10 mm, 100 Å), maintained at 40°C. The mobile phases were water + 0.1% formic acid / ACN + 0.1% formic acid with a flow rate of 0.4 mL/min for C18; and water + formiate NH4 (10mM) + 0.1% formic acid/ ACN + formiate NH4 (10mM) +0.1% formic with a flow rate of 0.4 mL/min for HILIC. The instrument operated at 70,000 resolutions during the full-scan acquisition, which ranged from 58 to 870 m/z.

The validation of the pre-analytical and analytical steps of the experiment was based on findings of QC samples (mix of samples analysed). Coefficients of variation [CV% = (the standard deviation/ mean) x 100], were calculated from all compounds. Metabolites having a CV > 30% in QCs were excluded from the final dataset. QCs were analyzed at the beginning of the run, every 10 samples and at the end of the run.

A library of standard compounds (Mass Spectroscopy Metabolite Library (MSML®) of standards, IROA Technologies™) was used to present a targeted analysis, including the identification step of metabolites based on the following criteria (1) retention time within ± 20 sec of the standard reference, (2) exact measured molecular mass within a range of 10 ppm around the known molecular mass of the reference compound, and (3) correspondence between isotopic ratios of the metabolite and the standard reference. Calculation of signal value was performed via Xcalibur® software (Thermo Fisher Scientific, San Jose, CA) after integration of the chromatographic peak area corresponding to the selected metabolites.

Statistical analyses

The data for phenotypic changes, MRI and western blot were evaluated with the GraphPad Prism 6.0 statistical analysis software. Data were analyzed by 2-way ANOVA with Sidak's post hoc test for multiple comparisons, unpaired t-tests, or Mann-Whitney U tests based on requirement. Results were considered statistically significant when p-values < 0.05.

Analysis for metabo-lipidomic profiles comparing Tg and WT mice were as follows:

Cohort 1: Serum T0, DBS at T1 and at T2, and modifications between T1-T2.

Cohort 2: Serum, brain, muscle, and liver at T1' according to non apriori strategy and based on analysis done on data from cohort 1.

Univariate analysis was done using the Metaboanalyst 6.0 computational software to compare the levels of metabolites between the different groups using the volcano plot of the False Discovery Rate.

Multivariate analysis of the metabolomic signatures was performed using the statistical software Simca-P+-17. Models were built to evaluate metabolomic profiles and their evolution during disease evolution for Tg mice compared with data from WT mice. Data were log-transformed, mean centered and unit variance scaled. To evaluate modifications of metabolomic profiles from DBS's collected at T1 and T2, the % of modification was calculated for each metabolite as follows: (levels of metabolite at T1-levels of metabolite at T2)/T1. Principal component analysis (PCA) was first performed to highlight any outliers and to evaluate and compare the metabolic variability within the group of Tg and WT mice. Orthogonal partial least-squares discriminant analysis (OPLS-DA) was used to evaluate the discrimination between Tg/WT mice, to evaluate some changes of metabolomics profiles between different time points and to identify the most discriminant metabolites between groups. Score plots and loading plots were drawn to visualize the models. Models were rejected if there was complete overlap of Q2 distributions [Q2(cum) < 0], we considered a model robust if Q2 > 40% and R2 > 70%. The set of models resulting from the cross-validation were used to determine the top 20 Variable Importance Parameters (VIP) > 1, ranking individual metabolites according to their contribution to the model. The models were cross validated as programmed in SIMCA(Westerhuis et al., 2010). The quality of the models was characterized by 4 main parameters: the CV ANOVA, R2 and Q2 values and the permutation plot.

Pathway analysis

According to the objectives of this study, we compared the common and different metabolites between Tg and WT mice (both cohorts); the different time points within the Tg and the WT group and between groups (cohort1); the different tissues of cohort 2 within the Tg and the WT group and between groups; and lastly determined main findings between cohort 1 and 2. Accordingly, Venn diagrams were used from the relevant metabolites highlighted from OPLS-DA models and univariate analysis. From the common metabolites but also from all the models generated, enrichment and pathway analysis were performed from the 20 best discriminant metabolites highlighted in the OPLS-DA models and univariate analysis using the

MetaboAnalyst software, based on KEGG pathway database(Assenov et al., 2008) (http://www.genome.jp/kegg/pathway.html).

Results

Characterization of disease evolution in Prp-TDP-43^{A315T} mice and determination of main stages in cohort 1

Phenotypic evolution of Prp-TDP-43^{A315T} mice

While monitoring disease progression in Tg mice, we designated 3 timepoints to refer to different stages of disease development (T0, T1 and T2); where T0 referred to a pre-symptomatic stage, T1 referred to a symptomatic stage, and T2 referred to end-stage disease stage (right before sacrifice). We began to monitor the body weight of mice at 50 days postnatal (PN). We observed no significant change in body weight between WT and Tg mice from 50-148 days PN (designated T0). Starting 154 until 250 days PN (designated T1), WT mice continued to grow with age while Tg mice gained less weight in comparison. During the T1 stage, we observed a significant 43.6% decrease in mean body weight of Prp-TDP-43^{A315T} Tg mice (26.3 ± 2.5 g) compared to C57Bl/6 WT (43.5 ± 11.5 g) beginning at 154 days PN (Figure 1A, C). Similar changes were observed when examining the hindlimb grip strength test, which measured the average maximum force generated by the hindlimb muscles. We observed a significant 44.6% decrease in grip strength performance of Tg mice (0.4 ± 0.1 N) compared to WT (0.7 ± 0.1 N) during T1, which continued to decline with age (Figure 1B, D). Additionally, we observed a significant decrease in tail position of Tg mice compared to WT which was also associated with an arbitrary score increase in gait impairment for all Tg mice (score 2) (data not shown). Based on the survival median per mouse, we allocated the end-stage symptom development (designated T2) as the last month of survival for each individual mouse. The median life expectancies for the Tg and WT mice were 176 days and 405 days, respectively (data not shown). Based on these phenotypic findings, we determined that the Prp-TDP-43^{A315T} strain does exhibit evidence of ALS pathology and deserved extended molecular characterization at the T1 stage.

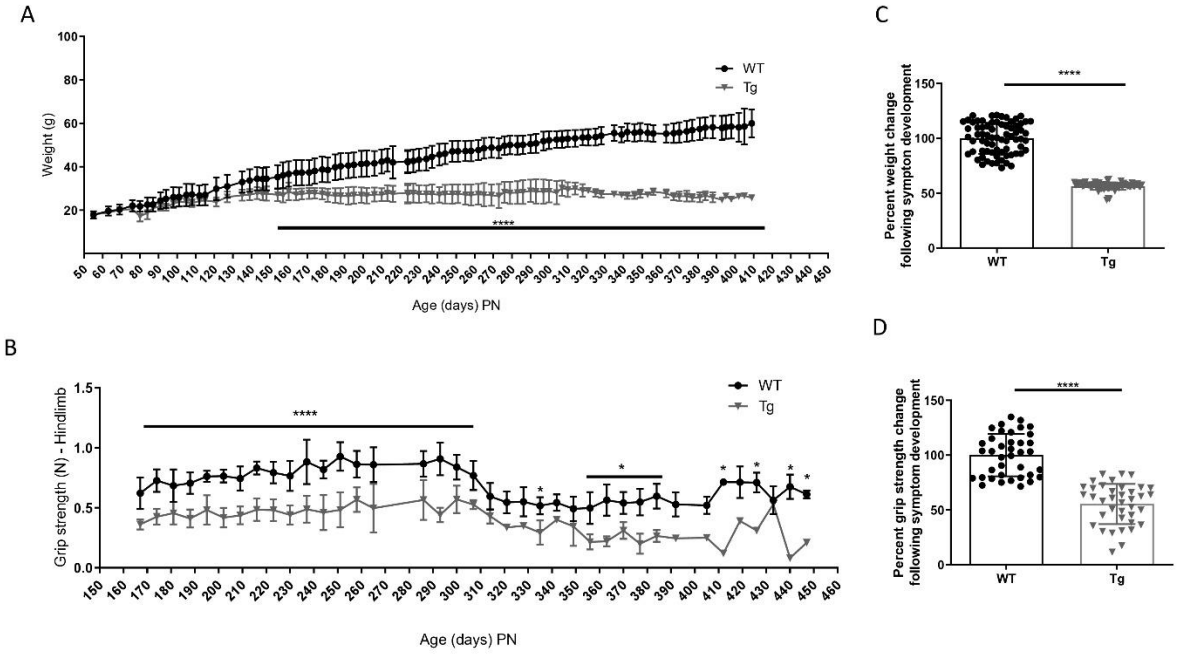

Figure 1. Decreased body weight and grip strength of Tg mice compared to WT. Change in mean +/- SD of body weight (g) from 50-450 days (A), and hindlimb grip strength (N) from 150-450 days PN (B) in WT and Tg mice. 2-way ANOVA, ****p<0.0001.
Percent change in body weight (C) and grip strength (D) in Tg mice relative to WT throughout T1 phase (150 – 250 days PN). Mann-Whitney test. ****p<0.0001. (N=12 WT, N=6 Tg).

MRI-related data of Prp-TDP-43^{A315T} mice

Axial images of the spinal cord of Tg and WT mice were taken (Figure 2A). Data was collected at T0, T1, and T2 to monitor for changes related to disease progression. Despite a small decline in diffusion coefficient for Tg mice at T1, no significant change in average diffusion coefficient was observed at any of the time points between Tg and WT mice (Figure 2B). However, a significant increase in insoluble TDP-43 was observed in the spinal cord of these mice at T0 and T2 (*p=0.01); this increase was not found to be significant at T1 (p=0.14) (Figure 2C-E). In addition, insoluble 35-kDa C-terminal fragment was detected in some of the Tg but not WT mice at the three timepoints that were analyzed (Figure 2C-E).

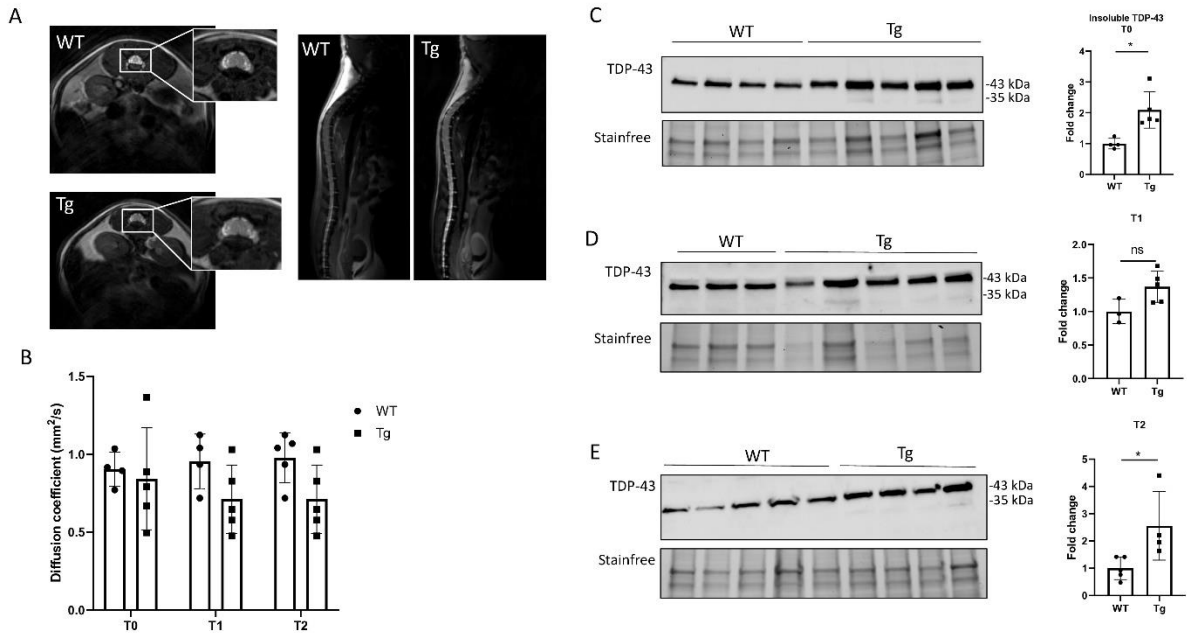

Figure 2. Increased insoluble TDP-43 in the spinal cord of Tg mice in the absence of MRI changes in the spinal cord. A) Representative MRI images of the axial spinal cord of WT and Tg mice. B) The calculated mean diffusion coefficient of the spinal cord of WT and Tg mice. One-way Anova. $p>0.05$. Immunoblot and quantification of insoluble TDP-43 in the spinal cord at T0 (C), T1 (D), and T2 (E). Fold change of Tg to WT was calculated following normalization of each condition to the corresponding stain-free gel. Mann-Whitney test, (N=4-5 WT, N=4-5 Tg), *$p=0.015$.

Metabolomic profile of Prp-TDP-43^{A315T} mice

We created score plots to visualize the OPLS-DA models and characterized the contribution of metabolites to the separation of classes using the loading plot and the contribution plot in cohorts 1 and 2. We obtained good model robustness and predictive capability for all sample data examined, as is represented in supplementary figure 1. These representative OPLS-DA score plots showed two distinct clusters between WT and Tg groups at T1 and T1', corresponding to specific metabolomic profiles for each group (Supp figure 1 A, B). For these scores, we observed CV-ANOVA determined pvalues < 0.01, Q2 values > 0.8, and validated models using permutation tests (Supp figure 1 C, D).

Multivariate analysis of the serum and DBS samples collected at T0, T1 and T2 demonstrated significant separations of metabolites between Tg and WT mice in cohort 1 (data not shown). Further univariate analysis of these samples demonstrated over 20 individual metabolites significantly modified at T0 in Tg mice relative to WT, with phenyllactic acid, adenosine and 2-

hydroxyadipic acid showing the largest fold change (Figure 3A). Though we did not identify any discriminating metabolites at T1, T2 DBS samples demonstrated PC (33_1) to significantly decrease in Tg mice (Figure 3B). Additionally, we evaluated modifications of metabolomic profiles from DBS's (T1-T2), in which we found no evidence of discriminating metabolites following univariate analysis (data not shown).

A Venn diagram was constructed to examine the common top 20 metabolites following multivariate and univariate analysis for all timepoints. We found creatinine to be in common at T0 and T1 at both multivariate and univariate levels, while uracil was in common between T0 and T2 at the univariate level (Figure 3C, D). Meanwhile, seven to ten metabolites were found in common between T1 and T2 samples across both multivariate and univariate levels, with glycine, L-lysine, PC (32_1), and SM (33_1) metabolites revealed in both methods of analysis (Figure 3C, D). Given the abundance of metabolites associated with T1 relative to other timepoints, we further examined how sample metabolites were altered at this timepoint for cohort 2.

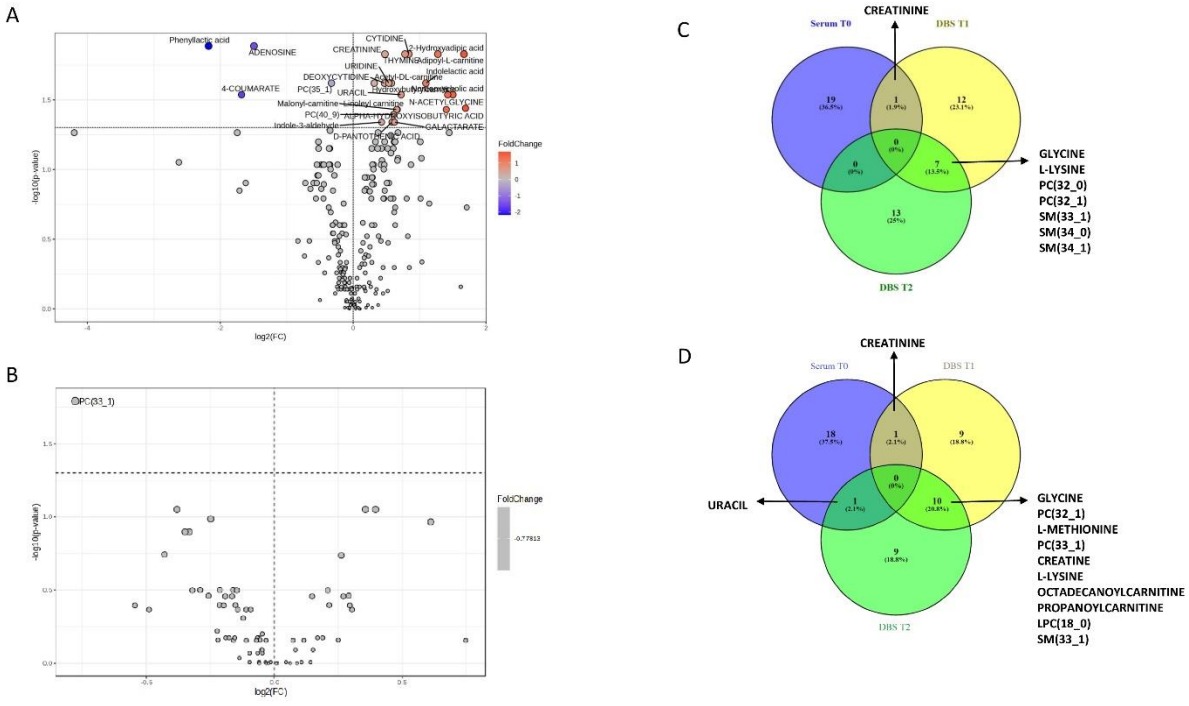

Figure 3. Analysis of serum and DBS metabolites from cohort 1 across all timepoints. Volcano plots demonstrating significant fold change in multiple metabolites in serum T0 (A), and DBS T2 (B) of Tg mice compared (FC=1 and FDR (adjusted p-value) cutoff = 0.05). C) Venn diagram representing common top 20 metabolites between all timepoints in cohort 1 based on multivariate analysis performed. D) Venn diagram representing common top 20

metabolites between all timepoints in cohort 1 based on univariate analysis performed. (N=12 WT, N=6 Tg).

Deeper characterization of Prp-TDP-43^{A315T} mice in cohort 2

Given that the cohort 1 group established certain phenotypic and metabolic findings across different timepoints of ALS disease progression, we then used cohort 2 to validate those same findings and add deeper molecular and metabolic knowledge in the characterization of these mice at T1 prime (T1'). With T1' relating to the same timeline established for cohort 1 at T1.

Alteration of specific targeted proteins in Prp-TDP-43^{A315T} mice at T1'

Prp-TDP-43^{A315T} mice exhibit an increase in TDP-43 and TDP-35 protein expression in the CNS

We examined TDP-43 protein expression in the brain and spinal cord of the cohort 2 at T1'. Analysis of the total protein (crude) lysates demonstrated a statistically significant 1.8-fold increase in TDP-43, an approximate 31-fold increase in TDP-35, a 7-fold increase in TDP-25, and a 2-fold increase in pTDP-43 in the brain of Tg mice compared to the normalized relative protein expression in WT mice (Figure 4A, Figure 5A). In the spinal cord, we did not detect the 25 kDa C-terminal fragment of TDP-43. However, we documented a statistically significant 1.9-fold increase in TDP-43, a 2.8-fold increase in TDP-35, and a 2.8-fold increase in pTDP-43, in Tg mice following normalization to the WT mice (Figure 4B, Figure 5B). Of added interest, we observed that Tg mice expressed a striking signal following incubation with the human TDP-43 antibody in brain and spinal cord crude protein fractions, that was not found in the WT mice, positively confirming the expression of mutated TDP-43 in the brain and spinal cord of Tg mice (Supp figure 2).

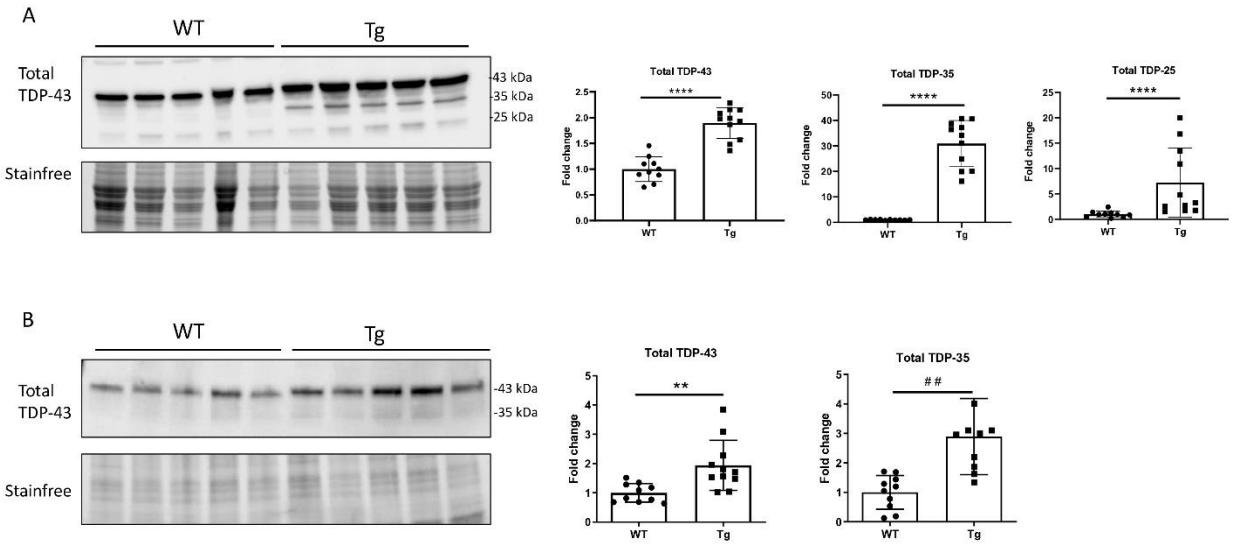

Figure 4. Increased expression of total full length TDP-43 and its C-terminal fragments in the brain and spinal cord of Tg mice. Representative immunoblots and quantification of total TDP-43 in the brain (A) and spinal cord (B) of WT and Tg mice. Fold change of Tg to WT was calculated following normalization of each condition to the corresponding stainfree gel. Mann-Whitney test (brain samples), ****p<0.0001. Unpaired t-test (spinal cord samples), **p=0.004, ##p=0.001. (N=10 WT, N=11 Tg).

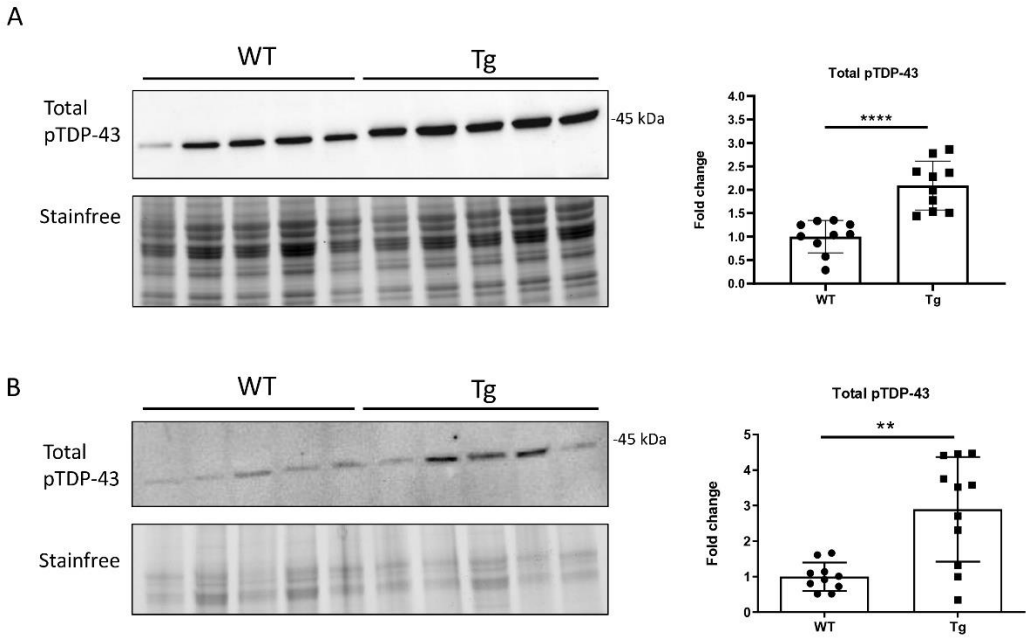

Figure 5. Increased expression of total pTDP-43 in the brain and spinal cord of Tg mice. Representative immunoblots and quantification of total pTDP-43 in the brain (A) and spinal cord (B) of WT and Tg mice. Fold change of Tg to WT was calculated following normalization of each

condition to the corresponding stainfree gel. Unpaired t-test, ****p<0.0001, **p=0.001. (N=10 WT, N=11 Tg).

As for the insoluble fractions, brain lysates of Tg mice revealed a statistically significant 1.5-fold and 5.5-fold increase in TDP-43 and TDP-35, respectively, and a 2-fold increase in pTDP-43 (Figure 6A, Figure 7A**).** In the spinal cord, we detected a 4-fold increase in full-length TDP-43, and a 1.6-fold decrease in pTDP-43 in Tg mice (Figure 6B, Figure 7B). Interestingly, a 75 kDa form of TDP-43 was only detected in the insoluble protein fraction of the spinal cord of both Tg and WT mice (Figure 6B). Its level increased in some but not all Tg mice and did not reach statistical significance overall.

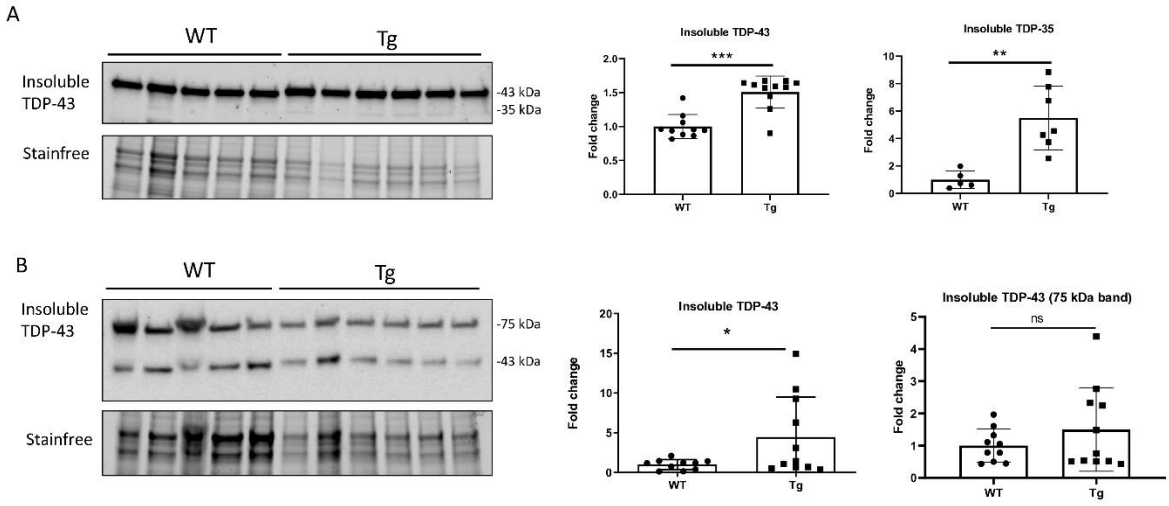

Figure 6. Increased expression of insoluble TDP-43 in the brain and spinal cord of Tg mice. Representative immunoblots and quantification of insoluble TDP-43 in the brain (A) and spinal cord (B) of WT and Tg mice. Fold change of Tg to WT was calculated following normalization of each condition to the corresponding stainfree gel. Mann-Whitney test (brain samples), **p=0.0025 ; ***p=0.0004. Unpaired t-test (spinal cord samples), *p=0.04. (N=10 WT, N=11 Tg).

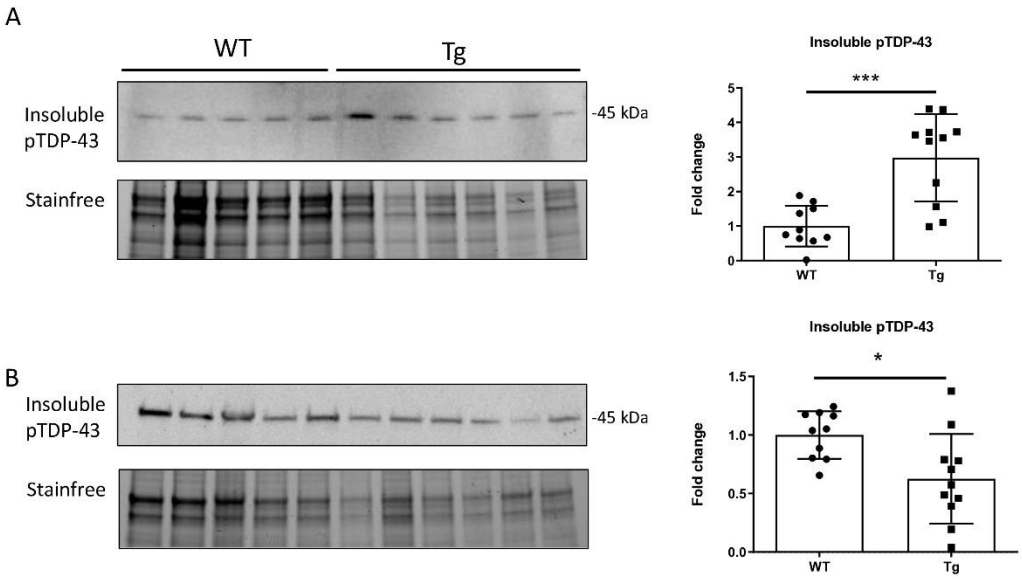

Figure 7. Increased expression of insoluble pTDP-43 in the brain and spinal cord of Tg mice. Representative immunoblots and quantification of insoluble TDP-43 in the brain (A) and spinal cord (B) of WT and Tg mice. Fold change of Tg to WT was calculated following normalization of each condition to the corresponding stainfree gel. Mann-Whitney test, (N=10 WT, N=11 Tg).

Prp-TDP-43^{A315T} mice exhibit a change in protein markers associated with ALS pathology

We further examined the expression of protein markers associated with the pathology of ALS. No change in the ratio of LC3 II/I was observed in either the brain or spinal cord for this cohort of mice (Supp figure 3). We found a 1.6-fold increase in glial fibrillary acidic protein (GFAP) expression (Figure 8A), a 0.6-fold change in the ratio of p-AMPK to AMPK (Figure 8B), and a 1.5-fold increase in erythroid-2 related factor 2 (NRF2) expression in the crude brain protein lysates of Tg mice compared to WT (Figure 8C). These markers were not found to be significantly altered in the crude spinal cord protein lysates of Tg mice compared to WT (Supp figure 4).

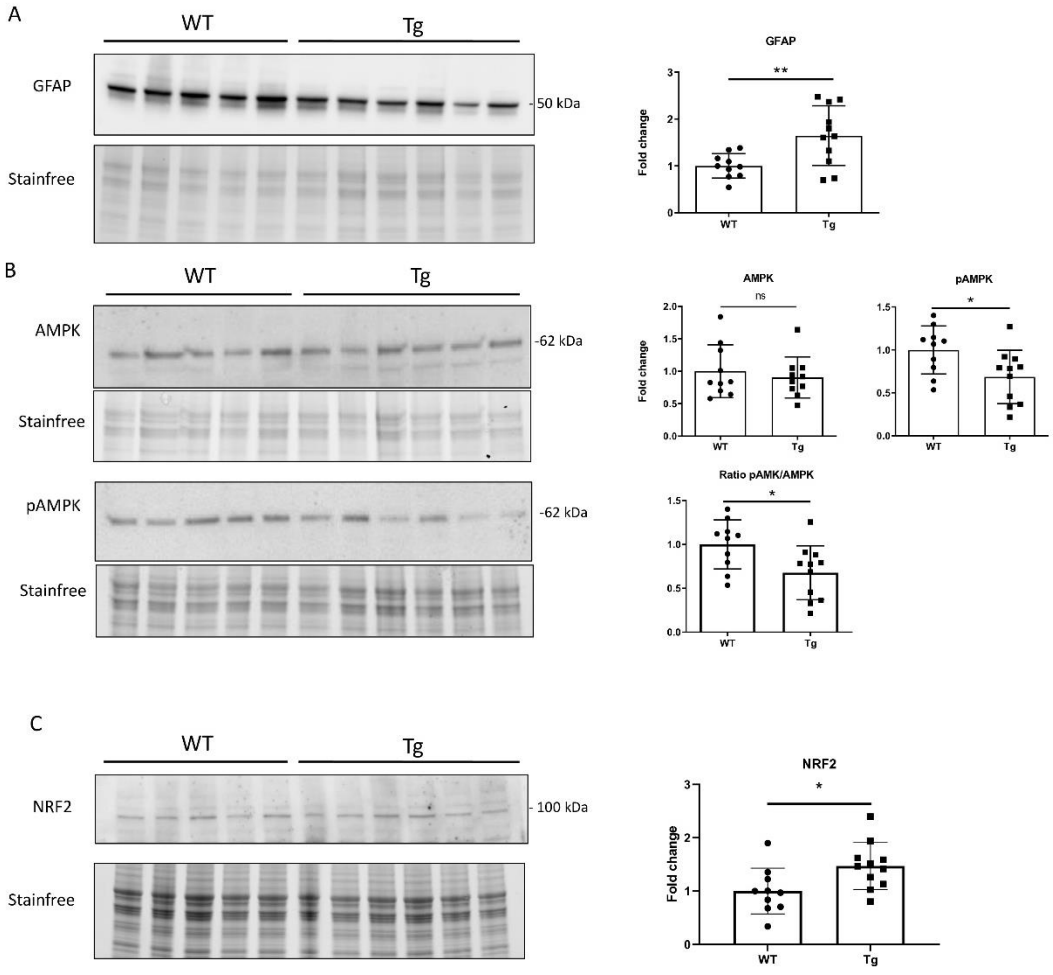

Figure 8. Increased GFAP, decreased pAMPK/AMPK ratio, and increased NRF2 in the brain of Tg mice. Representative immunoblots and quantification of GFAP (A), AMPK, pAMPK and their ratio (B), and NRF2 (C) in the brain of WT and Tg mice. Fold change of Tg to WT was calculated following normalization of each condition to the corresponding stainfree gel. Unpaired t-test, ***p*=0.008, **p*=0.02. WT (N=10 WT, N=11 Tg).

Metabolomic disturbances of Prp-TDP-43^{A315T} mice at T1'

Prp-TDP-43^{A315T} mice exhibit blood metabolic modifications associated with observed findings in cohort 1

In the second cohort of mice, we examined modifications in metabolites only focusing on the symptomatic period of the disease. In these mice, multivariate serum analysis showed a clear separation of metabolites between Tg and WT in the OPLSDA model. Though multivariate data demonstrated a significance following CV-ANOVA analysis (****p<0.0001), similar significance was not observed at a univariate level using the volcano plot of the FDR analysis (data not shown). However, upon comparing these serum metabolites with metabolites from the DBS T1 samples in cohort 1 we came across interesting findings. Venn diagram analysis demonstrated common metabolites at both the multivariate and univariate levels of these cohorts (Supp figure 5). Of note, sphingomyelin (33_1) was found to be an active player in both groups.

Prp-TDP-43^{A315T} mice exhibit tissue metabolic modifications associated with observed findings in cohort 1

We performed metabolite extraction and analysis on brain, liver and muscle tissues of mice from cohort 2 at T1'. Despite obtaining good and robust models for all tissue samples (data not shown), we did not find any significant discriminating metabolites in the muscle or liver. Interestingly, extracted metabolites from the brain demonstrated a significant difference between levels of taurine, D-glucose and D-xylose at both multivariate and univariate levels**.** These three metabolites had VIP values higher than 1, and ****p < 0.0001 following FDR analysis (Figure 9A) suggesting them to be discriminating molecules in the brain of Tg mice.

We examined the top 20 metabolites between all tissue samples following univariate analysis to determine common metabolites between samples. Phosphocholine was found to be a common metabolite between the brain and liver following multivariate analysis (Figure 9B). Of note, taurine, D-glucose and diethanolamine were found to be metabolites of interest in both the brain and muscle following the same analysis (Figure 9B). Venn diagrams from the univariate data revealed L-glutamine in common between brain and liver, histamine between muscle and liver, and D-glucose and diethanolamine in common between the brain and muscle tissue (Figure 9C).

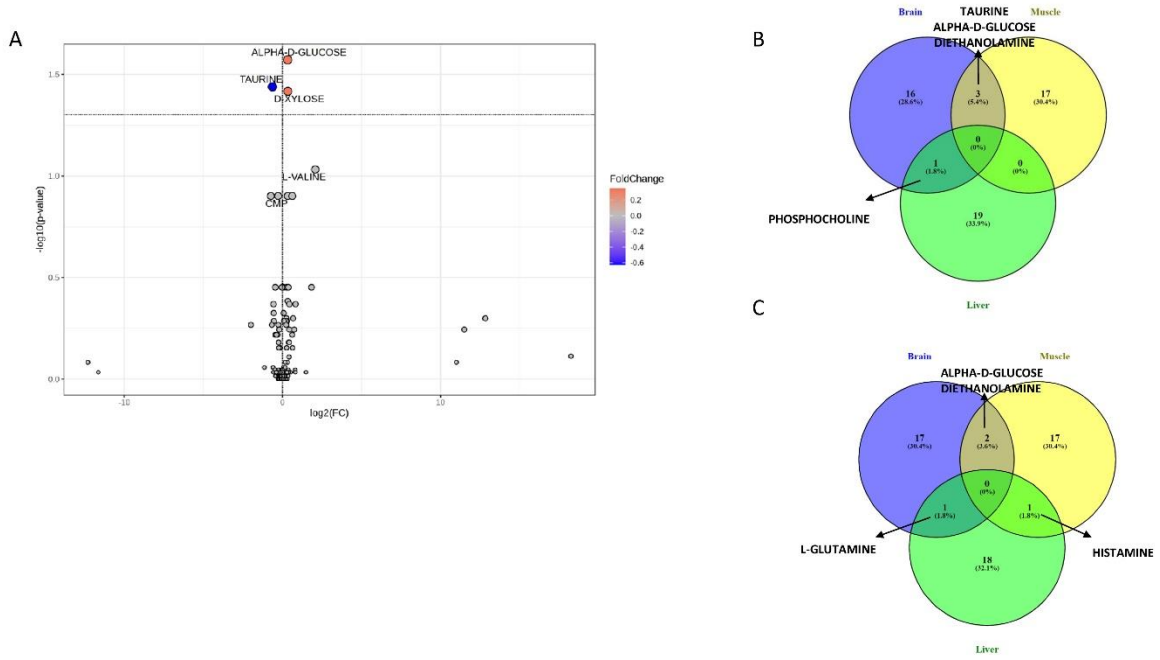

Figure 9. Analysis of tissue metabolites from cohort 2 at T1'. Volcano plots of Tg with respect to WT demonstrating significant fold change in multiple metabolites in the brain (A), where the main metabolites were alpha-d-glucose, D-xylose and taurine (FC=1 and FDR (adjusted p-value) cutoff = 0.05). B) Venn diagram representing common top 20 metabolites across all tissues at T1' in cohort 2 based on multivariate analysis performed. C) Venn diagram representing common top 20 metabolites across all tissues at T1' in cohort 2 based on univariate analysis performed. (N=10 WT, N=11 Tg).

Lipidomic disturbances of Prp-TDP-43^{A315T} mice at T1'

Lipid extraction and analysis was performed on serum, brain, liver and muscle tissues of mice from cohort 2 at T1'. Despite obtaining good and robust models for all samples (data not shown), we did not find any significant discriminating metabolites in the brain or serum. Lipids extracted from the liver demonstrated multivariate and univariate significance for phosphatidylcholine (O-16:0_20:4) and LPE (16:1) (Figure 10A). Of note, analysis from the muscle demonstrated significant changes between WT and Tg mice for 14 lipids across multiple subsets of classes. The main subsets involved were diacylglycerols (DG), fatty acyls (FA), phosphatidylcholine (PC), triglycerides (TG), and phosphatidylethanolamine (PE) (Figure 10B). Data collected from the TG lipid subset demonstrated an overall decrease in fold change of Tg mice compared to WT. However, we observed significant increases in the DG, FA, PC, and PE lipid subset profiles. Given the abundance of lipids that were found to be significant in

these tissues across both multivariate and univariate levels, we further generated Venn diagrams to examine the extent of discriminating metabolites from both analyses. We found a total of 12 common lipids in the liver and 14 significant lipids in the muscle (Figure 10C, D).

We examined the top 20 lipids between all samples following multivariate and univariate analysis. Venn diagram analysis of these lipids revealed LPC (16:1) in common between the serum and liver, PC (34:3) between the muscle and brain, and LPC (24:0) between the serum and brain following multivariate analysis (Supp figure 6). Venn diagram following univariate analysis revealed LPC (15:0) in common between the serum and liver, PA (27:1_18:0) between the muscle and liver, and LPC (24:0) and PC (45:4) between the serum and brain following univariate analysis (Supp figure 7).

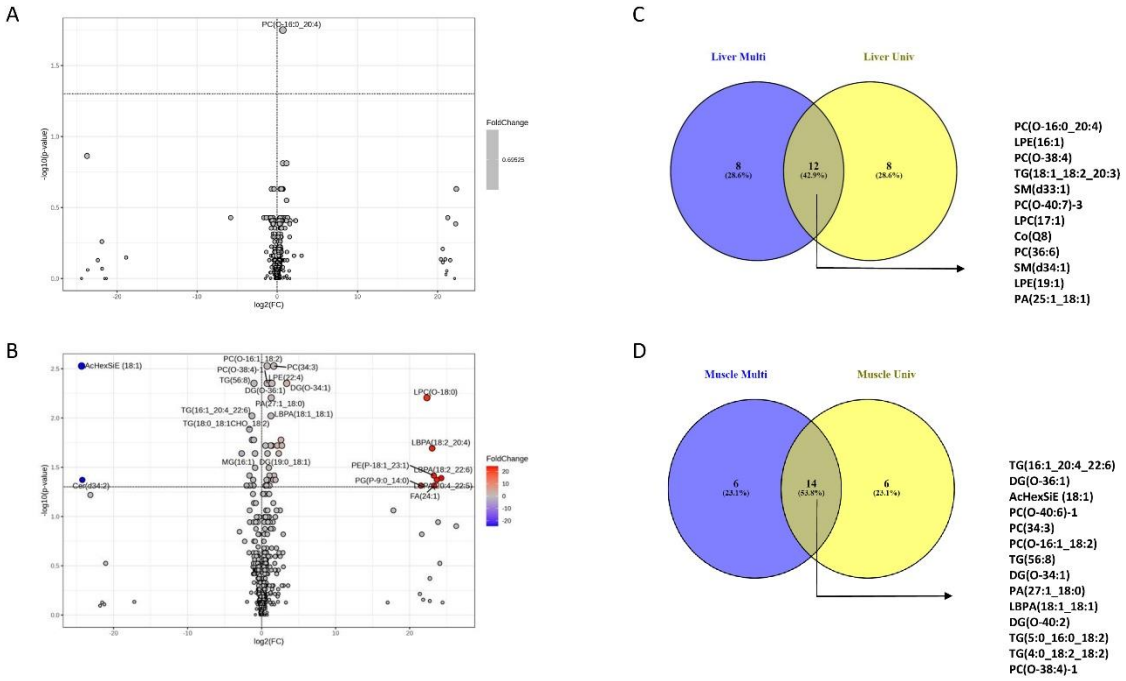

Figure 10. Analysis of lipid subclasses from cohort 2 at T1'. Volcano plots of Tg with respect to WT demonstrating significant fold changes in multiple lipid subclasses in the liver (A), where the main subset involved was PC, and muscle (B), where the main subsets involved were DG, FA, PC, PE, and TG. (FC=1 and FDR (adjusted p-value) cutoff = 0.05). Venn diagrams demonstrate common metabolites following multivariate and univariate analysis for the liver (C) and muscle (D). (N=10 WT, N=11 Tg).

Discussion

Phenotypic characterization of the Prp-TDP-43A315T mouse model of ALS

Several animal models have been developed to study ALS based on TDP-43. These models mainly aim to replicate the TDP-43 proteinopathy observed in ALS, which is characterized by the cytoplasmic mislocalization, cleavage, phosphorylation, and/or aggregation of the protein. The most commonly used models are the TDP-43 overexpression models, which are designed to drive the overexpression of either mutated or wildtype human TDP-43 using various promoters(Gendron & Petrucelli, 2011). Interestingly, the level of overexpression of TDP-43 (intermediate vs high) was found to generate different phenotypes, with varying disease onset, severity, and symptoms, highlighting a dose-dependent phenotype(Stallings et al., 2010; Wils et al., 2010). Although mutant TDP-43 is thought to be more toxic than wildtype TDP-43, it has been suggested that this toxicity can be linked to the mere overexpression of TDP-43 in either form(Y.-F. Xu et al., 2010). The development of motor deficits in different TDP-43 mouse models, despite differences observed at the level of TDP-43 proteinopathy and disease phenotypes, reflects the wide range of pathways that can be impacted by a dysfunction in TDP-43. This dysfunction eventually converging into an ALS-like phenotype. In that regard, the aim of this study was to provide more extensive characterization of the Prp-TDP43^{A315T} mouse model, in order to decipher the potential mechanisms that are implicated in the observed TDP-43 proteinopathy and ALS phenotype.

The Prp-TDP-43^{A315T} mouse model used in this study was first described in 2009(Wegorzewska et al., 2009). It expresses a mutant human *TARDBP* cDNA harboring an amino acid substitution associated with familial ALS. It has been shown to drive the overexpression of TDP-43 transgene at high levels in the nervous system. Given that this was a longitudinal study, we utilized female mice as male mice with ALS have a lower survival rate(Bargsted et al., 2017). We detected a significant reduction in weight and increased motor deficits around 150 days of age. While some studies reported that, despite being on a gel diet, the TDP-43^{A315T} mice started losing weight as the disease progressed(Herdewyn et al., 2014), others reported an increase in weight that was similar to that observed in the WT mice(Weerasekera et al., 2020). Here, we report that the Tg mice, which were on a high-fat diet, did not gain weight as the WT mice did, but did not show any weight loss either as the disease progressed. This confirms the presence of a hypermetabolic state and high energetic demands in Tg mice, a phenomenon that has been reported in this mouse model(Coughlan et al., 2016) and which is well documented in ALS(Fayemendy et al., 2021; He et al., 2022).

TDP-43 proteinopathy does not induce significant MRI changes in the spinal cord

Spinal cord MRI was conducted before and after the onset of symptoms, as well as towards the end stage of the disease. The goal was to identify potential structural changes at the level of the spinal cord by calculating the average diffusion coefficient. These values reflect the diffusion of water molecules in tissues, which can be either increased or decreased with changes in tissue micro-architecture and integrity(Rueda-Lopes et al., 2014; Werring, 2000). We noted no significant change in the diffusion coefficients at the analyzed timepoints. However, TDP-43 pathology and aggregation were well observed in the spinal cord of these mice, with an approximate 2-fold increase in detergent-insoluble TDP-43, suggesting that TDP-43 pathology is not associated with significant microstructural changes in the spinal cord at the time of symptom onset. A similar result has been previously observed in TDP-43^{A315T} mice at the level of the brain(Weerasekera et al., 2020).

Different patterns of TDP-43 proteinopathies in the brain and spinal cord of Prp-TDP-43A315T mice

We then carried out a more detailed characterization of Tg mice following the onset of symptoms (Cohort 2, T1'). We first assessed the expression level, fragmentation, and phosphorylation of TDP-43 in the central nervous system. Interestingly, different band patterns were observed in the brain and the spinal cord. In the total protein fraction, the 25 kDa band was not detected in the spinal cord but was detected in the brain of both WT and Tg mice. The 35 kDa fragment was not easily detected in the spinal cord, and its increase in Tg mice was also much less prominent in the spinal cord (2.8-fold) compared to the brain (31-fold).

The first study to describe this animal model did not note any TDP-43-positive aggregates in the brains of Tg mice(Wegorzewska et al., 2009). However, we detected a significant increase in the amount of TDP-43, its 35 kDa C-terminal fragment and of phosphorylated TDP-43 in the detergent-insoluble protein fraction. The insoluble 35 kDa fragment was only observed in the brain of some mice. Interestingly, a band around 75 kDa was solely observed in the insoluble protein fraction of the spinal cord in these mice. This band has been previously detected in the brain of individuals with frontotemporal lobar degeneration with TDP-43 pathology and in the insoluble protein fraction of HEK293T cells overexpressing the mutant TDP-43^{A315T} and was

shown to consist of covalently modified TDP-43(Guo et al., 2011). Similar to what has been previously reported, we found that this band was resistant to heating at 95°C, reducing conditions with DTT, and denaturation with urea. Studies have suggested that this band consisted of a hyperphosphorylated and acetylated form of TDP-43(Cohen et al., 2015; Guo et al., 2011). The exclusive detection of this band in the spinal cord and not the brain requires further investigation.

As for pTDP-43, we detected TDP-43 species phosphorylated at serine 409 and 410, which are consistently reported in ALS(Neumann et al., 2009). We observed a significant increase in pTDP-43, but pTDP-43 was easier to detect in the brain compared to the spinal cord. No phosphorylated TDP-43 C-terminal fragments were detected in either tissue. In the brain, there was also an increase in the amount of pTDP-43 in the insoluble protein fraction. Surprisingly, despite an increase in the total amount of pTDP-43, there was a decrease in the amount of insoluble pTDP-43 in the spinal cord of Tg mice, which can be due to a decreased burden of TDP-43 fragmentation in the spinal cord, or an increased elimination of pTDP-43. In fact, some studies have pointed to the role of phosphorylation in protecting against the aggregation of TDP-43 and that phosphorylation mainly took place after and not before the formation of TDP-43 aggregates(Brady et al., 2011; Gruijs Da Silva et al., 2022; H.-Y. Li et al., 2011). It should be noted that our results do not exclude the presence of pTDP-43 species other than those phosphorylated at S409/410. TDP-43 contains 64 sites that can be phosphorylated, with most of them located in the C-terminal domain(Eck et al., 2021).

Overall, our results concerning the presence/absence and levels of the different forms of TDP-43 in the brain and the spinal cord highlight the regional heterogeneity in their generation, modification and clearance, including but not limited to differences in protease activities, degradation pathways, and enzymes implicated in post-translational modifications.

Pronounced astrogliosis, metabolic and oxidative stress response in the brain

We then investigated the change in some ALS-associated disturbances including autophagy dysregulation, astrocyte activation, and the response of cells to energetic and oxidative stress. The ratio of the precursor and the active forms of the microtubule-associated protein light chain 3, LC 3 I/LC3 II, which is used as a macroautophagy marker(Kadowaki & Karim, 2009, p. 13), was not altered. This suggests that the autophagy-induced degradation pathway is not

altered in Tg mice during the early symptomatic phase. This was also observed in another study on 3 and 6 months old male TDP-43^{A315T} mice(Huang et al., 2020).

We observed a significant change in GFAP, activated AMP-activated protein kinase (AMPK), and the erythroid 2-related factor 2 (NRF2). The increase in the level of GFAP, an astrocytic intermediate filament protein, reflects a state of reactive astrogliosis early in the disease(Brahmachari et al., 2006). AMPK plays a crucial cellular energy sensor and regulator of metabolic homeostasis(J. Li & McCullough, 2010). No change in the level of AMPK was detected in Tg mice. However, we noted a decrease in pAMPK (and subsequently in the ratio of pAMPK/AMPK) in the brain of Tg mice, which was also observed a previous study performed on male TDP-43^{A315T} mice(The PLOS ONE Staff, 2014). These results reflect a decrease in the activation of AMPK in the brain of Tg mice compared to control mice, suggesting that cells are not responding adequately to energy stressors. This can be linked to subsequent metabolomic alterations, altered autophagy response to stress, and abnormal fatty acid and glucose metabolism(Barnaba et al., 2023; Muraleedharan & Dasgupta, 2022; Park et al., 2023). NRF2 is a transcription factor that plays a crucial role against oxidative stress and glutamate-induced excitotoxicity, through mechanisms that are mainly conferred by astrocytes(Habas et al., 2013). This is different from what is observed in male TDP-43^{A315T} mice, in which no change in NRF2 levels were detected in the brain(Lastres-Becker et al., 2022). The increase in NRF2 could reflect the induction of antioxidant cellular pathways in an attempt to reduce oxidative stress. A previous study showed that there was an activation of the NRF2 signaling pathway without a change in the NRF2 levels in the brain or spinal cord of male TDP-43^{A315T} mice(Lastres-Becker et al., 2022). However, an increase in the expression level of NRF2 was observed in the motor cortex of ALS patients (Lastres-Becker et al., 2022).

We observed no significant change in GFAP, NRF2 and pAMPK/AMPK in the spinal cord of Tg mice, despite noticing a significant difference in these markers in the brain. This can be due to the fact that the spinal cord was analyzed as a whole and was not divided into its different sections (i.e. cervical, thoracic and lumbar), excluding detection of potential specific regional changes. In addition, important differences in the ability of neurons to tolerate cellular stress exist between the brain and the spinal cord, which could explain their different responses to TDP-43 proteinopathy(Chestnut et al., 2011; Simandi et al., 2018).

Metabolic disturbances in Prp-TDP-43A315T mice

The ability to identify specific biomarkers associated with ALS provides the potential for earlier diagnosis, an essential aspect for optimal patient care and disease management. Accordingly, the use of metabolomics allows the identification of various individual metabolites and metabolic signatures that can help to discriminate between ALS and non-ALS cases(Hergesheimer et al., 2020; Lanznaster et al., 2018). In ALS, most metabolomic studies focused on mouse $SOD1^{G93A}$ mutants, as they are the most characterized models. Several of these studies have highlighted disturbances in energy metabolism. Previous studies published by our group used $SOD1^{G93A}$ mice for metabolomic and transcriptomic analysis compared to WT mice. Our group identified discriminating metabolites at the level of the muscle and cerebral cortex which were involved in tryptophan, arginine, and proline metabolic pathways(Patin et al., 2017). We also examined $SOD1^{G93A}$ mice injected with MR16-1 (a rat IgG1k monoclonal antibody with neutralizing activity on the effects of mouse IL-6). Metabolomic and transcriptomic analysis of these mice revealed that treatment with MR16-1 mainly altered branched-chain amino acid, lipid, arginine, and proline metabolism in $SOD1^{G93A}$ mice(Patin et al., 2016). Similar studies have also revealed alterations in the profile of sphingolipids, acetyl-CoA, and purines in the spinal cord of $SOD1^{G86R}$ and $SOD1^{G93A}$ mice(Henriques et al., 2018; Valbuena et al., 2019; X. Xu et al., 2023). Two studies have demonstrated that TDP-43 proteinopathies lead to metabolomic disturbances and can affect intermediates of the citric acid cycle, cellular redox pathways, NAD metabolism, and fatty acid metabolism in yeast and drosophila ALS models(Loganathan et al., 2022; Rajaratnam et al., 2023). Yet despite the abundance of TDP-43 mice models available, to the best of our knowledge, no studies to date have utilized such genetic models for metabolomic or lipidomic analysis.

In this study, we examined the metabolomic and lipidomic profiles of WT and Tg mice across blood and different tissue samples. We established significant predictive models and examined how metabolites were correlated across a multivariate and univariate level. Upon comparing serum metabolites from cohort 2 with metabolites from the DBS T1 samples in cohort 1 we found sphingomyelin to be an active player in both groups. This data is of interest as changes in sphingolipid metabolism have previously been implicated in the disease progression of ALS. An abnormal increase in sphingolipid levels (sphingomyelin, ceramide, cholesterol, etc.) has been observed in the spinal cord of ALS patients and in the spinal cord

of asymptomatic and symptomatic SOD1^{G93A} mice(Cutler et al., 2002). These findings are important as sphingomyelin is considered as a major component of oligodendrocytes and myelin sheaths(McCluskey et al., 2022), thus notably implicated in neurodegeneration and neuroinflammation in ALS.

We also demonstrated taurine, D-glucose and D-xylose to be discriminating metabolites in brain tissue of Tg mice. Glycolysis/gluconeogenesis pathways(Dodge et al., 2013; Manzo et al., 2019; Tefera et al., 2021), and to a smaller extent xylose metabolic dysfunction pathways(Wuolikainen et al., 2016) have been found to be implicated in different models of ALS. Our data is also in accordance with various studies that have found taurine metabolism to be highly implicated in the pathogenesis of ALS(Jung et al., 2013; Perry et al., 1987). Recently, plasma taurine was also found to be a significant biomarker associated with the survival and axonal excitability of motor neurons in 66 ALS patients(Nakazato et al., 2022). Though taurine has been shown to have neuroprotective effects in neurodegenerative diseases, our current study is the first to demonstrate differences in the Prp-TDP-43^{A315T} mouse model, further supporting its role as a potential biomarker in ALS.

Alterations in the lipidomic profile of ALS patients including, triglycerides, cholesterol, low/high-density lipoprotein concentrations, have been suggested as potential biomarkers of disease severity and life expectancy(Alessenko et al., 2023). Our data demonstrated that in the muscle of Prp-TDP-43^{A315T} mice, the main lipid subsets altered were DG, FA, PC, PE, and TG. The DG sub-pathway includes signalling molecules with roles in cytoskeletal, neuronal development, inflammation, immune cell signalling and apoptosis. Although these are all aspects of ALS pathology, the DG contribution specifically to ALS pathogenesis is still mostly unknown. On the other hand, phospholipids (including PC and PE), TGs and FAs have been shown to be involved in the physiopathology of Alzheimer disease, Parkinson disease and multiple sclerosis(Wei et al., 2023). Our team has previously demonstrated that in the brain of SOD1^{G93A} mice, there was evidence of significantly higher PC (36:2), PC (36:4), and PC (40:6) compared to controls (Blasco et al., 2017). This difference in PC content was also observed between ALS patients and controls, suggesting a specific involvement in ALS pathology(Blasco et al., 2017). In neurons, PC is especially important as it serves as a major choline reservoir for mediating neurotransmission, and has been shown to enhance neuronal differentiation and protect against neuronal alterations caused by inflammatory conditions in neural stem

cells(Magaquian et al., 2021). However, more studies are needed to determine how these lipids affect pathophysiological functions in TDP-43 proteinopathies.

Conclusion

This study provides a comprehensive analysis of the Prp-TDP-43^{A315T} transgenic mouse model. Our overall molecular results show a rather homogenous WT population and a heterogenous Tg population. This data highlights the individual differences observed in ALS pathologies and the differences in the adaptive responses of the organism to TDP-43-induced pathology. It also sheds light on the regional difference in handling TDP-43-related disturbances between the brain and the spinal cord and the important sex-related differences in TDP-43 pathologies in TDP-43^{A315T} mice. Additionally, our study is the first to examine the metabo-lipidomic profiles for this TDP-43 mouse model. This model shows numerous advantages as it recapitulates features (increased expression of TDP-43, motor impairments, distinct metabo-lipidomic profiles) described in other models with TDP-43 genetic variants, supporting the physiological relevance of these findings. Future studies examining differences in the microbiome, electrophysiological parameters of motor neurons, and gender-based deficits would provide added value to this TDP-43 mouse model of ALS, thus implementing the use of this model across different fields of research in ALS and, consequently other diseases associated with TDP-43 proteinopathies.

Author contributions

Y.A. S.O.: Conceptualization, data curation, formal analysis, investigation, methodology, visualization, writing (original draft). **H.A., P.E., C.V., L.G., P.C., C.A., P.V:** writing (review and editing) **D.L.:** conceptualization, formal analysis, project administration. **A.L., S.M, R.C:** data curation and formal analysis. **G.C.:** formal analysis. **F.M.:** data curation, formal analysis, methodology, writing (review and editing). **F.T.**: resources, project administration, supervision, writing (review and editing). **H.B.:** Conceptualization, formal analysis, funding acquisition, project administration, resources, supervision, writing (original draft).

Conflicts of interest. The authors declare that they have no conflicts of interest with the contents of this article.

Funding sources: This publication has been funded with support from Région Centre Val de Loire and the French National Research Agency under the program "Investissements d'avenir" Grant Agreement LabEx MAbImprove: ANR-10-LABX-53. We would like to thank the ARSLA for financial support. Funding sources had no participation in study design; in the collection, analysis, and interpretation of data; in the writing of the report; and in the decision to submit the article for publication.

Table 1: List of antibodies used in this study

Name of the antibody	Manufacturer (catalog #)	Species raised in	Dilution
C-terminal TDP-43	Proteintech (12892-1-AP)	Rabbit	1:5000
Phospho-TDP-43 (Ser409/410)	Proteintech (22309-1-AP)	Rabbit	1:5000
NRF2	Proteintech (16396-1-AP)	Rabbit	1:5000
GFAP	Proteintech (16825-1-AP)	Rabbit	1:2000
LC3 I/II	Thermo Fisher (PA1-16931)	Rabbit	1:2000
AMPK	Cell Signaling (2532S)	Rabbit	1:2000
Phospho-AMPK	Cell Signaling (2535S)	Rabbit	1:2000
Human TDP-43	Proteintech (60019-2-Ig)	Mouse	1:5000
HRP-conjugated anti-rabbit	Promega (W401B)	-	1:10 000
HRP-conjugated anti-mouse	Promega (W402B)	-	1:10 000

References

Alessenko, A. V., Gutner, U. A., & Shupik, M. A. (2023). Involvement of Lipids in the Pathogenesis of Amyotrophic Lateral Sclerosis. *Life*, *13*(2), 510. https://doi.org/10.3390/life13020510

Assenov, Y., Ramírez, F., Schelhorn, S.-E., Lengauer, T., & Albrecht, M. (2008). Computing topological parameters of biological networks. *Bioinformatics*, *24*(2), 282–284. https://doi.org/10.1093/bioinformatics/btm554

Bargsted, L., Medinas, D. B., Martínez Traub, F., Rozas, P., Muñoz, N., Nassif, M., Jerez, C., Catenaccio, A., Court, F. A., Hetz, C., & Matus, S. (2017). Disulfide cross-linked multimers of TDP-43 and spinal motoneuron

loss in a TDP-43A315T ALS/FTD mouse model. *Scientific Reports*, *7*(1), 14266. https://doi.org/10.1038/s41598-017-14399-5

Barnaba, C., Broadbent, D. G., Perez, G. I., & Schmidt, J. C. (2023). *AMPK Regulates Phagophore-to-Autophagosome Maturation*. https://doi.org/10.1101/2023.09.28.559981

Blasco, H., Veyrat-Durebex, C., Bocca, C., Patin, F., Vourc'h, P., Kouassi Nzoughet, J., Lenaers, G., Andres, C. R., Simard, G., Corcia, P., & Reynier, P. (2017). Lipidomics Reveals Cerebrospinal-Fluid Signatures of ALS. *Scientific Reports*, *7*(1), 17652. https://doi.org/10.1038/s41598-017-17389-9

Brady, O. A., Meng, P., Zheng, Y., Mao, Y., & Hu, F. (2011). Regulation of TDP-43 aggregation by phosphorylation andp62/SQSTM1: Regulation of TDP-43 aggregation by phosphorylation and p62. *Journal of Neurochemistry*, *116*(2), 248–259. https://doi.org/10.1111/j.1471-4159.2010.07098.x

Brahmachari, S., Fung, Y. K., & Pahan, K. (2006). Induction of Glial Fibrillary Acidic Protein Expression in Astrocytes by Nitric Oxide. *The Journal of Neuroscience*, *26*(18), 4930–4939. https://doi.org/10.1523/JNEUROSCI.5480-05.2006

Chestnut, B. A., Chang, Q., Price, A., Lesuisse, C., Wong, M., & Martin, L. J. (2011). Epigenetic Regulation of Motor Neuron Cell Death through DNA Methylation. *The Journal of Neuroscience*, *31*(46), 16619–16636. https://doi.org/10.1523/JNEUROSCI.1639-11.2011

Cohen, T. J., Hwang, A. W., Restrepo, C. R., Yuan, C.-X., Trojanowski, J. Q., & Lee, V. M. Y. (2015). An acetylation switch controls TDP-43 function and aggregation propensity. *Nature Communications*, *6*(1), 5845. https://doi.org/10.1038/ncomms6845

Coughlan, K. S., Halang, L., Woods, I., & Prehn, J. H. M. (2016). A high-fat jelly diet restores bioenergetic balance and extends lifespan in the presence of motor dysfunction and lumbar spinal cord motor neuron loss in TDP-43A315T mutant C57BL6/J mice. *Disease Models & Mechanisms*, *9*(9), 1029–1037. https://doi.org/10.1242/dmm.024786

Cutler, R. G., Pedersen, W. A., Camandola, S., Rothstein, J. D., & Mattson, M. P. (2002). Evidence that accumulation of ceramides and cholesterol esters mediates oxidative stress–induced death of motor neurons in amyotrophic lateral sclerosis. *Annals of Neurology*, *52*(4), 448–457. https://doi.org/10.1002/ana.10312

Dodge, J. C., Treleaven, C. M., Fidler, J. A., Tamsett, T. J., Bao, C., Searles, M., Taksir, T. V., Misra, K., Sidman, R. L., Cheng, S. H., & Shihabuddin, L. S. (2013). Metabolic signatures of amyotrophic lateral sclerosis reveal insights into disease pathogenesis. *Proceedings of the National Academy of Sciences*, *110*(26), 10812–10817. https://doi.org/10.1073/pnas.1308421110

Eck, R. J., Kraemer, B. C., & Liachko, N. F. (2021). Regulation of TDP-43 phosphorylation in aging and disease. *GeroScience*, *43*(4), 1605–1614. https://doi.org/10.1007/s11357-021-00383-5

Fayemendy, P., Marin, B., Labrunie, A., Boirie, Y., Walrand, S., Achamrah, N., Coëffier, M., Preux, P.-M., Lautrette, G., Desport, J.-C., Couratier, P., & Jésus, P. (2021). Hypermetabolism is a reality in amyotrophic lateral sclerosis compared to healthy subjects. *Journal of the Neurological Sciences*, *420*, 117257. https://doi.org/10.1016/j.jns.2020.117257

Gautam, M., Jara, J. H., Kocak, N., Rylaarsdam, L. E., Kim, K. D., Bigio, E. H., & Hande Özdinler, P. (2019). Mitochondria, ER, and nuclear membrane defects reveal early mechanisms for upper motor neuron

vulnerability with respect to TDP-43 pathology. *Acta Neuropathologica*, *137*(1), 47–69. https://doi.org/10.1007/s00401-018-1934-8

Gendron, T. F., & Petrucelli, L. (2011). Rodent Models of TDP-43 Proteinopathy: Investigating the Mechanisms of TDP-43-Mediated Neurodegeneration. *Journal of Molecular Neuroscience*, *45*(3), 486–499. https://doi.org/10.1007/s12031-011-9610-7

Gruijs Da Silva, L. A., Simonetti, F., Hutten, S., Riemenschneider, H., Sternburg, E. L., Pietrek, L. M., Gebel, J., Dötsch, V., Edbauer, D., Hummer, G., Stelzl, L. S., & Dormann, D. (2022). Disease-linked TDP-43 hyperphosphorylation suppresses TDP-43 condensation and aggregation. *The EMBO Journal*, *41*(8), e108443. https://doi.org/10.15252/embj.2021108443

Guo, W., Chen, Y., Zhou, X., Kar, A., Ray, P., Chen, X., Rao, E. J., Yang, M., Ye, H., Zhu, L., Liu, J., Xu, M., Yang, Y., Wang, C., Zhang, D., Bigio, E. H., Mesulam, M., Shen, Y., Xu, Q., … Wu, J. Y. (2011). An ALS-associated mutation affecting TDP-43 enhances protein aggregation, fibril formation and neurotoxicity. *Nature Structural & Molecular Biology*, *18*(7), 822–830. https://doi.org/10.1038/nsmb.2053

Habas, A., Hahn, J., Wang, X., & Margeta, M. (2013). Neuronal activity regulates astrocytic Nrf2 signaling. *Proceedings of the National Academy of Sciences*, *110*(45), 18291–18296. https://doi.org/10.1073/pnas.1208764110

Hardiman, O., Al-Chalabi, A., Chio, A., Corr, E. M., Logroscino, G., Robberecht, W., Shaw, P. J., Simmons, Z., & van den Berg, L. H. (2017). Amyotrophic lateral sclerosis. *Nature Reviews Disease Primers*, *3*(1), 17071. https://doi.org/10.1038/nrdp.2017.71

Hatzipetros, T., Bogdanik, L. P., Tassinari, V. R., Kidd, J. D., Moreno, A. J., Davis, C., Osborne, M., Austin, A., Vieira, F. G., Lutz, C., & Perrin, S. (2014). C57BL/6J congenic Prp-TDP43A315T mice develop progressive neurodegeneration in the myenteric plexus of the colon without exhibiting key features of ALS. *Brain Research*, *1584*, 59–72. https://doi.org/10.1016/j.brainres.2013.10.013

He, J., Fu, J., Zhao, W., Ren, C., Liu, P., Chen, L., Li, D., Tang, L., Zhou, L., Zhang, Y., Ma, X., Zhang, G., Li, N., & Fan, D. (2022). Hypermetabolism associated with worse prognosis of amyotrophic lateral sclerosis. *Journal of Neurology*, *269*(3), 1447–1455. https://doi.org/10.1007/s00415-021-10716-1

Henriques, A., Croixmarie, V., Bouscary, A., Mosbach, A., Keime, C., Boursier-Neyret, C., Walter, B., Spedding, M., & Loeffler, J.-P. (2018). Sphingolipid Metabolism Is Dysregulated at Transcriptomic and Metabolic Levels in the Spinal Cord of an Animal Model of Amyotrophic Lateral Sclerosis. *Frontiers in Molecular Neuroscience*, *10*, 433. https://doi.org/10.3389/fnmol.2017.00433

Herdewyn, S., Cirillo, C., Van Den Bosch, L., Robberecht, W., Vanden Berghe, P., & Van Damme, P. (2014). Prevention of intestinal obstruction reveals progressive neurodegeneration in mutant TDP-43 (A315T)mice. *Molecular Neurodegeneration*, *9*(1), 24. https://doi.org/10.1186/1750-1326-9-24

Hergesheimer, R., Lanznaster, D., Bourgeais, J., Hérault, O., Vourc'h, P., Andres, C. R., Corcia, P., & Blasco, H. (2020). Conditioned Medium from Cells Overexpressing TDP-43 Alters the Metabolome of Recipient Cells. *Cells*, *9*(10), 2198. https://doi.org/10.3390/cells9102198

Huang, S.-L., Wu, L.-S., Lee, M., Chang, C.-W., Cheng, W.-C., Fang, Y.-S., Chen, Y.-R., Cheng, P.-L., & Shen, C.-K. J. (2020). A robust TDP-43 knock-in mouse model of ALS. *Acta Neuropathologica Communications*, *8*(1), 3. https://doi.org/10.1186/s40478-020-0881-5

Jung, M.-K., Kim, K. Y., Lee, N.-Y., Kang, Y.-S., Hwang, Y. J., Kim, Y., Sung, J.-J., McKee, A., Kowall, N., Lee, J., & Ryu, H. (2013). Expression of Taurine Transporter (TauT) is Modulated by Heat Shock Factor 1 (HSF1) in Motor Neurons of ALS. *Molecular Neurobiology*, *47*(2), 699–710. https://doi.org/10.1007/s12035-012-8371-9

Kadowaki, M., & Karim, Md. R. (2009). Chapter 13 Cytosolic LC3 Ratio as a Quantitative Index of Macroautophagy. In *Methods in Enzymology* (Vol. 452, pp. 199–213). Elsevier. https://doi.org/10.1016/S0076-6879(08)03613-6

Lanznaster, D., De Assis, D. R., Corcia, P., Pradat, P.-F., & Blasco, H. (2018). Metabolomics Biomarkers: A Strategy Toward Therapeutics Improvement in ALS. *Frontiers in Neurology*, *9*, 1126. https://doi.org/10.3389/fneur.2018.01126

Lastres-Becker, I., De Lago, E., Martínez, A., & Fernández-Ruiz, J. (2022). New Statement about NRF2 in Amyotrophic Lateral Sclerosis and Frontotemporal Dementia. *Biomolecules*, *12*(9), 1200. https://doi.org/10.3390/biom12091200

Li, H.-Y., Yeh, P.-A., Chiu, H.-C., Tang, C.-Y., & Tu, B. P. (2011). Hyperphosphorylation as a Defense Mechanism to Reduce TDP-43 Aggregation. *PLoS ONE*, *6*(8), e23075. https://doi.org/10.1371/journal.pone.0023075

Li, J., & McCullough, L. D. (2010). Effects of AMP-Activated Protein Kinase in Cerebral Ischemia. *Journal of Cerebral Blood Flow & Metabolism*, *30*(3), 480–492. https://doi.org/10.1038/jcbfm.2009.255

Loganathan, S., Wilson, B. A., Carey, S. B., Manzo, E., Joardar, A., Ugur, B., & Zarnescu, D. C. (2022). TDP-43 Proteinopathy Causes Broad Metabolic Alterations including TCA Cycle Intermediates and Dopamine Levels in Drosophila Models of ALS. *Metabolites*, *12*(2), 101. https://doi.org/10.3390/metabo12020101

Lutz, C. (2018). Mouse models of ALS: Past, present and future. *Brain Research*, *1693*, 1–10. https://doi.org/10.1016/j.brainres.2018.03.024

Mackenzie, I. R. A., Bigio, E. H., Ince, P. G., Geser, F., Neumann, M., Cairns, N. J., Kwong, L. K., Forman, M. S., Ravits, J., Stewart, H., Eisen, A., McClusky, L., Kretzschmar, H. A., Monoranu, C. M., Highley, J. R., Kirby, J., Siddique, T., Shaw, P. J., Lee, V. M.-Y., & Trojanowski, J. Q. (2007). Pathological TDP-43 distinguishes sporadic amyotrophic lateral sclerosis from amyotrophic lateral sclerosis with SOD1 mutations. *Annals of Neurology*, *61*(5), 427–434. https://doi.org/10.1002/ana.21147

Magaquian, D., Delgado Ocaña, S., Perez, C., & Banchio, C. (2021). Phosphatidylcholine restores neuronal plasticity of neural stem cells under inflammatory stress. *Scientific Reports*, *11*(1), 22891. https://doi.org/10.1038/s41598-021-02361-5

Manzo, E., Lorenzini, I., Barrameda, D., O'Conner, A. G., Barrows, J. M., Starr, A., Kovalik, T., Rabichow, B. E., Lehmkuhl, E. M., Shreiner, D. D., Joardar, A., Liévens, J.-C., Bowser, R., Sattler, R., & Zarnescu, D. C. (2019). Glycolysis upregulation is neuroprotective as a compensatory mechanism in ALS. *eLife*, *8*, e45114. https://doi.org/10.7554/eLife.45114

Martias, C., Baroukh, N., Mavel, S., Blasco, H., Lefèvre, A., Roch, L., Montigny, F., Gatien, J., Schibler, L., Dufour-Rainfray, D., Nadal-Desbarats, L., & Emond, P. (2021). Optimization of Sample Preparation for Metabolomics Exploration of Urine, Feces, Blood and Saliva in Humans Using Combined NMR and UHPLC-HRMS Platforms. *Molecules*, *26*(14), Article 14. https://doi.org/10.3390/molecules26144111

McCluskey, G., Donaghy, C., Morrison, K. E., McConville, J., Duddy, W., & Duguez, S. (2022). The Role of Sphingomyelin and Ceramide in Motor Neuron Diseases. *Journal of Personalized Medicine*, *12*(9), 1418. https://doi.org/10.3390/jpm12091418

Muraleedharan, R., & Dasgupta, B. (2022). AMPK in the brain: Its roles in glucose and neural metabolism. *The FEBS Journal*, *289*(8), 2247–2262. https://doi.org/10.1111/febs.16151

Nakazato, T., Kanai, K., Kataura, T., Nojiri, S., Hattori, N., & Saiki, S. (2022). Plasma taurine is an axonal excitability-translatable biomarker for amyotrophic lateral sclerosis. *Scientific Reports*, *12*(1), 9155. https://doi.org/10.1038/s41598-022-13397-6

Neumann, M., Kwong, L. K., Lee, E. B., Kremmer, E., Flatley, A., Xu, Y., Forman, M. S., Troost, D., Kretzschmar, H. A., Trojanowski, J. Q., & Lee, V. M.-Y. (2009). Phosphorylation of S409/410 of TDP-43 is a consistent feature in all sporadic and familial forms of TDP-43 proteinopathies. *Acta Neuropathologica*, *117*(2), 137–149. https://doi.org/10.1007/s00401-008-0477-9

Neumann, M., Sampathu, D. M., Kwong, L. K., Truax, A. C., Micsenyi, M. C., Chou, T. T., Bruce, J., Schuck, T., Grossman, M., Clark, C. M., McCluskey, L. F., Miller, B. L., Masliah, E., Mackenzie, I. R., Feldman, H., Feiden, W., Kretzschmar, H. A., Trojanowski, J. Q., & Lee, V. M.-Y. (2006). Ubiquitinated TDP-43 in Frontotemporal Lobar Degeneration and Amyotrophic Lateral Sclerosis. *Science*, *314*(5796), 130–133. https://doi.org/10.1126/science.1134108

Park, J.-M., Lee, D.-H., & Kim, D.-H. (2023). Redefining the role of AMPK in autophagy and the energy stress response. *Nature Communications*, *14*(1), 2994. https://doi.org/10.1038/s41467-023-38401-z

Patin, F., Baranek, T., Vourc'h, P., Nadal-Desbarats, L., Goossens, J.-F., Marouillat, S., Dessein, A.-F., Descat, A., Hounoum, B. M., Bruno, C., Watier, H., Si-Tahar, M., Leman, S., Lecron, J.-C., Andres, C. R., Corcia, P., & Blasco, H. (2016). Combined Metabolomics and Transcriptomics Approaches to Assess the IL-6 Blockade as a Therapeutic of ALS: Deleterious Alteration of Lipid Metabolism. *Neurotherapeutics*, *13*(4), 905–917. https://doi.org/10.1007/s13311-016-0461-3

Patin, F., Corcia, P., Vourc'h, P., Nadal-Desbarats, L., Baranek, T., Goossens, J.-F., Marouillat, S., Dessein, A.-F., Descat, A., Madji Hounoum, B., Bruno, C., Leman, S., Andres, C. R., & Blasco, H. (2017). Omics to Explore Amyotrophic Lateral Sclerosis Evolution: The Central Role of Arginine and Proline Metabolism. *Molecular Neurobiology*, *54*(7), 5361–5374. https://doi.org/10.1007/s12035-016-0078-x

Perry, T. L., Hansen, S., & Jones, K. (1987). Brain glutamate deficiency in amyotrophic lateral sclerosis. *Neurology*, *37*(12), 1845–1845. https://doi.org/10.1212/WNL.37.12.1845

Rajaratnam, S., Soman, A. P., Phalguna, K. S., Pradhan, S. S., Manjunath, M., Rao, R. K., Dandamudi, R. B., Bhagavatham, S. K. S., Pulukool, S. K., Rathnakumar, S., Kocherlakota, S., Pargaonkar, A., Veeranna, R. P., Arumugam, N., Almansour, A. I., Choudhary, B., & Sivaramakrishnan, V. (2023). Integrated Omic Analysis Delineates Pathways Modulating Toxic TDP-43 Protein Aggregates in Amyotrophic Lateral Sclerosis. *Cells*, *12*(9), 1228. https://doi.org/10.3390/cells12091228

Rueda-Lopes, F. C., Hygino Da Cruz, L. C., Doring, T. M., & Gasparetto, E. L. (2014). Diffusion-Weighted Imaging and Demyelinating Diseases: New Aspects of an Old Advanced Sequence. *American Journal of Roentgenology*, *202*(1), W34–W42. https://doi.org/10.2214/AJR.13.11400

Shepheard, S. R., Parker, M. D., Cooper-Knock, J., Verber, N. S., Tuddenham, L., Heath, P., Beauchamp, N., Place, E., Sollars, E. S. A., Turner, M. R., Malaspina, A., Fratta, P., Hewamadduma, C., Jenkins, T. M., McDermott,

C. J., Wang, D., Kirby, J., & Shaw, P. J. (2021). Value of systematic genetic screening of patients with amyotrophic lateral sclerosis. *Journal of Neurology, Neurosurgery & Psychiatry*, *92*(5), 510–518. https://doi.org/10.1136/jnnp-2020-325014

Simandi, Z., Pajer, K., Karolyi, K., Sieler, T., Jiang, L.-L., Kolostyak, Z., Sari, Z., Fekecs, Z., Pap, A., Patsalos, A., Contreras, G. A., Reho, B., Papp, Z., Guo, X., Horvath, A., Kiss, G., Keresztessy, Z., Vámosi, G., Hickman, J., … Nagy, L. (2018). Arginine Methyltransferase PRMT8 Provides Cellular Stress Tolerance in Aging Motoneurons. *The Journal of Neuroscience*, *38*(35), 7683–7700. https://doi.org/10.1523/JNEUROSCI.3389-17.2018

Stallings, N. R., Puttaparthi, K., Luther, C. M., Burns, D. K., & Elliott, J. L. (2010). Progressive motor weakness in transgenic mice expressing human TDP-43. *Neurobiology of Disease*, *40*(2), 404–414. https://doi.org/10.1016/j.nbd.2010.06.017

Tefera, T. W., Steyn, F. J., Ngo, S. T., & Borges, K. (2021). CNS glucose metabolism in Amyotrophic Lateral Sclerosis: A therapeutic target? *Cell & Bioscience*, *11*(1), 14. https://doi.org/10.1186/s13578-020-00511-2

The PLOS ONE Staff. (2014). Correction: Mutant TDP-43 Deregulates AMPK Activation by PP2A in ALS Models. *PLoS ONE*, *9*(4), e95549. https://doi.org/10.1371/journal.pone.0095549

Valbuena, G. N., Cantoni, L., Tortarolo, M., Bendotti, C., & Keun, H. C. (2019). Spinal Cord Metabolic Signatures in Models of Fast- and Slow-Progressing SOD1G93A Amyotrophic Lateral Sclerosis. *Frontiers in Neuroscience*, *13*, 1276. https://doi.org/10.3389/fnins.2019.01276

Weerasekera, A., Crabbé, M., Tomé, S. O., Gsell, W., Sima, D., Casteels, C., Dresselaers, T., Deroose, C., Van Huffel, S., Rudolf Thal, D., Van Damme, P., & Himmelreich, U. (2020). Non-invasive characterization of amyotrophic lateral sclerosis in a hTDP-43A315T mouse model: A PET-MR study. *NeuroImage: Clinical*, *27*, 102327. https://doi.org/10.1016/j.nicl.2020.102327

Wegorzewska, I., & Baloh, R. H. (2011). TDP-43-Based Animal Models of Neurodegeneration: New Insights into ALS Pathology and Pathophysiology. *Neurodegenerative Diseases*, *8*(4), 262–274. https://doi.org/10.1159/000321547

Wegorzewska, I., Bell, S., Cairns, N. J., Miller, T. M., & Baloh, R. H. (2009). TDP-43 mutant transgenic mice develop features of ALS and frontotemporal lobar degeneration. *Proceedings of the National Academy of Sciences*, *106*(44), 18809–18814. https://doi.org/10.1073/pnas.0908767106

Wei, J., Wong, L. C., & Boland, S. (2023). Lipids as Emerging Biomarkers in Neurodegenerative Diseases. *International Journal of Molecular Sciences*, *25*(1), 131. https://doi.org/10.3390/ijms25010131

Werring, D. J. (2000). The pathogenesis of lesions and normal-appearing white matter changes in multiple sclerosis: A serial diffusion MRI study. *Brain*, *123*(8), 1667–1676. https://doi.org/10.1093/brain/123.8.1667

Westerhuis, J. A., Van Velzen, E. J. J., Hoefsloot, H. C. J., & Smilde, A. K. (2010). Multivariate paired data analysis: Multilevel PLSDA versus OPLSDA. *Metabolomics*, *6*(1), 119–128. https://doi.org/10.1007/s11306-009-0185-z

Wils, H., Kleinberger, G., Janssens, J., Pereson, S., Joris, G., Cuijt, I., Smits, V., Ceuterick-de Groote, C., Van Broeckhoven, C., & Kumar-Singh, S. (2010). TDP-43 transgenic mice develop spastic paralysis and

neuronal inclusions characteristic of ALS and frontotemporal lobar degeneration. *Proceedings of the National Academy of Sciences*, *107*(8), 3858–3863. https://doi.org/10.1073/pnas.0912417107

Wuolikainen, A., Jonsson, P., Ahnlund, M., Antti, H., Marklund, S. L., Moritz, T., Forsgren, L., Andersen, P. M., & Trupp, M. (2016). Multi-platform mass spectrometry analysis of the CSF and plasma metabolomes of rigorously matched amyotrophic lateral sclerosis, Parkinson's disease and control subjects. *Molecular BioSystems*, *12*(4), 1287–1298. https://doi.org/10.1039/C5MB00711A

Xu, X., Yang, Q., Liu, Z., Zhang, R., Yu, H., Wang, M., Chen, S., Xu, G., Shao, Y., & Le, W. (2023). Integrative analysis of metabolomics and proteomics unravels purine metabolism dysregulation in the SOD1G93A mouse model of amyotrophic lateral sclerosis. *Neurobiology of Disease*, *181*, 106110. https://doi.org/10.1016/j.nbd.2023.106110

Xu, Y.-F., Gendron, T. F., Zhang, Y.-J., Lin, W.-L., D'Alton, S., Sheng, H., Casey, M. C., Tong, J., Knight, J., Yu, X., Rademakers, R., Boylan, K., Hutton, M., McGowan, E., Dickson, D. W., Lewis, J., & Petrucelli, L. (2010). Wild-Type Human TDP-43 Expression Causes TDP-43 Phosphorylation, Mitochondrial Aggregation, Motor Deficits, and Early Mortality in Transgenic Mice. *Journal of Neuroscience*, *30*(32), 10851–10859. https://doi.org/10.1523/JNEUROSCI.1630-10.2010

Yu, C.-H., Davidson, S., Harapas, C. R., Hilton, J. B., Mlodzianoski, M. J., Laohamonthonkul, P., Louis, C., Low, R. R. J., Moecking, J., De Nardo, D., Balka, K. R., Calleja, D. J., Moghaddas, F., Ni, E., McLean, C. A., Samson, A. L., Tyebji, S., Tonkin, C. J., Bye, C. R., … Masters, S. L. (2020). TDP-43 Triggers Mitochondrial DNA Release via mPTP to Activate cGAS/STING in ALS. *Cell*, *183*(3), 636-649.e18. https://doi.org/10.1016/j.cell.2020.09.020

Supplementary figures

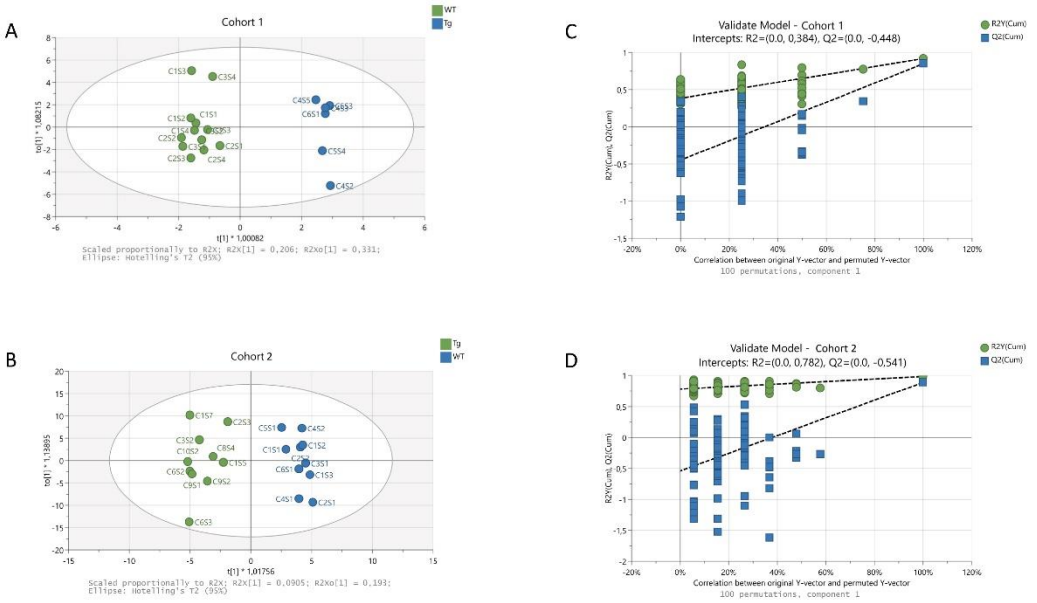

Supplementary figure 1. Representative validated score scatter plots for cohort 1 and 2 at T1 and T1', respectively. OPLS-DA score plot characterizing the contribution of metabolites to the separation of classes in cohort 1 at T1 (A) and 2 at T1' (B). Permutation tests used to validate the OPLS-DA models in cohort 1 at T1 (C) and 2 at T1' (D).

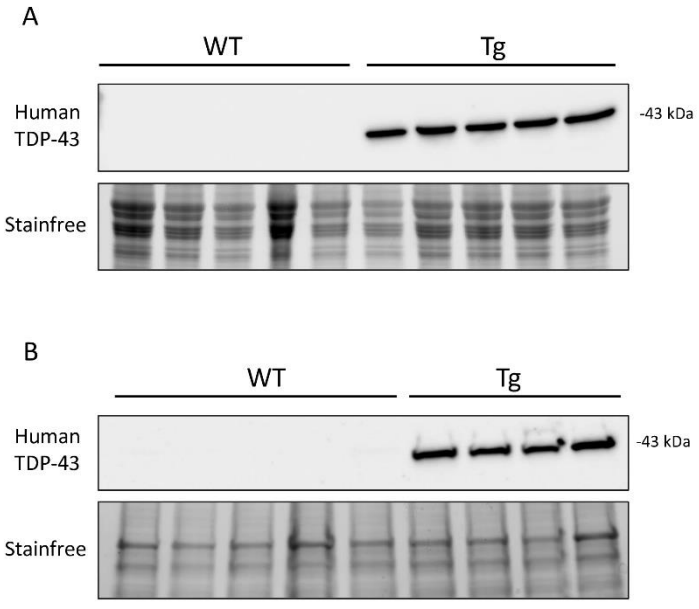

Supplementary figure 2. Representative immunoblots of mutant human TDP-43 in the brain (A) and spinal cord (B) of WT and Tg mice. (N=10 WT, N=11 Tg).

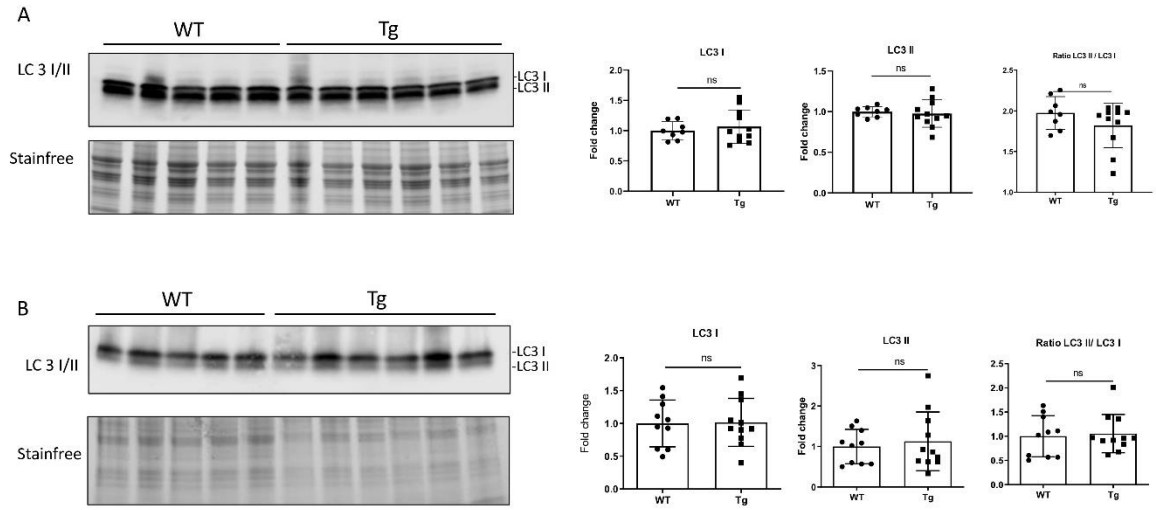

Supplementary figure 3. No significant change in LC3 I, LC3 II, or the ratio LC3 II/LC3 I in Tg mice. Representative immunoblots and quantification of LC3 I and LC3 II in the brain (A) and spinal cord (B) of WT and Tg mice. Fold change of Tg to WT was calculated following normalization of each condition to the corresponding stainfree gel. Unpaired t-test, p>0.05. (N=10 WT, N=11 Tg).

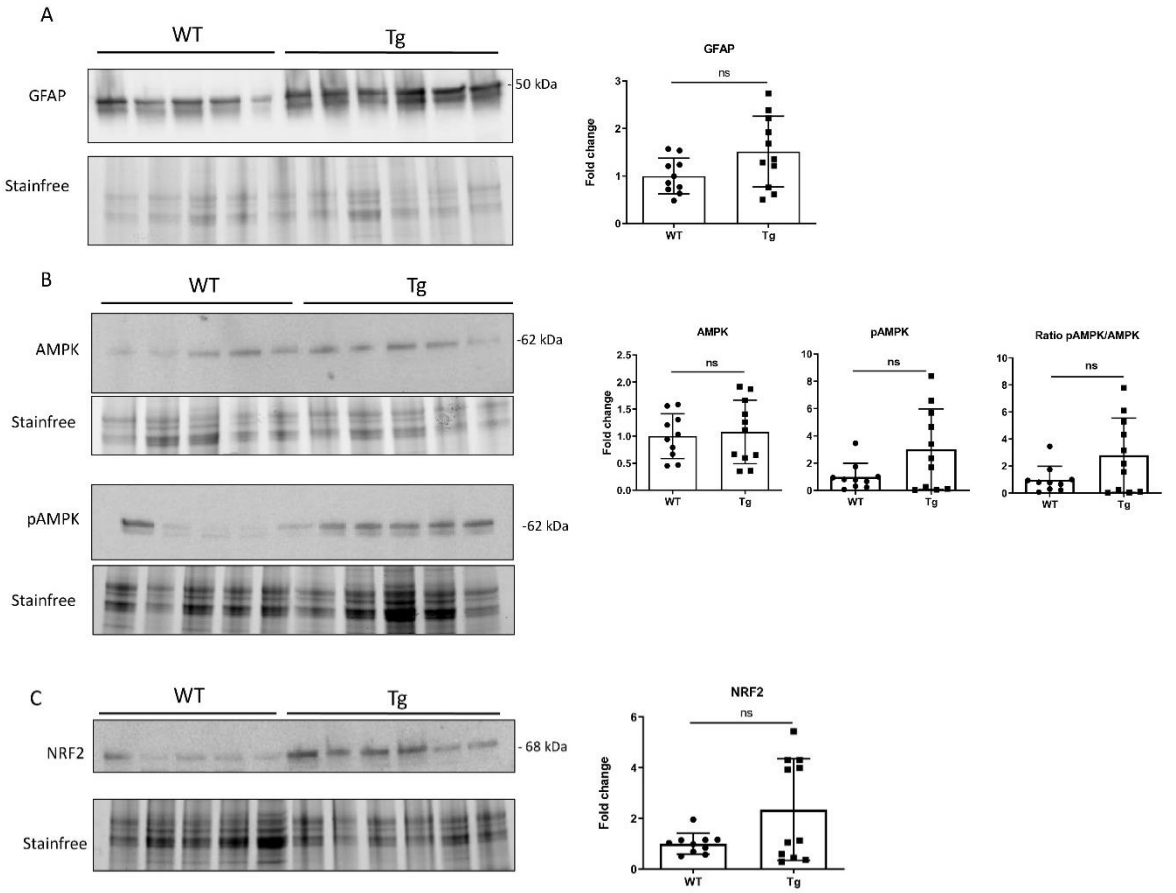

Supplementary figure 4. No significant change in GFAP, AMPK, pAMPK, the ratio pAMKP/AMPK, or NRF2 in the spinal cord of Tg mice. Representative immunoblots and quantification of GFAP (A),

AMPK and pAMPK (B), and NRF2 (C) in the spinal cord of WT and Tg mice. Fold change of Tg to WT was calculated following normalization of each condition to the corresponding stainfree gel. Unpaired t-

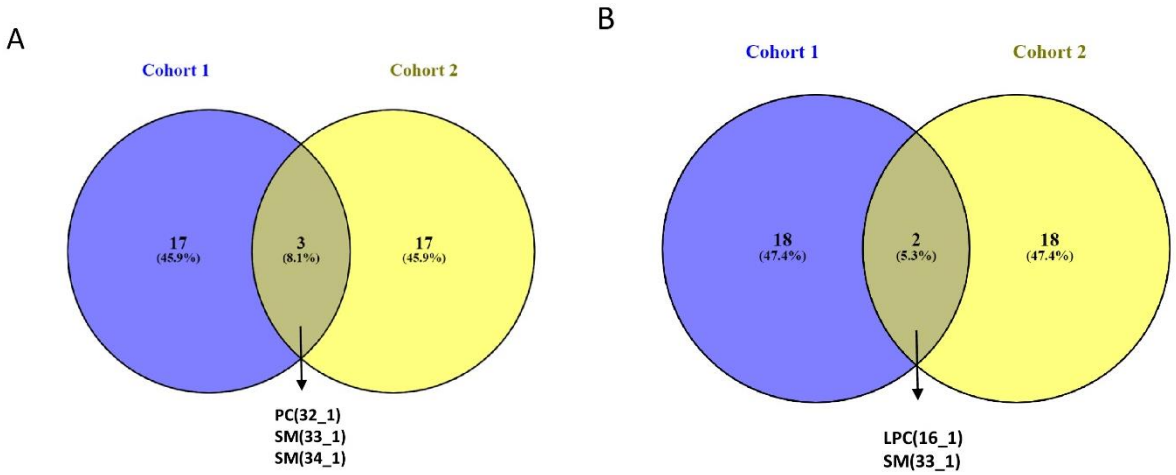

test, *p*>0.05. (N=10 WT, N=11 Tg).

Supplementary figure 5. Venn diagram examining common blood metabolites between cohort 1 and 2 at symptomatic stage. A) Top 20 metabolites collected from DBS T1 of cohort 1 and serum T1' of cohort 2 following multivariate analysis were examined for metabolites in common. B) Top 20 metabolites collected from DBS T1 of cohort 1 and serum T1' of cohort 2 following univariate analysis were examined for metabolites in common. (Cohort 1: N=12 WT and N=6 Tg; Cohort 2: N= 10 WT and N=11 Tg).

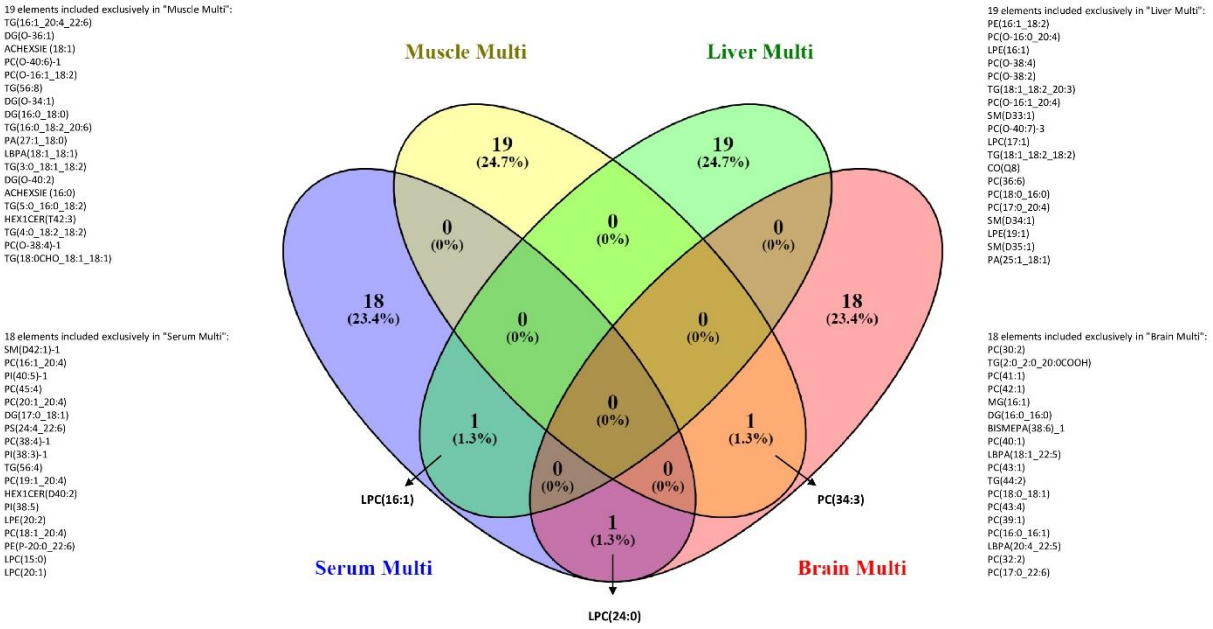

Supplementary figure 6. Multivariate analysis of lipid subclasses from cohort 2 at T1'.

Venn diagram representing common top 20 lipids between all samples in cohort 2 based on multivariate analysis performed. (N=10 WT, N=11 Tg).

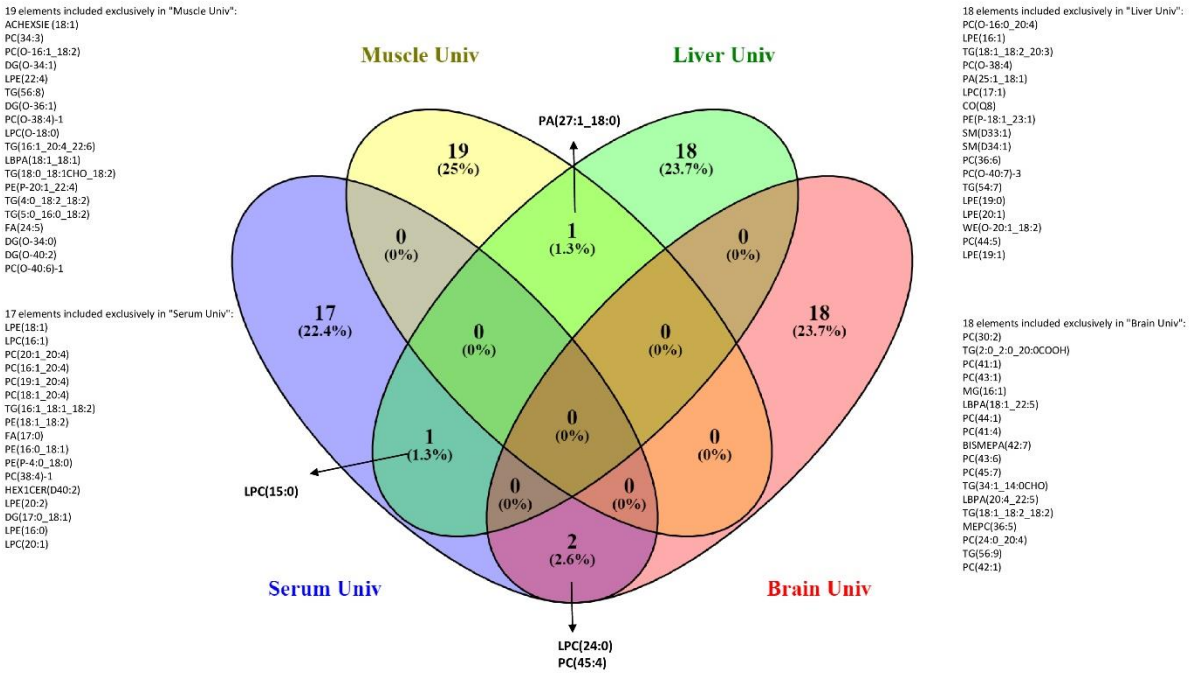

Supplementary figure 7. Univariate analysis of lipid subclasses from cohort 2 at T1'.

Venn diagram representing common top 20 lipids between all samples in cohort 2 based on univariate analysis performed. (N=10 WT, N=11 Tg).

e. Discussion

A well-characterized animal model is a cornerstone for developing effective treatments and understanding the underlying biology of ALS. We decided to conduct a detailed characterization of the Prp-TDP-43^{A315T} animal model, because it replicates several key aspects of TDP-43 proteinopathy in ALS. We also decided to use female mice which present with a slower progressing disease, allowing for a longer analysis in time, and providing additional information to the literature which was mainly conducted on male mice. Tg mice clearly showed motor dysfunction at the symptomatic stage, which was concomitant with a failure of these mice to gain weight, despite being on a high fat diet, confirming their hypermetabolic state which was also extensively reported in ALS patients (Fayemendy et al., 2021; J. He et al., 2022). However, the Tg group was much more heterogenous than the WT group, reflecting also the heterogeneity observed in ALS. The absence of modifications in the spinal cord MRI signal in Tg mice suggests the absence of important structural spinal cord changes even at symptomatic changes, even in the presence of TDP-43 proteinopathy in this tissue. The overall increase in the level of TDP-43 in the total and insoluble protein fractions in both the brain and spinal cord reflects the widespread TDP-43 proteinopathy in the CNS. TDP-43 CTF fragments were more observed in the brain than in the spinal cord of Tg mice, suggesting decreased TDP-43 fragmentation or increased degradation of these fragments in the spinal cord (Berning & Walker, 2019). This can also be reflected in the fact that insoluble pTDP-43 decreased in the spinal cord and increased in the brain. An interesting observation we made was the different patterns and degree of change of TDP-43 forms that were detected in the brain and spinal cord, implicating different handling of TDP-43 in these tissues. Similarly, the different ALS-related markers that were altered in the brain and not the spinal cord reflect the different tolerance and response of these tissues to stress conditions (Chestnut et al., 2011; Simandi et al., 2018). In the brain, the increase in GFAP levels reflected a state of astrogliosis, while the increase in NRF2 reflected the activation of the cellular response to stress, particularly oxidative stress (Habas et al., 2013). On the other hand, we noted a decrease in the ratio of pAMPK to AMPK, suggesting an inadequate response of brain cells to energetical stressors, which can be associated ultimately with various metabolomic alterations (Barnaba et al., 2023; Muraleedharan & Dasgupta, 2022; J.-M. Park et al., 2023). Indeed, alterations in various metabolites were detected in different tissues in Tg mice compared to WT. Alterations

were even detected in the serum at the presymptomatic stage at T0, suggesting that metabolomic dysfunction occurs early in the disease, and can therefore provide an avenue for the detection of early biomarkers. At the symptomatic stage, the increase in blood sphingomyelin was of particular interest because sphingolipid alterations were reported by other researchers in SOD1 mice and the spinal cord of ALS patients (Cutler et al., 2002). This result highlights the possible involvement of oligodendrocytes and myelination in the progression of the disease (McCluskey et al., 2022). We also detected changes in metabolites involved in glucose, xylose and taurine metabolisms, all of which have been reported to be implicated in ALS (Jung et al., 2013; Manzo et al., 2019; Nakazato et al., 2022; Perry et al., 1987; Tefera et al., 2021; Wuolikainen et al., 2016). Lipid metabolism, particularly in the muscle, was also highly altered in Tg mice compared to WT mice. The identified lipid subgroups were found to be associated with cytoskeletal function, inflammation, neuronal development and apoptosis (Blasco, Veyrat-Durebex, et al., 2017; Magaquian et al., 2021). Indeed, altered lipid metabolism in skeletal muscles has been previously found to be implicated in ALS (Quessada et al., 2021; Steyn et al., 2018, 2020). Overall, our results suggest that this model is a valuable tool to better our understanding of ALS and to help in the diagnostic and therapeutic development because it recapitulates important phenotypic, molecular, metabolomic and lipidomic changes observed in ALS.

After determining several parameters that are altered in transgenic Prp-TDP-43^{A315T} mice compared to controls, we could proceed with the final step of the project which is the administration of the scFv to these mice. In order to guarantee the delivery of the scFv into target cells in the CNS, we decided to use a recently developed AAV variant called AAV-CAP.B10, which transduces the neurons of the CNS. Here, we assessed the expression pattern of the scFv following the administration of the AAV to confirm the feasibility of our administration approach.

VIII. AAV-mediated delivery of the scFvs B1, D7 and 13R4.

A. Résumé en Français

L'administration de biothérapeutiques, telles que les anticorps ou fragments d'anticorps, pour cibler le SNC est compliquée par la barrière hémato-encéphalique (BHE) qui limite leur passage. Les méthodes de livraison actuelles sont peu efficaces pour traverser la BHE sans être invasives (Al Ojaimi et al., 2022). Dans cette étude, des vecteurs viraux adéno-associés (AAV), notamment l'AAV.CAP-B10, ont été utilisés pour exprimer les scFv anti-TDP-43 dans le SNC des souris sous le contrôle du promoteur de la synapsine. Après injection intraveineuse de 6-e11 VG chez des souris C57BL/6J, les différents tissus ont été prélevés après 4 et 8 semaines de l'injection pour analyser l'expression du scFv par RT-qPCR et western blot. On s'était concentrés sur le niveau d'expression et le tropisme tissulaire des AAV. Les scFv ont été bien exprimés dans le cerveau, le tronc cérébral et la moelle épinière après 4 et 8 semaines et aucun signal n'a été détecté dans les tissus périphériques, comme le foie, les reins ou les muscles. Il a été démontré que l'AAV-CAP.B10, qui est capable de traverser la BHE (Goertsen et al., 2022), ciblait principalement les neurones glutamatergiques du SNC (D. Brown et al., 2021), améliorant ainsi son efficacité et sécurité en minimisant ses effets sur les tissus périphériques (Jagadisan & Dhawan, 2023). Cependant, étant donné que les motoneurones supérieurs sont glutamatergiques (Stifani, 2014) il est crucial d'administrer l'AAV tôt dans la maladie pour éviter que la perte neuronale ne diminue son efficacité. Des recherches supplémentaires sont nécessaires pour évaluer la sécurité à long terme, les effets hors cible et la persistance de l'expression dans le temps du scFv. Le projet se poursuivra dans le contexte de l'appel d'offre iDEA-TECH Awards de Sanofi, en testant cet AAV chez des souris

Prp-TDP-43^{A315T} pour une période de 12 mois, avec une analyse approfondie des profils phénotypiques, moléculaires, métabolomiques, lipidomiques, et transcriptomiques.

B. Context

The administration of biotherapeutics, such as antibodies or antibody fragments, to target the CNS presents several challenges due to the unique and protective nature of the CNS. The most significant barrier is the BBB which severely restricts the passage of most biotherapeutics. There are limited delivery methods available that can effectively bypass the BBB without being invasive. Systemic administration routes, such as oral or intravenous delivery, often fail to deliver sufficient drug amounts to the CNS. Furthermore, the brain's complex environment, including its distinct cell types and extracellular matrix, poses additional challenges in ensuring that the biotherapeutics reach their specific targets within the CNS and maintain their efficacy over time. We have previously discussed the development of SPION-scFv nanoparticles that can potentially allow for the delivery of scFvs into the CNS in general, and the motor cortex in particular using magnetic targeting. However, this method has some limitations, and still requires further technological development and troubleshooting in order to meet its objectives. For this reason, to test the effect of the identified anti-TDP-43 scFvs *in vivo*, we decided to use adeno-associated viral (AAV) vectors which are capable of crossing the BBB and delivering the scFv directly into the CNS.

C. Materials and methods

a. Animals and AAV injection

An engineered variant of the AAV called AAV.CAP-B10 was acquired from the Bertarelli gene therapy platform (Geneva, Switzerland) to be used in this study. The CAP-B10 refers to a particular variant of the AAV capsid that was developed to improve the ability of the vector to deliver genes effectively to specific tissues, particularly neurons in the CNS (Goertsen et al., 2022). C57BL/6J wildtype female mice, aged six to eight weeks, were used to test the safety and expression pattern of the AAV-encoded scFv under the control of the synapsin promoter. For preliminary tests, only one mouse was used per timepoint, per scFv. A total of 12 mice were used. The AAV.CAP-B10 encoding either B1, D7, or the control scFv 13R4 was injected

into the tail vein of mice at an amount of 6-e11 viral genomes (VG). Mice injected with phosphate buffered saline (PBS) were used as controls.

b. Tissue and protein/RNA extraction

Samples were collected following isoflurane anaesthesia and cardiac perfusion with PBS. The brain, brainstem, spinal cord, kidneys, liver, gastrocnemius, and serum of mice were harvested at 4 weeks and 8 weeks post-injection. One group of mice was not euthanized to examine if the expression of the scFv persisted and if long-term side effects could be detected.

For protein extraction, the tissues were homogenized in 2 mL Precellys tubes containing ice-cold Cell Disruption Buffer (PARIS kit, Invitrogen™) supplemented with 1X Halt Protease Inhibitor Cocktail and Pierce Universal Nuclease (Thermo Fisher Scientific™). Following a 15 minutes incubation on ice, the homogenates were centrifuged at 1000xg for 5 min at 4°C. The supernatant was collected and the proteins were quantified using Pierce™ 660 Protein Assay Reagent. RNA extraction was only performed on tissues extracted from mice following 8 weeks of AAV injection. Mouse tissues were homogenized in 2 mL Precellys tubes containing Trizol® (Invitrogen). Total RNA extraction was performed using the Direct-zol™ RNA miniprep kit (Zymo Research) according to the manufacturer's protocol.

c. Western blot

A total of 40 µg of proteins were denatured at 95°C for 3 min in the presence of 1 mM DTT and resolved on 4-20% precast stain-free gels (Biorad). The proteins were then transferred onto a 0.2 µm nitrocellulose membrane and blocked for 2 hours at room temperature using 5% normal goat serum (Thermo Fisher Scientific™) in TBS-Tween (0.1%). Membranes were then incubated overnight at 4°C with an HRP-conjugated 6*His monoclonal antibody solution (1:10,000 ; Proteintech). Following washing, the blots were developed using the enhanced chemiluminescence solution (ECL, Biorad) and exposed using a ChemiDoc Imaging system (Biorad).

d. RT-qPCR

Following RNA extraction and quantification using a nanodrop, cDNA synthesis and qPCR amplification were performed using Luna Universal One-Step RT-qPCR kit following manufacturer's protocol. Briefly, the parameters used were as follows: reverse transcription at 55°C for 10 minutes, initial denaturation at 95°C for 1 minute, denaturation at 95°C for 10 seconds, extension at 60°C for 30 seconds, and melt curve at 60-95°C for 10 minutes at 0.5°C/5 seconds. A total of 45 cycles were performed. RT-qPCR experiments were carried out using 50ng RNA as template and SYBR Green I was used to measure DNA amplification after each PCR cycle. The primers used spanned common regions across all three scFvs (B1, D7, and 13R4) with forward primer used being AGCCTCTGGATTCACCTTCA and the reverse primer being GCGTTGTCTCTGGAGATGGT. The assays were performed in duplicate in a 3500 CFX (Biorad) in 20 µL reaction mixture. Quantification was carried out using a method derived from the $2^{-\Delta\Delta Cp}$ method. Normalized ratio was obtained for each target gene using CFX software, with qPCR efficiencies and values from non-injected mice considered, and *Gapdh* (glyceraldehyde 3-phosphate dehydrogenase) used as a reference gene for calculations. Reverse transcriptase negative (RT-) controls were used.

D. Results

a. scFv expression 4 weeks post-AAV administration

Following 4 weeks of AAV.CAP-B10 injection, the scFvs B1 and D7 were successfully expressed in the brain, brainstem and spinal cord. No signal was detected for the non-injected mice (Fig. 20.A). The expression of the scFvs was also limited to the CNS, with no signal detected for 13R4 in the kidneys, liver, muscle, or even in the serum (Fig. 20.B).

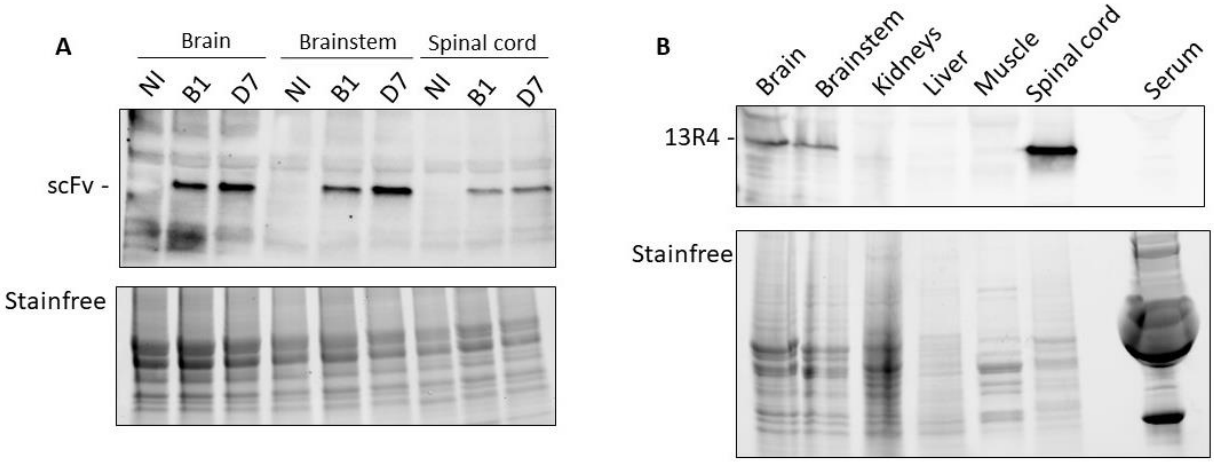

Figure 20: Exclusive AAV-mediated expression of the scFv in the CNS at 4 weeks post-administration. **A)** Immunoblot of 6*His-tagged scFv showing successful expression of the scFvs B1 and D7 in the brain, brainstem and spinal cord following 4 weeks of AAV administration into the tail vein of mice (N=1). NI: non-injected. **B)** Immunoblot of 6*His-tagged scFv showing that the expression of the control scFv 13R4 is restricted to the CNS following 4 weeks of AAV administration into the tail vein of mice (N=1).

b. scFv expression 8 weeks post-AAV administration

Western blot and RT-qPCR analyses revealed that the scFv was exclusively detected in the CNS with no signal in the peripheral tissues after 8 weeks of injection (Fig.21, 22). The RT- control ensured that any amplification observed in the qPCR step did not originate from residual genomic DNA rather than RNA, thereby validating the specificity of the RT+ reaction for scFv expression analysis.

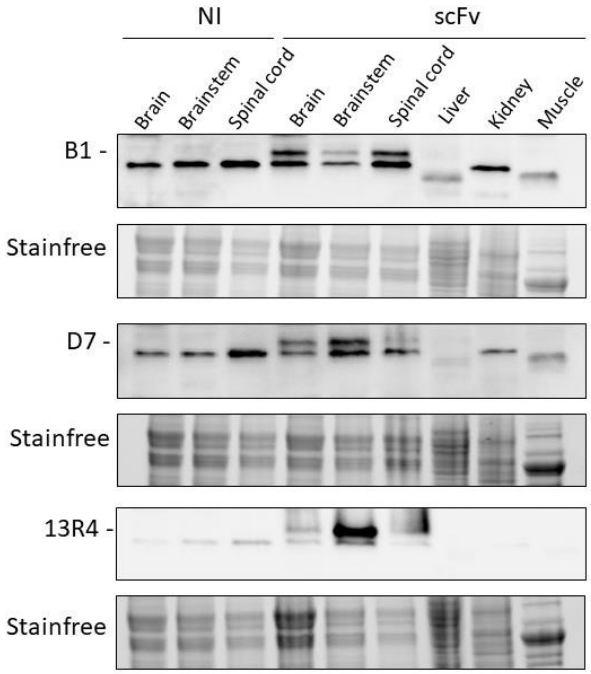

Figure 21: Exclusive AAV-mediated expression of the scFv in the CNS at 8 weeks post-administration. Immunoblot of 6*His-tagged scFv showing the successful expression of the scFvs B1, D7, and 13R4 in the brain, brainstem and spinal cord following 8 weeks of AAV administration into the tail vein of mice (N=1). NI: non-injected.

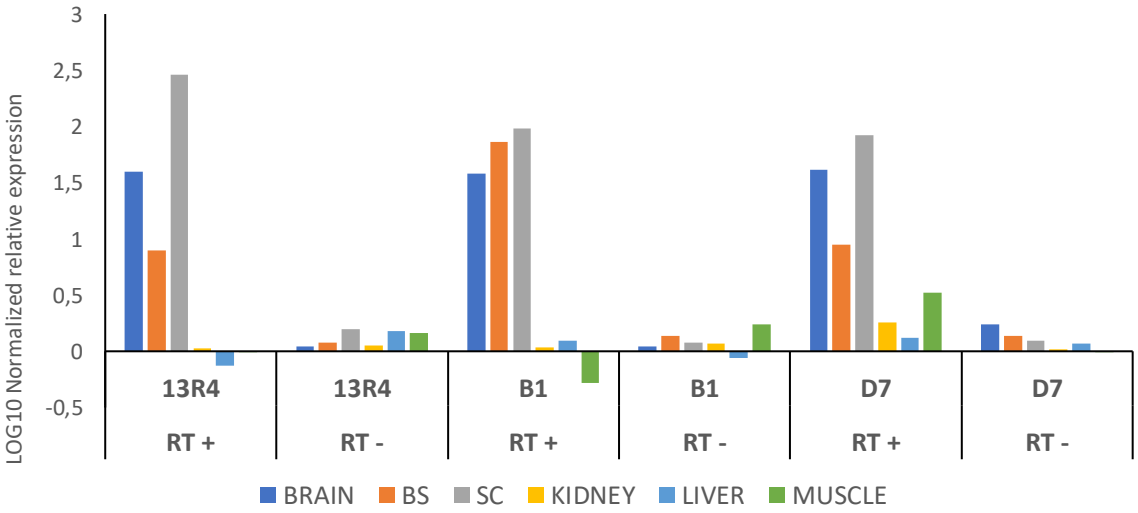

Figure 22: RT-qPCR results showing scFv expression exclusively in the CNS at 8 weeks post-AAV administration. Quantitative RT-qPCR results for scFv expression, presented as the mean relative expression levels (log10 scale) across different tissues. The expression levels were normalized to the housekeeping gene (*Gapdh*) and the non-injected group. RT+/-: reverse transcriptase positive/negative. (N=1).

E. Discussion

We investigated the expression profile of the engineered AAV-CAP.B10-encoded scFv in mice, focusing in a first place on its expression level and tissue tropism. AAV-CAP.B10 has been developed as a next-generation vector with enhanced ability to transduce target cells, particularly in challenging tissues such as the CNS (Goertsen et al., 2022). Our findings confirmed that AAV-CAP.B10 exhibited robust scFv expression in the CNS following 4 and 8 weeks of intravenous administration. No actual quantification was performed due to the restricted number of repeats. The enhanced CNS tropism could be attributed to the unique properties of the capsid, which allow for more efficient crossing of the blood-brain barrier and higher transduction rates in neuronal cells (Goertsen et al., 2022; Seo et al., 2022). Brown and his colleagues have shown by single-cell RNA sequencing that the AAV-CAP.B10 mainly targeted glutamatergic neurons in the CNS (D. Brown et al., 2021).This specific targeting that was restricted to the CNS can improve the efficacy and safety of this AAV tool by concentrating it in the CNS and minimizing its effect on peripheral tissues such as the liver (Jagadisan & Dhawan, 2023; Kubes & Jenne, 2018). However, since neurons in the CNS are the main target of the AAV-CAP.B10, caution should be given regarding the time of administration so that enough neurons are still present for the AAV transgene to be expressed. As the disease progresses and more neurons die, the efficiency of the treatment might be largely decreased.

Further investigations should evaluate long-term safety, potential off-target effects, and the persistence of the gene expression in time. As part of the Sanofi iDEA-TECH Awards, the next step of the project will be focused on delivering the AAV-CAP.B10 encoding the different scFvs to Prp-TDP-43^{A315T} mice at the early stages on the disease, and assessing the phenotypic, molecular, transcriptomic, metabolomic, and lipidomic profiles of these mice over a period of 12 months. The aim will be to investigate if the scFv B1 and/or D7 can bring back to normal some disease-associated alterations that have been studied in [Publication 6].

General discussion

In this project which aimed at developing scFv molecules to target TDP-43, different aspects of biotherapeutic selection, administration, and effects were evaluated. We were first interested in understanding how intracellular pH alterations, which are tightly linked to metabolic alterations, affect the behavior of TDP-43. Second, we characterized the effect of previously identified scFv molecules in a cellular model of ALS and demonstrated some protective effects. Third, in order to enhance the internalization of the scFv into target cells, we developed a nanoparticle-based delivery system by complexing the scFv to SPIONs. Fourth, following the assays *in vitro*, we decided to start the preclinical evaluation of the scFv. We started by the deep characterization of Prp-TDP-43^{A315T} animal model of ALS and identified measurable parameters that correlated with the disease state and that will be subsequently used to assess the effect of the scFv on the different pathophysiological alterations observed in ALS. Finally, we validated the administration of the scFv to the previously characterized mouse model using viral vectors, particularly the AAV-CAP.B10 variant which specifically transduces neurons in the CNS.

The importance of the intracellular environment when designing therapies

Intracellular environment can impact biotherapeutics and their target

When targeting intracellular proteins like TDP-43, one should carefully consider the intracellular environment in which the drug target resides. Intracellular targets, particularly proteins, are not static and can be affected by even the slightest alterations in the intracellular space. We know that in ALS, cellular homeostasis is greatly altered. Since metabolic changes, including mitochondrial dysfunction, oxidative stress and abnormal energy metabolism, are widely described in ALS, we decided to study a probable outcome of such changes which is the alteration of cellular pH.

pH is known to affect protein stability and folding. For instance, misfolding or denaturation of proteins due to pH changes can have an important impact on their functionality (Kristinsson & Hultin, 2003; Talley & Alexov, 2010), which could either enhance or diminish the effect of a drug designed to target that protein. Moreover, aberrant pH levels can affect the structure and assembly of proteins, potentially leading to increased aggregation (Pfefferkorn et al., 2010; Santos et al., 2020), which can alter the binding sites of drugs on their target, thus reducing drug efficacy or leading to unintended side effects. It should be noted

that the effect of the pH is not limited to the antigen but extends to the antibody as well (the scFv in our case). Therefore, in cases of perturbed metabolism and potentially altered intracellular pH, studies should also evaluate the stability and folding of the biotherapeutic in the intracellular environment, which might eventually lead to a change in the antigen-antibody interaction.

TDP-43 responds to intracellular pH changes

One outcome of pH alterations that was observed in our study was the increase in TDP-43-positive inclusions, an observation which can potentially be attributed to LLPS. This is a phenomenon in which biomolecules like proteins and nucleic acids demix into distinct liquid phases within a cell, forming membraneless organelles (Bratek-Skicki et al., 2022). These organelles are dynamic, reversible, and play a critical role in various cellular processes, including gene expression, signalling and stress response (Bratek-Skicki et al., 2022). Researchers have shown that proteins that have intrinsically disordered regions, which is the case of TDP-43, are more prone for LLPS (Chien et al., 2021; Pakravan et al., 2021). In fact, these intrinsically disordered regions, which are rich in hydrophilic amino acids (e.g. glycine, proline, serine…) but lack hydrophobic amino acids (e.g. valine, cysteine, leucine…) have a low complexity conformation which drives weak interactions with other molecules (Brocca et al., 2020; Martin & Holehouse, 2020). Changes in pH can influence such interactions, especially for those with ionizable amino acid residues that play a role in driving phase separation and LLPS (Pintado-Grima et al., 2022). In addition, for LLPS to occur, a saturation concentration of proteins needs to be reached, meaning that the concentration of the macromolecules needs to exceed a certain threshold to drive their condensation into liquid-like droplets (Harmon et al., 2017; J. Wang et al., 2018). This scenario has been replicated in our HEK293T cell model of ALS which overexpresses wildtype TDP-43. Aggregation of TDP-43 was reported in this model even at physiological pH, but an increase in LLPS was observed following just one hour of pH alterations. Longer treatments led to extensive cell death, which suggests that the long-term metabolic alterations that are reported in ALS might eventually cause cellular degeneration (Jin et al., 2022).

Concerning the aggregation of TDP-43, it is known to occur under certain pathological conditions, and intracellular pH can influence this process. A shift from LLPS-induced liquid-like droplets to insoluble aggregates might be occurring at times later than those reported in

our study. In fact, the involvement of intracellular pH alterations on age- and stress-induced LLPS and protein aggregation has been well-reported (Jin et al., 2022). An interesting study done on the tau protein, which also undergoes phase separation (Boyko & Surewicz, 2022), have shown a change in the propensity of tau for LLPS under varying pH conditions, with higher LLPS observed at pH values closer to the isoionic point (pI) of the protein (Ambadipudi et al., 2017). It should be noted that acidic rather than alkaline pH environments are often found in stressed or damaged cells and can promote protein misfolding and aggregation (Q. Liao et al., 2018; Marijan et al., 2019). As for TDP-43, which is intrinsically prone to aggregation, it can be especially affected by such pH changes. It can be thought that pH changes transmit a stress signal to cells, altering the solubility of proteins, and driving LLPS and the formation of liquid like droplets. Such phenomenon might be protective for the cell in the early stages and become cytotoxic if the cell fails to restore homeostasis.

Evaluating the intracellular pH of cells that have TDP-43 alterations is an interesting next step. In fact, understanding the relationship between intracellular pH and TDP-43 can influence the design of therapeutics, especially biotherapeutics, but could also lead to novel therapeutic strategies. In addition, it might reflect the need to consider cellular models of ALS that better recapitulate metabolic changes and subsequent pH alterations. For instance, designing therapeutics that target TDP-43 forms that are particularly observed in stressed cells can be an interesting approach. On the other hand, modulating intracellular pH to maintain it within an optimal range might also reduce TDP-43 dysfunction.

ALS - A neurodegenerative disease beyond motor neurons

Using omics to understand ALS

Understanding the pathophysiology of ALS relies on the understanding of the global cellular environment and not just focusing on one protein (e.g. TDP-43). We first started by conducting a metabolipidomic analysis *in vitro* on HEK293T cells overexpressing TDP-43. Although cellular models do not recapitulate the overall disease state, they can give us an idea about the mechanisms that are affected by TDP-43 proteinopathy. In our case they pointed towards the metabolism of lipids involving for example carnitines, glycerophospholipids, and phosphatidylcholine. To validate and complement these findings, *in vivo* studies using ALS animal models were the next logical step. The animal model provides a complete disease

environment, with the genetic background related to ALS, along with its molecular and phenotypic consequences.

Recent research suggests that ALS is not just a disorder confined to motor neurons but may be better understood as a systemic disease- a condition that involves multiple biological networks and systems, extending beyond the nervous system (Tortarolo et al., 2017). In fact, although ALS primarily affects motor neurons, evidence shows that other systems, including the immune system and muscle tissues are involved (Krasnianski et al., 2005; Le Gall et al., 2022; McCombe et al., 2020). Omics approaches, such as transcriptomics and metabolomics, which collect large datasets, can play a pivotal role in deciphering the complex interactions underlying the pathophysiology of ALS (Caldi Gomes et al., 2024; Humphrey et al., 2023; S. Park et al., 2021). For instance, metabolic abnormalities are common in ALS, including increased energy expenditure, lipid metabolism changes, and hypermetabolism (Guillot et al., 2021; J. Li et al., 2022; Steyn et al., 2018; Tandan et al., 2023). This approach is interesting for us when undertaking the preclinical evaluation of the scFv. We already observed several metabolic and lipidomic alterations outside of the CNS in the Prp-TDP-43^{A315T} mice compared to the controls (e.g. muscles, blood), highlighting the non-neuronal involvement in the disease, and the need to evaluate the system in a more global way. This method might allow us to look for new markers relating to general physiological mechanisms (e.g. metabolism), instead of being restricted to neuronal markers.

Metabolomics: a new tool for biomarker discovery, disease monitoring and therapeutic development in ALS

Metabolomics offers a direct snapshot of the biochemical activity within a cell, tissue or organism and provides a real-time functional readout of cellular processes. This data can help connect upstream biological events to downstream phenotypic outcomes (e.g. disease progression). It can allow the identification of biomarkers for disease diagnosis and prognosis, monitoring of disease progression and evaluating the response to potential treatments.

Metabolomics hold good potential for the discovery of early disease biomarkers. In fact, metabolic alterations were observed in presymptomatic patients even before any changes in neurofilament levels (Dorst et al., 2023). Further work is still needed to enhance this diagnostic

potential, eventually allowing an earlier access to treatments to patients before the development of symptoms.

Metabolomics can also enhance therapeutic approaches. For example, metabolic biomarkers identified in preclinical models can guide the development and use of new drugs through the identification of altered disease mechanisms. In humans, the identification of such biomarkers can also be used to select the right patient populations for clinical trials, increasing the chances of success. Metabolomic biomarkers can also serve as surrogate endpoints in clinical trials, providing early indications of whether a therapy is working. In one study for example, metabolomics was performed in order to determine if some metabolites correlated with disease progression in groups of ALS patients receiving different treatment (Blasco et al., 2018). Researchers were able to identify distinct metabolite changes that reflected the early response of patients to different treatments (Blasco et al., 2018). Additionally, by analyzing metabolic networks, researchers can understand the broader impact of targeting a specific pathway, predicting potential side effects and toxicity (Combrink et al., 2020; Quintás et al., 2021), or identifying compensatory mechanisms that could potentially reduce drug efficacy (Araújo et al., 2021; H. Huang et al., 2018; Wilhelmi et al., 2023). Moreover, since disease heterogeneity is a major problem in ALS clinical trials, metabolomics can be used to classify patients based on their metabolic profiles, leading to more personalized treatment strategies (Hussain et al., 2022; Wildberg et al., 2019).

Following this logic, we decided to rely on metabolipidomics for biomarker-guided drug development. We have analysed the metabolomic profile of Prp-TDP-43^{A315T} mice and identified metabolites and lipids that were different between WT and Tg groups in different tissues and at different time points during the progression of the disease. The next step would be the evaluation of whether these metabolic alterations that were observed in Tg mice can be rectified by the administration of the scFv. Additional analyses such as transcriptomics will also be performed to evaluate whether the function of TDP-43 has been restored (i.e. splicing patterns, RNA stability, or expression levels) (Humphrey et al., 2023; Morera et al., 2019; Seddighi et al., 2024).

Leveraging multi-omics to improve therapeutic approaches in ALS

In the context of ALS, a holistic multi-omics perspective (e.g. combination of metabolomics, lipidomics, transcriptomics, proteomics) enables researchers to identify novel therapeutic targets and biomarkers more effectively, allowing for more personalized and effective treatment strategies. An interesting recently published study investigated the early mechanisms underlying ALS by undertaking a multi-omics analysis approach on the prefrontal cortex of ALS patients (Caldi Gomes et al., 2024). The study revealed distinct molecular subclusters within the ALS population and was able to stratify patients into various subgroups. They were also able to identify significant sex differences, with females for example showing a stronger involvement of immune-related processes (Caldi Gomes et al., 2024). This implies that for drug development and clinical trials, sex-based differences need to be taken into consideration because males and females might not have the same response to drugs. Treatments might also need to be tailored to those differences in order to optimize their efficacy. Additionally, the study identified the MAPK pathway as a central driver of ALS pathophysiology in the various groups, which may serve as a promising therapeutic target (Caldi Gomes et al., 2024). This research is a representative example of how multi-omics approaches can provide researchers with the opportunity to go from a one-size-fits-all therapeutic approach to a more personalized approach, allowing for the targeting of the dominant dysfunctional mechanism in different patient subgroups.

Understanding the disease from a systems perspective helps address its heterogeneity by identifying common pathways while acknowledging individual variations. Due to the multifactorial and complex nature of ALS, future therapies may need to target several pathways at once, potentially combining drugs that address neuronal degeneration, inflammation, and metabolic dysfunction. Additionally, precision medicine approaches could tailor treatments based on a patient's specific molecular profile, considering factors like genetic mutations, sex differences, and environmental influences.

Targeting TDP-43: Good in theory, complicated in practice

Navigating unintended specificities when targeting TDP-43

The phage display screening we performed was targeting full-length TDP-43, rather than a specific domain. The full-length protein presents multiple epitopes, as was evident by our *in silico* prediction of TDP-43-scFv binding sites. This increases the chances of identifying binders that target different regions of the protein, or identifying novel binding sites, potentially opening new therapeutic avenues or insights into the protein's biology. In addition, many proteins, and particularly TDP-43, undergo posttranslational modifications and conformational changes which may expose different regions or domains at different times (Buratti, 2018; Ercan et al., 2017; François-Moutal et al., 2019). We therefore believe that targeting multiple sites across the entire protein may be more effective than focusing on a single domain.

Although the retained scFvs were selected against full-length TDP-43, its effect was limited to the 35-kDa CTF *in vitro*. This is probably due to several factors, some of which might be related to the distinct environments and assay conditions, and the difference between solutions and cellular environments. For instance, the 35 kDa CTF might have a more accessible conformation and expose different or more accessible epitopes after cleavage of TDP-43, making it more susceptible to scFv binding (Shenoy et al., 2020). The 35 kDa fragment is often associated with pathological aggregation in neurodegenerative diseases (M. Che et al., 2011b; M.-X. Che et al., 2015; Chhangani & Rincon-Limas, 2022; L.-L. Jiang et al., 2022; S. Xiao et al., 2015). These aggregates may expose distinct epitopes or provide more binding sites for the antibody, making it more effective in targeting it (Shenoy et al., 2020). Additionally, the 35 kDa fragment, being a cleaved product of full-length TDP-43, may be inherently less stable and more prone to degradation than the full-length protein (Chiang et al., 2016; Crippa et al., 2016). Antibody binding might exacerbate this instability, further marking the fragment for degradation through proteolytic pathways. In addition, in a cellular setting, post-translational modifications may alter the full-length TDP-43's structure or mask the epitope, making it harder for the antibody to bind (Ercan et al., 2017; Shenoy et al., 2020). Potential discrepancies between the initial therapeutic design and the resulting biological effects must therefore be carefully considered when targeting TDP-43 in ALS.

Is TDP-35 a good target form of TDP-43 in ALS?

TDP-43 proteinopathy is a hallmark of ALS, with debates ongoing about which form of TDP-43 should be the primary therapeutic target. Aggregated, mislocalized, and /or post-translationally modified TDP-43 seem to be the primary targets in ALS research aimed at mitigating the progression of the disease (Ojaimi et al., 2022). Some researchers also aimed at targeting extracellular TDP-43 in an attempt to block the spreading of TDP-43 pathology between cells (Chevalier et al., 2024).

In addition to full-length TDP-43, cleaved C-terminal fragments of TDP-43, which are prone to aggregation and believed to drive the formation of toxic inclusions (M. Che et al., 2011b; M.-X. Che et al., 2015; Chhangani & Rincon-Limas, 2022; L.-L. Jiang et al., 2022), are also worth targeting. For instance, one study showed that TDP-35 was more toxic and led to a more severe neurodegeneration than TDP-43 and TDP-25 in flies (Crippa et al., 2016). Reducing the formation or accumulation of these fragments could alleviate their harmful effects, prevent or reverse TDP-43 mislocalization, and restore TDP-43's nuclear function (Cicardi et al., 2018; Crippa et al., 2016). The selective targeting of TDP-35 CTF, which predominately accumulates in pathological conditions, could be an interesting approach. This approach might alleviate TDP-43 mislocalization and aggregation, while sparing the full-length, functional TDP-43, thus avoiding potential disruptions of its physiological roles.

Challenges of targeting TDP-43: multifaceted roles and broad impacts

Targeting TDP-43 in ALS appears promising in theory due to the central role of this protein in disease pathology (Ojaimi et al., 2022). However, implementing such strategies in practice is highly complicated due to the role of TDP-43 in both normal and pathological cellular processes. In addition, TDP-43 has a dual pathological role in ALS, involving both a loss of its normal function in the nucleus and a toxic gain of function in the cytoplasm through the formation of aggregates (M. C. Cao et al., 2023; W.-P. Huang et al., 2024; Kabashi et al., 2010; Sivakumar et al., 2018). Addressing both issues simultaneously is a major challenge. Any therapeutic approach must strike a delicate balance between reducing the toxic effects of TDP-43 aggregates and maintaining its essential functions in the nucleus. Additionally, TDP-43 proteinopathy extends beyond motor neurons, affecting multiple cell types and tissues, making it a systemic issue rather than a neuron-specific problem (Pattle et al., 2022; Peng et

al., 2020; Versluys et al., 2022). Moreover, the lack of clear biomarkers, difficulties in drug delivery, and the heterogeneity of ALS add additional layers of complexity. All these factors make TDP-43 a challenging but crucial target for future ALS treatments.

Assessing the downstream effects of targeting TDP-43 is complicated but crucial for ensuring the effectiveness of therapies. Due to the broad cellular pathways impacted by TDP-43, measuring the therapeutic response when targeting this protein can and should consider various parameters. In addition to the typical parameters including disease progression rate, symptoms severity, and survival, there exists other parameters that can provide valuable information about the treatment itself but also about the pathophysiology of the disease. These parameters include the direct changes in TDP-43 (e.g. localization, fragmentation, aggregation, post-translational modifications), as well as modifications in the cellular environments (e.g. neuroinflammation), metabolic alterations, transcriptomic changes, etc. Such evaluation is possible using multi-omics and trans-omics approaches (Ivanisevic & Sewduth, 2023; Kedaigle & Fraenkel, 2018; Yugi et al., 2016). For example, TDP-43 dysfunction affects lipid metabolism (Ceron-Codorniu et al., 2024; Hergesheimer et al., 2020), which is critical for membrane integrity, cellular signalling, and energy storage. Therapies that restore normal TDP-43 function should be expected to also normalize these lipid imbalances, which can be assessed through lipidomics. Another example is the use of metabolomics to track the change in TDP-43-induced mitochondrial dysfunction, which can lead to the accumulation of oxidative stress markers (e.g. malondialdehyde, 4-hydroxynonenal…) or the shift in energy-related metabolites (e.g. NADH, citric acid cycle intermediates…) (Ceron-Codorniu et al., 2024; Gautam et al., 2022; Kabuta et al., 2015; Y. Liu et al., 2014; Loganathan et al., 2022). A direct example of this is an interesting recent study that used passive immunization of mice against the glycine-rich domain and that have shown protective effects on processes involved in disease progression such as inflammation and neuronal damage (Riemenschneider et al., 2023). Their transcriptomic analysis revealed an improvement in neuroinflammation markers like TNF-α and NF-κB, which was used as a reflection of a good therapeutic potential (Riemenschneider et al., 2023).

All these parameters are not easy to assess *in vitro*, making animal models valuable for this purpose. However, going from *in vitro* assays to preclinical testing is complicated. It must first answer questions related to the choice of the animal model, the administration route,

the dosage, the number of administrations, and whether the treatment should be continuous or intermittent. Another important question is the time to start the treatment. Most animal models rely on drug administration in the pre-symptomatic phase in order to slow down the onset of the disease for example or delay its progression. However, this does not translate well into the clinical setting because most ALS cases are sporadic and treatment is only started after confirmed diagnosis. For this reason, our plan is to administer the AAV-encoded scFv upon the onset of symptoms.

Therapeutic delivery techniques depend on the drug format and desired outcome

Complicated delivery of recombinant scFvs targeting TDP-43 in the CNS

Prior to testing the scFv *in vivo*, we were faced with the question of the best administration technique, which can present good feasibility in humans in the future and allows primarily the targeting of the CNS with maximum efficiency and minimal side effects. For this reason, we first attempted to administer the scFv in its purified protein form, through the intravenous route via the tail vein (100 µg of endotoxin-free purified scFv). Since various studies provided evidence for BBB alterations and increased permeability in ALS (Alarcan et al., 2022), we assumed that the scFv might be able to cross the malfunctioning BBB and reach the CNS. However, we were not able to detect the scFv in any of the tissues we studied whether peripheral or central. We hypothesized that this might be due to 1) the short half-life of the scFv *in vivo* (Z. Li & Shah, 2019) or 2) the dilution of the scFv in biofluids and tissue parenchyma, preventing its effective detection by western blot or ELISA (H.-P. Chang et al., 2021). However, given that we attempted the detection of the scFv following various periods, ranging from 10 minutes to 24 hours post-injection, and given that the half-life of the scFv is not less than 10 minutes (Hutt et al., 2012; Z. Li & Shah, 2019), it is unlikely that the scFv was already eliminated from the body when the analysis was performed. Therefore, the second reason relating to very low scFv concentrations seemed to be more likely. Subsequently, we tried the intrathecal administration route (25 µg of endotoxin-free purified scFv), assuming that the scFv will be more concentrated in the CNS, and therefore easier to detect. Nevertheless, we also failed to detect a specific signal for the scFv in the brain or the spinal cord, pushing us to reconsider the administration formats and routes.

The administration of a drug targeting intracellular proteins in the CNS is particularly challenging because two barriers need to be overcome for the drug to reach its target: the BBB and the plasma membrane of target cells. As discussed in our review (Al Ojaimi et al., 2022), several techniques have been developed to deliver therapeutics across the BBB, including functionalized nanoparticles (Goulatis & Shusta, 2017) or transiently opening the BBB using focused ultrasounds (Dubey et al., 2020; Leinenga et al., 2020; Lesniak et al., 2019). For example, nanoparticles can be engineered to bind to receptors on the surface of the endothelial cells that make up the BBB, allowing substances to be transported across the barrier through receptor-mediated transcytosis. Some of the most commonly used receptors are the transferrin receptor and the insulin receptor (Pardridge, 2021; Thomsen et al., 2022). In the case of antibody therapeutics, the same logic can be applied by using bispecific antibodies targeting both a therapeutic target and the transferrin receptor for example (Couch et al., 2013; Rué et al., 2023; Syvänen et al., 2017; Y. J. Yu et al., 2014). However, these techniques do not ensure the delivery of therapeutics to specific target regions or to the cytoplasm of cells in the CNS, requiring further optimization.

Techniques to enhance the delivery of the scFv to target cells

First, we decided to develop PEGylated SPION-scFv complexes that can be directed using a localized magnetic field to the brain regions of interest, such as the motor cortex, and that can also cross the plasma membrane and be internalized by cells without substantial cytotoxicity (Balk et al., 2021; Gu et al., 2011; Gusliakova et al., 2024; Prijic et al., 2010). We were able to successfully obtain nanoparticles with the appropriate physicochemical characteristics that allowed them to be internalized by cells alongside the complexed scFv, even in the absence of a localized magnetic field. We could also envision functionalizing the SPION with an antibody fragment targeting BBB receptors to allow for its transcytosis into the brain parenchyma. However, due to several technical challenges, and the substantial workload it required to synthesize SPIONs and purify sufficient amounts of scFvs, we did not get the chance to extensively evaluate the behavior of these molecules in cells and optimize them for *in vivo* testing.

Therefore, to test the scFv *in vivo*, we decided to turn to gene therapy using AAVs for scFv delivery into target cells. AAV vectors are among the most widely used tools in gene therapy due to their ability to deliver therapeutic genes to specific cells with high precision

and relatively low immunogenicity (Baldrick et al., 2023; Bowles et al., 2012; Greig et al., 2024; Mendell et al., 2017). AAV vectors have revolutionized the field of gene therapy, offering a versatile and relatively safe platform for treating a wide range of genetic and acquired disorders, especially CNS diseases (L. Kang et al., 2023; Mendell et al., 2017). These vectors are particularly suited for conditions where long-term expression of a therapeutic gene is desired, as they can provide stable gene expression for years after a single administration, especially in cells that do not have a high turnover rate such as neurons (Brommel et al., 2020; Mendell et al., 2017). Since 2017, FDA approval was granted to six AAV-based gene therapies for certain types of the following disease (The Food and Drug Administration, 2024): retinal dystrophy (Luxturna®, 2017), spinal muscular atrophy (Zolgensma®, 2019), Hemophilia B (Hengenix®, 2022 and Beqvez®, 2024), Duchenne muscular dystrophy Elevidys®, 2023), and Hemophilia A (Roctavian®, 2023), .

In our case, to reduce off-target effects and primarily target neurons in the CNS, we chose to use the engineered AAV-CAP.B10 vector. This vector was developed by Goertsen and his colleagues in 2022 (Goertsen et al., 2022) using an advanced capsid engineering technique called directed evolution, that allowed for the selection of a capsid variant with enhanced CNS-specific delivery and reduced liver accumulation. Similar to what has been already reported (Goertsen et al., 2022), we observed that the AAV-CAP.B10 only transduced cells in the CNS and spared the liver, reducing the risk of triggering an immune response and causing hepatotoxicity (B. Gao, 2016; Jagadisan & Dhawan, 2023; Kubes & Jenne, 2018). Future immunohistological studies will be performed to determine the exact cells that were transduced by the AAV in the CNS of mice. In a previous study, single-cell RNA sequencing revealed that the neurons, particularly glutamatergic neurons, were the main cells that were targeted in the CNS by the AAV-CAP.B10 (D. Brown et al., 2021). It should be noted that upper motor neurons are mainly glutamatergic (Stifani, 2014), and therefore the time of administration and duration of transgene expression need to be carefully evaluated in order to ensure the presence of sufficient amounts of transducible motor neurons prior to extended neurodegeneration. As more motor neurons die, the scFv will probably be less expressed and therefore less efficient. The clinical use of AAVs continues to expand, with ongoing research aimed at monitoring for any long-term adverse effects, overcoming current limitations, and exploring new therapeutic applications.

The continuity of this project will be dedicated to the evaluation of the AAV-encoded scFv *in vivo*, by taking into consideration all the parameters that were identified during the characterization of the Prp-TDP-43^{A315T} mouse model that was described in Publication 6. The biodistribution, long-term expression, and effect on phenotypic, molecular, transcriptomic, metabolomic and lipidomic parameters will be evaluated at different timepoints, from disease onset to disease end-stage.

Conclusion and perspectives

In the quest to develop effective therapeutics for neurodegenerative diseases such as ALS, it is paramount to consider multiple facets of disease pathology and treatment strategies. First and foremost, targeting intracellular proteins requires a deep understanding of the intracellular environment in which the protein resides. Proteins do not function in isolation; they are part of complex networks influenced by various factors such as post-translational modifications, stress conditions, environmental exposures, and disease states. By comprehensively understanding these interactions, researchers can design more effective interventions that ensure proper delivery and function of therapeutic agents, thereby enhancing their efficacy.

Moreover, recognizing ALS as a systemic disorder rather than a localized neuronal disease shifts the focus toward a holistic approach in research and therapy. The application of omics technologies—proteomics, metabolomics, lipidomics, and transcriptomics—provides an integrated view of the disease, revealing systemic alterations that may contribute to disease progression. This perspective enables the identification of biomarkers and novel therapeutic targets beyond the affected neurons, ultimately leading to more comprehensive treatment strategies that can address the multifactorial nature of ALS and develop more personalized therapeutic strategies.

While TDP-43 is a central player in ALS pathology, focusing solely on this protein may overlook critical downstream alterations that significantly impact disease progression. TDP-43 mislocalization and aggregation disrupt numerous cellular processes, leading to the dysregulation of other proteins and signaling pathways. Thus, therapeutic strategies should also aim to mitigate these downstream effects. This broader targeting approach not only addresses the root cause but also counteracts the extensive cellular consequences associated with TDP-43 dysregulation.

Finally, the method of administration for therapeutic agents such as scFvs is crucial for their effectiveness. Consideration of diverse administration routes, including nanoparticles and adeno-associated viruses (AAV), holds promise for enhancing the delivery of these therapeutics directly to affected tissues. By optimizing administration strategies, we can improve therapeutic outcomes and pave the way for novel treatments that can alter the course of ALS. Overall, a multidimensional approach that encompasses the intracellular

environment, systemic implications of ALS, downstream alterations, and innovative delivery methods is essential for advancing therapeutic strategies in this challenging disorder.

References

Abdel-Khalik, J., Yutuc, E., Crick, P. J., Gustafsson, J.-Å., Warner, M., Roman, G., Talbot, K., Gray, E., Griffiths, W. J., Turner, M. R., & Wang, Y. (2017). Defective cholesterol metabolism in amyotrophic lateral sclerosis. Journal of Lipid Research, 58(1), 267–278. https://doi.org/10.1194/jlr.P071639

Abe, K., Aoki, M., Tsuji, S., Itoyama, Y., Sobue, G., Togo, M., Hamada, C., Tanaka, M., Akimoto, M., Nakamura, K., Takahashi, F., Kondo, K., Yoshino, H., Abe, K., Aoki, M., Tsuji, S., Itoyama, Y., Sobue, G., Togo, M., … Yoshino, H. (2017). Safety and efficacy of edaravone in well defined patients with amyotrophic lateral sclerosis: A randomised, double-blind, placebo-controlled trial. The Lancet Neurology, 16(7), 505–512. https://doi.org/10.1016/S1474-4422(17)30115-1

Abrahao, A., Abath Neto, O., Kok, F., Zanoteli, E., Santos, B., Pinto, W. B. V. D. R., Barsottini, O. G. P., Oliveira, A. S. B., & Pedroso, J. L. (2016). One family, one gene and three phenotypes: A novel VCP (valosin-containing protein) mutation associated with myopathy with rimmed vacuoles, amyotrophic lateral sclerosis and frontotemporal dementia. Journal of the Neurological Sciences, 368, 352–358. https://doi.org/10.1016/j.jns.2016.07.048

Afonso, G. J. M., Cavaleiro, C., Valero, J., Mota, S. I., & Ferreiro, E. (2023). Recent Advances in Extracellular Vesicles in Amyotrophic Lateral Sclerosis and Emergent Perspectives. Cells, 12(13), 1763. https://doi.org/10.3390/cells12131763

Afroz, T., Chevalier, E., Audrain, M., Dumayne, C., Ziehm, T., Moser, R., Egesipe, A.-L., Mottier, L., Ratnam, M., Neumann, M., Havas, D., Ollier, R., Piorkowska, K., Chauhan, M., Silva, A. B., Thapa, S., Stöhr, J., Bavdek, A., Eligert, V., … Seredenina, T. (2023). Immunotherapy targeting the C-terminal domain of TDP-43 decreases neuropathology and confers neuroprotection in mouse models of ALS/FTD. Neurobiology of Disease, 179, 106050. https://doi.org/10.1016/j.nbd.2023.106050

Ahmed, R. M., Phan, K., Highton-Williamson, E., Strikwerda-Brown, C., Caga, J., Ramsey, E., Zoing, M., Devenney, E., Kim, W. S., Hodges, J. R., Piguet, O., Halliday, G. M., & Kiernan, M. C. (2019). Eating peptides: Biomarkers of neurodegeneration in amyotrophic lateral sclerosis and frontotemporal dementia. Annals of Clinical and Translational Neurology, 6(3), 486–495. https://doi.org/10.1002/acn3.721

Aizawa, H., Sawada, J., Hideyama, T., Yamashita, T., Katayama, T., Hasebe, N., Kimura, T., Yahara, O., & Kwak, S. (2010). TDP-43 pathology in sporadic ALS occurs in motor neurons lacking the RNA editing enzyme ADAR2. Acta Neuropathologica, 120(1), 75–84. https://doi.org/10.1007/s00401-010-0678-x

Aizawa, H., Yamashita, T., Kato, H., Kimura, T., & Kwak, S. (2019). Impaired Nucleoporins Are Present in Sporadic Amyotrophic Lateral Sclerosis Motor Neurons that Exhibit Mislocalization of the 43-kDa TAR DNA-Binding Protein. Journal of Clinical Neurology, 15(1), 62. https://doi.org/10.3988/jcn.2019.15.1.62

Al Ojaimi, Y., Blin, T., Lamamy, J., Gracia, M., Pitiot, A., Denevault-Sabourin, C., Joubert, N., Pouget, J.-P., Gouilleux-Gruart, V., Heuzé-Vourc'h, N., Lanznaster, D., Poty, S., & Sécher, T. (2022). Therapeutic antibodies – natural and pathological barriers and strategies to overcome them. Pharmacology & Therapeutics, 233, 108022. https://doi.org/10.1016/j.pharmthera.2021.108022

Alami, N. H., Smith, R. B., Carrasco, M. A., Williams, L. A., Winborn, C. S., Han, S. S. W., Kiskinis, E., Winborn, B., Freibaum, B. D., Kanagaraj, A., Clare, A. J., Badders, N. M., Bilican, B., Chaum, E., Chandran, S., Shaw, C. E., Eggan, K. C., Maniatis, T., & Taylor, J. P. (2014). Axonal Transport of TDP-43 mRNA Granules Is Impaired by ALS-Causing Mutations. Neuron, 81(3), 536–543. https://doi.org/10.1016/j.neuron.2013.12.018

Alarcan, H., Al Ojaimi, Y., Lanznaster, D., Escoffre, J.-M., Corcia, P., Vourc'h, P., Andres, C. R., Veyrat-Durebex, C., & Blasco, H. (2022). Taking Advantages of Blood–Brain or Spinal Cord Barrier Alterations or Restoring Them to Optimize Therapy in ALS? Journal of Personalized Medicine, 12(7), 1071. https://doi.org/10.3390/jpm12071071

Al-Chalabi, A., Fang, F., Hanby, M. F., Leigh, P. N., Shaw, C. E., Ye, W., & Rijsdijk, F. (2010). An estimate of amyotrophic lateral sclerosis heritability using twin data. Journal of Neurology, Neurosurgery & Psychiatry, 81(12), 1324–1326. https://doi.org/10.1136/jnnp.2010.207464

Al-Chalabi, A., & Hardiman, O. (2013). The epidemiology of ALS: A conspiracy of genes, environment and time. Nature Reviews Neurology, 9(11), 617–628. https://doi.org/10.1038/nrneurol.2013.203

Allodi, I., Montañana-Rosell, R., Selvan, R., Löw, P., & Kiehn, O. (2021). Locomotor deficits in a mouse model of ALS are paralleled by loss of V1-interneuron connections onto fast motor neurons. Nature Communications, 12(1), 3251. https://doi.org/10.1038/s41467-021-23224-7

Alric, C., Aubrey, N., Allard-Vannier, É., Di Tommaso, A., Blondy, T., Dimier-Poisson, I., Chourpa, I., & Hervé-Aubert, K. (2016). Covalent conjugation of cysteine-engineered scFv to PEGylated magnetic nanoprobes for immunotargeting of breast cancer cells. RSC Advances, 6(43), 37099–37109. https://doi.org/10.1039/C6RA06076E

Altman, T., Ionescu, A., Ibraheem, A., Priesmann, D., Gradus-Pery, T., Farberov, L., Alexandra, G., Shelestovich, N., Dafinca, R., Shomron, N., Rage, F., Talbot, K., Ward, M. E., Dori, A., Krüger, M., & Perlson, E. (2021). Axonal TDP-43 condensates drive neuromuscular junction disruption through inhibition of local synthesis of nuclear encoded mitochondrial proteins. Nature Communications, 12(1), 6914. https://doi.org/10.1038/s41467-021-27221-8

Amanzadeh Jajin, E., Esmaeili, A., Rahgozar, S., & Noorbakhshnia, M. (2021). Quercetin-Conjugated Superparamagnetic Iron Oxide Nanoparticles Protect AlCl3-Induced Neurotoxicity in a Rat Model of Alzheimer's Disease via Antioxidant Genes, APP Gene, and miRNA-101. Frontiers in Neuroscience, 14, 598617. https://doi.org/10.3389/fnins.2020.598617

Ambadipudi, S., Biernat, J., Riedel, D., Mandelkow, E., & Zweckstetter, M. (2017). Liquid–liquid phase separation of the microtubule-binding repeats of the Alzheimer-related protein Tau. Nature Communications, 8(1), 275. https://doi.org/10.1038/s41467-017-00480-0

Andrés-Benito, P., Gelpi, E., Jové, M., Mota-Martorell, N., Obis, È., Portero-Otin, M., Povedano, M., Pujol, A., Pamplona, R., & Ferrer, I. (2021). Lipid alterations in human frontal cortex in ALS-FTLD-TDP43 proteinopathy spectrum are partly related to peroxisome impairment. Neuropathology and Applied Neurobiology, 47(4), 544–563. https://doi.org/10.1111/nan.12681

Andrew, A., Zhou, J., Gui, J., Harrison, A., Shi, X., Li, M., Guetti, B., Nathan, R., Tischbein, M., Pioro, E. P., Stommel, E., & Bradley, W. (2021). Pesticides applied to crops and amyotrophic lateral sclerosis risk in the U.S. NeuroToxicology, 87, 128–135. https://doi.org/10.1016/j.neuro.2021.09.004

Anson, D. S. (2004). The use of retroviral vectors for gene therapy-what are the risks? A review of retroviral pathogenesis and its relevance to retroviral vector-mediated gene delivery. Genetic Vaccines and Therapy, 2(1), 9. https://doi.org/10.1186/1479-0556-2-9

Anzilotti, S., Valente, V., Brancaccio, P., Franco, C., Casamassa, A., Lombardi, G., Palazzi, A., Conte, A., Paladino, S., Canzoniero, L. M. T., Annunziato, L., Pierantoni, G. M., & Pignataro, G. (2023). Chronic exposure to l-

BMAA cyanotoxin induces cytoplasmic TDP-43 accumulation and glial activation, reproducing an amyotrophic lateral sclerosis-like phenotype in mice. Biomedicine & Pharmacotherapy, 167, 115503. https://doi.org/10.1016/j.biopha.2023.115503

Araki, K., Araki, A., Honda, D., Izumoto, T., Hashizume, A., Hijikata, Y., Yamada, S., Iguchi, Y., Hara, A., Ikumi, K., Kawai, K., Ishigaki, S., Nakamichi, Y., Tsunekawa, S., Seino, Y., Yamamoto, A., Takayama, Y., Hidaka, S., Tominaga, M., … Katsuno, M. (2019). TDP-43 regulates early-phase insulin secretion via CaV1.2-mediated exocytosis in islets. Journal of Clinical Investigation, 129(9), 3578–3593. https://doi.org/10.1172/JCI124481

Araújo, A. M., Carvalho, F., Guedes De Pinho, P., & Carvalho, M. (2021). Toxicometabolomics: Small Molecules to Answer Big Toxicological Questions. Metabolites, 11(10), 692. https://doi.org/10.3390/metabo11100692

Arthur, K. C., Calvo, A., Price, T. R., Geiger, J. T., Chiò, A., & Traynor, B. J. (2016). Projected increase in amyotrophic lateral sclerosis from 2015 to 2040. Nature Communications, 7(1), 12408. https://doi.org/10.1038/ncomms12408

Ash, P. E. A., Dhawan, U., Boudeau, S., Lei, S., Carlomagno, Y., Knobel, M., Al Mohanna, L. F. A., Boomhower, S. R., Newland, M. C., Sherr, D. H., & Wolozin, B. (2019). Heavy Metal Neurotoxicants Induce ALS-Linked TDP-43 Pathology. Toxicological Sciences, 167(1), 105–115. https://doi.org/10.1093/toxsci/kfy267

Audrain, M., Egesipe, A.-L., Tentillier, N., Font, L., Ratnam, M., Mottier, L., Clavel, M., Le Roux-Bourdieu, M., Fenyi, A., Ollier, R., Chevalier, E., Guilhot, F., Fuchs, A., Piorkowska, K., Carlyle, B., Arnold, S. E., Berry, J. D., Luthi-Carter, R., Adolfsson, O., … Afroz, T. (2023). Targeting amyotrophic lateral sclerosis by neutralizing seeding-competent TDP-43 in CSF. Brain Communications, 5(6), fcad306. https://doi.org/10.1093/braincomms/fcad306

Azbill, R. D., Mu, X., & Springer, J. E. (2000). Riluzole increases high-affinity glutamate uptake in rat spinal cord synaptosomes. Brain Research, 871(2), 175–180. https://doi.org/10.1016/S0006-8993(00)02430-6

Babinchak, W. M., Haider, R., Dumm, B. K., Sarkar, P., Surewicz, K., Choi, J.-K., & Surewicz, W. K. (2019). The role of liquid–liquid phase separation in aggregation of the TDP-43 low-complexity domain. Journal of Biological Chemistry, 294(16), 6306–6317. https://doi.org/10.1074/jbc.RA118.007222

Babu, G. N., Kumar, A., Chandra, R., Puri, S. K., Singh, R. L., Kalita, J., & Misra, U. K. (2008). Oxidant–antioxidant imbalance in the erythrocytes of sporadic amyotrophic lateral sclerosis patients correlates with the progression of disease. Neurochemistry International, 52(6), 1284–1289. https://doi.org/10.1016/j.neuint.2008.01.009

Bakavayev, S., Stavsky, A., Argueti-Ostrovsky, S., Yehezkel, G., Fridmann-Sirkis, Y., Barak, Z., Gitler, D., Israelson, A., & Engel, S. (2023). Blocking an epitope of misfolded SOD1 ameliorates disease phenotype in a model of amyotrophic lateral sclerosis. Brain, 146(11), 4594–4607. https://doi.org/10.1093/brain/awad222

Baldrick, P., McIntosh, B., & Prasad, M. (2023). Adeno-associated virus (AAV)-based gene therapy products: What are toxicity studies in non-human primates showing us? Regulatory Toxicology and Pharmacology, 138, 105332. https://doi.org/10.1016/j.yrtph.2022.105332

Balk, M., Haus, T., Band, J., Unterweger, H., Schreiber, E., Friedrich, R. P., Alexiou, C., & Gostian, A.-O. (2021). Cellular SPION Uptake and Toxicity in Various Head and Neck Cancer Cell Lines. Nanomaterials, 11(3), 726. https://doi.org/10.3390/nano11030726

Banack, S. A., Dunlop, R. A., Stommel, E. W., Mehta, P., & Cox, P. A. (2022). miRNA extracted from extracellular vesicles is a robust biomarker of amyotrophic lateral sclerosis. Journal of the Neurological Sciences, 442, 120396. https://doi.org/10.1016/j.jns.2022.120396

Banka, V., Kelleher, A., Sehlin, D., Hultqvist, G., Sigurdsson, E. M., Syvänen, S., & Ding, Y.-S. (2023). Development of brain-penetrable antibody radioligands for in vivo PET imaging of amyloid-β and tau. Frontiers in Nuclear Medicine, 3, 1173693. https://doi.org/10.3389/fnume.2023.1173693

Barnaba, C., Broadbent, D. G., Perez, G. I., & Schmidt, J. C. (2023). AMPK Regulates Phagophore-to-Autophagosome Maturation. https://doi.org/10.1101/2023.09.28.559981

Baron, D. M., Fenton, A. R., Saez-Atienzar, S., Giampetruzzi, A., Sreeram, A., Shankaracharya, Keagle, P. J., Doocy, V. R., Smith, N. J., Danielson, E. W., Andresano, M., McCormack, M. C., Garcia, J., Bercier, V., Van Den Bosch, L., Brent, J. R., Fallini, C., Traynor, B. J., Holzbaur, E. L. F., & Landers, J. E. (2022). ALS-associated KIF5A mutations abolish autoinhibition resulting in a toxic gain of function. Cell Reports, 39(1), 110598. https://doi.org/10.1016/j.celrep.2022.110598

Baron, D. M., Kaushansky, L. J., Ward, C. L., Sama, R. R. K., Chian, R.-J., Boggio, K. J., Quaresma, A. J. C., Nickerson, J. A., & Bosco, D. A. (2013). Amyotrophic lateral sclerosis-linked FUS/TLS alters stress granule assembly and dynamics. Molecular Neurodegeneration, 8(1), 30. https://doi.org/10.1186/1750-1326-8-30

Basavarajappa, B. S., & Subbanna, S. (2021). Histone Methylation Regulation in Neurodegenerative Disorders. International Journal of Molecular Sciences, 22(9), 4654. https://doi.org/10.3390/ijms22094654

Bataveljić, D., Nikolić, L., Milosević, M., Todorović, N., & Andjus, P. R. (2012). Changes in the astrocytic aquaporin-4 and inwardly rectifying potassium channel expression in the brain of the amyotrophic lateral sclerosis SOD1 G93A rat model. Glia, 60(12), 1991–2003. https://doi.org/10.1002/glia.22414

Bates, A., & Power, C. A. (2019). David vs. Goliath: The Structure, Function, and Clinical Prospects of Antibody Fragments. Antibodies, 8(2), 28. https://doi.org/10.3390/antib8020028

Batulan, Z., Shinder, G. A., Minotti, S., He, B. P., Doroudchi, M. M., Nalbantoglu, J., Strong, M. J., & Durham, H. D. (2003). High Threshold for Induction of the Stress Response in Motor Neurons Is Associated with Failure to Activate HSF1. The Journal of Neuroscience, 23(13), 5789–5798. https://doi.org/10.1523/JNEUROSCI.23-13-05789.2003

Bäumer, D., Talbot, K., & Turner, M. R. (2014). Advances in motor neurone disease. Journal of the Royal Society of Medicine, 107(1), 14–21. https://doi.org/10.1177/0141076813511451

Bayer, H., Lang, K., Buck, E., Higelin, J., Barteczko, L., Pasquarelli, N., Sprissler, J., Lucas, T., Holzmann, K., Demestre, M., Lindenberg, K. S., Danzer, K. M., Boeckers, T., Ludolph, A. C., Dupuis, L., Weydt, P., & Witting, A. (2017). ALS-causing mutations differentially affect PGC-1α expression and function in the brain vs. Peripheral tissues. Neurobiology of Disease, 97, 36–45. https://doi.org/10.1016/j.nbd.2016.11.001

Beers, D. R., Henkel, J. S., Xiao, Q., Zhao, W., Wang, J., Yen, A. A., Siklos, L., McKercher, S. R., & Appel, S. H. (2006). Wild-type microglia extend survival in PU.1 knockout mice with familial amyotrophic lateral sclerosis. Proceedings of the National Academy of Sciences, 103(43), 16021–16026. https://doi.org/10.1073/pnas.0607423103

Beghi, E., Pupillo, E., Messina, P., Giussani, G., Chiò, A., Zoccolella, S., Moglia, C., Corbo, M., & Logroscino, G. (2011). Coffee and Amyotrophic Lateral Sclerosis: A Possible Preventive Role. American Journal of Epidemiology, 174(9), 1002–1008. https://doi.org/10.1093/aje/kwr229

Behzadi, A., Pujol-Calderón, F., Tjust, A. E., Wuolikainen, A., Höglund, K., Forsberg, K., Portelius, E., Blennow, K., Zetterberg, H., & Andersen, P. M. (2021). Neurofilaments can differentiate ALS subgroups and ALS from common diagnostic mimics. Scientific Reports, 11(1), 22128. https://doi.org/10.1038/s41598-021-01499-6

Beijer, D., Kim, H. J., Guo, L., O'Donovan, K., Mademan, I., Deconinck, T., Van Schil, K., Fare, C. M., Drake, L. E., Ford, A. F., Kochański, A., Kabzińska, D., Dubuisson, N., Van Den Bergh, P., Voermans, N. C., Lemmers, R. J. L. F., Van Der Maarel, S. M., Bonner, D., Sampson, J. B., … Baets, J. (2021). Characterization of HNRNPA1 mutations defines diversity in pathogenic mechanisms and clinical presentation. JCI Insight, 6(14), e148363. https://doi.org/10.1172/jci.insight.148363

Belzil, V. V., Bauer, P. O., Prudencio, M., Gendron, T. F., Stetler, C. T., Yan, I. K., Pregent, L., Daughrity, L., Baker, M. C., Rademakers, R., Boylan, K., Patel, T. C., Dickson, D. W., & Petrucelli, L. (2013). Reduced C9orf72 gene expression in c9FTD/ALS is caused by histone trimethylation, an epigenetic event detectable in blood. Acta Neuropathologica, 126(6), 895–905. https://doi.org/10.1007/s00401-013-1199-1

Ben Djemaa, S., David, S., Hervé-Aubert, K., Falanga, A., Galdiero, S., Allard-Vannier, E., Chourpa, I., & Munnier, E. (2018). Formulation and in vitro evaluation of a siRNA delivery nanosystem decorated with gH625 peptide for triple negative breast cancer theranosis. European Journal of Pharmaceutics and Biopharmaceutics, 131, 99–108. https://doi.org/10.1016/j.ejpb.2018.07.024

Benatar, M., Wuu, J., Andersen, P. M., Bucelli, R. C., Andrews, J. A., Otto, M., Farahany, N. A., Harrington, E. A., Chen, W., Mitchell, A. A., Ferguson, T., Chew, S., Gedney, L., Oakley, S., Heo, J., Chary, S., Fanning, L., Graham, D., Sun, P., … Fradette, S. (2022). Design of a Randomized, Placebo-Controlled, Phase 3 Trial of Tofersen Initiated in Clinically Presymptomatic SOD1 Variant Carriers: The ATLAS Study. Neurotherapeutics, 19(4), 1248–1258. https://doi.org/10.1007/s13311-022-01237-4

Benatar, M., Wuu, J., Andersen, P. M., Lombardi, V., & Malaspina, A. (2018). Neurofilament light: A candidate biomarker of presymptomatic amyotrophic lateral sclerosis and phenoconversion. Annals of Neurology, 84(1), 130–139. https://doi.org/10.1002/ana.25276

Benatar, M., Wuu, J., Lombardi, V., Jeromin, A., Bowser, R., Andersen, P. M., & Malaspina, A. (2019). Neurofilaments in pre-symptomatic ALS and the impact of genotype. Amyotrophic Lateral Sclerosis and Frontotemporal Degeneration, 20(7–8), 538–548. https://doi.org/10.1080/21678421.2019.1646769

Benatar, M., Wuu, J., & Turner, M. R. (2023). Neurofilament light chain in drug development for amyotrophic lateral sclerosis: A critical appraisal. Brain, 146(7), 2711–2716. https://doi.org/10.1093/brain/awac394

Bensimon, G., Lacomblez, L., & Meininger, V. (1994). A Controlled Trial of Riluzole in Amyotrophic Lateral Sclerosis. New England Journal of Medicine, 330(9), 585–591. https://doi.org/10.1056/NEJM199403033300901

Berdyński, M., Miszta, P., Safranow, K., Andersen, P. M., Morita, M., Filipek, S., Żekanowski, C., & Kuźma-Kozakiewicz, M. (2022). SOD1 mutations associated with amyotrophic lateral sclerosis analysis of variant severity. Scientific Reports, 12(1), 103. https://doi.org/10.1038/s41598-021-03891-8

Berger, M. M., Kopp, N., Vital, C., Redl, B., Aymard, M., & Lina, B. (2000). Detection and cellular localization of enterovirus RNA sequences in spinal cord of patients with ALS. Neurology, 54(1), 20–20. https://doi.org/10.1212/WNL.54.1.20

Bergmann, F., & Keller, B. U. (2004). Impact of mitochondrial inhibition on excitability and cytosolic Ca 2+ levels in brainstem motoneurones from mouse. The Journal of Physiology, 555(1), 45–59. https://doi.org/10.1113/jphysiol.2003.053900

Berning, B. A., & Walker, A. K. (2019). The Pathobiology of TDP-43 C-Terminal Fragments in ALS and FTLD. Frontiers in Neuroscience, 13, 335. https://doi.org/10.3389/fnins.2019.00335

Bissaro, M., & Moro, S. (2019). Rethinking to riluzole mechanism of action: The molecular link among protein kinase CK1δ activity, TDP-43 phosphorylation, and amyotrophic lateral sclerosis pharmacological treatment. Neural Regeneration Research, 14(12), 2083. https://doi.org/10.4103/1673-5374.262578

Blair, I. P., Williams, K. L., Warraich, S. T., Durnall, J. C., Thoeng, A. D., Manavis, J., Blumbergs, P. C., Vucic, S., Kiernan, M. C., & Nicholson, G. A. (2010). FUS mutations in amyotrophic lateral sclerosis: Clinical, pathological, neurophysiological and genetic analysis. Journal of Neurology, Neurosurgery & Psychiatry, 81(6), 639–645. https://doi.org/10.1136/jnnp.2009.194399

Blasco, H., Garcon, G., Patin, F., Veyrat-Durebex, C., Boyer, J., Devos, D., Vourc'h, P., Andres, C. R., & Corcia, P. (2017). Panel of Oxidative Stress and Inflammatory Biomarkers in ALS: A Pilot Study. Canadian Journal of Neurological Sciences / Journal Canadien Des Sciences Neurologiques, 44(1), 90–95. https://doi.org/10.1017/cjn.2016.284

Blasco, H., Patin, F., Descat, A., Garçon, G., Corcia, P., Gelé, P., Lenglet, T., Bede, P., Meininger, V., Devos, D., Gossens, J. F., & Pradat, P.-F. (2018). A pharmaco-metabolomics approach in a clinical trial of ALS: Identification of predictive markers of progression. PLOS ONE, 13(6), e0198116. https://doi.org/10.1371/journal.pone.0198116

Blasco, H., Veyrat-Durebex, C., Bocca, C., Patin, F., Vourc'h, P., Kouassi Nzoughet, J., Lenaers, G., Andres, C. R., Simard, G., Corcia, P., & Reynier, P. (2017). Lipidomics Reveals Cerebrospinal-Fluid Signatures of ALS. Scientific Reports, 7(1), 17652. https://doi.org/10.1038/s41598-017-17389-9

Boas, S. M., Joyce, K. L., & Cowell, R. M. (2021). The NRF2-Dependent Transcriptional Regulation of Antioxidant Defense Pathways: Relevance for Cell Type-Specific Vulnerability to Neurodegeneration and Therapeutic Intervention. Antioxidants, 11(1), 8. https://doi.org/10.3390/antiox11010008

Boehringer, A., Garcia-Mansfield, K., Singh, G., Bakkar, N., Pirrotte, P., & Bowser, R. (2017). ALS Associated Mutations in Matrin 3 Alter Protein-Protein Interactions and Impede mRNA Nuclear Export. Scientific Reports, 7(1), 14529. https://doi.org/10.1038/s41598-017-14924-6

Bogers, J. S., Bloem, B. R., & Den Heijer, J. M. (2023). The Etiology of Parkinson's Disease: New Perspectives from Gene-Environment Interactions. Journal of Parkinson's Disease, 13(8), 1281–1288. https://doi.org/10.3233/JPD-230250

Boillée, S., Yamanaka, K., Lobsiger, C. S., Copeland, N. G., Jenkins, N. A., Kassiotis, G., Kollias, G., & Cleveland, D. W. (2006). Onset and Progression in Inherited ALS Determined by Motor Neurons and Microglia. Science, 312(5778), 1389–1392. https://doi.org/10.1126/science.1123511

Bonnet, S., Prévot, G., Mornet, S., Jacobin-Valat, M.-J., Mousli, Y., Hemadou, A., Duttine, M., Trotier, A., Sanchez, S., Duonor-Cérutti, M., Crauste-Manciet, S., & Clofent-Sanchez, G. (2021). A Nano-Emulsion Platform Functionalized with a Fully Human scFv-Fc Antibody for Atheroma Targeting: Towards a Theranostic Approach to Atherosclerosis. International Journal of Molecular Sciences, 22(10), 5188. https://doi.org/10.3390/ijms22105188

Borg, R., Herrera, P., Purkiss, A., Cacciottolo, R., & Cauchi, R. J. (2023). Reduced levels of ALS gene DCTN1 induce motor defects in Drosophila. Frontiers in Neuroscience, 17, 1164251. https://doi.org/10.3389/fnins.2023.1164251

Bouteloup, C., Desport, J.-C., Clavelou, P., Guy, N., Derumeaux-Burel, H., Ferrier, A., & Couratier, P. (2009). Hypermetabolism in ALS patients: An early and persistent phenomenon. Journal of Neurology, 256(8), 1236–1242. https://doi.org/10.1007/s00415-009-5100-z

Bouyer, P., Bradley, S. R., Zhao, J., Wang, W., Richerson, G. B., & Boron, W. F. (2004). Effect of extracellular acid-base disturbances on the intracellular pH of neurones cultured from rat medullary raphe or hippocampus: Effect of acid-base disturbances on neurones. The Journal of Physiology, 559(1), 85–101. https://doi.org/10.1113/jphysiol.2004.067793

Bowles, D. E., McPhee, S. W., Li, C., Gray, S. J., Samulski, J. J., Camp, A. S., Li, J., Wang, B., Monahan, P. E., Rabinowitz, J. E., Grieger, J. C., Govindasamy, L., Agbandje-McKenna, M., Xiao, X., & Samulski, R. J. (2012). Phase 1 Gene Therapy for Duchenne Muscular Dystrophy Using a Translational Optimized AAV Vector. Molecular Therapy, 20(2), 443–455. https://doi.org/10.1038/mt.2011.237

Boyer, C., Whittaker, M. R., Bulmus, V., Liu, J., & Davis, T. P. (2010). The design and utility of polymer-stabilized iron-oxide nanoparticles for nanomedicine applications. NPG Asia Materials, 2(1), 23–30. https://doi.org/10.1038/asiamat.2010.6

Boyko, S., & Surewicz, W. K. (2022). Tau liquid–liquid phase separation in neurodegenerative diseases. Trends in Cell Biology, 32(7), 611–623. https://doi.org/10.1016/j.tcb.2022.01.011

Bozorgchami, N., Ahmadzadeh, M., Hatamabadi, D., Yazdani, A., Shahhosseini, S., & Mohit, E. (2024). Preparation, Characterization, and Radiolabeling of Anti-HER2 scFv With Technetium Tricarbonyl and Stability Studies. Journal of Labelled Compounds and Radiopharmaceuticals, 67(5), 168–179. https://doi.org/10.1002/jlcr.4090

Bradley, W. G., Andrew, A. S., Traynor, B. J., Chiò, A., Butt, T. H., & Stommel, E. W. (2018). Gene-Environment-Time Interactions in Neurodegenerative Diseases: Hypotheses and Research Approaches. Annals of Neurosciences, 25(4), 261–267. https://doi.org/10.1159/000495321

Bratek-Skicki, A., Van Nerom, M., Maes, D., & Tompa, P. (2022). Biological colloids: Unique properties of membraneless organelles in the cell. Advances in Colloid and Interface Science, 310, 102777. https://doi.org/10.1016/j.cis.2022.102777

Breevoort, S., Gibson, S., Figueroa, K., Bromberg, M., & Pulst, S. (2022). Expanding Clinical Spectrum of C9ORF72 -Related Disorders and Promising Therapeutic Strategies: A Review. Neurology Genetics, 8(3), e670. https://doi.org/10.1212/NXG.0000000000000670

Brehme, M., Voisine, C., Rolland, T., Wachi, S., Soper, J. H., Zhu, Y., Orton, K., Villella, A., Garza, D., Vidal, M., Ge, H., & Morimoto, R. I. (2014). A Chaperome Subnetwork Safeguards Proteostasis in Aging and

Neurodegenerative Disease. Cell Reports, 9(3), 1135–1150. https://doi.org/10.1016/j.celrep.2014.09.042

Brettschneider, J., Arai, K., Del Tredici, K., Toledo, J. B., Robinson, J. L., Lee, E. B., Kuwabara, S., Shibuya, K., Irwin, D. J., Fang, L., Van Deerlin, V. M., Elman, L., McCluskey, L., Ludolph, A. C., Lee, V. M.-Y., Braak, H., & Trojanowski, J. Q. (2014). TDP-43 pathology and neuronal loss in amyotrophic lateral sclerosis spinal cord. Acta Neuropathologica, 128(3), 423–437. https://doi.org/10.1007/s00401-014-1299-6

Briese, M., Saal-Bauernschubert, L., Lüningschrör, P., Moradi, M., Dombert, B., Surrey, V., Appenzeller, S., Deng, C., Jablonka, S., & Sendtner, M. (2020). Loss of Tdp-43 disrupts the axonal transcriptome of motoneurons accompanied by impaired axonal translation and mitochondria function. Acta Neuropathologica Communications, 8(1), 116. https://doi.org/10.1186/s40478-020-00987-6

Brocca, S., Grandori, R., Longhi, S., & Uversky, V. (2020). Liquid–Liquid Phase Separation by Intrinsically Disordered Protein Regions of Viruses: Roles in Viral Life Cycle and Control of Virus–Host Interactions. International Journal of Molecular Sciences, 21(23), 9045. https://doi.org/10.3390/ijms21239045

Brommel, C. M., Cooney, A. L., & Sinn, P. L. (2020). Adeno-Associated Virus-Based Gene Therapy for Lifelong Correction of Genetic Disease. Human Gene Therapy, 31(17–18), 985–995. https://doi.org/10.1089/hum.2020.138

Brooks, B. R. (1994). El escorial World Federation of Neurology criteria for the diagnosis of amyotrophic lateral sclerosis. Journal of the Neurological Sciences, 124, 96–107. https://doi.org/10.1016/0022-510X(94)90191-0

Brooks, B. R., Berry, J. D., Ciepielewska, M., Liu, Y., Zambrano, G. S., Zhang, J., & Hagan, M. (2022). Intravenous edaravone treatment in ALS and survival: An exploratory, retrospective, administrative claims analysis. eClinicalMedicine, 52, 101590. https://doi.org/10.1016/j.eclinm.2022.101590

Brooks, B. R., Heiman-Patterson, T., Wiedau-Pazos, M., Liu, S., Zhang, J., & Apple, S. (2022). Edaravone efficacy in amyotrophic lateral sclerosis with reduced forced vital capacity: Post-hoc analysis of Study 19 (MCI186-19) [clinical trial NCT01492686]. PLOS ONE, 17(6), e0258614. https://doi.org/10.1371/journal.pone.0258614

Brooks, B. R., Miller, R. G., Swash, M., & Munsat, T. L. (2000). El Escorial revisited: Revised criteria for the diagnosis of amyotrophic lateral sclerosis. Amyotrophic Lateral Sclerosis and Other Motor Neuron Disorders, 1(5), 293–299. https://doi.org/10.1080/146608200300079536

Brown, A.-L., Wilkins, O. G., Keuss, M. J., Hill, S. E., Zanovello, M., Lee, W. C., Bampton, A., Lee, F. C. Y., Masino, L., Qi, Y. A., Bryce-Smith, S., Gatt, A., Hallegger, M., Fagegaltier, D., Phatnani, H., NYGC ALS Consortium, Phatnani, H., Kwan, J., Sareen, D., … Fratta, P. (2022). TDP-43 loss and ALS-risk SNPs drive mis-splicing and depletion of UNC13A. Nature, 603(7899), 131–137. https://doi.org/10.1038/s41586-022-04436-3

Brown, D., Altermatt, M., Dobreva, T., Chen, S., Wang, A., Thomson, M., & Gradinaru, V. (2021). Deep Parallel Characterization of AAV Tropism and AAV-Mediated Transcriptional Changes via Single-Cell RNA Sequencing. Frontiers in Immunology, 12, 730825. https://doi.org/10.3389/fimmu.2021.730825

Bruijn, L. I., Becher, M. W., Lee, M. K., Anderson, K. L., Jenkins, N. A., Copeland, N. G., Sisodia, S. S., Rothstein, J. D., Borchelt, D. R., Price, D. L., & Cleveland, D. W. (1997). ALS-Linked SOD1 Mutant G85R Mediates Damage to Astrocytes and Promotes Rapidly Progressive Disease with SOD1-Containing Inclusions. Neuron, 18(2), 327–338. https://doi.org/10.1016/S0896-6273(00)80272-X

Bruniaux, J., Djemaa, S. B., Hervé-Aubert, K., Marchais, H., Chourpa, I., & David, S. (2017). Stealth magnetic nanocarriers of siRNA as platform for breast cancer theranostics. International Journal of Pharmaceutics, 532(2), 660–668. https://doi.org/10.1016/j.ijpharm.2017.05.022

Buchan, J. R., & Parker, R. (2009). Eukaryotic Stress Granules: The Ins and Outs of Translation. Molecular Cell, 36(6), 932–941. https://doi.org/10.1016/j.molcel.2009.11.020

Buckler, K. J., Vaughan-Jones, R. D., Peers, C., Lagadic-Gossmann, D., & Nye, P. C. (1991). Effects of extracellular pH, PCO2 and HCO3- on intracellular pH in isolated type-I cells of the neonatal rat carotid body. The Journal of Physiology, 444(1), 703–721. https://doi.org/10.1113/jphysiol.1991.sp018902

Bülow, P., Segal, M., & Bassell, G. J. (2022). Mechanisms Driving the Emergence of Neuronal Hyperexcitability in Fragile X Syndrome. International Journal of Molecular Sciences, 23(11), 6315. https://doi.org/10.3390/ijms23116315

Bunuales, M., Garduno, A., Chillon, M., Bosch, A., Gonzalez-Aparicio, M., Espelosin, M., Garcia-Gomara, M., Rico, A. J., Garcia-Osta, A., Cuadrado-Tejedor, M., Lanciego, J. L., & Hernandez-Alcoceba, R. (2024). Characterization of brain transduction capability of a BBB-penetrant AAV vector in mice, rats and macaques reveals differences in expression profiles. Gene Therapy, 31(9–10), 455–466. https://doi.org/10.1038/s41434-024-00466-w

Buratti, E. (2018). TDP-43 post-translational modifications in health and disease. Expert Opinion on Therapeutic Targets, 22(3), 279–293. https://doi.org/10.1080/14728222.2018.1439923

Cai, Y., Yu, X., Hu, S., & Yu, J. (2009). A Brief Review on the Mechanisms of miRNA Regulation. Genomics, Proteomics & Bioinformatics, 7(4), 147–154. https://doi.org/10.1016/S1672-0229(08)60044-3

Cai, Z., Jia, X., Liu, M., Yang, X., & Cui, L. (2022). Epigenome-wide DNA methylation study of whole blood in patients with sporadic amyotrophic lateral sclerosis. Chinese Medical Journal, 135(12), 1466–1473. https://doi.org/10.1097/CM9.0000000000002090

Calafatti, M., Cocozza, G., Limatola, C., & Garofalo, S. (2023). Microglial crosstalk with astrocytes and immune cells in amyotrophic lateral sclerosis. Frontiers in Immunology, 14, 1223096. https://doi.org/10.3389/fimmu.2023.1223096

Caldi Gomes, L., Hänzelmann, S., Hausmann, F., Khatri, R., Oller, S., Parvaz, M., Tzeplaeff, L., Pasetto, L., Gebelin, M., Ebbing, M., Holzapfel, C., Columbro, S. F., Scozzari, S., Knöferle, J., Cordts, I., Demleitner, A. F., Deschauer, M., Dufke, C., Sturm, M., … Lingor, P. (2024). Multiomic ALS signatures highlight subclusters and sex differences suggesting the MAPK pathway as therapeutic target. Nature Communications, 15(1), 4893. https://doi.org/10.1038/s41467-024-49196-y

Calvo-Rodriguez, M., Hou, S. S., Snyder, A. C., Kharitonova, E. K., Russ, A. N., Das, S., Fan, Z., Muzikansky, A., Garcia-Alloza, M., Serrano-Pozo, A., Hudry, E., & Bacskai, B. J. (2020). Increased mitochondrial calcium levels associated with neuronal death in a mouse model of Alzheimer's disease. Nature Communications, 11(1), 2146. https://doi.org/10.1038/s41467-020-16074-2

Cao, M. C., Ryan, B., Wu, J., Curtis, M. A., Faull, R. L. M., Dragunow, M., & Scotter, E. L. (2023). A panel of TDP-43-regulated splicing events verifies loss of TDP-43 function in amyotrophic lateral sclerosis brain tissue. Neurobiology of Disease, 185, 106245. https://doi.org/10.1016/j.nbd.2023.106245

Cao, W., Cao, Z., Tian, Y., Zhang, L., Wang, W., Tang, L., Xu, C., & Fan, D. (2023). Neutrophils Are Associated with Higher Risk of Incident Amyotrophic Lateral Sclerosis in a BMI - and Age-Dependent Manner. Annals of Neurology, 94(5), 942–954. https://doi.org/10.1002/ana.26760

Cappello, V., Vezzoli, E., Righi, M., Fossati, M., Mariotti, R., Crespi, A., Patruno, M., Bentivoglio, M., Pietrini, G., & Francolini, M. (2012). Analysis of neuromuscular junctions and effects of anabolic steroid administration in the SOD1G93A mouse model of ALS. Molecular and Cellular Neuroscience, 51(1–2), 12–21. https://doi.org/10.1016/j.mcn.2012.07.003

Carter, G. C., Hsiung, C.-H., Simpson, L., Yang, H., & Zhang, X. (2021). N-terminal Domain of TDP43 Enhances Liquid-Liquid Phase Separation of Globular Proteins. Journal of Molecular Biology, 433(10), 166948. https://doi.org/10.1016/j.jmb.2021.166948

Cassina, P., Cassina, A., Pehar, M., Castellanos, R., Gandelman, M., De León, A., Robinson, K. M., Mason, R. P., Beckman, J. S., Barbeito, L., & Radi, R. (2008). Mitochondrial Dysfunction in SOD1 G93A -Bearing Astrocytes Promotes Motor Neuron Degeneration: Prevention by Mitochondrial-Targeted Antioxidants. The Journal of Neuroscience, 28(16), 4115–4122. https://doi.org/10.1523/JNEUROSCI.5308-07.2008

Castle, M. J., Turunen, H. T., Vandenberghe, L. H., & Wolfe, J. H. (2016). Controlling AAV Tropism in the Nervous System with Natural and Engineered Capsids. In F. P. Manfredsson (Ed.), Gene Therapy for Neurological Disorders (Vol. 1382, pp. 133–149). Springer New York. https://doi.org/10.1007/978-1-4939-3271-9_10

Cavalli, G., & Heard, E. (2019). Advances in epigenetics link genetics to the environment and disease. Nature, 571(7766), 489–499. https://doi.org/10.1038/s41586-019-1411-0

Cedarbaum, J. M., Stambler, N., Malta, E., Fuller, C., Hilt, D., Thurmond, B., & Nakanishi, A. (1999). The ALSFRS-R: A revised ALS functional rating scale that incorporates assessments of respiratory function. Journal of the Neurological Sciences, 169(1–2), 13–21. https://doi.org/10.1016/S0022-510X(99)00210-5

Cermelli, C., Vinceti, M., Beretti, F., Pietrini, V., Nacci, G., Pietrosemoli, P., Bartoletti, A., Guidetti, D., Sola, P., Bergomi, M., Vivoli, G., & Portolani, M. (2002). Risk of sporadic amyotrophic lateral sclerosis associated with seropositivity for herpesviruses and echovirus-7. European Journal of Epidemiology, 18(2), 123–127. https://doi.org/10.1023/A:1023067728557

Ceron-Codorniu, M., Torres, P., Fernàndez-Bernal, A., Rico-Rios, S., Serrano, J. Ce., Miralles, M. P., Beltran, M., Garcera, A., Soler, R. M., Pamplona, R., & Portero-Otín, M. (2024). TDP-43 dysfunction leads to bioenergetic failure and lipid metabolic rewiring in human cells. Redox Biology, 75, 103301. https://doi.org/10.1016/j.redox.2024.103301

Chang, H.-P., Kim, S. J., & Shah, D. K. (2021). Whole-Body Pharmacokinetics of Antibody in Mice Determined using Enzyme-Linked Immunosorbent Assay and Derivation of Tissue Interstitial Concentrations. Journal of Pharmaceutical Sciences, 110(1), 446–457. https://doi.org/10.1016/j.xphs.2020.05.025

Chang, J., Shaw, T. B., Holdom, C. J., McCombe, P. A., Henderson, R. D., Fripp, J., Barth, M., Guo, C. C., Ngo, S. T., Steyn, F. J., & For the Alzheimer's Disease Neuroimaging Initiative. (2023). Lower hypothalamic volume with lower body mass index is associated with shorter survival in patients with amyotrophic lateral sclerosis. European Journal of Neurology, 30(1), 57–68. https://doi.org/10.1111/ene.15589

Chang, Q., & Martin, L. J. (2009). Glycinergic Innervation of Motoneurons Is Deficient in Amyotrophic Lateral Sclerosis Mice. The American Journal of Pathology, 174(2), 574–585. https://doi.org/10.2353/ajpath.2009.080557

Chaparro, C. I. P., Simões, B. T., Borges, J. P., Castanho, M. A. R. B., Soares, P. I. P., & Neves, V. (2023). A Promising Approach: Magnetic Nanosystems for Alzheimer's Disease Theranostics. Pharmaceutics, 15(9), 2316. https://doi.org/10.3390/pharmaceutics15092316

Che, M., Jiang, Y., Xie, Y., Jiang, L., & Hu, H. (2011a). Aggregation of the 35-kDa fragment of TDP-43 causes formation of cytoplasmic inclusions and alteration of RNA processing. The FASEB Journal, 25(7), 2344–2353. https://doi.org/10.1096/fj.10-174482

Che, M., Jiang, Y., Xie, Y., Jiang, L., & Hu, H. (2011b). Aggregation of the 35-kDa fragment of TDP-43 causes formation of cytoplasmic inclusions and alteration of RNA processing. The FASEB Journal, 25(7), 2344–2353. https://doi.org/10.1096/fj.10-174482

Che, M.-X., Jiang, L.-L., Li, H.-Y., Jiang, Y.-J., & Hu, H.-Y. (2015). TDP-35 sequesters TDP-43 into cytoplasmic inclusions through binding with RNA. FEBS Letters, 589(15), 1920–1928. https://doi.org/10.1016/j.febslet.2015.06.009

Chen, J., Yuan, X., Wei, P., Wang, D., Chen, C., Guo, Q., Luo, S.-Z., & Chen, L. (2022). The SGYS motif of TAF15 prion-like domain is critical to amyloid fibril formation. Biophysical Journal, 121(13), 2613–2623. https://doi.org/10.1016/j.bpj.2022.05.038

Chen, W., Yao, S., Wan, J., Tian, Y., Huang, L., Wang, S., Akter, F., Wu, Y., Yao, Y., & Zhang, X. (2021). BBB-crossing adeno-associated virus vector: An excellent gene delivery tool for CNS disease treatment. Journal of Controlled Release, 333, 129–138. https://doi.org/10.1016/j.jconrel.2021.03.029

Chen, W.-A., Chang, D.-Y., Chen, B.-M., Lin, Y.-C., Barenholz, Y., & Roffler, S. R. (2023). Antibodies against Poly(ethylene glycol) Activate Innate Immune Cells and Induce Hypersensitivity Reactions to PEGylated Nanomedicines. ACS Nano, 17(6), 5757–5772. https://doi.org/10.1021/acsnano.2c12193

Chen, X., Shi, C., He, M., Xiong, S., & Xia, X. (2023). Endoplasmic reticulum stress: Molecular mechanism and therapeutic targets. Signal Transduction and Targeted Therapy, 8(1), 352. https://doi.org/10.1038/s41392-023-01570-w

Chen, Z., Yuan, Z., Yang, S., Zhu, Y., Xue, M., Zhang, J., & Leng, L. (2023). Brain Energy Metabolism: Astrocytes in Neurodegenerative Diseases. CNS Neuroscience & Therapeutics, 29(1), 24–36. https://doi.org/10.1111/cns.13982

Cheng, K. K., Chan, P. S., Fan, S., Kwan, S. M., Yeung, K. L., Wáng, Y.-X. J., Chow, A. H. L., Wu, E. X., & Baum, L. (2015). Curcumin-conjugated magnetic nanoparticles for detecting amyloid plaques in Alzheimer's disease mice using magnetic resonance imaging (MRI). Biomaterials, 44, 155–172. https://doi.org/10.1016/j.biomaterials.2014.12.005

Cheng, L., Cai, B., Lu, D., & Zeng, H. (2023). The role of mitochondrial energy metabolism in neuroprotection and axonal regeneration after spinal cord injury. Mitochondrion, 69, 57–63. https://doi.org/10.1016/j.mito.2023.01.009

Cheng, Y.-F., Gu, X.-J., Yang, T.-M., Wei, Q.-Q., Cao, B., Zhang, Y., Shang, H.-F., & Chen, Y.-P. (2023). Signature of miRNAs derived from the circulating exosomes of patients with amyotrophic lateral sclerosis. Frontiers in Aging Neuroscience, 15, 1106497. https://doi.org/10.3389/fnagi.2023.1106497

Chestnut, B. A., Chang, Q., Price, A., Lesuisse, C., Wong, M., & Martin, L. J. (2011). Epigenetic Regulation of Motor Neuron Cell Death through DNA Methylation. The Journal of Neuroscience, 31(46), 16619–16636. https://doi.org/10.1523/JNEUROSCI.1639-11.2011

Chevalier, E., Audrain, M., Ratnam, M., Ollier, R., Fuchs, A., Piorkowska, K., Pfeifer, A., Kosco-Vilbois, M., Seredenina, T., & Afroz, T. (2024). Targeting the TDP-43 low complexity domain blocks spreading of pathology in a mouse model of ALS/FTD. Acta Neuropathologica Communications, 12(1), 156. https://doi.org/10.1186/s40478-024-01867-z

Chew, J., Cook, C., Gendron, T. F., Jansen-West, K., Del Rosso, G., Daughrity, L. M., Castanedes-Casey, M., Kurti, A., Stankowski, J. N., Disney, M. D., Rothstein, J. D., Dickson, D. W., Fryer, J. D., Zhang, Y.-J., & Petrucelli, L. (2019). Aberrant deposition of stress granule-resident proteins linked to C9orf72-associated TDP-43 proteinopathy. Molecular Neurodegeneration, 14(1), 9. https://doi.org/10.1186/s13024-019-0310-z

Chhangani, D., & Rincon-Limas, D. (2022). TDP-35, a truncated fragment of TDP-43, induces dose-dependent toxicity and apoptosis in flies. Neural Regeneration Research, 17(11), 2441. https://doi.org/10.4103/1673-5374.338997

Chi, L., Ke, Y., Luo, C., Gozal, D., & Liu, R. (2007). Depletion of reduced glutathione enhances motor neuron degeneration in vitro and in vivo. Neuroscience, 144(3), 991–1003. https://doi.org/10.1016/j.neuroscience.2006.09.064

Chiang, C.-H., Grauffel, C., Wu, L.-S., Kuo, P.-H., Doudeva, L. G., Lim, C., Shen, C.-K. J., & Yuan, H. S. (2016). Structural analysis of disease-related TDP-43 D169G mutation: Linking enhanced stability and caspase cleavage efficiency to protein accumulation. Scientific Reports, 6(1), 21581. https://doi.org/10.1038/srep21581

Chien, H.-M., Lee, C.-C., & Huang, J. J.-T. (2021). The Different Faces of the TDP-43 Low-Complexity Domain: The Formation of Liquid Droplets and Amyloid Fibrils. International Journal of Molecular Sciences, 22(15), 8213. https://doi.org/10.3390/ijms22158213

Chipika, R. H., Mulkerrin, G., Murad, A., Lope, J., Hardiman, O., & Bede, P. (2022). Alterations in somatosensory, visual and auditory pathways in amyotrophic lateral sclerosis: An under-recognised facet of ALS. Journal of Integrative Neuroscience, 21(3), 88. https://doi.org/10.31083/j.jin2103088

Chiu, M. L., Goulet, D. R., Teplyakov, A., & Gilliland, G. L. (2019). Antibody Structure and Function: The Basis for Engineering Therapeutics. Antibodies, 8(4), 55. https://doi.org/10.3390/antib8040055

Chou, C.-C., Zhang, Y., Umoh, M. E., Vaughan, S. W., Lorenzini, I., Liu, F., Sayegh, M., Donlin-Asp, P. G., Chen, Y. H., Duong, D. M., Seyfried, N. T., Powers, M. A., Kukar, T., Hales, C. M., Gearing, M., Cairns, N. J., Boylan, K. B., Dickson, D. W., Rademakers, R., … Rossoll, W. (2018). TDP-43 pathology disrupts nuclear pore complexes and nucleocytoplasmic transport in ALS/FTD. Nature Neuroscience, 21(2), 228–239. https://doi.org/10.1038/s41593-017-0047-3

Chowdhury, E. A., Meno-Tetang, G., Chang, H. Y., Wu, S., Huang, H. W., Jamier, T., Chandran, J., & Shah, D. K. (2021). Current progress and limitations of AAV mediated delivery of protein therapeutic genes and the importance of developing quantitative pharmacokinetic/pharmacodynamic (PK/PD) models. Advanced Drug Delivery Reviews, 170, 214–237. https://doi.org/10.1016/j.addr.2021.01.017

Chowdhury, G. M., Banasr, M., De Graaf, R. A., Rothman, D. L., Behar, K. L., & Sanacora, G. (2008). Chronic Riluzole Treatment Increases Glucose Metabolism in Rat Prefrontal Cortex and Hippocampus. Journal of Cerebral Blood Flow & Metabolism, 28(12), 1892–1897. https://doi.org/10.1038/jcbfm.2008.78

Ciazynska, K. (2023). TDP-43 folds shape disease. Nature Structural & Molecular Biology, 30(10), 1406–1406. https://doi.org/10.1038/s41594-023-01135-z

Cicardi, M. E., Cristofani, R., Rusmini, P., Meroni, M., Ferrari, V., Vezzoli, G., Tedesco, B., Piccolella, M., Messi, E., Galbiati, M., Boncoraglio, A., Carra, S., Crippa, V., & Poletti, A. (2018). Tdp-25 Routing to Autophagy and Proteasome Ameliorates its Aggregation in Amyotrophic Lateral Sclerosis Target Cells. Scientific Reports, 8(1), 12390. https://doi.org/10.1038/s41598-018-29658-2

Cicardi, M. E., Marrone, L., Azzouz, M., & Trotti, D. (2021). Proteostatic imbalance and protein spreading in amyotrophic lateral sclerosis. The EMBO Journal, 40(10), e106389. https://doi.org/10.15252/embj.2020106389

Ciryam, P., Kundra, R., Morimoto, R. I., Dobson, C. M., & Vendruscolo, M. (2015). Supersaturation is a major driving force for protein aggregation in neurodegenerative diseases. Trends in Pharmacological Sciences, 36(2), 72–77. https://doi.org/10.1016/j.tips.2014.12.004

Cistaro, A., Pagani, M., Montuschi, A., Calvo, A., Moglia, C., Canosa, A., Restagno, G., Brunetti, M., Traynor, B. J., Nobili, F., Carrara, G., Fania, P., Lopiano, L., Valentini, M. C., & Chiò, A. (2014). The metabolic signature of C9ORF72-related ALS: FDG PET comparison with nonmutated patients. European Journal of Nuclear Medicine and Molecular Imaging, 41(5), 844–852. https://doi.org/10.1007/s00259-013-2667-5

Clark, J. A., Southam, K. A., Blizzard, C. A., King, A. E., & Dickson, T. C. (2016). Axonal degeneration, distal collateral branching and neuromuscular junction architecture alterations occur prior to symptom onset in the SOD1G93A mouse model of amyotrophic lateral sclerosis. Journal of Chemical Neuroanatomy, 76, 35–47. https://doi.org/10.1016/j.jchemneu.2016.03.003

Combrink, M., Loots, D. T., & Du Preez, I. (2020). Metabolomics describes previously unknown toxicity mechanisms of isoniazid and rifampicin. Toxicology Letters, 322, 104–110. https://doi.org/10.1016/j.toxlet.2020.01.018

Conicella, A. E., Zerze, G. H., Mittal, J., & Fawzi, N. L. (2016). ALS Mutations Disrupt Phase Separation Mediated by α-Helical Structure in the TDP-43 Low-Complexity C-Terminal Domain. Structure, 24(9), 1537–1549. https://doi.org/10.1016/j.str.2016.07.007

Corrado, L., Carlomagno, Y., Falasco, L., Mellone, S., Godi, M., Cova, E., Cereda, C., Testa, L., Mazzini, L., & D'Alfonso, S. (2011). A novel peripherin gene (PRPH) mutation identified in one sporadic amyotrophic lateral sclerosis patient. Neurobiology of Aging, 32(3), 552.e1-552.e6. https://doi.org/10.1016/j.neurobiolaging.2010.02.011

Couch, J. A., Yu, Y. J., Zhang, Y., Tarrant, J. M., Fuji, R. N., Meilandt, W. J., Solanoy, H., Tong, R. K., Hoyte, K., Luk, W., Lu, Y., Gadkar, K., Prabhu, S., Ordonia, B. A., Nguyen, Q., Lin, Y., Lin, Z., Balazs, M., Scearce-Levie, K., … Watts, R. J. (2013). Addressing Safety Liabilities of TfR Bispecific Antibodies That Cross the Blood-Brain Barrier. Science Translational Medicine, 5(183). https://doi.org/10.1126/scitranslmed.3005338

Crippa, V., Cicardi, M. E., Ramesh, N., Seguin, S. J., Ganassi, M., Bigi, I., Diacci, C., Zelotti, E., Baratashvili, M., Gregory, J. M., Dobson, C. M., Cereda, C., Pandey, U. B., Poletti, A., & Carra, S. (2016). The chaperone HSPB8 reduces the accumulation of truncated TDP-43 species in cells and protects against TDP-43-

mediated toxicity. Human Molecular Genetics, 25(18), 3908–3924. https://doi.org/10.1093/hmg/ddw232

Cristofolini, T., Dalmina, M., Sierra, J. A., Silva, A. H., Pasa, A. A., Pittella, F., & Creczynski-Pasa, T. B. (2020). Multifunctional hybrid nanoparticles as magnetic delivery systems for siRNA targeting the HER2 gene in breast cancer cells. Materials Science and Engineering: C, 109, 110555. https://doi.org/10.1016/j.msec.2019.110555

Cutler, R. G., Pedersen, W. A., Camandola, S., Rothstein, J. D., & Mattson, M. P. (2002). Evidence that accumulation of ceramides and cholesterol esters mediates oxidative stress–induced death of motor neurons in amyotrophic lateral sclerosis. Annals of Neurology, 52(4), 448–457. https://doi.org/10.1002/ana.10312

Da Cruz, S., & Cleveland, D. W. (2011). Understanding the role of TDP-43 and FUS/TLS in ALS and beyond. Current Opinion in Neurobiology, 21(6), 904–919. https://doi.org/10.1016/j.conb.2011.05.029

Dadon-Nachum, M., Melamed, E., & Offen, D. (2011). The "Dying-Back" Phenomenon of Motor Neurons in ALS. Journal of Molecular Neuroscience, 43(3), 470–477. https://doi.org/10.1007/s12031-010-9467-1

Dafinca, R., Barbagallo, P., & Talbot, K. (2021). The Role of Mitochondrial Dysfunction and ER Stress in TDP-43 and C9ORF72 ALS. Frontiers in Cellular Neuroscience, 15, 653688. https://doi.org/10.3389/fncel.2021.653688

D'Amico, E., Grosso, G., Nieves, J. W., Zanghì, A., Factor-Litvak, P., & Mitsumoto, H. (2021). Metabolic Abnormalities, Dietary Risk Factors and Nutritional Management in Amyotrophic Lateral Sclerosis. Nutrients, 13(7), 2273. https://doi.org/10.3390/nu13072273

Daneshvar, D. H., Mez, J., Alosco, M. L., Baucom, Z. H., Mahar, I., Baugh, C. M., Valle, J. P., Weuve, J., Paganoni, S., Cantu, R. C., Zafonte, R. D., Stern, R. A., Stein, T. D., Tripodis, Y., Nowinski, C. J., & McKee, A. C. (2021). Incidence of and Mortality From Amyotrophic Lateral Sclerosis in National Football League Athletes. JAMA Network Open, 4(12), e2138801. https://doi.org/10.1001/jamanetworkopen.2021.38801

Daniel, B., Green, O., Viskind, O., & Gruzman, A. (2013). Riluzole increases the rate of glucose transport in L6 myotubes and NSC-34 motor neuron-like cells via AMPK pathway activation. Amyotrophic Lateral Sclerosis and Frontotemporal Degeneration, 14(5–6), 434–443. https://doi.org/10.3109/21678421.2013.808226

D'Antona, S., Caramenti, M., Porro, D., Castiglioni, I., & Cava, C. (2021). Amyotrophic Lateral Sclerosis: A Diet Review. Foods, 10(12), 3128. https://doi.org/10.3390/foods10123128

Darabi, S., Ariaei, A., Rustamzadeh, A., Afshari, D., Charkhat Gorgich, E. A., & Darabi, L. (2024). Cerebrospinal fluid and blood exosomes as biomarkers for amyotrophic lateral sclerosis; a systematic review. Diagnostic Pathology, 19(1), 47. https://doi.org/10.1186/s13000-024-01473-6

Dardiotis, E., Siokas, V., Sokratous, M., Tsouris, Z., Aloizou, A.-M., Florou, D., Dastamani, M., Mentis, A.-F. A., & Brotis, A. G. (2018). Body mass index and survival from amyotrophic lateral sclerosis: A meta-analysis. Neurology Clinical Practice, 8(5), 437–444. https://doi.org/10.1212/CPJ.0000000000000521

Davis, S. A., Itaman, S., Khalid-Janney, C. M., Sherard, J. A., Dowell, J. A., Cairns, N. J., & Gitcho, M. A. (2018). TDP-43 interacts with mitochondrial proteins critical for mitophagy and mitochondrial dynamics. Neuroscience Letters, 678, 8–15. https://doi.org/10.1016/j.neulet.2018.04.053

De Carvalho, M., Dengler, R., Eisen, A., England, J. D., Kaji, R., Kimura, J., Mills, K., Mitsumoto, H., Nodera, H., Shefner, J., & Swash, M. (2008). Electrodiagnostic criteria for diagnosis of ALS. Clinical Neurophysiology, 119(3), 497–503. https://doi.org/10.1016/j.clinph.2007.09.143

De Carvalho, M., & Swash, M. (2013). Fasciculation potentials and earliest changes in motor unit physiology in ALS. Journal of Neurology, Neurosurgery & Psychiatry, 84(9), 963–968. https://doi.org/10.1136/jnnp-2012-304545

De La Cruz, E., Esselin, F., Polge, A., Mouzat, K., & Guissart, C. (2024). Most SOD1 mutations are pathogenic, and their identification can lead to early access to treatment. Journal of Neurology, Neurosurgery & Psychiatry, jnnp-2024-333939. https://doi.org/10.1136/jnnp-2024-333939

De Marco, G., Lomartire, A., Manera, U., Canosa, A., Grassano, M., Casale, F., Fuda, G., Salamone, P., Rinaudo, M. T., Colombatto, S., Moglia, C., Chiò, A., & Calvo, A. (2022). Effects of intracellular calcium accumulation on proteins encoded by the major genes underlying amyotrophic lateral sclerosis. Scientific Reports, 12(1), 395. https://doi.org/10.1038/s41598-021-04267-8

De Vos, K. J., Chapman, A. L., Tennant, M. E., Manser, C., Tudor, E. L., Lau, K.-F., Brownlees, J., Ackerley, S., Shaw, P. J., McLoughlin, D. M., Shaw, C. E., Leigh, P. N., Miller, C. C. J., & Grierson, A. J. (2007). Familial amyotrophic lateral sclerosis-linked SOD1 mutants perturb fast axonal transport to reduce axonal mitochondria content. Human Molecular Genetics, 16(22), 2720–2728. https://doi.org/10.1093/hmg/ddm226

De Conti, L., Akinyi, M. V., Mendoza-Maldonado, R., Romano, M., Baralle, M., & Buratti, E. (2015). TDP-43 affects splicing profiles and isoform production of genes involved in the apoptotic and mitotic cellular pathways. Nucleic Acids Research, 43(18), 8990–9005. https://doi.org/10.1093/nar/gkv814

Deng, J., Wang, P., Chen, X., Cheng, H., Liu, J., Fushimi, K., Zhu, L., & Wu, J. Y. (2018). FUS interacts with ATP synthase beta subunit and induces mitochondrial unfolded protein response in cellular and animal models. Proceedings of the National Academy of Sciences, 115(41). https://doi.org/10.1073/pnas.1806655115

Desport, J. C., Preux, P. M., Magy, L., Boirie, Y., Vallat, J. M., Beaufrère, B., & Couratier, P. (2001). Factors correlated with hypermetabolism in patients with amyotrophic lateral sclerosis. The American Journal of Clinical Nutrition, 74(3), 328–334. https://doi.org/10.1093/ajcn/74.3.328

Dey, B., Kumar, A., & Patel, A. B. (2024). Pathomechanistic Networks of Motor System Injury in AmyotrophicLateral Sclerosis. Current Neuropharmacology, 22(11), 1778–1806. https://doi.org/10.2174/1570159X21666230824091601

Di Nardo, F., Cavalera, S., Baggiani, C., Giovannoli, C., & Anfossi, L. (2019). Direct vs Mediated Coupling of Antibodies to Gold Nanoparticles: The Case of Salivary Cortisol Detection by Lateral Flow Immunoassay. ACS Applied Materials & Interfaces, 11(36), 32758–32768. https://doi.org/10.1021/acsami.9b11559

Diaper, D. C., Adachi, Y., Lazarou, L., Greenstein, M., Simoes, F. A., Di Domenico, A., Solomon, D. A., Lowe, S., Alsubaie, R., Cheng, D., Buckley, S., Humphrey, D. M., Shaw, C. E., & Hirth, F. (2013). Drosophila TDP-43 dysfunction in glia and muscle cells cause cytological and behavioural phenotypes that characterize ALS and FTLD. Human Molecular Genetics, 22(19), 3883–3893. https://doi.org/10.1093/hmg/ddt243

Dietmann, A.-S., Kruse, N., Stork, L., Gloth, M., Brück, W., & Metz, I. (2023). Neurofilament light chains in serum as biomarkers of axonal damage in early MS lesions: A histological–serological correlative study. Journal of Neurology, 270(3), 1416–1429. https://doi.org/10.1007/s00415-022-11468-2

Dimitriadi, M., Kye, M. J., Kalloo, G., Yersak, J. M., Sahin, M., & Hart, A. C. (2013). The Neuroprotective Drug Riluzole Acts via Small Conductance Ca 2+ -Activated K + Channels to Ameliorate Defects in Spinal Muscular Atrophy Models. The Journal of Neuroscience, 33(15), 6557–6562. https://doi.org/10.1523/JNEUROSCI.1536-12.2013

Doble, A. (1996). The pharmacology and mechanism of action of riluzole. Neurology, 47(6_suppl_4). https://doi.org/10.1212/WNL.47.6_Suppl_4.233S

Dodge, J. C., Treleaven, C. M., Fidler, J. A., Tamsett, T. J., Bao, C., Searles, M., Taksir, T. V., Misra, K., Sidman, R. L., Cheng, S. H., & Shihabuddin, L. S. (2013). Metabolic signatures of amyotrophic lateral sclerosis reveal insights into disease pathogenesis. Proceedings of the National Academy of Sciences, 110(26), 10812–10817. https://doi.org/10.1073/pnas.1308421110

Dong, Q., Zhu, J., Liu, S., Yu, X., & Liu, R. (2018). An oligomer-specific antibody improved motor function and attenuated neuropathology in the SOD1-G93A transgenic mouse model of ALS. International Immunopharmacology, 65, 413–421. https://doi.org/10.1016/j.intimp.2018.10.032

Donnenfeld, H., Kascsak, R. J., & Bartfeld, H. (1984). Deposits of IgG and C3 in the spinal cord and motor cortex of ALS patients. Journal of Neuroimmunology, 6(1), 51–57. https://doi.org/10.1016/0165-5728(84)90042-0

Dormann, D., Rodde, R., Edbauer, D., Bentmann, E., Fischer, I., Hruscha, A., Than, M. E., Mackenzie, I. R. A., Capell, A., Schmid, B., Neumann, M., & Haass, C. (2010). ALS-associated fused in sarcoma (FUS) mutations disrupt Transportin-mediated nuclear import. The EMBO Journal, 29(16), 2841–2857. https://doi.org/10.1038/emboj.2010.143

Dorst, J., Weydt, P., Brenner, D., Witzel, S., Kandler, K., Huss, A., Herrmann, C., Wiesenfarth, M., Knehr, A., Günther, K., Müller, K., Weishaupt, J. H., Prudlo, J., Forsberg, K., Andersen, P. M., Rosenbohm, A., Schuster, J., Roselli, F., Dupuis, L., … Ludolph, A. C. (2023). Metabolic alterations precede neurofilament changes in presymptomatic ALS gene carriers. eBioMedicine, 90, 104521. https://doi.org/10.1016/j.ebiom.2023.104521

Dubey, S., Heinen, S., Krantic, S., McLaurin, J., Branch, D. R., Hynynen, K., & Aubert, I. (2020). Clinically approved IVIg delivered to the hippocampus with focused ultrasound promotes neurogenesis in a model of Alzheimer's disease. Proceedings of the National Academy of Sciences, 117(51), 32691–32700. https://doi.org/10.1073/pnas.1908658117

Duyckaerts, C., Maisonobe, T., Hauw, J.-J., & Seilhean, D. (2021). Charcot identifies and illustrates amyotrophic lateral sclerosis. Free Neuropathology, 12 Seiten. https://doi.org/10.17879/FREENEUROPATHOLOGY-2021-3323

Dzieciolowska, S., Drapeau, P., & Armstrong, G. A. B. (2017). Augmented quantal release of acetylcholine at the vertebrate neuromuscular junction following tdp-43 depletion. PLOS ONE, 12(5), e0177005. https://doi.org/10.1371/journal.pone.0177005

Dzik, K. P., Flis, D. J., Kaczor-Keller, K. B., Bytowska, Z. K., Karnia, M. J., Ziółkowski, W., & Kaczor, J. J. (2024). Spinal cord abnormal autophagy and mitochondria energy metabolism are modified by swim training in SOD1-

G93A mice. Journal of Molecular Medicine, 102(3), 379–390. https://doi.org/10.1007/s00109-023-02410-8

Echaniz-Laguna, A., Zoll, J., Ponsot, E., N'Guessan, B., Tranchant, C., Loeffler, J.-P., & Lampert, E. (2006). Muscular mitochondrial function in amyotrophic lateral sclerosis is progressively altered as the disease develops: A temporal study in man. Experimental Neurology, 198(1), 25–30. https://doi.org/10.1016/j.expneurol.2005.07.020

Egawa, N., Izumi, Y., Suzuki, H., Tsuge, I., Fujita, K., Shimano, H., Izumikawa, K., Takahashi, N., Tsukita, K., Enami, T., Nakamura, M., Watanabe, A., Naitoh, M., Suzuki, S., Seki, T., Kobayashi, K., Toda, T., Kaji, R., Takahashi, R., & Inoue, H. (2022). TDP-43 regulates cholesterol biosynthesis by inhibiting sterol regulatory element-binding protein 2. Scientific Reports, 12(1), 7988. https://doi.org/10.1038/s41598-022-12133-4

Egberink, R. O., Van Asbeck, A. H., Boswinkel, M., Muradjan, G., Dieker, J., & Brock, R. (2023). Deciphering Structural Determinants Distinguishing Active from Inactive Cell-Penetrating Peptides for Cytosolic mRNA Delivery. Bioconjugate Chemistry, 34(10), 1822–1834. https://doi.org/10.1021/acs.bioconjchem.3c00346

Eisen, A. (2021). The Dying Forward Hypothesis of ALS: Tracing Its History. Brain Sciences, 11(3), 300. https://doi.org/10.3390/brainsci11030300

Engelhardt, J. I., Tajti, J., & Appel, S. H. (1993). Lymphocytic Infiltrates in the Spinal Cord in Amyotrophic Lateral Sclerosis. Archives of Neurology, 50(1), 30–36. https://doi.org/10.1001/archneur.1993.00540010026013

Ercan, E., Eid, S., Weber, C., Kowalski, A., Bichmann, M., Behrendt, A., Matthes, F., Krauss, S., Reinhardt, P., Fulle, S., & Ehrnhoefer, D. E. (2017). A validated antibody panel for the characterization of tau post-translational modifications. Molecular Neurodegeneration, 12(1), 87. https://doi.org/10.1186/s13024-017-0229-1

Esselin, F., De La Cruz, E., Hirtz, C., Tiers, L., Alphandery, S., Baudesson, L., Taieb, G., Camu, W., & Lehmann, S. (2022). Repeated neurofilament light chain measurements did not capture Riluzole therapeutic effect in amyotrophic lateral sclerosis patients. CNS Neuroscience & Therapeutics, 28(10), 1532–1538. https://doi.org/10.1111/cns.13894

Fang, F., Kwee, L. C., Allen, K. D., Umbach, D. M., Ye, W., Watson, M., Keller, J., Oddone, E. Z., Sandler, D. P., Schmidt, S., & Kamel, F. (2010). Association Between Blood Lead and the Risk of Amyotrophic Lateral Sclerosis. American Journal of Epidemiology, 171(10), 1126–1133. https://doi.org/10.1093/aje/kwq063

Faresjö, R., Bonvicini, G., Fang, X. T., Aguilar, X., Sehlin, D., & Syvänen, S. (2021). Brain pharmacokinetics of two BBB penetrating bispecific antibodies of different size. Fluids and Barriers of the CNS, 18(1), 26. https://doi.org/10.1186/s12987-021-00257-0

Farg, M. A., Soo, K. Y., Walker, A. K., Pham, H., Orian, J., Horne, M. K., Warraich, S. T., Williams, K. L., Blair, I. P., & Atkin, J. D. (2012). Mutant FUS induces endoplasmic reticulum stress in amyotrophic lateral sclerosis and interacts with protein disulfide-isomerase. Neurobiology of Aging, 33(12), 2855–2868. https://doi.org/10.1016/j.neurobiolaging.2012.02.009

Farrawell, N. E., McAlary, L., Lum, J. S., Chisholm, C. G., Warraich, S. T., Blair, I. P., Vine, K. L., Saunders, D. N., & Yerbury, J. J. (2020). Ubiquitin Homeostasis Is Disrupted in TDP-43 and FUS Cell Models of ALS. iScience, 23(11), 101700. https://doi.org/10.1016/j.isci.2020.101700

Fassler, M., Benaim, C., & George, J. (2022). A Single Chain Fragment Variant Binding Misfolded Alpha-Synuclein Exhibits Neuroprotective and Antigen-Specific Anti-Inflammatory Properties. Cells, 11(23), 3822. https://doi.org/10.3390/cells11233822

Fatima, M., Tan, R., Halliday, G. M., & Kril, J. J. (2015). Spread of pathology in amyotrophic lateral sclerosis: Assessment of phosphorylated TDP-43 along axonal pathways. Acta Neuropathologica Communications, 3(1), 47. https://doi.org/10.1186/s40478-015-0226-y

Fayemendy, P., Marin, B., Labrunie, A., Boirie, Y., Walrand, S., Achamrah, N., Coëffier, M., Preux, P.-M., Lautrette, G., Desport, J.-C., Couratier, P., & Jésus, P. (2021). Hypermetabolism is a reality in amyotrophic lateral sclerosis compared to healthy subjects. Journal of the Neurological Sciences, 420, 117257. https://doi.org/10.1016/j.jns.2020.117257

Fecto, F. (2011). SQSTM1 Mutations in Familial and Sporadic Amyotrophic Lateral Sclerosis. Archives of Neurology, 68(11), 1440. https://doi.org/10.1001/archneurol.2011.250

Feng, S., Che, C., Feng, S., Liu, C., Li, L., Li, Y., Huang, H., & Zou, Z. (2019). Novel mutation in optineurin causing aggressive ALS+/−frontotemporal dementia. Annals of Clinical and Translational Neurology, 6(12), 2377–2383. https://doi.org/10.1002/acn3.50928

Fergani, A., Oudart, H., Gonzalez De Aguilar, J.-L., Fricker, B., René, F., Hocquette, J.-F., Meininger, V., Dupuis, L., & Loeffler, J.-P. (2007). Increased peripheral lipid clearance in an animal model of amyotrophic lateral sclerosis. Journal of Lipid Research, 48(7), 1571–1580. https://doi.org/10.1194/jlr.M700017-JLR200

Ferraiuolo, L., Higginbottom, A., Heath, P. R., Barber, S., Greenald, D., Kirby, J., & Shaw, P. J. (2011). Dysregulation of astrocyte–motoneuron cross-talk in mutant superoxide dismutase 1-related amyotrophic lateral sclerosis. Brain, 134(9), 2627–2641. https://doi.org/10.1093/brain/awr193

Ferraiuolo, L., Meyer, K., Sherwood, T. W., Vick, J., Likhite, S., Frakes, A., Miranda, C. J., Braun, L., Heath, P. R., Pineda, R., Beattie, C. E., Shaw, P. J., Askwith, C. C., McTigue, D., & Kaspar, B. K. (2016). Oligodendrocytes contribute to motor neuron death in ALS via SOD1-dependent mechanism. Proceedings of the National Academy of Sciences, 113(42). https://doi.org/10.1073/pnas.1607496113

Figlewicz, D. A., Krizus, A., Martinoli, M. G., Meininger, V., Dib, M., Rouleau, G. A., & Julien, J.-P. (1994). Variants of the heavy neurofilament subunit are associated with the development of amyotrophic lateral sclerosis. Human Molecular Genetics, 3(10), 1757–1761. https://doi.org/10.1093/hmg/3.10.1757

Figueroa-Romero, C., Mikhail, K. A., Gennings, C., Curtin, P., Bello, G. A., Botero, T. M., Goutman, S. A., Feldman, E. L., Arora, M., & Austin, C. (2020). Early life metal dysregulation in amyotrophic lateral sclerosis. Annals of Clinical and Translational Neurology, 7(6), 872–882. https://doi.org/10.1002/acn3.51006

Filareti, M., Luotti, S., Pasetto, L., Pignataro, M., Paolella, K., Messina, P., Pupillo, E., Filosto, M., Lunetta, C., Mandrioli, J., Fuda, G., Calvo, A., Chiò, A., Corbo, M., Bendotti, C., Beghi, E., & Bonetto, V. (2017). Decreased Levels of Foldase and Chaperone Proteins Are Associated with an Early-Onset Amyotrophic Lateral Sclerosis. Frontiers in Molecular Neuroscience, 10. https://doi.org/10.3389/fnmol.2017.00099

Fischer, L. R., Culver, D. G., Tennant, P., Davis, A. A., Wang, M., Castellano-Sanchez, A., Khan, J., Polak, M. A., & Glass, J. D. (2004). Amyotrophic lateral sclerosis is a distal axonopathy: Evidence in mice and man. Experimental Neurology, 185(2), 232–240. https://doi.org/10.1016/j.expneurol.2003.10.004

Fisse, A. L., Pitarokoili, K., Leppert, D., Motte, J., Pedreiturria, X., Kappos, L., Gold, R., Kuhle, J., & Yoon, M.-S. (2021). Serum neurofilament light chain as outcome marker for intensive care unit patients. Journal of Neurology, 268(4), 1323–1329. https://doi.org/10.1007/s00415-020-10277-9

Floare, M.-L., & Allen, S. P. (2020). Why TDP-43? Why Not? Mechanisms of Metabolic Dysfunction in Amyotrophic Lateral Sclerosis. Neuroscience Insights, 15, 263310552095730. https://doi.org/10.1177/2633105520957302

Fomin, V., Richard, P., Hoque, M., Li, C., Gu, Z., Fissore-O'Leary, M., Tian, B., Prives, C., & Manley, J. L. (2018). The C9ORF72 Gene, Implicated in Amyotrophic Lateral Sclerosis and Frontotemporal Dementia, Encodes a Protein That Functions in Control of Endothelin and Glutamate Signaling. Molecular and Cellular Biology, 38(22), e00155-18. https://doi.org/10.1128/MCB.00155-18

Frakes, A. E., Ferraiuolo, L., Haidet-Phillips, A. M., Schmelzer, L., Braun, L., Miranda, C. J., Ladner, K. J., Bevan, A. K., Foust, K. D., Godbout, J. P., Popovich, P. G., Guttridge, D. C., & Kaspar, B. K. (2014). Microglia Induce Motor Neuron Death via the Classical NF-κB Pathway in Amyotrophic Lateral Sclerosis. Neuron, 81(5), 1009–1023. https://doi.org/10.1016/j.neuron.2014.01.013

François-Moutal, L., Perez-Miller, S., Scott, D. D., Miranda, V. G., Mollasalehi, N., & Khanna, M. (2019). Structural Insights Into TDP-43 and Effects of Post-translational Modifications. Frontiers in Molecular Neuroscience, 12, 301. https://doi.org/10.3389/fnmol.2019.00301

François-Moutal, L., Scott, D. D., Ambrose, A. J., Zerio, C. J., Rodriguez-Sanchez, M., Dissanayake, K., May, D. G., Carlson, J. M., Barbieri, E., Moutal, A., Roux, K. J., Shorter, J., Khanna, R., Barmada, S. J., McGurk, L., & Khanna, M. (2022). Heat shock protein Grp78/BiP/HspA5 binds directly to TDP-43 and mitigates toxicity associated with disease pathology. Scientific Reports, 12(1), 8140. https://doi.org/10.1038/s41598-022-12191-8

Freibaum, B. D., Lu, Y., Lopez-Gonzalez, R., Kim, N. C., Almeida, S., Lee, K.-H., Badders, N., Valentine, M., Miller, B. L., Wong, P. C., Petrucelli, L., Kim, H. J., Gao, F.-B., & Taylor, J. P. (2015). GGGGCC repeat expansion in C9orf72 compromises nucleocytoplasmic transport. Nature, 525(7567), 129–133. https://doi.org/10.1038/nature14974

Friedrich, R. P., Janko, C., Unterweger, H., Lyer, S., & Alexiou, C. (2023). SPIONs and magnetic hybrid materials: Synthesis, toxicology and biomedical applications. Physical Sciences Reviews, 8(8), 1435–1464. https://doi.org/10.1515/psr-2019-0093

Fumagalli, E., Funicello, M., Rauen, T., Gobbi, M., & Mennini, T. (2008). Riluzole enhances the activity of glutamate transporters GLAST, GLT1 and EAAC1. European Journal of Pharmacology, 578(2–3), 171–176. https://doi.org/10.1016/j.ejphar.2007.10.023

Fumagalli, L., Young, F. L., Boeynaems, S., De Decker, M., Mehta, A. R., Swijsen, A., Fazal, R., Guo, W., Moisse, M., Beckers, J., Dedeene, L., Selvaraj, B. T., Vandoorne, T., Madan, V., Van Blitterswijk, M., Raitcheva, D., McCampbell, A., Poesen, K., Gitler, A. D., … Van Damme, P. (2021). C9orf72 -derived arginine-containing dipeptide repeats associate with axonal transport machinery and impede microtubule-based motility. Science Advances, 7(15), eabg3013. https://doi.org/10.1126/sciadv.abg3013

Gabery, S., Ahmed, R. M., Caga, J., Kiernan, M. C., Halliday, G. M., & Petersén, Å. (2021). Loss of the metabolism and sleep regulating neuronal populations expressing orexin and oxytocin in the hypothalamus in amyotrophic lateral sclerosis. Neuropathology and Applied Neurobiology, 47(7), 979–989. https://doi.org/10.1111/nan.12709

Gamez, J., & Carmona, F. (2021). Confirmation of early non-bulbar onset of amyotrophic lateral sclerosis in Spanish league soccer players. Journal of the Neurological Sciences, 428, 117586. https://doi.org/10.1016/j.jns.2021.117586

Ganne, A., Balasubramaniam, M., Ayyadevara, H., Kiaei, L., Shmookler Reis, R. J., Varughese, K. I., & Kiaei, M. (2023). In silico analysis of TUBA4A mutations in Amyotrophic Lateral Sclerosis to define mechanisms of microtubule disintegration. Scientific Reports, 13(1), 2096. https://doi.org/10.1038/s41598-023-28381-x

Gao, B. (2016). Basic liver immunology. Cellular & Molecular Immunology, 13(3), 265–266. https://doi.org/10.1038/cmi.2016.09

Gao, M., Zhu, L., Chang, J., Cao, T., Song, L., Wen, C., Chen, Y., Zhuo, Y., & Chen, F. (2023). Safety and Efficacy of Edaravone in Patients with Amyotrophic Lateral Sclerosis: A Systematic Review and Meta-analysis. Clinical Drug Investigation, 43(1), 1–11. https://doi.org/10.1007/s40261-022-01229-4

Garnier, C., Devred, F., Byrne, D., Puppo, R., Roman, A. Yu., Malesinski, S., Golovin, A. V., Lebrun, R., Ninkina, N. N., & Tsvetkov, P. O. (2017). Zinc binding to RNA recognition motif of TDP-43 induces the formation of amyloid-like aggregates. Scientific Reports, 7(1), 6812. https://doi.org/10.1038/s41598-017-07215-7

Gautam, M., Gunay, A., Chandel, N. S., & Ozdinler, P. H. (2022). Mitochondrial dysregulation occurs early in ALS motor cortex with TDP-43 pathology and suggests maintaining NAD+ balance as a therapeutic strategy. Scientific Reports, 12(1), 4287. https://doi.org/10.1038/s41598-022-08068-5

Gautam, M., Jara, J. H., Kocak, N., Rylaarsdam, L. E., Kim, K. D., Bigio, E. H., & Hande Özdinler, P. (2019). Mitochondria, ER, and nuclear membrane defects reveal early mechanisms for upper motor neuron vulnerability with respect to TDP-43 pathology. Acta Neuropathologica, 137(1), 47–69. https://doi.org/10.1007/s00401-018-1934-8

Gautam, M., Xie, E. F., Kocak, N., & Ozdinler, P. H. (2019). Mitoautophagy: A Unique Self-Destructive Path Mitochondria of Upper Motor Neurons With TDP-43 Pathology Take, Very Early in ALS. Frontiers in Cellular Neuroscience, 13, 489. https://doi.org/10.3389/fncel.2019.00489

Geevasinga, N., Menon, P., Nicholson, G. A., Ng, K., Howells, J., Kril, J. J., Yiannikas, C., Kiernan, M. C., & Vucic, S. (2015). Cortical Function in Asymptomatic Carriers and Patients With C9orf72 Amyotrophic Lateral Sclerosis. JAMA Neurology, 72(11), 1268. https://doi.org/10.1001/jamaneurol.2015.1872

Genge, A., Cedarbaum, J. M., Shefner, J., Chio, A., Al-Chalabi, A., Van Damme, P., McDermott, C., Glass, J., Berry, J., Van Eijk, R. P. A., Fournier, C., Grosskreutz, J., Andrews, J., Bertone, V., Bunte, T. M., Couillard, M., Cummings, C., Kittle, G., Polzer, J., … Van Den Berg, L. H. (2024). The ALSFRS-R Summit: A global call to action on the use of the ALSFRS-R in ALS clinical trials. Amyotrophic Lateral Sclerosis and Frontotemporal Degeneration, 25(3–4), 382–387. https://doi.org/10.1080/21678421.2024.2320880

Ghaderi, H., Alipour, A., Mohammadi Zadeh Holagh, A., Kazemi Lomedasht, F., Abdollahpour-Alitappeh, M., Kaghazian, H., & Shahsavarani, H. (2023). Recombinant antibody fragment therapeutics: Current status

and future prospects of scFv, nanobody, and mimotopes. Journal of Drug Delivery Science and Technology, 89, 105009. https://doi.org/10.1016/j.jddst.2023.105009

Ghadge, G. D., Kay, B. K., Drigotas, C., & Roos, R. P. (2019). Single chain variable fragment antibodies directed against SOD1 ameliorate disease in mutant SOD1 transgenic mice. Neurobiology of Disease, 121, 131–137. https://doi.org/10.1016/j.nbd.2018.08.021

Giampetruzzi, A., Danielson, E. W., Gumina, V., Jeon, M., Boopathy, S., Brown, R. H., Ratti, A., Landers, J. E., & Fallini, C. (2019). Modulation of actin polymerization affects nucleocytoplasmic transport in multiple forms of amyotrophic lateral sclerosis. Nature Communications, 10(1), 3827. https://doi.org/10.1038/s41467-019-11837-y

Gilodi, M., Lisi, S., F. Dudás, E., Fantini, M., Puglisi, R., Louka, A., Marcatili, P., Cattaneo, A., & Pastore, A. (2022). Selection and Modelling of a New Single-Domain Intrabody Against TDP-43. Frontiers in Molecular Biosciences, 8, 773234. https://doi.org/10.3389/fmolb.2021.773234

Glockshuber, R., Malia, M., Pfitzinger, I., & Plueckthun, A. (1990). A comparison of strategies to stabilize immunoglobulin Fv-fragments. Biochemistry, 29(6), 1362–1367. https://doi.org/10.1021/bi00458a002

Go, E. B., Lee, J. H., Cho, J. H., Kwon, N. H., Choi, J., & Kwon, I. (2024). Enhanced therapeutic potential of antibody fragment via IEDDA-mediated site-specific albumin conjugation. Journal of Biological Engineering, 18(1), 23. https://doi.org/10.1186/s13036-024-00418-3

Godoy-Corchuelo, J. M., Fernández-Beltrán, L. C., Ali, Z., Gil-Moreno, M. J., López-Carbonero, J. I., Guerrero-Sola, A., Larrad-Sainz, A., Matias-Guiu, J., Matias-Guiu, J. A., Cunningham, T. J., & Corrochano, S. (2022). Lipid Metabolic Alterations in the ALS–FTD Spectrum of Disorders. Biomedicines, 10(5), 1105. https://doi.org/10.3390/biomedicines10051105

Goertsen, D., Flytzanis, N. C., Goeden, N., Chuapoco, M. R., Cummins, A., Chen, Y., Fan, Y., Zhang, Q., Sharma, J., Duan, Y., Wang, L., Feng, G., Chen, Y., Ip, N. Y., Pickel, J., & Gradinaru, V. (2022). AAV capsid variants with brain-wide transgene expression and decreased liver targeting after intravenous delivery in mouse and marmoset. Nature Neuroscience, 25(1), 106–115. https://doi.org/10.1038/s41593-021-00969-4

Goldstein, L. H., & Abrahams, S. (2013). Changes in cognition and behaviour in amyotrophic lateral sclerosis: Nature of impairment and implications for assessment. The Lancet Neurology, 12(4), 368–380. https://doi.org/10.1016/S1474-4422(13)70026-7

González-Guevara, E., Cárdenas, G., Pérez-Severiano, F., & Martínez-Lazcano, J. C. (2020). Dysregulated Brain Cholesterol Metabolism Is Linked to Neuroinflammation in Huntington's Disease. Movement Disorders, 35(7), 1113–1127. https://doi.org/10.1002/mds.28089

Goodwin, M. S., Sinyavskaya, O., Burg, F., O'Neal, V., Ceballos-Diaz, C., Cruz, P. E., Lewis, J., Giasson, B. I., Davies, P., Golde, T. E., & Levites, Y. (2021). Anti-tau scFvs Targeted to the Cytoplasm or Secretory Pathway Variably Modify Pathology and Neurodegenerative Phenotypes. Molecular Therapy, 29(2), 859–872. https://doi.org/10.1016/j.ymthe.2020.10.007

Gorges, M., Vercruysse, P., Müller, H.-P., Huppertz, H.-J., Rosenbohm, A., Nagel, G., Weydt, P., Petersén, Å., Ludolph, A. C., Kassubek, J., & Dupuis, L. (2017). Hypothalamic atrophy is related to body mass index and age at onset in amyotrophic lateral sclerosis. Journal of Neurology, Neurosurgery & Psychiatry, 88(12), 1033–1041. https://doi.org/10.1136/jnnp-2017-315795

Goulatis, L. I., & Shusta, E. V. (2017). Protein engineering approaches for regulating blood–brain barrier transcytosis. Current Opinion in Structural Biology, 45, 109–115. https://doi.org/10.1016/j.sbi.2016.12.005

Goutman, S. A., Boss, J., Guo, K., Alakwaa, F. M., Patterson, A., Kim, S., Savelieff, M. G., Hur, J., & Feldman, E. L. (2020). Untargeted metabolomics yields insight into ALS disease mechanisms. Journal of Neurology, Neurosurgery & Psychiatry, 91(12), 1329–1338. https://doi.org/10.1136/jnnp-2020-323611

Goutman, S. A., Guo, K., Savelieff, M. G., Patterson, A., Sakowski, S. A., Habra, H., Karnovsky, A., Hur, J., & Feldman, E. L. (2022). Metabolomics identifies shared lipid pathways in independent amyotrophic lateral sclerosis cohorts. Brain, 145(12), 4425–4439. https://doi.org/10.1093/brain/awac025

Grad, L. I., Rouleau, G. A., Ravits, J., & Cashman, N. R. (2017). Clinical Spectrum of Amyotrophic Lateral Sclerosis (ALS). Cold Spring Harbor Perspectives in Medicine, 7(8), a024117. https://doi.org/10.1101/cshperspect.a024117

Gradisnik, L., & Velnar, T. (2023). Astrocytes in the central nervous system and their functions in health and disease: A review. World Journal of Clinical Cases, 11(15), 3385–3394. https://doi.org/10.12998/wjcc.v11.i15.3385

Gravel, M., Béland, L.-C., Soucy, G., Abdelhamid, E., Rahimian, R., Gravel, C., & Kriz, J. (2016). IL-10 Controls Early Microglial Phenotypes and Disease Onset in ALS Caused by Misfolded Superoxide Dismutase 1. The Journal of Neuroscience, 36(3), 1031–1048. https://doi.org/10.1523/JNEUROSCI.0854-15.2016

Gregory, J. M., Fagegaltier, D., Phatnani, H., & Harms, M. B. (2020). Genetics of Amyotrophic Lateral Sclerosis. Current Genetic Medicine Reports, 8(4), 121–131. https://doi.org/10.1007/s40142-020-00194-8

Greig, J. A., Martins, K. M., Breton, C., Lamontagne, R. J., Zhu, Y., He, Z., White, J., Zhu, J.-X., Chichester, J. A., Zheng, Q., Zhang, Z., Bell, P., Wang, L., & Wilson, J. M. (2024). Integrated vector genomes may contribute to long-term expression in primate liver after AAV administration. Nature Biotechnology, 42(8), 1232–1242. https://doi.org/10.1038/s41587-023-01974-7

Gschwendtberger, T., Thau-Habermann, N., Von Der Ohe, J., Luo, T., Hass, R., & Petri, S. (2023). Protective effects of EVs/exosomes derived from permanently growing human MSC on primary murine ALS motor neurons. Neuroscience Letters, 816, 137493. https://doi.org/10.1016/j.neulet.2023.137493

Gu, J., Xu, H., Han, Y., Dai, W., Hao, W., Wang, C., Gu, N., Xu, H., & Cao, J. (2011). The internalization pathway, metabolic fate and biological effect of superparamagnetic iron oxide nanoparticles in the macrophage-like RAW264.7 cell. Science China Life Sciences, 54(9), 793–805. https://doi.org/10.1007/s11427-011-4215-5

Güell-Bosch, J., Lope-Piedrafita, S., Esquerda-Canals, G., Montoliu-Gaya, L., & Villegas, S. (2020). Progression of Alzheimer's disease and effect of scFv-h3D6 immunotherapy in the 3xTg-AD mouse model: An in vivo longitudinal study using Magnetic Resonance Imaging and Spectroscopy. NMR in Biomedicine, 33(5), e4263. https://doi.org/10.1002/nbm.4263

Guillot, S. J., Bolborea, M., & Dupuis, L. (2021). Dysregulation of energy homeostasis in amyotrophic lateral sclerosis. Current Opinion in Neurology, 34(5), 773–780. https://doi.org/10.1097/WCO.0000000000000982

Günther, R., Pal, A., Williams, C., Zimyanin, V. L., Liehr, M., Von Neubeck, C., Krause, M., Parab, M. G., Petri, S., Kalmbach, N., Marklund, S. L., Sterneckert, J., Munch Andersen, P., Wegner, F., Gilthorpe, J. D., & Hermann, A. (2022). Alteration of Mitochondrial Integrity as Upstream Event in the Pathophysiology of SOD1-ALS. Cells, 11(7), 1246. https://doi.org/10.3390/cells11071246

Gupta, S. K., & Shukla, P. (2017). Microbial platform technology for recombinant antibody fragment production: A review. Critical Reviews in Microbiology, 43(1), 31–42. https://doi.org/10.3109/1040841X.2016.1150959

Gusliakova, O. I., Kurochkin, M. A., Barmin, R. A., Prikhozhdenko, E. S., Estifeeva, T. M., Rudakovskaya, P. G., Sindeeva, O. A., Galushka, V. V., Vavaev, E. S., Komlev, A. S., Lyubin, E. V., Fedyanin, A. A., Dey, K. K., & Gorin, D. A. (2024). Magnetically navigated microbubbles coated with albumin/polyarginine and superparamagnetic iron oxide nanoparticles. Biomaterials Advances, 158, 213759. https://doi.org/10.1016/j.bioadv.2024.213759

Gustavsson, T., Metzendorf, N. G., Wik, E., Roshanbin, S., Julku, U., Chourlia, A., Nilsson, P., Andersson, K. G., Laudon, H., Hultqvist, G., Syvänen, S., & Sehlin, D. (2023). Long-term effects of immunotherapy with a brain penetrating Aβ antibody in a mouse model of Alzheimer's disease. Alzheimer's Research & Therapy, 15(1), 90. https://doi.org/10.1186/s13195-023-01236-3

Guttenplan, K. A., Weigel, M. K., Adler, D. I., Couthouis, J., Liddelow, S. A., Gitler, A. D., & Barres, B. A. (2020). Knockout of reactive astrocyte activating factors slows disease progression in an ALS mouse model. Nature Communications, 11(1), 3753. https://doi.org/10.1038/s41467-020-17514-9

Gwathmey, K. G., Corcia, P., McDermott, C. J., Genge, A., Sennfält, S., De Carvalho, M., & Ingre, C. (2023). Diagnostic delay in amyotrophic lateral sclerosis. European Journal of Neurology, 30(9), 2595–2601. https://doi.org/10.1111/ene.15874

Habas, A., Hahn, J., Wang, X., & Margeta, M. (2013). Neuronal activity regulates astrocytic Nrf2 signaling. Proceedings of the National Academy of Sciences, 110(45), 18291–18296. https://doi.org/10.1073/pnas.1208764110

Hamilton, B. A., & Wright, J. F. (2021). Challenges Posed by Immune Responses to AAV Vectors: Addressing Root Causes. Frontiers in Immunology, 12, 675897. https://doi.org/10.3389/fimmu.2021.675897

Harmon, T. S., Holehouse, A. S., Rosen, M. K., & Pappu, R. V. (2017). Intrinsically disordered linkers determine the interplay between phase separation and gelation in multivalent proteins. eLife, 6, e30294. https://doi.org/10.7554/eLife.30294

He, J., Fu, J., Zhao, W., Ren, C., Liu, P., Chen, L., Li, D., Tang, L., Zhou, L., Zhang, Y., Ma, X., Zhang, G., Li, N., & Fan, D. (2022). Hypermetabolism associated with worse prognosis of amyotrophic lateral sclerosis. Journal of Neurology, 269(3), 1447–1455. https://doi.org/10.1007/s00415-021-10716-1

He, Z., Sun, B., Feng, F., Bai, J., Wang, H., Wang, H., Yang, F., Cui, F., & Huang, X. (2022). Time of symptoms beyond the bulbar region predicts survival in bulbar onset amyotrophic lateral sclerosis. Neurological Sciences, 43(3), 1817–1822. https://doi.org/10.1007/s10072-021-05556-w

Hergesheimer, R., Lanznaster, D., Bourgeais, J., Hérault, O., Vourc'h, P., Andres, C. R., Corcia, P., & Blasco, H. (2020). Conditioned Medium from Cells Overexpressing TDP-43 Alters the Metabolome of Recipient Cells. Cells, 9(10), 2198. https://doi.org/10.3390/cells9102198

Hervé, K., Douziech-Eyrolles, L., Munnier, E., Cohen-Jonathan, S., Soucé, M., Marchais, H., Limelette, P., Warmont, F., Saboungi, M. L., Dubois, P., & Chourpa, I. (2008). The development of stable aqueous suspensions of PEGylated SPIONs for biomedical applications. Nanotechnology, 19(46), 465608. https://doi.org/10.1088/0957-4484/19/46/465608

Hervé-Aubert, K., Allard-Vannier, E., Joubert, N., Lakhrif, Z., Alric, C., Martin, C., Viaud-Massuard, M.-C., Dimier-Poisson, I., Aubrey, N., & Chourpa, I. (2018). Impact of Site-Specific Conjugation of ScFv to Multifunctional Nanomedicines Using Second Generation Maleimide. Bioconjugate Chemistry, 29(5), 1553–1559. https://doi.org/10.1021/acs.bioconjchem.8b00091

Hideyama, T., Teramoto, S., Hachiga, K., Yamashita, T., & Kwak, S. (2012). Co-Occurrence of TDP-43 Mislocalization with Reduced Activity of an RNA Editing Enzyme, ADAR2, in Aged Mouse Motor Neurons. PLoS ONE, 7(8), e43469. https://doi.org/10.1371/journal.pone.0043469

Hideyama, T., Yamashita, T., Suzuki, T., Tsuji, S., Higuchi, M., Seeburg, P. H., Takahashi, R., Misawa, H., & Kwak, S. (2010). Induced Loss of ADAR2 Engenders Slow Death of Motor Neurons from Q/R Site-Unedited GluR2. The Journal of Neuroscience, 30(36), 11917–11925. https://doi.org/10.1523/JNEUROSCI.2021-10.2010

Higgins, C. M. J., Jung, C., Ding, H., & Xu, Z. (2002). Mutant Cu, Zn Superoxide Dismutase that Causes Motoneuron Degeneration Is Present in Mitochondria in the CNS. The Journal of Neuroscience, 22(6), RC215–RC215. https://doi.org/10.1523/JNEUROSCI.22-06-j0001.2002

Hinchcliffe, M., & Smith, A. (2017). Riluzole: Real-world evidence supports significant extension of median survival times in patients with amyotrophic lateral sclerosis. Degenerative Neurological and Neuromuscular Disease, Volume 7, 61–70. https://doi.org/10.2147/DNND.S135748

Hirabayashi, Y., Kwon, S.-K., Paek, H., Pernice, W. M., Paul, M. A., Lee, J., Erfani, P., Raczkowski, A., Petrey, D. S., Pon, L. A., & Polleux, F. (2017). ER-mitochondria tethering by PDZD8 regulates Ca 2+ dynamics in mammalian neurons. Science, 358(6363), 623–630. https://doi.org/10.1126/science.aan6009

Ho, W. Y., Chang, J.-C., Lim, K., Cazenave-Gassiot, A., Nguyen, A. T., Foo, J. C., Muralidharan, S., Viera-Ortiz, A., Ong, S. J. M., Hor, J. H., Agrawal, I., Hoon, S., Arogundade, O. A., Rodriguez, M. J., Lim, S. M., Kim, S. H., Ravits, J., Ng, S.-Y., Wenk, M. R., … Ling, S.-C. (2021). TDP-43 mediates SREBF2-regulated gene expression required for oligodendrocyte myelination. Journal of Cell Biology, 220(9), e201910213. https://doi.org/10.1083/jcb.201910213

Hop, P. J., Zwamborn, R. A. J., Hannon, E., Shireby, G. L., Nabais, M. F., Walker, E. M., Van Rheenen, W., Van Vugt, J. J. F. A., Dekker, A. M., Westeneng, H.-J., Tazelaar, G. H. P., Van Eijk, K. R., Moisse, M., Baird, D., Al Khleifat, A., Iacoangeli, A., Ticozzi, N., Ratti, A., Cooper-Knock, J., … Mill, J. (2022). Genome-wide study of DNA methylation shows alterations in metabolic, inflammatory, and cholesterol pathways in ALS. Science Translational Medicine, 14(633), eabj0264. https://doi.org/10.1126/scitranslmed.abj0264

Hu, C., Yang, J., Qi, Z., Wu, H., Wang, B., Zou, F., Mei, H., Liu, J., Wang, W., & Liu, Q. (2022). Heat shock proteins: Biological functions, pathological roles, and therapeutic opportunities. MedComm, 3(3), e161. https://doi.org/10.1002/mco2.161

Huang, C., Tong, J., Bi, F., Zhou, H., & Xia, X.-G. (2012). Mutant TDP-43 in motor neurons promotes the onset and progression of ALS in rats. Journal of Clinical Investigation, 122(1), 107–118. https://doi.org/10.1172/JCI59130

Huang, H., Van Dullemen, L. F. A., Akhtar, M. Z., Faro, M.-L. L., Yu, Z., Valli, A., Dona, A., Thézénas, M.-L., Charles, P. D., Fischer, R., Kaisar, M., Leuvenink, H. G. D., Ploeg, R. J., & Kessler, B. M. (2018). Proteo-metabolomics reveals compensation between ischemic and non-injured contralateral kidneys after reperfusion. Scientific Reports, 8(1), 8539. https://doi.org/10.1038/s41598-018-26804-8

Huang, W.-P., Ellis, B. C. S., Hodgson, R. E., Sanchez Avila, A., Kumar, V., Rayment, J., Moll, T., & Shelkovnikova, T. A. (2024). Stress-induced TDP-43 nuclear condensation causes splicing loss of function and STMN2 depletion. Cell Reports, 43(7), 114421. https://doi.org/10.1016/j.celrep.2024.114421

Huang, Y., Shih, C., Huang, C., Lin, C., Chou, C., Tsai, M., Liu, T. P., Chiu, J., & Chen, C. (2006). Effects of cadmium on structure and enzymatic activity of Cu,Zn-SOD and oxidative status in neural cells. Journal of Cellular Biochemistry, 98(3), 577–589. https://doi.org/10.1002/jcb.20772

Humphrey, J., Venkatesh, S., Hasan, R., Herb, J. T., De Paiva Lopes, K., Küçükali, F., Byrska-Bishop, M., Evani, U. S., Narzisi, G., Fagegaltier, D., NYGC ALS Consortium, Sleegers, K., Phatnani, H., Knowles, D. A., Fratta, P., & Raj, T. (2023). Integrative transcriptomic analysis of the amyotrophic lateral sclerosis spinal cord implicates glial activation and suggests new risk genes. Nature Neuroscience, 26(1), 150–162. https://doi.org/10.1038/s41593-022-01205-3

Hussain, H., Vutipongsatorn, K., Jiménez, B., & Antcliffe, D. B. (2022). Patient Stratification in Sepsis: Using Metabolomics to Detect Clinical Phenotypes, Sub-Phenotypes and Therapeutic Response. Metabolites, 12(5), 376. https://doi.org/10.3390/metabo12050376

Hutt, M., Färber-Schwarz, A., Unverdorben, F., Richter, F., & Kontermann, R. E. (2012). Plasma Half-life Extension of Small Recombinant Antibodies by Fusion to Immunoglobulin-binding Domains. Journal of Biological Chemistry, 287(7), 4462–4469. https://doi.org/10.1074/jbc.M111.311522

Ilieva, H., Vullaganti, M., & Kwan, J. (2023). Advances in molecular pathology, diagnosis, and treatment of amyotrophic lateral sclerosis. BMJ, e075037. https://doi.org/10.1136/bmj-2023-075037

Imperatore, J. A., McAninch, D. S., Valdez-Sinon, A. N., Bassell, G. J., & Mihailescu, M. R. (2020). FUS Recognizes G Quadruplex Structures Within Neuronal mRNAs. Frontiers in Molecular Biosciences, 7, 6. https://doi.org/10.3389/fmolb.2020.00006

Inagaki, H., Hosoda, N., Tsuiji, H., & Hoshino, S. (2020). Direct evidence that Ataxin-2 is a translational activator mediating cytoplasmic polyadenylation. Journal of Biological Chemistry, 295(47), 15810–15825. https://doi.org/10.1074/jbc.RA120.013835

Ingólfsson, H. I., Rizuan, A., Liu, X., Mohanty, P., Souza, P. C. T., Marrink, S. J., Bowers, M. T., Mittal, J., & Berry, J. (2023). Multiscale simulations reveal TDP-43 molecular level interactions driving condensation. Biophysical Journal, S0006349523006525. https://doi.org/10.1016/j.bpj.2023.10.016

Ishiguro, A., & Ishihama, A. (2023). ALS-linked TDP-43 mutations interfere with the recruitment of RNA recognition motifs to G-quadruplex RNA. Scientific Reports, 13(1), 5982. https://doi.org/10.1038/s41598-023-33172-5

Ishiguro, A., Kimura, N., Watanabe, Y., Watanabe, S., & Ishihama, A. (2016). TDP-43 binds and transports G-quadruplex-containing mRNAs into neurites for local translation. Genes to Cells, 21(5), 466–481. https://doi.org/10.1111/gtc.12352

Ishii, T., Kawakami, E., Endo, K., Misawa, H., & Watabe, K. (2017). Formation and spreading of TDP-43 aggregates in cultured neuronal and glial cells demonstrated by time-lapse imaging. PLOS ONE, 12(6), e0179375. https://doi.org/10.1371/journal.pone.0179375

Ising, C., Gallardo, G., Leyns, C. E. G., Wong, C. H., Jiang, H., Stewart, F., Koscal, L. J., Roh, J., Robinson, G. O., Remolina Serrano, J., & Holtzman, D. M. (2017). AAV-mediated expression of anti-tau scFvs decreases tau accumulation in a mouse model of tauopathy. Journal of Experimental Medicine, 214(5), 1227–1238. https://doi.org/10.1084/jem.20162125

Ito, H., Wate, R., Zhang, J., Ohnishi, S., Kaneko, S., Ito, H., Nakano, S., & Kusaka, H. (2008). Treatment with edaravone, initiated at symptom onset, slows motor decline and decreases SOD1 deposition in ALS mice. Experimental Neurology, 213(2), 448–455. https://doi.org/10.1016/j.expneurol.2008.07.017

Ivanisevic, T., & Sewduth, R. N. (2023). Multi-Omics Integration for the Design of Novel Therapies and the Identification of Novel Biomarkers. Proteomes, 11(4), 34. https://doi.org/10.3390/proteomes11040034

J Lukiw, W. (2021). Neurofilament Light (NF-L) Chain Protein from a Highly Polymerized Structural Component of the Neuronal Cytoskeleton to a Neurodegenerative Disease Biomarker in the Periphery. Journal of Alzheimer's & Neurodegenerative Diseases, 7(2), 1–9. https://doi.org/10.24966/AND-9608/100056

Jagadisan, B., & Dhawan, A. (2023). Hepatotoxicity in Adeno-Associated Viral Vector Gene Therapy. Current Hepatology Reports, 22(4), 276–290. https://doi.org/10.1007/s11901-023-00624-5

Jaiswal, M. K., Zech, W.-D., Goos, M., Leutbecher, C., Ferri, A., Zippelius, A., Carrì, M. T., Nau, R., & Keller, B. U. (2009). Impairment of mitochondrial calcium handling in a mtSOD1 cell culture model of motoneuron disease. BMC Neuroscience, 10(1), 64. https://doi.org/10.1186/1471-2202-10-64

Jamet, M., Dupuis, L., & Gonzalez De Aguilar, J.-L. (2024). Oligodendrocytes in amyotrophic lateral sclerosis and frontotemporal dementia: The new players on stage. Frontiers in Molecular Neuroscience, 17, 1375330. https://doi.org/10.3389/fnmol.2024.1375330

Jami, M.-S., Salehi-Najafabadi, Z., Ahmadinejad, F., Hoedt, E., Chaleshtori, M. H., Ghatrehsamani, M., Neubert, T. A., Larsen, J. P., & Møller, S. G. (2015). Edaravone leads to proteome changes indicative of neuronal cell protection in response to oxidative stress. Neurochemistry International, 90, 134–141. https://doi.org/10.1016/j.neuint.2015.07.024

Jiang, L.-L., Guan, W.-L., Wang, J.-Y., Zhang, S.-X., & Hu, H.-Y. (2022). RNA-assisted sequestration of RNA-binding proteins by cytoplasmic inclusions of the C-terminal 35-kDa fragment of TDP-43. Journal of Cell Science, 135(6), jcs259380. https://doi.org/10.1242/jcs.259380

Jiang, Y., Yamamoto, M., Kobayashi, Y., Yoshihara, T., Liang, Y., Terao, S., Takeuchi, H., Ishigaki, S., Katsuno, M., Adachi, H., Niwa, J., Tanaka, F., Doyu, M., Yoshida, M., Hashizume, Y., & Sobue, G. (2005). Gene expression profile of spinal motor neurons in sporadic amyotrophic lateral sclerosis. Annals of Neurology, 57(2), 236–251. https://doi.org/10.1002/ana.20379

Jin, X., Zhou, M., Chen, S., Li, D., Cao, X., & Liu, B. (2022). Effects of pH alterations on stress- and aging-induced protein phase separation. Cellular and Molecular Life Sciences, 79(7), 380. https://doi.org/10.1007/s00018-022-04393-0

Joukar, S., Bozorgchami, N., Hatamabadi, D., Yazdani, A., Mohit, E., Javani, E., Kordi, M., Khoshbakht, S., & Shahhosseini, S. (2022). In-house Optimization Radiolabeling of Recombinant scFv with 99mTc-

Tricarbonyl and Stability Studies: Radiolabeling scFv with technetium tricarbonyl. Trends in Peptide and Protein Sciences, 7(Vol. 7 (2022): Continuous Volume (in progress)), 1-6 (e10). https://doi.org/10.22037/tpps.v7i.39823

Jové, M., Mota-Martorell, N., Torres, P., Portero-Otin, M., Ferrer, I., & Pamplona, R. (2021). New insights into human prefrontal cortex aging with a lipidomics approach. Expert Review of Proteomics, 18(5), 333–344. https://doi.org/10.1080/14789450.2021.1940142

Ju, Y., Lee, W. S., Pilkington, E. H., Kelly, H. G., Li, S., Selva, K. J., Wragg, K. M., Subbarao, K., Nguyen, T. H. O., Rowntree, L. C., Allen, L. F., Bond, K., Williamson, D. A., Truong, N. P., Plebanski, M., Kedzierska, K., Mahanty, S., Chung, A. W., Caruso, F., … Kent, S. J. (2022). Anti-PEG Antibodies Boosted in Humans by SARS-CoV-2 Lipid Nanoparticle mRNA Vaccine. ACS Nano, 16(8), 11769–11780. https://doi.org/10.1021/acsnano.2c04543

Julian, T. H., Glascow, N., Barry, A. D. F., Moll, T., Harvey, C., Klimentidis, Y. C., Newell, M., Zhang, S., Snyder, M. P., Cooper-Knock, J., & Shaw, P. J. (2021). Physical exercise is a risk factor for amyotrophic lateral sclerosis: Convergent evidence from Mendelian randomisation, transcriptomics and risk genotypes. EBioMedicine, 68, 103397. https://doi.org/10.1016/j.ebiom.2021.103397

Jung, M.-K., Kim, K. Y., Lee, N.-Y., Kang, Y.-S., Hwang, Y. J., Kim, Y., Sung, J.-J., McKee, A., Kowall, N., Lee, J., & Ryu, H. (2013). Expression of Taurine Transporter (TauT) is Modulated by Heat Shock Factor 1 (HSF1) in Motor Neurons of ALS. Molecular Neurobiology, 47(2), 699–710. https://doi.org/10.1007/s12035-012-8371-9

Kabashi, E., Lin, L., Tradewell, M. L., Dion, P. A., Bercier, V., Bourgouin, P., Rochefort, D., Bel Hadj, S., Durham, H. D., Velde, C. V., Rouleau, G. A., & Drapeau, P. (2010). Gain and loss of function of ALS-related mutations of TARDBP (TDP-43) cause motor deficits in vivo. Human Molecular Genetics, 19(4), 671–683. https://doi.org/10.1093/hmg/ddp534

Kabuta, C., Kono, K., Wada, K., & Kabuta, T. (2015). 4-Hydroxynonenal induces persistent insolubilization of TDP-43 and alters its intracellular localization. Biochemical and Biophysical Research Communications, 463(1–2), 82–87. https://doi.org/10.1016/j.bbrc.2015.05.027

Kaiser, M., Maletzki, I., Hülsmann, S., Holtmann, B., Schulz-Schaeffer, W., Kirchhoff, F., Bähr, M., & Neusch, C. (2006). Progressive loss of a glial potassium channel (KCNJ10) in the spinal cord of the SOD1 (G93A) transgenic mouse model of amyotrophic lateral sclerosis. Journal of Neurochemistry, 99(3), 900–912. https://doi.org/10.1111/j.1471-4159.2006.04131.x

Kanai, K., Kuwabara, S., Misawa, S., Tamura, N., Ogawara, K., Nakata, M., Sawai, S., Hattori, T., & Bostock, H. (2006). Altered axonal excitability properties in amyotrophic lateral sclerosis: Impaired potassium channel function related to disease stage. Brain, 129(4), 953–962. https://doi.org/10.1093/brain/awl024

Kang, L., Jin, S., Wang, J., Lv, Z., Xin, C., Tan, C., Zhao, M., Wang, L., & Liu, J. (2023). AAV vectors applied to the treatment of CNS disorders: Clinical status and challenges. Journal of Controlled Release, 355, 458–473. https://doi.org/10.1016/j.jconrel.2023.01.067

Kang, S. H., Fukaya, M., Yang, J. K., Rothstein, J. D., & Bergles, D. E. (2010). NG2+ CNS Glial Progenitors Remain Committed to the Oligodendrocyte Lineage in Postnatal Life and following Neurodegeneration. Neuron, 68(4), 668–681. https://doi.org/10.1016/j.neuron.2010.09.009

Kang, S. H., Li, Y., Fukaya, M., Lorenzini, I., Cleveland, D. W., Ostrow, L. W., Rothstein, J. D., & Bergles, D. E. (2013). Degeneration and impaired regeneration of gray matter oligodendrocytes in amyotrophic lateral sclerosis. Nature Neuroscience, 16(5), 571–579. https://doi.org/10.1038/nn.3357

Kannan A. Nith, M., Kerry R. (1998). Corticomotor threshold is reduced in early sporadic amyotrophic lateral sclerosis." Muscle & Nerve. 20(9), 1137–1141.

Kasarskis, E. J., & Winslow, M. (1989). When did Lou Gehrig's personal illness begin? Neurology, 39(9), 1243–1243. https://doi.org/10.1212/WNL.39.9.1243

Kawahara, Y., Ito, K., Sun, H., Aizawa, H., Kanazawa, I., & Kwak, S. (2004). RNA editing and death of motor neurons. Nature, 427(6977), 801–801. https://doi.org/10.1038/427801a

Kedaigle, A., & Fraenkel, E. (2018). Turning omics data into therapeutic insights. Current Opinion in Pharmacology, 42, 95–101. https://doi.org/10.1016/j.coph.2018.08.006

Keifer, O. P., Gutierrez, J., Butt, M. T., Cramer, S. D., Bartus, R., Tansey, M., Deaver, D., Betourne, A., & Boulis, N. M. (2023). Spinal cord and brain concentrations of riluzole after oral and intrathecal administration: A potential new treatment route for amyotrophic lateral sclerosis. PLOS ONE, 18(8), e0277718. https://doi.org/10.1371/journal.pone.0277718

Kelaini, S., Chan, C., Cornelius, V. A., & Margariti, A. (2021). RNA-Binding Proteins Hold Key Roles in Function, Dysfunction, and Disease. Biology, 10(5), 366. https://doi.org/10.3390/biology10050366

Keller, M. F., Ferrucci, L., Singleton, A. B., Tienari, P. J., Laaksovirta, H., Restagno, G., Chiò, A., Traynor, B. J., & Nalls, M. A. (2014). Genome-Wide Analysis of the Heritability of Amyotrophic Lateral Sclerosis. JAMA Neurology, 71(9), 1123. https://doi.org/10.1001/jamaneurol.2014.1184

Kelley, K. W., Ben Haim, L., Schirmer, L., Tyzack, G. E., Tolman, M., Miller, J. G., Tsai, H.-H., Chang, S. M., Molofsky, A. V., Yang, Y., Patani, R., Lakatos, A., Ullian, E. M., & Rowitch, D. H. (2018). Kir4.1-Dependent Astrocyte-Fast Motor Neuron Interactions Are Required for Peak Strength. Neuron, 98(2), 306-319.e7. https://doi.org/10.1016/j.neuron.2018.03.010

Khademullah, C. S., Aqrabawi, A. J., Place, K. M., Dargaei, Z., Liang, X., Pressey, J. C., Bedard, S., Yang, J. W., Garand, D., Keramidis, I., Gasecka, A., Côté, D., De Koninck, Y., Keith, J., Zinman, L., Robertson, J., Kim, J. C., & Woodin, M. A. (2020). Cortical interneuron-mediated inhibition delays the onset of amyotrophic lateral sclerosis. Brain, 143(3), 800–810. https://doi.org/10.1093/brain/awaa034

Khalfallah, Y., Kuta, R., Grasmuck, C., Prat, A., Durham, H. D., & Vande Velde, C. (2018). TDP-43 regulation of stress granule dynamics in neurodegenerative disease-relevant cell types. Scientific Reports, 8(1), 7551. https://doi.org/10.1038/s41598-018-25767-0

Kim, E. G., Jeong, J., Lee, J., Jung, H., Kim, M., Zhao, Y., Yi, E. C., & Kim, K. M. (2020). Rapid Evaluation of Antibody Fragment Endocytosis for Antibody Fragment–Drug Conjugates. Biomolecules, 10(6), 955. https://doi.org/10.3390/biom10060955

Kim, H. J., Kim, N. C., Wang, Y.-D., Scarborough, E. A., Moore, J., Diaz, Z., MacLea, K. S., Freibaum, B., Li, S., Molliex, A., Kanagaraj, A. P., Carter, R., Boylan, K. B., Wojtas, A. M., Rademakers, R., Pinkus, J. L., Greenberg, S. A., Trojanowski, J. Q., Traynor, B. J., … Taylor, J. P. (2013). Mutations in prion-like domains in hnRNPA2B1 and hnRNPA1 cause multisystem proteinopathy and ALS. Nature, 495(7442), 467–473. https://doi.org/10.1038/nature11922

Kim, J.-A., Park, C., Sung, J.-J., Seo, D.-J., Choi, S.-J., & Hong, Y.-H. (2023). Small RNA sequencing of circulating small extracellular vesicles microRNAs in patients with amyotrophic lateral sclerosis. Scientific Reports, 13(1), 5528. https://doi.org/10.1038/s41598-023-32717-y

Kinoshita, Y., Ito, H., Hirano, A., Fujita, K., Wate, R., Nakamura, M., Kaneko, S., Nakano, S., & Kusaka, H. (2009). Nuclear Contour Irregularity and Abnormal Transporter Protein Distribution in Anterior Horn Cells in Amyotrophic Lateral Sclerosis: Journal of Neuropathology and Experimental Neurology, 68(11), 1184–1192. https://doi.org/10.1097/NEN.0b013e3181bc3bec

Klim, J. R., Williams, L. A., Limone, F., Guerra San Juan, I., Davis-Dusenbery, B. N., Mordes, D. A., Burberry, A., Steinbaugh, M. J., Gamage, K. K., Kirchner, R., Moccia, R., Cassel, S. H., Chen, K., Wainger, B. J., Woolf, C. J., & Eggan, K. (2019). ALS-implicated protein TDP-43 sustains levels of STMN2, a mediator of motor neuron growth and repair. Nature Neuroscience, 22(2), 167–179. https://doi.org/10.1038/s41593-018-0300-4

Koike, Y., Pickles, S., Estades Ayuso, V., Jansen-West, K., Qi, Y. A., Li, Z., Daughrity, L. M., Yue, M., Zhang, Y.-J., Cook, C. N., Dickson, D. W., Ward, M., Petrucelli, L., & Prudencio, M. (2023). TDP-43 and other hnRNPs regulate cryptic exon inclusion of a key ALS/FTD risk gene, UNC13A. PLOS Biology, 21(3), e3002028. https://doi.org/10.1371/journal.pbio.3002028

Kollewe, K., Mauss, U., Krampfl, K., Petri, S., Dengler, R., & Mohammadi, B. (2008). ALSFRS-R score and its ratio: A useful predictor for ALS-progression. Journal of the Neurological Sciences, 275(1–2), 69–73. https://doi.org/10.1016/j.jns.2008.07.016

Kontermann, R. E. (2009). Strategies to Extend Plasma Half-Lives of Recombinant Antibodies: BioDrugs, 23(2), 93–109. https://doi.org/10.2165/00063030-200923020-00003

Koppers, M., Van Blitterswijk, M. M., Vlam, L., Rowicka, P. A., Van Vught, P. W. J., Groen, E. J. N., Spliet, W. G. M., Engelen-Lee, J., Schelhaas, H. J., De Visser, M., Van Der Kooi, A. J., Van Der Pol, W.-L., Pasterkamp, R. J., Veldink, J. H., & Van Den Berg, L. H. (2012). VCP mutations in familial and sporadic amyotrophic lateral sclerosis. Neurobiology of Aging, 33(4), 837.e7-837.e13. https://doi.org/10.1016/j.neurobiolaging.2011.10.006

Korner, S., Kammeyer, J., Zapf, A., Kuzma-Kozakiewicz, M., Piotrkiewicz, M., Kuraszkiewicz, B., Goszczynska, H., Gromicho, M., Grosskreutz, J., Andersen, P. M., Carvalho, M. D., & Petri, S. (2019). Influence of Environment and Lifestyle on Incidence and Progress of Amyotrophic Lateral Sclerosis in A German ALS Population. Aging and Disease, 10(2), 205. https://doi.org/10.14336/AD.2018.0327

Kraft, A. D., Johnson, D. A., & Johnson, J. A. (2004). Nuclear Factor E2-Related Factor 2-Dependent Antioxidant Response Element Activation by tert -Butylhydroquinone and Sulforaphane Occurring Preferentially in Astrocytes Conditions Neurons against Oxidative Insult. The Journal of Neuroscience, 24(5), 1101–1112. https://doi.org/10.1523/JNEUROSCI.3817-03.2004

Krasnianski, A., Deschauer, M., Neudecker, S., Gellerich, F. N., Müller, T., Schoser, B. G., Krasnianski, M., & Zierz, S. (2005). Mitochondrial changes in skeletal muscle in amyotrophic lateral sclerosis and other neurogenic atrophies. Brain, 128(8), 1870–1876. https://doi.org/10.1093/brain/awh540

Kristinsson, H. G., & Hultin, H. O. (2003). Effect of Low and High pH Treatment on the Functional Properties of Cod Muscle Proteins. Journal of Agricultural and Food Chemistry, 51(17), 5103–5110. https://doi.org/10.1021/jf026138d

Krus, K. L., Strickland, A., Yamada, Y., Devault, L., Schmidt, R. E., Bloom, A. J., Milbrandt, J., & DiAntonio, A. (2022). Loss of Stathmin-2, a hallmark of TDP-43-associated ALS, causes motor neuropathy. Cell Reports, 39(13), 111001. https://doi.org/10.1016/j.celrep.2022.111001

Kubes, P., & Jenne, C. (2018). Immune Responses in the Liver. Annual Review of Immunology, 36(1), 247–277. https://doi.org/10.1146/annurev-immunol-051116-052415

Kuo, J. J., Siddique, T., Fu, R., & Heckman, C. J. (2005). Increased persistent Na + current and its effect on excitability in motoneurones cultured from mutant SOD1 mice. The Journal of Physiology, 563(3), 843–854. https://doi.org/10.1113/jphysiol.2004.074138

Kwon, S.-K., Sando, R., Lewis, T. L., Hirabayashi, Y., Maximov, A., & Polleux, F. (2016). LKB1 Regulates Mitochondria-Dependent Presynaptic Calcium Clearance and Neurotransmitter Release Properties at Excitatory Synapses along Cortical Axons. PLOS Biology, 14(7), e1002516. https://doi.org/10.1371/journal.pbio.1002516

Lacal, I., & Ventura, R. (2018). Epigenetic Inheritance: Concepts, Mechanisms and Perspectives. Frontiers in Molecular Neuroscience, 11, 292. https://doi.org/10.3389/fnmol.2018.00292

Lacomblez, L., Bensimon, G., Meininger, V., Leigh, P. N., Guillet, P., & Guillet, P. (1996). Dose-ranging study of riluzole in amyotrophic lateral sclerosis. The Lancet, 347(9013), 1425–1431. https://doi.org/10.1016/S0140-6736(96)91680-3

Laferriere, F., & Polymenidou, M. (2015). Advances and challenges in understanding the multifaceted pathogenesis of amyotrophic lateral sclerosis. Swiss Medical Weekly. https://doi.org/10.4414/smw.2015.14054

Laffita-Mesa, J. M., Rodríguez Pupo, J. M., Moreno Sera, R., Vázquez Mojena, Y., Kourí, V., Laguna-Salvia, L., Martínez-Godales, M., Valdevila Figueira, J. A., Bauer, P. O., Rodríguez-Labrada, R., Zaldívar, Y. G., Paucar, M., Svenningsson, P., & Pérez, L. V. (2013). De Novo Mutations in Ataxin-2 Gene and ALS Risk. PLoS ONE, 8(8), e70560. https://doi.org/10.1371/journal.pone.0070560

Lagier-Tourenne, C., Polymenidou, M., Hutt, K. R., Vu, A. Q., Baughn, M., Huelga, S. C., Clutario, K. M., Ling, S.-C., Liang, T. Y., Mazur, C., Wancewicz, E., Kim, A. S., Watt, A., Freier, S., Hicks, G. G., Donohue, J. P., Shiue, L., Bennett, C. F., Ravits, J., … Yeo, G. W. (2012). Divergent roles of ALS-linked proteins FUS/TLS and TDP-43 intersect in processing long pre-mRNAs. Nature Neuroscience, 15(11), 1488–1497. https://doi.org/10.1038/nn.3230

Lamanauskas, N., & Nistri, A. (2008). Riluzole blocks persistent Na + and Ca 2+ currents and modulates release of glutamate via presynaptic NMDA receptors on neonatal rat hypoglossal motoneurons in vitro. European Journal of Neuroscience, 27(10), 2501–2514. https://doi.org/10.1111/j.1460-9568.2008.06211.x

Lambert-Smith, I. A., Saunders, D. N., & Yerbury, J. J. (2022). Proteostasis impairment and ALS. Progress in Biophysics and Molecular Biology, 174, 3–27. https://doi.org/10.1016/j.pbiomolbio.2022.06.001

Lanznaster, D., Bourgeais, J., Bruno, C., Hergesheimer, R. C., Thepault, R.-A., Vourc'h, P., Corcia, P., Andres, C. R., Herault, O., & Blasco, H. (2019). TDP-43-Mediated Toxicity in HEK293T Cells: A Fast and Reproducible Protocol To Be Employed in the Search of New Therapeutic Options against Amyotrophic Lateral Sclerosis. Cells, 9(1), 68. https://doi.org/10.3390/cells9010068

Lanznaster, D., Veyrat-Durebex, C., Vourc'h, P., Andres, C. R., Blasco, H., & Corcia, P. (2020). Metabolomics: A Tool to Understand the Impact of Genetic Mutations in Amyotrophic Lateral Sclerosis. Genes, 11(5), 537. https://doi.org/10.3390/genes11050537

LaRocca, T. J., Mariani, A., Watkins, L. R., & Link, C. D. (2019). TDP-43 knockdown causes innate immune activation via protein kinase R in astrocytes. Neurobiology of Disease, 132, 104514. https://doi.org/10.1016/j.nbd.2019.104514

Larson, V. A., Mironova, Y., Vanderpool, K. G., Waisman, A., Rash, J. E., Agarwal, A., & Bergles, D. E. (2018). Oligodendrocytes control potassium accumulation in white matter and seizure susceptibility. eLife, 7, e34829. https://doi.org/10.7554/eLife.34829

Lawton, K. A., Brown, M. V., Alexander, D., Li, Z., Wulff, J. E., Lawson, R., Jaffa, M., Milburn, M. V., Ryals, J. A., Bowser, R., Cudkowicz, M. E., Berry, J. D., & On behalf of the Northeast ALS Consortium. (2014). Plasma metabolomic biomarker panel to distinguish patients with amyotrophic lateral sclerosis from disease mimics. Amyotrophic Lateral Sclerosis and Frontotemporal Degeneration, 15(5–6), 362–370. https://doi.org/10.3109/21678421.2014.908311

Le Blanc, G., Jetté Pomerleau, V., McCarthy, J., Borroni, B., Van Swieten, J., Galimberti, D., Sanchez-Valle, R., LaForce, R., Moreno, F., Synofzik, M., Graff, C., Masellis, M., Tartaglia, M. C., Rowe, J. B., Vandenberghe, R., Finger, E., Tagliavini, F., De Mendonça, A., Santana, I., … the Genetic Frontotemporal Dementia Initiative (GENFI). (2020). Faster Cortical Thinning and Surface Area Loss in Presymptomatic and Symptomatic C9orf72 Repeat Expansion Adult Carriers. Annals of Neurology, 88(1), 113–122. https://doi.org/10.1002/ana.25748

Le Gall, L., Duddy, W. J., Martinat, C., Mariot, V., Connolly, O., Milla, V., Anakor, E., Ouandaogo, Z. G., Millecamps, S., Lainé, J., Vijayakumar, U. G., Knoblach, S., Raoul, C., Lucas, O., Loeffler, J. P., Bede, P., Behin, A., Blasco, H., Bruneteau, G., … Pradat, P. F. (2022). Muscle cells of sporadic amyotrophic lateral sclerosis patients secrete neurotoxic vesicles. Journal of Cachexia, Sarcopenia and Muscle, 13(2), 1385–1402. https://doi.org/10.1002/jcsm.12945

Lee, B. J., Egi, Y., Van Leyen, K., Lo, E. H., & Arai, K. (2010). Edaravone, a free radical scavenger, protects components of the neurovascular unit against oxidative stress in vitro. Brain Research, 1307, 22–27. https://doi.org/10.1016/j.brainres.2009.10.026

Lee, H., Lee, J. J., Park, N. Y., Dubey, S. K., Kim, T., Ruan, K., Lim, S. B., Park, S.-H., Ha, S., Kovlyagina, I., Kim, K., Kim, S., Oh, Y., Kim, H., Kang, S.-U., Song, M.-R., Lloyd, T. E., Maragakis, N. J., Hong, Y. B., … Lee, G. (2021). Multi-omic analysis of selectively vulnerable motor neuron subtypes implicates altered lipid metabolism in ALS. Nature Neuroscience, 24(12), 1673–1685. https://doi.org/10.1038/s41593-021-00944-z

Lee, J. H., Chapman, D. V., & Saltzman, W. M. (2023). Nanoparticle Targeting with Antibodies in the Central Nervous System. BME Frontiers, 4, 0012. https://doi.org/10.34133/bmef.0012

Lee, J., Nguyen, P. T., Shim, H. S., Hyeon, S. J., Im, H., Choi, M.-H., Chung, S., Kowall, N. W., Lee, S. B., & Ryu, H. (2019). EWSR1, a multifunctional protein, regulates cellular function and aging via genetic and epigenetic pathways. Biochimica et Biophysica Acta (BBA) - Molecular Basis of Disease, 1865(7), 1938–1945. https://doi.org/10.1016/j.bbadis.2018.10.042

Lee, J.-M., Calkins, M. J., Chan, K., Kan, Y. W., & Johnson, J. A. (2003). Identification of the NF-E2-related Factor-2-dependent Genes Conferring Protection against Oxidative Stress in Primary Cortical Astrocytes Using

Oligonucleotide Microarray Analysis. Journal of Biological Chemistry, 278(14), 12029–12038. https://doi.org/10.1074/jbc.M211558200

Lee, S. E., Sias, A. C., Mandelli, M. L., Brown, J. A., Brown, A. B., Khazenzon, A. M., Vidovszky, A. A., Zanto, T. P., Karydas, A. M., Pribadi, M., Dokuru, D., Coppola, G., Geschwind, D. H., Rademakers, R., Gorno-Tempini, M. L., Rosen, H. J., Miller, B. L., & Seeley, W. W. (2017). Network degeneration and dysfunction in presymptomatic C9ORF72 expansion carriers. NeuroImage: Clinical, 14, 286–297. https://doi.org/10.1016/j.nicl.2016.12.006

Lee, S., Kim, S., Kang, H.-Y., Lim, H. R., Kwon, Y., Jo, M., Jeon, Y.-M., Kim, S. R., Kim, K., Ha, C. M., Lee, S., & Kim, H.-J. (2020). The overexpression of TDP-43 in astrocytes causes neurodegeneration via a PTP1B-mediated inflammatory response. Journal of Neuroinflammation, 17(1), 299. https://doi.org/10.1186/s12974-020-01963-6

Lee, Y. J., & Rio, D. C. (2024). A mutation in the low-complexity domain of splicing factor hnRNPA1 linked to amyotrophic lateral sclerosis disrupts distinct neuronal RNA splicing networks. Genes & Development, 38(1–2), 11–30. https://doi.org/10.1101/gad.351104.123

Lee, Y., Morrison, B. M., Li, Y., Lengacher, S., Farah, M. H., Hoffman, P. N., Liu, Y., Tsingalia, A., Jin, L., Zhang, P.-W., Pellerin, L., Magistretti, P. J., & Rothstein, J. D. (2012). Oligodendroglia metabolically support axons and contribute to neurodegeneration. Nature, 487(7408), 443–448. https://doi.org/10.1038/nature11314

Lehman, E. J., Hein, M. J., Baron, S. L., & Gersic, C. M. (2012). Neurodegenerative causes of death among retired National Football League players. Neurology, 79(19), 1970–1974. https://doi.org/10.1212/WNL.0b013e31826daf50

Leinenga, G., Bodea, L.-G., Koh, W. K., Nisbet, R. M., & Götz, J. (2020). Delivery of Antibodies into the Brain Using Focused Scanning Ultrasound. Journal of Visualized Experiments, 161. https://doi.org/10.3791/61372

Lemon, R. N. (2008). Descending Pathways in Motor Control. Annual Review of Neuroscience, 31(1), 195–218. https://doi.org/10.1146/annurev.neuro.31.060407.125547

Lesniak, W. G., Chu, C., Jablonska, A., Du, Y., Pomper, M. G., Walczak, P., & Janowski, M. (2019). A Distinct Advantage to Intraarterial Delivery of 89 Zr-Bevacizumab in PET Imaging of Mice With and Without Osmotic Opening of the Blood–Brain Barrier. Journal of Nuclear Medicine, 60(5), 617–622. https://doi.org/10.2967/jnumed.118.218792

Lewinski, F. V., & Keller, B. U. (2005). Ca2+, mitochondria and selective motoneuron vulnerability: Implications for ALS. Trends in Neurosciences, 28(9), 494–500. https://doi.org/10.1016/j.tins.2005.07.001

Li, D., Ding, L., Chen, Y., Wang, Z., Zeng, Z., Ma, X., Huang, H., Li, H., Qian, X., Yang, Z., & Zhu, H. (2024). Exploration of radionuclide labeling of a novel scFv-Fc fusion protein targeting CLDN18.2 for tumor diagnosis and treatment. European Journal of Medicinal Chemistry, 266, 116134. https://doi.org/10.1016/j.ejmech.2024.116134

Li, J., Cui, L., Sun, X., Shen, D., Yang, X., Liu, Q., & Liu, M. (2022). Alterations in metabolic biomarkers and their potential role in amyotrophic lateral sclerosis. Annals of Clinical and Translational Neurology, 9(7), 1027–1038. https://doi.org/10.1002/acn3.51580

Li, J., Zhou, Y., Su, Z., Li, X., Zhang, L., & Li, S. (2024). A Cell-Penetrating Peptide Improves Anti-HER2 Single-Chain Variable Fragment Internalization and Antitumor Activity against HER2-Positive Breast Cancer In Vitro and In Vivo. Molecules, 29(6), 1247. https://doi.org/10.3390/molecules29061247

Li, J.-Y., Cai, Z.-Y., Sun, X.-H., Shen, D., Yang, X.-Z., Liu, M.-S., & Cui, L.-Y. (2022). Blood–brain barrier dysfunction and myelin basic protein in survival of amyotrophic lateral sclerosis with or without frontotemporal dementia. Neurological Sciences, 43(5), 3201–3210. https://doi.org/10.1007/s10072-021-05731-z

Li, S., Yi, Y., Cui, K., Zhang, Y., Chen, Y., Han, D., Sun, L., Zhang, X., Chen, F., Zhang, Y., & Yang, Y. (2021). A Single-Chain Variable Fragment Antibody Inhibits Aggregation of Phosphorylated Tau and Ameliorates Tau Toxicity in vitro and in vivo. Journal of Alzheimer's Disease, 79(4), 1613–1629. https://doi.org/10.3233/JAD-191266

Li, Y., Chen, Z., Lu, Z., Yang, Q., Liu, L., Jiang, Z., Zhang, L., Zhang, X., & Qing, H. (2018). "Cell-addictive" dual-target traceable nanodrug for Parkinson's disease treatment via flotillins pathway. Theranostics, 8(19), 5469–5481. https://doi.org/10.7150/thno.28295

Li, Z., & Shah, D. K. (2019). Two-pore physiologically based pharmacokinetic model with de novo derived parameters for predicting plasma PK of different size protein therapeutics. Journal of Pharmacokinetics and Pharmacodynamics, 46(3), 305–318. https://doi.org/10.1007/s10928-019-09639-2

Liao, B., Zhao, W., Beers, D. R., Henkel, J. S., & Appel, S. H. (2012). Transformation from a neuroprotective to a neurotoxic microglial phenotype in a mouse model of ALS. Experimental Neurology, 237(1), 147–152. https://doi.org/10.1016/j.expneurol.2012.06.011

Liao, Q., Owen, M. C., Bali, S., Barz, B., & Strodel, B. (2018). Aβ under stress: The effects of acidosis, Cu 2+ -binding, and oxidation on amyloid β-peptide dimers. Chemical Communications, 54(56), 7766–7769. https://doi.org/10.1039/C8CC02263A

Liboux, A. L., Lefebvre, P., Roux, Y. L., Truffinet, P., Aubeneau, M., Kirkesseli, S., & Montay, G. (1997). Single- and Multiple-Dose Pharmacokinetics of Riluzole in White Subjects. The Journal of Clinical Pharmacology, 37(9), 820–827. https://doi.org/10.1002/j.1552-4604.1997.tb05630.x

Liddelow, S. A., Guttenplan, K. A., Clarke, L. E., Bennett, F. C., Bohlen, C. J., Schirmer, L., Bennett, M. L., Münch, A. E., Chung, W.-S., Peterson, T. C., Wilton, D. K., Frouin, A., Napier, B. A., Panicker, N., Kumar, M., Buckwalter, M. S., Rowitch, D. H., Dawson, V. L., Dawson, T. M., … Barres, B. A. (2017). Neurotoxic reactive astrocytes are induced by activated microglia. Nature, 541(7638), 481–487. https://doi.org/10.1038/nature21029

Lim, M. A., Selak, M. A., Xiang, Z., Krainc, D., Neve, R. L., Kraemer, B. C., Watts, J. L., & Kalb, R. G. (2012). Reduced Activity of AMP-Activated Protein Kinase Protects against Genetic Models of Motor Neuron Disease. The Journal of Neuroscience, 32(3), 1123–1141. https://doi.org/10.1523/JNEUROSCI.6554-10.2012

Lin, C.-L. G., Bristol, L. A., Jin, L., Dykes-Hoberg, M., Crawford, T., Clawson, L., & Rothstein, J. D. (1998). Aberrant RNA Processing in a Neurodegenerative Disease: The Cause for Absent EAAT2, a Glutamate Transporter, in Amyotrophic Lateral Sclerosis. Neuron, 20(3), 589–602. https://doi.org/10.1016/S0896-6273(00)80997-6

Liu, D., Zhu, M., Zhang, Y., & Diao, Y. (2021). Crossing the blood-brain barrier with AAV vectors. Metabolic Brain Disease, 36(1), 45–52. https://doi.org/10.1007/s11011-020-00630-2

Liu, F., Morderer, D., Wren, M. C., Vettleson-Trutza, S. A., Wang, Y., Rabichow, B. E., Salemi, M. R., Phinney, B. S., Oskarsson, B., Dickson, D. W., & Rossoll, W. (2022). Proximity proteomics of C9orf72 dipeptide repeat proteins identifies molecular chaperones as modifiers of poly-GA aggregation. Acta Neuropathologica Communications, 10(1), 22. https://doi.org/10.1186/s40478-022-01322-x

Liu, J., Jiang, Y., Zhang, G., Lin, Z., & Du, S. (2019). Protective effect of edaravone on blood-brain barrier by affecting NRF-2/HO-1 signaling pathway. Experimental and Therapeutic Medicine. https://doi.org/10.3892/etm.2019.7859

Liu, L., Song, Y., Zhao, M., Yi, Z., & Zeng, Q. (2015). Protective effects of edaravone, a free radical scavenger, on lipopolysaccharide-induced acute kidney injury in a rat model of sepsis. International Urology and Nephrology, 47(10), 1745–1752. https://doi.org/10.1007/s11255-015-1070-5

Liu, W., Yamashita, T., Tian, F., Morimoto, N., Ikeda, Y., Deguchi, K., & Abe, K. (2013). Mitochondrial Fusion and Fission Proteins Expression Dynamically Change in a Murine Model of Amyotrophic Lateral Sclerosis. Current Neurovascular Research, 10(3), 222–230. https://doi.org/10.2174/15672026113109990060

Liu, X., Lu, D., Bowser, R., & Liu, J. (2016). Expression of Carbonic Anhydrase I in Motor Neurons and Alterations in ALS. International Journal of Molecular Sciences, 17(11), 1820. https://doi.org/10.3390/ijms17111820

Liu, X., Lu, S., Liu, D., Zhang, L., Zhang, L., Yu, X., & Liu, R. (2019). ScFv-conjugated superparamagnetic iron oxide nanoparticles for MRI-based diagnosis in transgenic mouse models of Parkinson's and Huntington's diseases. Brain Research, 1707, 141–153. https://doi.org/10.1016/j.brainres.2018.11.034

Liu, X.-G., Zhang, L., Lu, S., Liu, D.-Q., Zhang, L.-X., Yu, X.-L., & Liu, R.-T. (2020). Multifunctional Superparamagnetic Iron Oxide Nanoparticles Conjugated with Aβ Oligomer-Specific scFv Antibody and Class A Scavenger Receptor Activator Show Early Diagnostic Potentials for Alzheimer's Disease. International Journal of Nanomedicine, Volume 15, 4919–4932. https://doi.org/10.2147/IJN.S240953

Liu, Y., Duan, W., Guo, Y., Li, Z., Han, H., Zhang, S., Yuan, P., & Li, C. (2014). A new cellular model of pathological TDP-43: The neurotoxicity of stably expressed CTF25 of TDP-43 depends on the proteasome. Neuroscience, 281, 88–98. https://doi.org/10.1016/j.neuroscience.2014.09.043

Liu, Y.-J., Ju, T.-C., Chen, H.-M., Jang, Y.-S., Lee, L.-M., Lai, H.-L., Tai, H.-C., Fang, J.-M., Lin, Y.-L., Tu, P.-H., & Chern, Y. (2015). Activation of AMP-activated protein kinase α1 mediates mislocalization of TDP-43 in amyotrophic lateral sclerosis. Human Molecular Genetics, 24(3), 787–801. https://doi.org/10.1093/hmg/ddu497

Liu, Z., Yang, C., Meng, X., Li, Z., Lv, C., & Cao, P. (2018). Neuroprotection of edaravone on the hippocampus of kainate-induced epilepsy rats through Nrf2/HO-1 pathway. Neurochemistry International, 112, 159–165. https://doi.org/10.1016/j.neuint.2017.07.001

Liu-Yesucevitz, L., Bilgutay, A., Zhang, Y.-J., Vanderwyde, T., Citro, A., Mehta, T., Zaarur, N., McKee, A., Bowser, R., Sherman, M., Petrucelli, L., & Wolozin, B. (2010). Tar DNA Binding Protein-43 (TDP-43) Associates with Stress Granules: Analysis of Cultured Cells and Pathological Brain Tissue. PLoS ONE, 5(10), e13250. https://doi.org/10.1371/journal.pone.0013250

Liu-Yesucevitz, L., Lin, A. Y., Ebata, A., Boon, J. Y., Reid, W., Xu, Y.-F., Kobrin, K., Murphy, G. J., Petrucelli, L., & Wolozin, B. (2014). ALS-Linked Mutations Enlarge TDP-43-Enriched Neuronal RNA Granules in the

Dendritic Arbor. The Journal of Neuroscience, 34(12), 4167–4174. https://doi.org/10.1523/JNEUROSCI.2350-13.2014

Lloyd, C. M., Richardson, M. P., Brooks, D. J., Al-Chalabi, A., & Leigh, P. N. (2000). Extramotor involvement in ALS: PET studies with the GABAA ligand [11C]flumazenil. Brain, 123(11), 2289–2296. https://doi.org/10.1093/brain/123.11.2289

Lo, A. S.-Y., Zhu, Q., & Marasco, W. A. (2008). Intracellular Antibodies (Intrabodies) and Their Therapeutic Potential. In Y. Chernajovsky & A. Nissim (Eds.), Therapeutic Antibodies (Vol. 181, pp. 343–373). Springer Berlin Heidelberg. https://doi.org/10.1007/978-3-540-73259-4_15

Loganathan, S., Wilson, B. A., Carey, S. B., Manzo, E., Joardar, A., Ugur, B., & Zarnescu, D. C. (2022). TDP-43 Proteinopathy Causes Broad Metabolic Alterations including TCA Cycle Intermediates and Dopamine Levels in Drosophila Models of ALS. Metabolites, 12(2), 101. https://doi.org/10.3390/metabo12020101

Logroscino, G., Piccininni, M., Marin, B., Nichols, E., Abd-Allah, F., Abdelalim, A., Alahdab, F., Asgedom, S. W., Awasthi, A., Chaiah, Y., Daryani, A., Do, H. P., Dubey, M., Elbaz, A., Eskandarieh, S., Farhadi, F., Farzadfar, F., Fereshtehnejad, S.-M., Fernandes, E., … Murray, C. J. L. (2018). Global, regional, and national burden of motor neuron diseases 1990–2016: A systematic analysis for the Global Burden of Disease Study 2016. The Lancet Neurology, 17(12), 1083–1097. https://doi.org/10.1016/S1474-4422(18)30404-6

Logroscino, G., Traynor, B. J., Hardiman, O., Chio, A., Mitchell, D., Swingler, R. J., Millul, A., Benn, E., Beghi, E., & for EURALS. (2010). Incidence of amyotrophic lateral sclerosis in Europe. Journal of Neurology, Neurosurgery & Psychiatry, 81(4), 385–390. https://doi.org/10.1136/jnnp.2009.183525

Lomen-Hoerth, C., Anderson, T., & Miller, B. (2002). The overlap of amyotrophic lateral sclerosis and frontotemporal dementia. Neurology, 59(7), 1077–1079. https://doi.org/10.1212/WNL.59.7.1077

Looser, Z. J., Faik, Z., Ravotto, L., Zanker, H. S., Jung, R. B., Werner, H. B., Ruhwedel, T., Möbius, W., Bergles, D. E., Barros, L. F., Nave, K.-A., Weber, B., & Saab, A. S. (2024). Oligodendrocyte–axon metabolic coupling is mediated by extracellular K+ and maintains axonal health. Nature Neuroscience, 27(3), 433–448. https://doi.org/10.1038/s41593-023-01558-3

Lu, S., Hu, J., Arogundade, O. A., Goginashvili, A., Vazquez-Sanchez, S., Diedrich, J. K., Gu, J., Blum, J., Oung, S., Ye, Q., Yu, H., Ravits, J., Liu, C., Yates, J. R., & Cleveland, D. W. (2022). Heat-shock chaperone HSPB1 regulates cytoplasmic TDP-43 phase separation and liquid-to-gel transition. Nature Cell Biology, 24(9), 1378–1393. https://doi.org/10.1038/s41556-022-00988-8

Ludolph, A., Dupuis, L., Kasarskis, E., Steyn, F., Ngo, S., & McDermott, C. (2023). Nutritional and metabolic factors in amyotrophic lateral sclerosis. Nature Reviews Neurology, 19(9), 511–524. https://doi.org/10.1038/s41582-023-00845-8

Luisier, R., Tyzack, G. E., Hall, C. E., Mitchell, J. S., Devine, H., Taha, D. M., Malik, B., Meyer, I., Greensmith, L., Newcombe, J., Ule, J., Luscombe, N. M., & Patani, R. (2018). Intron retention and nuclear loss of SFPQ are molecular hallmarks of ALS. Nature Communications, 9(1), 2010. https://doi.org/10.1038/s41467-018-04373-8

Luo, X., Zhao, W., Li, B., Zhang, X., Zhang, C., Bratasz, A., Deng, B., McComb, D. W., & Dong, Y. (2018). Co-delivery of mRNA and SPIONs through amino-ester nanomaterials. Nano Research, 11(10), 5596–5603. https://doi.org/10.1007/s12274-018-2082-0

Luque-Michel, E., Lemaire, L., & Blanco-Prieto, M. J. (2021). SPION and doxorubicin-loaded polymeric nanocarriers for glioblastoma theranostics. Drug Delivery and Translational Research, 11(2), 515–523. https://doi.org/10.1007/s13346-020-00880-8

M. Bordeau, B., & P. Balthasar, J. (2021). Strategies to enhance monoclonal antibody uptake and distribution in solid tumors. Cancer Biology and Medicine, 18(3), 649–664. https://doi.org/10.20892/j.issn.2095-3941.2020.0704

Mackenzie, I. R., Nicholson, A. M., Sarkar, M., Messing, J., Purice, M. D., Pottier, C., Annu, K., Baker, M., Perkerson, R. B., Kurti, A., Matchett, B. J., Mittag, T., Temirov, J., Hsiung, G.-Y. R., Krieger, C., Murray, M. E., Kato, M., Fryer, J. D., Petrucelli, L., … Rademakers, R. (2017). TIA1 Mutations in Amyotrophic Lateral Sclerosis and Frontotemporal Dementia Promote Phase Separation and Alter Stress Granule Dynamics. Neuron, 95(4), 808-816.e9. https://doi.org/10.1016/j.neuron.2017.07.025

Madji Hounoum, B., Mavel, S., Coque, E., Patin, F., Vourc'h, P., Marouillat, S., Nadal-Desbarats, L., Emond, P., Corcia, P., Andres, C. R., Raoul, C., & Blasco, H. (2017). Wildtype motoneurons, ALS-Linked SOD1 mutation and glutamate profoundly modify astrocyte metabolism and lactate shuttling. Glia, 65(4), 592–605. https://doi.org/10.1002/glia.23114

Magaquian, D., Delgado Ocaña, S., Perez, C., & Banchio, C. (2021). Phosphatidylcholine restores neuronal plasticity of neural stem cells under inflammatory stress. Scientific Reports, 11(1), 22891. https://doi.org/10.1038/s41598-021-02361-5

Magrané, J., Cortez, C., Gan, W.-B., & Manfredi, G. (2014). Abnormal mitochondrial transport and morphology are common pathological denominators in SOD1 and TDP43 ALS mouse models. Human Molecular Genetics, 23(6), 1413–1424. https://doi.org/10.1093/hmg/ddt528

Magrané, J., Sahawneh, M. A., Przedborski, S., Estévez, Á. G., & Manfredi, G. (2012). Mitochondrial Dynamics and Bioenergetic Dysfunction Is Associated with Synaptic Alterations in Mutant SOD1 Motor Neurons. The Journal of Neuroscience, 32(1), 229–242. https://doi.org/10.1523/JNEUROSCI.1233-11.2012

Mahmoudi, M., Quinlan-Pluck, F., Monopoli, M. P., Sheibani, S., Vali, H., Dawson, K. A., & Lynch, I. (2013). Influence of the Physiochemical Properties of Superparamagnetic Iron Oxide Nanoparticles on Amyloid β Protein Fibrillation in Solution. ACS Chemical Neuroscience, 4(3), 475–485. https://doi.org/10.1021/cn300196n

Malyala, S., Zhang, Y., Strubbe, J. O., & Bazil, J. N. (2019). Calcium phosphate precipitation inhibits mitochondrial energy metabolism. PLOS Computational Biology, 15(1), e1006719. https://doi.org/10.1371/journal.pcbi.1006719

Manzo, E., Lorenzini, I., Barrameda, D., O'Conner, A. G., Barrows, J. M., Starr, A., Kovalik, T., Rabichow, B. E., Lehmkuhl, E. M., Shreiner, D. D., Joardar, A., Liévens, J.-C., Bowser, R., Sattler, R., & Zarnescu, D. C. (2019). Glycolysis upregulation is neuroprotective as a compensatory mechanism in ALS. eLife, 8, e45114. https://doi.org/10.7554/eLife.45114

Marijan, D., Tse, R., Elliott, K., Chandhok, S., Luo, M., Lacroix, E., & Audas, T. E. (2019). Stress-specific aggregation of proteins in the amyloid bodies. FEBS Letters, 593(22), 3162–3172. https://doi.org/10.1002/1873-3468.13597

Marin, B., Boumédiene, F., Logroscino, G., Couratier, P., Babron, M.-C., Leutenegger, A. L., Copetti, M., Preux, P.-M., & Beghi, E. (2016). Variation in worldwide incidence of amyotrophic lateral sclerosis: A meta-analysis. International Journal of Epidemiology, dyw061. https://doi.org/10.1093/ije/dyw061

Marin, B., Logroscino, G., Boumédiene, F., Labrunie, A., Couratier, P., Babron, M.-C., Leutenegger, A. L., Preux, P. M., & Beghi, E. (2016). Clinical and demographic factors and outcome of amyotrophic lateral sclerosis in relation to population ancestral origin. European Journal of Epidemiology, 31(3), 229–245. https://doi.org/10.1007/s10654-015-0090-x

Marland, J. R. K., Hasel, P., Bonnycastle, K., & Cousin, M. A. (2016). Mitochondrial Calcium Uptake Modulates Synaptic Vesicle Endocytosis in Central Nerve Terminals. Journal of Biological Chemistry, 291(5), 2080–2086. https://doi.org/10.1074/jbc.M115.686956

Martin, E. W., & Holehouse, A. S. (2020). Intrinsically disordered protein regions and phase separation: Sequence determinants of assembly or lack thereof. Emerging Topics in Life Sciences, 4(3), 307–329. https://doi.org/10.1042/ETLS20190164

Martineau, É., Di Polo, A., Vande Velde, C., & Robitaille, R. (2018). Dynamic neuromuscular remodeling precedes motor-unit loss in a mouse model of ALS. eLife, 7, e41973. https://doi.org/10.7554/eLife.41973

Martínez-Palma, L., Miquel, E., Lagos-Rodríguez, V., Barbeito, L., Cassina, A., & Cassina, P. (2019). Mitochondrial Modulation by Dichloroacetate Reduces Toxicity of Aberrant Glial Cells and Gliosis in the SOD1G93A Rat Model of Amyotrophic Lateral Sclerosis. Neurotherapeutics, 16(1), 203–215. https://doi.org/10.1007/s13311-018-0659-7

Massart, R. (1981). Preparation of aqueous magnetic liquids in alkaline and acidic media. IEEE Transactions on Magnetics, 17(2), 1247–1248. https://doi.org/10.1109/TMAG.1981.1061188

Mateju, D., Franzmann, T. M., Patel, A., Kopach, A., Boczek, E. E., Maharana, S., Lee, H. O., Carra, S., Hyman, A. A., & Alberti, S. (2017). An aberrant phase transition of stress granules triggered by misfolded protein and prevented by chaperone function. The EMBO Journal, 36(12), 1669–1687. https://doi.org/10.15252/embj.201695957

Mattiazzi, M., D'Aurelio, M., Gajewski, C. D., Martushova, K., Kiaei, M., Beal, M. F., & Manfredi, G. (2002). Mutated Human SOD1 Causes Dysfunction of Oxidative Phosphorylation in Mitochondria of Transgenic Mice. Journal of Biological Chemistry, 277(33), 29626–29633. https://doi.org/10.1074/jbc.M203065200

Matveeva, A., Watters, O., Rukhadze, A., Khemka, N., Gentile, D., Perez, I. F., Llorente-Folch, I., Farrell, C., Lo Cacciato, E., Jackson, J., Piazzesi, A., Wischhof, L., Woods, I., Halang, L., Hogg, M., Muñoz, A. G., Dillon, E. T., Matallanas, D., Arijs, I., … Prehn, J. H. M. (2024). Integrated analysis of transcriptomic and proteomic alterations in mouse models of ALS/FTD identify early metabolic adaptions with similarities to mitochondrial dysfunction disorders. Amyotrophic Lateral Sclerosis and Frontotemporal Degeneration, 25(1–2), 135–149. https://doi.org/10.1080/21678421.2023.2261979

McCampbell, A., Cole, T., Wegener, A. J., Tomassy, G. S., Setnicka, A., Farley, B. J., Schoch, K. M., Hoye, M. L., Shabsovich, M., Sun, L., Luo, Y., Zhang, M., Thankamony, S., Salzman, D. W., Cudkowicz, M., Graham, D. L., Bennett, C. F., Kordasiewicz, H. B., Swayze, E. E., & Miller, T. M. (2018). Antisense oligonucleotides extend survival and reverse decrement in muscle response in ALS models. Journal of Clinical Investigation, 128(8), 3558–3567. https://doi.org/10.1172/JCI99081

McCluskey, G., Donaghy, C., Morrison, K. E., McConville, J., Duddy, W., & Duguez, S. (2022). The Role of Sphingomyelin and Ceramide in Motor Neuron Diseases. Journal of Personalized Medicine, 12(9), 1418. https://doi.org/10.3390/jpm12091418

McCombe, P. A., Lee, J. D., Woodruff, T. M., & Henderson, R. D. (2020). The Peripheral Immune System and Amyotrophic Lateral Sclerosis. Frontiers in Neurology, 11, 279. https://doi.org/10.3389/fneur.2020.00279

McGown, A., McDearmid, J. R., Panagiotaki, N., Tong, H., Al Mashhadi, S., Redhead, N., Lyon, A. N., Beattie, C. E., Shaw, P. J., & Ramesh, T. M. (2013). Early interneuron dysfunction in ALS: Insights from a mutant sod1 zebrafish model. Annals of Neurology, 73(2), 246–258. https://doi.org/10.1002/ana.23780

Mehta, P., Horton, D. K., Kasarskis, E. J., Tessaro, E., Eisenberg, M. S., Laird, S., & Iskander, J. (2017). CDC Grand Rounds: National Amyotrophic Lateral Sclerosis (ALS) Registry Impact, Challenges, and Future Directions. MMWR. Morbidity and Mortality Weekly Report, 66(50), 1379–1382. https://doi.org/10.15585/mmwr.mm6650a3

Mejia Maza, A., Jarvis, S., Lee, W. C., Cunningham, T. J., Schiavo, G., Secrier, M., Fratta, P., Sleigh, J. N., Fisher, E. M. C., & Sudre, C. H. (2021). NMJ-Analyser identifies subtle early changes in mouse models of neuromuscular disease. Scientific Reports, 11(1), 12251. https://doi.org/10.1038/s41598-021-91094-6

Melamed, Z., López-Erauskin, J., Baughn, M. W., Zhang, O., Drenner, K., Sun, Y., Freyermuth, F., McMahon, M. A., Beccari, M. S., Artates, J. W., Ohkubo, T., Rodriguez, M., Lin, N., Wu, D., Bennett, C. F., Rigo, F., Da Cruz, S., Ravits, J., Lagier-Tourenne, C., & Cleveland, D. W. (2019). Premature polyadenylation-mediated loss of stathmin-2 is a hallmark of TDP-43-dependent neurodegeneration. Nature Neuroscience, 22(2), 180–190. https://doi.org/10.1038/s41593-018-0293-z

Mendell, J. R., Al-Zaidy, S., Shell, R., Arnold, W. D., Rodino-Klapac, L. R., Prior, T. W., Lowes, L., Alfano, L., Berry, K., Church, K., Kissel, J. T., Nagendran, S., L'Italien, J., Sproule, D. M., Wells, C., Cardenas, J. A., Heitzer, M. D., Kaspar, A., Corcoran, S., … Kaspar, B. K. (2017). Single-Dose Gene-Replacement Therapy for Spinal Muscular Atrophy. New England Journal of Medicine, 377(18), 1713–1722. https://doi.org/10.1056/nejmoa1706198

Menon, P., Kiernan, M. C., & Vucic, S. (2015). Cortical hyperexcitability precedes lower motor neuron dysfunction in ALS. Clinical Neurophysiology, 126(4), 803–809. https://doi.org/10.1016/j.clinph.2014.04.023

Meyer, N., Richter, N., Fan, Z., Siemonsmeier, G., Pivneva, T., Jordan, P., Steinhäuser, C., Semtner, M., Nolte, C., & Kettenmann, H. (2018). Oligodendrocytes in the Mouse Corpus Callosum Maintain Axonal Function by Delivery of Glucose. Cell Reports, 22(9), 2383–2394. https://doi.org/10.1016/j.celrep.2018.02.022

Meyer, T., Schumann, P., Weydt, P., Petri, S., Weishaupt, J. H., Weyen, U., Koch, J. C., Günther, R., Regensburger, M., Boentert, M., Wiesenfarth, M., Koc, Y., Kolzarek, F., Kettemann, D., Norden, J., Bernsen, S., Elmas, Z., Conrad, J., Valkadinov, I., … Körtvélyessy, P. (2024). Clinical and patient-reported outcomes and neurofilament response during tofersen treatment in SOD1 -related ALS—A multicenter observational study over 18 months. Muscle & Nerve, 70(3), 333–345. https://doi.org/10.1002/mus.28182

Migliore, L., & Coppedè, F. (2022). Gene–environment interactions in Alzheimer disease: The emerging role of epigenetics. Nature Reviews Neurology, 18(11), 643–660. https://doi.org/10.1038/s41582-022-00714-w

Miller, T. M., Cudkowicz, M. E., Genge, A., Shaw, P. J., Sobue, G., Bucelli, R. C., Chiò, A., Van Damme, P., Ludolph, A. C., Glass, J. D., Andrews, J. A., Babu, S., Benatar, M., McDermott, C. J., Cochrane, T., Chary, S., Chew, S., Zhu, H., Wu, F., … Fradette, S. (2022). Trial of Antisense Oligonucleotide Tofersen for SOD1 ALS. New England Journal of Medicine, 387(12), 1099–1110. https://doi.org/10.1056/NEJMoa2204705

Mimoto, T., Miyazaki, K., Morimoto, N., Kurata, T., Satoh, K., Ikeda, Y., & Abe, K. (2012). Impaired antioxydative Keap1/Nrf2 system and the downstream stress protein responses in the motor neuron of ALS model mice. Brain Research, 1446, 109–118. https://doi.org/10.1016/j.brainres.2011.12.064

Miquel, E., Cassina, A., Martínez-Palma, L., Bolatto, C., Trías, E., Gandelman, M., Radi, R., Barbeito, L., & Cassina, P. (2012). Modulation of Astrocytic Mitochondrial Function by Dichloroacetate Improves Survival and Motor Performance in Inherited Amyotrophic Lateral Sclerosis. PLoS ONE, 7(4), e34776. https://doi.org/10.1371/journal.pone.0034776

Mitsumoto, H., Santella, R. M., Liu, X., Bogdanov, M., Zipprich, J., Wu, H.-C., Mahata, J., Kilty, M., Bednarz, K., Bell, D., Gordon, P. H., Hornig, M., Mehrazin, M., Naini, A., Flint Beal, M., & Factor-Litvak, P. (2008). Oxidative stress biomarkers in sporadic ALS. Amyotrophic Lateral Sclerosis, 9(3), 177–183. https://doi.org/10.1080/17482960801933942

Miyamoto, N., Maki, T., Pham, L.-D. D., Hayakawa, K., Seo, J. H., Mandeville, E. T., Mandeville, J. B., Kim, K.-W., Lo, E. H., & Arai, K. (2013). Oxidative Stress Interferes With White Matter Renewal After Prolonged Cerebral Hypoperfusion in Mice. Stroke, 44(12), 3516–3521. https://doi.org/10.1161/STROKEAHA.113.002813

Mompeán, M., Romano, V., Pantoja-Uceda, D., Stuani, C., Baralle, F. E., Buratti, E., & Laurents, D. V. (2016). The TDP-43 N-terminal domain structure at high resolution. The FEBS Journal, 283(7), 1242–1260. https://doi.org/10.1111/febs.13651

Moore, A. S., & Holzbaur, E. L. F. (2016). Dynamic recruitment and activation of ALS-associated TBK1 with its target optineurin are required for efficient mitophagy. Proceedings of the National Academy of Sciences, 113(24). https://doi.org/10.1073/pnas.1523810113

Morera, A. A., Ahmed, N. S., & Schwartz, J. C. (2019). TDP-43 regulates transcription at protein-coding genes and Alu retrotransposons. Biochimica et Biophysica Acta (BBA) - Gene Regulatory Mechanisms, 1862(10), 194434. https://doi.org/10.1016/j.bbagrm.2019.194434

Mortensen, C., Steffensen, K. D., Simonsen, E., Herskind, K., Madsen, J. S., Olsen, D. A., Iversen, D. B., Bergmann, T. K., Pottegård, A., & Stage, T. B. (2023). Neurofilament light chain as a biomarker of axonal damage in sensory neurons and paclitaxel-induced peripheral neuropathy in patients with ovarian cancer. Pain, 164(7), 1502–1511. https://doi.org/10.1097/j.pain.0000000000002840

Moser, J. M., Bigini, P., & Schmitt-John, T. (2013). The wobbler mouse, an ALS animal model. Molecular Genetics and Genomics, 288(5–6), 207–229. https://doi.org/10.1007/s00438-013-0741-0

Moujalled, D., Grubman, A., Acevedo, K., Yang, S., Ke, Y. D., Moujalled, D. M., Duncan, C., Caragounis, A., Perera, N. D., Turner, B. J., Prudencio, M., Petrucelli, L., Blair, I., Ittner, L. M., Crouch, P. J., Liddell, J. R., & White, A. R. (2017). TDP-43 mutations causing amyotrophic lateral sclerosis are associated with altered expression of RNA-binding protein hnRNP K and affect the Nrf2 antioxidant pathway. Human Molecular Genetics, 26(9), 1732–1746. https://doi.org/10.1093/hmg/ddx093

Mullard, A. (2023). NfL makes regulatory debut as neurodegenerative disease biomarker. Nature Reviews Drug Discovery, 22(6), 431–434. https://doi.org/10.1038/d41573-023-00083-z

Muraleedharan, R., & Dasgupta, B. (2022). AMPK in the brain: Its roles in glucose and neural metabolism. The FEBS Journal, 289(8), 2247–2262. https://doi.org/10.1111/febs.16151

Nabais, M. F., Lin, T., Benyamin, B., Williams, K. L., Garton, F. C., Vinkhuyzen, A. A. E., Zhang, F., Vallerga, C. L., Restuadi, R., Freydenzon, A., Zwamborn, R. A. J., Hop, P. J., Robinson, M. R., Gratten, J., Visscher, P. M., Hannon, E., Mill, J., Brown, M. A., Laing, N. G., … Wray, N. R. (2020). Significant out-of-sample classification from methylation profile scoring for amyotrophic lateral sclerosis. Npj Genomic Medicine, 5(1), 10. https://doi.org/10.1038/s41525-020-0118-3

Nagai, M., Re, D. B., Nagata, T., Chalazonitis, A., Jessell, T. M., Wichterle, H., & Przedborski, S. (2007). Astrocytes expressing ALS-linked mutated SOD1 release factors selectively toxic to motor neurons. Nature Neuroscience, 10(5), 615–622. https://doi.org/10.1038/nn1876

Nagano, S., Jinno, J., Abdelhamid, R. F., Jin, Y., Shibata, M., Watanabe, S., Hirokawa, S., Nishizawa, M., Sakimura, K., Onodera, O., Okada, H., Okada, T., Saito, Y., Takahashi-Fujigasaki, J., Murayama, S., Wakatsuki, S., Mochizuki, H., & Araki, T. (2020). TDP-43 transports ribosomal protein mRNA to regulate axonal local translation in neuronal axons. Acta Neuropathologica, 140(5), 695–713. https://doi.org/10.1007/s00401-020-02205-y

Nahm, M., Lim, S. M., Kim, Y.-E., Park, J., Noh, M.-Y., Lee, S., Roh, J. E., Hwang, S.-M., Park, C.-K., Kim, Y. H., Lim, G., Lee, J., Oh, K.-W., Ki, C.-S., & Kim, S. H. (2020). ANXA11 mutations in ALS cause dysregulation of calcium homeostasis and stress granule dynamics. Science Translational Medicine, 12(566), eaax3993. https://doi.org/10.1126/scitranslmed.aax3993

Naik, A., Kambli, P., Borana, M., Mohanpuria, N., Ahmad, B., Kelkar-Mane, V., & Ladiwala, U. (2015). Attenuation of lysozyme amyloid cytotoxicity by SPION-mediated modulation of amyloid aggregation. International Journal of Biological Macromolecules, 74, 439–446. https://doi.org/10.1016/j.ijbiomac.2014.12.040

Naito, M., Hideyama, T., Teramoto, S., Saito, T., Kato, H., Terashi, H., Kwak, S., & Aizawa, H. (2023). Pathological features of glial cells and motor neurons in the anterior horn of the spinal cord in sporadic ALS using ADAR2 conditional knockout mice. Journal of the Neurological Sciences, 444, 120520. https://doi.org/10.1016/j.jns.2022.120520

Nakazato, T., Kanai, K., Kataura, T., Nojiri, S., Hattori, N., & Saiki, S. (2022). Plasma taurine is an axonal excitability-translatable biomarker for amyotrophic lateral sclerosis. Scientific Reports, 12(1), 9155. https://doi.org/10.1038/s41598-022-13397-6

Nelson, A. T., & Trotti, D. (2022). Altered Bioenergetics and Metabolic Homeostasis in Amyotrophic Lateral Sclerosis. Neurotherapeutics, 19(4), 1102–1118. https://doi.org/10.1007/s13311-022-01262-3

Neumann, M., Sampathu, D. M., Kwong, L. K., Truax, A. C., Micsenyi, M. C., Chou, T. T., Bruce, J., Schuck, T., Grossman, M., Clark, C. M., McCluskey, L. F., Miller, B. L., Masliah, E., Mackenzie, I. R., Feldman, H., Feiden, W., Kretzschmar, H. A., Trojanowski, J. Q., & Lee, V. M.-Y. (2006). Ubiquitinated TDP-43 in Frontotemporal Lobar Degeneration and Amyotrophic Lateral Sclerosis. Science, 314(5796), 130–133. https://doi.org/10.1126/science.1134108

Neve, R. M., Nielsen, U. B., Kirpotin, D. B., Poul, M.-A., Marks, J. D., & Benz, C. C. (2001). Biological Effects of Anti-ErbB2 Single Chain Antibodies Selected for Internalizing Function. Biochemical and Biophysical Research Communications, 280(1), 274–279. https://doi.org/10.1006/bbrc.2000.4104

Ng, M., Ho, J. T., Ho, S., Lee, R., Li, G., Cheng, T., Song, Y., Ho, P. W., Fong, G. C., Mak, W., Chan, K., Li, L. S., Luk, K. D., Hu, Y., Ramsden, D. B., & Leong, L. L. (2008). Abnormal diffusion tensor in nonsymptomatic familial amyotrophic lateral sclerosis with a causative superoxide dismutase 1 mutation. Journal of Magnetic Resonance Imaging, 27(1), 8–13. https://doi.org/10.1002/jmri.21217

Nguyen, P. V., Hervé-Aubert, K., David, S., Lautram, N., Passirani, C., Chourpa, I., Aubrey, N., & Allard-Vannier, E. (2020). Targeted nanomedicine with anti-EGFR scFv for siRNA delivery into triple negative breast cancer cells. European Journal of Pharmaceutics and Biopharmaceutics, 157, 74–84. https://doi.org/10.1016/j.ejpb.2020.10.004

Nicholson, A. M., & Rademakers, R. (2016). What we know about TMEM106B in neurodegeneration. Acta Neuropathologica, 132(5), 639–651. https://doi.org/10.1007/s00401-016-1610-9

Nicolas, A., Kenna, K. P., Renton, A. E., Ticozzi, N., Faghri, F., Chia, R., Dominov, J. A., Kenna, B. J., Nalls, M. A., Keagle, P., Rivera, A. M., Van Rheenen, W., Murphy, N. A., Van Vugt, J. J. F. A., Geiger, J. T., Van Der Spek, R. A., Pliner, H. A., Shankaracharya, Smith, B. N., … Twine, N. A. (2018). Genome-wide Analyses Identify KIF5A as a Novel ALS Gene. Neuron, 97(6), 1267–1288. https://doi.org/10.1016/j.neuron.2018.02.027

Nieciecka, D., Celej, J., Żuk, M., Majkowska-Pilip, A., Żelechowska-Matysiak, K., Lis, A., & Osial, M. (2021). Hybrid System for Local Drug Delivery and Magnetic Hyperthermia Based on SPIONs Loaded with Doxorubicin and Epirubicin. Pharmaceutics, 13(4), 480. https://doi.org/10.3390/pharmaceutics13040480

Nieto-Gonzalez, J. L., Moser, J., Lauritzen, M., Schmitt-John, T., & Jensen, K. (2011). Reduced GABAergic Inhibition Explains Cortical Hyperexcitability in the Wobbler Mouse Model of ALS. Cerebral Cortex, 21(3), 625–635. https://doi.org/10.1093/cercor/bhq134

Nishimoto, Y., Ito, D., Yagi, T., Nihei, Y., Tsunoda, Y., & Suzuki, N. (2010). Characterization of Alternative Isoforms and Inclusion Body of the TAR DNA-binding Protein-43. Journal of Biological Chemistry, 285(1), 608–619. https://doi.org/10.1074/jbc.M109.022012

Nishimoto, Y., Nakagawa, S., Hirose, T., Okano, H., Takao, M., Shibata, S., Suyama, S., Kuwako, K., Imai, T., Murayama, S., Suzuki, N., & Okano, H. (2013). The long non-coding RNA nuclear-enriched abundant transcript 1_2 induces paraspeckle formation in the motor neuron during the early phase of amyotrophic lateral sclerosis. Molecular Brain, 6(1), 31. https://doi.org/10.1186/1756-6606-6-31

Niture, S. K., & Jaiswal, A. K. (2012). Nrf2 Protein Up-regulates Antiapoptotic Protein Bcl-2 and Prevents Cellular Apoptosis. Journal of Biological Chemistry, 287(13), 9873–9886. https://doi.org/10.1074/jbc.M111.312694

Nonaka, T., & Hasegawa, M. (2020). Prion-like properties of assembled TDP-43. Current Opinion in Neurobiology, 61, 23–28. https://doi.org/10.1016/j.conb.2019.11.018

Nonaka, T., Suzuki, G., Tanaka, Y., Kametani, F., Hirai, S., Okado, H., Miyashita, T., Saitoe, M., Akiyama, H., Masai, H., & Hasegawa, M. (2016). Phosphorylation of TAR DNA-binding Protein of 43 kDa (TDP-43) by Truncated Casein Kinase 1δ Triggers Mislocalization and Accumulation of TDP-43. Journal of Biological Chemistry, 291(11), 5473–5483. https://doi.org/10.1074/jbc.M115.695379

Nosrati, R., Abnous, K., Alibolandi, M., Mosafer, J., Dehghani, S., Taghdisi, S. M., & Ramezani, M. (2021). Targeted SPION siderophore conjugate loaded with doxorubicin as a theranostic agent for imaging and treatment of colon carcinoma. Scientific Reports, 11(1), 13065. https://doi.org/10.1038/s41598-021-92391-w

Oberdick, S. D., Jordanova, K. V., Lundstrom, J. T., Parigi, G., Poorman, M. E., Zabow, G., & Keenan, K. E. (2023). Iron oxide nanoparticles as positive T1 contrast agents for low-field magnetic resonance imaging at 64 mT. Scientific Reports, 13(1), 11520. https://doi.org/10.1038/s41598-023-38222-6

Oberstadt, M., Stieler, J., Simpong, D. L., Römuß, U., Urban, N., Schaefer, M., Arendt, T., & Holzer, M. (2018). TDP-43 self-interaction is modulated by redox-active compounds Auranofin, Chelerythrine and Riluzole. Scientific Reports, 8(1), 2248. https://doi.org/10.1038/s41598-018-20565-0

Obrador, E., Salvador-Palmer, R., López-Blanch, R., Jihad-Jebbar, A., Vallés, S. L., & Estrela, J. M. (2021). The Link between Oxidative Stress, Redox Status, Bioenergetics and Mitochondria in the Pathophysiology of ALS. International Journal of Molecular Sciences, 22(12), 6352. https://doi.org/10.3390/ijms22126352

Ojaimi, Y. A., Dangoumau, A., Alarcan, H., Hergesheimer, R., Vourc'h, P., Corcia, P., Lanznaster, D., & Blasco, H. (2022). TAR DNA-binding protein of 43 kDa (TDP-43) and amyotrophic lateral sclerosis (ALS): A promising therapeutic target. Expert Opinion on Therapeutic Targets, 26(6), 575–592. https://doi.org/10.1080/14728222.2022.2083958

Oliveira, J. P., Prado, A. R., Keijok, W. J., Antunes, P. W. P., Yapuchura, E. R., & Guimarães, M. C. C. (2019). Impact of conjugation strategies for targeting of antibodies in gold nanoparticles for ultrasensitive detection of 17β-estradiol. Scientific Reports, 9(1), 13859. https://doi.org/10.1038/s41598-019-50424-5

Ouali Alami, N., Schurr, C., Olde Heuvel, F., Tang, L., Li, Q., Tasdogan, A., Kimbara, A., Nettekoven, M., Ottaviani, G., Raposo, C., Röver, S., Rogers-Evans, M., Rothenhäusler, B., Ullmer, C., Fingerle, J., Grether, U., Knuesel, I., Boeckers, T. M., Ludolph, A., … Baumann, B. (2018). NF-κB activation in astrocytes drives a stage-specific beneficial neuroimmunological response in ALS. The EMBO Journal, 37(16), e98697. https://doi.org/10.15252/embj.201798697

Ovsepian, S. V., O'Leary, V. B., & Martinez, S. (2023). Selective vulnerability of motor neuron types and functional groups to degeneration in amyotrophic lateral sclerosis: Review of the neurobiological mechanisms and functional correlates. Brain Structure and Function, 229(1), 1–14. https://doi.org/10.1007/s00429-023-02728-6

Owen, S. C., Patel, N., Logie, J., Pan, G., Persson, H., Moffat, J., Sidhu, S. S., & Shoichet, M. S. (2013). Targeting HER2 + breast cancer cells: Lysosomal accumulation of anti-HER2 antibodies is influenced by antibody binding site and conjugation to polymeric nanoparticles. Journal of Controlled Release, 172(2), 395–404. https://doi.org/10.1016/j.jconrel.2013.07.011

Pablo, J., Banack, S. A., Cox, P. A., Johnson, T. E., Papapetropoulos, S., Bradley, W. G., Buck, A., & Mash, D. C. (2009). Cyanobacterial neurotoxin BMAA in ALS and Alzheimer's disease. Acta Neurologica Scandinavica, 120(4), 216–225. https://doi.org/10.1111/j.1600-0404.2008.01150.x

Pagani, M., Chiò, A., Valentini, M. C., Öberg, J., Nobili, F., Calvo, A., Moglia, C., Bertuzzo, D., Morbelli, S., De Carli, F., Fania, P., & Cistaro, A. (2014). Functional pattern of brain FDG-PET in amyotrophic lateral sclerosis. Neurology, 83(12), 1067–1074. https://doi.org/10.1212/WNL.0000000000000792

Pakravan, D., Michiels, E., Bratek-Skicki, A., De Decker, M., Van Lindt, J., Alsteens, D., Derclaye, S., Van Damme, P., Schymkowitz, J., Rousseau, F., Tompa, P., & Van Den Bosch, L. (2021). Liquid–Liquid Phase Separation

Enhances TDP-43 LCD Aggregation but Delays Seeded Aggregation. Biomolecules, 11(4), 548. https://doi.org/10.3390/biom11040548

Palamiuc, L., Schlagowski, A., Ngo, S. T., Vernay, A., Dirrig-Grosch, S., Henriques, A., Boutillier, A., Zoll, J., Echaniz-Laguna, A., Loeffler, J., & René, F. (2015). A metabolic switch toward lipid use in glycolytic muscle is an early pathologic event in a mouse model of amyotrophic lateral sclerosis. EMBO Molecular Medicine, 7(5), 526–546. https://doi.org/10.15252/emmm.201404433

Pan, Y., Li, W., Feng, Y., Xu, J., & Cao, H. (2019). Edaravone attenuates experimental asthma in mice through induction of HO-1 and the Keap1/Nrf2 pathway. Experimental and Therapeutic Medicine. https://doi.org/10.3892/etm.2019.8351

Pardo, A. C., Wong, V., Benson, L. M., Dykes, M., Tanaka, K., Rothstein, J. D., & Maragakis, N. J. (2006). Loss of the astrocyte glutamate transporter GLT1 modifies disease in SOD1G93A mice. Experimental Neurology, 201(1), 120–130. https://doi.org/10.1016/j.expneurol.2006.03.028

Pardo-Moreno, T., Mohamed-Mohamed, H., Suleiman-Martos, S., Ramos-Rodriguez, J. J., Rivas-Dominguez, A., Melguizo-Rodríguez, L., Gómez-Urquiza, J. L., Bermudez-Pulgarin, B., & Garcia-Morales, V. (2023). Amyotrophic Lateral Sclerosis and Serum Lipid Level Association: A Systematic Review and Meta-Analytic Study. International Journal of Molecular Sciences, 24(10), 8675. https://doi.org/10.3390/ijms24108675

Pardridge, W. M. (2021). Kinetics of Blood–Brain Barrier Transport of Monoclonal Antibodies Targeting the Insulin Receptor and the Transferrin Receptor. Pharmaceuticals, 15(1), 3. https://doi.org/10.3390/ph15010003

Park, J., Chariou, P. L., & Steinmetz, N. F. (2020). Site-Specific Antibody Conjugation Strategy to Functionalize Virus-Based Nanoparticles. Bioconjugate Chemistry, 31(5), 1408–1416. https://doi.org/10.1021/acs.bioconjchem.0c00118

Park, J.-M., Kim, S.-Y., Park, D., & Park, J.-S. (2020). Effect of edaravone therapy in Korean amyotrophic lateral sclerosis (ALS) patients. Neurological Sciences, 41(1), 119–123. https://doi.org/10.1007/s10072-019-04055-3

Park, J.-M., Lee, D.-H., & Kim, D.-H. (2023). Redefining the role of AMPK in autophagy and the energy stress response. Nature Communications, 14(1), 2994. https://doi.org/10.1038/s41467-023-38401-z

Park, S., Kim, D., Song, J., & Joo, J. W. J. (2021). An Integrative Transcriptome-Wide Analysis of Amyotrophic Lateral Sclerosis for the Identification of Potential Genetic Markers and Drug Candidates. International Journal of Molecular Sciences, 22(6), 3216. https://doi.org/10.3390/ijms22063216

Patel, A., Lee, H. O., Jawerth, L., Maharana, S., Jahnel, M., Hein, M. Y., Stoynov, S., Mahamid, J., Saha, S., Franzmann, T. M., Pozniakovski, A., Poser, I., Maghelli, N., Royer, L. A., Weigert, M., Myers, E. W., Grill, S., Drechsel, D., Hyman, A. A., & Alberti, S. (2015). A Liquid-to-Solid Phase Transition of the ALS Protein FUS Accelerated by Disease Mutation. Cell, 162(5), 1066–1077. https://doi.org/10.1016/j.cell.2015.07.047

Patel, P., Kriz, J., Gravel, M., Soucy, G., Bareil, C., Gravel, C., & Julien, J.-P. (2014). Adeno-associated Virus–mediated Delivery of a Recombinant Single-chain Antibody Against Misfolded Superoxide Dismutase for Treatment of Amyotrophic Lateral Sclerosis. Molecular Therapy, 22(3), 498–510. https://doi.org/10.1038/mt.2013.239

Patni, D., & Jha, S. K. (2021). Protonation–Deprotonation Switch Controls the Amyloid-like Misfolding of Nucleic-Acid-Binding Domains of TDP-43. The Journal of Physical Chemistry B, 125(30), 8383–8394. https://doi.org/10.1021/acs.jpcb.1c03262

Patni, D., & Jha, S. K. (2023). Thermodynamic modulation of folding and aggregation energy landscape by DNA binding of functional domains of TDP-43. Biochimica et Biophysica Acta (BBA) - Proteins and Proteomics, 1871(4), 140916. https://doi.org/10.1016/j.bbapap.2023.140916

Pattle, S. B., O'Shaughnessy, J., Rifai, O. M., Pate, J., Arends, M. J., Waldron, F. M., & Gregory, J. M. (2022). pTDP-43 aggregates accumulate in the gut and other non-central nervous system tissues prior to symptom onset in amyotrophic lateral sclerosis. https://doi.org/10.1101/2022.03.17.484805

Pegoraro, V., Marozzo, R., & Angelini, C. (2020). MicroRNAs and HDAC4 protein expression in the skeletal muscle of ALS patients. Clinical Neuropathology, 39(05), 105–114. https://doi.org/10.5414/NP301233

Pehar, M., Vargas, M. R., Robinson, K. M., Cassina, P., England, P., Beckman, J. S., Alzari, P. M., & Barbeito, L. (2006). Peroxynitrite transforms nerve growth factor into an apoptotic factor for motor neurons. Free Radical Biology and Medicine, 41(11), 1632–1644. https://doi.org/10.1016/j.freeradbiomed.2006.08.010

Peng, A. Y. T., Agrawal, I., Ho, W. Y., Yen, Y.-C., Pinter, A. J., Liu, J., Phua, Q. X. C., Koh, K. B., Chang, J.-C., Sanford, E., Man, J. H. K., Wong, P., Gutmann, D. H., Tucker-Kellogg, G., & Ling, S.-C. (2020). Loss of TDP-43 in astrocytes leads to motor deficits by triggering A1-like reactive phenotype and triglial dysfunction. Proceedings of the National Academy of Sciences, 117(46), 29101–29112. https://doi.org/10.1073/pnas.2007806117

Peric, M., Nikolic, L., Andjus, P. R., & Bataveljic, D. (2021). Dysfunction of oligodendrocyte inwardly rectifying potassium channel in a rat model of amyotrophic lateral sclerosis. European Journal of Neuroscience, 54(7), 6339–6354. https://doi.org/10.1111/ejn.15451

Perry, T. L., Hansen, S., & Jones, K. (1987). Brain glutamate deficiency in amyotrophic lateral sclerosis. Neurology, 37(12), 1845–1845. https://doi.org/10.1212/WNL.37.12.1845

Petri, S., Krampfl, K., Hashemi, F., Grothe, C., Hori, A., Dengler, R., & Bufler, J. (2003). Distribution of GABA A Receptor mRNA in the Motor Cortex of ALS Patients. Journal of Neuropathology & Experimental Neurology, 62(10), 1041–1051. https://doi.org/10.1093/jnen/62.10.1041

Pfefferkorn, C. M., McGlinchey, R. P., & Lee, J. C. (2010). Effects of pH on aggregation kinetics of the repeat domain of a functional amyloid, Pmel17. Proceedings of the National Academy of Sciences, 107(50), 21447–21452. https://doi.org/10.1073/pnas.1006424107

Philips, T., Bento-Abreu, A., Nonneman, A., Haeck, W., Staats, K., Geelen, V., Hersmus, N., Küsters, B., Van Den Bosch, L., Van Damme, P., Richardson, W. D., & Robberecht, W. (2013). Oligodendrocyte dysfunction in the pathogenesis of amyotrophic lateral sclerosis. Brain, 136(2), 471–482. https://doi.org/10.1093/brain/aws339

Philips, T., & Rothstein, J. D. (2017). Oligodendroglia: Metabolic supporters of neurons. Journal of Clinical Investigation, 127(9), 3271–3280. https://doi.org/10.1172/JCI90610

Phukan, J., Elamin, M., Bede, P., Jordan, N., Gallagher, L., Byrne, S., Lynch, C., Pender, N., & Hardiman, O. (2012). The syndrome of cognitive impairment in amyotrophic lateral sclerosis: A population-based study.

Journal of Neurology, Neurosurgery & Psychiatry, 83(1), 102–108. https://doi.org/10.1136/jnnp-2011-300188

Picciolini, S., Gualerzi, A., Vanna, R., Sguassero, A., Gramatica, F., Bedoni, M., Masserini, M., & Morasso, C. (2018). Detection and Characterization of Different Brain-Derived Subpopulations of Plasma Exosomes by Surface Plasmon Resonance Imaging. Analytical Chemistry, 90(15), 8873–8880. https://doi.org/10.1021/acs.analchem.8b00941

Pieri, M., Carunchio, I., Curcio, L., Mercuri, N. B., & Zona, C. (2009). Increased persistent sodium current determines cortical hyperexcitability in a genetic model of amyotrophic lateral sclerosis. Experimental Neurology, 215(2), 368–379. https://doi.org/10.1016/j.expneurol.2008.11.002

Pillai, M., & Jha, S. K. (2020). Early Metastable Assembly during the Stress-Induced Formation of Worm-like Amyloid Fibrils of Nucleic Acid Binding Domains of TDP-43. Biochemistry, 59(3), 315–328. https://doi.org/10.1021/acs.biochem.9b00780

Pintado-Grima, C., Bárcenas, O., & Ventura, S. (2022). In-Silico Analysis of pH-Dependent Liquid-Liquid Phase Separation in Intrinsically Disordered Proteins. Biomolecules, 12(7), 974. https://doi.org/10.3390/biom12070974

Pinto, S., Gromicho, M., Oliveira Santos, M. O., Swash, M., & De Carvalho, M. (2023). Respiratory onset in amyotrophic lateral sclerosis: Clinical features and spreading pattern. Amyotrophic Lateral Sclerosis and Frontotemporal Degeneration, 24(1–2), 40–44. https://doi.org/10.1080/21678421.2022.2067777

Piol, D., Robberechts, T., & Da Cruz, S. (2023). Lost in local translation: TDP-43 and FUS in axonal/neuromuscular junction maintenance and dysregulation in amyotrophic lateral sclerosis. Neuron, 111(9), 1355–1380. https://doi.org/10.1016/j.neuron.2023.02.028

Pirie, E., Oh, C., Zhang, X., Han, X., Cieplak, P., Scott, H. R., Deal, A. K., Ghatak, S., Martinez, F. J., Yeo, G. W., Yates, J. R., Nakamura, T., & Lipton, S. A. (2021). S-nitrosylated TDP-43 triggers aggregation, cell-to-cell spread, and neurotoxicity in hiPSCs and in vivo models of ALS/FTD. Proceedings of the National Academy of Sciences, 118(11), e2021368118. https://doi.org/10.1073/pnas.2021368118

Pirkalkhoran, S., Grabowska, W. R., Kashkoli, H. H., Mirhassani, R., Guiliano, D., Dolphin, C., & Khalili, H. (2023). Bioengineering of Antibody Fragments: Challenges and Opportunities. Bioengineering, 10(2), 122. https://doi.org/10.3390/bioengineering10020122

Pivovarova, N. B., & Andrews, S. B. (2010). Calcium-dependent mitochondrial function and dysfunction in neurons. The FEBS Journal, 277(18), 3622–3636. https://doi.org/10.1111/j.1742-4658.2010.07754.x

Pivovarova, N. B., Nguyen, H. V., Winters, C. A., Brantner, C. A., Smith, C. L., & Andrews, S. B. (2004). Excitotoxic Calcium Overload in a Subpopulation of Mitochondria Triggers Delayed Death in Hippocampal Neurons. The Journal of Neuroscience, 24(24), 5611–5622. https://doi.org/10.1523/JNEUROSCI.0531-04.2004

Plianwong, S., Opanasopit, P., Ngawhirunpat, T., & Rojanarata, T. (2013). Chitosan Combined with Poly-L-arginine as Efficient, Safe, and Serum-Insensitive Vehicle with RNase Protection Ability for siRNA Delivery. BioMed Research International, 2013, 1–9. https://doi.org/10.1155/2013/574136

Pollari, E., Goldsteins, G., Bart, G., Koistinaho, J., & Giniatullin, R. (2014). The role of oxidative stress in degeneration of the neuromuscular junction in amyotrophic lateral sclerosis. Frontiers in Cellular Neuroscience, 8. https://doi.org/10.3389/fncel.2014.00131

Polymenidou, M., Lagier-Tourenne, C., Hutt, K. R., Huelga, S. C., Moran, J., Liang, T. Y., Ling, S.-C., Sun, E., Wancewicz, E., Mazur, C., Kordasiewicz, H., Sedaghat, Y., Donohue, J. P., Shiue, L., Bennett, C. F., Yeo, G. W., & Cleveland, D. W. (2011). Long pre-mRNA depletion and RNA missplicing contribute to neuronal vulnerability from loss of TDP-43. Nature Neuroscience, 14(4), 459–468. https://doi.org/10.1038/nn.2779

Popuri, K., Beg, M. F., Lee, H., Balachandar, R., Wang, L., Sossi, V., Jacova, C., Baker, M., Shahinfard, E., Rademakers, R., Mackenzie, I. R. A., & Hsiung, G.-Y. R. (2021). FDG-PET in presymptomatic C9orf72 mutation carriers. NeuroImage: Clinical, 31, 102687. https://doi.org/10.1016/j.nicl.2021.102687

Pozzi, S., Thammisetty, S. S., Codron, P., Rahimian, R., Plourde, K. V., Soucy, G., Bareil, C., Phaneuf, D., Kriz, J., Gravel, C., & Julien, J.-P. (2019). Virus-mediated delivery of antibody targeting TAR DNA-binding protein-43 mitigates associated neuropathology. Journal of Clinical Investigation, 129(4), 1581–1595. https://doi.org/10.1172/JCI123931

Pradat, P.-F., Bruneteau, G., Gordon, P. H., Dupuis, L., Bonnefont-Rousselot, D., Simon, D., Salachas, F., Corcia, P., Frochot, V., Lacorte, J.-M., Jardel, C., Coussieu, C., Le Forestier, N., Lacomblez, L., Loeffler, J.-P., & Meininger, V. (2010). Impaired glucose tolerance in patients with amyotrophic lateral sclerosis. Amyotrophic Lateral Sclerosis, 11(1–2), 166–171. https://doi.org/10.3109/17482960902822960

Prijic, S., Scancar, J., Romih, R., Cemazar, M., Bregar, V. B., Znidarsic, A., & Sersa, G. (2010). Increased Cellular Uptake of Biocompatible Superparamagnetic Iron Oxide Nanoparticles into Malignant Cells by an External Magnetic Field. The Journal of Membrane Biology, 236(1), 167–179. https://doi.org/10.1007/s00232-010-9271-4

Putnam, R. W. (2001). Intracellular pH regulation of neurons in chemosensitive and nonchemosensitive areas of brain slices. Respiration Physiology, 129(1–2), 37–56. https://doi.org/10.1016/S0034-5687(01)00281-X

Qian, L., Bian, W., Wang, D., Ming, Z., Zhang, Y., Zhang, L., & Fu, L. (2023). Adeno-Associated Virus-Mediated Immunotherapy Based on Bispecific Tandem scFv for Alzheimer's Disease. Journal of Alzheimer's Disease, 93(2), 435–448. https://doi.org/10.3233/JAD-221088

Quessada, C., Bouscary, A., René, F., Valle, C., Ferri, A., Ngo, S. T., & Loeffler, J.-P. (2021). Skeletal Muscle Metabolism: Origin or Prognostic Factor for Amyotrophic Lateral Sclerosis (ALS) Development? Cells, 10(6), 1449. https://doi.org/10.3390/cells10061449

Quintás, G., Martínez-Sena, T., Conde, I., Pareja Ibars, E., Kleinjans, J., & Castell, J. V. (2021). Metabolomic analysis to discriminate drug-induced liver injury (DILI) phenotypes. Archives of Toxicology, 95(9), 3049–3062. https://doi.org/10.1007/s00204-021-03114-z

Rajabi, D., Khanmohammadi, S., & Rezaei, N. (2024). The role of long noncoding RNAs in amyotrophic lateral sclerosis. Reviews in the Neurosciences, 35(5), 533–547. https://doi.org/10.1515/revneuro-2023-0155

Raymond, J., Mehta, P., Larson, T., Factor-Litvak, P., Davis, B., & Horton, K. (2021). History of vigorous leisure-time physical activity and early onset amyotrophic lateral sclerosis (ALS), data from the national ALS registry: 2010–2018. Amyotrophic Lateral Sclerosis and Frontotemporal Degeneration, 22(7–8), 535–544. https://doi.org/10.1080/21678421.2021.1910308

Reineke, L. C., & Neilson, J. R. (2019). Differences between acute and chronic stress granules, and how these differences may impact function in human disease. Biochemical Pharmacology, 162, 123–131. https://doi.org/10.1016/j.bcp.2018.10.009

Renton, A. E., Chiò, A., & Traynor, B. J. (2014). State of play in amyotrophic lateral sclerosis genetics. Nature Neuroscience, 17(1), 17–23. https://doi.org/10.1038/nn.3584

Reyes-Ortega, F., Delgado, Á., & Iglesias, G. (2021). Modulation of the Magnetic Hyperthermia Response Using Different Superparamagnetic Iron Oxide Nanoparticle Morphologies. Nanomaterials, 11(3), 627. https://doi.org/10.3390/nano11030627

Rezvykh, A. P., Ustyugov, A. A., Chaprov, K. D., Teterina, E. V., Nebogatikov, V. O., Spasskaya, D. S., Evgen'ev, M. B., Morozov, A. V., & Funikov, S. Y. (2023). Cytoplasmic aggregation of mutant FUS causes multistep RNA splicing perturbations in the course of motor neuron pathology. Nucleic Acids Research, 51(11), 5810–5830. https://doi.org/10.1093/nar/gkad319

Richards, D., Morren, J. A., & Pioro, E. P. (2020). Time to diagnosis and factors affecting diagnostic delay in amyotrophic lateral sclerosis. Journal of the Neurological Sciences, 417, 117054. https://doi.org/10.1016/j.jns.2020.117054

Riemenschneider, H., Guo, Q., Bader, J., Frottin, F., Farny, D., Kleinberger, G., Haass, C., Mann, M., Hartl, F. U., Baumeister, W., Hipp, M. S., Meissner, F., Fernández-Busnadiego, R., & Edbauer, D. (2022). Gel-like inclusions of C-terminal fragments of TDP-43 sequester stalled proteasomes in neurons. EMBO Reports, 23(6), e53890. https://doi.org/10.15252/embr.202153890

Riemenschneider, H., Simonetti, F., Sheth, U., Katona, E., Roth, S., Hutten, S., Farny, D., Michaelsen, M., Nuscher, B., Schmidt, M. K., Flatley, A., Schepers, A., Gruijs Da Silva, L. A., Zhou, Q., Klopstock, T., Liesz, A., Arzberger, T., Herms, J., Feederle, R., … Edbauer, D. (2023). Targeting the glycine-rich domain of TDP-43 with antibodies prevents its aggregation in vitro and reduces neurofilament levels in vivo. Acta Neuropathologica Communications, 11(1), 112. https://doi.org/10.1186/s40478-023-01592-z

Rinchetti, P., Rizzuti, M., Faravelli, I., & Corti, S. (2018). MicroRNA Metabolism and Dysregulation in Amyotrophic Lateral Sclerosis. Molecular Neurobiology, 55(3), 2617–2630. https://doi.org/10.1007/s12035-017-0537-z

Rocha, M. C., Pousinha, P. A., Correia, A. M., Sebastião, A. M., & Ribeiro, J. A. (2013). Early Changes of Neuromuscular Transmission in the SOD1(G93A) Mice Model of ALS Start Long before Motor Symptoms Onset. PLoS ONE, 8(9), e73846. https://doi.org/10.1371/journal.pone.0073846

Roda, A. R., Montoliu-Gaya, L., Serra-Mir, G., & Villegas, S. (2020). Both Amyloid-β Peptide and Tau Protein Are Affected by an Anti-Amyloid-β Antibody Fragment in Elderly 3xTg-AD Mice. International Journal of Molecular Sciences, 21(18), 6630. https://doi.org/10.3390/ijms21186630

Rodrigues Martins, D., Sha, F., Van Der Elst, W., Shih, P.-Y., Devoght, J., Van Kolen, K., Mercken, M., Van Broeck, B., Declerck, P., & Theunis, C. (2023). Anti-tau intrabodies: From anti-tau immunoglobulins to the development of functional scFv intrabodies. Molecular Therapy - Methods & Clinical Development, 31, 101158. https://doi.org/10.1016/j.omtm.2023.101158

Rofo, F., Meier, S. R., Metzendorf, N. G., Morrison, J. I., Petrovic, A., Syvänen, S., Sehlin, D., & Hultqvist, G. (2022). A Brain-Targeting Bispecific-Multivalent Antibody Clears Soluble Amyloid-Beta Aggregates in Alzheimer's Disease Mice. Neurotherapeutics, 19(5), 1588–1602. https://doi.org/10.1007/s13311-022-01283-y

Rojas, F., Gonzalez, D., Cortes, N., Ampuero, E., HernÃ¡ndez, D. E., Fritz, E., Abarzua, S., Martinez, A., Elorza, A. A., Alvarez, A., Court, F., & Van Zundert, B. (2015). Reactive oxygen species trigger motoneuron death

in non-cell-autonomous models of ALS through activation of c-Abl signaling. Frontiers in Cellular Neuroscience, 09. https://doi.org/10.3389/fncel.2015.00203

Roos, E., Wärmländer, S. K. T. S., Meyer, J., Sholts, S. B., Jarvet, J., Gräslund, A., & Roos, P. M. (2021). Amyotrophic Lateral Sclerosis After Exposure to Manganese from Traditional Medicine Procedures in Kenya. Biological Trace Element Research, 199(10), 3618–3624. https://doi.org/10.1007/s12011-020-02501-4

Rosen, D. R., Siddique, T., Patterson, D., Figlewicz, D. A., Sapp, P., Hentati, A., Donaldson, D., Goto, J., O'Regan, J. P., Deng, H.-X., Rahmani, Z., Krizus, A., McKenna-Yasek, D., Cayabyab, A., Gaston, S. M., Berger, R., Tanzi, R. E., Halperin, J. J., Herzfeldt, B., … Brown, R. H. (1993). Mutations in Cu/Zn superoxide dismutase gene are associated with familial amyotrophic lateral sclerosis. Nature, 362(6415), 59–62. https://doi.org/10.1038/362059a0

Roshanbin, S., Xiong, M., Hultqvist, G., Söderberg, L., Zachrisson, O., Meier, S., Ekmark-Lewén, S., Bergström, J., Ingelsson, M., Sehlin, D., & Syvänen, S. (2022). In vivo imaging of alpha-synuclein with antibody-based PET. Neuropharmacology, 208, 108985. https://doi.org/10.1016/j.neuropharm.2022.108985

Rossi, S., Rompietti, V., Antonucci, Y., Giovannini, D., Scopa, C., Scaricamazza, S., Scardigli, R., Cestra, G., Serafino, A., Carrì, M. T., D'Ambrosi, N., & Cozzolino, M. (2020). UsnRNP trafficking is regulated by stress granules and compromised by mutant ALS proteins. Neurobiology of Disease, 138, 104792. https://doi.org/10.1016/j.nbd.2020.104792

Rothstein, J. D., Van Kammen, M., Levey, A. I., Martin, L. J., & Kuncl, R. W. (1995). Selective loss of glial glutamate transporter GLT-1 in amyotrophic lateral sclerosis. Annals of Neurology, 38(1), 73–84. https://doi.org/10.1002/ana.410380114

Rowland, L. P. (2001). How Amyotrophic Lateral Sclerosis Got Its Name: The Clinical-Pathologic Genius of Jean-Martin Charcot. Archives of Neurology, 58(3). https://doi.org/10.1001/archneur.58.3.512

Ruan, Y., Xiong, Y., Fang, W., Yu, Q., Mai, Y., Cao, Z., Wang, K., Lei, M., Xu, J., Liu, Y., Zhang, X., Liao, W., & Liu, J. (2022). Highly sensitive Curcumin-conjugated nanotheranostic platform for detecting amyloid-beta plaques by magnetic resonance imaging and reversing cognitive deficits of Alzheimer's disease via NLRP3-inhibition. Journal of Nanobiotechnology, 20(1), 322. https://doi.org/10.1186/s12951-022-01524-4

Rué, L., Jaspers, T., Degors, I. M. S., Noppen, S., Schols, D., De Strooper, B., & Dewilde, M. (2023). Novel Human/Non-Human Primate Cross-Reactive Anti-Transferrin Receptor Nanobodies for Brain Delivery of Biologics. Pharmaceutics, 15(6), 1748. https://doi.org/10.3390/pharmaceutics15061748

Ruf, W. P., Hannon, E., Freischmidt, A., Grozdanov, V., Brenner, D., Müller, K., Knehr, A., Günther, K., Dorst, J., Ammerpohl, O., Danzer, K. M., Mill, J., Ludolph, A. C., & Weishaupt, J. H. (2022). Methylome analysis of ALS patients and presymptomatic mutation carriers in blood cells. Neurobiology of Aging, 116, 16–24. https://doi.org/10.1016/j.neurobiolaging.2022.04.003

Ruffo, P., Strafella, C., Cascella, R., Caputo, V., Conforti, F. L., Andò, S., & Giardina, E. (2021). Deregulation of ncRNA in Neurodegenerative Disease: Focus on circRNA, lncRNA and miRNA in Amyotrophic Lateral Sclerosis. Frontiers in Genetics, 12, 784996. https://doi.org/10.3389/fgene.2021.784996

Rutter-Locher, Z., Turner, M. R., Leigh, P. N., & Al-Chalabi, A. (2016). Analysis of terms used for the diagnosis and classification of amyotrophic lateral sclerosis and motor neuron disease. Amyotrophic Lateral Sclerosis

and Frontotemporal Degeneration, 17(7–8), 600–604. https://doi.org/10.1080/21678421.2016.1181766

Ryan, M., Heverin, M., McLaughlin, R. L., & Hardiman, O. (2019). Lifetime Risk and Heritability of Amyotrophic Lateral Sclerosis. JAMA Neurology, 76(11), 1367. https://doi.org/10.1001/jamaneurol.2019.2044

Saab, A. S., Tzvetavona, I. D., Trevisiol, A., Baltan, S., Dibaj, P., Kusch, K., Möbius, W., Goetze, B., Jahn, H. M., Huang, W., Steffens, H., Schomburg, E. D., Pérez-Samartín, A., Pérez-Cerdá, F., Bakhtiari, D., Matute, C., Löwel, S., Griesinger, C., Hirrlinger, J., … Nave, K.-A. (2016). Oligodendroglial NMDA Receptors Regulate Glucose Import and Axonal Energy Metabolism. Neuron, 91(1), 119–132. https://doi.org/10.1016/j.neuron.2016.05.016

Saini, A., & Chawla, P. A. (2024). Breaking barriers with tofersen: Enhancing therapeutic opportunities in amyotrophic lateral sclerosis. European Journal of Neurology, 31(2), e16140. https://doi.org/10.1111/ene.16140

Saitoh, Y., & Takahashi, Y. (2020). Riluzole for the treatment of amyotrophic lateral sclerosis. Neurodegenerative Disease Management, 10(6), 343–355. https://doi.org/10.2217/nmt-2020-0033

Salamatina, A., Yang, J. H., Brenner-Morton, S., Bikoff, J. B., Fang, L., Kintner, C. R., Jessell, T. M., & Sweeney, L. B. (2020). Differential Loss of Spinal Interneurons in a Mouse Model of ALS. Neuroscience, 450, 81–95. https://doi.org/10.1016/j.neuroscience.2020.08.011

Salmon, K., Ross, J. P., Bertone, V., Gobbo, M., Anoja, N., Karamchandani, J., Dion, P. A., Rouleau, G. A., & Genge, A. (2022). The value of testing for ATXN2 intermediate repeat expansions in routine clinical practice for amyotrophic lateral sclerosis. European Journal of Human Genetics, 30(11), 1205–1207. https://doi.org/10.1038/s41431-022-01146-2

Samadhiya, S., Sardana, V., Bhushan, B., Maheshwari, D., Goyal, R., & Pankaj. (2022). Assessment of therapeutic response of edaravone and riluzole combination therapy in amyotrophic lateral sclerosis patients. Annals of Indian Academy of Neurology, 25(4), 692. https://doi.org/10.4103/aian.aian_1083_21

Sanati, M., Aminyavari, S., Khodagholi, F., Hajipour, M. J., Sadeghi, P., Noruzi, M., Moshtagh, A., Behmadi, H., & Sharifzadeh, M. (2021). PEGylated superparamagnetic iron oxide nanoparticles (SPIONs) ameliorate learning and memory deficit in a rat model of Alzheimer's disease: Potential participation of STIMs. NeuroToxicology, 85, 145–159. https://doi.org/10.1016/j.neuro.2021.05.013

Santos, J., Iglesias, V., Santos-Suárez, J., Mangiagalli, M., Brocca, S., Pallarès, I., & Ventura, S. (2020). pH-Dependent Aggregation in Intrinsically Disordered Proteins Is Determined by Charge and Lipophilicity. Cells, 9(1), 145. https://doi.org/10.3390/cells9010145

Sarkar, S. (2021). Mechanism of Gene-Environment Interactions Driving Glial Activation in Parkinson's Diseases. Current Environmental Health Reports, 8(3), 203–211. https://doi.org/10.1007/s40572-021-00320-w

Sarlette, A., Krampfl, K., Grothe, C., Neuhoff, N. V., Dengler, R., & Petri, S. (2008). Nuclear Erythroid 2-Related Factor 2-Antioxidative Response Element Signaling Pathway in Motor Cortex and Spinal Cord in Amyotrophic Lateral Sclerosis. Journal of Neuropathology & Experimental Neurology, 67(11), 1055–1062. https://doi.org/10.1097/NEN.0b013e31818b4906

Sasaki, S. (2010). Endoplasmic Reticulum Stress in Motor Neurons of the Spinal Cord in Sporadic Amyotrophic Lateral Sclerosis. Journal of Neuropathology & Experimental Neurology, 69(4), 346–355. https://doi.org/10.1097/NEN.0b013e3181d44992

Savica, R., Parisi, J. E., Wold, L. E., Josephs, K. A., & Ahlskog, J. E. (2012). High School Football and Risk of Neurodegeneration: A Community-Based Study. Mayo Clinic Proceedings, 87(4), 335–340. https://doi.org/10.1016/j.mayocp.2011.12.016

Saxena, S., Cabuy, E., & Caroni, P. (2009). A role for motoneuron subtype–selective ER stress in disease manifestations of FALS mice. Nature Neuroscience, 12(5), 627–636. https://doi.org/10.1038/nn.2297

Scekic-Zahirovic, J., Oussini, H. E., Mersmann, S., Drenner, K., Wagner, M., Sun, Y., Allmeroth, K., Dieterlé, S., Sinniger, J., Dirrig-Grosch, S., René, F., Dormann, D., Haass, C., Ludolph, A. C., Lagier-Tourenne, C., Storkebaum, E., & Dupuis, L. (2017). Motor neuron intrinsic and extrinsic mechanisms contribute to the pathogenesis of FUS-associated amyotrophic lateral sclerosis. Acta Neuropathologica, 133(6), 887–906. https://doi.org/10.1007/s00401-017-1687-9

Schaefer, A. M., Sanes, J. R., & Lichtman, J. W. (2005). A compensatory subpopulation of motor neurons in a mouse model of amyotrophic lateral sclerosis. The Journal of Comparative Neurology, 490(3), 209–219. https://doi.org/10.1002/cne.20620

Schlichtmann, B. W., Palanisamy, B. N., Malovic, E., Nethi, S. K., Padhi, P., Hepker, M., Wurtz, J., John, M., Ban, B., Anantharam, V., Kanthasamy, A. G., Narasimhan, B., & Mallapragada, S. K. (2023). Aggregation-Inhibiting scFv-Based Therapies Protect Mice against AAV1/2-Induced A53T-α-Synuclein Overexpression. Biomolecules, 13(8), 1203. https://doi.org/10.3390/biom13081203

Schmidt, E. J., Funes, S., McKeon, J. E., Morgan, B. R., Boopathy, S., O'Connor, L. C., Bilsel, O., Massi, F., Jégou, A., & Bosco, D. A. (2021). ALS-linked PFN1 variants exhibit loss and gain of functions in the context of formin-induced actin polymerization. Proceedings of the National Academy of Sciences, 118(23), e2024605118. https://doi.org/10.1073/pnas.2024605118

Schneider, E. L., Hearn, B. R., Pfaff, S. J., Fontaine, S. D., Reid, R., Ashley, G. W., Grabulovski, S., Strassberger, V., Vogt, L., Jung, T., & Santi, D. V. (2016). Approach for Half-Life Extension of Small Antibody Fragments That Does Not Affect Tissue Uptake. Bioconjugate Chemistry, 27(10), 2534–2539. https://doi.org/10.1021/acs.bioconjchem.6b00469

Schroeder, H. W., & Cavacini, L. (2010). Structure and function of immunoglobulins. Journal of Allergy and Clinical Immunology, 125(2), S41–S52. https://doi.org/10.1016/j.jaci.2009.09.046

Seddighi, S., Qi, Y. A., Brown, A.-L., Wilkins, O. G., Bereda, C., Belair, C., Zhang, Y.-J., Prudencio, M., Keuss, M. J., Khandeshi, A., Pickles, S., Kargbo-Hill, S. E., Hawrot, J., Ramos, D. M., Yuan, H., Roberts, J., Sacramento, E. K., Shah, S. I., Nalls, M. A., … Ward, M. E. (2024). Mis-spliced transcripts generate de novo proteins in TDP-43–related ALS/FTD. Science Translational Medicine, 16(734), eadg7162. https://doi.org/10.1126/scitranslmed.adg7162

Selles, M. C., Fortuna, J. T. S., Cercato, M. C., Santos, L. E., Domett, L., Bitencourt, A. L. B., Carraro, M. F., Souza, A. S., Janickova, H., Azevedo, C. V., Campos, H. C., De Souza, J. M., Alves-Leon, S., Prado, V. F., Prado, M. A. M., Epstein, A. L., Salvetti, A., Longo, B. M., Arancio, O., … Ferreira, S. T. (2023). AAV-mediated neuronal expression of an scFv antibody selective for Aβ oligomers protects synapses and rescues memory in Alzheimer models. Molecular Therapy, 31(2), 409–419. https://doi.org/10.1016/j.ymthe.2022.11.002

Seo, J. W., Ajenjo, J., Wu, B., Robinson, E., Raie, M. N., Wang, J., Tumbale, S. K., Buccino, P., Anders, D. A., Shen, B., Habte, F. G., Beinat, C., James, M. L., Reyes, S. T., Ravindra Kumar, S., Miles, T. F., Lee, J. T., Gradinaru, V., & Ferrara, K. W. (2022). Multimodal imaging of capsid and cargo reveals differential brain targeting and liver detargeting of systemically-administered AAVs. Biomaterials, 288, 121701. https://doi.org/10.1016/j.biomaterials.2022.121701

Shang, J., Yamashita, T., Nakano, Y., Morihara, R., Li, X., Feng, T., Liu, X., Huang, Y., Fukui, Y., Hishikawa, N., Ohta, Y., & Abe, K. (2017). Aberrant distributions of nuclear pore complex proteins in ALS mice and ALS patients. Neuroscience, 350, 158–168. https://doi.org/10.1016/j.neuroscience.2017.03.024

Shaw, P. J., Ince, P. G., Falkous, G., & Mantle, D. (1995). Oxidative damage to protein in sporadic motor neuron disease spinal cord. Annals of Neurology, 38(4), 691–695. https://doi.org/10.1002/ana.410380424

Sheets, M. D., Amersdorfer, P., Finnern, R., Sargent, P., Lindqvist, E., Schier, R., Hemingsen, G., Wong, C., Gerhart, J. C., & Marks, J. D. (1998). Efficient construction of a large nonimmune phage antibody library: The production of high-affinity human single-chain antibodies to protein antigens. Proceedings of the National Academy of Sciences, 95(11), 6157–6162. https://doi.org/10.1073/pnas.95.11.6157

Shefner, J. M., Al-Chalabi, A., Baker, M. R., Cui, L.-Y., De Carvalho, M., Eisen, A., Grosskreutz, J., Hardiman, O., Henderson, R., Matamala, J. M., Mitsumoto, H., Paulus, W., Simon, N., Swash, M., Talbot, K., Turner, M. R., Ugawa, Y., Van Den Berg, L. H., Verdugo, R., … Kiernan, M. C. (2020). A proposal for new diagnostic criteria for ALS. Clinical Neurophysiology, 131(8), 1975–1978. https://doi.org/10.1016/j.clinph.2020.04.005

Shellikeri, S., Karthikeyan, V., Martino, R., Black, S. E., Zinman, L., Keith, J., & Yunusova, Y. (2017). The neuropathological signature of bulbar-onset ALS: A systematic review. Neuroscience & Biobehavioral Reviews, 75, 378–392. https://doi.org/10.1016/j.neubiorev.2017.01.045

Sheng, Y., Chattopadhyay, M., Whitelegge, J., & Selverstone Valentine, J. (2013). SOD1 Aggregation and ALS: Role of Metallation States and Disulfide Status. Current Topics in Medicinal Chemistry, 12(22), 2560–2572. https://doi.org/10.2174/1568026611212220010

Shenoy, J., El Mammeri, N., Dutour, A., Berbon, M., Saad, A., Lends, A., Morvan, E., Grélard, A., Lecomte, S., Kauffmann, B., Theillet, F., Habenstein, B., & Loquet, A. (2020). Structural dissection of amyloid aggregates of TDP-43 and its C-terminal fragments TDP-35 and TDP-16. The FEBS Journal, 287(12), 2449–2467. https://doi.org/10.1111/febs.15159

Shibata, N., Nagai, R., Uchida, K., Horiuchi, S., Yamada, S., Hirano, A., Kawaguchi, M., Yamamoto, T., Sasaki, S., & Kobayashi, M. (2001). Morphological evidence for lipid peroxidation and protein glycoxidation in spinal cords from sporadic amyotrophic lateral sclerosis patients. Brain Research, 917(1), 97–104. https://doi.org/10.1016/S0006-8993(01)02926-2

Shibuya, K., Misawa, S., Arai, K., Nakata, M., Kanai, K., Yoshiyama, Y., Ito, K., Isose, S., Noto, Y., Nasu, S., Sekiguchi, Y., Fujimaki, Y., Ohmori, S., Kitamura, H., Sato, Y., & Kuwabara, S. (2011). Markedly reduced axonal potassium channel expression in human sporadic amyotrophic lateral sclerosis: An immunohistochemical study. Experimental Neurology, 232(2), 149–153. https://doi.org/10.1016/j.expneurol.2011.08.015

Shih, A. Y., Imbeault, S., Barakauskas, V., Erb, H., Jiang, L., Li, P., & Murphy, T. H. (2005). Induction of the Nrf2-driven Antioxidant Response Confers Neuroprotection during Mitochondrial Stress in Vivo. Journal of Biological Chemistry, 280(24), 22925–22936. https://doi.org/10.1074/jbc.M414635200

Shih, A. Y., Johnson, D. A., Wong, G., Kraft, A. D., Jiang, L., Erb, H., Johnson, J. A., & Murphy, T. H. (2003). Coordinate Regulation of Glutathione Biosynthesis and Release by Nrf2-Expressing Glia Potently Protects Neurons from Oxidative Stress. The Journal of Neuroscience, 23(8), 3394–3406. https://doi.org/10.1523/JNEUROSCI.23-08-03394.2003

Shirsat, S. D., Londhe, P. V., Gaikwad, A. P., Rizwan, M., Laha, S. S., Khot, V. M., Achal, V., Tabish, T. A., & Thorat, N. D. (2024). Endosomal escape in magnetic nanostructures: Recent advances and future perspectives. Materials Today Advances, 22, 100484. https://doi.org/10.1016/j.mtadv.2024.100484

Shoesmith, C. L., Findlater, K., Rowe, A., & Strong, M. J. (2007). Prognosis of amyotrophic lateral sclerosis with respiratory onset. Journal of Neurology, Neurosurgery & Psychiatry, 78(6), 629–631. https://doi.org/10.1136/jnnp.2006.103564

Si, Y., Cui, X., Crossman, D. K., Hao, J., Kazamel, M., Kwon, Y., & King, P. H. (2018). Muscle microRNA signatures as biomarkers of disease progression in amyotrophic lateral sclerosis. Neurobiology of Disease, 114, 85–94. https://doi.org/10.1016/j.nbd.2018.02.009

Sillerud, L. O., Solberg, N. O., Chamberlain, R., Orlando, R. A., Heidrich, J. E., Brown, D. C., Brady, C. I., Vander Jagt, T. A., Garwood, M., & Vander Jagt, D. L. (2013). SPION-Enhanced Magnetic Resonance Imaging of Alzheimer's Disease Plaques in AβPP/PS-1 Transgenic Mouse Brain. Journal of Alzheimer's Disease, 34(2), 349–365. https://doi.org/10.3233/JAD-121171

Simandi, Z., Pajer, K., Karolyi, K., Sieler, T., Jiang, L.-L., Kolostyak, Z., Sari, Z., Fekecs, Z., Pap, A., Patsalos, A., Contreras, G. A., Reho, B., Papp, Z., Guo, X., Horvath, A., Kiss, G., Keresztessy, Z., Vámosi, G., Hickman, J., … Nagy, L. (2018). Arginine Methyltransferase PRMT8 Provides Cellular Stress Tolerance in Aging Motoneurons. The Journal of Neuroscience, 38(35), 7683–7700. https://doi.org/10.1523/JNEUROSCI.3389-17.2018

Simpson, E. P., Henry, Y. K., Henkel, J. S., Smith, R. G., & Appel, S. H. (2004). Increased lipid peroxidation in sera of ALS patients: A potential biomarker of disease burden. Neurology, 62(10), 1758–1765. https://doi.org/10.1212/WNL.62.10.1758

Singh, N., Ray, S., & Srivastava, A. (2018). Clinical mimickers of amyotrophic lateral sclerosis-conditions we cannot afford to miss. Annals of Indian Academy of Neurology, 21(3), 173. https://doi.org/10.4103/aian.AIAN_491_17

Singh, T., Jiao, Y., Ferrando, L. M., Yablonska, S., Li, F., Horoszko, E. C., Lacomis, D., Friedlander, R. M., & Carlisle, D. L. (2021). Neuronal mitochondrial dysfunction in sporadic amyotrophic lateral sclerosis is developmentally regulated. Scientific Reports, 11(1), 18916. https://doi.org/10.1038/s41598-021-97928-7

Sivakumar, P., De Giorgio, F., Ule, A. M., Neeves, J., Nair, R. R., Bentham, M., Birsa, N., Humphrey, J., Plagnol, V., Acevedo-Arozena, A., Cunningham, T. J., Fisher, E. M. C., & Fratta, P. (2018). TDP-43 mutations increase HNRNP A1-7B through gain of splicing function. Brain, 141(12), e83–e83. https://doi.org/10.1093/brain/awy260

Sleigh, J. N., Tosolini, A. P., Gordon, D., Devoy, A., Fratta, P., Fisher, E. M. C., Talbot, K., & Schiavo, G. (2020). Mice Carrying ALS Mutant TDP-43, but Not Mutant FUS, Display In Vivo Defects in Axonal Transport of Signaling Endosomes. Cell Reports, 30(11), 3655-3662.e2. https://doi.org/10.1016/j.celrep.2020.02.078

Sloan, K. E., Gleizes, P.-E., & Bohnsack, M. T. (2016). Nucleocytoplasmic Transport of RNAs and RNA–Protein Complexes. Journal of Molecular Biology, 428(10), 2040–2059. https://doi.org/10.1016/j.jmb.2015.09.023

Smith, E. N., Lee, J., Prilutsky, D., Zicha, S., Wang, Z., Han, S., & Zach, N. (2024). Plasma neurofilament light levels show elevation two years prior to diagnosis of amyotrophic lateral sclerosis in the UK Biobank. Amyotrophic Lateral Sclerosis and Frontotemporal Degeneration, 25(1–2), 170–176. https://doi.org/10.1080/21678421.2023.2285428

So, E., Mitchell, J. C., Memmi, C., Chennell, G., Vizcay-Barrena, G., Allison, L., Shaw, C. E., & Vance, C. (2018). Mitochondrial abnormalities and disruption of the neuromuscular junction precede the clinical phenotype and motor neuron loss in hFUSWT transgenic mice. Human Molecular Genetics, 27(3), 463–474. https://doi.org/10.1093/hmg/ddx415

Solomon, D. A., Stepto, A., Au, W. H., Adachi, Y., Diaper, D. C., Hall, R., Rekhi, A., Boudi, A., Tziortzouda, P., Lee, Y.-B., Smith, B., Bridi, J. C., Spinelli, G., Dearlove, J., Humphrey, D. M., Gallo, J.-M., Troakes, C., Fanto, M., Soller, M., … Hirth, F. (2018). A feedback loop between dipeptide-repeat protein, TDP-43 and karyopherin-α mediates C9orf72-related neurodegeneration. Brain, 141(10), 2908–2924. https://doi.org/10.1093/brain/awy241

Sommer, B., Köhler, M., Sprengel, R., & Seeburg, P. H. (1991). RNA editing in brain controls a determinant of ion flow in glutamate-gated channels. Cell, 67(1), 11–19. https://doi.org/10.1016/0092-8674(91)90568-J

Song, C., Li, H., Zheng, C., Zhang, T., & Zhang, Y. (2023). Dual Efficacy of a Catalytic Anti-Oligomeric Aβ42 scFv Antibody in Clearing Aβ42 Aggregates and Reducing Aβ Burden in the Brains of Alzheimer's Disease Mice. Molecular Neurobiology, 60(10), 5515–5532. https://doi.org/10.1007/s12035-023-03406-8

Song, W., Song, Y., Kincaid, B., Bossy, B., & Bossy-Wetzel, E. (2013). Mutant SOD1G93A triggers mitochondrial fragmentation in spinal cord motor neurons: Neuroprotection by SIRT3 and PGC-1α. Neurobiology of Disease, 51, 72–81. https://doi.org/10.1016/j.nbd.2012.07.004

Soo, K. Y., & Atkin, J. D. (2015). Autophagy dysregulation by mutant fused in sarcoma—Implications for amyotrophic lateral sclerosis. Cell Death & Disease, 6(10), e1945–e1945. https://doi.org/10.1038/cddis.2015.311

Spencer, B., Brüschweiler, S., Sealey-Cardona, M., Rockenstein, E., Adame, A., Florio, J., Mante, M., Trinh, I., Rissman, R. A., Konrat, R., & Masliah, E. (2018). Selective targeting of 3 repeat Tau with brain penetrating single chain antibodies for the treatment of neurodegenerative disorders. Acta Neuropathologica, 136(1), 69–87. https://doi.org/10.1007/s00401-018-1869-0

Sreedharan, J., Blair, I. P., Tripathi, V. B., Hu, X., Vance, C., Rogelj, B., Ackerley, S., Durnall, J. C., Williams, K. L., Buratti, E., Baralle, F., de Belleroche, J., Mitchell, J. D., Leigh, P. N., Al-Chalabi, A., Miller, C. C., Nicholson, G., & Shaw, C. E. (2008). TDP-43 Mutations in Familial and Sporadic Amyotrophic Lateral Sclerosis. Science, 319(5870), 1668–1672. https://doi.org/10.1126/science.1154584

Staderini, T., Bigi, A., Lagrève, C., Marzi, I., Bemporad, F., & Chiti, F. (2024). Biophysical characterization of the phase separation of TDP-43 devoid of the C-terminal domain. Cellular & Molecular Biology Letters, 29(1), 104. https://doi.org/10.1186/s11658-024-00615-4

Staderini, T., Bigi, A., Mongiello, D., Cecchi, C., & Chiti, F. (2022). Biophysical characterization of full-length TAR DNA-binding protein (TDP -43) phase separation. Protein Science, 31(12), e4509. https://doi.org/10.1002/pro.4509

Stella, R., Bonadio, R. S., Cagnin, S., Massimino, M. L., Bertoli, A., & Peggion, C. (2021). Perturbations of the Proteome and of Secreted Metabolites in Primary Astrocytes from the hSOD1(G93A) ALS Mouse Model. International Journal of Molecular Sciences, 22(13), 7028. https://doi.org/10.3390/ijms22137028

Štětkářová, I., & Ehler, E. (2021). Diagnostics of Amyotrophic Lateral Sclerosis: Up to Date. Diagnostics, 11(2), 231. https://doi.org/10.3390/diagnostics11020231

Steyn, F. J., Ioannides, Z. A., Van Eijk, R. P. A., Heggie, S., Thorpe, K. A., Ceslis, A., Heshmat, S., Henders, A. K., Wray, N. R., Van Den Berg, L. H., Henderson, R. D., McCombe, P. A., & Ngo, S. T. (2018). Hypermetabolism in ALS is associated with greater functional decline and shorter survival. Journal of Neurology, Neurosurgery & Psychiatry, 89(10), 1016–1023. https://doi.org/10.1136/jnnp-2017-317887

Steyn, F. J., Li, R., Kirk, S. E., Tefera, T. W., Xie, T. Y., Tracey, T. J., Kelk, D., Wimberger, E., Garton, F. C., Roberts, L., Chapman, S. E., Coombes, J. S., Leevy, W. M., Ferri, A., Valle, C., René, F., Loeffler, J.-P., McCombe, P. A., Henderson, R. D., & Ngo, S. T. (2020). Altered skeletal muscle glucose-fatty acid flux in amyotrophic lateral sclerosis. Brain Communications, fcaa154. https://doi.org/10.1093/braincomms/fcaa154

Stifani, N. (2014). Motor neurons and the generation of spinal motor neuron diversity. Frontiers in Cellular Neuroscience, 8. https://doi.org/10.3389/fncel.2014.00293

Strong, M. J., Abrahams, S., Goldstein, L. H., Woolley, S., Mclaughlin, P., Snowden, J., Mioshi, E., Roberts-South, A., Benatar, M., HortobáGyi, T., Rosenfeld, J., Silani, V., Ince, P. G., & Turner, M. R. (2017). Amyotrophic lateral sclerosis - frontotemporal spectrum disorder (ALS-FTSD): Revised diagnostic criteria. Amyotrophic Lateral Sclerosis and Frontotemporal Degeneration, 18(3–4), 153–174. https://doi.org/10.1080/21678421.2016.1267768

Strubbe-Rivera, J. O., Schrad, J. R., Pavlov, E. V., Conway, J. F., Parent, K. N., & Bazil, J. N. (2021). The mitochondrial permeability transition phenomenon elucidated by cryo-EM reveals the genuine impact of calcium overload on mitochondrial structure and function. Scientific Reports, 11(1), 1037. https://doi.org/10.1038/s41598-020-80398-8

Sukockienė, E., Iancu Ferfoglia, R., Truffert, A., Héritier Barras, A.-C., Genton, L., Viatte, V., Leuchter, I., Escher, M., Horie, N., Poncet, A., Pasquina, P., Adler, D., & Janssens, J.-P. (2020). Multidisciplinary care in amyotrophic lateral sclerosis: A 4-year longitudinal observational study. Swiss Medical Weekly, 150(2324), w20258. https://doi.org/10.4414/smw.2020.20258

Sun, Z.-T., Ma, C., Li, G.-J., Zheng, X.-Y., Hao, Y.-T., Yang, Y., & Wang, X. (2021). Application of Antibody Fragments Against Aβ With Emphasis on Combined Application With Nanoparticles in Alzheimer's Disease. Frontiers in Pharmacology, 12, 654611. https://doi.org/10.3389/fphar.2021.654611

Surpi, A., Shelyakova, T., Murgia, M., Rivas, J., Piñeiro, Y., Greco, P., Fini, M., & Dediu, V. A. (2023). Versatile magnetic configuration for the control and manipulation of superparamagnetic nanoparticles. Scientific Reports, 13(1), 5301. https://doi.org/10.1038/s41598-023-32299-9

Swarup, V., Phaneuf, D., Bareil, C., Robertson, J., Rouleau, G. A., Kriz, J., & Julien, J.-P. (2011). Pathological hallmarks of amyotrophic lateral sclerosis/frontotemporal lobar degeneration in transgenic mice

produced with TDP-43 genomic fragments. Brain, 134(9), 2610–2626. https://doi.org/10.1093/brain/awr159

Swarup, V., Phaneuf, D., Dupré, N., Petri, S., Strong, M., Kriz, J., & Julien, J.-P. (2011). Deregulation of TDP-43 in amyotrophic lateral sclerosis triggers nuclear factor κB–mediated pathogenic pathways. Journal of Experimental Medicine, 208(12), 2429–2447. https://doi.org/10.1084/jem.20111313

Swinnen, B., & Robberecht, W. (2014). The phenotypic variability of amyotrophic lateral sclerosis. Nature Reviews Neurology, 10(11), 661–670. https://doi.org/10.1038/nrneurol.2014.184

Syvänen, S., Fang, X. T., Hultqvist, G., Meier, S. R., Lannfelt, L., & Sehlin, D. (2017). A bispecific Tribody PET radioligand for visualization of amyloid-beta protofibrils – a new concept for neuroimaging. NeuroImage, 148, 55–63. https://doi.org/10.1016/j.neuroimage.2017.01.004

Szelechowski, M., Amoedo, N., Obre, E., Léger, C., Allard, L., Bonneu, M., Claverol, S., Lacombe, D., Oliet, S., Chevallier, S., Le Masson, G., & Rossignol, R. (2018). Metabolic Reprogramming in Amyotrophic Lateral Sclerosis. Scientific Reports, 8(1), 3953. https://doi.org/10.1038/s41598-018-22318-5

Tadić, V., Adam, A., Goldhammer, N., Lautenschlaeger, J., Oberstadt, M., Malci, A., Le, T. T., Sengupta, S., Stubendorff, B., Keiner, S., Witte, O. W., & Grosskreutz, J. (2019). Investigation of mitochondrial calcium uniporter role in embryonic and adult motor neurons from G93AhSOD1 mice. Neurobiology of Aging, 75, 209–222. https://doi.org/10.1016/j.neurobiolaging.2018.11.019

Tadokoro, K., Yamashita, T., Shang, J., Ohta, Y., Nomura, E., Morihara, R., Omote, Y., Takemoto, M., & Abe, K. (2021). Switching the Proteolytic System from the Ubiquitin–Proteasome System to Autophagy in the Spinal Cord of an Amyotrophic Lateral Sclerosis Mouse Model. Neuroscience, 466, 47–57. https://doi.org/10.1016/j.neuroscience.2021.04.034

Takayasu, Y., Nakaki, J., Kawasaki, T., Koda, K., Ago, Y., Baba, A., & Matsuda, T. (2007). Edaravone, a Radical Scavenger, Inhibits Mitochondrial Permeability Transition Pore in Rat Brain. Journal of Pharmacological Sciences, 103(4), 434–437. https://doi.org/10.1254/jphs.SC0070014

Talbott, E. O., Malek, A. M., & Lacomis, D. (2016). The epidemiology of amyotrophic lateral sclerosis. In Handbook of Clinical Neurology (Vol. 138, pp. 225–238). Elsevier. https://doi.org/10.1016/B978-0-12-802973-2.00013-6

Talley, K., & Alexov, E. (2010). On the pH-optimum of activity and stability of proteins. Proteins: Structure, Function, and Bioinformatics, 78(12), 2699–2706. https://doi.org/10.1002/prot.22786

Tamaki, Y., Shodai, A., Morimura, T., Hikiami, R., Minamiyama, S., Ayaki, T., Tooyama, I., Furukawa, Y., Takahashi, R., & Urushitani, M. (2018). Elimination of TDP-43 inclusions linked to amyotrophic lateral sclerosis by a misfolding-specific intrabody with dual proteolytic signals. Scientific Reports, 8(1), 6030. https://doi.org/10.1038/s41598-018-24463-3

Tan, L. K. S., How, C. W., Low, L. E., Ong, B. H., Loh, J. S., Lim, S.-Y., Ong, Y. S., & Foo, J. B. (2023). Magnetic-guided targeted delivery of zerumbone/SPION co-loaded in nanostructured lipid carrier into breast cancer cells. Journal of Drug Delivery Science and Technology, 87, 104830. https://doi.org/10.1016/j.jddst.2023.104830

Tandan, R., Howard, D., & Matthews, D. E. (2023). Increased total daily energy expenditure in mild to moderate ALS: Greater contribution from physical activity energy expenditure than hyper-metabolism.

Amyotrophic Lateral Sclerosis and Frontotemporal Degeneration, 24(7–8), 661–668. https://doi.org/10.1080/21678421.2023.2240377

Tateo, S., Shinchi, H., Matsumoto, H., Nagata, N., Hashimoto, M., Wakao, M., & Suda, Y. (2023). Optimized immobilization of single chain variable fragment antibody onto non-toxic fluorescent nanoparticles for efficient preparation of a bioprobe. Colloids and Surfaces B: Biointerfaces, 224, 113192. https://doi.org/10.1016/j.colsurfb.2023.113192

Tefera, T. W., Steyn, F. J., Ngo, S. T., & Borges, K. (2021). CNS glucose metabolism in Amyotrophic Lateral Sclerosis: A therapeutic target? Cell & Bioscience, 11(1), 14. https://doi.org/10.1186/s13578-020-00511-2

Thakor, K., Naud, S., Howard, D., Tandan, R., & Waheed, W. (2021). Effect of riluzole on weight in short-term and long-term survivors of amyotrophic lateral sclerosis. Amyotrophic Lateral Sclerosis and Frontotemporal Degeneration, 22(5–6), 360–367. https://doi.org/10.1080/21678421.2021.1874992

Thakur, A., Parra, D. C., Motallebnejad, P., Brocchi, M., & Chen, H. J. (2022). Exosomes: Small vesicles with big roles in cancer, vaccine development, and therapeutics. Bioactive Materials, 10, 281–294. https://doi.org/10.1016/j.bioactmat.2021.08.029

The Food and Drug Administration. (2017, May 5). FDA approves drug to treat ALS [Online post]. https://www.fda.gov/news-events/press-announcements/fda-approves-drug-treat-als#:~:text=The%20U.S.%20Food%20and%20Drug,to%20as%20Lou%20Gehrig%27s%20disease.

The Food and Drug Administration. (2022, December 5). FDA Approves Oral Form for the treatment of adults with amyotrophic lateral sclerosis (ALS) [Online post]. https://www.fda.gov/drugs/news-events-human-drugs/fda-approves-oral-form-treatment-adults-amyotrophic-lateral-sclerosis-als#:~:text=FDA%20has%20approved%20Radicava%20ORS,to%20as%20Lou%20Gehrig%27s%20disease.

The Food and Drug Administration. (2023, April 25). FDA approves treatment of amyotrophic lateral sclerosis associated with a mutation in the SOD1 gene [Online post]. https://www.fda.gov/drugs/news-events-human-drugs/fda-approves-treatment-amyotrophic-lateral-sclerosis-associated-mutation-sod1-gene

The Food and Drug Administration. (2024, February 8). Approved Cellular and Gene Therapy Products [Online post]. https://www.fda.gov/vaccines-blood-biologics/cellular-gene-therapy-products/approved-cellular-and-gene-therapy-products

The Writing Group on Behalf of the Edaravone (MCI-186) ALS 18 Study Group. (2017). Exploratory double-blind, parallel-group, placebo-controlled study of edaravone (MCI-186) in amyotrophic lateral sclerosis (Japan ALS severity classification: Grade 3, requiring assistance for eating, excretion or ambulation). Amyotrophic Lateral Sclerosis and Frontotemporal Degeneration, 18(sup1), 40–48. https://doi.org/10.1080/21678421.2017.1361441

Thomsen, M. S., Johnsen, K. B., Kucharz, K., Lauritzen, M., & Moos, T. (2022). Blood–Brain Barrier Transport of Transferrin Receptor-Targeted Nanoparticles. Pharmaceutics, 14(10), 2237. https://doi.org/10.3390/pharmaceutics14102237

Thurber, G. M., Zajic, S. C., & Wittrup, K. D. (2007). Theoretic Criteria for Antibody Penetration into Solid Tumors and Micrometastases. Journal of Nuclear Medicine, 48(6), 995–999. https://doi.org/10.2967/jnumed.106.037069

Tibshirani, M., Tradewell, M. L., Mattina, K. R., Minotti, S., Yang, W., Zhou, H., Strong, M. J., Hayward, L. J., & Durham, H. D. (2015). Cytoplasmic sequestration of FUS/TLS associated with ALS alters histone marks through loss of nuclear protein arginine methyltransferase 1. Human Molecular Genetics, 24(3), 773–786. https://doi.org/10.1093/hmg/ddu494

Tohgi, H., Abe, T., Yamazaki, K., Murata, T., Ishizaki, E., & Isobe, C. (1999). Remarkable increase in cerebrospinal fluid 3-nitrotyrosine in patients with sporadic amyotrophic lateral sclerosis. Annals of Neurology, 46(1), 129–131. https://doi.org/10.1002/1531-8249(199907)46:1<129::AID-ANA21>3.0.CO;2-Y

Tollervey, J. R., Curk, T., Rogelj, B., Briese, M., Cereda, M., Kayikci, M., König, J., Hortobágyi, T., Nishimura, A. L., Župunski, V., Patani, R., Chandran, S., Rot, G., Zupan, B., Shaw, C. E., & Ule, J. (2011). Characterizing the RNA targets and position-dependent splicing regulation by TDP-43. Nature Neuroscience, 14(4), 452–458. https://doi.org/10.1038/nn.2778

Tortarolo, M., Lo Coco, D., Veglianese, P., Vallarola, A., Giordana, M. T., Marcon, G., Beghi, E., Poloni, M., Strong, M. J., Iyer, A. M., Aronica, E., & Bendotti, C. (2017). Amyotrophic Lateral Sclerosis, a Multisystem Pathology: Insights into the Role of TNF α. Mediators of Inflammation, 2017, 1–16. https://doi.org/10.1155/2017/2985051

Tradewell, M. L., Cooper, L. A., Minotti, S., & Durham, H. D. (2011). Calcium dysregulation, mitochondrial pathology and protein aggregation in a culture model of amyotrophic lateral sclerosis: Mechanistic relationship and differential sensitivity to intervention. Neurobiology of Disease, 42(3), 265–275. https://doi.org/10.1016/j.nbd.2011.01.016

Traynor, B. J., Codd, M. B., Corr, B., Forde, C., Frost, E., & Hardiman, O. M. (2000). Clinical Features of Amyotrophic Lateral Sclerosis According to the El Escorial and Airlie House Diagnostic Criteria: A Population-Based Study. Archives of Neurology, 57(8), 1171. https://doi.org/10.1001/archneur.57.8.1171

Tsai, Y.-L., Coady, T. H., Lu, L., Zheng, D., Alland, I., Tian, B., Shneider, N. A., & Manley, J. L. (2020). ALS/FTD-associated protein FUS induces mitochondrial dysfunction by preferentially sequestering respiratory chain complex mRNAs. Genes & Development, 34(11–12), 785–805. https://doi.org/10.1101/gad.335836.119

Tsirkas, I., Zur, T., Dovrat, D., Cohen, A., Ravkaie, L., & Aharoni, A. (2022). Protein fluorescent labeling in live yeast cells using scFv-based probes. Cell Reports Methods, 2(12), 100357. https://doi.org/10.1016/j.crmeth.2022.100357

Turner, M. R., Barnwell, J., Al-Chalabi, A., & Eisen, A. (2012). Young-onset amyotrophic lateral sclerosis: Historical and other observations. Brain, 135(9), 2883–2891. https://doi.org/10.1093/brain/aws144

Turner, M. R., Scaber, J., Goodfellow, J. A., Lord, M. E., Marsden, R., & Talbot, K. (2010). The diagnostic pathway and prognosis in bulbar-onset amyotrophic lateral sclerosis. Journal of the Neurological Sciences, 294(1–2), 81–85. https://doi.org/10.1016/j.jns.2010.03.028

Urbani, A., & Belluzzi, O. (2000). Riluzole inhibits the persistent sodium current in mammalian CNS neurons. European Journal of Neuroscience, 12(10), 3567–3574. https://doi.org/10.1046/j.1460-9568.2000.00242.x

Vahsen, B. F., Nalluru, S., Morgan, G. R., Farrimond, L., Carroll, E., Xu, Y., Cramb, K. M. L., Amein, B., Scaber, J., Katsikoudi, A., Candalija, A., Carcolé, M., Dafinca, R., Isaacs, A. M., Wade-Martins, R., Gray, E., Turner, M. R., Cowley, S. A., & Talbot, K. (2023). C9orf72-ALS human iPSC microglia are pro-inflammatory and

toxic to co-cultured motor neurons via MMP9. Nature Communications, 14(1), 5898. https://doi.org/10.1038/s41467-023-41603-0

Valdez, G., Tapia, J. C., Lichtman, J. W., Fox, M. A., & Sanes, J. R. (2012). Shared Resistance to Aging and ALS in Neuromuscular Junctions of Specific Muscles. PLoS ONE, 7(4), e34640. https://doi.org/10.1371/journal.pone.0034640

Van Blitterswijk, M., Van Es, M. A., Hennekam, E. A. M., Dooijes, D., Van Rheenen, W., Medic, J., Bourque, P. R., Schelhaas, H. J., Van Der Kooi, A. J., De Visser, M., De Bakker, P. I. W., Veldink, J. H., & Van Den Berg, L. H. (2012). Evidence for an oligogenic basis of amyotrophic lateral sclerosis. Human Molecular Genetics, 21(17), 3776–3784. https://doi.org/10.1093/hmg/dds199

Van Daele, S. H., Moisse, M., Van Vugt, J. J. F. A., Zwamborn, R. A. J., Van Der Spek, R., Van Rheenen, W., Van Eijk, K., Kenna, K., Corcia, P., Vourc'h, P., Couratier, P., Hardiman, O., McLaughin, R., Gotkine, M., Drory, V., Ticozzi, N., Silani, V., Ratti, A., De Carvalho, M., … Van Damme, P. (2023). Genetic variability in sporadic amyotrophic lateral sclerosis. Brain, 146(9), 3760–3769. https://doi.org/10.1093/brain/awad120

Van Den Bos, M. A. J., Higashihara, M., Geevasinga, N., Menon, P., Kiernan, M. C., & Vucic, S. (2018). Imbalance of cortical facilitatory and inhibitory circuits underlies hyperexcitability in ALS. Neurology, 91(18). https://doi.org/10.1212/WNL.0000000000006438

Van Laere, K., Vanhee, A., Verschueren, J., De Coster, L., Driesen, A., Dupont, P., Robberecht, W., & Van Damme, P. (2014). Value of 18 Fluorodeoxyglucose–Positron-Emission Tomography in Amyotrophic Lateral Sclerosis: A Prospective Study. JAMA Neurology, 71(5), 553. https://doi.org/10.1001/jamaneurol.2014.62

Vande Velde, C., Miller, T. M., Cashman, N. R., & Cleveland, D. W. (2008). Selective association of misfolded ALS-linked mutant SOD1 with the cytoplasmic face of mitochondria. Proceedings of the National Academy of Sciences, 105(10), 4022–4027. https://doi.org/10.1073/pnas.0712209105

Vangijzegem, T., Lecomte, V., Ternad, I., Van Leuven, L., Muller, R. N., Stanicki, D., & Laurent, S. (2023). Superparamagnetic Iron Oxide Nanoparticles (SPION): From Fundamentals to State-of-the-Art Innovative Applications for Cancer Therapy. Pharmaceutics, 15(1), 236. https://doi.org/10.3390/pharmaceutics15010236

Vázquez-Costa, J. F., Campins-Romeu, M., Martínez-Payá, J. J., Tembl, J. I., Del Baño-Aledo, M. E., Ríos-Díaz, J., Fornés-Ferrer, V., Chumillas, M. J., & Sevilla, T. (2018). New insights into the pathophysiology of fasciculations in amyotrophic lateral sclerosis: An ultrasound study. Clinical Neurophysiology, 129(12), 2650–2657. https://doi.org/10.1016/j.clinph.2018.09.014

Velappan, N., Close, D., Hung, L.-W., Naranjo, L., Hemez, C., DeVore, N., McCullough, D. K., Lillo, A. M., Waldo, G. S., & Bradbury, A. R. M. (2021). Construction, characterization and crystal structure of a fluorescent single-chain Fv chimera. Protein Engineering, Design and Selection, 34, gzaa029. https://doi.org/10.1093/protein/gzaa029

Veldink, J. H. (2017). ALS genetic epidemiology 'How simplex is the genetic epidemiology of ALS?' Journal of Neurology, Neurosurgery & Psychiatry, 88(7), 537–537. https://doi.org/10.1136/jnnp-2016-315469

Verde, F., Otto, M., & Silani, V. (2021). Neurofilament Light Chain as Biomarker for Amyotrophic Lateral Sclerosis and Frontotemporal Dementia. Frontiers in Neuroscience, 15, 679199. https://doi.org/10.3389/fnins.2021.679199

Verdile, V., Palombo, R., Ferrante, G., Ferri, A., Amadio, S., Volonté, C., & Paronetto, M. P. (2023). Dysregulation of alternative splicing underlies synaptic defects in familial amyotrophic lateral sclerosis. Progress in Neurobiology, 231, 102529. https://doi.org/10.1016/j.pneurobio.2023.102529

Versluys, L., Ervilha Pereira, P., Schuermans, N., De Paepe, B., De Bleecker, J. L., Bogaert, E., & Dermaut, B. (2022). Expanding the TDP-43 Proteinopathy Pathway From Neurons to Muscle: Physiological and Pathophysiological Functions. Frontiers in Neuroscience, 16, 815765. https://doi.org/10.3389/fnins.2022.815765

Vielhaber, S. (2000). Mitochondrial DNA abnormalities in skeletal muscle of patients with sporadic amyotrophic lateral sclerosis. Brain, 123(7), 1339–1348. https://doi.org/10.1093/brain/123.7.1339

Vijayvergiya, C., Beal, M. F., Buck, J., & Manfredi, G. (2005). Mutant Superoxide Dismutase 1 Forms Aggregates in the Brain Mitochondrial Matrix of Amyotrophic Lateral Sclerosis Mice. The Journal of Neuroscience, 25(10), 2463–2470. https://doi.org/10.1523/JNEUROSCI.4385-04.2005

Vucic, S., & Kiernan, M. C. (2010). Upregulation of persistent sodium conductances in familial ALS. Journal of Neurology, Neurosurgery & Psychiatry, 81(2), 222–227. https://doi.org/10.1136/jnnp.2009.183079

Vucic, S., Lin, C. S.-Y., Cheah, B. C., Murray, J., Menon, P., Krishnan, A. V., & Kiernan, M. C. (2013). Riluzole exerts central and peripheral modulating effects in amyotrophic lateral sclerosis. Brain, 136(5), 1361–1370. https://doi.org/10.1093/brain/awt085

Vucic, S., Nicholson, G. A., & Kiernan, M. C. (2008). Cortical hyperexcitability may precede the onset of familial amyotrophic lateral sclerosis. Brain, 131(6), 1540–1550. https://doi.org/10.1093/brain/awn071

Wahajuddin & Arora. (2012). Superparamagnetic iron oxide nanoparticles: Magnetic nanoplatforms as drug carriers. International Journal of Nanomedicine, 3445. https://doi.org/10.2147/IJN.S30320

Waller, R., Goodall, E. F., Milo, M., Cooper-Knock, J., Da Costa, M., Hobson, E., Kazoka, M., Wollff, H., Heath, P. R., Shaw, P. J., & Kirby, J. (2017). Serum miRNAs miR-206, 143-3p and 374b-5p as potential biomarkers for amyotrophic lateral sclerosis (ALS). Neurobiology of Aging, 55, 123–131. https://doi.org/10.1016/j.neurobiolaging.2017.03.027

Wang, B., Huang, M., Shang, D., Yan, X., Zhao, B., & Zhang, X. (2021). Mitochondrial Behavior in Axon Degeneration and Regeneration. Frontiers in Aging Neuroscience, 13, 650038. https://doi.org/10.3389/fnagi.2021.650038

Wang, G.-H., Jiang, Z.-L., Li, Y.-C., Li, X., Shi, H., Gao, Y.-Q., Vosler, P. S., & Chen, J. (2011). Free-Radical Scavenger Edaravone Treatment Confers Neuroprotection Against Traumatic Brain Injury in Rats. Journal of Neurotrauma, 28(10), 2123–2134. https://doi.org/10.1089/neu.2011.1939

Wang, H., Guan, L., & Deng, M. (2023). Recent progress of the genetics of amyotrophic lateral sclerosis and challenges of gene therapy. Frontiers in Neuroscience, 17, 1170996. https://doi.org/10.3389/fnins.2023.1170996

Wang, H., O'Reilly, É. J., Weisskopf, M. G., Logroscino, G., McCullough, M. L., Thun, M. J., Schatzkin, A., Kolonel, L. N., & Ascherio, A. (2011). Smoking and Risk of Amyotrophic Lateral Sclerosis: A Pooled Analysis of 5 Prospective Cohorts. Archives of Neurology, 68(2). https://doi.org/10.1001/archneurol.2010.367

Wang, H., Wang, Y., Yuan, C., Xu, X., Zhou, W., Huang, Y., Lu, H., Zheng, Y., Luo, G., Shang, J., & Sui, M. (2023). Polyethylene glycol (PEG)-associated immune responses triggered by clinically relevant lipid nanoparticles in rats. Npj Vaccines, 8(1), 169. https://doi.org/10.1038/s41541-023-00766-z

Wang, H.-M., Zhang, T., Huang, J.-K., Xiang, J.-Y., Chen, J., Fu, J.-L., & Zhao, Y.-W. (2017). Edaravone Attenuates the Proinflammatory Response in Amyloid-β-Treated Microglia by Inhibiting NLRP3 Inflammasome-Mediated IL-1β Secretion. Cellular Physiology and Biochemistry, 43(3), 1113–1125. https://doi.org/10.1159/000481753

Wang, J., Choi, J.-M., Holehouse, A. S., Lee, H. O., Zhang, X., Jahnel, M., Maharana, S., Lemaitre, R., Pozniakovsky, A., Drechsel, D., Poser, I., Pappu, R. V., Alberti, S., & Hyman, A. A. (2018). A Molecular Grammar Governing the Driving Forces for Phase Separation of Prion-like RNA Binding Proteins. Cell, 174(3), 688-699.e16. https://doi.org/10.1016/j.cell.2018.06.006

Wang, P., Deng, J., Dong, J., Liu, J., Bigio, E. H., Mesulam, M., Wang, T., Sun, L., Wang, L., Lee, A. Y.-L., McGee, W. A., Chen, X., Fushimi, K., Zhu, L., & Wu, J. Y. (2019). TDP-43 induces mitochondrial damage and activates the mitochondrial unfolded protein response. PLOS Genetics, 15(5), e1007947. https://doi.org/10.1371/journal.pgen.1007947

Wang, T., Tomas, D., Perera, N. D., Cuic, B., Luikinga, S., Viden, A., Barton, S. K., McLean, C. A., Samson, A. L., Southon, A., Bush, A. I., Murphy, J. M., & Turner, B. J. (2022). Ferroptosis mediates selective motor neuron death in amyotrophic lateral sclerosis. Cell Death & Differentiation, 29(6), 1187–1198. https://doi.org/10.1038/s41418-021-00910-z

Wang, T.-W., Wuu, J., Cooley, A., Yeh, T.-S., Benatar, M., & Weisskopf, M. (2023). Occupational lead exposure and survival with amyotrophic lateral sclerosis. Amyotrophic Lateral Sclerosis and Frontotemporal Degeneration, 24(1–2), 100–107. https://doi.org/10.1080/21678421.2022.2059379

Wang, W., Li, L., Lin, W.-L., Dickson, D. W., Petrucelli, L., Zhang, T., & Wang, X. (2013). The ALS disease-associated mutant TDP-43 impairs mitochondrial dynamics and function in motor neurons. Human Molecular Genetics, 22(23), 4706–4719. https://doi.org/10.1093/hmg/ddt319

Wang, W., Wang, L., Lu, J., Siedlak, S. L., Fujioka, H., Liang, J., Jiang, S., Ma, X., Jiang, Z., da Rocha, E. L., Sheng, M., Choi, H., Lerou, P. H., Li, H., & Wang, X. (2016). The inhibition of TDP-43 mitochondrial localization blocks its neuronal toxicity. Nature Medicine, 22(8), 869–878. https://doi.org/10.1038/nm.4130

Wang, Y.-J., Lin, M.-W., Lin, A.-A., & Wu, S.-N. (2008). Riluzole-induced block of voltage-gated Na+ current and activation of BKCa channels in cultured differentiated human skeletal muscle cells. Life Sciences, 82(1–2), 11–20. https://doi.org/10.1016/j.lfs.2007.10.015

Watanabe, K., Tanaka, M., Yuki, S., Hirai, M., & Yamamoto, Y. (2018). How is edaravone effective against acute ischemic stroke and amyotrophic lateral sclerosis? Journal of Clinical Biochemistry and Nutrition, 62(1), 20–38. https://doi.org/10.3164/jcbn.17-62

Watanabe, T., Morita, I., Nishi, H., & Murota, S.-I. (1988). Preventive effect of MCI-186 on 15-HPETE induced vascular endothelial cell injury in vitro. Prostaglandins, Leukotrienes and Essential Fatty Acids, 33(1), 81–87. https://doi.org/10.1016/0952-3278(88)90127-5

Waters, S., Swanson, M. E. V., Dieriks, B. V., Zhang, Y. B., Grimsey, N. L., Murray, H. C., Turner, C., Waldvogel, H. J., Faull, R. L. M., An, J., Bowser, R., Curtis, M. A., Dragunow, M., & Scotter, E. (2021). Blood-spinal cord

barrier leakage is independent of motor neuron pathology in ALS. Acta Neuropathologica Communications, 9(1), 144. https://doi.org/10.1186/s40478-021-01244-0

Wei, H., Chen, Q., Lin, L., Sha, C., Li, T., Liu, Y., Yin, X., Xu, Y., Chen, L., Gao, W., Li, Y., & Zhu, X. (2021). Regulation of exosome production and cargo sorting. International Journal of Biological Sciences, 17(1), 163–177. https://doi.org/10.7150/ijbs.53671

Wei, Y., Lim, L., Wang, L., & Song, J. (2016). Inter-domain interactions of TDP-43 as decoded by NMR. Biochemical and Biophysical Research Communications, 473(2), 614–619. https://doi.org/10.1016/j.bbrc.2016.03.158

Weishaupt, J. H., Bartels, C., Pölking, E., Dietrich, J., Rohde, G., Poeggeler, B., Mertens, N., Sperling, S., Bohn, M., Hüther, G., Schneider, A., Bach, A., Sirén, A., Hardeland, R., Bähr, M., Nave, K., & Ehrenreich, H. (2006). Reduced oxidative damage in ALS by high-dose enteral melatonin treatment. Journal of Pineal Research, 41(4), 313–323. https://doi.org/10.1111/j.1600-079X.2006.00377.x

Weishaupt, J. H., Körtvélyessy, P., Schumann, P., Valkadinov, I., Weyen, U., Hesebeck-Brinckmann, J., Weishaupt, K., Endres, M., Andersen, P. M., Regensburger, M., Dreger, M., Koch, J. C., Conrad, J., & Meyer, T. (2024). Tofersen decreases neurofilament levels supporting the pathogenesis of the SOD1 p.D91A variant in amyotrophic lateral sclerosis patients. Communications Medicine, 4(1), 150. https://doi.org/10.1038/s43856-024-00573-0

Weisskopf, M. G. (2004). Prospective Study of Cigarette Smoking and Amyotrophic Lateral Sclerosis. American Journal of Epidemiology, 160(1), 26–33. https://doi.org/10.1093/aje/kwh179

Wiedemann, F. R., Manfredi, G., Mawrin, C., Beal, M. F., & Schon, E. A. (2002). Mitochondrial DNA and respiratory chain function in spinal cords of ALS patients. Journal of Neurochemistry, 80(4), 616–625. https://doi.org/10.1046/j.0022-3042.2001.00731.x

Wijegunawardana, D., Vishal, S. S., Venkatesh, N., & Gopal, P. P. (2023). Ataxin-2 polyglutamine expansions aberrantly sequester TDP-43, drive ribonucleoprotein condensate transport dysfunction and suppress local translation. https://doi.org/10.1101/2023.01.30.526372

Wild, C. P. (2005). Complementing the Genome with an "Exposome": The Outstanding Challenge of Environmental Exposure Measurement in Molecular Epidemiology. Cancer Epidemiology, Biomarkers & Prevention, 14(8), 1847–1850. https://doi.org/10.1158/1055-9965.EPI-05-0456

Wildberg, C., Masuch, A., Budde, K., Kastenmüller, G., Artati, A., Rathmann, W., Adamski, J., Kocher, T., Völzke, H., Nauck, M., Friedrich, N., & Pietzner, M. (2019). Plasma Metabolomics to Identify and Stratify Patients With Impaired Glucose Tolerance. The Journal of Clinical Endocrinology & Metabolism, 104(12), 6357–6370. https://doi.org/10.1210/jc.2019-01104

Wilhelmi, P., Giri, V., Zickgraf, F. M., Haake, V., Henkes, S., Driemert, P., Michaelis, P., Busch, W., Scholz, S., Flick, B., Barenys, M., Birk, B., Kamp, H., Landsiedel, R., & Funk-Weyer, D. (2023). A metabolomics approach to reveal the mechanism of developmental toxicity in zebrafish embryos exposed to 6-propyl-2-thiouracil. Chemico-Biological Interactions, 382, 110565. https://doi.org/10.1016/j.cbi.2023.110565

Williams, K. L., Fifita, J. A., Vucic, S., Durnall, J. C., Kiernan, M. C., Blair, I. P., & Nicholson, G. A. (2013). Pathophysiological insights into ALS with C9ORF72 expansions. Journal of Neurology, Neurosurgery & Psychiatry, 84(8), 931–935. https://doi.org/10.1136/jnnp-2012-304529

Winton, M. J., Igaz, L. M., Wong, M. M., Kwong, L. K., Trojanowski, J. Q., & Lee, V. M.-Y. (2008). Disturbance of Nuclear and Cytoplasmic TAR DNA-binding Protein (TDP-43) Induces Disease-like Redistribution, Sequestration, and Aggregate Formation. Journal of Biological Chemistry, 283(19), 13302–13309. https://doi.org/10.1074/jbc.M800342200

Witzel, S., Frauhammer, F., Steinacker, P., Devos, D., Pradat, P.-F., Meininger, V., Halbgebauer, S., Oeckl, P., Schuster, J., Anders, S., Dorst, J., Otto, M., & Ludolph, A. C. (2021). Neurofilament light and heterogeneity of disease progression in amyotrophic lateral sclerosis: Development and validation of a prediction model to improve interventional trials. Translational Neurodegeneration, 10(1), 31. https://doi.org/10.1186/s40035-021-00257-y

Witzel, S., Maier, A., Steinbach, R., Grosskreutz, J., Koch, J. C., Sarikidi, A., Petri, S., Günther, R., Wolf, J., Hermann, A., Prudlo, J., Cordts, I., Lingor, P., Löscher, W. N., Kohl, Z., Hagenacker, T., Ruckes, C., Koch, B., Spittel, S., … German Motor Neuron Disease Network (MND-NET). (2022). Safety and Effectiveness of Long-term Intravenous Administration of Edaravone for Treatment of Patients With Amyotrophic Lateral Sclerosis. JAMA Neurology, 79(2), 121. https://doi.org/10.1001/jamaneurol.2021.4893

Woerner, A. C., Frottin, F., Hornburg, D., Feng, L. R., Meissner, F., Patra, M., Tatzelt, J., Mann, M., Winklhofer, K. F., Hartl, F. U., & Hipp, M. S. (2016). Cytoplasmic protein aggregates interfere with nucleocytoplasmic transport of protein and RNA. Science, 351(6269), 173–176. https://doi.org/10.1126/science.aad2033

Wojnilowicz, M., Glab, A., Bertucci, A., Caruso, F., & Cavalieri, F. (2019). Super-resolution Imaging of Proton Sponge-Triggered Rupture of Endosomes and Cytosolic Release of Small Interfering RNA. ACS Nano, 13(1), 187–202. https://doi.org/10.1021/acsnano.8b05151

Wolf, S. A., Boddeke, H. W. G. M., & Kettenmann, H. (2017). Microglia in Physiology and Disease. Annual Review of Physiology, 79(1), 619–643. https://doi.org/10.1146/annurev-physiol-022516-034406

Wolozin, B., & Ivanov, P. (2019). Stress granules and neurodegeneration. Nature Reviews Neuroscience, 20(11), 649–666. https://doi.org/10.1038/s41583-019-0222-5

Wood, H. (2022). Study reveals new ALS risk genes. Nature Reviews Neurology, 18(3), 128–128. https://doi.org/10.1038/s41582-022-00622-z

Wright, A., & Vissel, B. (2012). The essential role of AMPA receptor GluR2 subunit RNA editing in the normal and diseased brain. Frontiers in Molecular Neuroscience, 5. https://doi.org/10.3389/fnmol.2012.00034

Wu, D.-C., Ré, D. B., Nagai, M., Ischiropoulos, H., & Przedborski, S. (2006). The inflammatory NADPH oxidase enzyme modulates motor neuron degeneration in amyotrophic lateral sclerosis mice. Proceedings of the National Academy of Sciences, 103(32), 12132–12137. https://doi.org/10.1073/pnas.0603670103

Wu, J. J., Cai, A., Greenslade, J. E., Higgins, N. R., Fan, C., Le, N. T. T., Tatman, M., Whiteley, A. M., Prado, M. A., Dieriks, B. V., Curtis, M. A., Shaw, C. E., Siddique, T., Faull, R. L. M., Scotter, E. L., Finley, D., & Monteiro, M. J. (2020). ALS/FTD mutations in UBQLN2 impede autophagy by reducing autophagosome acidification through loss of function. Proceedings of the National Academy of Sciences, 117(26), 15230–15241. https://doi.org/10.1073/pnas.1917371117

Wu, M., Zhang, D., Zeng, Y., Wu, L., Liu, X., & Liu, J. (2015). Nanocluster of superparamagnetic iron oxide nanoparticles coated with poly (dopamine) for magnetic field-targeting, highly sensitive MRI and photothermal cancer therapy. Nanotechnology, 26(11), 115102. https://doi.org/10.1088/0957-4484/26/11/115102

Wuolikainen, A., Jonsson, P., Ahnlund, M., Antti, H., Marklund, S. L., Moritz, T., Forsgren, L., Andersen, P. M., & Trupp, M. (2016). Multi-platform mass spectrometry analysis of the CSF and plasma metabolomes of rigorously matched amyotrophic lateral sclerosis, Parkinson's disease and control subjects. Molecular BioSystems, 12(4), 1287–1298. https://doi.org/10.1039/C5MB00711A

Wymer, J., Apple, S., Harrison, A., & Hill, B. A. (2023). Pharmacokinetics, Bioavailability, and Swallowing Safety With Riluzole Oral Film. Clinical Pharmacology in Drug Development, 12(1), 57–64. https://doi.org/10.1002/cpdd.1168

Xia, L., Song, X., Yan, G., Quan, J., & Jin, G. (2022). Preparation and evaluation of LA-PEG-SPION, a targeted MRI contrast agent for liver cancer. Open Life Sciences, 17(1), 952–959. https://doi.org/10.1515/biol-2022-0074

Xia, R., Liu, Y., Yang, L., Gal, J., Zhu, H., & Jia, J. (2012). Motor neuron apoptosis and neuromuscular junction perturbation are prominent features in a Drosophila model of Fus-mediated ALS. Molecular Neurodegeneration, 7(1), 10. https://doi.org/10.1186/1750-1326-7-10

Xiao, S., Sanelli, T., Chiang, H., Sun, Y., Chakrabartty, A., Keith, J., Rogaeva, E., Zinman, L., & Robertson, J. (2015). Low molecular weight species of TDP-43 generated by abnormal splicing form inclusions in amyotrophic lateral sclerosis and result in motor neuron death. Acta Neuropathologica, 130(1), 49–61. https://doi.org/10.1007/s00401-015-1412-5

Xiao, X., Li, N., Wang, M., Xiong, C., Xie, D., Chu, X., Li, Y., Huang, Y., Ling, W., Li, Y., & Qiu, X. (2020). Delivery of plasmid DNA encoding Oct 4 with polyethylenimine-modified superparamagnetic iron oxide nanoparticles in HEK-293T cells. Journal of Nanoparticle Research, 22(5), 128. https://doi.org/10.1007/s11051-020-04864-0

Xu, L., Liu, T., Liu, L., Yao, X., Chen, L., Fan, D., Zhan, S., & Wang, S. (2020). Global variation in prevalence and incidence of amyotrophic lateral sclerosis: A systematic review and meta-analysis. Journal of Neurology, 267(4), 944–953. https://doi.org/10.1007/s00415-019-09652-y

Yamakawa, M., Ito, D., Honda, T., Kubo, K., Noda, M., Nakajima, K., & Suzuki, N. (2015). Characterization of the dipeptide repeat protein in the molecular pathogenesis of c9FTD/ALS. Human Molecular Genetics, 24(6), 1630–1645. https://doi.org/10.1093/hmg/ddu576

Yamamura, M., Miyamoto, Y., Mitsuno, M., Tanaka, H., Ryomoto, M., & Fukui, S. (2013). Edaravone Suppresses Reperfusion Injury following Leg Ischemia in Rats: A Transmission Electron Microscopic Study. International Journal of Angiology, 22(04), 267–270. https://doi.org/10.1055/s-0033-1357261

Yamashita, T., & Kwak, S. (2014). The molecular link between inefficient GluA2 Q/R site-RNA editing and TDP-43 pathology in motor neurons of sporadic amyotrophic lateral sclerosis patients. Brain Research, 1584, 28–38. https://doi.org/10.1016/j.brainres.2013.12.011

Yang, B., Pan, J., Zhang, X.-N., Wang, H., He, L., Rong, X., Li, X., & Peng, Y. (2023). NRF2 activation suppresses motor neuron ferroptosis induced by the SOD1G93A mutation and exerts neuroprotection in amyotrophic lateral sclerosis. Neurobiology of Disease, 184, 106210. https://doi.org/10.1016/j.nbd.2023.106210

Yang, Y., Hentati, A., Deng, H.-X., Dabbagh, O., Sasaki, T., Hirano, M., Hung, W.-Y., Ouahchi, K., Yan, J., Azim, A. C., Cole, N., Gascon, G., Yagmour, A., Ben-Hamida, M., Pericak-Vance, M., Hentati, F., & Siddique, T. (2001). The gene encoding alsin, a protein with three guanine-nucleotide exchange factor domains, is

mutated in a form of recessive amyotrophic lateral sclerosis. Nature Genetics, 29(2), 160–165. https://doi.org/10.1038/ng1001-160

Yerbury, J. J., Ooi, L., Blair, I. P., Ciryam, P., Dobson, C. M., & Vendruscolo, M. (2019). The metastability of the proteome of spinal motor neurons underlies their selective vulnerability in ALS. Neuroscience Letters, 704, 89–94. https://doi.org/10.1016/j.neulet.2019.04.001

Yin, P., Bai, D., Zhu, L., Deng, F., Guo, X., Li, B., Chen, L., Li, S., & Li, X.-J. (2021). Cytoplasmic TDP-43 impairs the activity of the ubiquitin-proteasome system. Experimental Neurology, 345, 113833. https://doi.org/10.1016/j.expneurol.2021.113833

Yin, S., Lopez-Gonzalez, R., Kunz, R. C., Gangopadhyay, J., Borufka, C., Gygi, S. P., Gao, F.-B., & Reed, R. (2017). Evidence that C9ORF72 Dipeptide Repeat Proteins Associate with U2 snRNP to Cause Mis-splicing in ALS/FTD Patients. Cell Reports, 19(11), 2244–2256. https://doi.org/10.1016/j.celrep.2017.05.056

Yoshikawa, M., Aizawa, S., Oppenheim, R. W., & Milligan, C. (2022). Neurovascular unit pathology is observed very early in disease progression in the mutant SOD1G93A mouse model of amyotrophic lateral sclerosis. Experimental Neurology, 353, 114084. https://doi.org/10.1016/j.expneurol.2022.114084

Yu, X., Wang, T., Chen, Y., Shen, Z., Gao, Y., Xiao, L., Zheng, J., & Zeng, P. (2020). Alcohol Drinking and Amyotrophic Lateral Sclerosis: An Instrumental Variable Causal Inference. Annals of Neurology, 88(1), 195–198. https://doi.org/10.1002/ana.25721

Yu, Y. J., Atwal, J. K., Zhang, Y., Tong, R. K., Wildsmith, K. R., Tan, C., Bien-Ly, N., Hersom, M., Maloney, J. A., Meilandt, W. J., Bumbaca, D., Gadkar, K., Hoyte, K., Luk, W., Lu, Y., Ernst, J. A., Scearce-Levie, K., Couch, J. A., Dennis, M. S., & Watts, R. J. (2014). Therapeutic bispecific antibodies cross the blood-brain barrier in nonhuman primates. Science Translational Medicine, 6(261). https://doi.org/10.1126/scitranslmed.3009835

Yugi, K., Kubota, H., Hatano, A., & Kuroda, S. (2016). Trans-Omics: How To Reconstruct Biochemical Networks Across Multiple 'Omic' Layers. Trends in Biotechnology, 34(4), 276–290. https://doi.org/10.1016/j.tibtech.2015.12.013

Yun, H., Kim, S., Kim, S., Park, H., & Jeong, H. (2024). Efficient generation of recombinant anti-HER2 scFv with high yield and purity using a simple method. Biotechnology Journal, 19(7), 2300745. https://doi.org/10.1002/biot.202300745

Zaepfel, B. L., & Rothstein, J. D. (2021). RNA Is a Double-Edged Sword in ALS Pathogenesis. Frontiers in Cellular Neuroscience, 15, 708181. https://doi.org/10.3389/fncel.2021.708181

Zarei, S., Carr, K., Reiley, L., Diaz, K., Guerra, O., Altamirano, P., Pagani, W., Lodin, D., Orozco, G., & Chinea, A. (2015). A comprehensive review of amyotrophic lateral sclerosis. Surgical Neurology International, 6(1), 171. https://doi.org/10.4103/2152-7806.169561

Zgorzynska, E., Dziedzic, B., & Walczewska, A. (2021). An Overview of the Nrf2/ARE Pathway and Its Role in Neurodegenerative Diseases. International Journal of Molecular Sciences, 22(17), 9592. https://doi.org/10.3390/ijms22179592

Zhang, K., Daigle, J. G., Cunningham, K. M., Coyne, A. N., Ruan, K., Grima, J. C., Bowen, K. E., Wadhwa, H., Yang, P., Rigo, F., Taylor, J. P., Gitler, A. D., Rothstein, J. D., & Lloyd, T. E. (2018). Stress Granule Assembly

Disrupts Nucleocytoplasmic Transport. Cell, 173(4), 958-971.e17. https://doi.org/10.1016/j.cell.2018.03.025

Zhang, S., Cooper-Knock, J., Weimer, A. K., Shi, M., Moll, T., Marshall, J. N. G., Harvey, C., Nezhad, H. G., Franklin, J., Souza, C. D. S., Ning, K., Wang, C., Li, J., Dilliott, A. A., Farhan, S., Elhaik, E., Pasniceanu, I., Livesey, M. R., Eitan, C., … Glass, J. D. (2022). Genome-wide identification of the genetic basis of amyotrophic lateral sclerosis. Neuron, 110(6), 992-1008.e11. https://doi.org/10.1016/j.neuron.2021.12.019

Zhang, Y., Qian, L., Kuang, Y., Liu, J., Wang, D., Xie, W., Zhang, L., & Fu, L. (2022). An adeno-associated virus-mediated immunotherapy for Alzheimer's disease. Molecular Immunology, 144, 26–34. https://doi.org/10.1016/j.molimm.2022.02.006

Zhao, B., Louadi, S., Dijkstra, A. A., Plotkin, S. S., Kaplan, J., & Cashman, N. R. (2021). Selective targeting of intracellular, misfolded, pathogenic TDP-43 with rationally designed intrabodies. Alzheimer's & Dementia, 17(S9). https://doi.org/10.1002/alz.055269

Zhao, P., Zhang, N., & An, Z. (2022). Engineering antibody and protein therapeutics to cross the blood–brain barrier. Antibody Therapeutics, 5(4), 311–331. https://doi.org/10.1093/abt/tbac028

Zhao, X., Zhang, E., Ren, X., Bai, X., Wang, D., Bai, L., Luo, D., Guo, Z., Wang, Q., & Yang, J. (2020). Edaravone alleviates cell apoptosis and mitochondrial injury in ischemia–reperfusion-induced kidney injury via the JAK/STAT pathway. Biological Research, 53(1), 28. https://doi.org/10.1186/s40659-020-00297-0

Zhao, Y., Lützen, U., Gohlke, P., Jiang, P., Herdegen, T., & Culman, J. (2021). Neuroprotective and antioxidative effects of pioglitazone in brain tissue adjacent to the ischemic core are mediated by PI3K/Akt and Nrf2/ARE pathways. Journal of Molecular Medicine, 99(8), 1073–1083. https://doi.org/10.1007/s00109-021-02065-3

Zhong, Z., Deane, R., Ali, Z., Parisi, M., Shapovalov, Y., O'Banion, M. K., Stojanovic, K., Sagare, A., Boillee, S., Cleveland, D. W., & Zlokovic, B. V. (2008). ALS-causing SOD1 mutants generate vascular changes prior to motor neuron degeneration. Nature Neuroscience, 11(4), 420–422. https://doi.org/10.1038/nn2073

Zhou, J., Li, A., Li, X., & Yi, J. (2019). Dysregulated mitochondrial Ca2+ and ROS signaling in skeletal muscle of ALS mouse model. Archives of Biochemistry and Biophysics, 663, 249–258. https://doi.org/10.1016/j.abb.2019.01.024

Ziff, O. J., Clarke, B. E., Taha, D. M., Crerar, H., Luscombe, N. M., & Patani, R. (2022). Meta-analysis of human and mouse ALS astrocytes reveals multi-omic signatures of inflammatory reactive states. Genome Research, 32(1), 71–84. https://doi.org/10.1101/gr.275939.12

Zoccolella, S., Beghi, E., Palagano, G., Fraddosio, A., Samarelli, V., Lamberti, P., Lepore, V., Serlenga, L., & Logroscino, G. (2006). Predictors of delay in the diagnosis and clinical trial entry of amyotrophic lateral sclerosis patients: A population-based study. Journal of the Neurological Sciences, 250(1–2), 45–49. https://doi.org/10.1016/j.jns.2006.06.027

Zou, Z.-Y., Zhou, Z.-R., Che, C.-H., Liu, C.-Y., He, R.-L., & Huang, H.-P. (2017). Genetic epidemiology of amyotrophic lateral sclerosis: A systematic review and meta-analysis. Journal of Neurology, Neurosurgery & Psychiatry, 88(7), 540–549. https://doi.org/10.1136/jnnp-2016-315018

Zuo, X., Zhou, J., Li, Y., Wu, K., Chen, Z., Luo, Z., Zhang, X., Liang, Y., Esteban, M. A., Zhou, Y., & Fu, X.-D. (2021). TDP-43 aggregation induced by oxidative stress causes global mitochondrial imbalance in ALS. Nature Structural & Molecular Biology, 28(2), 132–142. https://doi.org/10.1038/s41594-020-00537-7

Zürcher, N. R., Loggia, M. L., Lawson, R., Chonde, D. B., Izquierdo-Garcia, D., Yasek, J. E., Akeju, O., Catana, C., Rosen, B. R., Cudkowicz, M. E., Hooker, J. M., & Atassi, N. (2015). Increased in vivo glial activation in patients with amyotrophic lateral sclerosis: Assessed with [11C]-PBR28. NeuroImage: Clinical, 7, 409–414. https://doi.org/10.1016/j.nicl.2015.01.009

Yara ALOJAIMI

CHARACTERIZATION OF A THERAPEUTIC APPROACH TO TARGET TDP-43 IN AMYOTROPHIC LATERAL SCLEROSIS USING ANTIBODY FRAGMENTS

Résumé en français :

La Sclérose Latérale Amyotrophique (SLA) est une maladie neurodégénérative progressive caractérisée par la dégénérescence des motoneurones. Un marqueur pathologique clé de la SLA est l'accumulation cytoplasmique de la protéine TDP-43 dans les neurones et cellules gliales des patients, en faisant une cible thérapeutique prometteuse.

Dans ce projet, nous avons exploré plusieurs stratégies pour mieux comprendre la SLA en tant que protéinopathie liée à TDP-43 et cibler cette protéine. Nous avons d'abord démontré que les altérations du pH intracellulaire favorisent la délocalisation et l'accumulation de TDP-43 en punctas cytoplasmiques *in vitro*, soulignant ainsi l'impact du métabolisme sur TDP-43. Ensuite, nous avons testé deux fragments d'anticorps (scFv), B1 et D7, ciblant TDP-43 humaine sauvage. Le D7 a montré des effets protecteurs en réduisant les fragments insolbules 35 kDa de TDP-43 et en restaurant des altérations métaboliques dans des modèles cellulaires de SLA. Nous avons ensuite réalisé une caractérisation phénotypique, moléculaire et métabolipidomique détaillée du modèle murin Prp-TDP-43^{A315T} afin d'identifier des paramètres quantifiables de réponse aux thérapies. Ce modèle a reproduit les symptômes moteurs et l'agrégation de TDP-43, avec des altérations métabolipidomiques détectées avant l'apparition des symptômes, faisant de ce modèle un outil important pour l'étude des thérapies ciblant TDP-43. Pour surmonter les défis liés à la barrière hémato-encéphalique, nous avons teste différentes méthodes pour améliorer l'administration du scFv : des nanoparticules magnétiques (SPIONs) complexées avec le scFv qui ont permis l'internalisation su scFv *in vitro* et des vecteurs viraux adéno-associés (AAV.CAP-B10) qui ont permis l'expression du scFv dans le système nerveux central *in vivo*.

Ces résultats ouvrent des perspectives de développement de nouvelles thérapies ciblant TDP-43 dans la SLA et d'identification de nouveaux marqueurs de suivi thérapeutiques.

Mots clés : Biothérapies, Omique, scFv, SLA, TDP-43.

Summary :

Amyotrophic Lateral Sclerosis (ALS) is a progressive neurodegenerative disease characterized by motor neuron degeneration. A key pathological marker of ALS is the cytoplasmic accumulation of TDP-43 in neurons and glial cells, making it a promising therapeutic target.

This project explored several strategies to better understand ALS as a TDP-43 proteinopathy and to target this protein. First, we demonstrated that intracellular pH alterations promote the delocalization and accumulation of TDP-43 in cytoplasmic puncta *in vitro*, highlighting the impact of metabolism on TDP-43. Next, we tested two single-chain variable fragments (scFv), B1 and D7, targeting wildtype human TDP-43. The scFv D7 showed protective effects by reducing insoluble 35 kDa TDP-43 fragments and restoring metabolic alterations in cellular models of ALS. We then conducted a detailed phenotypic, molecular, and metabololipidomic characterization of the Prp-TDP-43^{A315T} mouse model to identify quantifiable parameters for therapeutic responses. This model reproduced motor symptoms and TDP-43 aggregation, with metabololipidomic alterations detected before symptom onset, making it an important tool for studying therapies targeting TDP-43. To overcome challenges related to the blood-brain barrier, we tested different methods to improve scFv delivery: magnetic nanoparticles (SPIONs) complexed with scFv, which enabled scFv internalization in *vitro*, and adeno-associated viral vectors (AAV.CAP-B10), which allowed scFv expression in the central nervous system *in vivo*.

These findings open up new prospects for developing TDP-43-targeted therapies for ALS and for identifying novel therapeutic follow-up markers.

Keywords : Biotherapeutics, Omics, scFv, ALS, TDP-43.